INTERNATIONAL JOURNAL OF PLANT BASED PHARMACEUTICALS

Discover the green world!

IJPBP

INTERNATIONAL JOURNAL OF PLANT BASED PHARMACEUTICALS
(IJPBP)

Int. J. Plant Bas. Pharm.

e-ISSN: 2791-7509

This is an international peer-reviewed Open Access journal and published two issues per year.

Corresponding Address
International Journal of Plant Based Pharmaceuticals
(IJPBP)
Prof. Dr. Bektas TEPE, Ph.D.
Kilis 7 Aralik University, Faculty of Science and Literature, Department of Molecular Biology and Genetics, 79000, Kilis-Türkiye
Phone: +90 348-814 26 66
Web: https://ijpbp.com
E-mail:
info@ijpbp.com

Publisher
Bektas TEPE Publications
Address:
Aydınlıkevler Mahallesi, Savun Caddesi, 2A/3, Altındağ, Ankara, Türkiye
Tel : +90 554 354 29 14

INTERNATIONAL JOURNAL OF PLANT BASED PHARMACEUTICALS
(IJPBP)
An International Peer Reviewed Open Access Journal
e-ISSN: 2791-7509

PUBLISHING (ADVISORY) BOARD

Bektas TEPE, Ph.D.
Editor-in-Chief
(Plant Biotechnology, Phytochemistry, Phytopharmaceuticals)
Kilis 7 Aralik University, Kilis-TÜRKİYE

Cengiz SARIKURKCU, Ph.D.
Co-Editor-in-Chief
(Biochemistry, Phytochemistry, Phytopharmaceuticals)
Afyonkarahisar Health Science University, Afyonkarahisar-TÜRKİYE

Filiz UCAN TURKMEN, Ph.D.
Co-Editor-in-Chief
(Plant Biotechnology, Phytochemistry, Phytopharmaceuticals)
Kilis 7 Aralik University, Kilis-TÜRKİYE

Marcello Iriti, Ph.D.
(Pharmaceutical Biology)
Milan University, Milan, ITALY

Sabiu Saheed, Ph.D.
(Biochemistry)
Durban University of Technology, KwaZuluNatal, SOUTH AFRICA

Prakash Murgeppa Bhuyar, Ph.D.
(Biotechnology, Environmental Engineering, Energy Efficiency, Renewable Energy, Biomass Conversion)
Energy Research Centre,, International College (MJU-IC), Maejo University, Nong Han, San Sai District, Chiang Mai 50290, THAILAND

Ekrem GUREL, Ph.D.
(Plant Physiology, Biotechnology)
Bolu Abant Izzet Baysal University,
Bolu- TÜRKİYE

Sanja Ćavar Zeljković, Ph.D.
(Plant Biotechnology, Natural Product Chemistry, Medicinal and Pharmaceutical Chemistry)
Palacký University, Olomouc-CZECH REPUBLIC

Mir Babak BAHADORI, Ph.D.
(Phytochemistry, Pharmacognosy, Chromatography, Spectroscopy, Food Chemistry)
Medicinal Plants Research Center, Maragheh-IRAN

Marcello LOCATELLI, Ph.D.
(Analytical Chemistry)
University "G. d'Annunzio" of Chieti-Pescara, Chieti-ITALY

Mejdi SNOUSSI, Ph.D.
(Microbiology, Phytochemistry)
Hail University, Ha'il-KSA

Jelena Popović-Djordjević, Ph.D.
(Chemistry of Natural Products, Organic Chemistry, Food Chemistry, Environmental Chemistry)
University of Belgrade, Belgrade-SERBIA

Adel KADRI, Ph.D.
(Biological Activity, Drug Design, ADMET, Docking)
University of Sfax, Sfax-TUNISIA

Walid ELFALLEH, Ph.D.
(Biomass Valorization for Medicinal and Food Applications)
Higher Institute of Applied Sciences and Technology of Gabes (ISSATGb), Gabes-TUNISIA

Paulo Augusto NETZ, Ph.D.
(Theoretical Chemistry)
Universidade Federal do Rio Grande do Soul,
Porto Alegre-BRASIL

Ryszard Amarowicz, Ph.D.
(Analytical Chemistry, Phenolic Compounds, Antioxidants, Chromatography)
Institute of Animal Reproduction and Food Research,
Olsztyn-POLAND

Gokhan ZENGIN, Ph.D.
(Biochemistry)
Selcuk University, Konya- TÜRKİYE

Leyla ACIK, Ph.D.
(Molecular Biology, Biotechnology)
Gazi University, Ankara- TÜRKİYE

Mustafa OSKAY, Ph.D.
(Biology, Microbiology, Bacteriology)
Manisa Celal Bayar University, Manisa- TÜRKİYE

Erman Salih ISTIFLI, Ph.D.
(Genetics, Molecular Docking, Molecular Dynamics, Drug Discovery)
Cukurova University, Adana- TÜRKİYE

Selami Selvi, Ph.D
(Plant Morphology and Anatomy, Plant Systematic, Ethnopharmacology, Plant Chemistry)
Balıkesir University, Balikesir- TÜRKİYE

Bulent KIRKAN, Ph.D.
(Analytical Chemistry, Phytochemistry)
Suleyman Demirel University, Isparta- TÜRKİYE

Muhsin Konuk, Ph.D
(Toxicology, Pharmacogenetics, Biotechnology, Bioactive compounds)
Uskudar University, Istanbul- TÜRKİYE

Yavuz Selim CAKMAK, Ph. D.
(Biology, Biochemistry, Biotechnology)
Aksaray University, Aksaray- TÜRKİYE

Mehdi Heidarian, Ph.D.
(Medicinal and Aromatic Plants)
Islamic Azad University, Tehran, IRAN

Sonia MALIK, Ph.D.
(Plant Biotechnology)
University of Orleans, Orleans, FRANCE

Language Editor
Erman Salih ISTIFLI, Ph.D.

INTERNATIONAL JOURNAL OF PLANT BASED PHARMACEUTICALS
(IJPBP)
An International Peer Reviewed Open Access Journal
e-ISSN: 2791-7509

JOURNAL INFORMATION

Journal Name:	International Journal of Plant Based Pharmaceuticals
Journal Abbreviation:	Int. J. Plant Bas. Pharm.
Scope & Subjects:	Researchers are cordially invited to submit their manuscripts to the International Journal of Plant Based Pharmaceuticals (IJPBP), an international and peer-reviewed open access journal devoted to the publish original research papers, review articles, short communications, letters to the editor/commentary and guest edited single topic issues in all areas of plant-based pharmaceuticals in English.
e-ISSN:	2791-7509
Publisher:	Bektas TEPE Publications
Language:	English
Frequency:	Biannually (June and December)
Type of Publication:	Peer Review Double-Blinded
Publication Fee:	No Submission or Processing Charges
Access type:	Open Access
Manuscript Submission System:	IJPBP uses the submission system given below: https://ijpbp.com
License:	Licensed under a Creative Commons Attribution 4.0 International License (CC BY).
Legal Responsibility:	Authors are responsible for content of articles that published in IJPBP
Indexing and Abstracting:	Google Scholar, DOAJ, EBSCO, Scilit, Asos Index, AcarIndex
Address:	Kilis 7 Aralik University, Faculty of Science and Literature, Department of Molecular Biology and Genetics, Kilis-Türkiye
Web:	https://ijpbp.com
Contact:	Phone: +90 348-814 26 66 E-mail: info@ijpbp.com

INTERNATIONAL JOURNAL OF PLANT BASED PHARMACEUTICALS
(IJPBP)
An International Peer Reviewed Open Access Journal
e-ISSN: 2791-7509

INSTRUCTION FOR AUTHORS

International Journal of Plant Based Pharmaceuticals is an international peer-reviewed open access journal publishing research on plant pharmaceuticals.

Ensure that the following items are present:

One author has been designated as the corresponding author with contact details:

- E-mail address
- Full postal address

All necessary files have been sent to the editorial office:

- Manuscript
- Include keywords
- All figures (include relevant captions)
- All tables (include titles, description, footnotes)
- Ensure all figure and table citations in the text match the files provided
- Supplementary files (where applicable)

Further considerations

- The manuscript fits within Aims and Scope of International Journal of Plant Based Pharmaceuticals. Please note that the Aims and Scope are regularly updated.
- The research is novel and has not been published previously (please see 'Responsible Research Publication: International Standards for Authors' from COPE for more information).
- Ethical consent has been obtained in case of work on animals and/or humans.
- Manuscript has been 'spell checked' and 'grammar checked'.
- All references mentioned in the Reference List are cited in the text and vice versa.
- Permission has been obtained for use of copyrighted material from other sources (including the Internet).
- A competing interest's statement is provided, even if the authors have no competing interests to declare.
- Journal policies detailed in this guide have been reviewed.
- Referee suggestions and contact details provided, based on journal requirements.

Types of paper

1. Original research papers

Original full-length research papers that have not been published previously, except in a preliminary form and should not exceed 7.500 words from introduction to conclusion (not including references) (including no more than six tables and figures combined-additional tables and figures can be submitted as supplementary material).

2. Review articles

Review articles (will be accepted in areas of topical interest) will normally focus on literature published over the previous years and should not exceed 10.000 words from introduction to conclusion (not including references) (including allowance for no more than six tables and figures combined). Review articles should not contain more than 120 references. If it is felt absolutely necessary to exceed these numbers (tables, figures, references), please contact the editorial office (bektastepe@yahoo.com) for advice before submission.

3. Short communications

Short communications of up to 3.000 words from introduction to conclusion (not including references), describing work that may be of a preliminary nature but merits publication. These papers should not contain more than 40 references.

4. Letters to the Editor/Commentary

Letters are published from time to time on matters of topical interest.

Special issues

If you would like to suggest a special issue, please contact our editorial office (info@ijpbp.com) with a proposal for the special issue including the rationale for the special issue topic, potential contributors and how you plan to attract high quality papers. Before submitting you proposal, please read our Guide for Guest Editors.

Ethics in publishing

The publication of an article in a peer-reviewed journal is an essential building block in the development of a coherent and respected network of knowledge. It is a direct reflection of the quality of the work of the authors and the institutions that support them. Peer-reviewed articles support and embody the scientific method.

It is therefore important to agree upon standards of expected ethical behavior for all parties involved in the act of publishing: the author, the journal editor, the peer reviewer, the published and the society of society-owned or sponsored journals.

The total similarity rate of the articles sent to IJPBP should not exceed 25% and the similarity rate to each source should not exceed 5%.

Conflict of interest

All authors must disclosure any financial and personal relationships with other people or organizations that could inappropriately influence (bias) their work. Examples of potential competing interests include employment, consultancies, stock ownership, honoraria, paid expert testimony, patent applications/registrations and grants or other funding. Authors should present the conflict of interest statement in the manuscript right after the 'Acknowledgment' section. If there is no interests to declare, please choose: ‘Conflict of interest: none’. This summary statement will be published within the article if accepted.

Submission declaration and verification

Submission of an article implies that the work described has not been published previously (except in the form of an abstract, a published lecture or academic thesis), that it is not under consideration for publication elsewhere, that its publication is approved by all authors and tacitly or explicitly by the responsible authorities where the work was carried out and that, if accepted, it will not be published elsewhere in the same form, in English or any other language, including electronically without the written consent of the copyright-holder. To verify originality, your article may be checked by the originality detection service Crossref Similarity Check.

Use of inclusive language

Inclusive language acknowledges diversity, conveys respect to all people, is sensitive to differences and promotes equal opportunities. Articles should make no assumptions about the beliefs or commitments of any reader, should contain nothing which might imply that one individual is superior to another on the grounds of race, sex, culture or any other characteristics and should use inclusive language throughout. Authors should ensure that writing is free from bias, for instance by using ‘he/she’, ‘his/her’ instead of ‘he’ or ‘his’, and by making use of job titles that free of stereotyping (e.g. ‘chairperson’ instead of ‘chairman’ and ‘flight attendant’ instead of ‘stewardess’).

Author contributions

For transparency, we encourage authors to submit an author statement in the manuscript outlining their individual contributions to the paper using the relevant CRediT roles:

- Conceptualization
- Data curation
- Formal analysis
- Funding acquisition
- Investigation
- Methodology
- Project administration
- Resources

- Software

- Supervision

- Validation

- Visualization

- Writing

- Review & Editing

Roles

- Writing original draft

- Writing-reviewing & editing

Authors statements should be formatted with the initials of the names of authors (e.g. T.H. for Thomas Hunt) and Credit role(s).

Changes to authorship

All authors should have made substantial contributions to all of the following:

- The conception and design of the study or acquisition of data or analysis and interpretation of data.

- Drafting the article or revising it critically for important intellectual content.

- Final approval of the version to be submitted.

If all 3 of these conditions are not met, a person does not qualify as an author and any contribution made by them should be mentioned in the Acknowledgements section of the manuscript.

Authors are expected to consider carefully the list and order of authors before submitting their manuscript and provide the definitive list of authors at the time of the original submission. Any addition, deletion or rearrangement of author names in the authorship list should be made only before the manuscript has been accepted and only if approved by the journal editor. To request such a change, the editor must receive the following from the corresponding author:

- the reason for the change in author list and

- written confirmation (e-mail, letter) from all authors that they agree with the addition, removal or rearrangement

In the case of addition or removal of authors, this includes confirmation from the author being added or removed.

Only in exceptional circumstances will the editor consider the addition, deletion or rearrangement of authors after the manuscript has been accepted. While the editor considers the request, publication of the manuscript will be suspended. If the manuscript has already been published in an online issue, any requests approved by the editor will result in a corrigendum.

Copyright

The Contributor(s) or, if applicable, the Contributor's Employer retains all proprietary rights, including copyright.

Role of funding source

Your are requested to identify who provided financial support for the conduct of the research and/or preparation of the article and to briefly describe the role of the sponsor(s), if any, in study design; in the collection, analysis and interpretation of data; in the writing of the report; and in the decision to submit the article for publication. If the funding source(s) had no such involvement then this should be stated.

Submission

The manuscript file prepared in .doc/.docx format to be sent to IJPBP, together with the cover letter and all other attachments, if any, by using the online manuscript submission system.

Peer review

This journal operates a single anonymized review process. All contributions will be initially assessed by the editor for suitability for the journal. Papers deemed suitable are then typically sent to a minimum of two independent expert reviewers to assess the scientific quality of the paper. The editor is responsible for the final decision regarding acceptance of rejection of articles. The editor’s decision is final. Editors are not involved in decisions about papers which they have written themselves or have been written by family members or colleagues or which relate to products or services in which the editor has an interest. Any such submission is subject to all of the journal’s usual procedures, with peer review handled independently of the relevant editor and their research groups.

Review Policy

The editor have the right to decline formal review of a manuscript when it is seemed that the manuscript

- is on a topic outside the scope of the journal

- makes no contribution to the advancement of the field of plant based pharmaceuticals

- is lacking technical or scientific merit

- is focused on the plant based pharmaceuticals that are of narrow regional scope and significance

- is fragmentary and providing marginally incremental results,

- reports only routine work (lacks novelty) or is poorly written.

Use of word processing software

It is important that the file be saved in the native format of the word processor used. The text should be in single-column format. Keep the layout of the text as simple as possible. Most formatting codes will be removed and replaced on processing the article. In particular, do not use the word processor's options to justify text or hyphenate words. However, do use bold face, italics, subscripts, superscripts etc. When preparing tables, if yo are using a table grid, use only one grid for each individual table and not a grid for each row. If no grid is used, use tabs, not spaces, to align columns. The electronic text should be prepared in a way very similar to that of conventional manuscripts. Note that source of files and figures, tables and text graphics will be required whether or not you embed your figures in the text. To avoid unnecessary errors you are strongly advised to use the 'spell-check' and 'grammar-check' functions of your word processor.

Article structure

Follow this order when typing manuscript: Title, Authors, Affiliations, Abstract (maximum 350 words), Keywords, Main text (Introduction, Material and Methods, Results and Discussion, Conclusion, Acknowledgements, Conflict of interest, CRediT authorship contribution statement, ORCID Numbers of the Authors, References, Tables, Figures and supplementary file (if any). The corresponding author should be identified with an asterisk and footnote. All other footnotes (except for table footnotes) should be identified with superscript numbers. The title of the paper should unambiguously reflect its contents.

Artwork

Electronic artwork

General points

- Make sure you use uniform lettering and sizing of your original artwork.

- Embed the used fonts if the application provides that option.

- Aim to use the following fonts in your illustrations: Arial, Courier, Times New Roman, Symbol, or use fonts that look similar.

- Number the illustrations according to their sequence in the text.

- Use a logical naming convention for your artwork files.

- Size the illustrations close to the desired dimensions of the published version.

- Submit each illustration as a separate file.

- Ensure that color images are accessible to all, including those with impaired color vision.

Formats

If your electronic artwork is created in a Microsoft Office application (Word, PowerPoint, Excel) then please supply 'as is' in the native document format.

Regardless of the application used other than Microsoft Office, when your electronic artwork is finalized, please 'Save as' or convert the images to one of the following formats (note the resolution requirements for line drawings, halftones, and line/halftone combinations given below):

EPS (or PDF): Vector drawings, embed all used fonts.

TIFF (or JPEG): Color or grayscale photographs (halftones), keep to a minimum of 300 dpi.

TIFF (or JPEG): Bitmapped (pure black & white pixels) line drawings, keep to a minimum of 1000 dpi.

TIFF (or JPEG): Combinations bitmapped line/half-tone (color or grayscale), keep to a minimum of 500 dpi.

Please do not:

- Supply files that are optimized for screen use (e.g., GIF, BMP, PICT, WPG); these typically have a low number of pixels and

limited set of colors;

- Supply files that are too low in resolution;

- Submit graphics that are disproportionately large for the content.

Color artwork

Please make sure that artwork files are in an acceptable format (TIFF (or JPEG), EPS (or PDF) or MS Office files) and with the correct resolution. If, together with your accepted article, you submit usable color figures then our editorial office will ensure, at no additional charge, that these figures will appear in color online (e.g., ScienceDirect and other sites).

Figure Captions

Ensure that each illustration has a caption. A caption should comprise a brief title (not on the figure itself) and a description of the illustration. Keep text in the illustrations themselves to a minimum but explain all symbols and abbreviations used.

Tables

Please submit tables as editable text and not as images. Tables can be placed either next to the relevant text in the article, or on separate page(s) at the end. Number tables consecutively in accordance with their appearance in the text and place any table notes below the table body. Be sparing in the use of tables and ensure that the data presented in them do not duplicate results described elsewhere in the article. Please avoid using vertical rules and shading in table cells.

References

Please note: EndNote users can download IJPBP's style file here.

Citation in text

Please ensure that every reference cited in the text is also present in the reference list (and vice versa). Any references cited in the abstract must be given in full. Unpublished results and personal communications are not recommended in the reference list, but may be mentioned in the text. If these references are included in the reference list they should follow the standard reference style of the journal and should include a substitution of the publication date with either 'Unpublished results' or 'Personal communication'. Citation of a reference as 'in press' implies that the item has been accepted for publication.

Reference links

Increased discoverability of research and high quality peer review are ensured by online links to the sources cited. In order to allow us to create links to abstracting and indexing services, such as Scopus, CrossRef and PubMed, please ensure that data provided in the references are correct. Please note that incorrect surnames, journal/book titles, publication year and pagination may prevent link creation. When copying references, please be careful as they may already contain errors. Use of the DOI is highly encouraged.

A DOI is guaranteed never to change, so you can use it as a permanent link to any electronic article. An example of a citation using DOI for an article not yet in an issue is: VanDecar J.C., Russo R.M., James D.E., Ambeh W.B., Franke M. (2003). Aseismic continuation of the Lesser Antilles slab beneath northeastern Venezuela. Journal of Geophysical Research,https://doi.org/10.1029/2001JB000884.

Please note the format of such citations should be in the same style as all other references in the paper.

Web references

As a minimum, the full URL should be given and the date when the reference was last accessed. Any further information, if known (DOI, author names, dates, reference to a source publication, etc.), should also be given. Web references can be listed separately (e.g., after the reference list) under a different heading if desired, or can be included in the reference list.

Data references

This journal encourages you to cite underlying or relevant datasets in your manuscript by citing them in your text and including a data reference in your Reference List. Data references should include the following elements: author name(s), dataset title, data repository, version (where available), year, and global persistent identifier. Add [dataset] immediately before the reference so we can properly identify it as a data reference. The [dataset] identifier will not appear in your published article.

References in a special issue

Please ensure that the words 'this issue' are added to any references in the list (and any citations in the text) to other articles in the same Special Issue.

Reference management software

Most of the journals have their reference template available in many of the most popular reference management software

products. These include all products that support Citation Style Language styles, such as Mendeley. Using citation plug-ins from these products, authors only need to select the appropriate journal template when preparing their article, after which citations and bibliographies will be automatically formatted in the journal's style. If no template is yet available for this journal, please follow the format of the sample references and citations as shown in this Guide. If you use reference management software, please ensure that you remove all field codes before submitting the electronic manuscript.

Reference style

Text: Citations in the text should follow the referencing style used by the American Psychological Association. You are referred to the Publication Manual of the American Psychological Association, Seventh Edition, ISBN 978-1-4338-3215-4, copies of which may be ordered online.

List: References should be arranged first alphabetically and then further sorted chronologically if necessary. More than one reference from the same author(s) in the same year must be identified by the letters 'a', 'b', 'c', etc., placed after the year of publication.

Examples:

Reference to a journal publication:

Van der Geer, J., Hanraads, J. A. J., & Lupton, R. A. (2010). The art of writing a scientific article. *Journal of Scientific Communications*, *163*(1), 51–59.

Reference to a journal publication with an article number:

Van der Geer, J., Hanraads, J. A. J., & Lupton, R. A. (2018). The art of writing a scientific article. *Heliyon*, *19*, Article e00205.

Reference to a book:

Strunk, W., & White, E. B. (2000). The elements of style (4th ed.). Longman (Chapter 4).

Reference to a chapter in an edited book:

Mettam, G.R., & Adams, L.B. (2009). How to prepare an electronic version of your article. In B.S. Jones, & R.Z. Smith (Eds.), Introduction to the electronic age (pp. 281–304). E-Publishing Inc.

Reference to a website:

Powertech Systems (2015). Lithium-ion vs lead-acid cost analysis. Retrieved from http://www.powertechsystems.eu/home/tech-corner/lithium-ion-vs-lead-acid-cost-analysis/. Accessed January 6, 2016.

Reference to a dataset:

[dataset] Oguro, M., Imahiro, S., Saito, S., & Nakashizuka, T. (2015). Mortality data for Japanese oak wilt disease and surrounding forest compositions. Mendeley Data, v1.

Reference to a conference paper or poster presentation:

Engle, E. K., Cash, T. F., & Jarry, J. L. (2009), November. The Body Image Behaviours Inventory-3: Development and validation of the Body Image Compulsive Actions and Body Image Avoidance Scales. Poster session presentation at the meeting of the Association for Behavioural and Cognitive Therapies, New York, NY.

Reference to software:

Coon, E., Berndt, M., Jan, A., Svyatsky, D., Atchley, A., Kikinzon, E., Harp, D., Manzini, G., Shelef, E., Lipnikov, K., Garimella, R., Xu, C., Moulton, D., Karra, S., Painter, S., Jafarov, E., & Molins, S. (2020), March 25. Advanced Terrestrial Simulator (ATS) v0.88 (Version 0.88). Zenodo. https://doi.org/10.5281/zenodo.3727209.

Journal abbreviations

Journal names should not be abbreviated.

Supplementary material

Supplementary material such as applications, images and sound clips, can be published with your article to enhance it. Submitted supplementary items are published exactly as they are received (Excel or PowerPoint files will appear as such online). Please submit your material together with the manuscript (at the end of the manuscript) and supply a concise, descriptive caption for each supplementary file. If you wish to make changes to supplementary material during any stage of the process, please make sure to provide an updated file. Do not annotate any corrections on a previous version. Please switch off the 'Track Changes' option in Microsoft Office files as these will appear in the published version.

Proof correction

To ensure a fast publication process of the article, we kindly ask authors to provide us with their proof corrections within two days. Corresponding authors will receive an e-mail containing proof produced by our editorial office and will review this file

and identify the sections to be corrected. We will do everything possible to get your article published quickly and accurately. Please use this proof only for checking the typesetting, editing, completeness and correctness of the text, tables and figures. Significant changes to the article as accepted for publication will only be considered at this stage with permission from the editor. It is important to ensure that all corrections are sent back to us in one communication. Please check carefully before replying, as inclusion of any subsequent corrections cannot be guaranteed. Proofreading is solely your responsibility.

Access to the final version of the article

The corresponding author will be notified and receive a link to the published version of the open access article at https://ijpbp.com. This link is in the form of an article DOI link that can be shared via email and social networks.

The authors are responsible for the content of the articles published in IJPBP. IJPBP does not accept any responsibility for the content of the article.

INTERNATIONAL JOURNAL OF PLANT BASED PHARMACEUTICALS
(IJPBP)
An International Peer Reviewed Open Access Journal
e-ISSN: 2791-7509

FROM THE EDITOR

International Journal of Plant BasedPharmaceuticals (IJPBP) is a peer-reviewed open access journal for original research articles, review articles and short communications related to all aspects of plant based pharmaceuticals and pharmaceutical analysis. IJPBP was launched in 2021, and published biannually.

IJPBP welcomes submissions from a diverse range of disciplines and geographic regions, reflecting its commitment to a truly global perspective on plant-based pharmaceuticals. Current areas of interest include, but are not limited to, the following topics:

- Analysis of traditional medicines and herbal formulations from various global traditions (e.g., Ayurveda, Traditional Chinese Medicine, and African ethnomedicine)
- Pharmaceutical analysis of complex systems in plant-derived drugs
- Quality control methodologies for biopharmaceuticals derived from plants
- Mechanisms of action and metabolism of plant-based compounds
- Quantitative and qualitative approaches in drug discovery and screening processes
- Applications of tracer analysis in molecular pharmacology and plant-based biopharmaceutics
- Clinical laboratory and bioanalytical methods for plant-based pharmaceuticals
- Analytical chemistry techniques for characterizing plant-derived molecules
- Toxicological and pharmacological activity analysis of plant-based drugs
- Development and application of advanced biochemistry methods for pharmaceutical research
- Emerging screening methods for bioactive compounds from plants
- Integration of molecular docking, dynamics simulations, and computational tools for plant-based drug research
- Novel formulations, including biomaterials, nanoparticles, and engineered cells from plant origins
- Biotechnology products such as plant-based peptides, proteins, and vaccines

IJPBP encourages contributions that explore new frontiers in plant-based pharmaceutical sciences and that demonstrate the global relevance and applicability of their findings. Submissions highlighting cross-disciplinary approaches or international collaborations are particularly welcome.

The journal has a distinguished editorial board with extensive academic qualifications, ensuring that the journal maintains high scientific standards and has a broad international coverage.

IJPBP seeks to publish original, high quality, peer-reviewed papers including original research articles and reviews as well as short communications. Submission would be encouraged on all aspects of plant based pharmaceutical analysis. The aim of this journal is to become a highly respected and trusted resource of leading knowledge in this field and to promote worldwide academic exchange.

Papers of IJPBP are opening accessible at the journal's homepage: https://ijpbp.com, and you are invited to read or download them freely for the academic exchanges.

Electronic versions of articles are published immediately and continuously once the manuscripts have been accepted. The average time between submission and final decision is 75 days and the average time between acceptance and final publication is 15 days. IJPBP does not charge authors who submit articles. The journal also does not charge authors for article processing or printing.

Sincerely,
Prof. Dr. Bektas TEPE, Ph.D.
Editor-in-Chief
International Journal of Plant Based Pharmaceuticas (IJPBP)
Contact: info@ijpbp.com

INTERNATIONAL JOURNAL OF PLANT BASED PHARMACEUTICALS
(IJPBP)
An International Peer Reviewed Journal
e-ISSN: 2791-7509

Table of Contents

Volume: 3 Issue: 1 June, 2023

Int. J. Plant Bas. Pharm. (2023) 3(1), 1-9

INTERNATIONAL JOURNAL OF PLANT BASED PHARMACEUTICALS

https://ijpbp.com

RESEARCH ARTICLE

OPEN ACCESS

Vernonia amygdalina leaf extract protects against carbon tetrachloride-induced hepatotoxicity and nephrotoxicity: a possible potential in the management of liver and kidney diseases

Temidayo Ogunmoyole[a*], Yetunde Beatrice Apanisile[b], Yusuff Adewale Akeem[c] Omowumi Jayeola Makun[d]

[a] *Ekiti State University, College of Medicine, Department of Medical Biochemistry, Ado Ekiti, Ekiti State, Nigeria*
[b] *Ekiti State University, Faculty of Science, Department of Science Laboratory Technology, Ado Ekiti, Ekiti State, Nigeria*
[c] *Osun State Primary Health Care Board , Osogbo, Nigeria*
[d] *Federal University of Petroleum Resources, Department of Environmental Management and Toxicology, Effurun, Delta State, Nigeria*

ARTICLE INFO

Article History:

Received: 08 July 2022
Revised: 25 September 2022
Accepted: 26 September 2022
Available online: 30 September 2022

Edited by: B. Tepe

Keywords:

Vernonia amygdalina
Rat
Kidney
Liver
Heart
Carbon tetrachloride

ABSTRACT

The rising prevalence of liver and kidney diseases is worrisome and constitutes a major threat to public health. The present study investigates the medicinal potentials of *Vernonia amygdalina* leaves in the management of liver and kidney diseases. Albino rats were randomly divided into five groups each containing 5 animals. In all groups, except group I (control), animals were exposed to 3 ml/kg bw of CCl_4 and then administered further different treatments. Groups III, IV, and V each were treated with 50 mg/kg bw, 100 mg/kg bw of bitter leaf extract, and 100 mg/kg bw of silymarin, respectively. Group II animals were left untreated after exposure to toxicant. Activities of creatine kinase (CK), aspartate aminotransferase (AST), alanine aminotransferase (ALT), alkaline phosphatase (ALP), as well as the level of urea, uric acid, and bilirubin were determined in the serum and tissue homogenates. Lipid profile as well as activities of superoxide dismutase (SOD) and catalase (CAT) were also determined. Exposure to CCl_4 resulted in a significant increase in CK, AST, ALP, and ALT levels as well as bilirubin, urea, and uric acid when compared to the control. Lipid profile was disrupted, activities of SOD and CAT were markedly inhibited and the level of GSH was significantly depleted. However, treatment with *V. amygdalina* reversed the toxic trend in a dose-dependent manner comparable to animals treated with silymarin. In conclusion, *V. amygdalina* leaf extract restored deranged lipid profile, distorted histoarchitecture as well as liver and kidney function markers. Hence, the plant is a potential candidate for the management of liver and kidney diseases.

1. Introduction

Since antiquity, nature has provided man with basic requirements such as healthcare, food, shelter as well as other necessities of human existence. Globally, medicinal plants occupy a central space and have dominated the healthcare system of developing countries where a very large percentage of the population depends on plants for therapy. As it stands, several developed and well-industrialized nations of the world are fast embracing the use of herbal extracts as complimentary therapy (Gurib-Fakim, 2006). Medicinal plants are not just important for healthcare but as an assured hope for the development of future medicines. At the moment, only about one-third of human diseases have readily available and efficacious therapies. There is, therefore, a dire need for medicinal plants with proven potency and safety

Reviewed by:
Recep Liman: Usak University, Usak, Türkiye
Ali Karadeniz: Ataturk University, Erzurum, Türkiye

* Corresponding author(s):
E-mail address:
tenidayo.ogunmoyole@eksu.edu.ng
(T. Ogunmoyole)
e-ISSN: 2791-7509
doi: https://doi.org/10.29228/ijpbp.10

Please cite this article as: Ogunmoyole, T., Apanisile, Y. B., Akeem, Y. A., & Makun, O. J. (2023). *Vernonia amygdalina* leaf extract protects against carbon tetrachloride-induced hepatotoxicity and nephrotoxicity: a possible potential in the management of liver and kidney diseases. *International Journal of Plant Based Pharmaceuticals*, *3*(1), 1-9, https://doi.org/10.29228/ijpbp.10.

that can serve as panacea to the menace of several diseases (Hamburger & Hostettmann, 1991). The World Health Organization (WHO) has endorsed and promoted the inclusion of herbal medicines in national healthcare programs due to ease of access, affordability, and safety (Singh & Singhi, 1981). Consequently, collaborative research efforts in the area of screening of plant extracts has led to the identification of pharmacologically active agents that can be exploited as drugs for the management of diseases (Rastogi & Meharotra, 1990).

Chronic liver disease (CLD) constitutes a major threat to global public health, causing increased morbidity and mortality worldwide (Marcellin & Kutala, 2018). Between 1980 and 2010, mortality as a result of liver disease increased by 46% globally (Mokdad et al., 2014) with higher prevalence in developing nations including Africa (Stepanova et al., 2017). Similarly, the global disease burden report in 2010 ranked chronic kidney disease as 27th on the list of causes of global death in 1990. However, in 2010, chronic kidney disease rose to the 18th position on the list (Stepanova et al., 2017). This rise in burden was second to HIV/AIDS. According to that report, the overall premature mortality was estimated at 82% which was the third largest coming after diabetes (93%) and HIV/AIDS (96%). Considering these data on various diseases that threaten global health as well as the sustainable development goal (Levin et al., 2017), there is a dire need to leverage on potent medicinal plants that could serve as a complimentary therapy to stem down the tide of these diseases.

Vernonia amygdalina (Del.) is a leafy vegetable widely noted for its bitter taste, hence it's popularly called 'bitter leaf'. Its leaves are normally employed in cooking delicious vegetable soup usually recommended for treating several ailments. *V. amygdalina* has been widely studied due to its versatile medicinal relevance such as in the treatment of diabetes, hypertension, and infertility (Kassebaum et al., 2016). Recent scientific evidence has given credence to its numerous medicinal benefits such as anti-obesity (Farombi & Owoeye, 2011), antioxidant (Adesanoye & Farombi, 2010), anticarcinogenic (Wong et al., 2013), antihyperglycemic (Jan Mohamed et al., 2015), anti-sickling (Clement et al., 2014), and in the management of cardiovascular disorders (Abdulmalik et al., 2016). Reports have indicated that leaf extract of *V. amygdalina* protects against brain degeneration thereby enhancing memory (Ebuehi & Ajagun-Ogunleye, 2017). Besides, extract of *V. amygdalina* leaf exhibits anti-helminthic, antiparasitic, and antimicrobial properties (Anibijuwon et al., 2012). In view of the rising burden of liver and kidney diseases, it is clear that there is a dire need to investigate the potential of *V. amygdalina* extract in the management of these diseases, that is, the motivating reason for this study.

2. Materials and methods

2.1. Plant materials

V. amygdalina leaves were obtained from a private farm in Ado Ekiti. The leaves were air dried, pulverized, and stored in an airtight container. Ethical approval for the study was obtained from the Office of Research and Development, Ekiti State University, Ado Ekiti.

2.2. Reagents and chemicals

All biochemical kits were of analytical grade and obtained from Randox laboratories, UK.

2.3. Extraction procedure

Bitter leaves were air-dried at room temperature and pulverized to obtain fine powder using a blender. 500 g of each of the powdered leaves of *V. amygdalina* was soaked in 5000 ml of distilled water for 72 hours to allow for extraction. It was then filtered using a cheesecloth, and freeze-dried to obtain the dried extract. The extract was kept in a closed container and kept inside the fridge at 4 °C for further studies.

2.4. Animals protocol

Twenty-five (25) male Wistar albino rats weighing 180–200 g were acclimatized for two weeks, housed in clean wire meshed cages under standard conditions (24 ± 1 °C), relative humidity, and 12/12-hour light and dark cycle. They were allowed to have free access (ad libitum) to food (commercial palletized diet from Vital Feed Mill) and drinking water daily. The rat beddings were changed and replaced every day throughout the experimental period.

2.4.1. Animal grouping and treatment

Experimental animals were administered different treatments as shown in Table 1.

Table 1. Animal treatment

Groups	Treatment
I	Drinking water only for 14 days
II	Single intraperitoneal injection of 3 ml CCl_4/kg body weight
III	3 ml CCl_4 + 50 mg/kg *V. amygdalina* extract by oral gavage for 14 days
IV	3 ml CCl_4 + 100 mg/kg *V. amygdalina* extract by oral gavage for 14 days
V	3 ml CCl_4 + 100 mg/kg silymarin by oral gavage for 14 days

2.5. Dissection of rats

The animals were decapitated under very light anesthesia to obtain the liver, kidney, and heart, while whole blood, collected by cardiac puncture, was allowed to stand for 1 hour in an EDTA tube. Serum was prepared by centrifugation at 3000 rpm for 15 min at 25 °C. The clear supernatant was collected and used for the estimation of serum biochemical parameters.

2.6. Preparation of homogenates

The liver, heart, and kidney were excised using scissors and forceps. They were trimmed of fatty tissue, washed in distilled water, blotted with filter paper, and weighed. They were then chopped into bits and homogenized in ten volumes of the homogenizing phosphate buffer (pH 7.4) using a Teflon homogenizer. The resulting homogenates were centrifuged at 3000 rpm at 4 °C for 30 mins. The supernatant obtained was collected and stored under 4 °C and then used for biochemical analyses.

2.7. Determination of serum creatine kinase (Ck-Mb) activity

Creatine kinase was measured by the method of Vanderlinde (1981). One thousand microliters of imidazole buffer (10 mM, pH 6.6), containing creatine phosphate (30 mM), glucose (20 mM), N-acetyl-cysteine (20 mM), magnesium acetate (10 mM), ethylenediaminetetraacetic acid (2 mM), ADP (2 mM), NADP (2 mM), AMP (5 mM), DAPP (10 µM), G6PDH (≥ 2.0 ku/l) and HK (≥ 2.15 ku/l) was incubated in a thermostatic cuvette at 37 °C after the addition of 50 µl of serum. Absorbance at 340 nm of the resulting mixture was read immediately for 5 min at 30-sec intervals. Change in absorbance per minute was estimated while enzyme activity was determined using the formula given below:

$$CK - Mb\ Activity\ (IU/l) = (\Delta Abs/min) \times 6667$$

2.8. Assay of aspartate aminotransferase (AST) activity

AST activity was determined following the principle described by Reitman & Frankel (1957). Briefly, 0.1 ml of organs' homogenates as well as the serum was mixed separately with phosphate buffer (100 mmol/l, pH 7.4), L-aspartate (100 mmol/l), and α-oxoglutarate (2 mmol/l), and the mixture incubated for exactly 30 min at 37 °C. Five hundred microliters of 2,4-dinitrophenyl hydrazine (2 mmol/l) were added to the reaction mixture and allowed to stand for exactly 20 min at 25 °C. Five milliliters of NaOH (0.4 mol/l) were then added and the absorbance of the mixture was read after 5 min at 546 nm against the reagent blank.

2.9. Assay of alanine aminotransferase (ALT) activity

The principle described by Reitman & Frankel (1957) was followed in the assay of ALT using a commercially available assay kit (Randox Laboratories, UK) according to the instructions of the manufacturer. Five hundred microliter of reagent I (R1) containing phosphate buffer (100 mmol/l, pH 7.4), L-alanine (200 mmol/l), and α-oxoglutarate (2 mol/l) was added to 0.1 ml of serum in a test tube and the mixture was incubated at 37 °C for 30 min. Exactly 0.5 ml of R2 containing 2,4-dinitrophenylhydrazine (2.0 mmol/l) was added and the solution was incubated again at 20 °C for 20 min. Finally, 5 ml of NaOH was added and the solution was allowed to stand for 5 min at 25 °C and the absorbance was read at 546 nm. The activity of ALT was obtained from the standard curve provided in the kit.

2.10. Assay of alkaline phosphatase (ALP) activity

The assay of serum ALP was based on the method of Englehardt (1970) using commercial assay kits (Randox Laboratories, UK) according to the instructions of the manufacturer. Exactly, 1.0 ml of the reagent (1 mol/l diethanolamine buffer pH 9.8, 0.5 mmol/l $MgCl_2$; substrate: 10 mmol/l *p*-nitrophenol phosphate) was added to 0.02 ml of the serum sample and mixed. The absorbance was taken at 405 nm for 3 minutes at intervals of 1 min. ALP activity was determined using the formula given below:

$$CALP\ activity\ (U/l) = 2760\ x\ \Delta Abs/min$$

2.11. Serum lipid profile

2.11.1. Estimation of total cholesterol level

The total cholesterol level was determined based on the method of Trinder (1969) using commercially available kits (Randox Laboratories, UK). Ten microliters (10 µl) of standard and 10 µl serum samples were measured into labeled test tubes. One milliliter (1 ml) of working reagent containing; Pipes buffer (80 mmol/l at pH 6.8), 4-amino antipyrine (0.25 mmol/l), phenol (6 mmol/l), peroxidase (≥ 0.5 U/ml), cholesterol esterase ion (≥ 0.15 U/ml), and cholesterol oxidase (0.10 U/ml) was added into all the tubes. The test tubes were mixed thoroughly and incubated for 10 min at 25 °C. The absorbance of the sample (Asample) was read at 500 nm against the reagent blank. Cholesterol concentration (mg/dl) was calculated using the formula given below:

$$Total\ Cholesterol\ \left(\frac{mg}{dl}\right) = \frac{Absorbance\ of\ sample}{Absorbance\ of\ standard} x\ Concentration\ of\ standard$$

2.11.2. Evaluation of concentration of triglyceride

Triglyceride levels were determined based on the method of Tietz (1995) using commercially available kits (Randox Laboratories, UK). Triglyceride standard (10 µl) and serum (10 µl) were measured into labeled test tubes. One milliliter of the working reagents; R1a (buffer) containing Pipes buffer (40 mmol/l, pH 7.6), 4-chloro-phenol (5.5 mmol/l), magnesium-ion (17.5 mmol/l); R1b (enzyme reagent containing 4-amino phenazone (0.5 mmol/l), ATP (1.0 mmol/l), lipase (≥ 150 U/ml), glycerol-kinase (≥ 0.4U/ml), glycerol-3-phosphate oxidase (≥ 1.5 U/ml), and peroxidase (≥ 0.5 U/ml) was added into all the tubes. The test tubes were mixed thoroughly and incubated for 10 min at room temperature. Absorbance was taken at 546 nm against the blank. Triglyceride concentration (mg/dl) was calculated using the formula given below:

$$Triglyceride\ concentration\ \left(\frac{mg}{dl}\right) = \frac{Absorbance\ of\ sample}{Absorbance\ of\ standard} x\ Concentration\ of\ standard$$

2.11.3. High-density lipoprotein-cholesterol (HDL-c) assay

High-density lipoprotein cholesterol was determined by the method of Grove (1979) in two stages:

I. Precipitation

A reaction mixture containing 200 µl of the serum, 200 µl of the cholesterol standard, and 500 µl of the diluted precipitant R1 (0.55 mM phosphotungstic acid, 25 mM magnesium chloride) was mixed and allowed to stand for 10 min at room temperature. It was then centrifuged for 10 min at 4000 rpm to obtain a clear supernatant. The clear supernatant was separated off within 2 h and the cholesterol content was determined by the CHOD-PAP reaction method.

II. Cholesterol CHOD-PAP Assay

One milliliter of cholesterol reagent was added to 100 µl of the sample supernatant in a test tube. The standard test tube contained 100 µl of the cholesterol standard supernatant and 1 ml of cholesterol reagent. The reagent mixture was mixed thoroughly and incubated for 10 min at 25 °C. The absorbance of the sample (A sample) and standard (Astandard) was then measured at 500 nm against the reagent blank within 1 h.

2.11.4. Low-density lipoprotein (LDL)-cholesterol determination

The concentration of low-density lipoprotein in the serum was calculated using the formula of Friedewald et al. (1972) given below:

$$LDL - Cholesterol\ \left(\frac{mg}{dl}\right) = \text{Total cholesterol} - \frac{Triglycerides}{5} - HDL - Cholesterol$$

2.12. Antioxidant assay

2.12.1. Determination of catalase activity

This experiment was carried out according to the method described by Sinha (1972). Two hundred microliters of serum and organs' homogenates were mixed separately with 0.8 ml of distilled water to give 1 in 5 dilutions of the sample. The assay mixture contained 2 ml of solution (800 µmol) and 2.5 ml of phosphate buffer in a 10 ml flat bottom flask. Properly diluted enzyme preparation (0.5 ml) was rapidly mixed with the reaction mixture by a gentle swirling motion. The reaction was run at room temperature. 1 ml portion of the reaction mixture was withdrawn and blown into 1 ml dichromate/acetic acid reagent at 60 seconds intervals. The hydrogen peroxide content of the withdrawn sample was determined by the method described below:

$$Catalase\ activity = [H_2O_2]\ Consumed = 800 - [H_2O_2]\ left$$

The concentration of H_2O_2 left was extrapolated from the standard curve for catalase activity.

2.12.2. Determination of superoxide dismutase (SOD) activity

The level of SOD activity was determined by the method of Misra & Fridovich (1972). A ten-fold dilution of the sample was prepared. An aliquot of the diluted sample was added to 2.5 ml of 0.05 M carbonate buffer (pH 10.2) to equilibrate in a spectrophotometer. The reaction was initiated by the addition of 0.3 ml of freshly prepared 0.3 mM adrenaline to the mixture which was quickly mixed by inversion. The reference cuvette contained 2.5 ml buffer, 0.3 ml of the substrate (adrenaline), and 0.2 ml of water. The increase in absorbance at 480 nm was monitored every 30 seconds for a total period of 150 seconds.

2.12.3. Determination of reduced glutathione level (GSH)

The method of Beutler (1963) was followed in estimating the level of reduced glutathione (GSH). Exactly 0.2 ml of supernatant was added to 1.8 ml of distilled water followed by the addition of 3 ml of the precipitating solution and then shaken thoroughly. The mixture was then allowed to stand for 5 min and then filtered. One milliliter of the filtrate was mixed with 4 ml of 0.1 M phosphate buffer at pH 7.4. Finally, 0.5 ml of the Ellman reagent was added. A blank was prepared with 4 ml of the 0.1 M phosphate buffer, 1 ml of diluted precipitating solution (3 parts to 2 parts of distilled water), and 0.5 ml of the Ellman reagent. The absorbance was measured at 412 nm against a reagent blank. The level of GSH in the serum was calculated from the standard curve.

2.12.4. Determination of total protein (TP) in serum

The Biuret method described by Weichselbaum (1946) was employed in the determination of total protein in the serum using commercially available kits (Randox Laboratories, UK). One milliliter of Reagent R1 containing sodium hydroxide (100 mmol/l), Na-K-tartrate (18 mmol/l), potassium iodide (15 mmol/l), and cupric sulfate (6 mmol/l) was added to 0.02 ml of the serum sample. The reaction mixture was incubated at 25 °C and absorbance was measured against the reagent blank at 546 nm. Total protein concentration (mg/ml) was calculated using the formula given below:

$$Total\ Protein\ Concentration\ \left(\frac{mg}{ml}\right) = \frac{Absorbance\ of\ sample}{Absorbance\ of\ standard} x\ Concentration\ of\ standard$$

2.13. Statistical analysis

All values were expressed as mean ± SD. Statistical evaluation was done using One Way Analysis of Variance (ANOVA) followed by Duncan's Multiple Range Test (DMRT) by using SPSS 11.09 for Windows. The significance level was set at $p < 0.05$.

3. Results and discussion

Table 1 shows the treatment protocol adopted for the experimental animals. Animals in group II were exposed to 3ml/kg bw of CCl_4 but not treated with the extracts, while the animals in groups III, IV, and V were exposed to 3ml/kg bw of CCl_4 and treated with 50, 100 mg/kg bw of *V. amygdalina* leaf extract and 100 mg/kg bw of silymarin, respectively. Group I animals received distilled water only and were not exposed to the toxicant at all. Exposure to CCl_4 caused a marked derangement in lipid profile (cholesterol, triglyceride, HDL-c, and LDL-c) regardless of the organ involved (Table 2A-D). Treatment with *V. amygdalina* resulted in the restoration of the lipid profile in a dose-dependent fashion comparable to animals treated with silymarin. Serum levels of alkaline phosphatase (ALP), alanine aminotransferase (ALT), and aspartate aminotransferase (AST), as well as bilirubin, were significantly raised relative to control animals (Table 3A-D). However, treatment of intoxicated animals with graded doses of *V. amygdalina* led to a restoration of the marker enzymes in a manner comparable with animals treated with silymarin (Table 3A-D). Urea, and uric acid as well as total bilirubin were elevated following exposure to CCl_4 (Table 3A-D). Administration of the leaf extract of *V. amygdalina* reversed the trend to a level comparable with animals that were not exposed to the toxicant (Table 3A-D). The activity of superoxide dismutase, catalase, and creatine kinase was significantly depleted when animals were exposed to CCl_4 but activity was restored to levels comparable with animals treated with silymarin following treatment with leaf extract of *V. amygdalina* (Table 4A-D). Reduced glutathione (GSH) was markedly decreased in the serum of animals exposed to CCl_4. However, GSH level was restored in the exposed animals following treatment with graded doses of *V. amygdalina* leaves extract. Administration of CCl_4 caused a marked distortion in hepatic, renal, and cardiac histoarchitecture but the distortion was reversed by treatment with *V. amygdalina* leaves extract (Table 4A-D). Photomicrograph of liver tissue of experimental animals under different treatments is as shown in Figure 1A-D.

The ever-increasing global burden of liver and kidney diseases calls for concerted efforts at stemming the tide which may threaten public health if left unchecked. Attainment of the sustainable development goal (SDG) on health requires not only conventional drugs but the complementary effort of herbal medicines. Animal models of liver and kidney diseases have been routinely used to assess the therapeutic potentials of medicinal plants in managing such diseases. Derangement of lipid profile is a potent toxicity mechanism of several toxicants. Hyperlipidemia has been identified as a major culprit in the onset and progression of cardiovascular diseases (Ugwu Okechukwu et al., 2013). Routinely, notable signs of toxicity include high cholesterol, high triglycerides, high LDL, and depleted HDL in exposed animals (Khafar & Kakey, 2020). In the present study, exposure of experimental animals to carbon tetrachloride (CCl_4) (Table 1) caused a marked derangement in the lipid profile regardless of the organ involved (Table 2A-D). Specifically, there was a surge in cholesterol levels in the liver, kidney heart, and serum following exposure to CCl_4. This observation implies that CCl_4 triggered a derangement in critical membrane lipids leading to a compromise in membrane function. However, treatment with *V. amygdalina* leaf extract restored the cholesterol level to a level comparable with animals treated with silymarin. Undoubtedly, such an effect could be linked to the flavonoids and other polyphenols present in the extract. Triglyceride levels in the serum and organs' homogenates were significantly increased following exposure of experimental animals to CCl_4 (Table 2A-D). However, treatment with *V. amygdalina* leaf extract reversed the trend in a manner that was dose-dependent and comparable to animals treated with silymarin. This further suggests the potential of the plant as an efficacious alternative in the management of multiple organ diseases. The level of high-density lipoprotein has been used to predict the antioxidant status and overall well-being of the animals. In the present study, CCl_4 exposure caused a marked depletion in the level of HDL in the serum, liver, kidney, and heart homogenates of experimental animals. This observation points to the free radical-induced depletion of antioxidants in the animals. Administration of *V. amygdalina* extract relieved the oxidative stress on the organs as the level of HDL was restored to normal. Detailed phytochemical contents of the leaf extract of *V. amygdalina* have been reported. The relief experienced by experimental animals following treatment with the plant extract can be attributed to the flavonoid and polyphenolic content of the plant. On the other hand,

low-density lipoprotein (LDL) otherwise called 'bad cholesterol' was increased following exposure to CCl_4. Administration of *V. amygdalina* extract brought the LDL level back to a basal level comparable to silymarin. Invariably, the surge in LDL was due to increased free radicals triggered by the toxicant. Treatment of intoxicated animals with *V. amygdalina* extract relieved the toxicity imposed by CCl_4, further buttressing its potential in the management of diseases related to these organs. Treatment of CCl_4 exposed animals with *V. amygdalina* leaves resulted in a dose-dependent reversal of total cholesterol, triglycerides, and LDL-cholesterol in a manner comparable to the negative control and animals treated with the standard drug (Table 2A-D). This may be due to the presence of bioactive ingredients such as flavonoids in the extract.

Table 2. Effect of *V. amygdalina* leaf extract on lipid profile in the serum, liver, kidney, and heart of CCl_4-exposed rat

A. Serum

Parameter	I	II	III	IV	V
Total Cholesterol (mg/dl)	73.28 ± 1.84^a	140.21 ± 0.00^b	79.61 ± 0.25^a	69.17 ± 0.31^a	77.76 ± 0.96^a
Triglyceride (mg/dl)	23.05 ± 1.30^a	46.22 ± 1.18^b	27.17 ± 1.39^a	26.25 ± 0.11^a	25.35 ± 0.81^a
HDL (mg/dl)	15.91 ± 0.68^a	10.10 ± 0.04^b	10.38 ± 0.20^b	11.87 ± 0.05^a	13.35 ± 0.28^a
LDL (mg/dl)	54.10 ± 4.53^a	120.87 ± 0.46^b	13.74 ± 0.31^a	12.05 ± 0.38^a	59.34 ± 1.22^a

B. Liver

Parameter	I	II	III	IV	V
Total Cholesterol (mg/dl)	72.96 ± 1.01^a	119.75 ± 1.52^b	83.67 ± 1.26^a	95.48 ± 1.77^a	86.63 ± 1.95^a
Triglyceride (mg/dl)	1.40 ± 0.16^a	25.8 ± 0.27^b	8.57 ± 1.63^a	1.07 ± 1.12^a	1.20 ± 0.92^a
HDL (mg/dl)	53.62 ± 0.11^a	34.19 ± 0.10^b	40.13 ± 0.08^a	49.42 ± 0.30^a	36.29 ± 0.08^a
LDL (mg/dl)	6.53 ± 1.06^a	67.44 ± 3.41^b	27.82 ± 1.26^a	13.84 ± 1.69^a	6.26 ± 1.76^a

C. Kidney

Parameter	I	II	III	IV	V
Total Cholesterol (mg/dl)	30.58 ± 0.50^a	57.46 ± 0.76^b	42.55 ± 1.13^a	42.11 ± 1.58^a	34.65 ± 0.95^a
Triglyceride (mg/dl)	17.34 ± 0.09^a	36.17 ± 0.20^b	32.01 ± 0.38^a	33.79 ± 15.00^a	34.81 ± 0.44^a
HDL (mg/dl)	11.27 ± 0.19^a	8.31 ± 0.01^b	9.61 ± 0.24^a	10.13 ± 0.09^a	10.47 ± 0.23^a
LDL (mg/dl)	16.11 ± 0.57^a	41.93 ± 0.74^b	28.01 ± 1.03^a	25.22 ± 4.18^a	19.19 ± 0.75^a

D. Heart

Parameter	I	II	III	IV	V
Total Cholesterol (mg/dl)	23.96 ± 1.80^a	38.49 ± 0.65^b	28.89 ± 0.00^a	22.11 ± 0.79^a	23.08 ± 2.53^a
Triglyceride (mg/dl)	7.75 ± 0.65^a	11.6 ± 0.50^b	9.65 ± 0.20^a	9.89 ± 0.08^a	8.22 ± 0.04^a
HDL (mg/dl)	6.40 ± 0.07^a	3.57 ± 0.11^b	4.71 ± 0.29^a	4.91 ± 0.02^a	5.70 ± 0.14^a
LDL (mg/dl)	16.01 ± 1.71^a	32.6 ± 0.68^b	24.25 ± 0.28^a	15.95 ± 0.01^a	15.73 ± 2.53^a

Data represent mean ± SEM of experiment performed in triplicate. I: Administered water only, II: Administered CCl_4 only, III: Treated with *V.amygdalina* at 50 mg/kg bw after exposure, IV: Treated with *V.amygdalina* at 100 mg/kg bw after exposure, V: Treated with silymarin at 100 mg/kg bw after exposure, 'b' represents significant difference from the control 'a' at $p < 0.05$.

Monitoring the integrity of the liver and kidney involves the assessment of specific biomarkers such as ALP, ALT, and AST (Khafar & Kakey, 2020). Whenever there is an unusual increase in the level of these biomarkers in the blood, hepatic injury can be inferred (Udem et al., 2010). In the present study, the significant increase in ALP in the serum and organs homogenates following exposure to CCl_4 toxicity (Table 3A-D) could be a result of an obstruction in bile flow, heart failure, dehydration, and a decrease in renal blood flow (Whitby et al., 1984). The most fundamental explanation is that CCl_4 deranged the membrane lipid profile, hence, these biomarkers that are normally compartmentalized within the membrane-surrounded cell, leaked into the bloodstream, leading to an elevation in their level in the serum. Treatment with *V. amygdalina* leaves extract caused a dose-dependent restoration of these biomarkers suggesting a curative effect on the organ injury caused by the toxicant. This effect can be linked to the presence of antioxidant phytochemicals present in the extract. Bilirubin is a product of heme degradation in the spleen, liver, and bone marrow. Under normal circumstances, bilirubin is conjugated with glucuronic acid to form a soluble product that is excreted. Unusually high bilirubin is a type of an injured liver or too high a level of heme degradation. Serum and liver bilirubin levels of experimental rats exposed to CCl_4 toxicity were significantly increased relative to the control. This, perhaps, suggests that the toxicant upregulates heme degradation causing a derangement in the process. It can also be traced to the free radical-induced oxidative injury on the hepatocytes. Administration of *V. amygdalina* leaves extract relieved the toxicity imposed by the toxicant restoring the bilirubin level to that comparable with animals that were not exposed at all (Table 3A-D). This indicates the potential of the plant as a therapeutic remedy for liver diseases.

Urea, one of the products of nitrogen metabolism in mammals has been employed as a routine marker for chronic kidney diseases (Borghi et al., 2020). In the present study, intoxicated animals that were treated with graded doses of *V. amygdalina* showed signs of recovery as indicated in the reversal of urea to levels comparable with animals treated with silymarin (Table 3A-D). This suggests the presence of antioxidant phytochemicals such as flavonoids and other polyphenols in the extract which produced the observed effect. It also implies the possible therapeutic relevance of the plant in the management of kidney diseases.

Uric acid, the product of purine degradation in humans has been suggested as central to the development of gout. Recent reports have suggested an intricate link between high serum levels of uric acid and certain pathological conditions such as hypertension, diabetes, obesity, and renal insufficiency (Xiong et al., 2019). In the present study, exposure of experimental animals to CCl_4 caused a surge in the serum level of uric acid relative to the control. *V. amygdalina* showed a potent ameliorative effect when administered

to animals under the toxic effect of CCl_4. The uric acid level dropped back to levels comparable to animals that were not exposed to the toxicant, following treatment with *V. amygdalina* leaves extract (Table 3A-D). This suggests the potential of the plant in the management of chronic kidney disease.

Table 3. Effect of *V. amygdalina* leaf extract on selected biomarkers in organs of CCl_4 exposed rat

A. Serum

Parameter	I	II	III	IV	V
ALP (U/l)	85.37 ± 0.00^a	145.96 ± 0.00^b	109.61 ± 0.00^a	92.46 ± 1.07^a	96.39 ± 0.00^a
ALT (U/l)	66.09 ± 0.88^a	106.69 ± 1.72^b	79.51 ± 0.65^a	69.69 ± 2.25^a	66.92 ± 0.46^a
AST (U/l)	75.19 ± 1.06^a	113.01 ± 1.08^b	78.20 ± 0.87^a	69.41 ± 1.44^a	73.36 ± 0.49^a
Total Bilirubin (mg/dl)	63.73 ± 0.43^a	102.48 ± 0.36^b	78.34 ± 0.38^a	72.33 ± 0.88^a	68.11 ± 0.67^a
Urea mg/dl)	42.80 ± 0.68^a	99.61 ± 0.66^b	72.69 ± 0.00^a	57.12 ± 0.82^a	50.77 ± 0.57^a
Creatine kinase (U/l)	41.73 ± 1.41^a	62.93 ± 2.34^b	46.18 ± 1.86^a	42.29 ± 1.44^a	13.93 ± 2.10^a
Uric acid (mg/dl)	28.40 ± 0.10^a	50.80 ± 0.23^b	33.77 ± 0.66^a	26.35 ± 0.14^a	31.11 ± 0.53^a

B. Liver

Parameter	I	II	III	IV	V
ALP (U/l)	55.08 ± 0.00^a	112.91 ± 0.00^b	97.08 ± 1.60^a	60.59 ± 34.98^a	65.41 ± 1.38^a
ALT (U/l)	44.99 ± 3.23^a	116.55 ± 3.18^b	89.32 ± 1.10^a	83.21 ± 0.39^a	66.03 ± 0.96^a
AST (U/l)	69.07 ± 1.55^a	104.59 ± 4.32^b	77.57 ± 0.83^a	75.02 ± 1.01^a	68.64 ± 1.74^a
Total Bilirubin (mg/dl)	24.85 ± 1.28^a	46.48 ± 0.18^b	37.20 ± 0.576^a	28.67 ± 0.061^a	26.65 ± 1.15^a

C. Kidney

Parameter	I	II	III	IV	V
ALP (U/l)	85.37 ± 0.00^a	145.96 ± 0.00^b	14.70 ± 41.31^a	93.64 ± 0.00^a	6.39 ± 0.00^a
ALT (U/l)	56.14 ± 0.94^a	158.71 ± 7.56^b	64.20 ± 0.87^a	58.43 ± 2.25^a	4.06 ± 0.97^a
AST (U/l)	69.58 ± 1.28^a	99.74 ± 1.08^b	93.03 ± 1.55^a	89.12 ± 1.06^a	5.27 ± 1.47^a
Urea mg/dl)	52.69 ± 0.67^a	93.08 ± 0.00^b	71.83 ± 50.18^a	65.77 ± 0.00^a	58.85 ± 0.00^a
Uric acid (mg/dl)	24.36 ± 0.29^a	50.48 ± 0.33^b	41.63 ± 0.44^a	32.50 ± 0.41^a	25.55 ± 0.55^a

D. Heart

Parameter	I	II	III	IV	V
ALP (U/l)	23.87 ± 1.59^a	38.56 ± 0.00^b	34.43 ± 1.15^a	27.54 ± 0.00^a	7.54 ± 0.00^a
ALT (U/l)	2.18 ± 0.49^a	15.05 ± 0.39^b	11.48 ± 0.72^a	6.13 ± 0.26^a	4.56 ± 0.47^a
AST (U/l)	11.97 ± 0.77^a	27.09 ± 1.44^b	21.86 ± 1.57^a	14.34 ± 0.00^a	9.88 ± 1.05^a
Creatine kinase (U/l)	51.88 ± 1.41^a	83.91 ± 1.17^a	54.00 ± 0.01^a	50.16 ± 0.01^a	41.45 ± 1.11^a

Data represent mean ± SEM of experiment performed in triplicate. I: Administered water only, II: Administered CCl_4 only, III: Treated with *V.amygdalina* at 50 mg/kg bw after exposure, IV: Treated with *V.amygdalina* at 100 mg/kg bw after exposure, V: Treated with silymarin at 100 mg/kg bw after exposure, 'b' represents significant difference from the control 'a' at $p < 0.05$.

Table 4. Effect of *V. amygdalina* leaf on reduced glutathione, total protein and selected antioxidant enzymes activity in CCl_4 exposed rats

A. Serum

Parameter	I	II	III	IV	V
SOD (U/mg protein)	8.47 ± 0.49^a	5.02 ± 0.35^b	5.17 ± 1.68^a	6.20 ± 0.95^a	7.80 ± 1.04^a
CAT (U/mg protein)	4.36 ± 0.18^a	1.84 ± 0.05^b	1.92 ± 0.62^a	2.44 ± 0.14^a	3.77 ± 0.60^a
GSH (mM/g tissue)	6.81 ± 1.10^a	4.53 ± 1.22^b	5.27 ± 0.65^a	5.88 ± 0.32^a	6.04 ± 0.87^a
Total protein (mg/ml)	3.75 ± 0.20^a	1.67 ± 0.60^b	2.73 ± 0.27^a	3.02 ± 0.81^a	2.59 ± 0.18^a

B. Liver

Parameter	I	II	III	IV	V
SOD (U/mg protein)	2.04 ± 0.10^a	1.42 ± 0.42^b	1.37 ± 0.17^a	1.79 ± 0.29^a	2.11 ± 0.32^a
CAT (U/mg protein)	1.14 ± 0.13^a	0.26 ± 0.21^b	0.28 ± 1.21^a	0.61 ± 0.67^a	0.97 ± 0.22^a
GSH (mM/g tissue)	1.93 ± 0.03^a	0.39 ± 0.01^b	0.92 ± 0.18^a	1.16 ± 0.01^a	1.79 ± 0.03^a
Total protein (mg/ml)	1.88 ± 0.13^a	1.07 ± 0.09^b	1.18 ± 0.21^a	1.44 ± 0.34^a	1.58 ± 0.43^a

C. Kidney

Parameter	I	II	III	IV	V
SOD (U/mg protein)	5.26 ± 0.02^a	2.28 ± 0.12^b	2.95 ± 0.63^a	3.46 ± 0.44^a	3.62 ± 0.21^a
CAT (U/mg protein)	1.36 ± 0.11^a	0.64 ± 0.07^b	0.77 ± 0.19^a	1.05 ± 0.31^a	1.47 ± 0.60^a
GSH (mM/g tissue)	2.52 ± 0.17^a	0.93 ± 0.02^b	1.56 ± 0.87^a	1.93 ± 0.09^a	1.95 ± 0.04^a
Total protein (mg/ml)	2.97 ± 0.02^a	2.14 ± 0.01^b	2.22 ± 0.13^a	2.37 ± 0.17^a	2.74 ± 0.11^a

Table 4. *Continues*

D. Heart

Parameter	I	II	III	IV	V
SOD (U/mg protein)	4.31 ± 1.47[a]	2.08 ± 0.75[b]	2.35 ± 0.49[a]	3.63 ± 1.27[a]	4.22 ± 0.43[a]
CAT (U/mg protein)	3.16 ± 0.10[a]	1.90 ± 0.15[b]	2.27 ± 0.19[a]	2.89 ± 0.41[a]	3.02 ± 0.23[a]
GSH (mM/g tissue)	3.89 ± 0.03[a]	1.05 ± 0.05[b]	2.15 ± 1.40[a]	3.24 ± 1.84[a]	2.65 ± 0.02[a]
Total protein (mg/ml)	6.47 ± 1.21[a]	2.43 ± 0.68[b]	2.77 ± 1.01[a]	3.37 ± 1.17[a]	5.43 ± 1.84[a]

Data represent mean ± SEM of experiment performed in triplicate. I: Administered water only, II: Administered CCl_4 only, III: Treated with *V.amygdalina* at 50 mg/kg bw after exposure, IV: Treated with *V.amygdalina* at 100 mg/kg bw after exposure, V: Treated with silymarin at 100 mg/kg bw after exposure, 'b' represents significant difference from the control 'a' at $p < 0.05$.

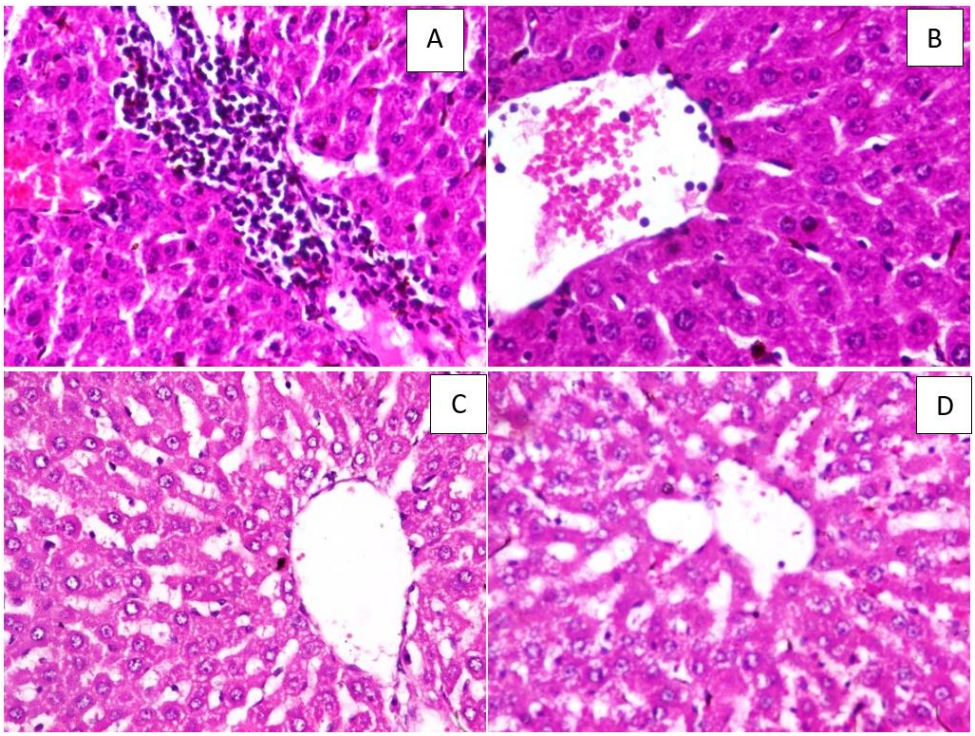

Figure 1. Histoarchitecture of liver tissue slices of experimental animals under different experimental treatments at 400x magnification

A. Photomicrograph of liver slices of animals that were not exposed to carbon tetrachloride toxicity at all. It showed no sign of histological distortion of the hepatocytes. Tissue histomorphology was normal and the nuclei was rightly located in the cytoplasm.

B. Photomicrograph of liver slices of animals exposed to CCl_4 (3 ml/kg bw) without treatment. It showed fatty liver with cholestasis.

C. Photomicrograph of liver slices of animals treated with *V. amygdalina* (100 mg/kg bw) after exposure to CCl_4. It showed no sign of distorted hepatic histoarchitecture.

D. Photomicrograph of liver slices of animals treated with silymarin at 100 mg/kg bw after initial exposure to CCl_4. It showed unperturbed hepatic histomorphology without any sign of histopathological distortion.

Antioxidant enzymes such as superoxide dismutase and catalase (CAT) are critical in shielding the physiological system from the menace of free radicals (Nandi et al., 2019). In terms of this mechanism, SOD dismutates superoxide radicals converting them to hydrogen peroxide which is scavenged by catalase (Zhang & Feng, 2018). In the present study, exposure of experimental animals to CCl_4 resulted in depletion in the level of SOD and catalase in the serum and organs homogenates (Table 4A-D). This is probably due to the surge in the level of superoxide anion radicals occasioned by the toxicant. However, treatment with *V. amygdalina* extract caused a restoration of SOD and CAT levels to that comparable with normal animals (Table 4A-D). This implies that certain phytochemicals in the extract exhibited potent antioxidant activity in scavenging both superoxide anions and breaking hydrogen peroxide viz-a-viz the activation of SOD and catalase respectively. This observation can be attributed to the flavonoids and polyphenols present in the extract.

Reduced glutathione GSH is a non-enzymic thiol often used to measure the health status of the organism. Any species that depletes the GSH level of an organism is toxic. In the present study, administration of CCl_4 depleted the GSH level in the serum and organs homogenates suggesting the multiorgan toxicity of CCl_4 (Table 4A-D). However, treatment with *V. amygdalina* leaf extract restored the GSH level in a dose-dependent manner comparable to animals treated with silymarin. This suggests that the potential of *V. amygdalina* leaves in the management of multiorgan disorders.

Hepatic histoarchitecture distorted by exposure to CCl_4 was restored by treatment with *V. amygdalina* leaf extract (Figure 1A-D). This is an indication that the oxidative injury inflicted on the liver by CCl_4 was healed by phytochemicals present in the extract, suggesting the medicinal potential of the plant in the treatment of liver diseases.

4. Conclusions

V. amygdalina leaf extract restored deranged lipid profile, reactivated inhibited antioxidant enzymes, and reversed oxidative injury to the liver, kidney, and heart. Distorted histoarchitecture of the hepatic, renal, and cardiac tissues was also restored following treatment with *V. amygdalina* (Figure 1A-D). Hence, this plant is a potential therapeutic agent that can be exploited in the management of diseases relating to these critical organs.

Acknowledgments

The authors wish to acknowledge the technical support of Mr. Oyelade of the Department of Science Laboratory Technology, Federal Polytechnic Ado Ekiti, Nigeria.

Conflict of interest

The authors confirm that there are no known conflicts of interest.

Statement of ethics

Ethical approval for this study was obtained from the Office of Research and Development, Ekiti State University, Ado Ekiti (Date: August 23, 2021, Number: ORD/AD/EAC/19/0081).

Availability of data and materials

All data generated or analyzed during this study are included in this published article.

Funding

The authors declare that the study did not receive any financial support/grant from any public or private organization.

CRediT authorship contribution statement

Temidayo Ogunmoyole: Conceptualization, Investigation, Writing - original and final draft, Supervision
Yetunde Beatrice Apanisile: Resources, Formal analysis, Investigation, Methodology
Yusuff Adewale Akeem: Formal analysis, Investigation, Software
Omowumi Jayeola Makun: Formal analysis, Investigation, Software

ORCID Numbers of the Authors

T. Ogunmoyole: 0000-0002-6185-0602
Y. B. Apanisile: 0000-0002-5778-7524
Y. A. Akeem: 0000-0001-7929-2111
O. J. Makun: 0000-0002-6278-1418

Supplementary File

None.

Publisher's Note

All claims expressed in this article are solely those of the authors and do not necessarily represent those of their affiliated organizations, or those of the publisher, the editors and the reviewers. Any product that may be evaluated in this article, or claim that may be made by its manufacturer, is not guaranteed or endorsed by the publisher.

This is an open-access article distributed under the terms of the Creative Commons Attribution 4.0 International License (CC BY). The use, distribution or reproduction in other forums is permitted, provided the original author(s) and the copyright owner(s) are credited and that the original publication in this journal is cited, in accordance with accepted academic practice. No use, distribution or reproduction is permitted which does not comply with these terms.

References

Abdulmalik, O., Oladapo, O. O., & Bolaji, M. O. (2016). Effect of aqueous extract of *Vernonia amygdalina* on atherosclerosis in rabbits. *ARYA Atherosclerosis*, *12*(1), 35-40.
Adesanoye, O. A., & Farombi, E. O. (2010). Hepatoprotective effects of *Vernonia amygdalina* (Astereaceae) in rats treated with carbon tetrachloride. *Experimental and Toxicologic Pathology*, *62*(2), 197-206.
Anibijuwon, I. I., Oladejo, B. O., Adetitun, D. O., & Kolawole, O. M. (2012). Antimicrobial activities of *Vernonia amygdalina* against oral microbes. *Global Journal of Pharmacology*, *6*(3), 178-185.
Beutler, E. (1963). Improved method for the determination of blood glutathione. *Journal of Laboratory and Clinical Medicine*, *61*, 882-888.
Borghi, C., Agabiti-Rosei, E., Johnson, R. J., Kielstein, J. T., Lurbe, E., Mancia, G., & Tsioufis, K. P. (2020). Hyperuricaemia and gout in cardiovascular, metabolic and kidney disease. *European Journal of Internal Medicine*, *80*, 1-11.
Clement, E., Erharuyi, O., Vincent, I., Joy, A., Christopher, A., Anthony, A., & Abiodun, F. (2014). Significance of bitter leaf (*Vernonia amagdalina*) in tropical diseases and beyond: a review. *Malaria Chemotherapy Control & Elimination*, *3*(120), 1-10.
Ebuehi, O. A., & Ajagun-Ogunleye, M. O. (2017). Neurochemical impact of the aqueous extract of *Vernonia amygdalina* and *Talinum triangulare* on learning and memory in male Wistar rats. *International Journal of Brain and Cognitive Sciences*, *6*(5), 81-88.
Englehardt, A. (1970). Measurement of alkaline phosphatase. *Aerztl Labor*, *16*(42), 1.
Farombi, E. O., & Owoeye, O. (2011). Antioxidative and chemopreventive properties of *Vernonia amygdalina* and *Garcinia biflavonoid*. *International Journal of Environmental Research and Public Health*, *8*(6), 2533-2555.
Friedewald, W. T., Levy, R. I., & Fredrickson, D. S. (1972). Estimation of the concentration of low-density lipoprotein cholesterol in plasma, without use of their preparative ultracentrifuge. *Clinical Chemistry*, *18*, 499–502.
Grove, T. H. (1979). Effect of reagent pH on determination of high-density lipoprotein cholesterol by precipitation with sodium phosphotungstate-magnesium. *Clinical Chemistry*, *25*(4), 560-564.
Gurib-Fakim, A. (2006). Medicinal plants: traditions of yesterday and drugs of tomorrow. *Molecular Aspects of Medicine*, *27*(1), 1-93.
Hamburger, M., & Hostettmann, K. (1991). 7. Bioactivity in plants: the link between phytochemistry and medicine. *Phytochemistry*, *30*(12), 3864-3874.
Jan Mohamed, H. J. B., Yap, R. W. K., Loy, S. L., Norris, S. A., Biesma, R., & Aagaard-Hansen, J. (2015). Prevalence and determinants of overweight, obesity, and type 2 diabetes mellitus in adults in Malaysia. *Asia Pacific Journal of Public Health*, *27*(2), 123-135.
Kassebaum, N. J., Arora, M., Barber, R. M., Bhutta, Z. A., Brown, J., Carter, A., & Biryukov, S. (2016). Global, regional, and national disability-adjusted life-years (DALYs) for 315 diseases and injuries and healthy life expectancy (HALE), 1990–2015: a systematic analysis for the Global Burden of Disease Study 2015. *The Lancet*, *388*(10053), 1603-1658.
Khafar, K. R., & Kakey, E. S. (2020). Hepatorenal Function Markers Alteration in Aged and Aged Related Disease in Human. *Indian Journal of Public Health Research & Development*, *11*(5), 844–849.
Levin, A., Tonelli, M., Bonventre, J., Coresh, J., Donner, J. A., Fogo, A. B., & Yang, C. W. (2017). Global kidney health 2017 and beyond: a roadmap for closing gaps in care, research, and policy. *The Lancet*, *390*(10105), 1888-1917.
Marcellin, P., & Kutala, B. K. (2018). Liver diseases: A major, neglected global public health problem requiring urgent actions and large-scale screening. *Liver International*, *38*, 2-6.
Misra, H. P., & Fridovich, I. (1972). The role of superoxide anion in the autoxidation of epinephrine and a simple assay for superoxide dismutase. *Journal of Biological Chemistry*, *247*(10), 3170-3175.
Mokdad, A. A., Lopez, A. D., Shahraz, S., Lozano, R., Mokdad, A. H., Stanaway, J., & Naghavi, M. (2014). Liver cirrhosis mortality in 187 countries between 1980 and 2010: a systematic analysis. *BMC Medicine*, *12*(1), 145.
Nandi, A., Yan, L. J., Jana, C. K., & Das, N. (2019). Role of catalase in oxidative stress-and age-associated degenerative diseases. *Oxidative Medicine and Cellular Longevity*, *2019*, 9613090.
Rastogi, R. P., & Mehrotra, B. N. (1990). Compendium of Indian medicinal plants, vol. 1. CSIR, New Delhi, 118-122.
Reitman, S., & Frankel, S. (1957). Glutamic–pyruvate transaminase assay by colorimetric method. *American Journal of Clinical Pathology*, *28*(1), 56-63.
Singh, P., & Singhi, C. L. (1981). Chemical investigation of clerodendron-fragrans. *Journal of the Indian Chemical Society*, *58*(6), 626-627.
Sinha, A. K. (1972). Colorimetric assay of catalase. *Analytical Biochemistry*, *47*(2), 389-394.
Stepanova, M., De Avila, L., Afendy, M., Younossi, I., Pham, H., Cable, R., & Younossi, Z. M. (2017). Direct and indirect economic burden of chronic liver disease in the United States. *Clinical Gastroenterology and Hepatology*, *15*(5), 759-766.
Tietz, N. W. (1995). Clinical guide to laboratory tests. In Clinical guide to laboratory tests (pp. 1096-1096), 3rd ed. Philadelphia: Saunders and Co. Publishers.
Trinder, P. (1969). A simple Turbidimetric method for the determination of serum cholesterol. *Annals of Clinical Biochemistry*, *6*(5), 165-166.

Udem, S. C., Obidoa, O., & Asuzu, I. U. (2010). Acute and chronic toxicity studies of *Erythrina senegalensis* DC stem bark extract in mice. *Comparative Clinical Pathology*, *19*(3), 275-282.

Ugwu Okechukwu, P. C., Nwodo Okwesili, F. C., Joshua Parker, E., Odo Christian, E., & Ossai Emmanuel, C. (2013). Effect of ethanol leaf extract of *Moringa oleifera* on lipid profile of mice. *Research Journal of Pharmaceutical, Biological and Chemical Sciences*, *4*(1), 1324-1332.

Vanderlinde, R. E. (1981). Urinary enzyme measurements in the diagnosis of renal disorders. *Annals of Clinical & Laboratory Science*, *11*(3), 189-201.

Weichselbaum, C. T. (1946). An accurate and rapid method for the determination of proteins in small amounts of blood serum and plasma. *American Journal of Clinical Pathology*, *16*(3), 40-49.

Whitby, L. G., Percy-Robb, I. W., & Smith, A. F. (1984). Enzymes test in diagnosis. *Lecture Notes on Clinical Chemistry*, 3rd ed., Blackwell Sci. Publication, London, pp. 138–168.

Wong, F. C., Woo, C. C., Hsu, A., & Tan, B. K. H. (2013). The anti-cancer activities of *Vernonia amygdalina* extract in human breast cancer cell lines are mediated through caspase-dependent and p53-independent pathways. *PLOS ONE*, *8*(10), e78021.

Xiong, Q., Liu, J., & Xu, Y. (2019). Effects of uric acid on diabetes mellitus and its chronic complications. *International Journal of Endocrinology*, *2019*, 9691345.

Zhang, L. B., & Feng, M. G. (2018). Antioxidant enzymes and their contributions to biological control potential of fungal insect pathogens. *Applied Microbiology and Biotechnology*, *102*(12), 4995-5004.

Int. J. Plant Bas. Pharm. (2023) 3(1), 10-17

INTERNATIONAL JOURNAL OF PLANT BASED PHARMACEUTICALS

https://ijpbp.com

RESEARCH ARTICLE

OPEN ACCESS

Variation in chemical composition, insecticidal and antioxidant activities of essential oils from the leaves, stem barks, and roots of *Blighia unijugata* (Baker) and *B. sapida* (K. D. Koenig)

Ganiyat K. Oloyede[a]*, Patricia A. Onocha[a], ThankGod R. Ikiroma[a], Olusegun W. Olusola[a]

[a] *University of Ibadan, Department of Chemistry, Organic Chemistry Unit, Ibadan, Nigeria*

ARTICLE INFO

Article History:

Received: 16 July 2022
Revised: 26 September 2022
Accepted: 27 September 2022
Available online: 02 October 2022

Edited by: B. Tepe

Keywords:

Blighia unijugata
Blighia sapida
Sitophillus zeamaise
Essential oil
Antioxidant
Insecticidal

ABSTRACT

Blighia unijugata (Baker) and *B. sapida* (K.D. Koenig) (Sapindaceae) are forest trees widespread in Tropical Africa. They are used in folk medicine for the treatment of rheumatism, cardiovascular diseases, yellow fever, dysentery, and epilepsy. The essential oils of the air-dried leaves, stem bark, and roots of the plants were extracted using the hydrodistillation method and were analyzed by Gas Chromatography-Mass Spectrometry (GC-MS). The antioxidant activity was determined using the 2,2-diphenyl-1-picrylhydrazyl (DPPH) radical method using α-tocopherol and ascorbic acid as standards. The insecticidal activity of the oils was investigated by determining the percentage mortality of the grain insects (*Sitophilus zeamaise*). Results showed that the yield of the colorless oils (% w/w) from the leaves, stem bark, and roots of the plants were 0.91%, 0.42%, and 0.34% for *B. unijugata* and 0.67%, 0.32%, and 0.48% for *B. sapida*, respectively. The most abundant compounds in *B. unijugata* leaves were pentadecanoic acid (14-methyl-, methyl ester) (38.34%), carbonic acid, propyl-en-2-yl undecylpropyl ester (36.79%), and 9-octadecanoic acid *(Z)*-methyl ester (24.86%). The stem bark was rich in 1,3-dimethoxybenzene (79.01%) while the root contained limonene (20.51%), *trans*-13-octadecanoic acid (16.74 %), and *cis*-vaccenic acid (9.50%). The leaf essential oil of *B. sapida* had hexahydrofarnesyl acetone (21.43%), phytol (20.45%), geosmin (16.258%), and α-ionone (8.271%) as the major constituents. The stem bark had cholesterol (38.66%) as the major constituent while the root contained nonanal (18.09%) and 4-cyclopropyl carbonyl tetradecane (11.6%). The antioxidant analysis revealed that *B. unijugata* root had 83.96% inhibition at 100 mg/ml, while *B. sapida* stem had 79.73% inhibition, better than α-tocopherol. No significant insecticidal activity was observed in the essential oils of the plants against *S. zeamaise* except for *B. sapida* stem which showed 50% toxicity to the maize weevils. However, the two plants can be the source of antioxidant agents against oxidative stress and related diseases.

1. Introduction

Plants play a very important role in human society due to their secondary metabolites which serve as the source of medicine and food (Akerele, 1991; Farnsworth & Soejarto, 1991; Tapsell et al., 2006, Oloyede et al., 2019a, Onanuga & Oloyede, 2021). The biological function of essential oils in a variety of fields has made them very important natural products especially their use in food, cosmetics, deodorants, biocides, insecticides or pharmaceutical industries, personal care, and perfumery (Bakkali et al., 2008; Abdelouaheb & Amadou, 2012; Oloyede et al., 2021). Essential oils are obtained by hydrodistillation, enfleurage, solvent extraction, expression, and CO_2 hypercritical methods. Other modern techniques include microwave distillation, headspace trapping, solid phase micro-extraction (SPME), supercritical fluid extraction (SPE), and simultaneous distillation extraction (SDE). Therapeutic activities of essenti-

Reviewed by:
Ibrahim Halil Kenger: Gaziantep Islamic Science and Technology University, Gaziantep, Türkiye
Imen Dridi: Carthage University, Zarzouna, Tunisia

* Corresponding author(s):
E-mail address:
oloyedegk@gmail.com (G. K. Oloyede)
e-ISSN: 2791-7509
doi: https://doi.org/10.29228/ijpbp.11

al oils are due to the presence of compounds of terpene origin, olefinic double bonds, and functional groups such as hydroxyl and aldehydes (Bowles, 2003; Edris, 2007; Sell, 2010, Oloyede et al., 2019a, b).

The Sapindaceae (Soapberry) family are trees, shrubs, or lianas widely distributed in tropical to sub-tropical regions. Many of its members contain latex, milky sap, and mildly toxic saponins with soap-like qualities in the foliage and/or the seeds or roots. *Blighia* is a genus of three species of flowering plants (*B. sapida*, *B. unijugata*, and *B. welwitschii*) (Watson & Dalwitz, 2007). *B. welwitschii* however is not available in Nigeria. *B. unijugata* is a shrub that is small to medium-sized, but occasionally grows up to 30 to 35 m tall (Bekele-Tesemma & Tengnäs, 2007; Oderinde et al., 2008) (Figure 1). In some African countries, the leaves are used as vegetables to prepare meals. Various parts of the tree are known to have anti-malarial, sedative, and analgesic properties, for the treatment of rheumatism, kidney pain, and stiffness. Bark pulp is applied as enema or bark decoction is taken to treat fever, and as purgative (Burkill, 2000; Hyde et al., 2002). The wood of *B. unijugata* is commonly used for light construction, furniture, and charcoal production (Katende et al., 1995). Macroscopical investigation showed the stem bark outer layer is greyish and, the inner layer is pale reddish brown, with a disagreeable odor, while microscopical screening revealed the presence of starch grains, trichomes, and sclerenchyma and chemomicroscopic result revealed the presence of lignin, starch, calcium oxalate, cellulose, stone cells (Osuala, 2020). Significant inhibitory activity against the pathogenic microorganisms was observed when the nutritional elements, comparative study of the antimicrobial and cytotoxicity of the root, stem bark, and leaf essential oils, and crude extract of *B. unijugata* was investigated (Oderinde et al., 2008; Adewuyi, et al., 2009). Phytochemical screening showed the presence of polyphenols, polyterpenes, and flavonoids while extract of the fruits and butanol fraction from the leaves of *B. unijugata* was reported not to be toxic in animal studies (Aquaisua et al., 2011; Bléyéré et al., 2013; Osuala, 2020). Hydrogen peroxide and DPPH free radical scavenging activities of leaf, stem bark, root, flower, and fruit of *B. unijugata* was reported by Ajiboye et al. (2017a, b) and the essential oil compositions were reported (Dorcas et al., 2017) indicating the presence of terpenes.

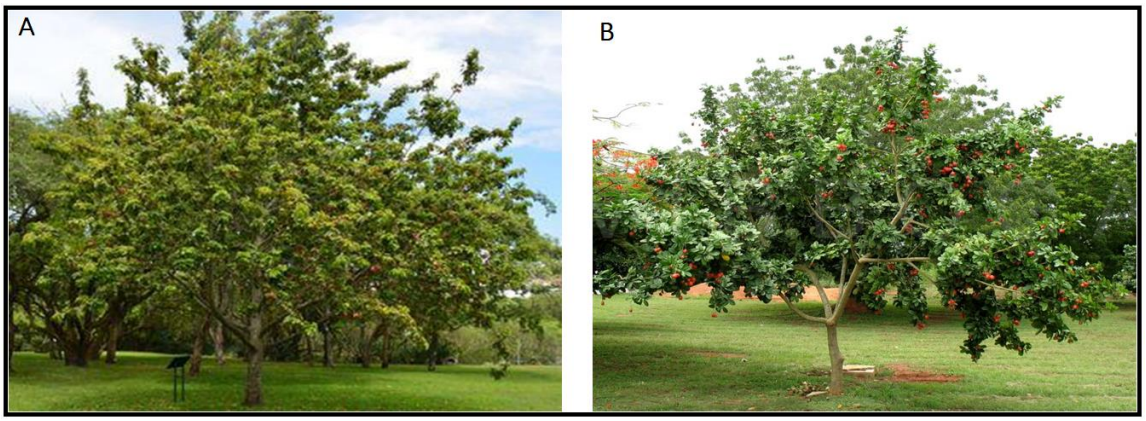

Figure 1. *B. unijugata* (A) and *B. sapida* (B)

B. sapida is a woody perennial multipurpose fruit tree species native to the Guinean forests of West Africa (Orwa et al., 2009) (Figure 1). The fruit of *B. sapida* is edible when fully ripped (Moya, 2001). The fruit produces lather with water and is therefore used for laundering purposes in some West African countries. Crushed fruits are used as fish poison while various preparation and combination of the extract have been made for the treatment of diseases such as dysentery, epilepsy, and yellow fever (Gbolade, 2009; Hamzah et al., 2013). The plant has been reported to be effective against cold, pain, and emulsion properties (Elizabeth et al., 2012) and is used as an insecticidal agent. The extract of the flowers is used as cologne while the pulverized bark is mixed with grounded hot peppers and rubbed on the body as a stimulant. Capsules of the fruits have the property of producing saponins, which lather in water and are used for washing (Ekué et al., 2010). Alkaloids, saponins, cardiac glycosides, reducing sugar, carbohydrates, flavonoids, phenol, and tannin were found in *B. sapida* fruits and root bark (Oyeleke, et al., 2013; Dossou et al., 2014). Aqueous extract of *B. sapida* decreased blood glucose levels of rats in a separate experiment and was the most potent inhibitor of α-amylase while ethanolic extract inhibited α-glucosidase most effectively (Howélé et al., 2010; Kazeem et al., 2013).

These two plants are sometimes used interchangeably and previous work done only focused on *B. unijugata*. Therefore, the main objective of this study is to compare the composition of the essential oil extracted from the leaves, roots, and stem bark of *B. unijugata* and *B. sapida* and to investigate their antioxidants [using the 2,2-diphenyl-1-picrylhydrazyl (DPPH) radical method] and insecticidal potential using the maize pest (*Sitophilus zeamaise*) method (Oloyede et al., 2019a, b).

2. Materials and methods

2.1. Materials

2.1.1. Plant collection and identification

Fresh leaves, roots, and stem bark of *B. unijugata* and *B. sapida* were collected at the Botanical Garden and identified at the Herbarium, Department of Botany, University of Ibadan, Nigeria in January 2016. The samples were air-dried, pulverized, and placed in air-tight polythene bags before extraction to prevent any loss of volatile components.

2.1.2. Reagents

Hexane, methanol, ascorbic acid, and butylated hydroxyanisole (BHA) were purchased from BDH chemicals. 2,2-Diphenyl-1-picrylhydrazyl (DPPH) were purchased from Sigma-Aldrich.

2.1.3. Equipment/Apparatus

Hydro-distillation flask, Clevenger apparatus, glass condenser, heating mantle, electronic weighing balance (OHAUS), oven (Carbolite), syringes, sample bottles, GC-MS (Agilent Technologies, Model-7890A) gas chromatograph, and UV spectrophotometer (Unico1200 & Perkin Elmer Lambda 25 model, UK).

2.2. Methods

2.2.1. Extraction of essential oil

Hydro-distillation method using the Clevenger apparatus was used to extract oils. 300 g of each of the pulverized samples was weighed and placed in a 5 liter round bottom flask fitted with a heating mantle and water was added until the sample was fully immersed. The extraction process was carried out for 3 hours at a regulated temperature according to the European Pharmacopoeia (1996) specification. The volatile oil trapped in 1.0 ml of hexane was carefully collected using a syringe and placed in a sample vial. The weight of the oil was recorded and stored in the refrigerator until further analysis (Burt, 2004; Oloyede & Egbewole, 2014).

2.2.2. Gas chromatography-mass spectrometry (GC-MS) analysis

The essential oils were analyzed using GC-MS (Agilent Technologies, Model-7890A) gas chromatograph, coupled with a 5975C mass spectrometer (Agilent Technology). The gas chromatograph capillary column type was an HP-5MS, with a column length of 30 m; internal diameter of 0.320 mm, and film thickness of 0.25 µm. The carrier gas used was helium at a constant flow rate of 1.4123 ml/min and an average velocity of 43.311 cm/sec, while the pressure was put at 1.5 psi. Temperature programming started with an initial column temperature set at 80 °C for 2 mins and was increased to 240 °C at the rate of 10 °C/min. The volume of the sample injected was 1µl (Cronin & Caplan, 1987; Baser & Buchbauer, 2015; Onocha et al., 2016).

2.2.3. Identification of components

Flame ionization detector (FID) set at a temperature of 300 °C was used to identify the constituents and their percentage compositions obtained from electronic integration measurement. The peak numbers and relative percentages of the characterized compounds were recorded while the individual components of the oil were identified based on their retention indices determined with reference to *n*-alkanes and by comparison of their mass spectra fragmentation pattern (NIST0.8 L Database/Chem. Station System) with previously reported data (Lawless, 2013; Adams 2007; Las Heras et al., 2003). The peak numbers and relative percentages of the characterized components are given in Tables 1 and 2.

2.2.4. Insecticidal activity assay

Maize weevil insects, *S. zeamais*, that were used in this study were cultured at the Department of Crop Protection and Environmental Biology, University of Ibadan, Nigeria. A standard culture was maintained for 4 weeks without exposure to any insecticide. Following the methods of Karpouhtsis et al. (1998) and Isman (2000) with little modification, six insects (three males and three females) were used for each assay. The insects were placed in air penetrating containers containing 10 g of maize to avoid mortality by suffocation. 0.2 ml of test samples, *B. unijugata* leaves (BUL), *B. unijugata* stem (BUS), *B. unijugata* roots (BUR), *B. sapida* leaves (BSL), *B. sapida* stem (BSS), *B. sapida* roots (BSR), were applied onto a piece of sterilized Whatman filter paper (No: 1) and introduced into the different containers to determine its toxicity against the insects either via inhalation or contact. A control experiment of the same number of insects, but without test samples, was also performed. Three different concentrations of the essential oils, 25%-100% were prepared by serial dilution with hexane. Analysis was done in triplicate. Insects were monitored at 12-72 hours. Percentage (%) mortality of insects was calculated using the formula given below:

$$Corrected\ mortality\ (\%) = 1 - \frac{n\ in\ Co\ before\ treatment\ x\ n\ in\ T\ after\ treatment}{n\ in\ Co\ after\ treatment\ \times\ n\ in\ T\ before\ treatment} x\ 100$$

Where 'n' is insect population, 'T' is treated diet with sample, and 'Co' is control.

2.2.5. Antioxidant screening

The antioxidant activity of the essential oils of the samples was determined using DPPH radical scavenging method. Various concentrations (25 mg/ml – 100 mg/ml) of the test sample (1 ml of each essential oil) were mixed with 0.2 mm methanol-DPPH solution (2.0 ml), prepared by dissolving 7.81 mg of DPPH in 100 ml of methanol. The mixture was shaken vigorously and left to incubate for 30 minutes in the dark at room temperature and the absorbance was then measured at 517 nm and recorded using GS UV-12, UV-VIS spectrophotometer. In its radical form, DPPH absorbs, but upon reduction by an antioxidant species, its absorption reduces. A blank experiment was carried out applying the same procedure without the test sample (DPPH/methanol) and the absorbance was recorded. Ascorbic acid (vitamin C) and α-tocopherol (vitamin E) were used as standard.

2.2.6. Statistical analysis for determination of percentage inhibition in the DPPH analysis

Determination of the free radical scavenging activity in the DPPH analysis of each test oil solution was calculated as percentage inhibition using the equation given below (Ayoola et al., 2008; Onocha et al., 2016):

$$Inhibition\ (\%) = 1 - \frac{Ablank - Asample}{Ablank} x\ 100$$

This was statistically determined from the absorbance measurement of samples. Graph showing % inhibition against concentration (mg/ml) was shown as a column chart in Figure 2.

3. Results and discussion

The percentage yields (w/w) of the colourless essential oils were as follows: BUL: 0.91%, BUS: 0.42%, BUR: 0.34%, BSL: 0.67%, BSS: 0.48%, and BSR: 0.32%.

Three non-terpenoid constituents yielding a total of 99.99% identified in *B. unijugata* leaf essential oil (Table 1) were pentadecanoic acid, 14-methyl, methyl ester (38.34%), carbonic acid, prop-1-en-2-yl undecylpropyl ester (36.79%), and 9-octadecanoic acid *(Z)*-methyl ester (24.86%). Twelve constituents were identified in the root essential oil of *B. unijugata* representing a total of 99.94%, comprising one monoterpene (limonene), and eleven non-terpenoids, mainly acids, esters, and hydrocarbon. The major constituents were: limonene (20.51%), *trans*-13-octadecanoic acid (16.74%), *cis*-vaccenic acid (9.50%), 1,2-benzene dicarboxylic acid, butyl-2-methyl propyl ester (9.74%), and 2,5-norbornanediol (8.36%). Other constituents present were 3-methylheptadecane (7.42%), *cis*-13-octadecanoic acid, *(E)* (6.40%), hexadecanoic acid (5.93%), heptadecanolide (4.0%), octadec-9-enoic acid (3.21%), 9-

octadecanoic acid *(Z)*-2,3-dihydroxy propylester (2.96%) and 9-octadecanoic acid *(E)* (0.32%). Fifteen compounds were detected in the stem bark oil of *B. unijugata* with a non-terpenoid 1,3-dimethoxybenzene as the major constituent (79.01%), however, longifolene (4.22%), 4-penta-1-one, 1-(1H, imidazole-2-yl)-4-isopropenyl cyclo hexanone (2.54%), α-ionone (2.40%), phenol, 4-methoxy-3-methyl (2.20%), *trans*-β-ionone (1.51%), benzothiazole, 3-methyl (1.26%), 2,5-nornanediol (1.18%), hexahydro farnesyl acetone (1.13%), tricosane (0.83%), 1,16-hexadecanediol (0.81%), 5-*t*-butyl-4-methylimidazole (0.78%), 2-piperidine, N-(4-bromo, *n*-butyl) (0.58%), farnesyl acetone (0.57%), and octadecane,1-bromo (0.48%) were detected in trace amount. It was observed that only 2,5-norbornanediol was common to both the root and stem bark essential oil of *B. unijugata* (Table 1). Geranyl acetone is common to root and leaves of *B. sapida*, on the other hand, hexahydrofarnesyl acetone, farnesyl acetone, and cembrene A were found in stem and leaves, whereas the oleic acid was detected in stem and root.

Table 1. Chemical constituents of leaves, stem, and roots of *B. unijugata*

No	RT (min)	Constituents	Composition (%)*		
			BUL	BUS	BUR
1	4.34	1,16-Hexadecanediol	-	0.81	-
2	5.67	Dimethylresorcinol	-	79.01	-
3	11.17	α-Ionone	-	2.40	-
4	11.63	5-*t*-Butyl-4-methylimidazole	-	0.78	-
5	11.73	4-Methoxy-3-methyl phenol	-	2.20	-
6	12.41	β-Ionone	-	1.51	-
7	15.39	2,5-Norbornanediol	-	1.18	8.36
8	15.95	Longifolene	-	4.22	-
9	16.57	Octadecane,1-bromo	-	0.48	-
10	17.85	Limonene	-	-	20.51
11	17.58	4-penta-1-one,1-(1H-Imidazol-2-yl)-4-isopropenylcyclohexanone	-	2.54	-
12	19.30	Hexahydrofarnesyl acetone	-	1.13	-
13	19.36	Carbonic acid, prop-1-en-2-yl undecyl ester	36.79	-	-
14	20.63	Farnesyl acetone	-	0.57	-
15	20.76	Methyl isohexadecanoate	38.34	-	-
16	21.27	Heptadecane, 3-methyl	-	-	7.42
17	21.43	1,2-Benzenedicarboxylic acid, butyl-2-methyl propyl ester	-	-	9.14
18	21.88	Hexadecanoic acid	-	-	5.93
19	23.38	Octadec-9-enoic acid	-	-	3.21
20	23.63	Oleic acid, methyl ester	24.86	-	-
21	23.80	Heptadecanolide	-	-	4.00
22	24.03	9-Octadecanoic acid *(Z)*-2,3-dihydroxypropyl ester	-	-	2.96
23	24.67	*cis*-Vaccenic acid	-	-	9.50
24	25.05	*cis*-13-Octadecenoic acid	-	-	6.40
25	25.23	9-Octadecanoic acid, *(E)*	-	-	0.32
26	26.52	2-Piperidinone, N-(4-bromo *n*-butyl)	-	0.58	-
27	27.88	*trans*-13-Octadecenoic acid	-	-	16.74
28	27.95	Docosane	-	0.25	-
29	29.26	Tricosane	-	0.83	-
30	30.26	Benzothiazole 3-methyl		1.26	
		Total	99.99	99.75	94.49

*Percentages were calculated from the flame ionization detection data. RT: Retention time on HP-5MS column, BUL: *B. unijugata* leaves, BUS: *B. unijugata* stem, BUR: *B. unijugata* roots.

Seventeen components were identified in the leaf essential oil of *B. sapida* and contained hexahydrofarnesyl acetone (21.43%), phytol (20.45%), geosmin (16.25%), and α-ionone (8.27%) as the major constituents, while β-ionone (4.41%), β-eudesmol (2.20%), aromadendrene (1.36%), coniferyl aldehyde and *n*-propyl ether (2.94%) were also detected. Twenty-one compounds were observed in *B. sapida* stem essential oil, with the major constituent being cholesterol (38.66%). The root with twenty two compounds had nonanal (18.09%), 4-cyclopropyl carbonyl tetradecane (11.60%), 3-methyl-4-(phenylthio)-2-prop-2-enyl-2,5-dihydro thiophene-1,1-dioxide (11.49%) as the principal components, while *n*-hexanoic acid (9.60%), ascorbyl palmitate (1.35%), (2)-6-octadecanoic acid (0.87%), 6-methoxy-2,7,8-trimethyl-2-(4,8,12-trimethyl decyl) chroman (0.52%), stearin (0.34%), and oleic acid (0.26%) were also found in the oil. Cembrene A, hexahydrofarnesyl acetone, and farnesyl acetone were common to both *B. sapida* stem and leaf, while oleic acid was present in *B. sapida* stem and root and was also detected in *B. unijugata* (Table 2).

Mass fragmentation of the major and common components in *B. unijugata* and *B. sapida* leaves, stem bark, and root were also presented in Table 3.

3.1. Insecticidal activity

The use of natural products from plants is considered a useful alternative for the control of stored grain pests (Ho et al., 1996; Isman, 2000). Essential oils have also been employed as green pesticides (Obeng-Ofori & Reichmuth, 1999; Koul et al., 2008). The result of the insecticidal analysis showed that only *B. unijugata* leaves (BSL) and *B. sapida* stem (BSS) showed 50% and 33.3% toxicity to the maize weevils, respectively (Table 4) and justify their use in ethnomedicine as pesticides. The low insecticidal activity observed may have been due to the absence of certain phytochemicals such as α-pinene, β-pinene, camphor, linalool, and other related compounds in the plant essential oils which were reported to be responsible for the toxicity of stored grain pests (Huang et al., 1998; Lee et al., 2001). The extracts may however have pronounced activity.

3.2. Antioxidant activity

The essential oils scavenged free radicals in the antioxidant screening assay, with comparable activity to the standards, ascorbic acid, and α-tocopherol. *B. unijugata* root (83.96%) showed the highest activity and better activity than α-tocopherol (75.08%) but lower than ascorbic acid (91.60%) at 100 mg/ml. BUL and BUS exhibited 79.19% and 77.28% inhibition at the same concentration, respectively. The activity of *B. sapida* stem essential oil (79.73%) was

higher than that of the root (79.61%) at 100 mg/ml. The leaf essential oil gave the least antioxidant activity (74.96%). These values are comparable to that of one of the standard, α-tocopherol (75.08%) but less than that of ascorbic acid (91.60%). The antioxidant activities of the oils were concentration-dependent (Figure 2). The results indicated that the essential oils are good scavengers of free radicals as the reduction in absorbance values were observed in all the oil samples after incubation in DPPH.

Table 2. Chemical composition of the essential oil of leaves, stem, and roots of *B. sapida*

No	RT (min)	Constituents	Composition (%)*		
			BSL	BSS	BSR
1	3.464	Benzene acetyldehyde	-	1.93	-
2	3.514	2,4,4-Trimethyl-2-hexen-1-ol	2.21	-	-
3	3.802	Octan-1-ol	-	-	3.82
4	4.322	Nonanal	-	-	18.09
5	4.328	1,10-Decanediol	-	4.71	-
6	4.335	2-Methyl cyclohexanol	2.44	-	-
7	5.427	*(E)*-Non-2-enal	-	-	3.89
8	5.724	Veratrole	-	2.98	-
9	5.701	Butylcyclopentane	-	-	2.89
10	5.902	*(2E,4E)*-3,7-Dimethyl-2,4-octadiene	-	1.74	-
11	7.304	Acetaldehyde, (3,3-dimethylcyclohexylidene)	1.17	-	-
12	8.877	*(E,E)*-2,4-Decadienal	-	-	4.33
13	10.649	Geosmin	16.25	-	-
14	11.174	α-Ionone	8.26	-	-
15	11.715	Geranyl acetone	3.14	-	3.07
16	11.733	3,5-Dimethyl-1-adamantanol	-	3.81	-
17	12.373	Eremophylene	-	3.66	-
18	12.417	β-Ionone	4.41	-	-
19	13.878	*cis*-Chrysanthemol	-	1.54	-
20	14.82	Caryophyllene oxide	-	-	1.47
21	15.546	β-Eudesmol	2.20	-	-
22	16.157	Aromandendrene	1.35	-	-
23	16.558	Coniferyl aldehyde, *n*-propyl ether	2.94	-	-
24	17.575	2-(1H-Imidazole-5-yl)bicyclo[1,1,1]pentan-2-ol	-	1.51	-
25	19.297	Hexahydrofarnesyl acetone	21.44	2.03	-
26	20.607	Farnesyl acetone	7.01	1.34	-
27	21.101	Isophytol	1.21	-	-
28	21.27	Cembrene A	1.19	3.03	-
29	21.803	*n*-Hexanoic acid	-	-	9.60
30	21.929	Ascorbyl palmitate	-	-	1.35
31	21.998	1-Hexacosene	-	-	2.03
32	22.106	*(Z)*-9-Tricosene	-	-	1.73
33	22.112	Verticilla-4(20),7,11-triene	-	2.59	-
34	22.232	1,3,6,10-Cyclo-tetra decatetraene-3,7,11-trimethyl	-	1.99	-
35	23.194	2-Octylcyclopropaneoctanal	-	-	3.26
36	23.291	Stearin	-	-	0.34
37	23.819	Phytol	20.45	-	-
38	23.823	*(E)*-3-Eicosene	-	2.15	-
39	24.287	Linoleic acid	-	0.76	-
40	25.03	Petroselinic acid	-	0.13	-
41	25.242	Dodecyl myristate	-	0.19	-
42	26.501	Oleic acid	-	1.30	0.27
43	27.348	*(E)*-Octadecanoic acid	-	-	4.79
44	27.399	(2)-6-Octadecanoic acid	-	-	0.88
45	27.954	Vinyl stearyl ether	-	0.60	-
46	27.956	*trans*-13-Octadecenoic acid	2.41	-	-
47	28.652	Squalene	-	-	10.75
48	29.35	2-Hydroxy-cyclopentadecanone	-	1.23	-
49	29.364	Batilol	1.83	-	-
50	29.802	3-Methyl-4-(phenyl thio)-2-prop-2-enyl-2,5-dihydrothiophene-1,1-dioxide	-	-	11.5
51	30.93	Cholesterol	-	38.66	-
52	31.05	δ-Tocopherol	-	-	3.09
53	31.073	*O*-Acetyl-δ-tocopherol	-	-	0.734
54	31.302	4-Cyclo propyl carbonyl tetradecane	-	-	11.6
55	31.997	6-Methoxy-2,7,8-trimethyl-2-(4,8,12-trimethyl decyl)chroman	-	-	0.522
		Total	100	75.88	87.15

*Percentages were calculated from the flame ionization detection data. RT: Retention time on HP-5MS column, BSL: *B. spida* leaves, BSS: *B. spida* stem, BSR: *B. unijugata* roots.

The presence of oxygenated terpenoids has been reported to greatly enhance the free radical scavenging activity of plant metabolites (Fang et al., 2002; Oloyede & Egbewole, 2014; Ajiboye et al., 2017a, b; Oloyede et al, 2019a, b) and may also be responsible for the observed activity in these plants.

4. Conclusions

Comparative evaluation of the chemical composition of the essential oils from the leaves, stem bark, and roots of *B. unijugata* and *B. sapida* showed that they were rich in oxygenated terpenoids and non-terpenoids with few monoterpenes such as limonene (20.51%) in *B. unijugata*. 2, 5-norbornanediol was found to be present in both the root and stem bark essential oils of the plant. Cembrene A, hexahydrofarnesyl acetone, and farnesyl acetone were found in both *B. sapida* stem and leaf. Oleic acid was also found in *B. unijugata* and *B. sapida* stem and root. Toxic effects against the maize weevil, *S. zeamaise*, and significant free radical scavenging when compared to standards of ascorbic acid and α-tocopherol justify the use of the plants in traditional medicine.

Table 3. Mass fragmentation of the major and common components in *B. unijugata* and *B. sapida* leaves, stem bark, and root

No	Major/Common constituents	Molecular formula	Molecular weight (g/mol)	Mass fragmentation *(m/z)* values
1	*trans*-13-Octadecenoic acid	$C_{18}H_{34}O_2$	282	282 (M^+) ($C_{18}H_{34}O_2)^+$, 264, 246, 235, 222, 211, 196, 180, 165, 151, 137, 123, 111, 97, 83, 69, 60, 55, 41, 29, 15
2	Limonene	$C_{10}H_{16}$	136	136 (M^+), ($C_{10}H_{16})^+$, 121, 107, 93, 79, 68, 55, 53, 41, 39, 29
3	Oleic acid, methyl ester	$C_{19}H_{36}O_2$	296	296 (M^+) ($C_{19}H_{36}O_2)^+$, 278, 264, 246, 207, 193, 180, 152, 137, 129, 111, 97, 87, 83, 74, 69, 59, 55, 41, 33, 29, 15
4	Carbonic acid, prop-1-en-2-yl undecyl ester	$C_{15}H_{28}O_3$	256	256 (M^+) ($C_{15}H_{28}O_3)^+$, 199, 154, 126, 111, 97, 85, 71, 67, 57, 43, 29
5	Methyl isohexadecanoate	$C_{17}H_{34}O_2$	270	270 (M^+) ($C_{17}H_{34}O_2)^+$, 239, 227, 213, 199, 185, 171, 157, 143, 129, 111, 97, 87, 74, 69, 59, 55, 43, 29
6	Dimethyl resorcinol	$C_8H_{10}O_2$	138	138 (M^+) ($C_8H_{10}O_2)^+$, 123, 109, 95, 78, 65, 57, 52 43, 29
7	Cholesterol	$C_{27}H_{40}O$	386	386 (M^+) ($C_{27}H_{40}O)^+$, 386, 353, 301, 275, 255, 247, 231, 173, 159, 145, 133, 119, 107, 95, 81, 69, 57, 43
8	Hexahydrofarnesyl acetone*	$C_{18}H_{36}O$	268	250 (M^+) ($C_{18}H_{36}O)^+$, 250, 210, 124, 109, 95, 58, 43, 29
9	Phytol	$C_{20}H_{40}O$	296	296 (M^+) ($C_{20}H_{40}O)^+$, 137, 123, 111, 95, 81, 71, 57, 43, 29
10	Nonanal	$C_9H_{18}O$	142	142 (M^+) ($C_9H_{18}O)^+$,114, 98, 95, 82, 70, 57, 41, 39, 29
11	Geosmin	$C_{12}H_{22}O$	182	182 (M^+)($C_{12}H_{22}O)^+$,125, 112, 97, 83, 71, 69, 57, 69, 57, 56, 53, 43, 39
12	2,5-Norbornanediol*	$C_7H_{12}O_2$	128	128 (M^+) ($C_7H_{12}O_2)^+$, 126, 110 (100), 95, 92, 88, 86, 84, 83, 82, 81, 79, 73, 71, 68, 67, 65, 57, 54, 49, 45, 43, 41
13	Geranyl acetone*	$C_{13}H_{22}O$	194	194 (M^+) ($C_{13}H_{22}O)^+$, 151, 136, 125, 121, 109, 95, 83, 79, 69, 43, 41,39, 27
14	Farnesyl acetone*	$C_{18}H_{30}O$	262	262 (M^+) ($C_{18}H_{30}O)^+$, 138, 125, 121, 107, 95, 93, 81, 69, 43,41, 29
15	Cembrene A*	$C_{20}H_{32}$	272	272 (M^+) ($C_{20}H_{32})^+$, 257, 229, 187, 173, 159, 145, 133, 119, 105, 91, 79, 67, 55
16	Oleic acid*	$C_{18}H_{34}O_2$	282	282 (M^+) ($C_{18}H_{34}O_2)^+$, 264, 151, 125, 131, 111, 97, 83, 69, 57, 55, 43, 41, 39, 29, 27

*Compounds that are common to the leaf, stem bark, and root essential oils. The individual components of the oil were identified based on their retention indices determined with reference to *n*-alkanes and by comparison of their mass spectra fragmentation pattern (NIST0.8 L Database/Chem. Station System) with previously reported data. Structures were obtained from the literature (Lawless, 2013; Adams, 2007; Las Heras et al., 2003).

Table 4. Insecticidal activity of *B.unijugata* and *B. sapida* leaves, stem, and root essential oil on *S. zeamaise**

T (hr)	Insects killed at different concentrations (%)																		
	BUL			BUS			BUR			BSL			BSS			BSR			C
	25	50	100	25	50	100	25	50	100	25	50	100	25	50	100	25	50	100	
3	-	1	-	-	-	-	-	-	-	-	-	-	-	-	-	-	-	-	-
6	1	-	-	-	-	-	-	-	-	-	-	-	-	-	-	-	-	-	-
12	-	-	-	-	-	-	1	-	-	-	-	-	-	-	-	-	-	1	-
18	2	-	-	-	-	-	-	-	-	-	-	1	-	-	-	-	-	-	-
24	-	-	-	-	-	-	-	-	-	-	1	-	1	-	1	-	-	-	-
36	-	-	-	-	-	-	-	-	-	-	-	-	-	-	-	-	-	-	-
48	-	-	-	-	-	-	-		-	-	-	-	-	1	-	-	-	-	-
72	-	-	-	-	-	-	-	-	-	-	-	-	-	-	1	-	-	-	-
No-i	6	6	6	6	6	6	6	6	6	6	6	6	6	6	6	6	6	6	-
No-d	3	1	0	0	0	0	0	0	0	0	1	1	1	1	2	0	0	1	-
% M	50.0	16.7	0	0	0	0	16.7	0	0	0	16.7	16.7	16.7	16.7	33.3	0	0	16.7	-

*BUL: *B. unijugata* leaves. BUS: *B. unijugata* stem bark, BUR: *B. unijugata* roots, BSL: *B. sapida* leaves, BSS: *B. sapida* stem bark, BSR: *B. sapida* roots, T: Time (hours), No-i = Number of insects used, No-d = Number of dead insects, % M = Percentage mortality.

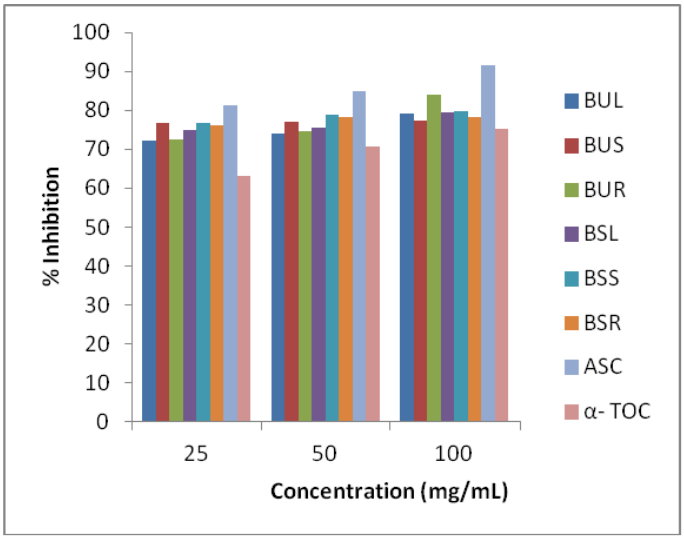

Figure 4. Percentage inhibition of DPPH free radical scavenging activities of BUL (*B. unijugata* leaves), BUS (*B. unijugata* stem bark), BUR (*B. unijugata* roots), BSL (*B. sapida* leaves), BSS (*B. sapida* stem bark) and BSR (*B. sapida* roots), standards ascorbic (ASC) and α-tocopherol (α-TOC).

Acknowledgments

The authors appreciate the Department of Chemistry, University of Ibadan for the use of UV-Visible Spectrophotometer used for the antioxidant screening and also the staff of Central Science Laboratory, University of Lagos for the use of GC/GC-MS equipment. We also acknowledge and appreciate the tremendous support and assistance of the H.O.D and members of staff of the Department of Crop Protection and Environmental Biology, especially Mr. Oyelade for their assistance in culturing the grain insects used for insecticidal screening. G.K. Oloyede also acknowledges GKO Publishers Ltd for sponsoring part of this research through grant No. (04GKO2016) used for editorial work.

Conflict of interest

The authors confirm that there are no known conflicts of interest.

Statement of ethics

In this study, no method requiring the permission of the "Ethics Committee" was used.

Availability of data and materials

All data generated or analyzed during this study are included in this published article.

Funding

The editorial work related to this project was funded by GKO Publishers Ltd. (Grant No: 04GKO2016).

CRediT authorship contribution statement

Ganiyat K. Oloyede: Conceptualization, Methodology, Investigation, Data analysis, Writing-original draft, Supervision
Patricia A. Onocha: Conceptualization, Supervision, Methodology, Resources, Conceptualization, Visualization, Formal analysis, Investigation, Methodology
ThankGod R. Ikiroma: Laboratory investigation, Practicals, Investigation, Result analysis
Olusegun W. Olusola: Laboratory investigation, Practicals, Investigation, Result analysis

ORCID Numbers of the Authors

G. K. Oloyede: 0000-0002-9057-7502
P. A. Onocha: 0000-0002-7952-5920
T. R. Ikiroma: 0000-0003-1303-0789
O. W. Olusola: 0000-0002-1776-0570

Supplementary File

The supplementary file accompanying this article is available at https://ijpbp.com/index.php/ijpbp/libraryFiles/downloadPublic/13.

Publisher's Note

All claims expressed in this article are solely those of the authors and do not necessarily represent those of their affiliated organizations, or those of the publisher, the editors and the reviewers. Any product that may be evaluated in this article, or claim that may be made by its manufacturer, is not guaranteed or endorsed by the publisher.

This is an open-access article distributed under the terms of the Creative Commons Attribution 4.0 International License (CC BY). The use, distribution or reproduction in other forums is permitted, provided the original author(s) and the copyright owner(s) are credited and that the original publication in this journal is cited, in accordance with accepted academic practice. No use, distribution or reproduction is permitted which does not comply with these terms.

References

Abdelouaheb, D., & Amadou, D. (2012). The Therapeutic Benefits of Essential Oils, Nutrition, Well-Being and Health, Dr. Jaouad Bouayed (Ed.), pp. 160. ISBN: 978-953-51-0125-3.

Adams, R. P. (2007). Identification of essential oil components by gas chromatography/mass spectrometry (Vol. 456, pp. 544-545). Carol Stream: Allured Publishing Corporation.

Adewuyi, A., Oderinde, R. A., & Omotosho, M. A. (2009). Comparative Study of the Antibacterial and Cyctotoxicity of the Essential Oils from the Leaves, Stem Bark and Roots of *Blighia unijugata* Baker (Sapinadaceae). *Medicinal and Aromatic Plant Science and Biotechnology*, *3*(SI1), 97-99.

Ajiboye, C. O. , Moronkola, D. O., Adesomoju, A. A. (2017a). Hydrogen Peroxide Free Radical Scavenging Activities of Leaf, Stem Bark,Root, Flower and Fruit of *Blighia unijugata* Baker (Sapindaceae) Extracts. *Journal of Chemical and Pharmaceutical Research*, *9*(8):8-12.

Ajiboye, C. O., Moronkola, D. O., & Adesomoju, A. A. (2017b). DPPH free radical scavenging activities of leaf, stem bark, root, flower and fruit of *Blighia unijugata* Baker (Sapindaceae) extracts. *Journal of Chemical, Biological and Physical Sciences*, *7*(4), 1190-1197.

Akerele, O. (1991). Medicinal plants and primary health care: an agenda for action. *Eastern Mediterranean Region Drugs Digest*, 8(2), 11-25.

Apel, K., & Hirt, H. (2004). Reactive oxygen species: metabolism, oxidative stress, and signaling transduction. *Annual Review of Plant Biology*, *55*, 373-399.

Aquaisua, A. N., Bassey, R. B., Ikpeme, B. M., & Bassey, E. I. (2011). Effect of crude extracts of *Blighia unijugata* on histology of the liver and kidney of adult Wistar rats. *International Research Journal of Pharmacy and Pharmacology*, *1*, 17-22.

Ayoola, G. A., Coker, H. A., Adesegun, S. A., Adepoju-Bello, A. A., Obaweya, K., Ezennia, E. C., & Atangbayila, T. O. (2008). Phytochemical screening and antioxidant activities of some selected medicinal plants used for malaria therapy in Southwestern Nigeria. *Tropical Journal of Pharmaceutical Research*, *7*(3), 1019-1024.

Bakkali, F., Averbeck, S., Averbeck, D., & Idaomar, M. (2008). Biological effects of essential oils–a review. *Food and Chemical Toxicology*, *46*(2), 446-475.

Baser, K. H. C., & Buchbauer, G. (2015). Handbook of essential oils: science, technology, and applications. Handbook of essential oils: science, technology, and applications., (Ed. 2), FL. Taylor and Francis Group.

Bekele-Tesemma, A., & Tengnäs, B. (2007). Useful trees and shrubs of Ethiopia: identification, propagation, and management for 17 agroclimatic zones (p. 552). Nirobi: RELMA in ICRAF Project, World Agroforestry Centre, Eastern Africa Region.

Bléyéré, N. M., N'dia, K. F., Kouakou, K. L., Abo, K. J., & Ehilé, E. E. (2013). Acute toxicity in mice and effects of a butanol extract from the leaves of *Blighia unijugata* bak.(Sapindaceae) on electrocardiogram of rabbits. *Scholars Academic Journal of Pharmacy*, *2*(6), 429-435.

Bowles, E. J. (2003). The chemistry of aromatherapeutic oils (ed.). Crowns Nest NSW, Australia: Allen & Unwin.

Burkill, H. M. (2000). Useful plants of West Tropical Africa. 2nd ed. Vol. 5, Families S-Z, United Kingdom, Royal Botanic Gardens, Kew, Richmond, 686.

Burt, S. (2004). Essential oils: their antibacterial properties and potential applications in foods—a review. *International Journal of Food Microbiology*, *94*(3), 223-253.

Cronin, D. A., & Caplan, P. J. (1987). Application of GC/MS to identification of flavour compounds in foods. Applications of mass spectrometry in food science/edited by John Gilbert, Elsevier Applied Science,

Dorcas, O. M., Usman, Z. F., Oludoyin, A. A., & Clement, O. A. (2017). Essential oil compositions of leaf, stem-bark, stem, root, flower, and fruit with seed of *Blighia unijugata* Baker (Sapindaceae). *African Journal of Pharmacy and Pharmacology*, *11*(7), 108-119.

Dossou, V. M., Agbenorhevi, J. K., Combey, S., & Afi-Koryoe, S. (2014). Ackee (*Blighia sapida*) fruit arils: Nutritional, phytochemicals and antioxidant properties. *International Journal of Nutrition and Food Sciences*, *3*(6), 534-537.

Edris, A. E. (2007). Pharmaceutical and therapeutic potentials of essential oils and their individual volatile constituents: a review. *Phytotherapy Research: An International Journal Devoted to Pharmacological and Toxicological Evaluation of Natural Product Derivatives*, *21*(4), 308-323.

Ekué, M. R., Sinsin, B., Eyog-Matig, O., & Finkeldey, R. (2010). Uses, traditional management, perception of variation and preferences in ackee (*Blighia sapida* KD Koenig) fruit traits in Benin: implications for domestication and conservation. *Journal of Ethnobiology and Ethnomedicine*, *6*(1), 1-14.

Elizabeth, N., Amusa, S. A., & Nilza, J. S. (2012). Physico-chemical properties of *Blighia sapida* (ackee) oil extract and its potential application as emulsion base. *African Journal of Pharmacy and Pharmacology*, *6*(3), 200-210.

European Pharmacopoeia (1996). Saint Ruffine: Conseil de 1' Europe Maisonneure S.A. NCCLS. 1999. National Committee for Clinical Laboratory Standards, Performance Standards for Antimicrobial Susceptibility Testing, 6th edition. Approved Standards, M2-A6, Wayne, Pennsylvania.

Fang, Y. Z., Yang, S., & Wu, G. (2002). Free radicals, antioxidants, and nutrition. *Nutrition*, *18*(10), 872-879.

Farnsworth, N. R., & Soejarto, D. D. (1991). Global importance of medicinal plants. *The Conservation of Medicinal Plants*, *26*, 25-51.

Gbolade, A. A. (2009). Inventory of antidiabetic plants in selected districts of Lagos State, Nigeria. *Journal of Ethnopharmacology*, *121*(1), 135-139.

Hamzah, R. U., Egwim, E. C., Kabiru, A. Y., & Muazu, M. B. (2013). . Phytochemical And Invitro Antioxidant Properties Of The Methanolic Extract Of Fruits Of *Blighia sapida*, *Vitellaria paradoxa* And *Vitex doniana*. *Oxidant and Antioxidant in Medical Science*, *2*(3), 217-223.

Ho, S. H., Koh, L., Ma, Y., Huang, Y., & Sim, K. Y. (1996). The oil of garlic, Allium sativum L.(Amaryllidaceae), as a potential grain protectant against Tribolium castaneum (Herbst) and Sitophilus zeamais Motsch. Postharvest Biology and Technology, 9(1), 41-48.

Howélé, O., Bobelé, N., Théodor, D., & Seraphi, K. C. (2010). Nutritional composition studies of sun dried *Blighia sapida* (K. Koenig) aril from Côte d'Ivoire. *Journal of Applied Biosciences*, *32*, 1989-1994.

Huang, Y., Hee, S. K., & Ho, S. H. (1998). Antifeedant and growth inhibitory effects of α-pinene on the stored-product insects, *Tribolium castaneum* (Herbst) and *Sitophilus zeamais* Motsch. *International Pest Control*, *40*(1), 18-20.

Hyde, M. A., Wursten, B., Ballings, P., & Coates Palgrave, M. (2002). Flora of zimbabwe: species information: *Blighia unijugata*. CITIS Harare: pp. 317-318.

Isman, M. B. (2000). Plant essential oils for pest and disease management. *Crop Protection*, *19*(8-10), 603-608.

Karpouhtsis, I., Pardali, E., Feggou, E., Kokkini, S., Scouras, Z. G., & Mavragani-Tsipidou, P. (1998). Insecticidal and genotoxic activities of oregano essential oils. *Journal of Agricultural and Food Chemistry*, *46*(3), 1111-1115.

Katende, A. B., Birnie, A., & Tengnas, B. O. (1995). Useful trees and shrubs for Uganda. Identification, propagation and management for agricultural and pastoral communities. Regional soil conservation unit (RSCU), Swedish International Development Authority (SIDA), 1-710.

Kazeem, M. I., Raimi, O. G., Balogun, R. M., & Ogundajo, A. L. (2013). Comparative study on the α-amylase and α-glucosidase inhibitory potential of different extracts of *Blighia sapida* Koenig. *American Journal of Research Communication*, *1*(7), 178-192.

Koul, O., Walia, S., & Dhaliwal, G. S. (2008). Essential oils as green pesticides: potential and constraints. *Biopesticides International*, *4*(1), 63-84.

Las Heras, B., Rodriguez, B., Bosca, L., & Villar, A. M. (2003). Terpenoids: sources, structure elucidation and therapeutic potential in inflammation. *Current Topics in Medicinal Chemistry*, *3*(2), 171-185.

Lawless, J. (2013). The Encyclopedia of essential oils: the complete guide to the use of aromatic oils in aromatherapy, herbalism, health, and well being. Conari Press.

Lee, B. H., Choi, W. S., Lee, S. E., & Park, B. S. (2001). Fumigant toxicity of essential oils and their constituent compounds towards the rice weevil, *Sitophilus oryzae* (L.). *Crop Protection*, *20*(4), 317-320.

Moya, J. (2001). Ackee (*Blighia sapida*) poisoning in the Northern Province, Haiti, 2001. *Epidemiological Bulletin*, *22*(2), 8-9.

Obeng-Ofori, D., & Reichmuth, C. H. (1999). Plant oils as potentiation agents of monoterpenes for protection of stored grains against damage by stored product beetle pests. *International Journal of Pest Management*, *45*(2), 155-159.

Oderinde, R. A., Ajayi, I. A., & Adewuyi, A. (2008). Nutritional elements, antibacterial activity and cytotoxicity of the leaf, root and stem bark of Blighia unijugata Baker (Sapindaceae). *Medicinal and Aromatic Plant Science and Biotecthnology*, *2*, 137-140.

Oloyede, G. (2019b). Enzyme inhibition, free radical scavenging and insecticidal activities of crude extracts and isolates from *Laportea aestuans* (Gaud). In Abstracts of Papers of The American Chemical Society (Vol. 257). 1155 16th St, Nw, Washington, DC 20036 USA, American Chemical Society.

Oloyede, G. K., & Egbewole, I. S. (2014). Chemical constituents and antimicrobial activity of essential oil of *Combretum hispidum* leaves. *AU J Tech*, *18* (2), 69-74.

Oloyede, G. K., Ibok, M. G., & Ojo, T. K. (2021). Chemical constituents, antimicrobial and antioxidant activities of *Leptoderris brachyptera* (Benth.) Dunn and *Leptoderris micrantha* Dunn essential oils. *Trends in Phytochemical Research*, *5*(1), 13-23.

Oloyede, G., Alli, M., & Lateef, M. (2019a). Enzyme inhibition, antioxidant, and insecticidal activities of flavonoids and fixed oil from *Albizia zygia* (JF Macbr). In Abstracts of Papers of The American Chemical Society (Vol. 258). 1155 16th St, Nw, Washington, DC 20036 USA, American Chemical Society.

Onanuga, A. O., & Oloyede, G. K. (2021). Two new biologically active steroids from *Costus lucanusianus* (Costaceae). *Steroids*, *175*, 108913.

Onocha, P. A., Oloyede, G. K., Abegunde, L. M., & Oluwafemi, A. K. (2016). Antioxidant, Toxicity and Phytochemical Screening of Extracts Obtained from *Mariscus alterifolious Vahl Journal of Natural Sciences Research*, *6*(5), 1-7.

Orwa, C., Mutua, A., Kindt, R., Jamnadass, R., & Simons, A. (2009). Agroforestree Database: a tree reference and selection guide. Version 4. Agroforestree Database: a tree reference and selection guide. Retrieved at http://www.worldagroforestry.org/sites/treedbs/treedatabases.asp.

Osuala, F. N., Odoh, U. E., Onuigbo, V., & Ohadoma, S. C. (2020). Pharmacognostic Screening and Anti-inflammatory Investigation of the Methanol extract of stem bark of *Blighia unijugata* Baker (Sapindaceae). *Journal of Drug Delivery and Therapeutics*, *10*(4), 146-152.

Oyeleke, G. O., Oyetade, O. A., Afolabi, F., & Adegoke, B. M. (2013). Nutrients, antinutrients and physicochemical compositions of *Blighia sapida* pulp and pulp oil (ackee apple). *IOSR Journal of Applied Chemistry*, *4*(1), 5-8.

Sell, C. (2010). Chemsitry of Essential Oils in The Handbook of Essential Oils, Science, Technology and Appplication, CRC Press. ISBN 978-1-4200-6315.

Tapsell, L. C., Hemphill, I., Cobiac, L., Sullivan, D. R., Fenech, M., Patch, C. S., & Inge, K. E. (2006). Health benefits of herbs and spices: the past, the present, the future. *Medicinal Journal of Australia 185*, S4-S24.

Watson, L., & Dalwitz, M. J. (2007). Sapindaceae Juss. The Families of Flowering Plants: Descriptions, Illustrations, Identification, and Information Retrieval. Retrieved 21-06-2016.

Int. J. Plant Bas. Pharm. (2023) 3(1), 18-31

INTERNATIONAL JOURNAL OF PLANT BASED PHARMACEUTICALS

https://ijpbp.com

REVIEW

OPEN ACCESS

A review on the pathogenesis of cutaneous non-melanoma skin cancer (NMSC) and selected herbs as chemoprotective agents

Aniqa Aniqa[a], Sarvnarinder Kaur[a]*, Shilpa Sadwal[a]

[a] *Panjab University, Department of Biophysics, Chandigarh, India*

ARTICLE INFO

Article History:

Received: 28 July 2022
Revised: 24 August 2022
Accepted: 30 September 2022
Available online: 06 October 2022

Edited by: B. Tepe

Keywords:

Skin cancer
NMSC
Chemoprevention
Azadirachta indica
Catharanthus roseus
Ocimum sanctum
Phyllanthus emblica
Santalum album
Tinospora cordifolia
Withania somnifera

ABSTRACT

The high incidence of NMSC (non-melanoma skin cancer) and the side effects of the available treatments disrupt the quality of life in more than one way. Particularly in the later stages, pain management and palliative care is the sole mean of alleviating the agony, all this warrants the need for alternative strategies with enhanced efficacy, better tolerance, and wide safety margins. Therefore, herbs in NMSC prevention and intervention are engaging due to their accessibility, efficacy, cost-effectiveness, and tolerated nature. Various components in the crude extracts follow 'Pharmacodynamic synergy', augment the beneficial effects of the active constituents, and reduce the likelihood of drug resistance. The extracts/active constituents of *Azadirachta indica*, *Catharanthus roseus*, *Ocimum sanctum*, *Phyllanthus emblica*, *Santalum album*, *Tinospora cordifolia*, and *Withania somnifera* demonstrated the anti-cancerous effect on distinct cancerous cells and animal models. Nonetheless, there is a lack of in vivo investigations validating its chemopreventive efficacy in experimental models of skin carcinogenesis. Therefore, the current review suggests the scientific community emphasize the extensive research on these herbs to obtain an efficacious drug as well as the people around the globe incorporate these herbs in their daily dietary habits/meals to obtain maximum benefit from these herbs.

List of Abbreviations

ACC1: Acetyl-CoA carboxylase 1
Akt/PI-3K: Ak strain transforming/phosphoinositide 3-kinases
AP-1: Activator protein 1
ATM: Ataxia telangiectasia mutated
BCC: Basal cell carcinoma
BRAF: v-Raf murine sarcoma viral oncogene
CAT: Catalase
CDK4: Cyclin-dependent kinase-4
CDKN2A: Cyclin-dependent kinase inhibitor 2A
CDKN2A: Cyclin-dependent kinase inhibitor 2A
CEA: Carcinoembryonic antigen
COX-2: Cyclooxygenase 2
CYP: Cytochrome P450

Reviewed by:
Yahyea Baktiar Laskar: Assam University, Silchar, Assam, India
Mehmet Tahir Husunet: Gaziantep Islamic Science and Technology University, Gaziantep, Türkiye

* Corresponding author(s):
E-mail address:
sarvnarinder@pu.ac.in (S. Kaur)
e-ISSN: 2791-7509
doi: https://doi.org/10.29228/ijpbp.12

Please cite this article as: Aniqa, A., Kaur, S., & Sadwal, S. (2023). A review on the pathogenesis of cutaneous non-melanoma skin cancer (NMSC) and selected herbs as chemoprotective agents. *International Journal of Plant Based Pharmaceuticals*, *3*(1), 18-31, https://doi.org/10.29228/ijpbp.12.

DMBA: 7,12-dimethyl Benz(a)anthracene
DTD: D-Tyr-tRNATyr deacylase
ECM: Extracellular matrix
EDC: Electrodesiccation and curettage
EMT: Epithelial-mesenchymal transformation
ERBB4: Erb-b2 receptor tyrosine kinase 4
FBXW7: F-Box and WD repeat domain containing 7
GAGs: Glycosaminoglycans
Gli1/Gli: GLI family zinc finger 1/GLI family zinc finger 2
GPX: Glutathione peroxidase
GR: Glutathione reductase
GRIN2A: Glutamate receptor ionotropic NMDA type subunit 2A
GRM3: Glutamate metabotropic receptor 3
GRM8: Glutamate metabotropic receptor 8
GSH: Glutathione
Ha-ras/ Ki-ras: Harvey ras/Kirsten ras
IDH1: Isocitrate Dehydrogenase 1
JAK-STAT: Janus kinase/signal transducers and activators of transcription
KEAP1: Kelch-like ECH associated protein 1
KIT: KIT proto-oncogene, receptor tyrosine kinase
KNSTRN: Kinetochore localized astrin (SPAG5) binding protein
LDH: Lactate dehydrogenase
LPO: Lipid peroxidation
MAPK1/2: Mitogen activated protein kinase 1/2
MSC: Melanoma skin cancer
mTOR: Mammalian target of rapamycin
NF-κB: Nuclear factor kappa light chain enhancer of B cells
NMSC: Non-melanoma skin cancer
NRAS/N-ras: Neuroblastoma RAS viral oncogene homolog
ODC: Ornithine decarboxylase
PN: Peroxynitrite
POC: People of color
PREX2: Phosphatidylinositol 3,4,5-trisphosphate-dependent Rac exchanger 2
PTCH1: PATCHED1
RAC1: Ras related C3 botulinum toxin substrate 1
RUNX1T1: RUNX1 partner transcriptional co-repressor 1
SCC: Squamous cell carcinoma
SMO: Smoothened (frizzled class receptor)
SOD: Superoxide dismutase
SPF: Sun protection formula
STAT 1: Signal transducer and activator of transcription 1
STAT3: Signal transducer and activator of transcription 3
SUFU: Suppressor of fused protein
TYR: Tyrosine
UDP-GT: Uridine diphosphate glucuronyl transferase
UV: Ultraviolet
α-MSH: Alpha-melanocyte-stimulating hormone

1. Introduction

Skin cancers, including melanoma skin cancer (MSC) and non-melanoma skin cancer (NMSC), are frequent in Caucasians, and their incidence is steadily increasing worldwide (Bray et al., 2018; Labani et al., 2021). Figure 1 portrays the different types of skin cancers along with risk factors contributing to the onset of skin cancers. The high incidence of skin cancers imposes a burden on the healthcare system as well as the patient via associated morbidity, social impact, and healthcare cost (Fitzmaurice et al., 2017). Although people of color (POC) are less afflicted, they are more likely to die from skin cancers owing to the scarcity of awareness, late-stage diagnosis, and socioeconomic barriers hampering access to care (Gupta et al., 2016).

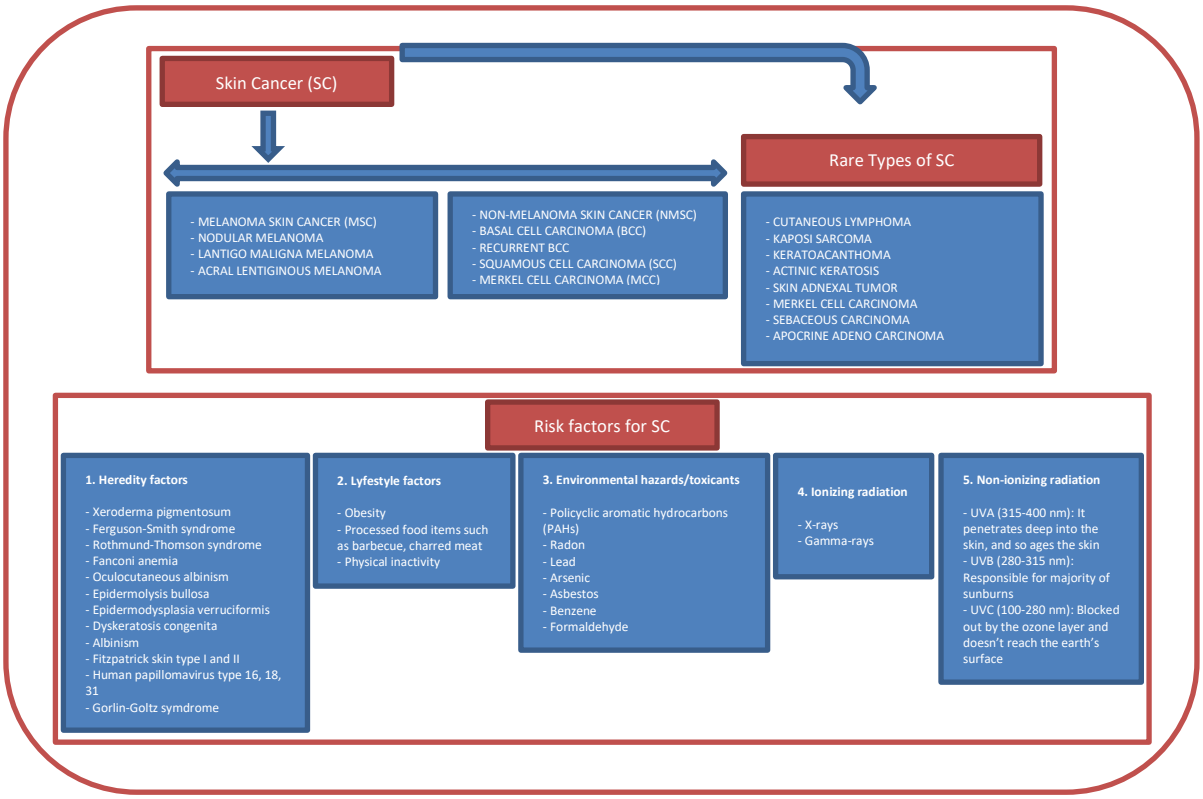

Figure 1. Different types of skin cancers (common and rare) and various risk factors responsible for the onset of skin cancer

Possible causes of NMSC pathogenesis include exposure to ultraviolet (UV) radiation, ionizing radiations, environmental toxicants/pollutants, lifestyle habits, toxic xenobiotics such as radon, lead, arsenic, polycyclic aromatic hydrocarbons (PAHs), and hereditary factors (Didona et al., 2018; Rees et al., 2014). Although site-specific treatments are effective in skin cancer, they have some limitations (aesthetic issues viz., pigmentary changes, atrophy, fibrosis, and cost burden) (Sobanko et al., 2015). Modulations in signaling pathways, high mutational burden, as well as increased risk among immunosuppressed patients led to a new landscape in skin cancer therapeutics such as epidermal growth factor receptor (EGFR) therapy, inhibitors of hedgehog signaling, BRAF, and MEK, checkpoint inhibitors, and immunotherapy such as intratumoral, oncolytic viral therapy, non-viral oncolytic therapy (Cives et al., 2020). The treatments available for metastatic tumors have many adverse effects such as weakened immunity, hair/weight loss, fatigue, sleep disturbances, fertility problems, morbidity, psychological problems in cancer survivors, and decreased quality of life. It is noteworthy that even after several therapy sessions, a high relapse rate (due to inevitable exposure to UV radiation, environmental toxicants, and chemoresistance) brings a financial burden along with significant morbidity to the patient (Sloan & Gelband, 2007). In Australia, treatment of skin cancer accounts for AUS$ 511 million in 2010 (Gordon et al., 2018). According to United States statistics, the usual annual amount of treatment for skin cancers is doubled within five years (Wu et al., 2015). Thus, there is a desperate demand for complementary treatment with minimum or nil side effects. Herbal remedies have long been used since ancient times to tackle diverse ailments, due to their easy accessibility, safe nature, effectiveness, and no toxicity (Lengai et al., 2020; Thomasset et al., 2007). Currently, we are focusing on the pathogenesis of NMSC, and alternative herbal remedies to combat the NMSC, as well as the role of selected herbs as an adjuvant along with the conventional therapies to reduce its side effects.

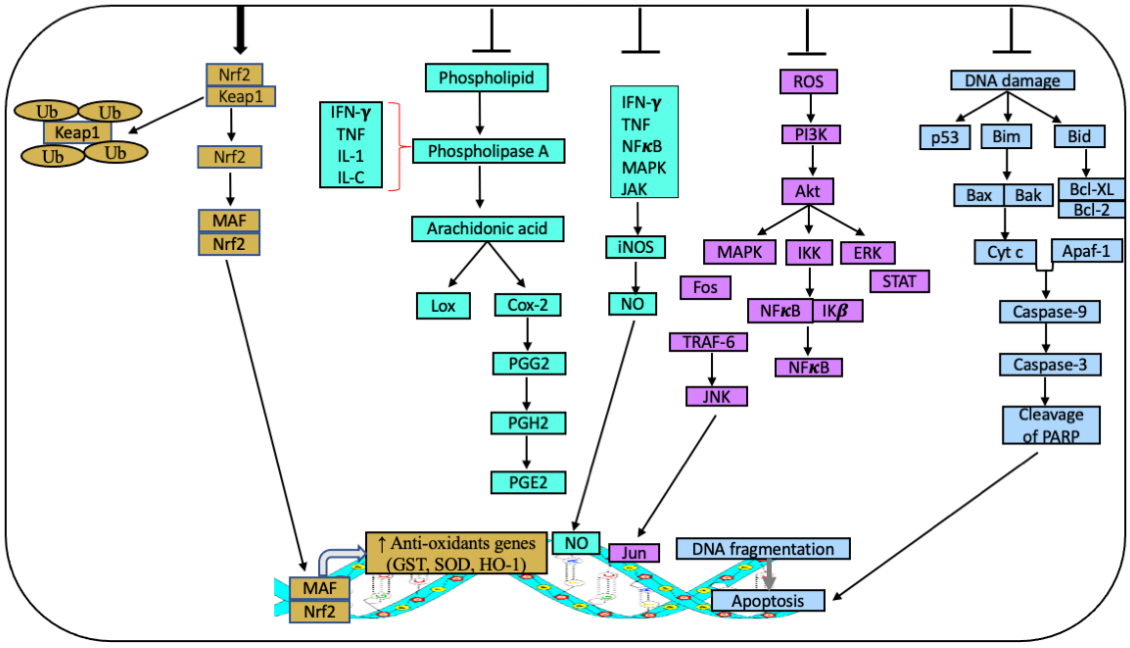

Figure 2. Mechanism of chemopreventive action of selected herbs against NMSC

Several authors have already discussed the protective role of botanicals/phytochemicals such as vitamin C and E, selenium, and carotenoids, among others against skin cancers (Chaiprasongsuk & Panich, 2022; F'guyer et al., 2003; Gan et al., 2021; Ijaz et al., 2018; Katta & Brown, 2015; Millsop et al., 2013). This review will give new insights into the selected herbs, namely *Azadirachta indica*, *Catharanthus roseus*, *Ocimum sanctum*, *Phyllanthus emblica*, *Santalum album*, *Tinospora cordifolia*, and *Withania somnifera*, and the main targets of these herbs. Figure 2 portrays how these herbs modulate/inhibit various perturbed signaling pathways and impede NMSC. The reason for choosing these herbs is that these herbs are very common in Asian countries, especially India. These herbs have already shown promising chemoprotective effects against NMSC in a few in vivo studies, but there is a lack of clinical trials on these herbs. These herbs warrant extensive research for novel drug discovery.

2. Materials and methods

For the review, reports on the cell lines and animal models were searched using scientific databases (PubMed and Google Scholar) against non-melanocytic skin cancer. In the current review, the beneficial effects of chosen herbs viz., *A. indica*, *C. roseus*, *O. sanctum*, *P. emblica*, *S. album*, *T. cordifolia*, and *W. somnifera* and their active-constituents against NMSC were described. Various databases (such as PubMed and Google Scholar) were utilized to extract the pertinent information. Various combinations of major keywords included were: *Azadirachta indica*, *Catharanthus roseus*, *Ocimum sanctum*, *Phyllanthus emblica*, *Santalum album*, *Tinospora cordifolia*, *Withania somnifera*, chemoprotective, chemotherapeutic, and chemoprotection.

3. Results and discussion

NMSC, also known as "cancer of keratinocytes," is among the most common human malignancies and is mainly classified as BCC & SCC, which account for about 99% of all NMSCs (Katalinic et al., 2003). Rare forms of NMSCs are sebaceous carcinoma, apocrine adenocarcinoma, Merkel cell carcinoma, and other rare tumors (Wollina et al., 2017). Sung et al. (2021) stated that there were

1,198,073 new cases, and 63,731 deaths occurred from NMSC in 2020.

BCC is the abnormal division of mutated basal cells and is the predominant type of NMSC (Apalla et al., 2017; Koh et al., 2003). Patients with Gorlin-Goltz syndrome, Fitzpatrick skin (I and II), are at higher risk of developing BCC (Didona et al., 2018). Although BCC develops at a slower rate, it is capable of widespread tissue destruction and causes significant morbidity. Mutation in the PATCHED1 (PTCH1, a tumor-suppressor gene) is a driving force for BCC (Lauth et al., 2004). Along with that, mutations in the genes such as c-Myc, Ras, Harvey (Ha)-ras, Kirsten (Ki)-ras, cyclin-dependent kinase inhibitor 2A (CDKN2A), NRAS, TP53, GLI family zinc finger 1 (Gli1), kinetochore localized astrin (SPAG5) binding protein (KNSTRN), GLI family zinc finger 2 (Gli2), suppressor of fused protein (SUFU), or smoothened (SMO), commence to BCC (Boeckmann et al., 2020).

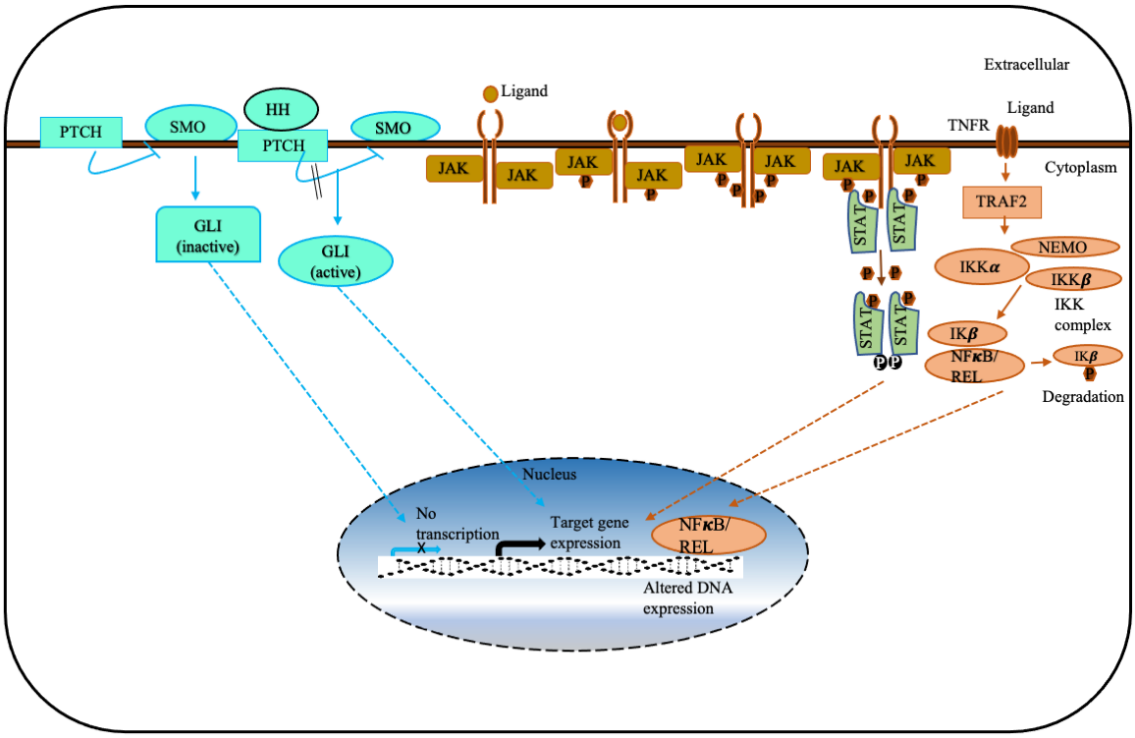

Figure 3. Various signaling pathways altered during NMSC
Mutation in the PTCH1 is a driving force for BCC.
Modulation in the JAK-STAT pathway leads to activation of NFkB signaling and commence to SCC.

SCC is the abnormal division of mutated squamous cells (Queen, 2017). Depending upon the tumor size, depth, perineural invasion, immunity of the patient, and anatomical location, SCC has enough potential for recurrence (Lee & Miller, 2009). People with human papillomavirus, Fitzpatrick skin type I and II, xeroderma pigmentosum, and albinism (Didona et al., 2018) are at higher risk of developing SCC. Almost 55% of SCC develops in the area of the head and neck, 18% on the hands and forearms, and 13% on the legs (Apalla et al., 2017; Leiter et al., 2017). Mutations in the genes such as p53, glutamate receptor 8 (GRM8), ERBB4, RUNX1 partner transcriptional co-repressor 1 (RUNX1T1), Kelch-like ECH-associated protein 1 (KEAP1), and F-box leads to SCC. In addition, mutations in the WD repeat domain containing 7 (FBXW7), and KRAS causes SCC (Kan et al., 2010). Figure 2 portrays the dysregulated signaling pathways connected to NMSC.

The side-effects of surgery (the gold standard for resecting primary skin tumors), and other treatments (Mohs micrographic surgery, curettage, and electrodesiccation) compel investigators for innovative complementary remedies with minimal adverse effects. The cost burden of the conventional modalities warrants the need for cancer prevention by primary prevention (abolishing contact with the carcinogen) or secondary prevention (repairing the already built pathologies) (Seite et al., 2017). Also, healthy individuals have the likelihood of evolving skin cancer owing to continuous exposure to UV rays exposure and environmental pollutants. Since it is impossible to avoid sun exposure, dietary habits and chemoprevention through natural products could effectively prevent skin cancer (Stoj et al., 2022).

3.1. Herbs as chemoprotective agents for NMSC

Cancer chemoprevention involves preventing, inhibiting, or reversing carcinogenesis by administering chemically synthesized or natural agents (George et al., 2021). Chemically synthesized drugs exert positive effects; however, in a long run, they instigate detrimental effects, which warrants the need to utilize the diverse medicinal potential of natural agents/herbal medicines, which are easily accessible, and considered safe, and cost-effective, for cancer management. Skin cancer involves three stages viz., initiation, promotion, and progression (Arora & Koul, 2014). Thus, the complexity of cancer can be tackled by using herbs in the form of galenical preparations (tincture, extracts, tonic) or as active components that target multiple deranged pathways. Galenical preparations follow 'pharmacodynamic synergy', in which the presence of numerous components acts in synergism and enhances the medicinal effects of active components as well as antagonizes its toxicity (Arora & Koul, 2014). It is revealed that 80% of developing nations utilize traditional medicine (Anquez-Traxler, 2011). Also, alternative medicine is gaining popularity as a complementary way of care in developed countries (Deng & Cassileth, 2013). Most

people look for substitutes that can be easily integrated into their diet to cure their illnesses (Naja et al., 2015).

Herbs, along with serving as a food and medicine for generations, also hold a unique place under modern-day "nutraceuticals" to manage high cholesterol, osteoporosis, diabetes, arthritis, diminished memory, and constipation among others along with showing anti-cancer effects (Hussain et al., 2015). Active components present within herbs such as flavonoids, terpenoids, polyphenols, carotenoids, catechins, anthocyanins, etc. have beneficial properties (Alzohairy, 2016; Guldiken et al., 2018). The next section discusses the importance of selected herbs in preventing/combating NMSC. Figure 3 shows the various phytochemicals isolated from these herbs.

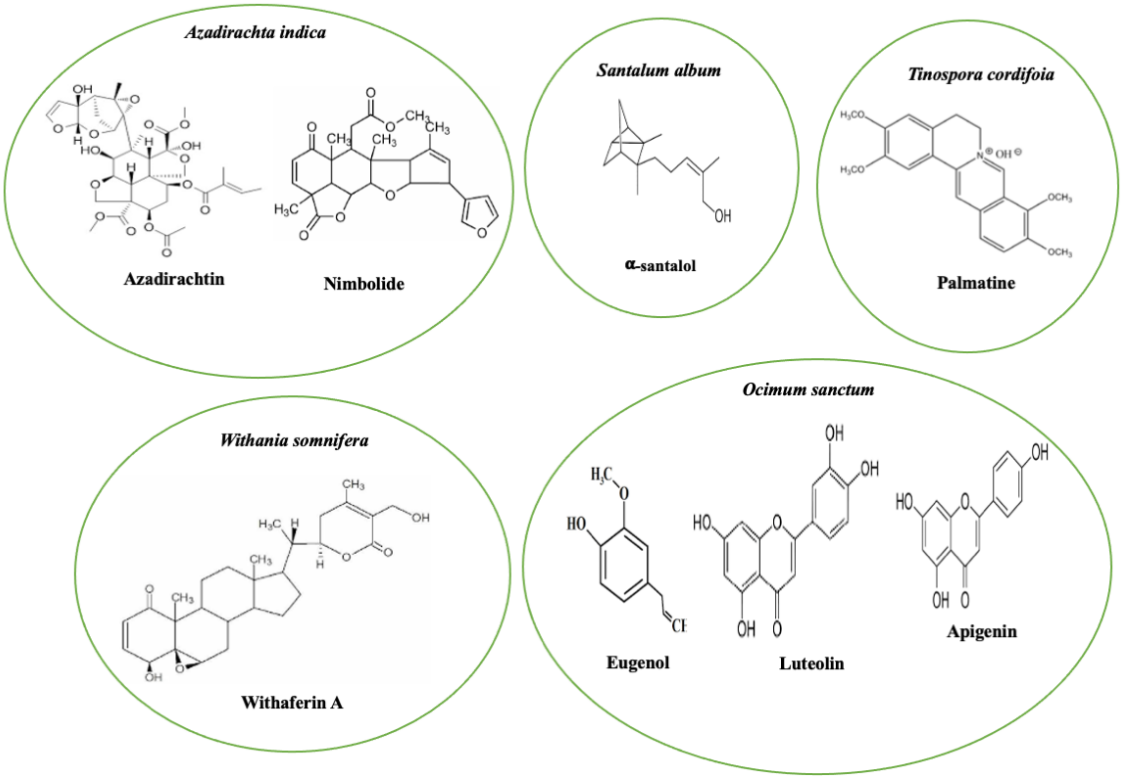

Figure 4. Active phytochemicals from selected herbs and their chemical structure

3.1.1. A. indica (Neem)

A. indica (Meliaceae) is indigenous to India, Pakistan, Burma, Nepal, and Bangladesh. *A. indica* defends the skin from harmful UV rays and other chemical contaminants, as well as skin infections and wounds (Treichel et al., 2020). The vitamins and fatty acids found in neem help minimize wrinkles and fine lines on the skin and provide an anti-aging benefit. Dasgupta et al. (2004a) reported the chemoprotective effect of *A. indica* leaves against dimethylbenz[a]anthracene (DMBA)-induced papilloma formation by increasing the antioxidant defense mechanism in albino mice. Koul et al. (2006) found that aqueous *A. indica* leaf extract (AAILE) reduced the tumor statistics, significantly improved the antioxidant enzymes in DMBA-treated mice, and thus prevented skin carcinogenesis in mice. Akihisa et al. (2009) observed that limonoids treatment to the B16 melanoma cells as well as TPA-treated mice markedly inhibited melanin production as well as decreased the inflammation in TPA-treated mice. Akihisa et al. (2011) further observed that limonoids, salanin, and 3-deacetylsalanin caused a significant reduction in melanin content in B16 melanoma cells, and markedly alleviated the inflammation in TPA-treated mice. Arora et al. (2011a) reported that AAILE treatment caused a significant improvement in skin histology and surface structure as revealed through scanning electron microscopy, and also modulated the STAT-1, AP-1, and NFkB genes expression in DMBA/TPA treated mice. Further, they also found that AAILE treatment caused a marked reduction in tumor incidence, tumor burden, and tumor volume. Also, AAILE treatment caused a significant increase in apoptosis of cancerous cells as revealed via expressions of Bcl-2, Bax, caspase-9, and caspase-3 (Arora et al., 2011b). Arora et al. (2013) also showed in a study that AAILE treatment significantly decreased the cytochrome p450 levels, and increased the DTD, UDP-GT, and LPO in skin/tumors, and liver tissues of tumor-bearing mice, which showed its chemopreventive effect. Arora et al. (2013) also found that AAILE caused a significant decrease in PCNA, and cyclin D1, which are cell-cycle proteins responsible for cell proliferation. Also, AAILE treatment caused markedly increased expressions of p53 and p21. Ali et al. (2015) observed that stigmasterol treatment had a chemopreventive effect against DMBA/croton oil-induced skin cancer in mice as revealed via the reduction in tumor size, number, decreased DNA damage, and increase in antioxidant enzymes. Chugh et al. (2018) observed that AAILE treatment caused a marked reduction in skin papilloma formation as unveiled via scrutinizing the cell proliferation, cell count, DNA/amide ratio, ODC, ATM, and LDH within skin/papilloma of mice. After that, Chugh and Koul (2021) observed that AAILE treatment decreased the GAGs levels, collagen levels, and CEA levels, and thus modulated the ECM to reduce the metastasis of skin carcinoma in the DMBA/TPA-induced murine skin cancer model. Table 1 lists a few findings validating its protective role against NMSC.

3.1.2. C. roseus (Sadabahaar)

C. roseus, also known as "periwinkle" (Apocynaceae), is indigenous to Madagascar, hence the name "Madagascar periwinkle." Now, it is available in almost all of the world's warm areas. It has found a role in both western medicine and traditional therapies and has shown extensive health benefits. Ayurvedic physicians used the flowers of *C. roseus* to treat eczema, dermatitis, and other skin issues (Nayak & Pinto Pereira, 2006). Pham et al. (2018) observed that *n*-butanol extract of *C. roseus* caused significant cytotoxicity on *Escherichia coli* and *Staphylococcus lugdunensis*. Rezadoost et al. (2019) showed that methanolic extract of *C. roseus* significantly increased the apoptosis of MCF-7, A431, and U87-MG cancerous cells. Pham et al. (2019) also observed that the root extract of *C. roseus* markedly inhibited the growth of *E. coli*, *Enterobacter aerogenes*, *S. lugdunensis*, *Candida albicans* , and *Aspergillus* spp. Table 2 lists a few findings validating its protective role against NMSC.

Table 1. Different reports on the chemoprotective efficacy of *A. indica* against NMSC

Extract/active component	Cell line/animal model	Dose	Duration	Effects	Mechanism of action	References
Ethanolic extract of *A. indica* leaves	DMBA-induced skin papilloma genesis in Swiss albino mice	250 and 500 mg per kilogram (kg) body weight (bw)	for 15 days	Chemopreventive	↑ Phase-II enzyme ↑GST, DT-diaphorase (in extrahepatic), GR (in extrahepatic), GPX, SOD, and CAT ↓ Tumor incidence/burden, number of papilloma ↑ Antioxidant enzymes	(Dasgupta et al., 2004a)
Aqueous *A. indica* leaf extract (AAILE)	DMBA-induced skin tumors in male mice	400 mg/kg bw	for 14 weeks	Chemopreventive	↓ Mean tumor burden and tumor volume, CAT, SOD ↑LPO, GSH, GPx, and GR ↓ Mean tumor burden, tumor volume, & hyperchromatia ↑LPO	(Koul et al., 2006)
Limonoids from seed extract of neem	B16 melanoma cells 12-*O*-tetradecanoylphorbol-13-acetate (TPA)-induced inflammation in mice	25 mg/ml	for 20 weeks	Anti-inflammatory & Chemopreventive	↓ Melanin production (74–91%) ↓ Inflammation ↓ Epstein-Barr Virus Early Antigen (EBV-EA)	(Akihisa et al., 2009)
Several limonoids from *n*-hexane extract of Neem seeds Salanin and & 3-deacetylsalanin	B16 melanoma cells & TPA-induced inflammation in mice	25µg/ml	for 3 hours	Cytotoxic as well as anti-inflammatory	70-74% reduction in melanin content 79-85% cell viability 2,3,5,6, and 9-15 showed marked anti-inflammatory activity	(Akihisa et al., 2011)
Aqueous *A. indica* leaf extract (AAILE)	Skin carcinogenesis in LACA mice by topical application of DMBA followed by TPA	300mg/kg bw	On alternate days	Chemopreventive	↑ Regions of degeneration in histology & SEM ↑ STAT 1 and AP-1 ↓ NF-κB	(Arora et al., 2011a)
Aqueous *A. indica* leaf extract (AAILE)	Skin carcinogenesis in mice	300mg/kg bw	for 20 weeks	Apoptotic	↓ Tumor incidence (58.3%), mean tumor burden (54.5%), and mean tumor volume (45.6%) ↑ Bax, caspase 3, caspase 9 ↓ Bcl-2	(Arora et al., 2011b)
Aqueous *A. indica* leaf extract (AAILE)	Effect of skin carcinogenesis induced by DMBA/TPA on skin and hepatic tissue's biochemical status in mice	300mg/kg bw	for 10 weeks	Anti-cancer	↓ Cytochrome p450 (CYP) & GSH level (in liver & skin) ↑ DTD, UDP-GT (in liver & skin), and UDP-GT activity (in liver) ↑ LPO (in liver & skin)	(Arora et al., 2013)
Aqueous *A. indica* leaf extract (AAILE)	Skin carcinogenesis induced by DMBA/TPA in male LACA mice	300mg/kg bw	for 20 weeks	Chemopreventive	↓ PCNA and cyclin D1 ↑ p53 and p21 ↑ LPO	(Arora et al., 2013)
Stigmasterol from *A. indica*	DMBA/Croton oil-induced skin cancer in mice	200 mg/kg and 400 mg/kg bw	for 16 weeks	Chemopreventive	↑ Latency period ↓ Tumor size, number of papillomas, LPO, aspartate aminotransferase, alanine aminotransferase, alkaline phosphatase, and bilirubin ↓ DNA damage ↑ Glutathione, SOD, and CAT	(Ali et al., 2015)
Aqueous *A. indica* leaf extract (AAILE)	DMBA/TPA-induced skin papilloma genesis in mice	300mg/kg bw	for 10 weeks	Growth inhibitory	↓ Papilloma incidence and number ↓ Cell proliferation, epidermal thickness & cell count, DNA/amide I ratio ↓ ODC, ATM ↓ LDH	(Chugh et al., 2018)
Aqueous *A. indica* leaf extract (AAILE)	DMBA/TPA-induced skin cancer in mice	300mg/kg bw	for 22 weeks	Chemopreventive	↓ Collagen and glycosaminoglycans (GAG) levels ↓ Carcinoembryonic antigen (CEA)	(Chugh & Koul, 2021)

Table 2. Different reports on the chemoprotective efficacy of *C. roseus* against NMSC

Extract/active component	Cell line/animal model	Dose	Duration	Effects	Mechanism of action	References
Extract of *C. roseus* stem & its *n*-butanol fraction	A2780 (ovarian), H460 (lung), A431 (skin), MIA PaCa-2 (pancreas), Du145 (prostate), HT29 (colon), MCF-7 (breast), BE2-C (neuroblastoma), SJ-G2, U87, and SMA (glioblastoma)	GI_{50} values of 5.2-21.0 µg/ml	for 0-72 hours	Cytotoxic	↓ Activity of *E. coli* & *S. lugdunensis*	(Pham et al., 2018)
Methanolic extract of *C. roseus*	MCF-7 breast cancer cells, A431 epidermal cell line, and U87-MG glioma cell line that were compared to HGF-1 as normal cells	50 µg/ml	for 0-72 hours	Apoptotic	↑ Apoptosis of cancer cells	(Rezadoost et al., 2019)
C. roseus root extract (RE) and its sub-fractions: saponin-enriched (SE) and aqueous (AQ) fractions	A2780 (ovarian), H460 (lung), A431 (skin), MIA PaCa-2 (pancreas), Du145 (prostate), HT29 (colon), MCF-7 (breast), BE2-C (neuroblastoma), SJ-G2, U87, and SMA (glioblastoma)	100 µg/ml	for 0-72 hours	Antioxidative & growth inhibitory	↓ Growth of *E. coli*, *E. aerogenes*, and *S. lugdunensis* and fungi (*C. albicans* and *A. niger*)	(Pham et al., 2019)

Table 3. Different reports on the chemoprotective efficacy of *O. sanctum* against NMSC

Extract/active component	Cell line/animal model	Dose	Duration	Effects	Mechanism of action	References
Apigenin	DMBA-initiated and TPA promoted skin tumorigenesis in SENCAR mice	1 to 20 µmol	for 33 weeks	Chemopreventive	↓ Tumor incidence ↓ ODC ↓ Papilloma incidence and numbers ↑ Latency period of tumor appearance ↓ Incidence of carcinoma, & numbers ↓ Ratio of carcinomas/papilloma	(Wei et al., 1990)
Eugenol	DMBA-induced and croton oil promoted	2 mg	for 6 weeks	Free-radical scavenging	↓ SOD, LPO ↓ Number of papillomas (84%) ↓ Number of tumor	(Sukumaran et al., 1994)
Ethanolic tulsi leaf extract	DMBA-induced skin papillomagenesis in swiss albino male mice	150 µl	for 15 days	Chemopreventive	↓ Tumor incidence (papillomas) ↓ Average number of tumors, cumulative number of papillomas ↑GSH, GST	(Prashar et al., 1994)
Ethanolic leaf extract of *O. sanctum*	DMBA/ croton oil-induced papillomagenesis in the skin of male Swiss albino mice	800 mg/kg bw	for 15 days	Chemopreventive	↓ Number of tumor, cumulative number of papillomas, and mean number of tumors ↑GST ↑ Glutathione level	(Prashar & Kumar, 1995)
Apigenin	UVB-induced skin carcinogenesis in mice	5 µM/200 µl DMSO 10 µM (0-100 µM)	for 11 weeks	Chemopreventive	↓ ODC (25-45% inhibition) activity ↓ Cancer incidence (52% inhibition) ↑ Tumor free survival	(Birt et al., 1997)
Hydroalcoholic extract of the fresh leaves of Tulsi	Benzo(a)pyrene-induced forestomach and DMBA-initiated skin papilloma genesis in mice	200 and 400 mg/kg bw	for 15 days	Chemopreventive	↑ Phase II enzymes, GST, DT-diaphorase, GR, SOD, GSH, and CAT in hepatic and extrahepatic organs ↑ GST and DT-diaphorase (in forestomach, kidney, and lung) ↓ Phase I enzyme, LPO and LDH ↓ Tumor burden, percentage of tumor bearing-animals	(Dasgupta et al., 2004b)
Alcoholic extract of the Tulsi leaves	Carcinogens viz., 3-mthylcholanthrene (MCA), DMBA and aflatoxin B1 (AFB1)-initiated TPA promoted by following 2-stage Skin tumorigenesis in a mouse model	100 µl	for 24 weeks	Antiproliferative Immunomodulatory & antioxidant	↓ Number of tumors ↓ Cutaneous γ-glutamyl transpeptidase (GGT) and glutathione-*S*-transferase-P (GST-P) ↑ Infiltration of polymorphonuclear, mononuclear and lymphocytic cells ↓ ODC activity ↑ Interleukin-1β (IL-1β), TNF-α (serum) ↓ Phase I enzymes ↑Phase II enzymes ↑ Glutathione levels ↓ LPO, heat shock protein	(Rastogi et al., 2007)

Extract/active component	Cell line/animal model	Dose	Duration	Effects	Mechanism of action	References
Apigenin	UVB-induced mouse and human 308 keratinocyte cell line	5-50 µM	for 22 hours	Chemopreventive	↓ COX-2	(Van Dross et al., 2007)
Luteolin	UV-induced skin cancer & JB6 P+ cell line and the SKH-1 hairless mouse model	10 or 20 µmol/l	for 0-12 hours	Chemopreventive	↓ Protein kinase C (epsilon), c-Src activities, activator protein-1, and nuclear factor-κB activity ↓ Phosphorylation of mitogen-activated protein kinases and the Akt signaling pathway ↓ Tumor incidence,multiplicity, and overall size ↓ Cyclooxygenase-2, tumor necrosis factor-α, PCNA, PKCε, and Src kinase	(Byun et al., 2010)
Eugenol	DMBA initiated and TPA promoted skin tumorigenesis	30 µL	for 28 weeks	Antiproliferative, anti-inflammatory, & antioxidative	↓ Oxidative stress, inflammation, cell proliferation ↑ Apoptosis ↓ IL-6, TNF-α, and PGE_2 ↓ NF-κB	(Kaur et al., 2010)
Luteolin	UV-induced damages in human keratinocytes in vitro, ex vivo, and in vivo	12 µg/mL	for 0-24 hours	Antioxidative & anti-inflammatory	↓ Cyclobutane pyrimidine dimers ↓ Skin erythema ↓ Cyclooxygenase-2, prostaglandin E_2 production	(Wölfle et al., 2011)

3.1.3. *O. sanctum* (Tulsi)

O. sanctum, also famous as "Queen of Herbs", is a member of the Labiatae family that originated in north-central India and now grows throughout the eastern world tropics (Africa, America, Asia, China). In ancient times, it was topically applied to the skin to heal acne and wounds (Marwat et al., 2011). Tulsi also protected the skin by avoiding blackheads and treating fungal infections (Khan et al., 2010) and wounds (Mandal et al., 2022). Wei et al. (1990) showed the chemopreventive efficacy of apigenin against DMBA/TPA-induced skin tumorigenesis in mice as evidenced by the reduction in tumor incidence, ODC, papilloma incidence, and carcinoma incidence. Sukumaran et al. (1994) observed that eugenol treatment caused a significant decrease in LPO, SOD, number of papillomae, and number of tumor-bearing mice and thus showed free radical scavenging potential. Prashar et al. (1994) found that ethanolic tulsi leaf extract markedly reduced the tumor incidence, and the average number of tumors, and significantly improved the activity of the antioxidant enzymes in DMBA-treated mice. Prashar and Kumar (1995) reported that ethanolic extract of tulsi caused a marked reduction in the number of tumors, papillomas, and significantly improved the GST, and GSH levels within DMBA-induced mice. Birt et al. (1997) observed that apigenin reduced the UVB-induced skin carcinogenesis in mice by reducing the cancer incidence as well as the expression of ODC in mice. Dasgupta et al. (2004b) reported that tulsi leaf extract significantly improved the antioxidant defense mechanism of benzopyrene-induced tumor-bearing mice. Van Dross et al. (2007) found that apigenin showed chemopreventive efficacy against UVB-induced carcinoma in mice and keratinocyte cells. Rastogi et al. (2007) observed that alcoholic extract of Tulsi enhanced the endogenous antioxidant enzymes, and decreased the number of tumors, inflammation, and ODC in tumor-bearing mice. Byun et al. (2010) found that luteolin decreased tumor incidence, tumor size, cyclooxygenase-2 activity, protein kinase C activity, and modulated the MAPK and Akt signaling in JB6 P+ cells and SKH-1 mouse model, and thus showed a chemoprotective effect. Kaur et al. (2010) stated that eugenol markedly attenuated oxidative stress, inflammation, cell proliferation, and substantially increased the apoptosis of tumor cells in DMBA/TPA treated mice. Wölfle et al. (2011) reported that luteolin decreased the formation of cyclobutene pyrimidine dimers, skin erythema, cyclooxygenase-2, and prostaglandin E2 production against UV-induced damages in keratinocytes. Table 3 lists a few findings validating the protective role of *O. sanctum* against NMSC.

3.1.4. *P. emblica* (Amla)

P. emblica, or "Indian gooseberry" (Euphorbiaceae), is indigenous to Asia, China, India, Nepal, and Sri Lanka (Ahmad et al., 2021). It has been reported that *P. emblica* reduces the UV-induced erythema and strikingly reduces the free radicals (Fujii et al., 2008). Its seeds are also used to heal scabies and itches (Mehmood et al., 2011). Amla also aids in treating freckles and age spots (Singh et al., 2012). Sancheti et al. (2005) observed that amla fruit extract decreased the tumor incidence, tumor burden, and tumor yield in DMBA/croton oil-induced skin carcinogenesis in a murine model and thus showed a chemoprotective effect. Majeed et al. (2011) showed that the amla fruit extract significantly decreased the collagen damage as well as ROS level in normal fibroblast cells exposed to UVB. Fujii et al. (2013) observed that amla extract and collagen peptide significantly reduced epidermal hyperplasia, and skin wrinkle formation in UVB-induced hairless mice. Table 4 lists a few findings validating the protective role of *P. emblica* against NMSC.

3.1.5. *S. album* (Chandan)

S. album, or "Royal Tree" (Santalaceae), is indigenous to Asia, Australia, Hawaii, and Pacific Islands (Santha & Dwivedi, 2015). Sandalwood is the most commonly utilized incense among Chinese and Japanese people (Goswami & Tah, 2018; Khan et al., 2021). The Egyptians used its wood for embalming the deceased to venerate the god (Kumar et al., 2012). Sandalwoods are under the Padma (lotus) group in Buddhism and ascribed to the bodhisattva Amitabha. It is perhaps one of the most often used scents in incense offerings to the Buddha (Goswami & Tah, 2018). In 1997, it is categorized under 'vulnerable' species by the International Union for Conservation of Nature (IUCN) (Kumar et al., 2012). *S. album* also can cure skin diseases such as pimples, scars, and eczema. Its essential oil is mainly used in Ayurvedic medicine to alleviate anxiety. This essential oil is also used for skin toning and treating skin problems. It also has anti-aging and anti-tanning properties. Alpha-santalol is the main active constituent of sandalwood oil, which showed promising anti-inflammatory, chemopreventive, and fungicidal effects (Bommareddy et al., 2019). Dwivedi and Abu-Ghazaleh (1997) showed that sandalwood oil significantly decreased the papilloma incidence, and papilloma multiplicity, and reduced the ODC expressions against DMBA/TPA-induced skin papilloma genesis in mice. Further, Dwivedi and Zhang (1999) observed that sandalwood oil reduced the papilloma incidence as well as

multiplicity in CD-1 mice. Dwivedi et al. (2003) observed that α-santalol treatment caused a marked decrement in papilloma incidence, and ODC activity in DMBA/TPA-induced mice. Dwivedi et al. (2006) found that α-santalol treatment markedly decreased the tumor incidence, ODC activity, DNA synthesis, and incorporation of 3H thymidine in DNA in DMBA/TPA treated mice. Kaur et al. (2005) showed that sandalwood oil significantly decreased the cell number, and increased the apoptosis, and autophagy of A431 carcinoma cells. Dwivedi et al. (2006) stated that α-santalol treatment markedly reduced the tumor incidence, multiplicity and ODC activity in UVB/TPA treated mice. Bommareddy et al. (2007) found that α-santalol markedly decreased the tumor multiplicity and LPO in UVB-treated female mice. Arasada et al. (2008) observed that α-santalol significantly decreased tumor incidence, multiplicity, and increased the apoptosis of mutated cells in UVB-treated mice. Zhang et al. (2010) showed that α-santalol markedly decreased the cell viability, downregulated the expression of mutated cell cycle genes, and increased the p21 expression in A431 carcinoma as well as UACC-62 melanoma cells. Chilampalli et al. (2013) observed that α-santalol markedly reduced the tumor multiplicity, cell viability, cell proliferation, and induced apoptosis in A431 carcinoma cells as well as UVB-treated mice. Dickinson et al. (2014) stated that sandalwood oil markedly decreased the PARP cleavage, and AP-1 activity, and increased the apoptosis as well as autophagy in HaCaT keratinocytes. Table 5 lists the findings that showed Sandalwood's chemopreventive efficacy against skin cancer.

Table 4. Different reports on the chemoprotective efficacy of *P. emblica* against NMSC

Extract/active component	Cell line/animal model	Dose	Duration	Effects	Mechanism of action	References
Amla fruit extract	DMBA/croton oil-induced skin carcinogenesis in mice	-	for 16 weeks	Chemopreventive	↓ Tumor incidence, tumor yield, tumor burden, cumulative number of papilloma	(Sancheti et al., 2005)
Amla fruit extrac	Human skin fibroblast cells	0-40µg/ml	for 0-48 hours	Chemopreventive	↑Cell-proliferation, TIMP-1, and production of procollagen ↓ Matrix metalloproteinase-1 (MMP-1) production	(Fujii et al., 2008)
Amla fruit extract	Normal human dermal fibroblasts exposed with UVB irradiation	0.5 mg/ml	for 0-24 hours	Photoprotective	↓ Collagen damage ↓ ROS	(Majeed et al., 2011)
Amla extract and collagen peptide	Photoaging induced by UVB irradiation in Male Hos:HR-1 hairless mice	5%	for 7 weeks	Photoprotective	↓ 8- OHdG-positive cells and epidermal hyperplasia ↓ Skin wrinkle formation in the mice	(Fujii et al., 2013)

Table 5. Different reports on the chemoprotective efficacy of *S. album* against NMSC

Extract/active component	Cell line/animal model	Dose	Duration	Effects	Mechanism of action	References
Sandalwood oil (5% in acetone, w/v)	DMBA-initiated and TPA-promoted skin papillomas in mice	100 µl	for 20 weeks	Chemopreventive	↓ Papilloma incidence by 67% & multiplicity by 96% ↓ ODC activity by 70%	(Dwivedi & Abu-Ghazaleh, 1997)
Sandalwood oil	CD-1 mice	5% pre-treated	-	Chemopreventive	↓ Papilloma incidence and multiplicity	(Dwivedi & Zhang, 1999)
α-Santalol	DMBA-initiated and TPA-promoted skin tumors in CD-1 and SENCAR mice	5%	for 20 weeks	Chemopreventive	↓ Papilloma development ↓ ODC activity ↓ Incorporation of ^{3}H-thymidine in DNA	(Dwivedi et al., 2003)
α-Santalol	DMBA-initiated and TPA-promoted skin cancer in mice	1.25% and 2.5%	for 20 weeks	Chemopreventive	↓ Tumor incidence and multiplicity ↓ ODC activity and DNA synthesis ↓ Incorporation of ^{3}H-thymidine in DNA	(Dwivedi et al., 2006)
East Indian sandalwood oil & α-santalol (about 25–75 µM)	Human epidermoid carcinoma A431 cells	25-75 mM	for 0-48 hours	Apoptotic & anti-proliferative	↓ Cell number ↑ Caspase-3, poly(ADP-ribose) polymerase cleavage, caspase-8 and caspase-9 ↓ Mitochondrial membrane potential ↑ Cytochrome C ↑ Autophagy through stimulation of microtubule-associated protein 1 light chain 3 (LC3)	(Kaur et al., 2005)
α-Santalol	UVB-induced skin tumorigenesis of SKH-1 hairless mice under three different protocols (DMBA-initiated and UVB-promoted; UVB-initiated and TPA-promoted and UVB-initiated and UVB promoted)	5%	for 30 weeks	Chemopreventive	↓ Tumor incidence and multiplicity ↓ ODC activity	(Dwivedi et al., 2006)
α-Santalol	UVB-induced skin tumour development in female SKH-1 mice	1.25%, 2.5%, and 5%	for 30 weeks	Antioxidant and anti-cancer activity	↓ Tumor multiplicity ↓ LPO (in skin and liver microsomes)	(Bommareddy et al., 2007)

Extract/active component	Cell line/animal model	Dose	Duration	Effects	Mechanism of action	References
α-Santalol	UVB-induced skin tumor development in SKH-1 mice	5%	for 30 weeks	Apoptosis	↓ Tumor incidence and multiplicity ↑ Caspase-3, caspase-8 levels, and p53 ↓ Development of tumors	(Arasada et al., 2008)
α-Santalol	Mutated human epidermoid carcinoma A431 cells and p53 wild-type human melanoma UACC-62 cells	50-100 µM 50–75 µM	for 0-72 hours	Anti-proliferative	↓ Cell viability ↑ G2/M phase cell cycle arrest ↑ Cyclin A, cyclin B1, Cdc2, Cdc25c, p-Cdc25c, and Cdk-2 ↑ p21, wild-type p53 ↓ Mutated p53 in UACC-62 cells ↑ Depolymerization of microtubules	(Zhang et al., 2010)
α-Santalol, honokiol and magnolol isolated from *Magnolia officinalis* bark extract	Chemically and UVB-induced skin cancer development in mice & humans epidermoid carcinoma A431 cells	Combination treatment of α-santalol (5 mg in 100 µl acetone) and honokiol (30 µg in 100 µl acetone)	for 30 weeks	Apoptotic	↓ Tumor multiplicity, cell viability, cell-proliferation (90% reduction) ↑ Apoptosis	(Chilampalli et al., 2013)
East Indian sandalwood oil (EISO)	HaCaT keratinocytes (UV-signature mutations, dysfunctional p53 and a defective NFkB signaling pathway)	0.0005% & 0.001%	for 0-24 hours	Anti-cancer	↓PARP cleavage ↑Apoptosis ↓ AP-1 activity ↓ Plasma membrane integrity ↑ Cleavage of LC3 ↑ Autophagy ↓ Multiplication of cells	(Dickinson et al., 2014)

3.1.6. T. cordifolia (Guduchi)

T. cordifolia, also known as "Giloy" (Menispermaceae), is abundant in South Asia, Indonesia, the Philippians, Bangladesh, Thailand, Myanmar, China, and Srilanka (Upadhyay et al., 2010). It is the best remedy for skin problems such as black spots, pimples, fine lines, wrinkles, and acne and slows down the aging process (Yates et al., 2022). Goyal et al. (2007) showed that root extract of *T. cordifolia* significantly decreased the tumor incidence, tumor yield, and tumor burden in DMBA/TPA treated mice. Chaudhary et al. (2008) showed that *T. cordifolia* extract significantly decreased the papilloma number, tumor burden, and LPO, and markedly increased the phase-II detoxifying enzymes in DMBA/croton oil treated mice. Ali and Dixit (2013) reported that palmatine significantly decreased the tumor size, and number, and significantly increased the antioxidant enzyme activities, restoring the DNA damage in DMBA/croton oil treated mice. Table 6 summarizes a few studies that demonstrated the protective potential of *T. cordifolia* against NMSC.

Table 6. Different reports on the chemoprotective efficacy of *T. cordifolia* against NMSC

Extract/active component	Cell line/animal model	Dose	Duration	Effects	Mechanism of action	References
Root extract of *T. cordifolia* plant extract (TCE)	Two-stage skin carcinogenesis process in Swiss albino mice	-	for 16 weeks	Anti-tumor	↓ Tumor incidence, tumor yield, tumor burden, and cumulative number of papillomas	(Goyal et al., 2007)
T. cordifolia extract	Two-stage skin carcinogenesis model in mouse using DMBA/croton oil	100 mg/kg bw	for 16 weeks	Anti-oncogenic	↓ Cumulative number of papillomas, tumor yield, tumor burden, and tumor weight ↑ Phase II detoxifying enzymes ↓ LPO	(Chaudhary et al., 2008)
Alkaloid palmatine extracted from *T. cordifolia*	DMBA/croton oil induced skin carcinogenesis in Swiss albino mice	200 mg/kg bw	for 16 weeks	Anticancer	↓ Tumor size, number ↑ GSH, SOD, CAT, restored the increased DNA damage	(Ali & Dixit, 2013)

3.1.7. W. somnifera (Ashwagandha)

Ashwagandha, or "Indian ginseng" (Solanaceae), is grown in Afghanistan, India, Egypt, Morocco, Nepal, Sri Lanka, China, Jordan, Congo, Baluchistan, South Africa, and Yemen (Mandlik & Namdeo, 2021). Ashwagandha benefits the skin by replenishing natural oils and creating skin-enriching compounds such as hyaluronan, elastin, and collagen, giving skin hydration and suppleness, and strength. Davis and Kuttan (2001) showed that 1-oxo-5b, 6b-epoxy-with a-2-enolide isolated from the chloroform root extracts of *W. somnifera* markedly enhanced the antioxidant enzyme activities, and decreased the LPO in DMBA-treated mice. Prakash et al. (2002) reported that hydroalcoholic root extract of *W. somnifera* markedly decreased the incidence as well as the number of skin tumors, and enhanced the antioxidant enzyme activities in DMBA-treated mice. Mathur et al. (2004) found that 1-oxo-5b, 6b-epoxy-with a-2-enolide isolated from the chloroform root extracts of *W. somnifera* markedly increased the p53 foci in UVB exposed rats, and thus showed anti-cancerous activity. Padmavathi et al. (2005) showed that *W. somnifera* root extract significantly decreased the phase I xenobiotic metabolizing enzymes, and increased the phase II antioxidative enzymes, decreased the tumor incidence, and multiplicity in benzopyrene and DMBA treated mice. Li and Zhao (2013) showed that withaferin A markedly decreased cell proliferation, LDH, and IDH-1, and increased the mitochondrial membrane potential, complex-I activity, and mitochondrial respiration in JBP6+ cells as well as TPA-treated mice. Maliyakkal et al. (2015) found that ethanolic extracts of *W. somnifera* (WS-ET) and *T. cordifolia* markedly decreased the side population, ABC-B1, and ABC-G2 transporters in CSCs. Li et al. (2016) showed that withaferin A attenuated the cell proliferation, ACC-1, and AP-1 and thus showed a chemopreventive effect against chemically induced skin

carcinogenesis in the murine model. Xu et al. (2019) observed that withaferin A decreased tumor promotion via stabilizing the IDH-1, and inactivating HIF-1A in TPA-treated mice. Table 7 lists a few findings that indicate the protective role of Ashwagandha against NMSC.

Table 7. Different reports on the chemoprotective efficacy of *W. somnifera* against NMSC

Extract/active component	Cell line/animal model	Dose	Duration	Effects	Mechanism of action	References
W. somnifera	DMBA-treated group	20 mg/kg bw i.p.	-	Anti-cancer	↓ LPO ↑ GSH, GST, GPx, and CAT	(Davis & Kuttan, 2001)
W. somnifera hydroalcoholic root extract (WSRE)	DMBA-induced skin cancer in mice	400 mg/kg orally	-	Chemopreventive	↓ Incidence and an average number of skin lesions ↑ GSH, LPO, SOD, CAT, GPX, and GST ↓ MRN complex protein NBS-1	(Prakash et al., 2002)
1-*oxo*-5b, 6b-epoxy-with a-2-enolide isolated from the chloroform root extracts of *W. somnifera*	Skin tumors in rats by UVB radiation followed by topical treatment with benzoyl peroxide	20 mg/kg bw	for 12 weeks	Anti-cancer	↑ p53+foci (clusters of cells containing the mutated p53 protein)	(Mathur et al., 2004)
W. somnifera root extract	Benzo(a)pyrene-induced forestomach papilloma genesis and DMBA-induced skin papilloma genesis in the Swiss albino mice	2.5% and 5% (w/w)	for 14 days	Chemopreventive	↓ Phase I xenobiotic metabolizing enzymes ↑ Phase II and Antioxidant enzymes (liver) ↓ Tumor incidence and multiplicity (in stomach and skin) ↓ MDSC ↓ Metastasis of tumor	(Padmavathi et al., 2005)
Withaferin A (WA)	Skin epidermal JB6 P+ cells, a well-established TPA model for tumor promotion in mouse	20 µg	-	Chemopreventive	↓ Cell proliferation ↓ LDH & isocitrate dehydrogenase 1 (IDH1) ↑ Mitochondrial membrane potential, complex I activity and mitochondrial respiration ↑ α-Ketoglutarate	(Li & Zhao, 2013)
Ethanolic extracts of *W. somnifera* (WS-ET) and *T. cordifolia* (TC-ET)	Cancer stem cells (CSCs)	WS-ET (20 µg/ml) and TC-ET (50 µg/ml)	for 0-96 hours	Tumor sensitizing & cytotoxic	↓ Side-population (SP), ABC-B1, and ABC-G2 transporters	(Maliyakkal et al., 2015)
Withaferin A	Chemically-induced skin carcinogenesis mouse model	20 µg	for 14 weeks	Chemopreventive	↓ Cell proliferation, acetyl-CoA carboxylase 1 (ACC1), activator protein (AP) 1	(Li et al., 2016)
Withaferin A	TPA-induced skin cancer	-	-	Chemopreventive	↓ Tumor promotion via stabilizing IDH1, & inactivating HIF-1α signaling	(Xu et al., 2019)

3.2. Challenges faced by herbs

The major challenge is the lack of pharmacokinetics studies (absorption, distribution, metabolism, excretion, and toxicity profile) on these herbs, and only a few pre-clinical studies on the defending efficacy of these plants against NMSC are present, that's why these herbs have not been used in clinical trials till date. This review draws the attention of scientists worldwide to explore these herbs for the discovery of new medicines. Also, this review emphasizes the importance of these herbs and suggests that people worldwide get the maximum benefit from these herbs by incorporating them into daily food. Combining traditional and pharmacological expertise could lead to new, less expensive, and potentially successful anticancer drugs.

4. Conclusions

In conclusion, the above-discussed herbs showed promising anti-cancerous efficacy against cell lines and animal models. However, there is a need for extensive research on different parts of these herbs viz., leaf, stem, root, seed, etc. to bring these herbs into clinical trials and further isolation of active phytochemicals for the discovery of safer drugs.

Acknowledgments

None.

Conflict of interest

The authors declare that they have no potential conflict of interest.

Statement of ethics

In this study, no method requiring the permission of the "Ethics Committee" was used.

Availability of data and materials

All data generated or analyzed during this study are included in this published article.

Funding

None.

CRediT authorship contribution statement

Aniqa Aniqa: Conceptualization, Data curation, Investigation, Writing-reviewing & editing the manuscript, Reviewing the manuscript
Sarvanrinder Kaur: Conceptualization,Reviewing the manuscript
Shilpa Sadwal: Reviewing the manuscript

ORCID Numbers of the Authors

A. Aniqa: 0000-0002-5425-3287
S. Kaur: 0000-0001-9279-1855
S. Sadwal: 0000-0003-0587-5191

Supplementary File

None.

Publisher's Note

All claims expressed in this article are solely those of the authors and do not necessarily represent those of their affiliated organizations, or those of the publisher, the editors and the reviewers. Any product that may be evaluated in this article, or claim that may be made by its manufacturer, is not guaranteed or endorsed by the publisher.

This is an open-access article distributed under the terms of the Creative Commons Attribution 4.0 International License (CC BY). The use, distribution or reproduction in other forums is permitted, provided the original author(s) and the copyright owner(s) are credited and that the original publication in this journal is cited, in accordance with accepted academic practice. No use, distribution or reproduction is permitted which does not comply with these terms.

References

Ahmad, B., Hafeez, N., Rauf, A., Bashir, S., Linfang, H., Rehman, M. U., Mubarak, M. S., Uddin, M. S., Bawazeer, S., *et al.* (2021). *Phyllanthus emblica*: A comprehensive review of its therapeutic benefits. *South African Journal of Botany, 138*, 278-310.

Akihisa, T., Noto, T., Takahashi, A., Fujita, Y., Banno, N., Tokuda, H., Koike, K., Suzuki, T., Yasukawa, K., *et al.* (2009). Melanogenesis inhibitory, anti-inflammatory, and chemopreventive effects of limonoids from the seeds of *Azadirachta indicia* A. Juss.(neem). *Journal of Oleo Science, 58*(11), 581-594.

Akihisa, T., Takahashi, A., Kikuchi, T., Takagi, M., Watanabe, K., Fukatsu, M., Fujita, Y., Banno, N., Tokuda, H., *et al.* (2011). The melanogenesis-inhibitory, anti-inflammatory, and chemopreventive effects of limonoids in *n*-hexane extract of *Azadirachta indica* A. Juss.(neem) seeds. *Journal of Oleo Science, 60*(2), 53-59.

Ali, H., & Dixit, S. (2013). Extraction optimization of *Tinospora cordifolia* and assessment of the anticancer activity of its alkaloid palmatine. *The Scientific World Journal, 2013*, 376216.

Ali, H., Dixit, S., Ali, D., Alqahtani, S. M., Alkahtani, S., & Alarifi, S. (2015). Isolation and evaluation of anticancer efficacy of stigmasterol in a mouse model of DMBA-induced skin carcinoma. *Drug Design, Development and Therapy, 9*, 2793.

Alzohairy, M. A. (2016). Therapeutics role of *Azadirachta indica* (Neem) and their active constituents in diseases prevention and treatment. *Evidence-Based Complementary and Alternative Medicine, 2016*, 7382506.

Anquez-Traxler, C. (2011). The legal and regulatory framework of herbal medicinal products in the European Union: a focus on the traditional herbal medicines category. *Drug Information Journal, 45*(1), 15-23.

Apalla, Z., Nashan, D., Weller, R. B., & Castellsagué, X. (2017). Skin cancer: epidemiology, disease burden, pathophysiology, diagnosis, and therapeutic approaches. *Dermatology and Therapy, 7*(1), 5-19.

Arasada, B. L., Bommareddy, A., Zhang, X., Bremmon, K., & Dwivedi, C. (2008). Effects of α-santalol on proapoptotic caspases and p53 expression in UVB irradiated mouse skin. *Anticancer Research, 28*(1A), 129-132.

Arora, N., Bansal, M., & Koul, A. (2011a). *Azadirachta indica* exerts chemopreventive action against murine skin cancer: studies on histopathological, ultrastructural changes and modulation of NF-κB, AP-1, and STAT1. *Oncology Research Featuring Preclinical and Clinical Cancer Therapeutics, 19*(5), 179-191.

Arora, N., Bansal, M., & Koul, A. (2013). *Azadirachta indica* acts as a pro-oxidant and modulates cell cycle associated proteins during DMBA/TPA induced skin carcinogenesis in mice. *Cell Biochemistry and Function, 31*(5), 385-394.

Arora, N., & Koul, A. (2014). A 'complex solution'to a 'complex'problem. *European Journal of Cancer Prevention, 23*(6), 568-578.

Arora, N., Koul, A., & Bansal, M. (2011b). Chemopreventive activity of *Azadirachta indica* on two-stage skin carcinogenesis in murine model. *Phytotherapy Research, 25*(3), 408-416.

Birt, D. F., Mitchell, D., Gold, B., Pour, P., & Pinch, H. C. (1997). Inhibition of ultraviolet light induced skin carcinogenesis in SKH-1 mice by apigenin, a plant flavonoid. *Anticancer Research, 17*(1A), 85-91.

Boeckmann, L., Martens, M. C., & Emmert, S. (2020). Molecular biology of basal and squamous cell carcinomas. *Sunlight, Vitamin D and Skin Cancer, 1268*, 171-191.

Bommareddy, A., Brozena, S., Steigerwalt, J., Landis, T., Hughes, S., Mabry, E., Knopp, A., VanWert, A. L., & Dwivedi, C. (2019). Medicinal properties of alpha-santalol, a naturally occurring constituent of sandalwood oil. *Natural Product Research, 33*(4), 527-543.

Bommareddy, A., Hora, J., Cornish, B., & Dwivedi, C. (2007). Chemoprevention by α-santalol on UVB radiation-induced skin tumor development in mice. *Anticancer Research, 27*(4B), 2185-2188.

Bray, F., Ferlay, J., Soerjomataram, I., Siegel, R. L., Torre, L. A., & Jemal, A. (2018). Global cancer statistics 2018: GLOBOCAN estimates of incidence and mortality worldwide for 36 cancers in 185 countries. *CA: A Cancer Journal for Clinicians, 68*(6), 394-424.

Byun, S., Lee, K. W., Jung, S. K., Lee, E. J., Hwang, M. K., Lim, S. H., Bode, A. M., Lee, H. J., & Dong, Z. (2010). Luteolin inhibits protein kinase Cε and c-Src activities and UVB-induced skin cancer. *Cancer Research, 70*(6), 2415-2423.

Chaiprasongsuk, A., & Panich, U. (2022). Role of Phytochemicals in Skin Photoprotection via Regulation of Nrf2. *Frontiers in Pharmacology, 13*, 823881.

Chaudhary, R., Jahan, S., & Goyal, P. K. (2008). Chemopreventive potential of an Indian medicinal plant (*Tinospora cordifolia*) on skin carcinogenesis in mice. *Journal of Environmental Pathology, Toxicology and Oncology, 27*(3), 233-243.

Chilampalli, C., Zhang, X., Kaushik, R. S., Young, A., Zeman, D., Hildreth, M. B., Fahmy, H., & Dwivedi, C. (2013). Chemopreventive effects of combination of honokiol and magnolol with α-santalol on skin cancer developments. *Drug Discoveries & Therapeutics, 7*(3), 109-115.

Chugh, N., & Koul, A. (2021). Altered presence of extra cellular matrix components in murine skin cancer: Modulation by *Azadirachta indica* leaf extract. *Journal of Traditional and Complementary Medicine, 11*(3), 197-208.

Chugh, N. A., Bansal, M. P., & Koul, A. (2018). The effect of *Azadirachta indica* leaf extract on early stages of chemically induced skin cancer in mice. *Journal of Herbs, Spices & Medicinal Plants, 24*(3), 257-271.

Cives, M., Mannavola, F., Lospalluti, L., Sergi, M. C., Cazzato, G., Filoni, E., Cavallo, F., Giudice, G., Stucci, L. S., *et al.* (2020). Non-melanoma skin cancers: Biological and clinical features. *International Journal of Molecular Sciences, 21*(15), 5394.

Dasgupta, T., Banerjee, S., Yadava, P., & Rao, A. (2004a). Chemopreventive potential of *Azadirachta indica* (Neem) leaf extract in murine carcinogenesis model systems. *Journal of Ethnopharmacology, 92*(1), 23-36.

Dasgupta, T., Rao, A., & Yadava, P. (2004b). Chemomodulatory efficacy of basil leaf (*Ocimum basilicum*) on drug metabolizing and antioxidant enzymes, and on carcinogen-induced skin and forestomach papillomagenesis. *Phytomedicine, 11*(2-3), 139-151.

Davis, L., & Kuttan, G. (2001). Effect of *Withania somnifera* on DMBA induced carcinogenesis. *Journal of Ethnopharmacology, 75*(2-3), 165-168.

Deng, G., & Cassileth, B. (2013). Complementary or alternative medicine in cancer care—myths and realities. *Nature Reviews Clinical Oncology, 10*(11), 656-664.

Dickinson, S. E., Olson, E. R., Levenson, C., Janda, J., Rusche, J. J., Alberts, D. S., & Bowden, G. T. (2014). A novel chemopreventive mechanism for a traditional medicine: East Indian sandalwood oil induces autophagy and cell death in proliferating keratinocytes. *Archives of Biochemistry and Biophysics, 558*, 143-152.

Didona, D., Paolino, G., Bottoni, U., & Cantisani, C. (2018). Non melanoma skin cancer pathogenesis overview. *Biomedicines, 6*(1), 6.

Dwivedi, C., & Abu-Ghazaleh, A. (1997). Chemopreventive effects of sandalwood oil on skin papillomas in mice. *European Journal of Cancer Prevention, 6*(4), 399-401.

Dwivedi, C., Guan, X., Harmsen, W. L., Voss, A. L., Goetz-Parten, D. E., Koopman, E. M., Johnson, K. M., Valluri, H. B., & Matthees, D. P. (2003). Chemopreventive effects of α-santalol on skin tumor development in CD-1 and SENCAR mice. *Cancer Epidemiology Biomarkers & Prevention, 12*(2), 151-156.

Dwivedi, C., Valluri, H. B., Guan, X., & Agarwal, R. (2006). Chemopreventive effects of α-santalol on ultraviolet B radiation-induced skin tumor development in SKH-1 hairless mice. *Carcinogenesis, 27*(9), 1917-1922.

Dwivedi, C., & Zhang, Y. (1999). Sandalwood oil prevents skin tumour development in CD1 mice. *European Journal of Cancer Prevention, 8*(5), 449-455.

F'guyer, S., Afaq, F., & Mukhtar, H. (2003). Photochemoprevention of skin cancer by botanical agents. *Photodermatology, Photoimmunology & Photomedicine, 19*(2), 56-72.

Fitzmaurice, C., Allen, C., Barber, R. M., Barregard, L., Bhutta, Z. A., Brenner, H., Dicker, D. J., Chimed-Orchir, O., Dandona, R., *et al.* (2017). Global, regional, and national cancer incidence, mortality, years of life lost, years lived with disability, and disability-adjusted life-years for 32 cancer groups, 1990 to 2015: a systematic analysis for the global burden of disease study. *JAMA Oncology, 3*(4), 524-548.

Fujii, T., Okuda, T., Yasui, N., Wakaizumi, M., Ikami, T., & Ikeda, K. (2013). Effects of amla extract and collagen peptide on UVB-induced photoaging in hairless mice. *Journal of Functional Foods, 5*(1), 451-459.

Fujii, T., Wakaizumi, M., Ikami, T., & Saito, M. (2008). Amla (*Emblica officinalis* Gaertn.) extract promotes procollagen production and inhibits matrix metalloproteinase-1 in human skin fibroblasts. *Journal of Ethnopharmacology, 119*(1), 53-57.

Gan, C., Zi, C., Sheng, J., Wang, X., & Xu, H. (2021). Recent Advances on Anti-skin Cancer Activity of Phytochemicals and Underlying Molecular Mechanisms. *Medicine Research, 5*(2), 210006.

George, B., Chandran, R., & Abrahamse, H. (2021). Role of Phytochemicals in Cancer Chemoprevention: Insights. *Antioxidants (Basel), 10*(9), 1455.

Gordon, L. G., Elliott, T. M., Olsen, C. M., Pandeya, N., & Whiteman, D. C. (2018). Multiplicity of skin cancers in Queensland and their cost burden to government and patients. *Australian and New Zealand Journal of Public Health, 42*(1), 86-91.

Goswami, N. B., & Tah, J. (2018). White sandal (*Santalum album* L.), a precious medicinal and timber yielding plant: a short review. *Plant Archives, 18*(1), 1048-1056.

Goyal, P., Chaudhary, R., Jahan, S., & Gupta, U. (2007). Chemo preventive efficacy of tinospora cordifolia (a medicinal plant) against chemical induced skin papillomagenesis in mice. *Cancer Epidemiology Biomarkers & Prevention, 16*(12_Supplement), B5-B5.

Guldiken, B., Ozkan, G., Catalkaya, G., Ceylan, F. D., Yalcinkaya, I. E., & Capanoglu, E. (2018). Phytochemicals of herbs and spices: Health versus toxicological effects. *Food and Chemical Toxicology, 119*, 37-49.

Gupta, A. K., Bharadwaj, M., & Mehrotra, R. (2016). Skin cancer concerns in people of color: risk factors and prevention. *Asian Pacific Journal of Cancer Prevention, 17*(12), 5257-5264.

Hussain, S. A., Panjagari, N. R., Singh, R., & Patil, G. (2015). Potential herbs and herbal nutraceuticals: food applications and their interactions with food components. *Critical Reviews in Food Science and Nutrition, 55*(1), 94-122.

Ijaz, S., Akhtar, N., Khan, M. S., Hameed, A., Irfan, M., Arshad, M. A., Ali, S., & Asrar, M. (2018). Plant derived anticancer agents: A green approach towards skin cancers. *Biomedicine & Pharmacotherapy, 103*, 1643-1651.

Kan, Z., Jaiswal, B. S., Stinson, J., Janakiraman, V., Bhatt, D., Stern, H. M., Yue, P., Haverty, P. M., Bourgon, R., *et al.* (2010). Diverse somatic mutation patterns and pathway alterations in human cancers. *Nature, 466*(7308), 869-873.

Katalinic, A., Kunze, U., & Schäfer, T. (2003). Epidemiology of cutaneous melanoma and non-melanoma skin cancer in Schleswig-Holstein, Germany: incidence, clinical subtypes, tumour stages and localization (epidemiology of skin cancer). *British Journal of Dermatology, 149*(6), 1200-1206.

Katta, R., & Brown, D. N. (2015). Diet and skin cancer: The potential role of dietary antioxidants in nonmelanoma skin cancer prevention. *Journal of Skin Cancer, 2015*, 893149.

Kaur, G., Athar, M., & Alam, M. S. (2010). Eugenol precludes cutaneous chemical carcinogenesis in mouse by preventing oxidative stress and inflammation and by inducing apoptosis. *Molecular Carcinogenesis: Published in Cooperation with the University of Texas MD Anderson Cancer Center, 49*(3), 290-301.

Kaur, M., Agarwal, C., Singh, R. P., Guan, X., Dwivedi, C., & Agarwal, R. (2005). Skin cancer chemopreventive agent, α-santalol, induces apoptotic death of human epidermoid carcinoma A431 cells via caspase activation together with dissipation of mitochondrial membrane potential and cytochrome c release. *Carcinogenesis, 26*(2), 369-380.

Khan, A., Ahmad, A., Akhtar, F., Yousuf, S., Xess, I., Khan, L. A., & Manzoor, N. (2010). *Ocimum sanctum* essential oil and its active principles exert their antifungal activity by disrupting ergosterol biosynthesis and membrane integrity. *Research in Microbiology, 161*(10), 816-823.

Khan, S., Ikram, M., & Faisal, M. (2021). Commercial, Cosmetic, and Medicinal Importance of Sandal (*Santalum album*): A Valuable Forest Resource. In *Non-Timber Forest Products* (pp. 129-144): Springer.

Koh, D., Wang, H., Lee, J., Chia, K., Lee, H., & Goh, C. (2003). Basal cell carcinoma, squamous cell carcinoma and melanoma of the skin: analysis of the Singapore Cancer Registry data 1968–97. *British Journal of Dermatology, 148*(6), 1161-1166.

Koul, A., Ghara, A. R., & Gangar, S. C. (2006). Chemomodulatory effects of *Azadirachta indica* on the hepatic status of skin tumor bearing mice. *Phytotherapy Research, 20*(3), 169-177.

Kumar, A. A., Joshi, G., & Ram, H. M. (2012). Sandalwood: history, uses, present status and the future. *Current Science, 103*(12), 1408-1416.

Labani, S., Asthana, S., Rathore, K., & Sardana, K. (2021). Incidence of melanoma and nonmelanoma skin cancers in Indian and the global regions. *Journal of Cancer Research and Therapeutics, 17*(4), 906-911.

Lauth, M., Unden, A. B., & Toftgård, R. (2004). Non-melanoma skin cancer: pathogenesis and mechanisms. *Drug Discovery Today: Disease Mechanisms, 1*(2), 267-272.

Lee, D. A., & Miller, S. J. (2009). Nonmelanoma skin cancer. *Facial Plastic Surgery Clinics of North America, 17*(3), 309-324.

Leiter, U., Keim, U., Eigentler, T., Katalinic, A., Holleczek, B., Martus, P., & Garbe, C. (2017). Incidence, mortality, and trends of nonmelanoma skin cancer in Germany. *Journal of Investigative Dermatology, 137*(9), 1860-1867.

Lengai, G. M., Muthomi, J. W., & Mbega, E. R. (2020). Phytochemical activity and role of botanical pesticides in pest management for sustainable agricultural crop production. *Scientific African, 7*, e00239.

Li, W., Zhang, C., Du, H., Huang, V., Sun, B., Harris, J. P., Richardson, Q., Shen, X., Jin, R., *et al.* (2016). Withaferin A suppresses the up-regulation of acetyl-coA carboxylase 1 and skin tumor formation in a skin carcinogenesis mouse model. *Molecular Carcinogenesis, 55*(11), 1739-1746.

Li, W., & Zhao, Y. (2013). Withaferin A suppresses tumor promoter 12-*O*-tetradecanoylphorbol 13-acetate-induced decreases in isocitrate dehydrogenase 1 activity and mitochondrial function in skin epidermal JB 6 cells. *Cancer Science, 104*(2), 143-148.

Majeed, M., Bhat, B., Anand, S., Sivakumar, A., Paliwal, P., & Geetha, K. (2011). Inhibition of UV-induced ROS and collagen damage by *Phyllanthus emblica* extract in normal human dermal fibroblasts. *Journal of Cosmetic Science, 62*(1), 49-56.

Maliyakkal, N., Appadath Beeran, A., Balaji, S. A., Udupa, N., Ranganath Pai, S., & Rangarajan, A. (2015). Effects of *Withania somnifera* and *Tinospora cordifolia* extracts on the side population phenotype of human epithelial cancer cells: toward targeting multidrug resistance in cancer. *Integrative Cancer Therapies, 14*(2), 156-171.

Mandal, A. K., Poudel, M., Neupane, N. P., & Verma, A. (2022). Phytochemistry, Pharmacology, and Applications of Ocimum sanctum (Tulsi): Springer Link.

Mandlik, D. S., & Namdeo, A. G. (2021). Immunomodulators and Phytodrugs. In *Evidence Based Validation of Traditional Medicines* (pp. 901-920): Springer.

Marwat, S. K., Khan, M. S., Ghulam, S., Anwar, N., Mustafa, G., & Usman, K. (2011). Phytochemical constituents and pharmacological activities of sweet Basil-*Ocimum basilicum* L.(Lamiaceae). *Asian Journal of Chemistry, 23*(9), 3773.

Mathur, S., Kaur, P., Sharma, M., Katyal, A., Singh, B., Tiwari, M., & Chandra, R. (2004). The treatment of skin carcinoma, induced by UV B radiation, using 1-*oxo*-5β, 6β-epoxy-witha-2-enolide, isolated from the roots of *Withania somnifera*, in a rat model. *Phytomedicine, 11*(5), 452-460.

Mehmood, M. H., Siddiqi, H. S., & Gilani, A. H. (2011). The antidiarrheal and spasmolytic activities of *Phyllanthus emblica* are mediated through dual blockade of muscarinic receptors and Ca^{2+} channels. *Journal of Ethnopharmacology, 133*(2), 856-865.

Millsop, J. W., Sivamani, R. K., & Fazel, N. (2013). Botanical agents for the treatment of nonmelanoma skin cancer. *Dermatology Research and Practice, 2013*, 837152.

Naja, F., Fadel, R. A., Alameddine, M., Aridi, Y., Zarif, A., Hariri, D., Mugharbel, A., Khalil, M., Nahleh, Z., *et al.* (2015). Complementary and alternative medicine use and its association with quality of life among Lebanese breast cancer patients: a cross-sectional study. *BMC Complementary and Alternative Medicine, 15*(1), 1-10.

Nayak, B., & Pinto Pereira, L. M. (2006). *Catharanthus roseus* flower extract has wound-healing activity in Sprague Dawley rats. *BMC Complementary and Alternative Medicine, 6*(1), 1-6.

Padmavathi, B., Rath, P. C., Rao, A. R., & Singh, R. P. (2005). Roots of *Withania somnifera* inhibit forestomach and skin carcinogenesis in mice. *Evidence-Based Complementary and Alternative Medicine, 2*(1), 99-105.

Pham, H. N. T., Sakoff, J. A., Van Vuong, Q., Bowyer, M. C., & Scarlett, C. J. (2018). Screening phytochemical content, antioxidant, antimicrobial and cytotoxic activities of *Catharanthus roseus* (L.) G. Don stem extract and its fractions. *Biocatalysis and Agricultural Biotechnology, 16*, 405-411.

Pham, H. N. T., Sakoff, J. A., Vuong, Q. V., Bowyer, M. C., & Scarlett, C. J. (2019). Phytochemical, antioxidant, anti-proliferative and antimicrobial properties of *Catharanthus roseus* root extract, saponin-enriched and aqueous fractions. *Molecular Biology Reports, 46*(3), 3265-3273.

Prakash, J., Gupta, S. K., & Dinda, A. K. (2002). *Withania somnifera* root extract prevents DMBA-induced squamous cell carcinoma of skin in Swiss albino mice. *Nutrition and Cancer, 42*(1), 91-97.

Prashar, R., & Kumar, A. (1995). Chemopreventive action of *Ocimum sanctum* on 2, 12-dimethylbenz (a) anthracene DMBA-induced papillomagenesis in the skin of mice. *International Journal of Pharmacognosy, 33*(3), 181-187.

Prashar, R., Kumar, A., Banerjee, S., & Rao, A. (1994). Chemopreventive action by an extract from *Ocimum sanctum* on mouse skin papillomagenesis and its enhancement of skin glutathione S-transferase activity and acid soluble sulfydryl level. *Anti-Cancer Drugs, 5*(5), 567-572.

Queen, L. (2017). *Skin cancer: causes, prevention, and treatment.* (Senior Honors Theses). Liberty University, (648).

Rastogi, S., Shukla, Y., Paul, B. N., Chowdhuri, D. K., Khanna, S. K., & Das, M. (2007). Protective effect of *Ocimum sanctum* on 3-methylcholanthrene, 7, 12-dimethylbenz (a) anthracene and aflatoxin B1 induced skin tumorigenesis in mice. *Toxicology and Applied Pharmacology, 224*(3), 228-240.

Rees, J. R., Zens, M. S., Gui, J., Celaya, M. O., Riddle, B. L., & Karagas, M. R. (2014). Non melanoma skin cancer and subsequent cancer risk. *PloS One, 9*(6), e99674.

Rezadoost, M. H., Kumleh, H. H., & Ghasempour, A. (2019). Cytotoxicity and apoptosis induction in breast cancer, skin cancer and glioblastoma cells by plant extracts. *Molecular Biology Reports, 46*(5), 5131-5142.

Sancheti, G., Jindal, A., Kumari, R., & Goyal, P. (2005). Chemopreventive action of *Emblica officinalis* on skin carcinogenesis in mice. *Asian Pacific Journal of Cancer Prevention, 6*(2), 197-201.

Santha, S., & Dwivedi, C. (2015). Anticancer effects of sandalwood (*Santalum album*). *Anticancer Research, 35*(6), 3137-3145.

Seite, S., Del Marmol, V., Moyal, D., & Friedman, A. (2017). Public primary and secondary skin cancer prevention, perceptions and knowledge: an international cross-sectional survey. *Journal of the European Academy of Dermatology and Venereology, 31*(5), 815-820.

Singh, E., Sharma, S., Pareek, A., Dwivedi, J., Yadav, S., & Sharma, S. (2012). Phytochemistry, traditional uses and cancer chemopreventive activity of Amla (*Phyllanthus emblica*): The Sustainer. *Journal of Applied Pharmaceutical Science, 2*(1), 176-183.

Sloan, F. A., & Gelband, H. (2007). Defining resource-level-appropriate cancer control. In *Cancer Control Opportunities in Low-and Middle-Income Countries*: National Academies Press (US).

Sobanko, J. F., Sarwer, D. B., Zvargulis, Z., & Miller, C. J. (2015). Importance of physical appearance in patients with skin cancer. *Dermatologic Surgery, 41*(2), 183-188.

Stoj, V., Shahriari, N., Shao, K., & Feng, H. (2022). Nutrition and nonmelanoma skin cancers. *Clinics in Dermatology, 40*(2), 173-185.

Sukumaran, K., Unnikrishnan, M., & Kuttan, R. (1994). Inhibition of tumour promotion in mice by eugenol. *Indian Journal of Physiology and Pharmacology, 38*(4), 306-308.

Sung, H., Ferlay, J., Siegel, R. L., Laversanne, M., Soerjomataram, I., Jemal, A., & Bray, F. (2021). Global cancer statistics 2020: GLOBOCAN estimates of incidence and mortality worldwide for 36 cancers in 185 countries. *CA: A Cancer Journal for Clinicians, 71*(3), 209-249.

Thomasset, S. C., Berry, D. P., Garcea, G., Marczylo, T., Steward, W. P., & Gescher, A. J. (2007). Dietary polyphenolic phytochemicals—promising cancer chemopreventive agents in humans? A review of their clinical properties. *International Journal of Cancer, 120*(3), 451-458.

Treichel, T. L. E., do Prado, T. D., do Amaral, A. S. Z., de Sousa Gomes, Y., da Rocha Pinto, L., Martins, G. T., Martins, A. T., & Cagnini, D. Q. (2020). Use of Ointment or Aqueous Extract of Neem (*Azadirachta indica*) for the Repair of Experimental Skin Lesions in Sheep. *American Journal of Plant Sciences, 11*(5), 100290.

Upadhyay, A. K., Kumar, K., Kumar, A., & Mishra, H. S. (2010). *Tinospora cordifolia* (Willd.) Hook. f. and Thoms.(Guduchi)–validation of the Ayurvedic pharmacology through experimental and clinical studies. *International Journal of Ayurveda Research, 1*(2), 112-121.

Van Dross, R. T., Hong, X., Essengue, S., Fischer, S. M., & Pelling, J. C. (2007). Modulation of UVB-induced and basal cyclooxygenase-2 (COX-2) expression by apigenin in mouse keratinocytes: Role of USF transcription factors. *Molecular Carcinogenesis: Published in Cooperation with the University of Texas MD Anderson Cancer Center, 46*(4), 303-314.

Wei, H., Tye, L., Bresnick, E., & Birt, D. F. (1990). Inhibitory effect of apigenin, a plant flavonoid, on epidermal ornithine decarboxylase and skin tumor promotion in mice. *Cancer Research, 50*(3), 499-502.

Wollina, U., Koch, A., Schönlebe, J., & Tchernev, G. (2017). Carcinosarcoma of skin (sarcomatoid carcinoma)-A rare non-melanoma slin cancer (Case Review). *Georgian Medical News, 263*, 7-10.

Wölfle, U., Esser, P. R., Simon-Haarhaus, B., Martin, S. F., Lademann, J., & Schempp, C. M. (2011). UVB-induced DNA damage, generation of reactive oxygen species, and inflammation are effectively attenuated by the flavonoid luteolin in vitro and in vivo. *Free Radical Biology and Medicine, 50*(9), 1081-1093.

Wu, X., Elkin, E. E., & Marghoob, A. A. (2015). Burden of basal cell carcinoma in USA. *Future Oncology, 11*(22), 2967-2974.

Xu, K., Zhang, C., Li, Y., Xi, X., Zheng, L., Meng, M., Liu, T., Zhao, Y., & Li, W. (2019). Withaferin A suppresses skin tumor promotion by inhibiting proteasome-dependent isocitrate dehydrogenase 1 degradation. *Translational Cancer Research, 8*(6), 2449.

Yates, C. R., Bruno, E. J., & Yates, M. E. (2022). *Tinospora cordifolia*: A review of its immunomodulatory properties. *Journal of Dietary Supplements, 19*(2), 271-285.

Zhang, X., Chen, W., Guillermo, R., Chandrasekher, G., Kaushik, R. S., Young, A., Fahmy, H., & Dwivedi, C. (2010). Alpha-santalol, a chemopreventive agent against skin cancer, causes G2/M cell cycle arrest in both p53-mutated human epidermoid carcinoma A431 cells and p53 wild-type human melanoma UACC-62 cells. *BMC Research Notes, 3*(1), 1-15.

Int. J. Plant Bas. Pharm. (2023) 3(1), 32-40

INTERNATIONAL JOURNAL OF PLANT BASED PHARMACEUTICALS

https://ijpbp.com

RESEARCH ARTICLE

OPEN ACCESS

Ruellia simplex C. Wright (Acanthaceae): Antinociceptive, anti-inflammatory, and antidiabetic activities of a novel fatty acid isolated from its leaf extract

Cletus Anes Ukwubile[a*], Henry Nettey[b], Troy Salvia Malgwi[a], Nnamdi David Menkiti[c]

[a] *University of Maiduguri, Faculty of Pharmacy, Department of Pharmacognosy, Nigeria*
[b] *University of Ghana, School of Pharmacy, Department of Pharmaceutics and Pharmaceutical Microbiology, Legon, Accra, Ghana*
[c] *Ahmadu Bello University, Faculty of Physical Sciences, Department of Chemistry, Zaria, Nigeria*

ARTICLE INFO

Article History:

Received: 12 August 2022
Revised: 27 September 2022
Accepted: 05 October 2022
Available online: 07 October 2022

Edited by: B. Tepe

Keywords:

Ruellia simplex
Antinociceptive
Anti-inflammatory
Antidiabetics
Fatty acid

ABSTRACT

Ruellia simplex is a medicinal plant whose leaf is used to treat pains, inflammation, and diabetes in Nigeria. The current study was undertaken to determine the antinociceptive (analgesics), anti-inflammatory, and antidiabetic activities of a novel fatty acid isolated from the leaf extract of *R. simplex*. Isolation of a novel fatty acid from the most active fraction was carried out on silica gel column chromatography while, antinociceptive, anti-inflammatory, and antidiabetic activities of the isolated compound were evaluated by acetic acid, carrageenan, and alloxan-induced animal models respectively. The chemical structure of the new compound was elucidated by FT-IR, NMR, GC-MS, and LC-MS. The isolated fatty acid showed inhibition of pains by decreasing abdominal writhing in mice in dose dependent fashion as well as reduced paw volume in the carrageenan-induced paw edema in rats at IC_{50} = 12.5 ± 1.08 µg/ml and 10.21 ± 1.02 µg/ml, respectively, whereas the antidiabetic activity showed a dose dependent reduction in blood sugar levels with IC_{50} = 6.02 ± 0.01 µg/ml. The compound showed the following features: R-COOH functional group at 3327 wavelength cm^{-1} by FTIR; EI-MS $[M]^{+*}$ at *m/z* 467, peak area 62.231% and RT 14.086 min by GC-MS; singly charged fragments at *m/z* 116.1 and *m/z* 465.1, RT 1.31 min by LC-MS and eight proton signals consisting of singlets and multiplets (^{1}H), thirty carbon atoms (^{13}C) NMR data. From the study, the novel fatty acid from *R. simplex* extract was potentially active for the treatment of pains, inflammation, and diabetes.

1. Introduction

The discovery of drugs from indigenous herbal plants has progressed with many civilizations. This is because medicinal plants have been used to treat different types of diseases for decades (Tabuti et al., 2012). In most cases, the science or mechanism for the use of these plants is not clear or known to herbalists or traditional medicine practitioners, yet the scientific validation for the use of most of these plants has been done only in recent times (Boadu & Asase, 2017). Moreover, the significant advances in experimental and molecular biology techniques applied to these plants have paved the way for pharmacognosist and natural products researchers to find out the potential use of secondary metabolites to treat or manage an array of diseases such as cancers, hypertension, diabetes, ulcers, pains, inflammation, infections, among other diseases (Schippmann et al., 2006).

For instance, pain or analgesia is characterized as an unwanted experience and nervous agitati-

Reviewed by:
Yavuz Selim Cakmak: Aksaray University, Aksaray, Türkiye
Menderes Suicmez: Hitit University, Corum, Türkiye

* Corresponding author(s):
E-mail address:
doccletus@yahoo.com
caukwubile@unimaid.edu.ng
(C. A. Ukwubile)
e-ISSN: 2791-7509
doi: https://doi.org/10.29228/ijpbp.13

on with either short or prolonged tissue degeneration. All analgesic drugs selectively exert pain-relieving effects without pronounced change of consciousness by acting on the central nervous system or the peripheral pain receptors (Belachew et al., 2020; Nguyen et al., 2020). Despite the use of these analgesics as pain reduction agents, some of them have been classified recently as proton pump inhibitors (PPIs) indicating their beneficial off-target effects. Similarly, inflammation is an immunological response by the body against infection. For example, the febrile response is a classical sign of an inflammatory response to an invading harmful stimulus involving several mediators such as interleukins (Yeshwante et al., 2009). In addition, inflammation is usually followed by pain. For this reason, nonsteroidal anti-inflammatory drugs (NSAIDs) are the standard treatment for pains and inflammation because they inhibit the activity of cyclooxygenase enzymes, which play crucial roles in the production of prostaglandins (PGAs); endogenous mediators known to initiate pains and inflammation. The use of these NSAIDs has increased the risk of anomalies in some organs and/or tissues in the body such as the liver, kidney, GIT, and heart (Padmanabhan & Jangle, 2012; Ukwubile et al., 2021). Hence, natural product researchers have been looking for alternative herbal treatments with low side effects.

On the other hand, diabetes is a disease characterized by high blood glucose levels (known as hyperglycemia). The disease is usually associated with frequent urination and is occasionally accompanied by high blood pressure resulting in about 40% of deaths annually globally (Ibrahim et al., 2014; Ojo et al., 2018). Currently, the exact number of people living with type 2 diabetes in Nigeria has doubled in the last decades (the highest in Africa), and current chemotherapeutic drugs have not yielded the desired result, thus, the use of herbal plants for the treatment of diabetes is now being embraced globally as a better alternative to the prevailing medicinal approach, in which *Ruellia simplex* C. Wright (Acanthaceae) is one of such plants.

R. simplex is commonly called Mexican petunia or Texas petunia. It is a woody-based, rhizomatous annual plant that is grown as an ornamental herb. It originated in Mexico and has been distributed in many countries of west Africa such as Nigeria, Ghana, and the Ivory Coast (Iwu, 2014). The plants' branches from the ground into several woody-based stems with purple elongated leaves. Some species in the genus are suspected to be poisonous, especially those with reddish inflorescence or flowers. These species are often scarce and endemic to the Mediterranean regions extending sparsely into the tropics for example the *R. brittonianna* (Iwu, 2014).

Most species of the genus *Ruellia* have been used as antipyretic, antioxidant, analgesic, anti-spasmolytic, antiviral, antihypertensive, antifungal, antiulcer, antidiabetic, and anti-inflammatory agents in Nigeria. The plant *R. simplex* was reported to contain various secondary metabolites such as glycosides, alkaloids, flavonoids, and triterpenoids (Sharma et al., 2001).

The present study was carried out to evaluate the antinociceptive, anti-inflammatory, and antidiabetic potentials of an isolated novel fatty acid from the leaf methanol extract of *R. simplex*.

2. Materials and methods

2.1. Materials

2.1.1 Chmicals and reagents

Methanol, ethyl acetate, acetic acid, alloxan-monohydrate, carrageenan, and chloroform (analytical grades; JoeChem Nig. Ltd. for Sigma-Aldrich, St Lous Mo, USA), *n*-hexane (Benrock, Nig. Ltd.), distilled water, ibuprofen tablet (Alapharm, Nig. Ltd.), diclofenac sodium (Hovid, Nig. Ltd.), silica gel 60-120 mesh, silica gel 60 F254 TLC plates (Merk, Germany), LH-20 Sephadex (Sigma-Aldrich, St Lous Mo, USA).

2.1.2. Apparatus and instruments

Magnifying lens, NMR 850 MHz, LC-MS (Bruker, UK), GC-MS 790A (Agilent Technologies, UK), alpha II FTIR (UK), glass column (95 x 35 mm), vernier caliper, vacuum rotary evaporator (Buchi type, Shan, Model No: 130VRE, Haryana, India).

2.2. Methods

2.2.1. Collection and preparation of plant material

The fresh leaves of *R. simplex* were collected in the early morning hours between 5:30 am and 6:30 am in Eburu-Mmiri, Nsukka Enugu State, in March 2022, and authenticated by Mr. C. A. Ukwubile. A voucher specimen (No: FGO/002501) was deposited at the Archives of Medicinal Plants, Forest Guide, Ogurugu. The leaves were shade-dried for two weeks and pulverized into fine powders, weighed, and stored in a clean sample bottle before extracting with methanol for the extract.

2.2.2. Preparation of ethyl acetate fraction of R. simplex extract

Using liquid-liquid partitioning (LLP), 40 g of the obtained methanol extract was suspended in a separating funnel containing 700 ml of distilled water mixed with 300 ml of methanol. It was then successively partitioned with *n*-hexane (400 ml) (x 3), chloroform (400 ml) (x 3), and ethyl acetate (400 ml) (x 3). The fractions were dried using a rotary evaporator at 45 °C and separately weighed, kept in sample bottles, and stored in a refrigerator at 5 °C for subsequent use. Each fraction was tested for biological activities to obtain the most active fraction. The ethyl acetate fraction (EF) was the most bioactive fraction from the preliminary assays and was used in the current study.

2.2.3. Phytochemical screening

The EF was screened to determine the presence of some secondary metabolites which are likely to contain fatty acids like alkaloids, flavonoids, saponins, tannins, triterpenes, cardiac glycosides, carbohydrates, and fats/oils. The methods previously described by (Evans, 2002) were used for this purpose.

2.2.3.1. Isolation and characterization of novel fatty acid from the EF

The EF was subjected to silica gel (60-120 mesh size) open-column chromatography. Elution was carried out by gradient technique using *n*-hexane, chloroform, and acetone (2:4:4), respectively in the increasing order of their polarities. A total of twenty-five sub-fractions were collected and grouped into two based on their profiles on the TLC plate. Each sub-fraction was bio-monitored to select the most active sub-fraction. The most active sub-fraction

was subjected to comparative TLC using oleanolic acid as a marker compound for fatty acid. The separated compound showed similar color and Rf value with the authentic fatty acid used as standard. Finally, the isolated compound was checked for purity using the HPLC and then subjected to melting point determination, FT-IR, GC-MS, LC-MS, and NMR analysis to identify and elucidate the structure (Evans, 2002; Kumar et al., 2012).

2.2.3.2. Determination of melting point of the compound

The melting point of the isolated novel fatty acid was determined by using an IA9000 Series digital melting point apparatus (Electrothermal Engineering Ltd., UK). Briefly, 0.5 mg of the compound was introduced into a capillary tube and inserted into the heating bath of the melting point machine apparatus, and heated to determine the temperature after melting (Jothy et al., 2011).

2.2.3.3. FT-IR analysis of isolated compound

The fourier transform infrared (FT-IR) analysis of the compound was carried out using an Alpha II type FT-IR (Bruker, UK). The compound was scanned at 400-4000 cm^{-1} wavelength.

2.2.3.4. GC-MS analysis of isolated compound

GC-MS analysis of isolated compounds was carried out using Agilent 5977B GC/MSD with the following conditions: HP-5 capillary column (30 mm x 0.25 mm internal diameter., 0.25 µm thickness), oven temperature from 50 °C for 1 min, and increased to 250 °C at the value of 25 °C/min for 10 min, to a final temperature of 300 °C at the value of 20 °C/min. Head pressure was 15 psi, injector temperature, was 250 °C, injection mode 0.2 min splitless, injected volume 0.1 µl, the temperature of detector 270 °C, carrier gas helium. Mass spectra conditions: ion source temperature 225 °C, electron impact: 50 eV, acquisition mode scan (*m/z* 50–600) (Jothy et al., 2011).

2.2.3.5. LC-MS analysis of isolated compound

The liquid chromatography was performed using the quadrupole time-of-flight LC/-MS 6546 LC/Q-TOF (Agilent Technologies, UK) using the following experimental conditions: Zorbax SB C18, 2.1 x 50 mm column, 100% MilliQ water þ 0.1% formic acid 1.81 solvent A, 100% acetonitrile þ 0.1% formic acid solvent B, 0.3 ml/min flow rate, 3.1 µl injection volume, 30 min run time, and gradient elution technique was used (Siddiqui et al., 2011).

2.2.3.6. NMR analysis of isolated compound

The nuclear magnetic resonance (NMR) spectroscopy (^{1}H and ^{13}C NMR) was performed with a Bruker 850 MHz apparatus at the NMR laboratory of King Abdulaziz University, Jedda, Saudi Arabia. The isolated compound was dissolved in 2.5 µl deuterated chloroform ($CDCl_3$) and placed in the NMR tube. Then 0.1 µl of the solution was injected into the NMR port. The chemical shifts (δ) were reported as part per million (ppm) with reference to tetra-methyl-silane (TMS) as the internal standard solvent. The characteristics of the identified protons and carbons of the compound were compared with the proposed structure from the NIST library and other identification chemical libraries for organic compounds.

2.2.4. Antinociceptive activity of isolated novel fatty acid

To evaluate the antinociceptive activity, we investigated the peripheral and central antinociceptive activities of the compound. For peripheral antinociceptive activity, the acetic acid-induced writhing method in mice was used (Abotsi et al., 2017). Briefly, twenty mice of the opposite sex were grouped into four groups (five animals in each) and allowed to acclimatize in the laboratory for one week before evaluation. Group I is the negative control group which received 1% Tween-80 in normal saline solution, group II is the positive control group which received 50 mg/kg bw diclofenac sodium standard drug, while groups III and IV received 2 and 4 mg/kg bw doses of isolated compound intraperitoneal (i.p.), respectively before administration of 0.5% acetic acid (i.p.) 10 min later. After 15 min, the writhing of the abdomen was observed on each mouse every 5 min for 30 min using a magnifying lens. The analgesic activity was then expressed as follows:

$$Writhing\ inhibition\ (\%) = \frac{Wc - Ws}{\mathrm{Wc}} x\ 100$$

where Wc is the mean number of writhing in the control group and Ws is the mean number of the writhing of the treated groups.

On the other hand, the central antinociceptive activity was carried out using the tail immersion method, with morphine as the standard drug.

2.2.5. Anti-inflammatory activity evaluation

In determining the anti-inflammatory effect of the isolated fatty acid, carrageenan-induced paw edema of the rat model was used. Briefly, rats were grouped randomly into different groups. The plethysmometer was used to measure the rat's pedal volume to the ankle joint. Thereafter, the animals were injected with 100 µl normal saline,10 mg/kg bw of ibuprofen as well as 2 and 4 mg/kg bw of isolated fatty acid, respectively via intraperitoneal (i.p.) route 1 h before the injection of 50 µl of 1% carrageenan in the right hind paw of the rats (Abotsi et al., 2017). After the induction of edema in the rats, the volume of the paw was measured at intervals of 5, 10, 15, 20, 25, 30, 35, 40, 45, 50, 55, and 60 min. The edema volume was calculated using the formula below:

$$Change\ in\ paw\ edema\ volume = Final\ paw\ volume - \ Initial\ paw\ volume$$

2.2.6. Antidiabetic activity evaluation

The antidiabetic activity was evaluated using a glucose tolerance test (GTT), as was previously described by Mohamed et al. (2012) with moderate modification. Briefly, mice were first randomly selected and divided into four groups of three mice per group. Group I was administered 1% Tween-80 in normal saline (i.e., 0.1 ml/10 g bw) which served as the negative control group, and group II was administered 10 mg/kg bw Glibenclamide tablet (May & Baker Nig., Plc) standard drug, while groups III and IV were administered isolated fatty acid at doses of 5 and 10 mg/kg bw, respectively (i.p.). Then one hour later, all animals were administered i.p. in the penial vein with 1.5 ml 1% alloxan monohydrate (Sigma-Aldrich St. Lous Mo, USA). Six hours after alloxan monohydrate administration (i.p.), blood samples were then collected from each animal by the tail tips in 30, 60, 120, 180, and 240 min. Finally, the blood glucose levels were determined using a glucometer (ACCU-CHEK Softclix, Roche), after noting the glucose baseline in each mouse of each group.

2.3. Statistical analysis

The data generated from the studies were subjected to a one-way analysis of variance (One-way ANOVA) using SPSS statistical software (version 22). Values are expressed as mean ± SD for various groups. The values of $p < 0.05$ were taken as statistically significant.

3. Results and discussion

3.1. Preliminary phytochemical screening

In the current study, preliminary phytochemical screening of the leaf extract revealed the presence of alkaloids, tannins, saponins, flavonoids, and triterpenes as well cardiac glycosides (Table 1).

Table 1. Phytochemical contents of *R. simplex* leaf methanol extract

Constituents	Interference
Carbohydrate	+
Saponins	+
Alkaloids	++
Flavonoids	++
Tannins	+
Triterpenes	+
Phytosterols	++
Cardiac glycosides	+
Fats/oils	++
Proteins	-
Anthracene	-

+: Moderately detected, ++: Largely detected, -: Not detected

3.2. Structural elucidation of isolated fatty acid

The isolated fatty acid was an amorphous yellow compound with a fine smell like groundnut oil typical of fatty acid. The structure of the isolated fatty acid was elucidated using various techniques previously described. FTIR showed a non-bonded OH group (3000 cm^{-1}), symmetrical stretching of OH groups (2984 and 2500 cm^{-1}) of fatty acids, an α-unsaturated carboxylic acid group (2000 cm^{-1}), and mono-substituted aromatic rings (1500 and 1000 cm^{-1}) stretching, which are an indication of fatty acids (Kumar et al., 2017). The MS data: EIMS $[M]^+$ at *m/z* 467, while the LC-MS data showed pseudomolecular ions $[M+H]^-$ at 465.1 and $[M+H]^+$ at 617.1 *m/z*; RT, 2.756 min. ^{1}H-NMR spectrum analysis revealed a signal δ 0.772 ppm (H-1, d, 0.777) of methylene carbon C-2, characteristic of fatty acids. The proton H-13 at δ 1.468 ppm (s) indicated an olefinic ring of unsaturated fatty acids The results obtained were represented in Figure 1, Table 2, Figure 2, Figure 3, Figure 4, and supplementary files (S1-S5).

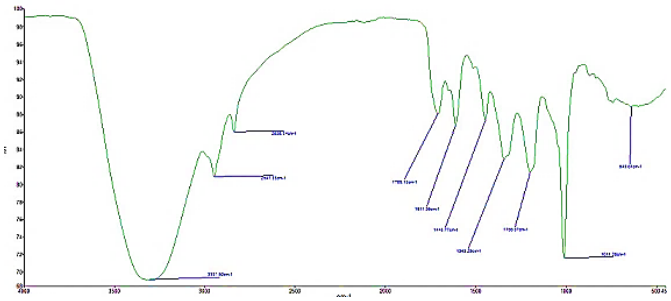

Figure 1. FTIR spectrum of isolated novel fatty acid

Table 2. ^{1}H and ^{13}C (850 MHz) NMR data of isolated novel compound in CDCL3

Peak No.	δ_H ppm (850 MHz)	δ_C ppm (850 MHz)
2	0.772 (d, 0.777)	33.08
3	0.885 (m)	32.91
4	0.902 (s)	32.92
5	0.918 (d, 0.925)	32.62
6	0.968 (q)	32.43
7	0.984 (s)	31.95
8	1.079 (s)	31.45
9	1.132 (s)	31.01
10	1.281 (m)	30.69
11	1.330 (s)	30.57
12	1.453 (q)	30.19
13	1.468 (s)	29.73, 29.69
14	1.733 (m)	29.40
15	1.782 (s)	29.28, 28.14, 28.10, 27.98, 27.67, 27.16, 27.12, 26.99, 26.48, 25.94, 24.12, 23.62, 23.59, 23.40, 23.29, 22.94, 22.73

3.3. Antinociceptive and anti-inflammatory effects of novel fatty acid (2,4-PHPBEa)

The result obtained showed that the compound *2,4-PHPBEa* significantly reduced the withing of abdominal pains in the rats in a dose-dependent fashion from 2 to 4 mg/kg bw. The novel fatty acid from *R. simplex* greatly inhibited the peripheral pains induced by acetic acid in 30 min, as the doses increased from 2 to 4 mg/kg with 66.19% and 82.71% inhibition of writhing, respectively (Table 3). These results were statistically significant ($p < 0.05$; one-way ANOVA) when compared to the standard drug diclofenac sodium. On the other hand, the central antinociceptive activity (Table 4) of the novel fatty acid at the same doses showed significant dose-dependent decreases in response to tail flicking or licking after 120 min administration when compared to the standard drug morphine ($p < 0.05$).

3.4. Antidiabetic effect of novel fatty acid 2,4-PHPBEa

There was a dose-dependent reduction in the level of plasma glucose in the alloxan-induced diabetic rats from 30 to 240 min (Figure 7). However, the standard drug did not show a significant decrease in hyperglycemic effect within this period ($p < 0.05$).

Fatty acids are a group of organic compounds which are structurally made up of long chains of carbons terminating two functional groups of a carboxylic acid and a methyl group on different sides. Naturally occurring fatty acids often possess mostly even number of carbon atoms, which are saturated or unsaturated depending on the bonds existing between the carbon atoms. Medicinal plants and vegetable oils contain palmitic acid, stearic acid, oleic acid, and linoleic acid. These fatty acids are saturated and unsaturated in nature consisting of single and double bonds respectively (Pinto et al., 2017). These fatty acids have been isolated from various plant families where they are used for treating many diseases such as pain, inflammation, diabetes, cancers, hemorrhoids, etc. Some of these fatty acids have been used for the formulation of various dosage forms by pharmaceutical industries for therapeutic purposes.

An evaluation of the phytochemical contents of plants (Table 1), is important to elucidate the various classes of secondary metabolites that are present in the plant. This is very crucial in that secondary metabolites such as alkaloids, saponins, and flavonoids, for example, have been used as anticancer, anti-hemorrhoid, and antioxidant agents, respectively (González et al., 2011). It has been reported that a plant's therapeutic activities are also solely dependent on the

type of metabolites it contained at a given period (Valdés et al., 2020). These phytochemicals play crucial roles in ameliorating various human diseases in traditional medicine. For instance, saponin and flavonoid groups of phytochemicals possessed compounds that are used as analgesics and anti-inflammatory agents, while alkaloids and triterpenes showed both anticancer and antimalarial properties, respectively. Tannins, on the other hand, also possess an anti-diabetic effect, whereas cardiac glycosides help to stimulate the cardiac muscles in hypertension conditions (Jacobs et al., 1990). The roles played by these metabolites were not at variance from their roles in this study. In the fractionation and isolation of novel fatty acid, a total of twenty-five fractions were collected and grouped into four (I, II, III, IV) based on their TLC profiles, and were bio-monitored for antinociceptive, anti-inflammatory, and antidiabetic effects. Group II (i.e., fractions 9-15) showed the biologically most potent activity. Further fractionation of group II using normal phase short column silica gel chromatography eluted by gradient elution using *n*-hexane:chloroform (1:2), and *n*-hexane:ethyl acetate (2:8) yielded 2.8 mg compound A and 28 mg compound B, respectively. Compound B showed 75% (antinociceptive), 86.4% (anti-inflammatory), and 78.12% (antidiabetic) effects, while compound A produced less than 2% biological activities within 24 h testing.

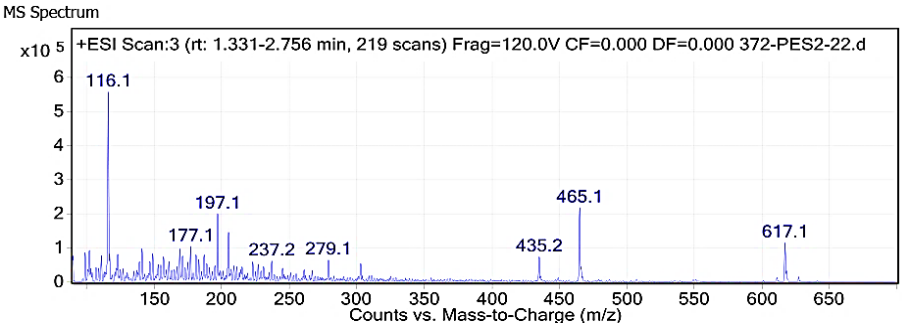

Figure 2. LC-MS of isolated novel fatty acid

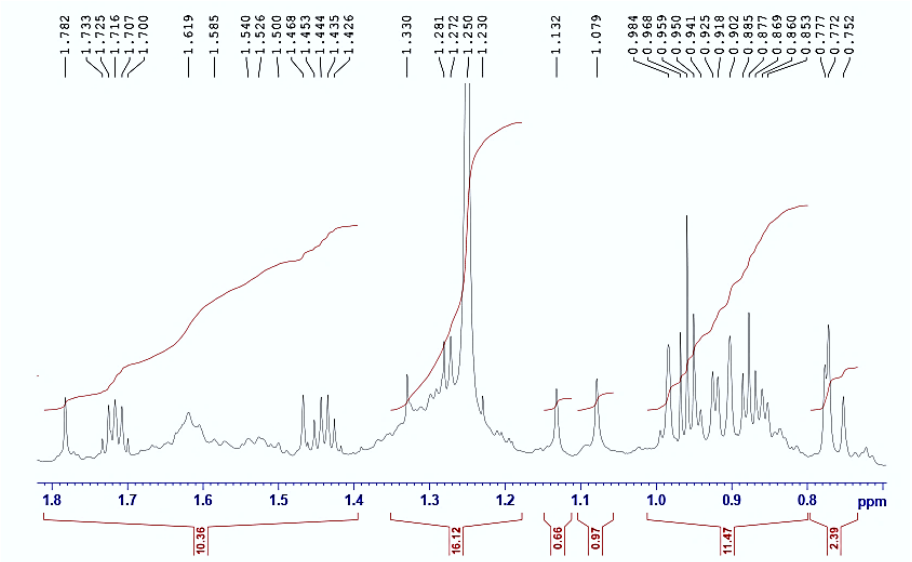

Figure 3. ^{1}H-NMR spectrum of isolated novel fatty acid

The isolated novel compound in the current study possessed the following properties: physical properties; yellow amorphous in appearance (28 mg), melting point; 164.4 °C, the UV data: [MeOH] λmax 217.8 and 308.3 nm, [MeOH+NaOH] λmax 227.5 and 406.2 nm (Figure S1a, b). The FTIR spectrum showed the presence of a non-bonded OH group (3000 cm^{-1}), symmetrical stretching of OH groups (2984 and 2500 cm^{-1}) of fatty acids, an α-unsaturated carboxylic acid group (2000 cm^{-1}), and mono-substituted aromatic rings (1500 and 1000 cm^{-1}) stretching (Figure 1), which are indicative of the presence of fatty acids (Kumar et al., 2017). The MS data showed EIMS $[M]^+$ at *m/z* 467 with molecular formula; $C_{28}H_{26}O_6$ (Figure S2), while the LC-MS data (Figure 2) showed pseudomolecular ions $[M+H]^-$ at 465.1 and $[M+H]^+$ at 617.1 *m/z*; RT, 2.756 min. The NMR analysis of the compound revealed the following: ^{1}H-NMR spectrum (Table 2, Figure 3) analysis revealed a signal δ 0.772 ppm (H-1, d, 0.777) of methylene carbon C-2, characteristic of fatty acids. The proton H-13 at δ 1.468 ppm (s) indicated an olefinic ring of unsaturated fatty acids while the proton H-15 at δ 1.782 ppm (s) contained OH groups linked to a carbonyl carbon which are typical of fatty acids. The ^{1}H-^{1}H COSY correlations of (Figure S3) showed that the proton H-10 (δ 0.82 ppm) correlates with H-3 (δ 0.79 ppm), H-7 (δ 0.89 ppm), and H-9 (δ 1.09 ppm); proton H-12 (δ 0.89 ppm) correlates with H6, and H-15 (δ 1.42 ppm) correlates with H-12 and H-13. These patterns of correlations indicated various linkages between aromatic rings of benzene. The HMBC correlations (Figure S4) showed that the proton H-9 was double bonds connected with C-7 and C-16, H-11 was connected by double bonds to C-18 and C-20, while the proton at H-12 was double bonds connected to the carbonyl carbon C-26 of carboxylic acid. The HSQC spectrum (Figure S5) did not show multiple bond corrections and was typical of fatty acids. The ^{13}C-NMR spectrum of the compound (Table 2, Figure 4) showed mainly methylene carbons

with few methine carbons at δ 33.08 to 22.73 ppm. In all, the ^{13}C-NMR spectrum indicated twenty-eight (28) carbon atoms with no quaternary and methane carbon signals. When these NMR spectral data were compared with chemical libraries, the NIST library, and published literature, there was no match to the isolated fatty acid found, hence, it was concluded that the compound was novel. However, following IUPAC rules for naming of organic compounds, the fatty acid was identified as (2*E*,4*E*)-4-(4'-(2-phenyl-4,4a,6,8a-tetrahydropyrano[3,2-d] [1,3]dioxin-6-yl)-[1,1'-biphenyl]-3(4H)-ylidene) but-2-enoic acid (Figure 5); *m/z*: 470.17 (100.0%); exact mass: 470.17; elemental analysis: C (74.03), O (20.40), H (5.57). The addition of three extra atoms as opposed to that of the MS data (467) could be due to the overlapping of some peaks in the MS or the resolution of some other elements such as esters that are naturally attached to most unsaturated fatty acids (Jacobs et al., 1990). Our study identified the novel compound as a type of fatty acid because of the information derived from the spectroscopic data described above.

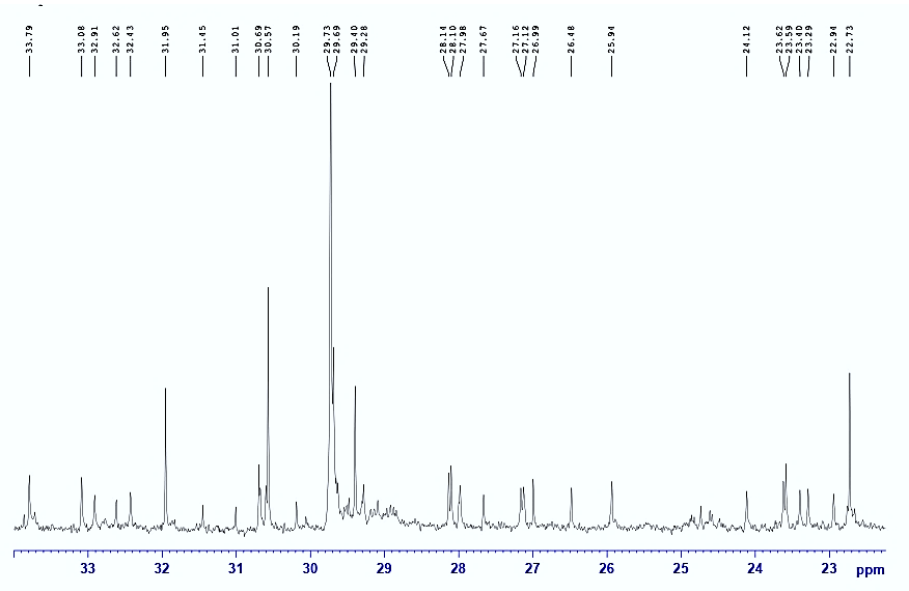

Figure 4. ^{13}C-NMR spectrum of isolated novel fatty acid

It has been previously reported that fatty acids such as linoleic, arachidic, and palmitic acids showed analgesic and anti-inflammatory potentials in inflammation-induced rat models (Forman et al., 2006). This report was not different from that obtained in the current study, where the isolated fatty acid showed dose-dependent antinociceptive and anti-inflammatory effects at higher doses. The isolated novel fatty acid showed significant inhibition in abdominal writhing in the animals within the experimental periods. The presence of olefinic rings and repeated chains of oxygen-bonded aromatic rings could be responsible for the biological activities of this compound. Again, many fatty acids originate from secondary metabolites, such as flavonoids, were reported to have anti-inflammatory potential. This is because they inhibit the production of mediators of inflammation by altering pathways like arachidonic acid, thereby, inhibiting many enzymes like prostaglandin, ATPase, lipoxygenase, cyclooxygenase, NADH oxidase, phospholipases, protein kinase, peroxidases, tyrosinases, and hydrolases. Thus, this novel fatty acid must have acted in a similar way to achieve the obtained result in the current study (Padmanabhan & Jangle, 2012). The number of abdominal writhing displayed by the compound showed its antinociceptive potential which was achieved through the prevention of prostaglandin production, that is peripheral pain inhibition mechanism investigated in this study. Therefore, the novel fatty acid must have achieved this biological activity by modulation of the peripheral and central routes of impulse (De Farias Freire et al., 1993; Pan et al., 2010).

Table 3. Peripheral antinociceptive activity of novel *2,4-PHPBEa* in acetic acid induced rats

Group	Number of writhing (± SD)	Inhibition of writhing (%)
Normal saline	18.04 ± 1.02	-
Standard drug	10.21 ± 0.24	43.40
2 mg/kg	6.10 ± 0.01*	66.19*
4 mg/kg	3.12 ± 0.02*	82.71*

Values are mean ± SD (n = 5)
*Statistically significant at $p < 0.05$ compared with the standard drug diclofenac sodium (one-way ANOVA followed by Duncan's multiple range test).

Similarly, inflammation is usually associated with signs like edema, redness, pain, as well as dysfunction of organs and organs tissues, and it is also associated with secretions of pain mediators (Vane & Botting, 1998). In the current study, at the doses of 2 and 4 mg/kg bw of the novel fatty acid, the diameters of carrageenan-induced paw edema decreased progressively within 60 min (Figure 6). The compound was able to achieve this by inhibiting the release of numerous mediators of inflammation like interleukin-6, nitric oxide, and α-tumor necrosis factor, which are body's innate immune mediators and prostaglandins (PGE2) (Dhasmana et al., 2014). The ability of *2,4-PHPBEa* to prohibit the production of these promoters of inflammation makes it an excellent agent of inflammation which was capable of preventing the expression of these pro-inflammatory factors. The result obtained was statistically significant when compared with the standard drug ibuprofen ($p < 0.05$).

Table 4. Central antinociceptive activity of novel fatty *2,4-PHPBEa* by tail immersion

Group	Number of responses (in 2 hours)			
	30 min	60 min	90 min	120 min
Normal saline	15.01 ± 1.11	14.06 ± 1.10	8.00 ± 0.11	7.01 ± 0.01
Standard drug	12.22 ± 1.02	12.00 ± 0.20	12.24 ± 1.21*	8.04 ± 0.28*
2 mg/kg	8.22 ± 1.21	8.00 ± 0.10	7.24 ± 0.12	7.10 ± 0.01*
4 mg/kg	4.08 ± 0.01	3.14 ± 0.01	3.01 ± 0.02	2.14 ± 0.01*

Values are mean ± SD (n = 5).
*Statistically significant at $p < 0.05$ compared with the standard drug morphine (one-way ANOVA followed by Duncan's multiple range test).

One of the largest worldwide health challenges currently is diabetes which has resulted in various types of life-threatening sicknesses like stroke, hypertension, and cardiac myopathy (Maritim et al., 2003). Since there are no guaranteed drugs currently to effectively manage and treat diabetes, there is a need to search for novel compounds with significant antidiabetic effects to serve as preferred drugs to the existing ones. In this present study, the result showed that there was a significant difference in plasma glucose baseline levels in all the groups before oral administration of the control standard drug Glibenclamide and various doses of *2,4-PHPBEa* (2 and 4 mg/kg bw). The ability of this compound to significantly reduce the glucose level in the animals was due to inhibition of the activity of α-glucosidase which facilitates the production of excess insulin (Wiernsperger, 2003). Some fatty acids have also been reported to be effective in ameliorating diabetic conditions, thus, the current novel fatty acid should also belong to this class of compounds.

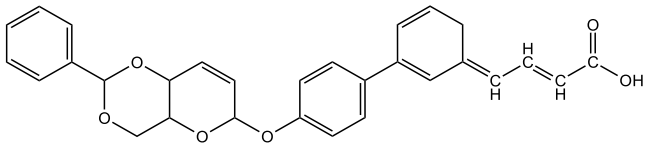

Figure 5. Proposed structure of novel fatty acid
(2*E*,4*E*)-4-(4'-(2-phenyl-4,4a,6,8a-tetrahydropyrano[3,2-d][1,3]dioxin-6-yl)-[1,1'-biphenyl]-3(4H)-ylidene)but-2-enoic acid
($C_{28}H_{26}O_6$), *m/z*: 470.17 (100.0%); exact mass: 470.17; elemental analysis: C (74.03), O (20.40), H (5.57).
The fatty acid was abbreviated as *2,4-PHPBEa*.

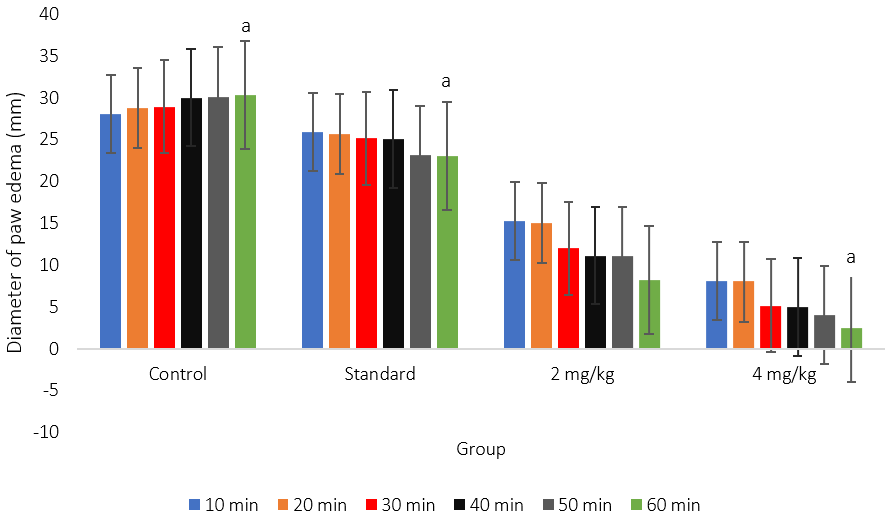

Figure 6. Effects of novel isolated fatty acid *2,4-PHPBEa* on diameter of carrageenan-induced paw edema in rats
Results are mean ± SD (n = 5). 'a' means statistically significant vs control ($p < 0.05$; one-way ANOVA)

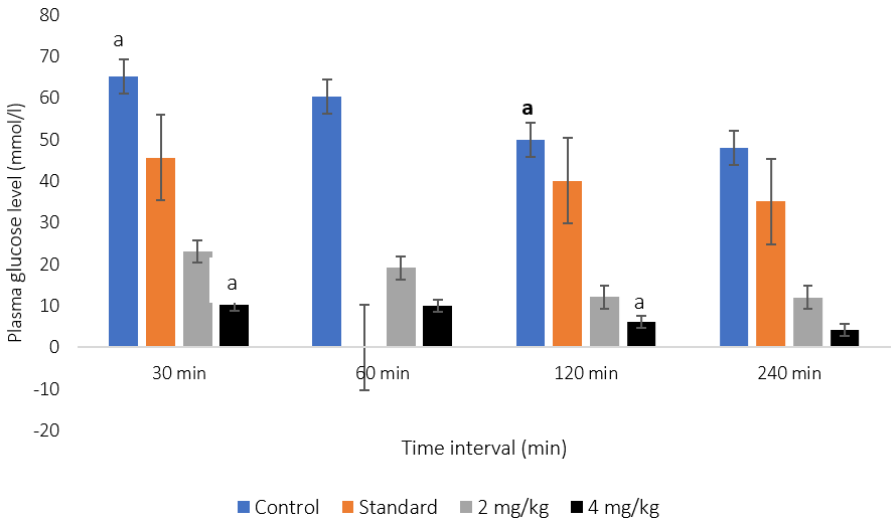

Figure 7. Effects of novel isolated fatty acid *2,4-PHPBEa* on plasma glucose level of alloxan-induced diabetic rats.
Results are mean ± SD (n = 5). 'a' means statistically significant vs control ($p < 0.05$; one-way ANOVA)

4. Conclusions

Our study showed that the novel fatty acid *2,4-PHPBEa* possessed potential antinociceptive, anti-inflammatory, and antidiabetic activities, in correlation with the inhibition of various promoters of pains, inflammation, and diabetes by blocking their metabolic pathways responsible for the negative effects on health. Furthermore, the current study design covered structural elucidation procedures to characterize the novel compound, which finally affirmed it as an unsaturated fatty acid. The ability of the characterized novel compound to act significantly on pain, inflammation (NSAIDs-like), and diabetes showed that it could be the promising'hit' bioactive compound in *R. simplex* which may be used against these illnesses, and further justifies its ethnomedicinal use in folkloric medicine. Finally, it is suggested that the mechanism of action of this novel fatty acid in pain, inflammation, and diabetes should be investigated for future research.

Acknowledgments

The authors were grateful to Dr. Mary Chama from the Department of Chemistry, University of Ghana, Legon, Ghana for helping out in some of the spectroscopic studies as well as Prof. Regina Appiah-Opong from the Department of Clinical Pathology, Noguchi, Memorial Institute for Medical Research, University of Ghana, Legon, Accra, Ghana.

Conflict of interest

The authors confirm that there are no known conflicts of interest.

Statement of ethics

Ethical approval for this study was obtained from the Research Ethical Committee of the University of Jos, Nigeria with approval number of UJ/FPS/F17-00379.

Availability of data and materials

All data generated or analyzed during this study are included in this published article.

Funding

None.

CRediT authorship contribution statement

Cletus Anes Ukwubile: Conceptualization, Investigation, Methodology, Final analysis, Writing -original and final draft
Henry Nettey: Resources, Formal analysis, Supervision
Troy Salvia Malgwi: Formal analysis, Investigation, Methodology, Software
Nnamdi David Menkiti: Formal analysis, Investigation, Software

ORCID Numbers of the Authors

C. A. Ukwubile: 0000-0001-7183-4510
H. Nettey: 0000-0002-5408-5957
T. S. Malgwi: 0000-0001-5051-8754
N. D. Menkiti: 0000-0001-6979-0088

Supplementary File

The supplementary file accompanying this article is available at https://ijpbp.com/index.php/ijpbp/libraryFiles/downloadPublic/14.

Publisher's Note

All claims expressed in this article are solely those of the authors and do not necessarily represent those of their affiliated organizations, or those of the publisher, the editors and the reviewers. Any product that may be evaluated in this article, or claim that may be made by its manufacturer, is not guaranteed or endorsed by the publisher.

This is an open-access article distributed under the terms of the Creative Commons Attribution 4.0 International License (CC BY). The use, distribution or reproduction in other forums is permitted, provided the original author(s) and the copyright owner(s) are credited and that the original publication in this journal is cited, in accordance with accepted academic practice. No use, distribution or reproduction is permitted which does not comply with these terms.

References

Abotsi, W. K. M., Lamptey, S. B., Afrane, S., Boakye-Gyasi, E., Umoh, R. U., & Woode, E. (2017). An evaluation of the anti-inflammatory, antipyretic and analgesic effects of hydroethanol leaf extract of *Albizia zygia* in animal models. *Pharmaceutical Biology, 55*(1), 338-348.

Belachew, T. F., Asrade, S., Geta, M., & Fentahun, E. (2020). In vivo evaluation of wound healing and anti-inflammatory activity of 80% methanol crude flower extract of *Hagenia abyssinica* (Bruce) JF Gmel in mice. *Evidence-Based Complementary and Alternative Medicine, 2020*, 9645792.

Boadu, A. A., & Asase, A. (2017). Documentation of Herbal Medicines Used for the Treatment and Management of Human Diseases by Some Communities in Southern Ghana. *Evidence-Based Complementary and Alternative Medicine, 2017*, 3043061.

De Farias Freire, S. M., Da Silva Emim, J. A., Lapa, A. J., Souccar, C., & Torres, L. M. B. (1993). Analgesic and antiinflammatory properties of *Scoparia dulcis* L. extracts and glutinol in rodents. *Phytotherapy Research, 7*(6), 408-414.

Dhasmana, D., Hathorn, E., McGrath, R., Tariq, A., & Ross, J. D. (2014). The effectiveness of nonsteroidal anti-inflammatory agents in the treatment of pelvic inflammatory disease: a systematic review. *Systematic Reviews, 3*(79), 1-6.

Evans, W. (2002). *Trease and Evans Pharmacognosy*: Souders Elsevier.

Forman, G. S., Bellabarba, R. M., Tooze, R. P., Slawin, A. M., Karch, R., & Winde, R. (2006). Metathesis of renewable unsaturated fatty acid esters catalysed by a phoban-indenylidene ruthenium catalyst. *Journal of Organometallic Chemistry, 691*(24-25), 5513-5516.

González, R., Ballester, I., López-Posadas, R., Suárez, M., Zarzuelo, A., Martínez-Augustin, O., & Medina, F. S. D. (2011). Effects of flavonoids and other polyphenols on inflammation. *Critical Reviews in Food Science and Nutrition, 51*(4), 331-362.

Ibrahim, M. A., Koorbanally, N. A., & Islam, M. S. (2014). Anti-oxidative activity and inhibition of key enzymes linked to type 2 diabetes (α-glucosidase and α-amylase) by *Khaya senegalensis*. *Acta Pharmaceutica, 64*(3), 311-324.

Iwu, M. M. (2014). *The Medicinal plants of West tropical Africa. 2nd Edition*: Taylor & Francis.

Jacobs, H., Singh, T., Reynolds, W. F., & McLean, S. (1990). Isolation and ^{13}C-NMR Assignments of Cucurbitacins from *Cayaponia angustiloba*, *Cayaponia racemosa*, and *Gurania subumbellata*. *Journal of Natural Products, 53*(6), 1600-1605.

Jothy, S. L., Zakaria, Z., Chen, Y., Lau, Y. L., Latha, L. Y., Shin, L. N., & Sasidharan, S. (2011). Bioassay-directed isolation of active compounds with antiyeast activity from a *Cassia fistula* seed extract. *Molecules, 16*(9), 7583-7592.

Kumar, D., Kumar, H., Vedasiromoni, J., & Pal, B. C. (2012). Bio-assay guided isolation of α-glucosidase inhibitory constituents from *Hibiscus mutabilis* Leaves. *Phytochemical Analysis, 23*(5), 421-425.

Kumar, N., Devineni, S. R., Gajjala, P. R., Dubey, S. K., & Kumar, P. (2017). Synthesis, isolation, identification and characterization of new process-related impurity in isoproterenol hydrochloride by HPLC, LC/ESI-MS and NMR. *Journal of Pharmaceutical Analysis, 7*(6), 394-400.

Maritim, A., Sanders, R., & Watkins, J. (2003). Diabetes, oxidative stress, and antioxidants: a review. *Journal of Biochemical and Molecular Toxicology, 17*(1), 24-38.

Mohamed, E. A. H., Siddiqui, M. J. A., Ang, L. F., Sadikun, A., Chan, S. H., Tan, S. C., Asmawi, M. Z., & Yam, M. F. (2012). Potent α-glucosidase and α-amylase inhibitory

activities of standardized 50% ethanolic extracts and sinensetin from *Orthosiphon stamineus* Benth as anti-diabetic mechanism. *BMC Complementary and Alternative Medicine, 12*(176), 1-7.

Nguyen, T., Chen, X., Chai, J., Li, R., Han, X., Chen, X., Liu, S., Chen, M., & Xu, X. (2020). Antipyretic, anti-inflammatory and analgesic activities of *Periplaneta americana* extract and underlying mechanisms. *Biomedicine & Pharmacotherapy, 123*, 109753.

Ojo, O. A., Ajiboye, B. O., Imiere, O. D., Adeyonu, O., Olayide, I., & Fadaka, A. (2018). Antioxidative properties of *Blighia sapida* KD Koenig stem bark extract and inhibitory effects on carbohydrate hydrolyzing enzymes associated with non-insulin dependent diabetes mellitus. *Pharmacognosy Journal, 10*(2), 376-383.

Padmanabhan, P., & Jangle, S. (2012). Evaluation of in-vitro anti-inflammatory activity of herbal preparation, a combination of four medicinal plants. *International Journal of Basic and Applied Medical Sciences, 2*(1), 109-116.

Pan, M.-H., Lai, C.-S., & Ho, C.-T. (2010). Anti-inflammatory activity of natural dietary flavonoids. *Food & Function, 1*(1), 15-31.

Pinto, M. E., Araujo, S. G., Morais, M. I., Sa, N. P., Lima, C. M., Rosa, C. A., Siqueira, E. P., Johann, S., & Lima, L. A. (2017). Antifungal and antioxidant activity of fatty acid methyl esters from vegetable oils. *Anais da Academia Brasileira de Ciências, 89*(3), 1671-1681.

Schippmann, U., Leaman, D., & Cunningham, A. (2006). *Plants as source of medicines: new perspectives* (Vol. 17). Netherlands: Springer, Dordrecht.

Sharma, H. K., Chhangte, L., & Dolui, A. K. (2001). Traditional medicinal plants in Mizoram, India. *Fitoterapia, 72*(2), 146-161.

Siddiqui, M. J. A., Ismail, Z., & Saidan, N. H. (2011). Simultaneous determination of secondary metabolites from *Vinca rosea* plant extractives by reverse phase high performance liquid chromatography. *Pharmacognosy Magazine, 7*(26), 92-96.

Tabuti, J. R., Kukunda, C. B., Kaweesi, D., & Kasilo, O. M. (2012). Herbal medicine use in the districts of Nakapiripirit, Pallisa, Kanungu, and Mukono in Uganda. *Journal of Ethnobiology and Ethnomedicine, 8*, 35.

Ukwubile, C. A., Ikpefan, E. O., Malgwi, T. S., Dibal, M. Y., Famurewa, A. C., Rasheed-Jada, H., Milagawanda, H. H., & Suleiman, A. U. (2021). Antioxidant, anti-inflammatory, analgesic and in vitro-in vivo cytotoxicity effects of *Spondias venulosa* (Engl.) Engl. leaf extracts on MCF-7/S0. 5 and OV7 cancer cell lines. *Scientific African, 13*, e00917.

Valdés, E., González, C., Díaz, K., Vásquez-Martínez, Y., Mascayano, C., Torrent, C., Cabezas, F., Mejias, S., Montoya, M., *et al.* (2020). Biological properties and absolute configuration of flavanones from *Calceolaria thyrsiflora* Graham. *Frontiers in Pharmacology, 11*, 1125.

Vane, J. R., & Botting, R. M. (1998). Anti-inflammatory drugs and their mechanism of action. *Inflammation Research, 47*(2), 78-87.

Wiernsperger, N. (2003). Oxidative stress as a therapeutic target in diabetes: revisiting the controversy. *Diabetes & Metabolism, 29*(6), 579-585.

Yeshwante, S., Juvekar, A., Nagmoti, D., Wankhede, S., Shah, A., Pimprikar, R., & Saindane, D. (2009). Anti-inflammatory activity of methanolic extracts of Dillenia indica L. leaves. *Journal of Young Pharmacists, 1*(1), 63.

Int. J. Plant Bas. Pharm. (2023) 3(1), 41-46

INTERNATIONAL JOURNAL OF PLANT BASED PHARMACEUTICALS

https://ijpbp.com

RESEARCH ARTICLE

OPEN ACCESS

Antioxidant potential of *Drosera peltata* in Dalton Ascites Lymphoma (DAL) bearing mice

Raju Asirvatham[a*], Arockiasamy Josphin Maria Christina[b]

[a] *St. Joseph's College of Pharmacy, Department of Pharmacology, Cherthala, Kerala, India*
[b] *Ahalia School of Pharmacy, Department of Pharmacology, Palakkad, Kerala, India*

ARTICLE INFO

Article History:

Received: 19 September 2022
Revised: 7 October 2022
Accepted: 10 October 2022
Available online: 14 October 2022

Edited by: B. Tepe

Keywords:

Drosera peltata
Dalton Ascites Lymphoma
Glutathione
Malondialdehyde

ABSTRACT

Cancer is one of the prominent causes of death reported by World Health Organization (WHO). The purpose of this study was to measure the antioxidant status of animals treated with 250 and 500 mg/kg doses of ethanol and aqueous extract of *Drosera peltata* on Dalton Ascites Lymphoma (DAL) inoculated mice. A total of 70 mice were divided into 7 groups, each group with ten mice. The first group (negative control) received normal food and water for 14 days and was kept under normal conditions. The second group also received normal food and water for 14 days, which was used as a cancer (positive) control. The third group received 5-fluorouracil (20 mg/kg, i.p.) once a day for 14 days. The fourth and fifth group animals received 250 and 500 mg/kg of ethanol extracts of *D. peltata* (EEDP) whereas the sixth and seventh groups of mice received 250 and 500 mg/kg of aqueous extracts of *D. peltata* (AEDP), orally for 14 days. All the groups were inoculated with DAL (2×10^6 cells/mouse, i.p.) except group I, 24 hours before the commencement of the drug treatment. After the completion of treatment, blood was drawn retro-orbitally and the animals were sacrificed to isolate the liver, lungs, kidneys, and brain for observing tissue antioxidant status. The parameters analyzed were total protein (TP), catalase (CAT), malondialdehyde (MDA), superoxide dismutase (SOD), peroxidase (P), and glutathione (GSH) from the tissues apart, and the protein carbonyl content (PCC) also measured from the blood sample. Treatment with EEDP and AEDP significantly lowered the MDA levels from 23 to 10 mmol/ml in the blood, whereas from 28 to 4 nm/g in tissue isolates of the liver, lungs, kidneys, and brain. It also raised the TP, GSH, SOD, CAT, and P levels in the blood and in the tissue samples of the cancer cell line inoculated animals, where their levels were close to those observed in control (negative) group animals. The results proposed that both extracts of *D. peltata* ameliorated various tissue antioxidant levels in mice with DAL cancer lines comparable to the negative control.

1. Introduction

Ayurveda, the Indian medical system, treats a variety of illnesses, including cancer, primarily using herbal medicines or formulations. It is one of the oldest medical systems covering thousands of medical concepts and hypotheses. Interestingly, Ayurveda can treat many chronic diseases that modern medicine cannot treat, such as cancer, diabetes, arthritis, and asthma (Parasuraman et al., 2014). Cancer is one of the prominent causes of death reported by WHO (WHO, 2022). There are several ways to treat cancer in modern medicine. These include chemotherapy, radiation therapy, and surgery. Chemotherapy is currently considered to be the most effective way to treat cancer (Baskar et al., 2012). The high toxicity of most anticancer drugs has facilitated the development of less toxic and cheaper complements. Plants have long been used to treat cancer. An important strategy for developing effective anti-cancer drugs is the discovery of phytochemicals with anti-cancer activity from natural resources. Plant-derived

Reviewed by:
Sujin Johny M. Pharm: Kuwait University, Kuwait
Alen Joel: King Kalid Unuversity, Abha, Saudi Arabia

* Corresponding author(s):
E-mail address:
rajuasirvatham@gmail.com (R. Asirvatham)
e-ISSN: 2791-7509
doi: https://doi.org/10.29228/ijpbp.14

anticancer compounds and their derivatives are effective in cancer treatment. Natural plant-derived substances such as flavonoids, terpenoids, and steroids have received a great deal of attention in recent years due to their various pharmacological actions, such as antioxidants and antitumors (Desai et al., 2008). Similarly, they have proven useful in the prevention and control of adverse pathophysiological conditions and complex diseases including cancer. One of the plants rich in therapeutically important compounds as well as used in Ayurvedic formulations is *Drosera*. The genus *Drosera* is commonly known as Sandew. It is one of the largest genera of more than 170 species of carnivorous plants belonging to the Droseraceae family. In India, three *Drosera* plants were identified namely *Drosera indica* L., *D. burmannii* Vahl., and *D. peltata* J.Sm. These include 1,4 naphthoquinone, plumbagin, ramantaseon and its glucosiderosoliside, and flavonoids such as quercetin and hyperoside. In both Plumbaginaceae and Droseraceae, a yellow color pigment was found as a main phytoconstituent, named plumbagin (5-hydroxy-2-methyl-1,4-naphthoquinone). Plumbagin is a major active ingredient with a variety of pharmacological actions, including anti-fertility, anti-malaria, anti-viral, anti-bacterial, anti-convulsant, anti-cancer, and leishmania drugs. Plumbagin and quercetin are the biologically active important phytoconstituents found in *Drosera*. Pharmacological effects are based on the number of constituents present in each plant (Asirvatam & Christina, 2018). HPTLC method was used to quantify the plumbagin and quercetin content among the three Indian *Drosera* species (Asirvatham et al., 2020). The above species are used in several clinical manifestations, such as memory loss, vision loss, infertility, general weakness of the body, the development of premature aging, and bronchial asthma. It is used as an important ingredient in Ayurveda preparations ('Swarnabhasma'-Golden ash) for rheumatoid arthritis, diabetes, and neuropathy (Asirvatham et al., 2013). Cold decoration of *D. indica* is used to remove corn and these species are mentioned in the list of endangered medicinal plants (Reddy et al., 2001). Earlier in this report, the in vitro antioxidant and anticancer potential as well as the in vivo effect of *D. peltata* have been reported for different in vitro antioxidant and anticancer models (Balaji & Asirvatham, 2015). This study aimed to determine the ability of cells to recover and retain the antioxidant enzymes with the treatment of ethanol and an aqueous extract of 250 and 500 mg/kg *D. peltata* in Dalton Ascites Lymphoma (DAL) bearing mice.

2. Materials and methods

2.1. Plant material and extraction

The whole plant of *D. peltata* (Figure 1) was collected from Munnar, Kerala, India (10.0889° N, 77.0595° E) in December 2008. Air-dried, coarsely powdered whole plants (350 g) were defatted with petroleum ether (60-80 °C), and followed the merc was extracted with ethanol solvent in a Soxhlet extractor for 72 hours. The obtained ethanol extract was concentrated and allowed to dry under a controlled temperature (40-50 °C). The obtained merc was soaked in water containing chloroform for 2 days, filtered, concentrated, and allowed dry to get the aqueous extract (Asirvatham et al., 2013). Ethanol extract of *D. peltata* (EEDP) and aqueous extract of *D. peltata* (AEDP) were reconstituted with distilled water for animal study.

2.2. Experimental animal and study approval

The treatment protocol (A. Raju 0903PH2254/JNTUH 2009) was initially presented to the Institutional Animal Ethical Committee. After reviewing the procedure, the committee had permitted to conduct the study. Adult male and female Swiss albino mice weighing approximately 20 to 25 g were acclimated to experimental conditions for approximately 2 weeks before subjecting to the experimental procedure. Tumor cell line-Dalton Ascites Lymphoma (DAL) cells-were obtained from the Amala Cancer Institute in Thrissur, Kerala, India. DAL cells were maintained in mice by weekly intraperitoneal (i.p.) inoculation of 2 x 10^6 cells/mouse.

2.3. Treatment protocol

It was a 14-day study, in which a total of 70 mice were divided into seven groups containing ten animals in each (Christina et al., 2004). All the mice were inoculated with DAL cells (2 × 10^6 cells/mouse, i.p.) 24 hours before the commencement of the drug treatment, except mice belonging to group I (negative control).

Group I: The animals received normal food and water for 14 days
Group II (DAL control): The animals received normal food and water for 14 days
Group III (DAL cells): The animals received 5- fluorouracil (20 mg/kg, i.p) for 14 days
Group IV (DAL cells): The animals received EEDP (250 mg/kg, p.o.) for 14 days
Group V (DAL cells): The animals received EEDP (500 mg/kg, p.o.) for 14 days
Group VI (DAL cells): The animals received AEDP (250 mg/kg, p.o.) for 14 days
Group VII (DAL cells): The animals received AEDP (500 mg/kg, p.o.) for 14 days

On the 15th day, blood was collected by retro-orbital puncture and was allowed to stand for 45 minutes at room temperature. Serum was collected after centrifugation at 2500 rpm at 30 °C for 15 minutes to estimate antioxidant enzyme levels (Demirci et al., 2011) in serum such as malondialdehyde (MDA), catalase (CAT), glutathione (GSH), superoxide dismutase (SOD), and protein carbonyl content (PCC).

After the collection of blood, mice were sacrificed with excessive anesthesia, and the liver, lung, kidney, and brain samples were removed for the measurement of tissue antioxidant status. To estimate the content of antioxidants in the tissue, the isolated organ was divided into two parts to prepare tissue homogenates (Vani et al., 1990). The first homogenate (10%, w/v) was prepared with potassium chloride (KCl, 0.15 M) and the content was centrifuged at 8000 rpm for 10 minutes, and the supernatant was used to measure total protein (TP), peroxidase (P), catalase (CAT), and malondialdehyde (MDA). Similarly, the second homogenate (10%, w/v) was prepared with sucrose phosphate buffer (5M, pH 7.4) and the test tube content was centrifuged at 8000 rpm for 10 minutes, and the supernatant was used for the measurement of glutathione peroxidase (GSH) and superoxide dismutase (SOD). The determination of the levels of mentioned antioxidant enzymes from tissue homogenates was done by COBAS MIRA PLUS–S autoanalyzer (Roche, Switzerland) using antioxidant estimation assay kits from Agappe Diagnostics, India (Raju et al., 2022).

2.4. Statistical analysis

The results obtained after statistical analysis were expressed in terms of mean ± SEM. To present the results, the data were evaluated using a one-way ANOVA followed by Newman Keul's multiple comparison tests.

3. Results and discussion

Ayurvedic treatment is very effective, but the proper pharmacovigilance, mechanism of action, pharmacokinetics, and other important aspects of Ayurvedic drugs are not yet fully understood. Moreover, due to the lack of evidence, the basic ideologies in Ayurveda are not scientifically acceptable. With the help of advanced research methodologies, validated research, and advanced technology, the Western medicine system has been almost at the forefront of the medical system. Therefore, there is an urgent need for research methodologies to validate the fundamental concept of Ayurveda treatment because a perfect health restoration including maintenance is possible in Ayurvedic drug treatment (Parasuraman et al., 2014).

Figure 1. *D. peltata* (from https://flowersofindia.net/catalog/)

The generation of free radicals is the basic etiology of most human diseases condition, and there is an increasing need to develop techniques for measuring free radicals and their responses in vivo. These free radicals are so reactive that they have a short lifespan because of that, are not suitable for direct assays, and are determined by indirect methods where various end products of the target molecule like lipids, proteins, and DNA are measured quantitatively (Sara et al., 2015). The end product formed from the reactions of free radicals and biomolecules is more stable than free radicals. Measurements of these end products concerning the oxidation target are an important aspect of the treatment modulation. MDA and PCC are the by-products of lipid peroxidation and oxidized proteins respectively (Ahmad et al., 2008).

Medicinal plants have various phytoconstituents which are an excellent source of lead compounds to develop therapeutic drugs including anticancer agents. Therefore, many studies have been conducted on herbs for various ethnobotany reasons (Newman & Cragg, 2009) The antitumor properties of the extracts from these plant species have already been reported (Raju et al., 2012).

Table 1 shows the status of various blood antioxidants in DAL cancer cell line-bearing mice. In this study, MDA levels were increased significantly ($p < 0.001$) in DAL control mice (positive control) when compared to negative controls. After treatment with EEDP and AEDP at the doses of 250, and 500 mg/kg, levels of MDA were reduced, and the other free radical protective enzymes were slightly increased when compared to the positive control group. Similarly, serum PCC was raised in DAL-controlled group mice (positive control), but 14 days of extract treatment at doses of 250, 500 mg/kg EEDP and AEDP significantly re-established PCC ($p < 0.001$) like the negative control group mice. Inoculation of DAL cells also caused a significant increase in the level of MDA in tissues of the liver, brain, lungs, and kidneys when compared to the negative control animals, and simultaneous significant ($p < 0.001$) reductions in SOD, TP, GSH, P, and CAT levels were also observed in the above tissue samples. 14 days of continuous treatment with EEDP (250 and 500 mg/kg) brought back the alteration of internal antioxidant status to normal levels (Tables 2-5). Most of the parameters were returned to normal levels upon the administration of a high dose of EEDP and AEDP. Almost the same results like restoration of SOD, TP, GSH, P, and CAT and reduction of MDA were observed with 5-fluorouracil-treated mice. EEDP at 250 mg/kg and AEDP at 250 mg/kg treatment showed a non-significant ($p > 0.05$) effect on the restoration of P in the liver and kidney.

This study was conducted to estimate the antioxidant status in blood and various organs and the effectiveness of EEDP and AEDP on the restoration of these parameters in cancer-bearing animals. Significantly increased levels of MDA and SOD in serum, liver, brain, lung, and kidney were found in the tumor-bearing animal, which causes tissue damage and loss of functional completeness of cell membranes (Gupta et al., 2004). Lipid peroxidation is an autocatalytic chain reaction initiated by free radicals which affect the pathological state of cells. MDA, the marker compound of lipid peroxidation, is found at a high concentration in cancerous tissues than in normal organs (Yagi, 1987). GSH, an effective inhibitor of neoplastic cell processes, and a part of the endogenous antioxidant system plays an important role in cell proliferation. It is biosynthesized especially in high concentrations in the liver and is known to have important functions in the protection process against free radicals (Shaik & Mehvar, 2006). Excessive production of free

radicals leads to oxidative stress and damage to macromolecules which affects many functions of important organs, especially in the liver, kidneys, brain, and lungs, even if the tumor site does not directly interfere with these organs (DeWys, 1982). The generated oxygen radicals destruct the cell membranes by lipid peroxidation and can lead to tissue and/or organ damage (Koca et al., 2005) followed by the reduction of other enzyme systems such as SOD, CAT, and GSH that counteract the harmful effects of reactive oxygen species (Ichimura et al., 2004). The reduction in SOD, CAT, GSH, and P in the DAL group is due to the loss of Mn^{2+} in mitochondria (Sun et al., 1989). Tumor growth also reduces the level of SOD and CAT and arrests the functional activity in cancer-bearing mice.

Table 1. Effect of EEDP and AEDP on blood antioxidant status of DAL bearing mice

Blood	CAT U/ml serum	SOD U/ml serum	P U/ml serum	GSH U/l	MDA nmol/ml	PCC nmol/mg protein
Normal	14.4 ± 0.13	7.5 ± 0.67	34.5 ± 1.25	73.98 ± 0.51	8.65 ± 0.17	1.9 ± 0.8
DAL (control)	4.48 ± 0.19	2.63 ± 0.11	21.35 ± 0.54	43.2 ± 0.4	21.65 ± 0.15	8.6 ± 1.6
DAL + 5FU (20 mg/kg)	12.63 ± 0.23	6.68 ± 0.11	33.13 ± 0.72	73.5 ± 0.15	7.68 ± 0.18	2.2 ± 0.7
DAL + EEDP (250 mg/kg)	10.85 ± 0.13[a]	4.6 ± 0.24[a]	29.08 ± 0.61[a]	63.95 ± 0.58[a]	11.63 ± 0.11[a]	4.3 ± 1.1[a]
DAL + EEDP (500 mg/kg)	13.3 ± 0.11[a]	5.68 ± 0.25[a]	33.88 ± 0.31[a]	73.15 ± 0.42[a]	8.68 ± 0.18[a]	2.1 ± 0.54[a]
DAL + AEDP (250 mg/kg)	5.73 ± 0.18[a]	4.55 ± 0.1[a]	23.63 ± 0.51[b]	49.15 ± 0.84[a]	17.83 ± 0.15[a]	6.5 ± 1.5[a]
DAL + AEDP (500 mg/kg)	9.53 ± 0.2[a]	4.58 ± 0.18[a]	28.23 ± 0.54[a]	56.9 ± 1.77[a]	14.75 ± 0.12[a]	5.5 ± 0.6[a]

The data were expressed as mean ± SEM, n = 10. The data were analyzed by One Way Analysis of Variance (ANOVA) followed by Newman-Keul's multiple comparison test where a: $p < 0.001$. All the data were compared with cancer control group.

Table 2. Effect of EEDP and AEDP on the liver antioxidant status of DAL bearing-mice

Liver	TP mg/dl	CAT U/mg tissue	SOD U/mg tissue	P nm/100mg tissue	GSH nm/100mg tissue	MDA nm/g protein
Normal	12.25 ± 0.66	10.45 ± 0.1	4.35 ± 0.06	22.78 ± 0.29	53.05 ± 0.21	4.65 ± 0.06
DAL (control)	5.37 ± 0.15	1.83 ± 0.02	14.93 ± 0.36	16.7 ± 0.22	43.05 ± 0.21	24.85 ± 0.27
DAL + 5FU (20 mg/kg)	11.55 ± 0.29	9.13 ± 0.3	5.2 ± 0.44	21.9 ± 1.21	50.95 ± 3.66	5.7 ± 0.14
DAL + EEDP (250 mg/kg)	11.97 ± 0.27[a]	8.28 ± 0.38[a]	5.6 ± 0.2[a]	21.27 ± 0.43[a]	54.1 ± 0.48[a]	5.5 ± 0.18
DAL + EEDP (500 mg/kg)	12.55 ± 0.28[a]	9.75 ± 0.15[a]	3.2 ± 0.1[a]	23.9 ± 0.56[a]	56.4 ± 0.35[a]	3.6 ± 0.12[a]
DAL + AEDP (250 mg/kg)	9.95 ± 0.14[a]	7.75 ± 0.25[a]	8.07 ± 0.43[a]	19.95 ± 0.33[b]	51.07 ± 0.51[b]	13.2 ± 0.46[a]
DAL + AEDP (500 mg/kg)	11 ± 0.36[a]	9 ± 0.19[a]	6.17 ± 0.16[a]	21.83 ± 0.73[a]	53.15 ± 0.54[a]	7.5 ± 0.15[a]

The data were expressed as mean ± SEM, n = 10. The data were analyzed by One Way Analysis of Variance (ANOVA) followed by Newman-Keul's multiple comparison test where a: $p < 0.001$, b: $p < 0.01$. All the data were compared with cancer control group.

Table 3. Effect of EEDP and AEDP on the kidney antioxidant status of DAL bearing mice

Kidney	TP mg/dl	CAT U/mg tissue	SOD U/mg tissue	P nm/100mg tissue	GSH nm/100mg tissue	MDA nm/g protein
Normal	22.68 ± 0.27	11.48 ± 0.14	23.55 ± 0.4	77.5 ± 3.23	101.85 ± 0.61	12.87 ± 0.67
DAL (control)	16.6 ± 0.22	4.92 ± 0.32	12.83 ± 0.08	55.65 ± 1.88	50.75 ± 0.06	22.03 ± 0.11
DAL + 5FU (20 mg/kg)	21.53 ± 0.05	10.35 ± 0.13	20.75 ± 0.2	72.18 ± 0.94	96.82 ± 0.79	10.73 ± 0.86
DAL + EEDP (250 mg/kg)	22.4 ± 0.16[a]	10.5 ± 0.01[a]	19.53 ± 0.11[a]	75.98 ± 0.94[a]	87.87 ± 0.75[a]	10 ± 0.24[a]
DAL + EEDP (500 mg/kg)	21.75 ± 0.06[a]	10.35 ± 0.06[a]	22.05 ± 0.59[a]	79.62 ± 0.39[a]	94.23 ± 0.69[a]	11 ± 0.4[a]
DAL + AEDP (250 mg/kg)	21.2 ± 0.34[a]	10.9 ± 0.15[a]	19.85 ± 0.06[a]	66.75 ± 0.59[b]	63.63 ± 1.26[a]	14.65 ± 0.19[a]
DAL + AEDP (500 mg/kg)	21.63 ± 0.33[a]	10.93 ± 0.35[a]	16.05 ± 0.42[a]	71.23 ± 0.39[a]	71.95 ± 1.26[a]	15.72 ± 0.35[a]

The data were expressed as mean ± SEM, n = 10. The data were analyzed by One Way Analysis of Variance (ANOVA) followed by Newman-Keul's multiple comparison test where a: $p < 0.001$, b: $p < 0.01$. All the data were compared with cancer control group.

Table 4. Effect of EEDP and AEDP on the brain antioxidant status of DAL bearing mice

Brain	TP mg/dl	CAT U/mg tissue	SOD U/mg tissue	P nm/100mg tissue	GSH nm/100mg tissue	MDA nm/g protein
Normal	41.82 ± 2.83	22.1 ± 0.59	33.3 ± 0.58	34.66 ± 0.66	82.48 ± 0.94	8.48 ± 0.38
DAL (control)	9.82 ± 0.28	8.4 ± 1.67	15.64 ± 0.39	10.36 ± 0.33	38.16 ± 0.18	27.06 ± 0.66
DAL + 5FU (20 mg/kg)	35.84 ± 1.35	21.22 ± 0.37	30.64 ± 0.77	29.04 ± 0.69	79.68 ± 1.25	10.08 ± 0.32
DAL + EEDP (250 mg/kg)	26.22 ± 0.58[a]	16.58 ± 0.77[a]	25.06 ± 0.49[a]	23.42 ± 0.89[a]	69.44 ± 0.34[a]	15.92 ± 0.9[a]
DAL + EEDP (500 mg/kg)	40.62 ± 0.92[a]	21 ± 0.46[a]	31.68 ± 0.62[a]	31.92 ± 1.2[a]	80.92 ± 0.72[a]	9 ± 0.32[a]
DAL + AEDP (250 mg/kg)	24.78 ± 0.41[a]	14.28 ± 0.53[a]	22.74 ± 1.1[a]	20.98 ± 2.15[a]	57.28 ± 1.28[a]	16.92 ± 0.9[a]
DAL + AEDP (500 mg/kg)	33.08 ± 0.69[a]	17.56 ± 1.04[a]	27.68 ± 0.57[a]	29.48 ± 0.71[a]	64.3 ± 1.55[a]	15.06 ± 0.98[a]

The data were expressed as mean ± SEM, n = 10. The data were analyzed by One Way Analysis of Variance (ANOVA) followed by Newman-Keul's multiple comparison test where a: $p < 0.001$. All the data were compared with cancer control group.

Table 5. Effect of EEDP and AEDP on the lung antioxidant status of DAL bearing mice

Lung	TP mg/dl	CAT U/mg tissue	SOD U/mg tissue	P nm/100mg tissue	GSH nm/100mg tissue	MDA nm/g protein
Normal	26.55 ± 0.39	20.55 ± 0.28	13.63 ± 0.28	42.18 ± 0.51	62.73 ± 0.35	7.65 ± 0.17
DAL (control)	16.03 ± 0.73	6.48 ± 0.15	4.68 ± 0.11	30.63 ± 6.33	22.95 ± 1.11	23.05 ± 0.22
DAL + 5FU (20 mg/kg)	23.5 ± 0.48	20.05 ± 0.23	12.7 ± 0.18	38.15 ± 0.31	60.65 ± 0.19	6.75 ± 0.36
DAL + EEDP (250 mg/kg)	22.9 ± 0.44[a]	18.8 ± 0.19[a]	11.93 ± 0.32[a]	40.75 ± 0.27[a]	59.63 ± 0.25[a]	6.28 ± 0.08[a]
DAL + EEDP (500 mg/kg)	28.65 ± 0.92[a]	20.8 ± 0.21[a]	10.5 ± 0.2[a]	43.6 ± 0.11[a]	63.95 ± 0.12[a]	8.35 ± 0.12[a]
DAL + AEDP (250 mg/kg)	24.18 ± 0.49[a]	18.07 ± 0.29[a]	10.52 ± 0.17[a]	38.87 ± 0.54[a]	54.2 ± 0.89[a]	10.53 ± 0.25[a]
DAL + AEDP (500 mg/kg)	26.33 ± 0.4[a]	20.35 ± 0.29[a]	12.57 ± 0.26[a]	48.8 ± 2.18[a]	60.88 ± 0.32[a]	6.63 ± 0.14[a]

The data were expressed as mean ± SEM, n = 10. The data were analyzed by One Way Analysis of Variance (ANOVA) followed by Newman-Keul's multiple comparison test where a: $p < 0.001$. All the data were compared with cancer control group.

The PCC of blood has increased significantly in the positive control group mice. The carbonyl content of proteins has been reported to be a sensitive and early marker of oxidative stress on tissues compared to lipid peroxidation (Rajesh et al., 2004). Elevated levels

of PCC have been reported in patients with brain tumors. Elevated values of PCC strongly suggest that oxidative stress (OS) may play a vital role in the carbonylation of protein in the brain which is an oxidation reaction mediated by Fe^{2+} and Cu^{2+}. Free radicals bind to the cation binding site of a protein in presence of H_2O_2 or O_2, which converts the side chain of the amino acid to a carbonyl group. Accumulation of carbonyl groups in a protein causes many chemical modifications to form the oxidation product of the protein (Levine et al., 2000). In this study, a significant increase was determined in PCC levels in DAL-inoculated mice. The PCC levels were recovered after the administration of two doses of EEDP and AEDP. Administration of EEDP and AEDP significantly increased the SOD and CAT levels.

Plant extracts containing antioxidative components such as plumbagin have been reported to be cytotoxic to tumor cells (Ruby et al., 1995) and have antitumor activity in experimental animals (Liu et al., 1998). Induction of apoptosis and cell cycle arrest during the G_2/M phase are the two main mechanisms behind the antioxidative and antitumor activity. The effects of free radicals on the initiation of cancer are well documented (Maity et al., 2000). Mice treated with 250, and 500 mg/kg EEDP and AEDP showed inhibition of lipid peroxidation, reflected as a reduction in MDA and PCC. Furthermore, EEDP and AEDP administration also restored the antioxidant enzyme systems of the blood, liver, brain, kidney, and lungs to almost normal levels.

4. Conclusions

Natural antioxidants may enhance the endogenous antioxidant defenses against ROS disruption and restore optimal balance by neutralizing reactive species. They are becoming more and more important because of their important role in disease prevention. Ethanol extracts of *D. peltata* showed significantly higher activity than the aqueous extracts. The possible mechanism of the antitumor activity of *D. peltata* may be due to the antioxidant activity of its ethanol extract. Maintaining endogenous antioxidant status during the treatment of cancer has the advantage of minimization of serious adverse effects and reducing the treatment course period. A medicinal plant, *D. peltata*, that has anticancer and antioxidant potential, may help expect a better outcome from the disease condition.

Acknowledgments

None.

Conflict of interest

The authors confirm that there are no known conflicts of interest.

Statement of ethics

This study required permission from the “Institutional Animal Ethical Committee (IAEC)”. The study, treatment and handling of the animals was submitted to the IAEC prior to the start of the study and the committee approved the proposal number as A. Raju 0903PH2254/JNTUH 2009.

Availability of data and materials

All data generated or analyzed during this study are included in this published article.

Funding

None.

CRediT authorship contribution statement

Raju Asirvatham: Conceptualization, Investigation, Data curation, Writing - original draft
Arockiasamy Josphin Maria Christina: Supervision, Resources, Visualization, Formal analysis, Investigation, Methodology

ORCID Numbers of the Authors

R. Asirvatham: 0000-0002-7939-4975
A. J. M. Christina: 0000-0003-1552-1266

Supplementary File

None.

Publisher’s Note

All claims expressed in this article are solely those of the authors and do not necessarily represent those of their affiliated organizations, or those of the publisher, the editors and the reviewers. Any product that may be evaluated in this article, or claim that may be made by its manufacturer, is not guaranteed or endorsed by the publisher.

This is an open-access article distributed under the terms of the Creative Commons Attribution 4.0 International License (CC BY). The use, distribution or reproduction in other forums is permitted, provided the original author(s) and the copyright owner(s) are credited and that the original publication in this journal is cited, in accordance with accepted academic practice. No use, distribution or reproduction is permitted which does not comply with these terms.

References

Ahmad, R., Tripathi, A. K., Tripathi, P., Singh, S., Singh, R., & Singh, R. K. (2008). Malondialdehyde and protein carbonyl as biomarkers for oxidative stress and disease progression in patients with chronic myeloid leukemia. *in vivo, 22*(4), 525-528.

Asirvatam, R., & Christina, A. J. M. (2018). Free radical scavenging potential of *Drosera indica* L in presence of Dalton Ascites lymphoma (DAL) tumor bearing mice. *Indonesian Journal of Pharmacy, 29*(3), 127-135.

Asirvatham, R., Christina, A. J. M., & Murali, A. (2013). In vitro antioxidant and anticancer activity studies on *Drosera indica* L. (Droseraceae). *Advanced Pharmaceutical Bulletin, 3*(1), 115-120.

Asirvatham, R., Mathew, A. A., & Dawn, V. T. (2020). In vivo antianemic study of two species of *Murva* on phenylhydrazine induced anaemia in rats. *Adıyaman Üniversitesi Sağlık Bilimleri Dergisi, 6*(2), 243-247.

Balaji, V. R., & Asirvatham, R. (2015). In vitro anticancer and antioxidant activity studies on *Drosera peltata* JE Sm. *Spatula DD, 5*(3), 183-199.

Baskar, R., Lee, K. A., Yeo, R., & Yeoh, K. W. (2012). Cancer and radiation therapy: current advances and future directions. *International Journal of Medical Sciences, 9*(3), 193-199.

Christina, A., Joseph, D. G., Packialakshmi, M., Kothai, R., Robert, S. J. H., Chidambaranathan, N., & Ramasamy, M. (2004). Anticarcinogenic activity of *Withania somnifera* Dunal against Dalton’s ascitic lymphoma. *Journal of Ethnopharmacology, 93*(2-3), 359-361.

Demirci, S., Ozsaran, Z., Celik, H. A., Aras, A. B., & Aydin, H. H. (2011). The interaction between antioxidant status and cervical cancer: a case control study. *Tumori Journal, 97*(3), 290-295.

Desai, A. G., Qazi, G. N., Ganju, R. K., El-Tamer, M., Singh, J., Saxena, A. K., Bedi, Y. S., Taneja, S. C., & Bhat, H. K. (2008). Medicinal plants and cancer chemoprevention. *Current Drug Metabolism, 9*(7), 581-591.

DeWys, W. D. (1982). Pathophysiology of cancer cachexia: current understanding and areas for future research. *Cancer Research, 42*(2_Supplement), 721-725.

Gupta, M., Mazumder, U. K., Kumar, R. S., Sivakumar, T., & Vamsi, M. L. M. (2004). Antitumor activity and antioxidant status of *Caesalpinia bonducella* against Ehrlich ascites carcinoma in Swiss albino mice. *Journal of Pharmacological Sciences, 94*(2), 177-184.

Ichimura, Y., Habuchi, T., Tsuchiya, N., Wang, L., Oyama, C., Sato, K., Nishiyama, H., Ogawa, O., & Kato, T. (2004). Increased risk of bladder cancer associated with a glutathione peroxidase 1 codon 198 variant. *The Journal of Urology, 172*(2), 728-732.

Koca, R., Armutcu, F., Altinyazar, C., & Gürel, A. (2005). Evaluation of lipid peroxidation, oxidant/antioxidant status, and serum nitric oxide levels in *Alopecia areata*. *Medical Science Monitor: International Medical Journal of Experimental and Clinical Research, 11*(6), 296-299.

Levine, R. L., Wehr, N., Williams, J. A., Stadtman, E. R., & Shacter, E. (2000). Determination of carbonyl groups in oxidized proteins. *Stress Response, 99*, 15-24.

Liu, M., Pelling, J. C., Ju, J., Chu, E., & Brash, D. E. (1998). Antioxidant action via p53-mediated apoptosis. *Cancer Research, 58*(8), 1723-1729.

Maity, P., Chakraborty, S., & Bhattacharya, P. (2000). Neovascularisation offers a new perspective to glutamine related therapy. *Indian Journal of Experimental Biology, 38*(1), 88-90.

Newman, D. J., & Cragg, G. M. (2009). Natural product scaffolds as leads to drugs. *Future Medicinal Chemistry, 1*(8), 1415-1427.

Parasuraman, S., Thing, G. S., & Dhanaraj, S. A. (2014). Polyherbal formulation: Concept of ayurveda. *Pharmacognosy Reviews, 8*(16), 73-80.

Rajesh, M., Sulochana, K. N., Coral, K., Punitham, R., Biswas, J., Babu, K., & Ramakrishnan, S. (2004). Determination of carbonyl group content in plasma proteins as a useful marker to assess impairment in antioxidant defense in patients with Eales' disease. *Indian Journal of Ophthalmology, 52*(2), 139-144.

Raju, A., Christina, M., & Murali, A. (2012). Antitumor activity of ethanol and aqueous extracts of *Drosera burmannii* vahl. in EAC bearing mice. *Spatula DD, 2*(2), 83-88.

Raju, A., Salwa, A. S., Daisy, P. A., Aparna, A. M., & Boby, J. (2022). Neuroprotective effect of *Vanda tessellata* as "Rasna" Species, on aluminium chloride induced Alzheimer's in rats: Neuroprotective study of Rasna. *Journal of Microbiology, Biotechnology and Food Sciences, 12*(1), e5164.

Reddy, C. S., Reddy, K., & Jadhav, S. (2001). Threatened (medicinal) plants of Andhra Pradesh. *Medicinal Plants Conservation Center*, 1-39.

Ruby, A. J., Kuttan, G., Babu, K. D., Rajasekharan, K., & Kuttan, R. (1995). Anti-tumour and antioxidant activity of natural curcuminoids. *Cancer Letters, 94*(1), 79-83.

Sara, J., Abdolrasoul, E., Ahmad, K., & Hossain, B. (2015). Evaluation of antioxidant activity of *Malus domestica* fruit extract from Kashan area. *African Journal of Agricultural Research, 10*(20), 2136-2140.

Shaik, I. H., & Mehvar, R. (2006). Rapid determination of reduced and oxidized glutathione levels using a new thiol-masking reagent and the enzymatic recycling method: application to the rat liver and bile samples. *Analytical and Bioanalytical Chemistry, 385*(1), 105-113.

Sun, Y., Oberley, L. W., Elwell, J. H., & Sierra-Rivera, E. (1989). Antioxidant enzyme activities in normal and transformed mouse liver cells. *International Journal of Cancer, 44*(6), 1028-1033.

Vani, M., Reddy, G. P., Reddy, G. R., Thyagaraju, K., & Reddanna, P. (1990). Glutathione-S-transferase, superoxide dismutase, xanthine oxidase, catalase, glutathione peroxidase and lipid peroxidation in the liver of exercised rats. *Biochemistry International, 21*(1), 17-26.

WHO (World Health Organization). (2022). Cancer. Retrieved from https://www.who.int/news-room/fact-sheets/detail/cancer. Accessed 3 February 2022.

Yagi, K. (1987). Lipid peroxides and human diseases. *Chemistry and Physics of Lipids, 45*(2-4), 337-351.

Int. J. Plant Bas. Pharm. (2023) 3(1), 47-53

INTERNATIONAL JOURNAL OF PLANT BASED PHARMACEUTICALS

https://ijpbp.com

RESEARCH ARTICLE

OPEN ACCESS

The effects of *Sideritis akmanii* on endoplasmic reticulum stress, inflammation, and DNA damage in experimentally ER-stress-induced MCF-7 cancer cells

Ibrahim Hakkı Cigerci[a*], Halil Turhan[a], Omer Hazman[b], Nilay Isitez[c]

[a] *Afyon Kocatepe University, Faculty of Science and Literature, Department of Molecular Biology and Genetics, Afyonkarahisar, Türkiye*
[b] *Afyon Kocatepe University, Faculty of Science and Literature, Department of Chemistry, Afyonkarahisar, Türkiye*
[c] *Afyonkarahisar Health Sciences University, Faculty Of Pharmacy, Department Of Basic Pharmaceutical Sciences, Afyonkarahisar, Türkiye*

ARTICLE INFO

Article History:

Received: 23 September 2022
Revised: 02 November 2022
Accepted: 06 November 2022
Available online: 08 November 2022

Edited by: B. Tepe

Keywords:

MCF-7
ER-stress
Comet assay
Sideritis akmanii
Cytotoxicity
Genotoxicity

ABSTRACT

Cancer is one of the diseases that became a social problem that can happen with uncontrolled proliferation, growth, differentiation, and spread of cells in our body. Breast cancer, on the other hand, is one of the types of cancer with the highest incidence in women. In our study, endoplasmic reticulum (ER) stress is induced by thapsigargin (T) in MCF-7 cells and then, the effects of *Sideritis akmanii* acetone extract (SAE) on cell viability, ER stress, inflammation, and DNA damage were investigated. The MTT [3-(4,5-dimethylthiazol-2-yl)-2,5-diphenyltetrazolium bromide] test was used to determine the effect of SAE on cytotoxicity and the comet (SCGE; single-cell gel electrophoresis) assay was used for the effects on genotoxicity. Additionally, the mRNA expression levels of both ER stress parameters (ATF4: activating transcription factor 4, ATF6: activating transcription factor 6, PERK: protein kinase RNA-like ER kinase, GRP78: glucose-regulated protein 78) and inflammation-related parameters (TNF alpha: tumor necrosis factor-alpha, IFN-gamma: interferon-gamma, IL-6: interleukin-6, IL-8: interleukin-8, IL-12: interleukin-12) were determined by qPCR. The results showed that DNA damage levels increased as a result of T treatment, DNA damage caused by T decreased when a low dose of SAE was administered and a high dose of SAE further increased DNA damage levels. It was determined that SAE, administered in different doses with T or alone in experimental groups, increased mRNA expression levels of all ER stress and inflammatory genes compared to the control group. As a result, it has been determined that *S. akmanii*, especially at high doses, may exhibit anticarcinogenic effects through its effects on genotoxic, cytotoxic, and ER stress in MCF-7 cells.

1. Introduction

Cancer is a disease that is the second most cause of death after cardiovascular diseases both in the world and in our country. Cancer is caused by the uncontrolled proliferation, growth, differentiation, and spread of cells in our body. Breast cancer is one of the most common types of cancer among women (Ferlay et al., 2015). Breast cancer is a multifactorial disease in which there is a strong interaction between genetic and environmental factors (McPherson et al., 2000). Many studies have shown that oxidative stress and inflammation, which can become chronic under the influence of environmental factors, can be associated with the development and progression of cancer. Inflammation and oxidative stress can be effective in stimulating oncogenic factors through both DNA damage and endoplasmic reticulum (ER) stress. However, chemotherapeutic agents such as carboplatin, which have many anticarcinogenic effects, and bioactive substances of plants that have antioxidant effects can show anticarcinogenic effects by increasing oxidative stress, inflammation, and ER stress (Hazman et al., 2018).

Reviewed by:
Muhammad Mudassir Ali: University of Veterinary and Animal Sciences, Lahore, Pakistan
Elif Gulbahce Mutlu: KTO Karatay University, Konya, Türkiye
Dudu Erkoc Kaya: Selcuk University, Konya, Turkey

* Corresponding author(s):
E-mail address:
cigerci@aku.edu.tr (I. H. Cigerci)
e-ISSN: 2791-7509
doi: https://doi.org/10.29228/ijpbp.15

There is a linear relationship between the reactive oxygen species (ROS) that occur in cancer cells and the level of DNA damage caused by them and ER stress can occur due to DNA damage through ROS (Evyapan et al., 2019). Both DNA damage and ER stress-mediated programmed cell death (apoptosis) is effective in maintaining growth, development, and homeostasis in healthy individuals, while in cancer patients they can be used to eliminate cancer cells (Hazman et al., 2018).

ER has numerous important functions such as regulating intracellular calcium storage, post-translational modification, folding, and delivery of newly synthesized proteins (Mori, 2000). These functions of the ER are essential for the vital continuity of the cell. ER damage or a defect in ER functions causes errors in protein folding or intracellular calcium storage dysregulation, leading to a condition defined as ER stress (Sancho-Martínez et al., 2012). ER transmembrane proteins called IRE1 (inositol-requiring enzyme 1), PERK, and ATF6 which are stimulated as a result of ER stress would lead to the development of unfolded protein response (UPR) and activate signal transduction pathways that lead the cell to apoptosis (Fribley et al., 2009; Mori, 2000; Treiman, 2002). Normally, IRE1, PERK, and ATF6 proteins are bound by the ER chaperone protein named GRP78 (ER-chaperone glucose-regulated protein 78) and are in an inactive form. However, UPR, which develops due to protein folding suppression which happens due to the factors such as oxidative stress, DNA damage, and inflammation, which are caused by the effect of various factors in the tissues/cells in the organism, triggers apoptosis via caspase 12 by separating GRP78 from these 3 proteins (IRE1, PERK, and ATF6) localized in the ER transmembrane (Çelik et al., 2015; Hazman et al., 2018).

In this study, presented in this context, we investigated the effects of *Sideritis akmanii*, an endemic sage species, on ER stress and DNA damage in breast cancer (MCF-7) cells. For this purpose, *S. akmanii* acetone extract (SAE) was prepared first and then the cytotoxicity of this extract was determined. ER stress, inflammation, and DNA damage levels were detected after the application of different doses of SAE.

2. Materials and methods

2.1. Acetone extraction of S. akmanii

The plants were collected from the Kumalar plateau in the countryside of Suhut District of Afyonkarahisar province on July 16, 2015, when flowering was at its highest level. The plants dried in the shade were pulverized. 20 g of the plant material was weighed and extracted with 250 ml of acetone in the Soxhlet device for 24 hours. After the extraction process, acetone was evaporated with the help of a rotary and it was kept at +4 °C until it was used.

2.2. Determination of SAE cytotoxicity levels in MCF-7 cells

The MTT solution used in the study was prepared by dissolving the MTT salt (Sigma) in a phosphate buffer (pH: 7.4) at a concentration of 5 µg/ml. MTT solution was prepared fresh for each use.

$1x10^5$ MCF-7 cells were seeded into each well of the 24-well plate using the cell suspension, whose number of cells per ml was determined with the trypan blue method. The plates were incubated at 37 °C in the incubator (Panasonic) containing 5% CO_2 (carbon dioxide). When the density of the cells on the plate surface reached 50-60%, SAE doses were administered as 1000, 750, 500, 250, 100, 50, and 10 µg/ml. 1% DMSO was used as a control. The plates were placed into the incubator, which had 5% CO_2, to be incubated for 24 hours at 37 °C. After incubation, MTT solution with a temperature of 37 °C was added to each well at a rate of 10% of the well's volume and incubated again for 3 hours. At the end of the incubation, the formazan crystals in the wells of the plate were removed with an automatic pipette without damaging the cells. Subsequently, the formazan crystals remaining at the bottom of the wells on the plate were dissolved in 800 µl of DMSO added to each well (Hazman et al., 2021). Immediately after, absorbance values were determined at 540 nm with a microplate reader spectrophotometer (BioTek ELx-800). Cell viability of the control group which was not treated with SAE was considered 100%, and the effect of each dose on cell viability was calculated using the formula shown below (Günay et al., 2016; Ulasli et al., 2013). At least three repetitions were performed for each dose in the MTT analysis used to determine cell viability.

$$Cell\ viability\ (\%) = 100\ \mathrm{x}\frac{Absorbance\ of\ sample}{Absorbance\ of\ control}$$

2.3. Creation of experimental groups and experimental model

SAE doses to be applied to experimental groups were determined according to cytotoxicity analysis. To obtain cell lysates to be used as samples in the analysis, $5x10^5$ cells were seeded in 25 cm^2 flasks in a 5 ml medium. When the confluent ratio reached 50-70%, ER stress was induced by applying 50 µl 10-8 M T to each flask in the respective groups. SAE at doses of 10, 50, and 100 µg/ml was applied to flasks with and without ER stress. Experimental groups created in the study and applications used on experimental groups are presented in Table 1.

Table 1. The design of the experimental groups

Experimental groups*	Applications to cells
Group 1: Control	After the cells were seeded, no application was made other than medium.
Group 2: DMSO	DMSO, the solvent of T and SAE, was applied to the cells at a rate of 1%.
Group 3: Thapsigargin (T)	To create ER stress in cells, T was applied at a final concentration of 10^{-8} M.
Group 4: SAE_{10}	SAE was applied to the cells at a final concentration of 10 µg/ml.
Group 5: T + SAE_{10}	SAE at 10 µg/ml was applied to the cells together with T at 10^{-8} M concentration.
Group 6: SAE_{50}	SAE was applied to the cells at a final concentration of 50 µg/ml.
Group 7: T + SAE_{50}	SAE at 50 µg/ml was applied to the cells together with T at 10^{-8} M concentration.
Group 8: SAE_{100}	SAE was applied to the cells at a final concentration of 100 µg/ml.
Group 9: T + SAE_{100}	SAE at 100 µg/ml was applied to the cells together with T at 10^{-8} M concentration.

* Studies with experimental groups were carried out with at least 3 repetitions.

2.4. Determination of DNA damage

After SAE and T applications were performed on MCF-7 cells, DNA damage in samples was determined using the comet assay. 24 hours after the experimental groups mentioned in Table 1, the cells were collected from the base of the flask by trypsinization and detrypsinization. Cell suspensions belonging to experimental groups created in 1 ml of phosphate-buffered saline (PBS) were used in the

analysis. For this purpose, 20 µl of cell suspension was taken and mixed with 100 µl of low melting agarose (LMA) in eppendorf. All of the cell-LMA mixtures in the eppendorf were taken and prepared in slides by treating them with normal melting agarose (NMA) one day in advance. Following the stages of lysis and electrophoresis, each preparation was stained. The stained preparations were scored by counting 100 cells in a fluorescence microscope (Singh et al., 1988).

2.5. RNA isolation, cDNA synthesis, and gene expression levels

In MCF-7 cells, mRNA expression levels were determined by using total RNA isolated from experimental groups, and complementary DNA (cDNAs) was determined by Reverse Transcription-Polymerase Chain Reaction (RT-PCR) method using a commercial cDNA synthesis kit (GeneMatrix). In the analyses, total RNAs belonging to MCF-7 cells were isolated using a commercial kit (GeneMatrix). The amount of RNAs obtained was determined through the optic density (OD_{260}/OD_{280}) in nanodrop (BioTek, Epoch 2). RNAs with an OD_{260}/OD_{280} ratio of 1.7-2.2 were used in the study (Hazman et al., 2021).

Syber Green PCR Master Mix (10 µl) and primer pair (oligonucleotide) were added to 1 µl of the cDNA of each sample obtained by following the manufacturer's protocols. Primers are specific for each transcription analysis and were determined using studies in the literature (Günay et al., 2016). The primers presented in Table 2 were used at the level of 100 ng in each RT-PCR reaction.

Table 2. Expression primers used in real-time PCR analysis

Genes	Primers	
B-actin	F: 5'-CACCCCAGCCATGTACGTTGC-3'	R: 5'-CCGGAGTCCATCACGATGCCA-3'
IFN-γ	F: 5'-GCAATCTGAGCCAGTGC-3'	R: 5'-TTTGGAAGCACCAGGCA-3'
TNF-α	F: 5'-GAGTGACAAGCCTGTAGCCCA-3'	R: 5'-GCTGGTTATCTCTCAGCTCCACG-3'
IL 12	F: 5'-GACCCAGGAATGTTCCCATGC-3'	R: 5'-TTTCTGGAGGCCAGGCAACTC-3'
IL-6	F: 5'-GGTACATCCTCGACGGCATCT-3'	R: 5'-GTGCCTCTTTGCTGCTTTCAC-3'
IL-8	F: 5'-GACAAGAGCCAGGAAGAAAC-3'	R: 5'-CTACAACAGACCCACACAATAC-3'
GRP78	F: 5'-GCCTGTATTTCTAGACCTGCC-3'	R: 5'-TTCATCTTGCCAGCCAGTTG-3'
PERK	F: 5'-CCCCAACAAGGCCAGCCTGG-3'	R: 5'-GGACAGCCAGCCGTGTTCCC-3'
ATF4	F: 5'-TCAAACCTCATGGGTTCTCC-3'	R: 5'-GTGTCATCCAACGTGGTCAG-3'
ATF6	F: 5'-CTCCGAGATCAGCAGAGGAA-3'	R: 5'-AATGACTCAGGGATGGTGCT-3'

Table 3. Determination of cytotoxicity levels of SAE in MCF-7 cells

Concentration (µg/ml)	MCF-7 cell viability levels (%)
1000	29.86 ± 3.44
750	32.29 ± 3.24
500	2986 ± 5.66
250	24.82 ± 1.65
100	20.65 ± 0.89
50	44.27 ± 0.69
25	81.07 ± 7.48
0	100.00 ± 8.41

The data are presented as mean ± standard deviation ($n \geq 3$). A group of cells without any SAE treatment (dose 0) were used as the control group.

Table 4. Lethal doses of SAE in MCF-7 cells

Lethal doses (LDs)*	Concentration (µg/ml)
LD_0	0.002
LD_5	0.036
LD_{10}	0.169
LD_{15}	0.479
LD_{50}	38.851

* Lethal doses were determined as a result of calculating % viability rates (Table 3) obtained from MTT analysis after applying different doses of SAE to MCF-7 cells through the probit analysis program.

In the qPCR analysis performed, the protocol was applied for the β-actin gene for 10 minutes at 95 °C, 1 minute at 94 °C, 1 minute at 61 °C and 1 minute at 72 °C. The application for ATF6, PERK, ATF4, and IL-6 was performed for 10 min at 95 °C, 1 min at 94 °C, 1 min at 60 °C and 1 min at 72 °C. The protocol applied is as follows: For GRP78, 10 minutes at 95 °C, 30 seconds at 95 °C, 1 minute at 58 °C, and 30 seconds at 72 °C; for TNF-α and IL-12 for 10 minutes at 95 °C, 30 seconds at 95 °C, 1 minute at 54 °C and 30 seconds at 72 °C; for TNF-α and IL-12 for 10 minutes at 95 °C, 30 seconds at 95 °C, 1 minute at 54 °C and 30 seconds at 72 °C. A total of 40 cycles were performed in all analyses. Gene expression values were calculated according to the formula 2-ΔΔCt. The calculation of the ΔΔCt values used in this study was performed with the formula presented below (Pfaffle, 2001).

$$\Delta\Delta Ct = (\text{Cttarget gene} - \text{Ctβactin})\text{experimental group} - (Cttarget\ gene - Ct\beta actin)control\ group$$

3. Results and discussion

3.1. Effect of SAE on cytotoxicity levels in MCF-7 cells

The viability rates (%) obtained as a result of MTT analysis performed to determine the cytotoxicity of SAE on the MCF-7 cell line and the SAE lethal doses calculated using these rates are presented in Table 3 and Table 4, respectively.

When the data in Table 3 and Table 4 are examined, it was seen that the toxicity of SAE in MCF-7 cells begins from low doses. In the study, 3 doses have been administered to MCF cells were determined by taking into account the cytotoxic doses of SAE (Table 3 and Table 4). The analyzes were continued by using 10 µg/ml of SAE extract, which is lower than the LD_{50} dose as a low dose, a dose close to the LD_{50} dose (50 µg/ml) as the medium dose, and 100 µg/ml SAE extract as the high dose.

3.2. Effect of SAE on DNA damage in MCF-7 cells

Statistical evaluation of the data obtained from comet assay is presented in Table 5. Compared to the control group, only T administration and high (50 and 100 µg/ml) doses of SAE applications were found to increase DNA damage scores in the experimental groups. It was observed that this increase was greater in the groups in which T was administered together with high doses of SAE. It was observed that the DNA damage did not change in the experimental groups in which a low dose of SAE was applied, compared to the control and DMSO groups.

Table 5. Effect of SAE on DNA damage in MCF-7 cells

Experimental groups	DNA damage levels
Control	9.67 ± 2.08^{a}
DMSO	14.33 ± 3.79^{ab}
T	45.00 ± 5.00^{c}
SAE_{10}	17.33 ± 5.77^{ab}
T + SAE_{10}	18.33 ± 7.64^{b}
SAE_{50}	68.67 ± 1.53^{d}
T + SAE_{50}	92.00 ± 3.00^{f}
SAE_{100}	82.00 ± 3.00^{e}
T + SAE_{100}	94.00 ± 5.29^{f}

The data are presented as mean ± standard deviation (n = 5). ^{a,b,c,d,e,f}: The difference between mean values carrying different exponential expressions on the same row is statistically significant ($p < 0.05$). Abbreviations: DMSO; dimethyl sulfoxide, T; Thapsigargin, SAE; *S. akmanii* acetone extract.

Table 6. The effect of SAE on mRNA levels of some genes related to ER stress and inflammation in MCF-7 cells

Experimental groups	Genes whose mRNA expression levels are determined								
	ATF6	ATF4	PERK	Grp78	IL-6	IL-8	IL-12	TNF-α	IFN-γ
*SAE_{10}	+ 0.43	+ 30.27	+ 0.71	+ 0.26	+ 4.29	+ 0.46	+ 0.23	+ 0.19	+ 0.27
*T + SAE_{10}	+ 0.53	+ 27.92	+ 0.68	+ 0.52	+ 1.60	+ 0.97	+ 0.52	+ 0.29	+ 0.51
*SAE_{50}	+ 5.72	+ 0.75	+ 0.75	+ 1.60	+ 12.20	+ 2.47	+ 0.17	+ 0.96	+ 1
*T + SAE_{50}	+ 1.61	+ 0.84	+ 0.84	+ 1.27	+ 1.31	+ 0.48	+ 0.38	+ 0.54	+ 0.68
*SAE_{100}	+ 0.28	+ 50.09	+ 0.56	+ 0.84	+ 6.16	+ 6.77	+ 0.14	+ 0.33	+ 0.38
*T + SAE_{100}	+ 0.23	+ 124.40	+ 1.24	+ 0.93	+ 16.14	+ 5.54	+ 0.65	+ 0.47	+ 0.53

* It shows the experimental groups whose stimulation and suppression conditions were expressed compared to the control group. Data expressed by '+' indicates that the data of the specified experimental group of the relevant gene is stimulated compared to the data of the control group of the relevant gene. Abbreviations: DMSO; dimethyl sulfoxide, T; thapsigargin, SAE; *S. akmanii* extract, ATF4; activating transcription factor 4, ATF6; activating transcription factor 6, PERK; protein kinase RNA-like ER kinase, GRP78; glucose regulating protein 78; TNF-α; tumor necrosis factor-alpha, IFN-γ; Interferon-gamma, IL-6; Interleukin-6, IL-8; Interleukin-8, IL-12; Interleukin-12.

3.3. Effects of SAE on ER stress and inflammation in MCF-7 cells

In the presented study as stated before, the expression levels of ATF6, ATF4, PERK, and GRP78 mRNA of the ER stress genes and expression levels of IL-6, IL-8, IL-12, TNF α, and IFN-γ mRNA of the inflammatory and pro-inflammatory genes were calculated by normalizing with the β-actin gene. The findings showed that SAE, administered to experimental groups with T or in different doses alone, increased mRNA expression levels of ER stress and inflammation-related genes compared to the control group. The findings are presented in Table 6.

We conducted this study using cell culture (MCF-7 cells) and included control groups in our experiments. The advantage of cell culture experiments is that they can promptly allow the observation of the biological effects of the test substance in question. Besides, the use of cells that grow unlimitedly in cell culture does not require the ethics committee report encountered when conducting studies with experimental animals. Therefore, cell culture studies are widely used in cancer research, biochemistry, cytogenetics, and molecular biology studies worldwide. In our study, the cytotoxic effects of SAE on MCF-7 cells were investigated by the MTT method. It was observed that the cytotoxic effect of SAE on MCF-7 cells increased depending on the increase in concentration. In 24-hour application, the LD_{50} dose of SAE was found to be 38.851 µg/ml. Due to low doses of the LD_{50} dose (38.851 µg/ml) of SAE, it may be recommended to investigate the anticarcinogenic activity of this sample in further studies. Similar to our study, Yumrutas et al. (2015), in their study on MCF-7 cells, found that 100 µg/ml dose of methanol extract of *S. syriaca* reduced cell viability in MCF-7 cells (54.91 % of the control group).

Loizzo et al. (2007) extracted the essential oils of *S. perfoliata* in their study and detected 15 monoterpenes, 17 sesquiterpenes, and 1 diterpene in the essential oil. In their cell culture studies with essential oils, they determined that essential oils showed high activity on human melanoma (C32) cells and kidney adenocarcinoma (ACHN) cells, and their IC_{50} values were determined as 98.58 and 100.90 µg/ml, respectively. In our study, it was determined that SAE, which is in the same family as *S. perfoliata*, decreased cell viability in MCF-7 cells depending on the increasing concentration.

Todorova and Trendafilova (2014) determined in their study with S. scardica that 100 µg/ml of the plant's diethyl ether extract decreased cell viability in B16 and HL-60 cells by 51.3% and 77.5%, respectively. They have shown that decreased cell viability is caused by flavonoids (apigenin, luteolin, and their glycosides). In line with this information, it is thought that flavonoids contained in SAE may cause cytotoxicity observed on MCF-7.

The comet assay is a widely used method for assessing DNA damage in vitro and in vivo. It is also known as single-cell gel electrophoresis (SCGE). It is based on a run with electrophoresis after the lysis of cells embedded in agarose gel. While the undamaged DNA remains intact in the cell nucleus during the electrophoresis process, breaks emerge as a result of DNA fragmentation. The fragments of broken DNA extend toward the anode, forming a comet-shaped structure. This comet-shaped DNA is then made visible using a DNA-binding dye. To assess the extent of DNA damage, the comet's shape, size, and amount of DNA in it is measured. Types of analysis protocols of the comet method are the measurement of DNA crosslinks (e.g. thymine dimers), and DNA single- and double-strand breaks. The advantages of the comet assay are that it requires a small number of

cells per sample and provides individual damage data per cell. Scoring comets in the comet assay can be done either visually or with image analysis software (Tice et al., 2000).

In our study, we aimed to investigate the possible genotoxic effects of SAE on MCF-7 cells. Compared to the control group, only T administration and high doses (50 and 100 µg/ml) of SAE applications were found to increase DNA damage scores in the experimental groups. It was observed that this increase was greater in the groups in which T was administered together with high doses of SAE. It was observed that the DNA damage did not change in the experimental groups in which low-dose SAE was applied, compared to the control and DMSO groups. These data indicate that low-dose SAE can be used for preventive and therapeutic purposes as it does not affect DNA damage, while high doses may show anticarcinogenic effects on cancer cells due to increased DNA damage.

In their study with flavonoids, Das et al. (2017) found that combined flavonoid applications induced DNA damage in human erythroleukemic cell line (K562) cells. For example, they have shown that the combination of quercetin and myricetin leads to maximum DNA damage. In our study, it is thought that the presence of combined flavonoids in SAE increases the DNA damage on MCF-7 cells depending on the increase in the dose.

Guo et al. (2016) showed that Jungermannenon A and B diterpenoids initiate ROS production on PC3 (prostate cancer), which leads to the induction of mitochondrial damage and permanent DNA damage. In our study, the combination of diterpenoids' presence in SAE may cause the induction of mitochondrial damage and permanent DNA damage by initiating ROS production in MCF-7 cells.

Chronic inflammation affects immune system components that are directly linked to cancer progression. Under normal conditions, immune cells, which include granulocytes, macrophages, mast cells, lymphocytes, dendritic cells, and natural killer cells, act as a preliminary defense against pathogens. When tissue damage occurs, macrophages and mast cells secrete cytokines and chemokines to direct circulating leukocytes to the damaged area to destroy pathogens (Samadi et al., 2015).

In our study, expression levels of IL-6 cytokine of SAE on MCF-7 cells increased in all application groups compared to the control. Gene expression levels of IL-8, a chemokine, were increased in SAE10, T+SAE10, and T+SAE50 applications, while they increased in other applications. The effect of SAE on the IL-12 and TNF-α genes was found to be similar and suppressed in all application groups. While the IFN-γ gene showed a similar effect with control at a concentration of 50 µg/ml, it was suppressed in other administration groups. In our study, it is thought that SAE has a similar effect on the effect of tissue damage by increasing the expression of IL-6 cytokine.

IL-8 greatly affects the tumor microenvironment. It is the chemokine that promotes the activation of endothelial cells, angiogenesis, neutrophil infiltration in the tumor site, and cancer development through increased autocrine signaling. Inhibition of IL-8 in cancer cells is crucial as it reduces the proliferation and progression of cancer cells. Especially in prostate cancer, IL-8 plays an important key role in the adhesion of cancer cells to the endothelium and extracellular matrix by increasing the risk of cancer and cell survival. Aqueous extract of *S. syriaca* was observed to significantly lower IL-8 levels on stimulated human colon cancer cell line 29 (HT29) and human prostate cancer cell line 3 (PC3) cells (Kogiannou et al., 2013). In our findings, IL-8 gene expression levels in MCF-7 cells of SAE were suppressed in SAE10, T+SAE10, and T+SAE50 applications, while they increased in SAE50, SAE100, and T+SAE100 applications. These results suggest that the consumption of *S. akmanii* as a tea by the people in Anatolia may be medicinally effective. It can be considered that it indirectly slows the development and progression of cancer in low doses when consumed by the public as tea.

ER is very sensitive to changes occurring at the physiological and biochemical level, such as ion balance in its lumen, and synthesis charge. Glucose deprivation, calcium depletion, exposure to free radicals, impairment of glycosylation, excessive cholesterol load and disruption of cell control mechanisms due to some pathological and physiological reasons associated with oxidative stress induction causes the accumulation of misfolded proteins and subsequently an increase in ER stress (Imai et al., 2016; Sozen & Ozer, 2017). The accumulation of misfolded proteins in the ER generates the UPR response as a protective reaction that reduces incipient protein synthesis, facilitates protein folding, and increases proteasomal degradation of misfolded proteins (Christen & Fent, 2016). UPR is primarily a survival response that activates protein misfolding mechanisms. However, prolonged ER stress conditions can disrupt cell life. The three pathways activated by ER stress are IRE1, PERK, and ATF6. In cases where there is no ER stress, these three pathways are suppressed by the GRP78/BIP chaperon (Kapuy et al., 2014).

Zhou et al. (2014), in their study, investigated the relationship between ER stress and apoptosis by inducing ER stress with T in MCF-7 cells. They showed that in MCF-7 cells induced by ampelopsin (an important bioactive component of *Ampelopsis grossedentata*), T increased the expression of the GRP78 gene. They also determined that T increased ampelopsin-induced cell growth inhibition and apoptosis. In our study, it was observed that the expression levels of the GRP78 gene, which plays a role in the UPR response in ER stress, in the SAE50 and T+SAE50 application groups increased compared to the control. It was observed that the PERK gene involved in UPR response in ER stress was suppressed in all application groups, but there was an increase in T+SAE100 administration compared to the control. Also, ATF6, which is involved in UPR response and is under GRP78 control in ER stress, was found to increase in SAE50 and T+SAE50 application groups such as GRP78. This suggests that GRP78 reacts to ER stress by activating ATF-6 in the case of ER stress. ATF4, which is under PERK control in the case of ER stress, was observed to have increased expression levels at low and high concentrations and expression levels were suppressed at a dose of 50 µg/ml SAE. This situation suggests that ATF4 is activated differently from PERK.

4. Conclusions

In line with the results obtained from this study, it was determined that SAE has genotoxic and cytotoxic effects on MCF-7 cells. As an endemic species, this plant was found to cause ER stress in MCF-7 cells and could be effective in inflammation. This study will help to investigate the apoptosis process associated with ER stress in the future. It is thought that this study can also lead the path of studies to explain the possible phytotherapeutic effects of *S. akmanii*.

Acknowledgments

The authors thank Afyon Kocatepe University Scientific Research Projects Coordination Unit for their support to this study with the project numbered 15.FEN.BIL.45.

Conflict of interest

The authors confirm that there are no known conflicts of interest.

Statement of ethics

In this study, no method requiring the permission of the "Ethics Committee" was used.

Availability of data and materials

All data generated or analyzed during this study are included in this published article.

Funding

This project was funded by Afyon Kocatepe University Scientific Research Projects Coordination Unit (Grant No: 15.FEN.BIL.45).

CRediT authorship contribution statement

Ibrahim Hakkı Cigerci: Conceptualization, Investigation, Data curation, Project administration, Writing - original draft, Supervision, Methodology
Halil Turhan: Investigation, Data curation, Resources, Conceptualization, Writing – original draft, Methodology, Visualization, Formal analysis
Omer Hazman: Formal analysis, Methodology, Investigation, Supervision, Validation, Writing – original draft, Review & Editing
Nilay Isitez: Conseptualization, Formal analysis, Resources, Review & Editing, Writing-reviewing & editing

ORCID Numbers of the Authors

I. H. Cigerci: 0000-0002-3626-7730
H. Turhan: 0000-0002-0515-1874
O. Hazman: 0000-0002-2702-6847
N. Isitez: 0000-0002-1928-7158

Supplementary File

None.

Publisher's Note

All claims expressed in this article are solely those of the authors and do not necessarily represent those of their affiliated organizations, or those of the publisher, the editors and the reviewers. Any product that may be evaluated in this article, or claim that may be made by its manufacturer, is not guaranteed or endorsed by the publisher.

This is an open-access article distributed under the terms of the Creative Commons Attribution 4.0 International License (CC BY). The use, distribution or reproduction in other forums is permitted, provided the original author(s) and the copyright owner(s) are credited and that the original publication in this journal is cited, in accordance with accepted academic practice. No use, distribution or reproduction is permitted which does not comply with these terms.

References

Christen, V., & Fent, K. (2016). Silica nanoparticles induce endoplasmic reticulum stress response and activate mitogen activated kinase (MAPK) signalling. *Toxicology Reports, 3*, 832-840.
Çelik, S., Serkan, S., & Hazman, Ö. (2015). Endoplasmik retikulum stresine cevap yolakları ve tip 2 diyabet patogenezinde endoplasmik retikulum stres aracılı beta hücre apoptosisinin rolü. *Kocatepe Tıp Dergisi, 16*(3), 227-237.
Das, A., Majumder, D., & Saha, C. (2017). Correlation of binding efficacies of DNA to flavonoids and their induced cellular damage. *Journal of Photochemistry and Photobiology B: Biology, 170*, 256-262.
Evyapan, G., Ay, G., Cömertpay, G., & Luleyap, H. (2019). Role of endoplasmic reticulum stress response in tumorogenesis. *Cukurova Medical Journal, 44*(1), 241-248.
Ferlay, J., Soerjomataram, I., Dikshit, R., Eser, S., Mathers, C., Rebelo, M., Parkin, D. M., Forman, D., & Bray, F. (2015). Cancer incidence and mortality worldwide: sources, methods and major patterns in GLOBOCAN 2012. *International Journal of Cancer, 136*(5), E359-E386.
Fribley, A., Zhang, K., & Kaufman, R. J. (2009). Regulation of apoptosis by the unfolded protein response. In *Apoptosis* (pp. 191-204): Springer.
Guo, Y. X., Lin, Z. M., Wang, M. J., Dong, Y. W., Niu, H. M., Young, C. Y., Lou, H. X., & Yuan, H. Q. (2016). Jungermannenone A and B induce ROS-and cell cycle-dependent apoptosis in prostate cancer cells in vitro. *Acta Pharmacologica Sinica, 37*(6), 814-824.
Günay, E., Celik, S., Sarinc-Ulasli, S., Özyürek, A., Hazman, Ö., Günay, S., Özdemir, M., & Ünlü, M. (2016). Comparison of the anti-inflammatory effects of proanthocyanidin, quercetin, and damnacanthal on benzo (a) pyrene exposed A549 alveolar cell line. *Inflammation, 39*(2), 744-751.
Hazman, Ö., Bozkurt, M. F., Fidan, A. F., Uysal, F. E., & Çelik, S. (2018). The effect of boric acid and borax on oxidative stress, inflammation, ER stress and apoptosis in cisplatin toxication and nephrotoxicity developing as a result of toxication. *Inflammation, 41*(3), 1032-1048.
Hazman, Ö., Sarıova, A., Bozkurt, M. F., & Ciğerci, İ. H. (2021). The anticarcinogen activity of β-arbutin on MCF-7 cells: Stimulation of apoptosis through estrogen receptor-α signal pathway, inflammation and genotoxicity. *Molecular and Cellular Biochemistry, 476*(1), 349-360.
Imai, T., Kosuge, Y., Saito, H., Uchiyama, T., Wada, T., Shimba, S., Ishige, K., Miyairi, S., Makishima, M., *et al.* (2016). Neuroprotective effect of S-allyl-l-cysteine derivatives against endoplasmic reticulum stress-induced cytotoxicity is independent of calpain inhibition. *Journal of Pharmacological Sciences, 130*(3), 185-188.
Kapuy, O., Vinod, P., & Bánhegyi, G. (2014). mTOR inhibition increases cell viability via autophagy induction during endoplasmic reticulum stress–An experimental and modeling study. *FEBS Open Bio, 4*, 704-713.
Kogiannou, D. A., Kalogeropoulos, N., Kefalas, P., Polissiou, M. G., & Kaliora, A. C. (2013). Herbal infusions; their phenolic profile, antioxidant and anti-inflammatory effects in HT29 and PC3 cells. *Food and Chemical Toxicology, 61*, 152-159.
Loizzo, M. R., Tundis, R., Menichini, F., Saab, A. M., Statti, G. A., & Menichini, F. (2007). Cytotoxic activity of essential oils from Labiatae and Lauraceae families against in vitro human tumor models. *Anticancer Research, 27*(5A), 3293-3299.
McPherson, K., Steel, C., & Dixon, J. (2000). Breast cancer—epidemiology, risk factors, and genetics. *British Medical Journal, 321*(7261), 624-628.
Mori, K. (2000). Tripartite management of unfolded proteins in the endoplasmic reticulum. *Cell, 101*(5), 451-454.
Pfaffle, M. (2001). A new mathematical model for relative quantification in real-time RT-PCR. *Nucleic Acids Research, 29*, 2002-2007.
Samadi, A. K., Bilsland, A., Georgakilas, A. G., Amedei, A., Amin, A., Bishayee, A., Azmi, A. S., Lokeshwar, B. L., Grue, B., *et al.* (2015). *A multi-targeted approach to suppress tumor-promoting inflammation.* Paper presented at the Seminars in Cancer Biology.
Sancho-Martínez, S. M., Prieto-García, L., Prieto, M., Lopez-Novoa, J. M., & López-Hernández, F. J. (2012). Subcellular targets of cisplatin cytotoxicity: an integrated view. *Pharmacology & Therapeutics, 136*(1), 35-55.
Singh, N. P., McCoy, M. T., Tice, R. R., & Schneider, E. L. (1988). A simple technique for quantitation of low levels of DNA damage in individual cells. *Experimental Cell Research, 175*(1), 184-191.
Sozen, E., & Ozer, N. K. (2017). Impact of high cholesterol and endoplasmic reticulum stress on metabolic diseases: An updated mini-review. *Redox Biology, 12*, 456-461.
Tice, R. R., Agurell, E., Anderson, D., Burlinson, B., Hartmann, A., Kobayashi, H., Miyamae, Y., Rojas, E., Ryu, J. C., *et al.* (2000). Single cell gel/comet assay: guidelines for in vitro and in vivo genetic toxicology testing. *Environmental and Molecular Mutagenesis, 35*(3), 206-221.
Todorova, M., & Trendafilova, A. (2014). *Sideritis scardica* Griseb., an endemic species of Balkan peninsula: Traditional uses, cultivation, chemical composition, biological activity. *Journal of Ethnopharmacology, 152*(2), 256-265.
Treiman, M. (2002). Regulation of the endoplasmic reticulum calcium storage during the unfolded protein response—significance in tissue ischemia? *Trends in Cardiovascular Medicine, 12*(2), 57-62.
Ulasli, S. S., Celik, S., Gunay, E., Ozdemir, M., Hazman, O., Ozyurek, A., Koyuncu, T., & Unlu, M. (2013). Anticancer effects of thymoquinone, caffeic acid phenethyl ester and

resveratrol on A549 non-small cell lung cancer cells exposed to benzo (a) pyrene. *Asian Pacific Journal of Cancer Prevention, 14*(10), 6159-6164.

Yumrutas, O., Oztuzcu, S., Pehlivan, M., Ozturk, N., Poyraz, I. E., Igci, Y. Z., Cevik, M. O., Bozgeyik, I., Aksoy, A. F., *et al.* (2015). Cell viability, anti-proliferation and antioxidant activities of *Sideritis syriaca*, *Tanacetum argenteum* sub sp. *argenteum* and *Achillea aleppica* subsp. *zederbaueri* on human breast cancer cell line (MCF-7). *Journal of Applied Pharmaceutical Science, 5*(3), 1-5.

Zhou, Y., Shu, F., Liang, X., Chang, H., Shi, L., Peng, X., Zhu, J., & Mi, M. (2014). Ampelopsin induces cell growth inhibition and apoptosis in breast cancer cells through ROS generation and endoplasmic reticulum stress pathway. *PLoS ONE, 9*(2), e89021.

Int. J. Plant Bas. Pharm. (2023) 3(1), 54-61

INTERNATIONAL JOURNAL OF PLANT BASED PHARMACEUTICALS

https://ijpbp.com

RESEARCH ARTICLE

OPEN ACCESS

The inclusion of garlic and turmeric powder in high-fructose diets protects against the development of metabolic syndrome in Wistar rats

Ali Siddiq Idoko[a*], Aliyu Abdullahi[b], Masud Eneji Sadiq[c], Bilkis Muhammad Maibalangu[d]

[a] *Federal University Dutsin-Ma, Department of Biochemistry and Molecular Biology, Katsina State, Nigeria*
[b] *Alqalam University, Department of Biological Sciences, Katsina State, Nigeria*
[c] *Usmanu Danfodiyo University, Department of Biochemistry and Molecular Biology, Sokoto, Nigeria*
[d] *College of Education Azare, Department of Chemistry, Bauchi State, Nigeria*

ARTICLE INFO

Article History:

Received: 10 September 2022
Revised: 26 October 2022
Accepted: 25 November 2022
Available online: 02 December 2022

Edited by: B. Tepe

Keywords:

Metabolic syndrome
Turmeric
Garlic
Dyslipidaemia
Insulin resistance
Oxidative stress

ABSTRACT

The worldwide prevalence of the metabolic syndrome is largely attributable to excessive consumption of high-energy food sweeteners and lifestyle practices that encourage physical inactivity. This study was designed to evaluate the potential benefits of garlic and/or turmeric in down-regulating the risk factors associated with metabolic syndrome. Twenty-four male Wistar rats were divided into 8 groups of 3 rats per group. Group 1 received standard rat chow, Group 2 received a high-fructose diet only, while Group 3 received a 2% turmeric-supplemented high-fructose diet. Groups 4 and 5 were fed a standard diet supplemented with 2% each of garlic and turmeric:garlic (50% w/w), respectively. Groups 6, 7, and 8 were respectively fed a high-fructose diet supplemented with 2% garlic, a standard diet supplemented with 2% turmeric, and a high-fructose diet supplemented with 2% turmeric:garlic (50% w/w). Feed intake and changes in body weight were monitored weekly and after 56 days, the rats were sacrificed. Activities of serum antioxidant enzymes, lipid profile, and atherogenic indices were determined. Homeostasis Model Assessment of Insulin Resistance (HOMA-IR) was computed from the measured blood glucose and insulin levels. The positive control (Group 2) gained weight significantly ($p < 0.05$) when compared with groups that received diet supplementation. Total cholesterol, triglycerides, low-density lipoprotein, and atherogenic indices of diet-supplemented groups were significantly low ($p < 0.05$) when compared with the positive control. Interestingly, while no differences ($p > 0.05$) were observed in the catalase and glutathione peroxidase enzyme activities in the high-fat diet group supplemented with 2% mixed turmeric:garlic when compared with the normal control, activities of these enzymes in the garlic and/or turmeric supplemented high-fructose diet groups were significantly elevated ($p < 0.05$) when compared with the positive control. The HOMA-IR and atherogenic indices results revealed the inclusion of turmeric and garlic in a high-fat diet had anti-dyslipidemic effects, decreased oxidative stress, and reduced coronary risk factors. Our findings strongly suggest supplementation of high-calorie diets with garlic and/or turmeric powder has potential long-term health benefits in individuals exposed to the risks of developing metabolic syndrome.

Reviewed by:
Khalid Hussain: University of Punjab, Lahore, Pakistan
Manobendro Nath Ray: University of Rajshahi, Rajshahi, Bangladesh
Teeraporn Katisart: Mahasarakham University, Maha Sarakham, Thailand
* Corresponding author(s):
E-mail address:
asidoko1@gmail.com (A. S. Idoko)
e-ISSN: 2791-7509
doi: https://doi.org/10.29228/ijpbp.16

1. Introduction

Unhealthy lifestyles such as smoking, alcoholism, and overconsumption of sweetened beverages are increasing the prevalence of metabolic syndrome (MetS); a cluster of risk factors for the development of cardiovascular-related diseases. The clustering abnormalities often include hyperglycemia, dyslipidemia, central obesity, insulin resistance, and high blood pressure (Alberti et al., 2009) which individually or synergistically increase the risk of cardiovascular complications (Sperling et al., 2015; Tune et al., 2017).

Please cite this article as: Idoko, A. S., Abdullahi, A., Sadiq, M. E., & Maibalangu, B. M. (2023). The inclusion of garlic and turmeric powder in high-fructose diets protects against the development of metabolic syndrome in Wistar rats. *International Journal of Plant Based Pharmaceuticals*, *3*(1), 54-61, https://doi.org/10.29228/ijpbp.16.

Although the global prevalence of the syndrome is about 25% and 19% in the populations of adults and children respectively (do Vale Moreira et al., 2020), it is feared that the prevalence could hit 53% by the year 2035 (Gierach et al., 2014). Despite the varied definitions of MetS, the disease prevalence notwithstanding correlates positively with increasing body mass index (Engin, 2017; Nguyen et al., 2008). Central obesity (visceral adiposity) usually caused by overfeeding and excessive consumption of sweetened beverages triggers inflammation and oxidative stress (Huang et al., 2015; Rehman & Akash, 2016). These two conditions can individually and collectively cause cardiovascular damage directly or activate pathways that result in the development of the syndrome (Pekgor et al., 2019).

Since unhealthy lifestyle such as overfeeding and consumption of alcohol and sweetened drinks predisposes to metabolic syndrome, lifestyle modifications including the consumption of antioxidant-rich functional foods could be helpful in the management of MetS (Rodriguez-Cano et al., 2015; Tian et al., 2018). Existing literature on garlic and turmeric suggests these spices possess remarkable antioxidant properties (Anand et al., 2007; Coban et al., 2012; Panyod & Sheen, 2020). The present study, therefore, explores the potential benefits of garlic and turmeric both singly and in combination as food supplements in mitigating the effects of high-fat diet predisposition to MetS.

2. Materials and methods

2.1. Chemicals and feed ingredients

All the chemicals and reagents including methionine, premix minerals, and vitamins used were of analytical grades. Commercial assay kits for antioxidant enzymes (Cayman Chemical Michigan, USA), lipid profile, and insulin ELISA kits (Randox Laboratories Ltd., UK) were purchased for biochemical assays. Feed ingredients including rice bran, corn starch, bone meal, soybean meal, and palmitic acid (16:0) were sourced locally from Dutsin-Ma Central Market, Katsina State.

Table 1. Composition of formulated rat diet

Feed ingredient	Control diet g/100 g	High-fructose g/100 g
Corn starch	55.45	-
Fructose	-	55.45
Soybean meal	32	32
Cellulose	4.50	4.50
Palm oil	6	6
Bone meal	1.25	1.25
Salt mix	0.30	0.30
Vitamin/mineral mix	0.25	0.25
Methionine	0.25	0.25
Total	100	100

Mineral mix (g/kg): $CaCO_3$ (15.258), $COCl_2.6H_2O$ (0.001), $ZnCl_2$ (0.001), $CuSO_4.5H_2O$ (0.019), $FeSO_4.7H_2O$ (1.078), $MgSO_4$ (2.929), $MnSO_4.2H_2O$ (0.178), KI (0.032), KH_2PO_4 (15.559), and NaCl (5.573), Vitamin mix (g/kg diets): thiamine (0.02), riboflavin (0.03), pyridoxine (0.01), *p*-aminobenzoic acid (0.20), myo-inositol (2.00), biotin (0.001), menadione (0.01), ergocalciferol (0.4), choline-HCl (2.0), and cellulose (3.31), α–tocopherol acetate (50), retinal palmitate (0.4), calcium pantothenate (0.0016), and folic acid (0.0002)

2.2. Spice supplements

Turmeric and garlic were bought from Dutsin-Ma Central Market in the Katsina State of Nigeria and were identified as *Curcuma longa* (FUDMA/PSB/00143) and *Allium sativum* (FUDMA/PSB/0019) in the Herbarium of the Department of Biological Sciences, Federal University Dutsin-Ma (FUDMA) The spices were carefully screened, washed, air dried then pulverized using electronic blender and finally sieved through a 0.05 mm sieve. Equal amounts (w/w) of the processed spices were mixed and stored in air-tight containers.

2.3. Formulation of the standard rat diet

Standard rat chow was formulated following the methods of Idoko et al. (2022) and Imam et al. (2022). Briefly, corn starch, cellulose, soybean meal (SBM), vitamin, and mineral mix, were mixed as summarized in Table 1.

2.4. Supplementation of formulated diet

The formulated standard diet was mixed with garlic, turmeric, and garlic:turmeric powders in the ratio 98:2 (w/w) to obtain a 2% spice-supplemented diet.

2.5. Experimental design

Male Wistar rats (24) with an average weight of 120 ± 5.20 g were purchased from National Veterinary Research Institute, Vom, Plateau State, Nigeria. The animals were housed in plastic cages and were maintained according to the guidelines of the National Research Council (2011) for experimental animals. As previously described (Idoko et al., 2022), the rats were divided into 8 groups of 3 rats per group and the formulated diets were randomly assigned as follows:

Group 1 = Standard diet (normal control)
Group 2 = High-fructose diet (positive control)
Group 3 = High-fructose diet + 2% turmeric
Group 4 = Standard diet + 2% garlic
Group 5 = Standard diet + 2% mixed turmeric:garlic (50% w/w)
Group 6 = High-fructose diet + 2% garlic
Group 7 = Standard diet + 2% turmeric
Group 8 = High-fructose diet + 2% mixed turmeric:garlic (50% w/w)

Feeding was ad libitum for a period of eight (8) weeks.

2.6. Determination of feed intake and change in body weight

The rats were fed three times daily and feed was withdrawn two hours after access. The weekly feed intake was estimated by subtracting the leftover amount from the total amount served. The rats were also weighed weekly to estimate the change in body weights.

2.7. Blood sample collection

On the 56th day of the experiment, the rats were weighed, anesthetized, and sacrificed by cutting the jugular vein after a 12-

hour fasting period. Blood was collected in plain sample containers and then centrifuged at 1500 g for 15 minutes to obtain serum for further biochemical analyses.

2.8. Determination of insulin and HOMA-IR

The blood glucose levels were determined using a glucometer (Acuu chek) according to the manufacturer`s protocol. ELISA kit was used to determine serum insulin levels while the index for Homeostasis Model Assessment of Insulin Resistance (HOMA-IR) was calculated as follows (Yin et al., 2013):

$$HOMA-IR = \frac{fasting\ insulin\ (mU/l) x\ fasting\ glucose\ (mmol/l)}{22.5} x\ Concentration\ of\ standard$$

2.9. Determination of lipid profile parameters

2.9.1. Determination of total cholesterol (TC)

Serum total cholesterol was estimated spectrophotometrically using Randox kits following methods described by the manufacturer. Briefly, 10 µl of serum was added to 1000 µl of the reagent (4-aminoantipyrine, phenol, peroxidase, cholesterol esterase, cholesterol oxidase, and PIPES buffer) in a tube. A standard was similarly prepared by adding 10 µl of the standard reagent to 1000 µl of the reagent. Finally, the blank solution for instrument calibration was equally constituted by replacing serum with 10 µl distilled water. Prepared solutions were incubated at 37 °C for 5 minutes after which absorbance was taken at 546 nm. Total cholesterol (mg/dl) was calculated using the relationship:

$$Total\ Cholesterol\ \left(\frac{mg}{dl}\right) = \frac{Absorbance\ of\ sample}{Absorbance\ of\ standard} x\ Concentration\ of\ standard$$

2.9.2. Determination of serum triglycerides (TG)

Serum triglyceride concentration was determined based on an enzymatic hydrolysis procedure using Randox kits as described by the manufacturer. To 10 µl of a serum sample, 1000 µl of reagent (4-amonophenazone, ATP, lipases, glycerol-kinase, glycerol-3-phosphate oxidase, and peroxidase, PIPES buffer, 4-chloro-phenol, and magnesium-ions) was added. Similar preparations were done for the standard solution (1000 µl of the reagent + 10 µl of the standard reagent) and blank (1000 µl + 10 µl distilled water). These were mixed properly and the absorbance of the sample was read against the blank at 546 nm. Triglyceride concentration was calculated as follows:

$$Triglyceride\ concentration\ \left(\frac{mg}{dl}\right) = \frac{Absorbance\ of\ sample}{Absorbance\ of\ standard} x\ Concentration\ of\ standard$$

2.9.3. Determination of HDL-cholesterol (HDL-C)

High-density lipoprotein-cholesterol (HDL-cholesterol) was determined based on first-stage quantitative precipitation of low-density lipoprotein (LDL), very low-density lipoprotein (VLDL), and chylomicron fractions by the addition of phosphotungstic acid in the presence of magnesium ions. The second stage involves the CHOP-PAP assay as described by the manufacturer. Two separate tubes containing 200 µl each of serum sample and standard were mixed with 500 µl of Randox kit reagent (phosphotungstic acid and magnesium chloride), incubated at 28 °C for 10 minutes then centrifuged at 4000 rpm for 10 minutes. For the second stage estimation of HDL-cholesterol, exactly 100 µl of recovered supernatants were mixed with 1000 µl of working reagent. A blank solution was similarly prepared using 10 µl of distilled water. The reaction constituents in each tube were thoroughly mixed and incubated at 37 °C for 5 minutes. The absorbance was read at 546 nm and HDL-cholesterol was estimated using the relationship:

$$HDL-C\ \left(\frac{mg}{dl}\right) = \frac{Absorbance\ of\ sample}{Absorbance\ of\ standard} x\ Concentration\ of\ standard$$

2.9.4. Determination of LDL-Cholesterol (LDL-C)

Low-density lipoprotein-cholesterol (LDL-cholesterol) was calculated from estimated values obtained from TC, TG, and HDL assays (Friedewald et al., 1972):

$$LDL-C\ \left(\frac{mg}{dl}\right) = \text{TC} - \frac{TG}{5} - HDL-C$$

The method of Kazemi et al. (2018) was used to calculate the atherogenic index (AI) and coronary risk index (CRI) as follows:

$$Atherogenic\ Index\ (AI) = \frac{LDL-C}{HDL-C}$$

$$Coronary\ risk\ index\ (CRI) = \frac{TC}{HDL-C}$$

2.10. Determination of the serum antioxidant enzymes

2.10.1. Superoxide dismutase (SOD) assay

The determination was based on using tetrazolium salt to detect superoxide radicals produced by the action of xanthine oxidase on hypoxanthine. Exactly 200 µl of the appropriately diluted radical detector was pipetted into well-labeled microtitre plate wells after which 10 µl each of the prepared standard and serum samples were added in separate wells. The reaction in each well was initiated by dispensing 20 µl diluted xanthine oxidase. The wells were then covered and incubated on a shaker at room temperature for 20 minutes. The absorbance was read at 450 nm using Rayto (RT 6000) plate reader.

2.10.2. Determination of serum catalase activity

The 4-amino-3-hydrazino-5-mercapto-1,2,4-triazole (Purpald) spectrophotometric method was used to determine catalase activity. Into three microtiter wells labeled sample, standard, and control, 100 µl of assay buffer and 30 µl of methanol were added. Twenty microliters of each of the prepared standard and serum samples were added into appropriate wells, then 20 µl H_2O_2 was added to each well to initiate the reaction. The plate was covered and incubated on a shaker for 20 minutes at room temperature after which KOH (30 µl) was added to each well to terminate the reaction. This was followed by the addition of 30 µl of purpald chromogen. The plate was incubated on a shaker for 10 minutes at room temperature. Potassium periodate (10 µl) was pipetted into each well and incubated on a shaker for another 5 minutes and the absorbance was read at 540 nm using Rayto (RT 6000) plate reader.

2.10.3. Determination of glutathione peroxidase activity

Glutathione peroxidase activity was determined by a coupling reaction with glutathione reductase. Oxidized glutathione is produced when hydroperoxide is reduced by glutathione peroxidase. The oxidized glutathione is recycled to its reduced form by the action of glutathione reductase in the presence of NADPH. This decreases the absorbance at 340 nm. Briefly, a microtitre plate was prepared by adding 20 µl serum sample, 100 µl of assay buffer, and 50 µl of the co-substrate mixture. A non-enzymatic well was similarly prepared to contain 50 µl of the co-substrate mixture and

120 µl of assay buffer. The positive control well contained 100 µl of assay buffer, 20 µl of diluted GPx, and 50 µl of the co-substrate mixture. The reaction was initiated by dispensing 20 µl of cumenehydroperoxide to each well. The plates were shaken for a few seconds. The decrease in absorbance was read at 340 nm using Rayto (RT-2100C) plate reader once every 3 minutes.

2.11. Statistical analysis

The results are presented as means ± standard error of the mean (SEM) for triplicate determinations. SPSS statistical software package for windows version 16 (IBM Corp.) was used for one-way analysis of variance (ANOVA) while means were compared for significance using posthoc Ducan's new multiple range test at 95% confidence interval.

3. Results and discussion

3.1. Feed intake, change in body weight, and HOMA-IR of experimental rats fed garlic and turmeric-supplemented diet

Table 2 presents the results of feed intake and body weight changes of experimental rats fed the high-fructose diet supplemented with garlic and turmeric. The positive control group (G2) consumed significantly more feed when compared with all other groups ($p < 0.05$) with a commensurate increased gain in body weight ($p < 0.05$). Feed consumed by groups fed high-fructose diets supplemented with 2% turmeric (G3), 2% mixed turmeric:garlic (G5), and standard diet + 2% mixed turmeric:garlic compared favorably ($p > 0.05$) with the standard diet normal control group (G1) while feed consumed by G4 (standard diet + 2% garlic), G6 (high-fructose diet + 2% garlic) and G7 (standard diet + 2% turmeric) in the range 328.54 ± 2.05 - 330.00 ± 1.10 g was significantly higher ($p < 0.05$) when compared to feed consumed by G1 (normal control). However, no differences in body weight changes ($p > 0.05$) were observed between groups G1, G4, G5, and G7 while the group with the least gain in body weights include G3 and G6 both of which received a high-fructose diet supplemented with 2% turmeric and 2% garlic respectively.

The values of blood glucose, insulin, and HOMA-IR were significantly ($p < 0.05$) lower in the groups fed supplemented diets when compared with the positive group (G2) as shown in Table 3. No differences were observed in the HOMA-IR values for groups that received standard diets with or without supplementation. Interestingly, circulating insulin and HOMA-IR values were observed for a high-fructose diet + 2% mixed turmeric:garlic (G8) compared ($p > 0.05$) with that observed for normal control (G1).

Table 2. Weight gain and feed intake by rats fed garlic and/or turmeric supplemented high-fructose diets

Group	Weight (g)	Feed intake (g)
G1	8.97 ± 1.70^{b}	324.66 ± 2.18^{a}
G2	17.86 ± 2.12^{c}	500.96 ± 2.17^{c}
G3	3.72 ± 1.13^{a}	321.58 ± 1.66^{a}
G4	10.44 ± 0.84^{b}	328.54 ± 2.05^{b}
G5	10.16 ± 3.09^{b}	313.36 ± 3.01^{a}
G6	2.68 ± 1.36^{a}	334.70 ± 1.32^{b}
G7	10.57 ± 2.89^{b}	330.00 ± 1.10^{b}
G8	8.55 ± 2.27^{b}	324.66 ± 3.01^{a}

Values are presented as mean ± SEM for 8 determinations. Values with different superscripts along the same column are significantly different ($p < 0.05$). Group 1 = Standard diet (normal control), Group 2 = High-fructose diet (positive control), Group 3 = High-fructose diet + 2% turmeric, Group 4 = Standard diet + 2% garlic, Group 5 = Standard diet + 2% mixed turmeric:garlic (50% w/w), Group 6 = High-fructose diet + 2% garlic, Group 7 = Standard diet + 2% turmeric; Group 8 = High-fructose diet +2% mixed turmeric:garlic (50% w/w)

Table 3. Glucose, insulin and homeostasis model assessment (HOMA-IR)

Group	Glucose (mmol/l)	Insulin (µU/l)	HOMA-IR
G1	4.59 ± 0.40^{d}	9.33 ± 0.33^{ab}	1.92 ± 0.24^{a}
G2	6.19 ± 0.67^{e}	26.67 ± 0.33^{e}	7.33 ± 0.07^{d}
G3	3.85 ± 0.81^{c}	15.33 ± 0.33^{c}	2.62 ± 0.76^{b}
G4	4.00 ± 0.24^{c}	9.67 ± 0.33^{ab}	1.71 ± 0.54^{a}
G5	4.31 ± 0.49^{c}	17.33 ± 0.33^{d}	3.32 ± 0.80^{c}
G6	3.94 ± 0.64^{c}	17.00 ± 0.58^{d}	2.98 ± 0.13^{c}
G7	4.46 ± 0.11^{d}	10.33 ± 0.33^{b}	2.05 ± 0.80^{a}
G8	4.93 ± 0.13^{d}	8.67 ± 0.33^{a}	1.90 ± 0.08^{a}

Values are presented as mean ± SEM for 3 determinations. Values with different superscripts along the same column are significantly different ($p < 0.05$). Group 1 = Standard diet (normal control), Group 2 = High-fructose diet (positive control), Group 3 = High-fructose diet + 2% turmeric, Group 4 = Standard diet + 2% garlic, Group 5 = Standard diet + 2% mixed turmeric:garlic (50% w/w), Group 6 = High-fructose diet + 2% garlic, Group 7 = Standard diet + 2% turmeric; Group 8 = High-fructose diet +2% mixed turmeric:garlic (50% w/w)

Palatability plays important role in the rate at which sweetened diets such as high-fructose diet is consumed thereby altering the hunger and satiety homeostasis (Lindqvist et al., 2008). Two important diet regulatory hormones insulin and leptin necessary for the metabolism of energy molecules are not elicited following the intake of fructose-rich diets (Arslan & Şanlıer, 2016; Lustig, 2010). Instead, ghrelin, a hormone that promotes overfeeding is increased following fructose consumption (Teff et al., 2004). Furthermore, fructose is a source of unregulated production of acetyl-CoA used in hepatic de novo lipogenesis (Samuel, 2011; Taskinen et al., 2017). High-fructose consumption has also been associated with obesity and other metabolic diseases (Hannou et al., 2018; Malik et al., 2019) which are mainly due to an uncontrolled supply of acetyl-CoA intermediates. Moreover, fructose has also been shown to induce the synthesis of enzymes required for the synthesis of fatty acids (Softic et al., 2017) and stimulate sterol regulatory element–binding protein 1c (SREBP1c) and carbohydrate-responsive element–binding protein (ChREBP) (Herman & Samuel, 2016) even in the absence of insulin which are both regulators of de novo lipogenesis (Ramos et al., 2017). ChREBP is activated by glucose while SREBP-1c is activated by insulin and both respectively upregulate gene expressions of glycolytic and lipogenic enzymes particularly in the liver (Linden et al., 2018).

Our results show that the inclusion of garlic and/or turmeric in the diets could antagonize the effects of fructose on feed intake and weight gain and this probably explains the relative weight decrease observed in the groups fed high-fructose diets supplemented with garlic and/or ginger. Lai et al. (2014) report that garlic up-regulates lipolytic genes and down-regulates sterol regulatory element-

binding protein-1c (SREBP1c), a lipogenic gene while curcumin, the main bioactive component of turmeric was found to inhibit (SREBP) expression (Vafaeipour et al., 2022). In another study with mice, garlic administration was shown to have stimulatory effects on AMP-activated protein kinase (AMPK) and decreased gene expressions of adipogenesis leading to decreased body weight gain and epididymal fat accumulation (Kim & Kim, 2011). AMPK balances nutrient supply with energy demand. Furthermore, Lee et al. (2011) reported that dietary supplementation with garlic decreases the expression of genes for adipogenesis and stimulates the expression of UCP in mice with high-fat diet-induced obesity which resulted in a decreased mass of the adipose tissue. Besides the direct weight-reducing effects of garlic, garlic stimulates the secretion of norepinephrine thereby enhancing triglyceride catabolism and thermogenesis (Oi et al., 1999).

Table 4. Lipid profile and atherogenic indices of rats fed garlic and/or turmeric supplemented high-fructose diets

Group	Total cholesterol (mg/dl)	Triglycerides (mg/dl)	HDL (mg/dl)	LDL (mg/dl)
G1	97.67 ± 0.88^{bc}	52.00 ± 0.73^{b}	20.00 ± 1.15^{bc}	67.27 ± 1.70^{bc}
G2	132.33 ± 1.45^{f}	82.67 ± 0.67^{d}	15.33 ± 0.88^{a}	100.47 ± 1.39^{e}
G3	89.00 ± 1.00^{a}	46.00 ± 0.00^{a}	23.00 ± 1.00^{c}	56.80 ± 0.00^{a}
G4	101.33 ± 2.40^{c}	51.67 ± 2.03^{b}	23.67 ± 0.88^{c}	67.33 ± 1.68^{bc}
G5	109.00 ± 1.00^{d}	60.50 ± 2.50^{c}	28.50 ± 1.50^{d}	68.40 ± 1.00^{c}
G6	118.67 ± 0.67^{e}	61.00 ± 1.00^{c}	30.00 ± 1.73^{d}	76.67 ± 2.18^{d}
G7	114.00 ± 3.06^{d}	81.67 ± 0.88^{d}	16.67 ± 0.67^{ab}	81.00 ± 2.34^{d}
G8	93.00 ± 3.02^{ab}	54.67 ± 1.33^{b}	20.00 ± 1.15^{bc}	73.37 ± 0.81^{ab}

Values are presented as mean ± SEM for 3 determinations. Values with different superscripts along the same column are significantly different ($p < 0.05$). HDL: High-density lipoprotein cholesterol, LDL: Low-density lipoprotein cholesterol, Group 1 = Standard diet (normal control), Group 2 = High-fructose diet (positive control), Group 3 = High-fructose diet + 2% turmeric, Group 4 = Standard diet + 2% garlic, Group 5 = Standard diet + 2% mixed turmeric:garlic (50% w/w), Group 6 = High-fructose diet + 2% garlic, Group 7 = Standard diet + 2% turmeric; Group 8 = High-fructose diet +2% mixed turmeric:garlic (50% w/w)

Table 5. Atherogenic and coronary risk indices of rats fed garlic and/or turmeric supplemented high-fructose diets

Group	Atherogenic index	Coronary risk index
G1	3.40 ± 0.28^{a}	4.92 ± 0.31^{b}
G2	6.60 ± 0.40^{c}	8.68 ± 0.47^{d}
G3	2.47 ± 0.11^{a}	3.88 ± 0.13^{a}
G4	2.85 ± 0.09^{a}	4.29 ± 0.09^{ab}
G5	2.41 ± 0.16^{a}	3.83 ± 0.17^{a}
G6	2.57 ± 0.22^{a}	3.98 ± 0.25^{a}
G7	4.86 ± 0.06^{b}	6.85 ± 0.10^{c}
G8	3.12 ± 0.17^{a}	4.67 ± 0.20^{ab}

Values are presented as mean ± SEM for 3 determinations. Values with different superscripts along the same column are significantly different ($p < 0.05$). HDL: High-density lipoprotein cholesterol, LDL: Low-density lipoprotein cholesterol, Group 1 = Standard diet (normal control), Group 2 = High-fructose diet (positive control), Group 3 = High-fructose diet + 2% turmeric, Group 4 = Standard diet + 2% garlic, Group 5 = Standard diet + 2% mixed turmeric:garlic (50% w/w), Group 6 = High-fructose diet + 2% garlic, Group 7 = Standard diet + 2% turmeric; Group 8 = High-fructose diet +2% mixed turmeric:garlic (50% w/w)

Curcumin has also been shown to have anti-obesity activities by inducing apoptosis of 3T3-L1 adipocytes, inhibiting adipogenesis, and activating lipolysis (Wu et al., 2019). According to Kang and Kim (2010), curcumin decreases glucose levels by inhibiting glucose-6-phosphatase and phosphoenolpyruvate carboxykinase and thus activates glycolytic and glycogenic pathways while downregulating gluconeogenesis. Curcumin has also been reported to stimulate insulin production in hyperglycemic individuals to maintain a euglycemic state (Na et al., 2011). Also, curcumin increases adiponectin release and lowers the levels of pro-inflammatory interleukin (IL)-6 IL-1β and tumor necrosis factor-α in patients with type 2 diabetes mellitus.

As observed in this study, the improved insulin sensitivity in the groups fed high-fructose diets supplemented with garlic and/or turmeric (Table 3) could partly be due to the anti-obesity activities of the spices. Insulin resistance is usually associated with an increase in body weight in several ways including the interference with inefficient energy utilization arising from a surplus supply of high-energy molecules (Samuel & Shulman, 2016), interference with insulin signaling by toxic metabolites formed from ectopic deposits of lipids (Lee et al., 2011) or triggering of inflammation which could inhibit insulin receptor substrate 1 (IRS-1) and insulin receptor (IR) in the insulin signal transduction pathway (Ye & Gimble, 2011). Therefore, by regulating energy intake and weight gain as discussed, the inclusion of these spices could protect against insulin resistance. From our results, the inclusion of garlic and/or turmeric powder in the diets probably mediates weight control and insulin sensitivities in high-fat diet-exposed Wistar rats.

3.2. Lipid profiles and atherogenic indices of rats fed garlic and/or turmeric-supplemented high-fructose diets

Table 4 shows the lipid profile and atherogenic indices of rats fed garlic and/or turmeric-supplemented high-fructose diet. Except for the high-fructose diet + 2% mixed turmeric:garlic group (G8), the lipid profiles of all other groups were elevated ($p < 0.05$) when compared with the normal control group (G1). However, the lipid profiles of all the high-fructose diet groups that received supplements had significantly ($p < 0.05$) lower serum total cholesterol, triglycerides, and LDL-C and significantly ($p < 0.05$) higher HDL when compared with the positive control (G2). Interestingly, total cholesterol, serum triglycerides, HDL, and LDL levels of the group fed a 2% turmeric-supplemented normal diet did not differ significantly ($p > 0.05$) from that of the normal control group (G1).

As shown in Table 5, there is an elevated coronary risk in the group fed a high-fructose diet only (positive control group). The atherogenic index of groups that received supplemented high-fructose diets was comparable to the normal control group ($p < 0.05$) but significantly different ($p < 0.05$) from the positive control group (G2). Except for the positive control group (G2), the group fed a turmeric-supplemented normal diet (G7) had significantly higher AI and CRI compared with the other experimental groups.

As results indicate improvements in weight, blood glucose levels, and reduced likelihood for insulin resistance in the groups of rats fed garlic and/or turmeric-supplemented diets, the anti-dyslipidemic

traits observed in Table 5 for the treatment groups are quite expected. Dyslipidemia is an independent risk factor component of metabolic syndrome for atherosclerotic patients (Ginsberg et al., 2006). In insulin resistance, for example, there is poor VLDL clearance due to a decrease in lipoprotein lipase (LPL) mRNA expression (Rashid et al., 2003). Fructose metabolism supplies abundant triose-phosphates which are the precursors of both glycerol- and the fatty-acyl moieties of VLDL-triglycerides. Furthermore, stimulation of SREBP by fructose activates HMG-CoA reductase and fatty acid synthase (FAS) which play important roles in cholesterol and fatty acid biosynthesis respectively. The observed anti-dyslipidemic effect of turmeric and/or garlic supplementation in a high-fructose diet is consistent with reported anti-cardiometabolic functions as well as the cardioprotective role of curcuminoids (Johnston et al., 2017; Qin et al., 2017). In another study, garlic and its bioactive component, allicin have been shown to also decrease the HMG-CoA reductase activity and the expression of HMG-CoA reductase mRNA in rats with hypercholesterolemia (Gupta & Porter, 2001; Rai et al., 2009). LXR-α is a lipogenic transcription factor that causes the induction of SREBP-1c. Garlic and turmeric as reported by Mohammadi and Oshaghi (2014) inhibit LXR-α expression in the liver but stimulate LXR-α expression in the intestine. Decreasing LXR-α expression in the liver will decrease SREBP1c and therefore decrease the expression of lipogenic enzymes like ACC and FAS as earlier discussed. On the other hand, by stimulating LXR-α in the intestine, garlic reduces intestinal absorption of cholesterol. Sahebkar et al. (2014) also noted that curcumin decreases lipogenic gene expressions in diet-induced metabolic syndrome and therefore, is a regulator of plasma lipid concentration. Besides decreasing the hepatic expression of lipogenic transcription factors LXR-α and SREBP1c (Maithilikarpagaselvi et al., 2016), curcumin has also been reported to covalently modify FAS by competitively binding to malonyl/acetyltransferase domain resulting in decreased TAG synthesis. Our results suggest the long-term consumption of diets supplemented with turmeric and/or garlic could prevent dyslipidemia and thus reduce cardiometabolic risks associated with excessive consumption of metabolic syndrome-causing diets.

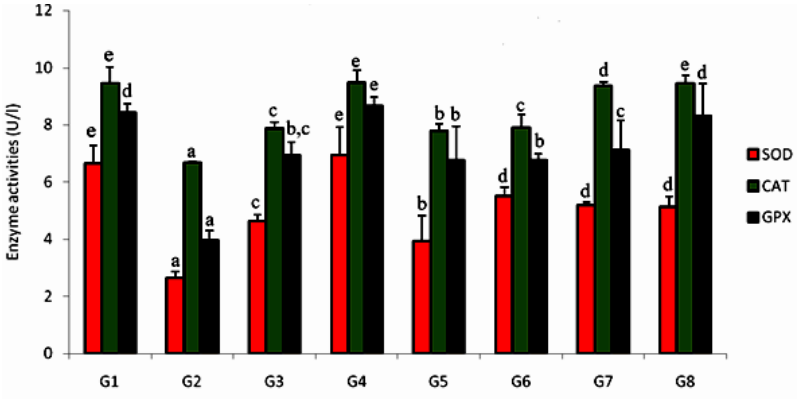

Figure 1. Serum antioxidant enzymes activities in rats fed high-fructose diets supplemented with garlic and/or turmeric

Values are presented as mean ± SEM. Columns with different superscripts for a given enzyme are significantly different ($p < 0.05$). SOD = Superoxide dismutase, CAT = Catalase, GPx = Glutathione peroxidase, G1 = Standard diet (normal control), G2 = High-fructose diet (positive control), G3 = High-fructose diet + 2% turmeric, G4 = Standard diet + 2% garlic, G5 = Standard diet + 2% mixed turmeric:garlic (50% w/w), G6 = High-fructose diet + 2% garlic, G7 = Standard diet + 2% turmeric; G8 = High-fructose diet +2% mixed turmeric:garlic (50% w/w)

3.3. Activities of antioxidant enzymes in rats fed garlic and/or turmeric-supplemented high-fructose diets

Figure 1 presents the activities of serum antioxidant enzymes of rats fed a high-fructose diet supplemented with garlic and/or turmeric. The serum enzyme activities of all the studied antioxidant enzymes (SOD, catalase, and glutathione peroxidase) were significantly higher in all groups fed garlic and/or turmeric-supplemented diets as compared with the positive control group, but mostly lower than the activities in the normal control (Figure 1).

Oxidative stress is an important component of metabolic syndrome and thus a risk factor for the development of cardiometabolic diseases. Imam et al. (2022) noted in their study that intake of high-fructose diets results in hyperglycemia and insulin resistance - two leading causes of oxidative stress. Thus excess energy-rich substrates in the metabolic pool especially in obese individuals increase the likelihood of excess production of free radicals (McMurray et al., 2016). The elevated activities of the antioxidant enzymes are consistent with the observed changes in body weight, and reduced risks of insulin resistance and dyslipidemia in the groups fed a high-fructose diet supplemented with garlic and/or turmeric. Oxidative stress is not only a major pathogenesis of these conditions, it is further exacerbated by the conditions (Maslov et al., 2019). In our previous report (Idoko et al., 2022), it was suggested that the hepatoprotective and nephroprotective effects of these supplements may also have a balancing effect on oxidative redox. Earlier reports (Afrin et al., 2017; Coban et al., 2012) demonstrated that curcumin lowers the production of free radicals and stimulates the synthesis of antioxidant enzymes. Similarly, allicin was found to increase concentrations of glutathione in the liver (Panyod & Sheen, 2020). Therefore findings in this study and earlier reports suggest the inclusion of the spices may not only retard conditions that lead to oxidative stress but also directly scavenge free radicals. Our finding strongly suggests that the inclusion of garlic and/or turmeric in high-fructose diets improved the oxidative status exhibited by experimental rats that received supplementation.

4. Conclusions

In conclusion, our results reveal that the inclusion of garlic and/or turmeric powder in a metabolic syndrome-causing diet was beneficial in improving the atherogenic and coronary risk indices, as well as the HOMA-IR of experimental rats that received supplementation, and this could prevent long-term excess fat accumulation, dyslipidemia, and oxidative stress. Thus, the inclusion of garlic and/or turmeric powder in the diet may forestall the development of the physical and biochemical components of metabolic syndrome risk factors which were maintained on a high-fructose diet for 8 weeks in rats.

Acknowledgments

None.

Conflict of interest

The authors confirm that there are no known conflicts of interest.

Statement of ethics

The rats were kept according to the standards for keeping experimental rodents as approved by the Federal University Dutsin-Ma Ethical Committee on the use of experimental animals and human subjects (FUDMA/IEC/2021205).

Availability of data and materials

All data generated or analyzed during this study are included in this published article.

Funding

None.

CRediT authorship contribution statement

Ali Siddiq Idoko: Conceptualization and interpretation of data, Writing original draft
Aliyu Abdullahi: Methodology, Formal analysis
Masud Eneji Sadiq: Literature review, Formal analysis, Proofreading
Bilkis Muhammad Maibalangu: Experimental investigation, Data collection

ORCID Numbers of the Authors

A. S. Idoko: 0000-0003-1700-7631
A. Abdullahi: 0000-0002-4020-0459
M. E. Sadiq: 0000-0001-5193-4338
B. M. Maibalangu: 0000-0003-3781-7682

Supplementary File

None.

Publisher's Note

All claims expressed in this article are solely those of the authors and do not necessarily represent those of their affiliated organizations, or those of the publisher, the editors and the reviewers. Any product that may be evaluated in this article, or claim that may be made by its manufacturer, is not guaranteed or endorsed by the publisher.

This is an open-access article distributed under the terms of the Creative Commons Attribution 4.0 International License (CC BY). The use, distribution or reproduction in other forums is permitted, provided the original author(s) and the copyright owner(s) are credited and that the original publication in this journal is cited, in accordance with accepted academic practice. No use, distribution or reproduction is permitted which does not comply with these terms.

References

Afrin, R., Arumugam, S., Rahman, A., Wahed, M. I. I., Karuppagounder, V., Harima, M., Suzuki, H., Miyashita, S., Suzuki, K., *et al.* (2017). Curcumin ameliorates liver damage and progression of NASH in NASH-HCC mouse model possibly by modulating HMGB1-NF-κB translocation. *International Immunopharmacology, 44*, 174-182.

Alberti, K. G., Eckel, R. H., Grundy, S. M., Zimmet, P. Z., Cleeman, J. I., Donato, K. A., Fruchart, J. C., James, W. P. T., Loria, C. M., *et al.* (2009). Harmonizing the metabolic syndrome: a joint interim statement of the international diabetes federation task force on epidemiology and prevention; national heart, lung, and blood institute; American heart association; world heart federation; international atherosclerosis society; and international association for the study of obesity. *Circulation, 120*(16), 1640-1645.

Anand, P., Kunnumakkara, A. B., Newman, R. A., & Aggarwal, B. B. (2007). Bioavailability of curcumin: problems and promises. *Molecular Pharmaceutics, 4*(6), 807-818.

Arslan, S., & Şanlıer, N. (2016). Relationship between daily dietary fructose intake, body composition and biochemical parameters patients with type 2 diabetes. *Journal of Human Sciences, 13*(2), 2642-2655.

Coban, D., Milenkovic, D., Chanet, A., Khallou-Laschet, J., Sabbe, L., Palagani, A., Vanden Berghe, W., Mazur, A., & Morand, C. (2012). Dietary curcumin inhibits atherosclerosis by affecting the expression of genes involved in leukocyte adhesion and transendothelial migration. *Molecular Nutrition & Food Research, 56*(8), 1270-1281.

National Research Council (2011). Guide for the care and use of laboratory animals, National Academies Press. *Washington, DC.*

do Vale Moreira, N. C., Hussain, A., Bhowmik, B., Mdala, I., Siddiquee, T., Fernandes, V. O., Júnior, R. M. M., & Meyer, H. E. (2020). Prevalence of metabolic syndrome by different definitions, and its association with type 2 diabetes, pre-diabetes, and cardiovascular disease risk in Brazil. *Diabetes & Metabolic Syndrome: Clinical Research & Reviews, 14*(5), 1217-1224.

Engin, A. (2017). The definition and prevalence of obesity and metabolic syndrome. Obesity and Lipotoxicity. *Advances in Experimental Medicine and Biology,* (Vol. 960): Springer, Cham.

Friedewald, W. T., Levy, R. I., & Fredrickson, D. S. (1972). Estimation of the concentration of low-density lipoprotein cholesterol in plasma, without use of the preparative ultracentrifuge. *Clinical Chemistry, 18*(6), 499-502.

Gierach, M., Gierach, J., Ewertowska, M., Arndt, A., & Junik, R. (2014). Correlation between body mass index and waist circumference in patients with metabolic syndrome. *International Scholarly Research Notices, 2014*, 514589.

Ginsberg, H. N., Zhang, Y. L., & Hernandez-Ono, A. (2006). Metabolic syndrome: focus on dyslipidemia. *Obesity, 14*(2S), 41S-49S.

Gupta, N., & Porter, T. D. (2001). Garlic and garlic-derived compounds inhibit human squalene monooxygenase. *The Journal of Nutrition, 131*(6), 1662-1667.

Hannou, S. A., Haslam, D. E., McKeown, N. M., & Herman, M. A. (2018). Fructose metabolism and metabolic disease. *The Journal of Clinical Investigation, 128*(2), 545-555.

Herman, M. A., & Samuel, V. T. (2016). The sweet path to metabolic demise: fructose and lipid synthesis. *Trends in Endocrinology & Metabolism, 27*(10), 719-730.

Huang, C. J., McAllister, M. J., Slusher, A. L., Webb, H. E., Mock, J. T., & Acevedo, E. O. (2015). Obesity-related oxidative stress: the impact of physical activity and diet manipulation. *Sports Medicine-Open, 1*(1), 32.

Idoko, A., Abdullahi, A., Maibulangu, B., Nura, L., Imam, N., Bonomi, Z., Muhammed, F., & Umar, S. (2022). *Allium sativum* and *Curcuma longa* Powder Protect Against Hepatotoxic and Nephrotoxic Effects of High-fructose Diet. *FUOYE Journal of Pure and Applied Sciences (FJPAS), 7*(1), 59-78.

Imam, N., Idoko, A., Osibemhe, M., Lawal, N., & Zaharaddeen, A. (2022). Obesity and Insulin Resistance Components of Metabolic Syndrome Induced by High-fructose Diet in Wistar Rats could be attenuated by Spices-Supplemented Diets. *Journal of Applied Sciences and Environmental Management, 26*(5), 893-901.

Johnston, T., Korolenko, T., Pirro, M., & Sahebkar, A. (2017). Preventing cardiovascular heart disease: Promising nutraceutical and non-nutraceutical treatments for cholesterol management. *Pharmacological Research, 120*, 219-225.

Kang, C., & Kim, E. (2010). Synergistic effect of curcumin and insulin on muscle cell glucose metabolism. *Food and Chemical Toxicology, 48*(8-9), 2366-2373.

Kazemi, T., Hajihosseini, M., Moossavi, M., Hemmati, M., & Ziaee, M. (2018). Cardiovascular risk factors and atherogenic indices in an Iranian population: Birjand East of Iran. *Clinical Medicine Insights: Cardiology, 12*, 1179546818759286.

Kim, M., & Kim, H. (2011). Effect of garlic on high fat induced obesity. *Acta Biologica Hungarica, 62*(3), 244-254.

Lai, Y. S., Chen, W. C., Ho, C. T., Lu, K. H., Lin, S. H., Tseng, H. C., Lin, S. Y., & Sheen, L. Y. (2014). Garlic essential oil protects against obesity-triggered nonalcoholic fatty liver disease through modulation of lipid metabolism and oxidative stress. *Journal of Agricultural and Food Chemistry, 62*(25), 5897-5906.

Lee, M. S., Kim, I. H., Kim, C. T., & Kim, Y. (2011). Reduction of body weight by dietary garlic is associated with an increase in uncoupling protein mRNA expression and activation of AMP-activated protein kinase in diet-induced obese mice. *The Journal of Nutrition, 141*(11), 1947-1953.

Linden, A. G., Li, S., Choi, H. Y., Fang, F., Fukasawa, M., Uyeda, K., Hammer, R. E., Horton, J. D., Engelking, L. J., *et al.* (2018). Interplay between ChREBP and SREBP-1c coordinates postprandial glycolysis and lipogenesis in livers of mice [S]. *Journal of Lipid Research, 59*(3), 475-487.

Lindqvist, A., Baelemans, A., & Erlanson-Albertsson, C. (2008). Effects of sucrose, glucose and fructose on peripheral and central appetite signals. *Regulatory Peptides, 150*(1-3), 26-32.

Lustig, R. H. (2010). Fructose: metabolic, hedonic, and societal parallels with ethanol. *Journal of the American Dietetic Association, 110*(9), 1307-1321.

Maithilikarpagaselvi, N., Sridhar, M. G., Swaminathan, R. P., Sripradha, R., & Badhe, B. (2016). Curcumin inhibits hyperlipidemia and hepatic fat accumulation in high-fructose-fed male Wistar rats. *Pharmaceutical Biology, 54*(12), 2857-2863.

Malik, V. S., Li, Y., Pan, A., De Koning, L., Schernhammer, E., Willett, W. C., & Hu, F. B. (2019). Long-term consumption of sugar-sweetened and artificially sweetened beverages and risk of mortality in US adults. *Circulation, 139*(18), 2113-2125.

Maslov, L. N., Naryzhnaya, N. V., Boshchenko, A. A., Popov, S. V., Ivanov, V. V., & Oeltgen, P. R. (2019). Is oxidative stress of adipocytes a cause or a consequence of the metabolic syndrome? *Journal of Clinical & Translational Endocrinology, 15*, 1-5.

McMurray, F., Patten, D. A., & Harper, M. E. (2016). Reactive oxygen species and oxidative stress in obesity—recent findings and empirical approaches. *Obesity, 24*(11), 2301-2310.

Mohammadi, A., & Oshaghi, E. A. (2014). Effect of garlic on lipid profile and expression of LXR alpha in intestine and liver of hypercholesterolemic mice. *Journal of Diabetes & Metabolic Disorders, 13*, 20.

Na, L. X., Zhang, Y. L., Li, Y., Liu, L. Y., Li, R., Kong, T., & Sun, C. H. (2011). Curcumin improves insulin resistance in skeletal muscle of rats. *Nutrition, Metabolism and Cardiovascular Diseases, 21*(7), 526-533.

Nguyen, N. T., Magno, C. P., Lane, K. T., Hinojosa, M. W., & Lane, J. S. (2008). Association of hypertension, diabetes, dyslipidemia, and metabolic syndrome with obesity: findings from the National Health and Nutrition Examination Survey, 1999 to 2004. *Journal of the American College of Surgeons, 207*(6), 928-934.

Oi, Y., Kawada, T., Shishido, C., Wada, K., Kominato, Y., Nishimura, S., Ariga, T., & Iwai, K. (1999). Allyl-containing sulfides in garlic increase uncoupling protein content in brown adipose tissue, and noradrenaline and adrenaline secretion in rats. *The Journal of Nutrition, 129*(2), 336-342.

Panyod, S., & Sheen, L. Y. (2020). Beneficial effects of Chinese herbs in the treatment of fatty liver diseases. *Journal of Traditional and Complementary Medicine, 10*(3), 260-267.

Pekgor, S., Duran, C., Berberoglu, U., & Eryilmaz, M. A. (2019). The role of visceral adiposity index levels in predicting the presence of metabolic syndrome and insulin resistance in overweight and obese patients. *Metabolic Syndrome and Related Disorders, 17*(5), 296-302.

Qin, S., Huang, L., Gong, J., Shen, S., Huang, J., Ren, H., & Hu, H. (2017). Efficacy and safety of turmeric and curcumin in lowering blood lipid levels in patients with cardiovascular risk factors: a meta-analysis of randomized controlled trials. *Nutrition Journal, 16*, 68.

Rai, S. K., Sharma, M., & Tiwari, M. (2009). Inhibitory effect of novel diallyldisulfide analogs on HMG-CoA reductase expression in hypercholesterolemic rats: CREB as a potential upstream target. *Life Sciences, 85*(5-6), 211-219.

Ramos, V. W., Batista, L. O., & Albuquerque, K. T. (2017). Effects of fructose consumption on food intake and biochemical and body parameters in Wistar rats. *Revista Portuguesa de Cardiologia (English Edition), 36*(12), 937-941.

Rashid, S., Watanabe, T., Sakaue, T., & Lewis, G. F. (2003). Mechanisms of HDL lowering in insulin resistant, hypertriglyceridemic states: the combined effect of HDL triglyceride enrichment and elevated hepatic lipase activity. *Clinical Biochemistry, 36*(6), 421-429.

Rehman, K., & Akash, M. S. H. (2016). Mechanisms of inflammatory responses and development of insulin resistance: how are they interlinked? *Journal of Biomedical Science, 23*, 87.

Rodriguez-Cano, A., Mier-Cabrera, J., Balas-Nakash, M., Muñoz-Manrique, C., Legorreta-Legorreta, J., & Perichart-Perera, O. (2015). Dietary changes associated with improvement of metabolic syndrome components in postmenopausal women receiving two different nutrition interventions. *Menopause (New York, NY), 22*(7), 758-764.

Sahebkar, A., Chew, G. T., & Watts, G. F. (2014). Recent advances in pharmacotherapy for hypertriglyceridemia. *Progress in Lipid Research, 56*, 47-66.

Samuel, V. T. (2011). Fructose induced lipogenesis: from sugar to fat to insulin resistance. *Trends in Endocrinology & Metabolism, 22*(2), 60-65.

Samuel, V. T., & Shulman, G. I. (2016). The pathogenesis of insulin resistance: integrating signaling pathways and substrate flux. *The Journal of Clinical Investigation, 126*(1), 12-22.

Softic, S., Gupta, M. K., Wang, G. X., Fujisaka, S., O'Neill, B. T., Rao, T. N., Willoughby, J., Harbison, C., Fitzgerald, K., *et al.* (2017). Divergent effects of glucose and fructose on hepatic lipogenesis and insulin signaling. *The Journal of Clinical Investigation, 127*(11), 4059-4074.

Sperling, L. S., Mechanick, J. I., Neeland, I. J., Herrick, C. J., Després, J. P., Ndumele, C. E., Vijayaraghavan, K., Handelsman, Y., Puckrein, G. A., *et al.* (2015). The cardiometabolic health alliance: working toward a new care model for the metabolic syndrome. *Journal of the American College of Cardiology, 66*(9), 1050-1067.

Taskinen, M. R., Söderlund, S., Bogl, L., Hakkarainen, A., Matikainen, N., Pietiläinen, K., Räsänen, S., Lundbom, N., Björnson, E., *et al.* (2017). Adverse effects of fructose on cardiometabolic risk factors and hepatic lipid metabolism in subjects with abdominal obesity. *Journal of Internal Medicine, 282*(2), 187-201.

Teff, K. L., Elliott, S. S., Tschöp, M., Kieffer, T. J., Rader, D., Heiman, M., Townsend, R. R., Keim, N. L., D'alessio, D., *et al.* (2004). Dietary fructose reduces circulating insulin and leptin, attenuates postprandial suppression of ghrelin, and increases triglycerides in women. *The Journal of Clinical Endocrinology & Metabolism, 89*(6), 2963-2972.

Tian, Y., Su, L., Wang, J., Duan, X., & Jiang, X. (2018). Fruit and vegetable consumption and risk of the metabolic syndrome: A meta-analysis. *Public Health Nutrition, 21*(4), 756-765.

Tune, J. D., Goodwill, A. G., Sassoon, D. J., & Mather, K. J. (2017). Cardiovascular consequences of metabolic syndrome. *Translational Research, 183*, 57-70.

Vafaeipour, Z., Razavi, B. M., & Hosseinzadeh, H. (2022). Effects of turmeric (*Curcuma longa*) and its constituent (curcumin) on the metabolic syndrome: An updated review. *Journal of Integrative Medicine, 20*(3), 193-203.

Wu, L. Y., Chen, C. W., Chen, L. K., Chou, H. Y., Chang, C. L., & Juan, C. C. (2019). Curcumin attenuates adipogenesis by inducing preadipocyte apoptosis and inhibiting adipocyte differentiation. *Nutrients, 11*(10), 2307.

Ye, J., & Gimble, J. M. (2011). Regulation of stem cell differentiation in adipose tissue by chronic inflammation. *Clinical and Experimental Pharmacology and Physiology, 38*(12), 872-878.

Yin, J., Li, M., Xu, L., Wang, Y., Cheng, H., Zhao, X., & Mi, J. (2013). Insulin resistance determined by Homeostasis Model Assessment (HOMA) and associations with metabolic syndrome among Chinese children and teenagers. *Diabetology & Metabolic Syndrome, 5*, 71.

Int. J. Plant Bas. Pharm. (2023) 3(1), 62-67

INTERNATIONAL JOURNAL OF PLANT BASED PHARMACEUTICALS

https://ijpbp.com

RESEARCH ARTICLE

OPEN ACCESS

Investigation of apoptotic, cytotoxic, and antioxidant effects of *Juglans regia* against MDA-MB-231 and A549 cell lines

Lütfiye Kadıoğlu Dalkılıç[a]*, Semih Dalkılıç[a], Lütfü Uygur[a]

[a] *Firat University, Faculty of Science, Department of Biology, 23000, Elazığ, Türkiye*

ARTICLE INFO

Article History:

Received: 05 January 2023
Revised: 18 January 2023
Accepted: 26 January 2023
Available online: 31 January 2023

Edited by: B. Tepe

Keywords:

Cell line
Anticancer
Antioxidant
Juglans regia
MTT assay

ABSTRACT

Cancer is one of the most common pathologies in the world, which for centuries has led to a decline in the standard of living and even death of many people. In short, cancer is a disease that occurs when mutations in genes that limit and regulate cell proliferation, survival, and movement are reflected in somatic cells. In recent years, there have been many new and promising developments in the world of science for cancer treatment. However, due to the side effects of some treatments, the cost of others, and the fact that some drugs are still in the trial phase, it has not yet reached the expected level of treatment and success. This has encouraged the scientific community to investigate natural agents due to their lower cost and limited side effects. *Juglans regia* L., popularly known as walnut, is a plant containing many natural compounds that have been used both as a foodstuff and for various medicinal purposes from past to present. As a result of the literature review, it is known that walnut has many medicinal and biological properties, especially anti-inflammatory, antifungal and antiallergic properties. In this study, the outer shells of *J. regia* were used and the components of these shells were extracted with three different solvents: methanol, ethanol, and hexane. These extracts were used in cytotoxic activity and antioxidant activity assays. The antioxidant activity of the extract was determined using a DPPH assay. Cytotoxic activity was determined by MTT assay using a breast cancer cell line (MDA-MB-231). *J. regia* extracts were found to have significant cytotoxic activity on the MDA-MB-231 cell line. It has been observed that the outer bark of *J. regia* showed more potent anticancer effects than antioxidant activity. According to the results obtained from the study, the antioxidant and cytotoxic effect of the outer bark of *J. regia* is thought to contribute significantly to the identification of new active substances for cancer treatment. Therefore, further studies are needed to fully determine the effects of the outer bark of *J. regia*.

1. Introduction

Cancer is one of the 20th century's most dreaded diseases, cancer is still occurring with persistence and increasing incidence. The situation is so alarming that one in four people is at a lifetime risk of cancer (Roy & Saikia, 2016). With more than 10 million deaths per year, cancer is one of the most important health problems on earth, and both its diagnosis and treatment have become a major challenge for the scientific community (Siddiqui et al., 2022). Breast cancer is the most common type of cancer and one of the most common causes of cancer death in women (Khan et al., 2022). Although treatments for breast cancer have made significant progress in recent years, many patients continue to experience metastasis and tumor growth due to chemoresistance as well as many disadvantages associated with chemotherapy and radiotherapy. For this reason, researchers are exploring new methods to better understand cancer cells' behavior and develop more effective therapies against them. Due to the serious side effects of synthetic drugs used for treatment and the medical and economic problems they cause, treatment with herbs has become popular (Akkol et al., 2020).

Reviewed by:
Aynur Karadag Gurel: Usak University, Usak, Türkiye
Muhsin Aydın: Adiyaman University, Adiyaman, Türkiye

* Corresponding author(s):
E-mail address:
tkadioglu85@gmail.com (L. Kadıoğlu Dalkılıç)
e-ISSN: 2791-7509
doi: https://doi.org/10.29228/ijpbp.17

Herbal medicines have become a very safe, non-toxic, and readily available source for compounds that treat cancer. Plants are believed to neutralize the effects of diseases in the body due to their various properties (Khan et al., 2019). Oilseeds and nuts play an important role in the nutrition of cancer patients because they are rich in biocomponents (Deniz Güneş & Acar Tek, 2021).

Juglans regia L., popularly known as walnut, is one of 64 species belonging to the Juglandaceae family. It is a plant thought to be native to the Middle East, Anatolia, northern parts of Iran, and the Himalayas. Since ancient times, *J. regia* has been used not only as a food but also in fields such as pharmacology and cosmetics with its different parts. It has also proved to be effective against coronary heart disease, diabetes, obesity, and rheumatism with regular use. Considering the results of the previous studies, it is seen that the regular consumption of walnuts causes a decrease in the incidence of cancer (Catanzaro et al., 2015; Schmiech et al., 2019).

2. Materials and methods

2.1. Extract preparation

J. regia was collected from the Cip district of Elazığ in Turkey. The outer reddish shells were separated, dried, and ground to give one gram of powder. Then, 1 g was taken and kept for 72 hours with 10 ml of methanol, ethanol, and hexane solvents in a shaker incubator. All extracts were filtered with Whatman filter paper to remove extra particles of outer shells. The final stock was mixed with 10 ml of DMEM medium to gain the desired concentration, as shown in (Figure 1).

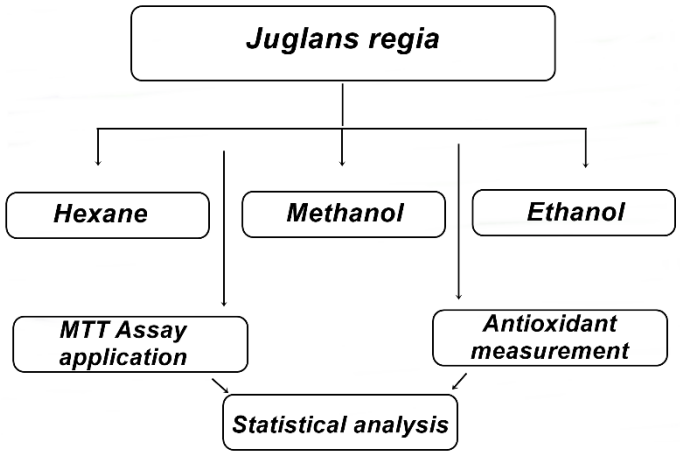

Figure 1. Experiment flowchart
The general design of the experiment has shown applied methods on the outer shells of *J. regia*.
Three different solvents; hexane, methanol, and ethanol were used to evaluate cytotoxic and antioxidant activities.

2.2. Supply of cell line

MDA-MB-231 and A549 cell lines were obtained from Fırat University. Both cell lines were grown in DMEM [1% L-Glutamine, 1% Penicillin-Streptomycin, and 10% FBS (Fetal Bovine Serum)] in 25cm^2 flasks at 37 °C and 5% CO_2 atmosphere conditions.

2.2.1. Cell culture and cell line

When both cell lines grown in 25cm^2 flasks became 90% confluent, the medium in the flask was removed and washed with 5ml sterile PBS solution. 1ml Trypsin-EDTA was added to the flasks and incubated at 37 °C for 2 minutes in an incubator with 5% CO_2 and Trypsin-EDTA was inactivated with 5ml medium. Cells were removed from the flask and centrifuged at 1200 rpm for 5 minutes, then the supernatant was removed, the cell pellet was diluted with DMEM and 100 µl was seeded into 96-well plates according to the calculation after cell counting. Only medium was added to the first row to be used as blank and incubated for 24 hours at 37 °C in an incubator containing 5% CO_2. After incubation, *J. regia* outer shell extract diluted with the medium was added in three different concentrations, 12 replicates of each concentration, and incubated for 72 hours at 37 °C in an incubator containing 5% CO_2. 2.5 µg/ml doxorubicin was used as the positive control and DMEM was used as the negative control. MTT test was performed after incubation.

2.3. MTT assay application

The MTT [3-(4,5-dimethylthiazol-2-yl)-2,5-diphenyltetrazolium bromide] assay is a method used for measuring cell viability, proliferation, and cytotoxicity. The MTT method is based on the active mitochondria in living cells, reducing the MTT, a tetrazolium salt that can pass through the cell membrane, by taking electrons inside the cell and converting it into purple water-insoluble formazan crystals (Dalkilic et al., 2021; Riss & Moravec, 2004). The effect of plant extracts on cell viability at the end of incubation was determined by the MTT method. First, 20µl 5 mg/ml MTT solution was added to the wells containing cells from stock MTT (Thermo Fisher, USA) prepared in sterile phosphate buffer (pH: 7.2) and incubated for 4 hours at 37 °C in a dark environment containing 5% CO_2. After incubation, the medium was removed and formazan crystals were dissolved with 100µl DMSO (dimethylsulphoxide). The absorbance values were then determined using a plate reader (Synergy HT USA) device at a wavelength of 570 nm. By reading the control wells, the absorbance values obtained were averaged and this value was accepted as 100% live cell. The absorbance values obtained from the wells of plant extract were compared to the control absorbance value and percent viability values were calculated (Coskun et al., 2021; Dalkilic et al., 2021). The absorbance values measured with the plate reader device were recorded, then the measured absorbance values were compared with the control groups.

2.4. Antioxidant measurement

The antioxidant properties of *J. regia* were determined by DPPH free radical scavenging activity. DPPH (Sigma-Aldrich, USA) was prepared in methanol as a free radical. A stock solution of extracts was prepared and diluted with methanol as 2, 1, 0.5, 0.25, and 0.125 mg/ml. Methanol (2.5 ml) was used as a negative control. 0.3 mM DPPH methanol solution was added to the samples. The plate was left under incubation for 30 minutes in a dark environment, and the spectrophotometer absorbance values were measured at 517 nm. Due to the reduced absorbance, the remaining DPPH is detected as free radical removal activity (Flieger & Flieger, 2020; Huang et al., 2005).

Results were calculated based on the formula given below:

$$Antioxidant\ activity\ (\%) = \frac{Control\ ABS - Sample\ ABS}{Control\ ABS} x\ 100$$

3. Results and discussion

The inhibition percentage of the DPPH radical in different concentrations of the methanol extract of the *J. regia* shell is mentioned in (Figure 2). According to the results, outer shell extracts of *J. regia* have shown antioxidant activities in a dose-dependent manner. The cytotoxic activity of the shell extract of *J. regia*, with ethanol, methanol, and hexane on the MDA-MB-231 (breast cancer) cell line at concentrations of 1/1000, 1/2000, and 1/4000 µg/ml were investigated. According to the results obtained from the study, methanol and hexane extracts exhibited significant differences compared to the control (p <0.05) at 1/1000 µg/ml concentration.

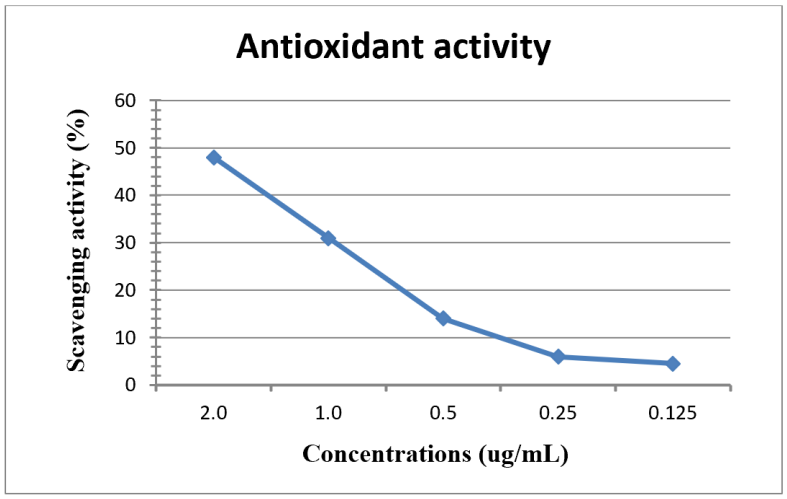

Figure 2. Percent inhibition of DPPH free radical scavenging activities
Percentage change of DPPH radical scavenging inhibition activity of methanol extract of *J. regia* according to concentrations.

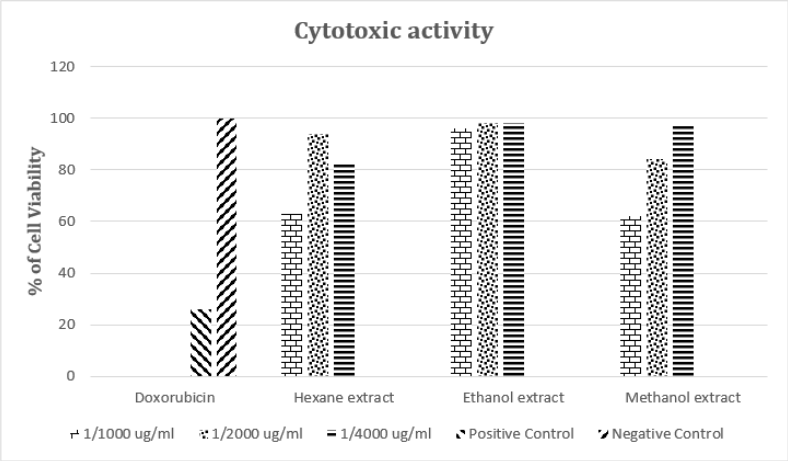

Figure 3. Results of cytotoxic activity in the MDA-MB-231 cell line
Represents the percentage of live cells, three extracts, three different concentrations, and analysis with MTT assay to observe effects of *J. regia* on MDA-MB 231 cell lines, DMEM: negative control (-), doxorubicin (2.5 µg/ml): positive control (+).

Cell viability was reduced and it was observed to have a cytotoxic effect at 1/1000 µg/ml concentration. While ethanol extract of *J. regia* showed non-significant differences compared to the control. Cell viability is not reduced and it was observed to have no cytotoxic effect at all concentrations. Also, similar results were detected in methanol and hexane extracts at (1/1000 µg/ml, 1/2000 µg/ml) concentration as shown in Figure 3. It was clear that the ethanol extract of *J. regia* did not show any cytotoxic activity at the concentrations of 1/1000 µg/ml, 1/2000 µg/ml, and 1/4000 µg/ml against the MDA-MB-231 cell line.

The nuclear morphology images in the A549 cell line treated with the methanol and ethanol extracts of *J. regia* bark at a dose of 2.0 µg/ml are shown in Figure 4. Images were taken with a fluorescence-inverted microscope at 10X magnification. Cells were stained with Hoechst 33258 dye to visualize cell death [Positive control (doxorubicin 2.5 µg/ml), negative control (untreated cells)]. Hoechst stain was used to visualize the nuclear morphology of the cells.

Methanol and ethanol extract applied in the A549 cell line induced apoptosis in cells. However, when the two extracts were compared, it was observed that the methanol extract showed higher apoptotic activity than the ethanol extract.

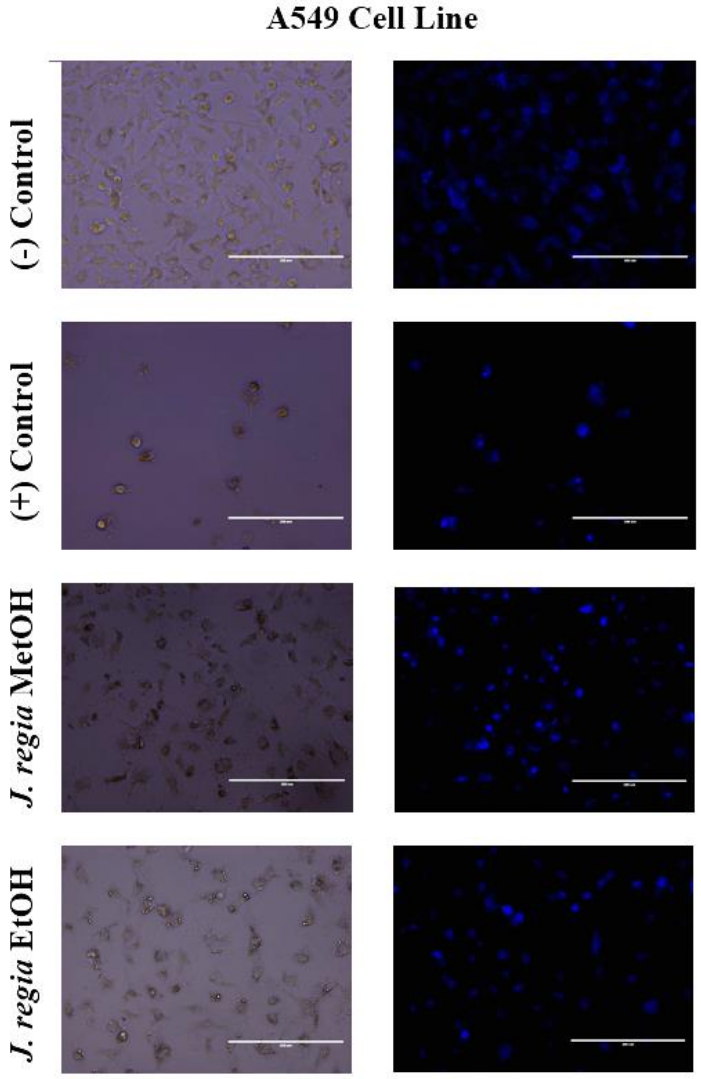

Figure 4. Results of the double staining method
Blue stained areas represent propidium iodide stain, (-) control represents untreated cells, and (+) control represents doxorubicin-treated cells.

J. regia flowers are known to contain multiple polyphenolic compounds that exhibit antioxidant effects through various mechanisms (Żurek et al., 2022). In addition, it has been reported by many authors that *J. regia* is one of the nuts with the highest antioxidant activity (Halvorsen et al., 2002; Kornsteiner et al., 2006; Mishra et al., 2010). Among various dried fruits, the methanolic extract of *J. regia* has been found to have very high antioxidant activity. Studies have also suggested that the shell or seed coat surrounding the kernel also has high antioxidant activity (Jahanban-Esfahlan et al., 2019). Some studies in the literature have shown that *J. regia* green bark has an antioxidant effect in the presence of polyphenolic compounds (Oliveira et al., 2008; Zhou et al., 2015). In a study, *J. regia* seed, green bark, and leaf parts were extracted with methanol and petroleum ether, and their antioxidant effect was investigated. As a result, it was observed that the radical effect increased with the increase in the concentrations of all methanolic extracts. At the same time, it was determined that the extracts of walnut leaf and green shell prepared with petroleum ether had the lowest radical effect (Carvalho et al., 2010). In another study, the antioxidant activity of *J. regia* green peel was determined by comparing the maturity stages. The results showed that the antioxidant capacity of ripe green peel was higher (Soto-Madrid et al., 2021). The flavonoids of *J. regia* leaves are known to have strong antioxidant properties (Zhao et al., 2014). In a previous study, *J. regia* leaves were powdered and their antioxidant effect was examined by dissolving with methanol. At the end of the study, it was seen that it had a higher value than ascorbic acid used as a reference, and the results obtained were determined to be significant (Shah et al., 2018). In another study, the antioxidant activity of the extract of powdered *J. regia* leaves with methanol

was determined at different concentrations, and in line with the results obtained, it was determined that it exhibited an effective scavenging capacity depending on the concentrations (Pereira et al., 2007).

Natural products are a good source of oncogene protein modulators and many of them or their derivatives have been developed as anticancer drugs such as doxorubicin and bleomycin (Yuan et al., 2020). In the current era, natural agents have a very important place in the treatment of cancer, either because of their various components or as a whole (Catanzaro et al., 2018). *J. regia* peel is part of the residue from the consumption of the fruit and its components are used as antimicrobial, anticancer, and antioxidant agents (Vieira et al., 2020; Yin et al., 2019; Zakavi et al., 2013). In a study, the cytotoxicity of the membrane surrounding the *J. regia* nucleus was determined in MCF-7, Caco-2, and a primary fibroblast cell line (HFF-1) with different concentrations of *J. regia* nucleus membrane. The results showed a significant decrease in the Caco-2 cell line at 24 and 48 hours. However, no cytotoxic effect was found on HFF-1 and MCF-7 cell lines (D'Angeli et al., 2021). In another study, the anticancer effect of the extract from *J. regia* seeds on breast cancer cell line MDA-MB231 and colon cancer cell line HT-29 was determined using MTT [3-(4, 5-dimethyl thiazolyl)-2,5-diphenyl-tetrazolium bromide]. In line with the results obtained, it was determined that *J. regia* seeds showed inhibitory properties in HT-29 and MDA-MB231 cells and had the same antioxidant effect (Jahanbani et al., 2016). In another study, the polyphenol fraction isolated from the pollen of male flowers of the *J. regia* tree was investigated for its antioxidant and anticancer effects in cell lines such as breast cancer cell line (MCF-7), colorectal cancer cell lines (DLD-1, Caco-2) and glioblastoma cell line (U87MG). According to the results of this study, the strongest cytotoxic activity of *J. regia* pollen was observed in Caco-2 and MCF-7 cell lines, while the lowest cytotoxic activity was observed in melanoma (SK-Mel-29) and astrocytoma (U251MG) cell lines (Żurek et al., 2022). The anticancer effect of *J. regia* extracts on the human neuroblastoma cell line (IMR-32); human breast epithelial cell line (HBL-100); human osteosarcoma cell line (U2OS) was investigated. The results obtained from this study emphasized that the *J. regia* tree constitutes a very good source of effective natural antioxidants that can act as anti-cancer agents, considering that *J. regia* extracts exhibited greater cell viability in U2OS cells versus IMR-32 and HBL-100 cells (Shah et al., 2018).

4. Conclusions

When the apoptotic, cytotoxic, and antioxidant activities of *J. regia* against MDA-MB-231 and A549 cell lines were examined, the highest effect in the antioxidant study was reported at a concentration of 2.0 µg/ml of *J. regia* bark prepared in methanol solvent, and the lowest effect was reported at a concentration of 0.125 µg/ml. When the cytotoxic activity assay results were examined, the most effective result in the MDA-MB-231 cell line was seen in the highest concentrations of methanol and ethanol extracts of a walnut shell. When the results of apoptotic activity were examined, the shell extracts of *J. regia* showed evident apoptotic activity even if it was not as potent as doxorubicin. Our results indicate that *J. regia* bark extract may be an effective agent in the fight against cancer, and also support previous studies.

Acknowledgments

Thanks to Prof. Dr. Mustafa KAPLAN, Fırat University, Faculty of Medicine, Department of Parasitology, for his kind contribution to provide the laboratory environment for this study.

Conflict of interest

The authors confirm that there are no known conflicts of interest.

Statement of ethics

In this study, no method requiring the permission of the "Ethics Committee" was used.

Availability of data and materials

All data generated or analyzed during this study are included in this published article.

Funding

This research received no external funding.

CRediT authorship contribution statement

Lütfiye Kadıoğlu Dalkılıç: Project administration, Conceptualization
Semih Dalkılıç: Data curation, Supervision, Validation
Lütfü Uygur: Writing-reviewing & editing

ORCID Numbers of the Authors

Lütfiye Kadıoğlu Dalkılıç: 0000-0002-6791-3811
Semih Dalkılıç: 0000-0002-6892-247X
Lütfü Uygur: 0000-0002-5113-2703

Supplementary File

None.

Publisher's Note

All claims expressed in this article are solely those of the authors and do not necessarily represent those of their affiliated organizations, or those of the publisher, the editors and the reviewers. Any product that may be evaluated in this article, or claim that may be made by its manufacturer, is not guaranteed or endorsed by the publisher.

This is an open-access article distributed under the terms of the Creative Commons Attribution 4.0 International License (CC BY). The use, distribution or reproduction in other forums is permitted, provided the original author(s) and the copyright owner(s) are credited and that the original publication in this journal is cited, in accordance with accepted academic practice. No use, distribution or reproduction is permitted which does not comply with these terms.

References

Akkol, E. K., Dereli, F. T. G., Sobarzo-Sánchez, E., & Khan, H. (2020). Roles of medicinal plants and constituents in gynecological cancer therapy: Current literature and future directions. *Current Topics in Medicinal Chemistry, 20*(20), 1772-1790.

Carvalho, M., Ferreira, P. J., Mendes, V. S., Silva, R., Pereira, J. A., Jerónimo, C., & Silva, B. M. (2010). Human cancer cell antiproliferative and antioxidant activities of *Juglans regia* L. *Food and Chemical Toxicology, 48*(1), 441-447.

Catanzaro, D., Rancan, S., Orso, G., Dall'Acqua, S., Brun, P., Giron, M. C., Carrara, M., Castagliuolo, I., Ragazzi, E., *et al.* (2015). *Boswellia serrata* preserves intestinal epithelial barrier from oxidative and inflammatory damage. *PloS One, 10*(5), e0125375.

Catanzaro, E., Greco, G., Potenza, L., Calcabrini, C., & Fimognari, C. (2018). Natural products to fight cancer: A focus on *Juglans regia*. *Toxins, 10*(11), 469.

Coskun, D., Dalkilic, S., Dalkilic, L. K., & Coskun, M. F. (2021). The Synthesis, Characterization, and Anticancer Activity of New 2-acetylbenzofuran-Chalcone Hybrids. *Iranian Journal of Science and Technology, Transactions A: Science, 45*(5), 1561-1569.

D'Angeli, F., Malfa, G. A., Garozzo, A., Li Volti, G., Genovese, C., Stivala, A., Nicolosi, D., Attanasio, F., Bellia, F., *et al.* (2021). Antimicrobial, antioxidant, and cytotoxic activities of *Juglans regia* l. *pellicle* extract. *Antibiotics, 10*(2), 159.

Dalkilic, S., Dalkilic, L. K., İnci, S., Korkmaz, İ., & Kirbag, S. (2021). Investigation of cytotoxic effect of black mulberry (*Morus nigra* L.) fruit. *Indian Journal of Traditional Knowledge, 20*(1), 54-58.

Deniz Güneş, B., & Acar Tek, N. (2021). Meme Kanserinden Korunmada ve Meme Kanseri Tedavisinde Akdeniz Diyetinin Etkisi. *Adnan Menderes Üniversitesi Sağlık Bilimleri Fakültesi Dergisi, 5*(2), 442-454.

Flieger, J., & Flieger, M. (2020). The [DPPH●/DPPH-H]-HPLC-DAD method on tracking the antioxidant activity of pure antioxidants and goutweed (*Aegopodium podagraria* L.) hydroalcoholic extracts. *Molecules, 25*(24), 6005.

Halvorsen, B., Holte, K., Myhrstad, M. C., Barikmo, I., Hvattum, E., Remberg, S. F., Wold, A. B., & Haffner, K. (2002). A Systematic Screening of Total Antioxidants in Dietary Plants. *Journal of Nutrition, 132*, 461-471.

Huang, D., Ou, B., & Prior, R. L. (2005). The chemistry behind antioxidant capacity assays. *Journal of Agricultural and Food Chemistry, 53*(6), 1841-1856.

Jahanban-Esfahlan, A., Ostadrahimi, A., Tabibiazar, M., & Amarowicz, R. (2019). A comparative review on the extraction, antioxidant content and antioxidant potential of different parts of walnut (*Juglans regia* L.) fruit and tree. *Molecules, 24*(11), 2133.

Jahanbani, R., Ghaffari, S. M., Salami, M., Vahdati, K., Sepehri, H., Sarvestani, N. N., Sheibani, N., & Moosavi-Movahedi, A. A. (2016). Antioxidant and anticancer activities of walnut (*Juglans regia* L.) protein hydrolysates using different proteases. *Plant Foods for Human Nutrition, 71*, 402-409.

Khan, M. I., Bouyahya, A., Hachlafi, N. E., Menyiy, N. E., Akram, M., Sultana, S., Zengin, G., Ponomareva, L., Shariati, M. A., *et al.* (2022). Anticancer properties of medicinal plants and their bioactive compounds against breast cancer: a review on recent investigations. *Environmental Science and Pollution Research, 29*(17), 24411-24444.

Khan, T., Ali, M., Khan, A., Nisar, P., Jan, S. A., Afridi, S., & Shinwari, Z. K. (2019). Anticancer plants: A review of the active phytochemicals, applications in animal models, and regulatory aspects. *Biomolecules, 10*(1), 47.

Kornsteiner, M., Wagner, K. H., & Elmadfa, I. (2006). Tocopherols and total phenolics in 10 different nut types. *Food Chemistry, 98*(2), 381-387.

Mishra, N., Dubey, A., Mishra, R., & Barik, N. (2010). Study on antioxidant activity of common dry fruits. *Food and Chemical Toxicology, 48*(12), 3316-3320.

Oliveira, I., Sousa, A., Ferreira, I. C., Bento, A., Estevinho, L., & Pereira, J. A. (2008). Total phenols, antioxidant potential and antimicrobial activity of walnut (*Juglans regia* L.) green husks. *Food and Chemical Toxicology, 46*(7), 2326-2331.

Pereira, J. A., Oliveira, I., Sousa, A., Valentão, P., Andrade, P. B., Ferreira, I. C., Ferreres, F., Bento, A., Seabra, R., *et al.* (2007). Walnut (*Juglans regia* L.) leaves: Phenolic compounds, antibacterial activity and antioxidant potential of different cultivars. *Food and Chemical Toxicology, 45*(11), 2287-2295.

Riss, T. L., & Moravec, R. A. (2004). Use of multiple assay endpoints to investigate the effects of incubation time, dose of toxin, and plating density in cell-based cytotoxicity assays. *Assay and Drug Development Technologies, 2*(1), 51-62.

Roy, P., & Saikia, B. (2016). Cancer and cure: A critical analysis. *Indian Journal of Cancer, 53*(3), 441-442.

Schmiech, M., Lang, S. J., Ulrich, J., Werner, K., Rashan, L. J., Syrovets, T., & Simmet, T. (2019). Comparative investigation of frankincense nutraceuticals: Correlation of boswellic and lupeolic acid contents with cytokine release inhibition and toxicity against triple-negative breast cancer cells. *Nutrients, 11*(10), 2341.

Shah, U. N., Mir, J. I., Ahmed, N., Jan, S., & Fazili, K. M. (2018). Bioefficacy potential of different genotypes of walnut *Juglans regia* L. *Journal of Food Science and Technology, 55*, 605-618.

Siddiqui, A. J., Jahan, S., Singh, R., Saxena, J., Ashraf, S. A., Khan, A., Choudhary, R. K., Balakrishnan, S., Badraoui, R., *et al.* (2022). Plants in anticancer drug discovery: from molecular mechanism to chemoprevention. *BioMed Research International, 2022*, 5425485.

Soto-Madrid, D., Gutiérrez-Cutiño, M., Pozo-Martínez, J., Zúñiga-López, M. C., Olea-Azar, C., & Matiacevich, S. (2021). Dependence of the ripeness stage on the antioxidant and antimicrobial properties of walnut (*Juglans regia* L.) green husk extracts from industrial by-products. *Molecules, 26*(10), 2878.

Vieira, V., Pereira, C., Abreu, R. M., Calhelha, R. C., Alves, M. J., Coutinho, J. A., Ferreira, O., Barros, L., & Ferreira, I. C. (2020). Hydroethanolic extract of *Juglans regia* L. green husks: A source of bioactive phytochemicals. *Food and Chemical Toxicology, 137*, 111189.

Yin, Q., Liu, M., & Ren, H. (2019). Biochar produced from the co-pyrolysis of sewage sludge and walnut shell for ammonium and phosphate adsorption from water. *Journal of Environmental Management, 249*, 109410.

Yuan, S., Gopal, J. V., Ren, S., Chen, L., Liu, L., & Gao, Z. (2020). Anticancer fungal natural products: Mechanisms of action and biosynthesis. *European Journal of Medicinal Chemistry, 202*, 112502.

Zakavi, F., Golpasand Hagh, L., Daraeighadikolaei, A., Farajzadeh Sheikh, A., Daraeighadikolaei, A., & Leilavi Shooshtari, Z. (2013). Antibacterial effect of *Juglans regia* bark against oral pathologic bacteria. *International Journal of Dentistry, 2013*, 854765.

Zhao, M. H., Jiang, Z. T., Liu, T., & Li, R. (2014). Flavonoids in *Juglans regia* L. leaves and evaluation of in vitro antioxidant activity via intracellular and chemical methods. *The Scientific World Journal, 2014*, 303878.

Zhou, X., Cai, J., Zhu, W., Zhao, H., Wang, K., & Zhang, X. (2015). Boswellic acid attenuates asthma phenotype by downregulation of GATA3 via nhibition of PSTAT6. *Genetics and Molecular Research, 14*(3), 7463-7468.

Żurek, N., Pycia, K., Pawłowska, A., & Kapusta, I. T. (2022). Phytochemical Screening and Bioactive Properties of *Juglans regia* L. Pollen. *Antioxidants, 11*(10), 2046.

Int. J. Plant Bas. Pharm. (2023) 3(1), 68-72

INTERNATIONAL JOURNAL OF PLANT BASED PHARMACEUTICALS

https://ijpbp.com

RESEARCH ARTICLE

OPEN ACCESS

Phytochemical evaluation and acute oral toxicity of crude methanol extract of *Pleurotus tuber-regium* (Fr.) Singer in laboratory mice (*Mus musculus*)

Sarah Princess Edoh[a], Dahiru Sani[b*], Christian Emeka Mbah[a], Hindatu Yusuf[c], Abubakar Nuhu Ishaq[d], Tabita Gaba Sule[d,e], Kalen Ephraim Audu[d]

[a] *Ahmadu Bello University, Faculty of Life Sciences, Department of Zoology, Zaria, Nigeria*
[b] *Ahmadu Bello University, Faculty of Veterinary Medicine, Department of Veterinary Pharmacology and Toxicology, Zaria, Nigeria*
[c] *Federal University, Faculty of Science, Department of Microbiology and Biotechnology, Dutse, Nigeria*
[d] *Ahmadu Bello University, Faculty of Life Sciences, Department of Biology, Zaria, Nigeria*
[e] *Umar Suleiman College of Education, Department of Biology, Gashu'a, Nigeria*

ARTICLE INFO

Article History:

Received: 30 August 2022
Revised: 10 January 2023
Accepted: 04 February 2023
Available online: 08 February 2023

Edited by: B. Tepe

Keywords:

Acute oral toxicity
Methanol
Pleurotus tuber-regium
Phytochemicals
Laboratory mice

ABSTRACT

This research aimed to evaluate the phytochemical components of the crude methanol extract (CME) of *Pleurotus tuber-regium* and its acute toxicity in mice, *Mus musculus*. Before being filtered and evaporated, the crushed mushroom was macerated in 70% methanol for 72 hours. The phytochemical screening and acute oral toxicity were carried out using standard procedures. The CME consists of alkaloids, cardiac glycosides, saponins, phenolic compounds, tannins, steroids, carbohydrates, flavonoids, and terpenoids. When given orally, the LD_{50} was shown to be greater than 5000 mg/kg with no outward symptoms of toxicity. Haematology showed a significant ($p < 0.05$) decrease in packed cell volume, hemoglobin concentration, total red blood cell, and neutrophil counts in the treatment group as compared to the control group, while total white blood cell and lymphocyte counts significantly ($p < 0.05$) increased. On serum biochemistry, a significant ($p < 0.05$) increase in aspartate aminotransferase, alanine transferase, alanine phosphatase, blood urea nitrogen, and creatinine was observed in the treated group. There was however no significant ($p > 0.05$) difference in serum albumin and total protein. In conclusion, 5000 mg/kg of extract had a significant influence on the hematological and biochemical profiles of mice but didn't cause irreparable liver and kidney damage.

1. Introduction

Pleurotus tuber-regium, (Pleurotaceae) can be found on dead trees and fallen logs of *Daniella oliveri* in the wild (Vishwakarma et al., 2018). The mushroom produces a sclerotium, or underground tuber and both the sclerotium and mushroom are edible. When ripe, the cap curls upward to form a cup-like shape, similar to that of an oyster mushroom (*Pleurotus ostreatus*) (Lin et al., 2020). In Nigeria, sclerotium is nutritiously consumed as food, with folkloric claims that they have potent medicinal properties against asthma, high blood pressure, cancer, inflammation, hyperlipidemia, and hyperglycemia (Okolo et al., 2020; Vishwakarma et al., 2018). Plant-botanical interactions can cause poisoning, which can end in harm or death. Toxicological information can be utilized to forecast the effects of plant botanicals used by humans and animals (Shirish, 2011). Nonetheless, complementary and alternative medicine

Reviewed by:
Florence Nalimu: Mbarara University of Science and Technology, Mbarara, Uganda
Nilay İşitez: Afyonkarahisar Health Sciences University, Afyonkarahisar, Türkiye

* Corresponding author(s):
E-mail address:
mdsani77@gmail.com (D. Sani)
e-ISSN: 2791-7509
doi: https://doi.org/10.29228/ijpbp.18

(CAM) continues to be marginalized in global discourses about public health (Aliyu et al., 2017). There's also the assumption that because herbal therapies are derived from nature, they don't have the same unpleasant or dangerous side effects as pharmaceuticals (Olaniyan et al., 2016). Despite positive ethnomedical reports from all around the world, the safety profile of several medicinal plants used in complementary and alternative therapies is unknown (Muia et al., 2020). Toxicity should be evaluated for proper and documented herbal medical products, as it is for conventional orthodox pharmaceuticals that have been properly researched and manufactured, according to Olaniyan et al. (2016); nevertheless, the toxicity of traditional herbal therapies is rarely assessed. As a result, consumers frequently focus on herbal drugs' medical benefits while ignoring their negative effects on other organs. *P. tuber-regium* was investigated for its qualitative phytochemical components and acute oral toxicity.

2. Materials and methods

2.1. P. tuber-regium collection, identification, and processing

P. tuber-regium was obtained from Yaba College of Technology's Mushroom Research and Training Laboratory. A mycologist (Dr. Ofodile Lauretta) from the Department of Botany taxonomically identified the mushroom with the voucher number of YCT 001 2021. The mushroom was cleansed in a salt solution to remove any microbial contamination before being transported and preserved in the laboratory for future use.

2.2. Preparation of crude methanol extract

The whole mushroom was air-dried at room temperature for 2 weeks in the laboratory. Thereafter, normal milling equipment (Model E Scale, Model Number ES0, China) was used to pulverize 500 g of the *P. tuber-regium*. The pulverized material was macerated in 5000 ml of 70% methanol for 72 hours (Itodo et al., 2022). The filtrate was then concentrated with a rotary evaporator (Model BUCHI, Model Number R110, England) and evaporated to dryness on a water bath (Model BATH, Model Number B11, China) at 50 °C, and the percentage yield was calculated (weight of dry extract/weight of dry plant × 100). Before further experimentation and analysis, the dried extracts were properly stored in an airtight container at 4 ± 2 °C in a refrigerator.

2.3. Phytochemical screening of crude methanol extract

The crude methanol extract was screened for qualitative phytochemicals using standard laboratory protocols (Khandelwal, 2005).

2.4. Source of experimental animals

Adult male mice (*Mus musculus*), weighing 15-18 g, were obtained from the Veterinary Pharmacology and Toxicology animal house at Ahmadu Bello University in Zaria. The experimental animals were housed at 25 – 27 °C temperature and 50-60% humidity in 15 × 30 cm cages with metal tops that were thoroughly cleaned, the bedding materials consisted of wood shavings (sawdust) which were changed twice a week. The experimental animals were allowed to acclimatize for two weeks before the commencement of the study. They were fed ordinary mice pellets and allowed access to unrestricted clean water.

2.5. Acute toxicity study

The up-and-down acute toxicity test procedure was utilized according to the guidelines of the Organization for Economic Cooperation and Development (OECD) 425 (OECD, 2008). Ten mice were randomly distributed into two groups of five each. The mice were fasted for 12 hours before the commencement of the oral administration of extracts. Using an orogastric tube, five mice (*M. musculus*) were sequentially administered 5.000 mg/kg body weight of *P. tuber-regium* once while the remaining five served as control. The mice were observed for any change in behavior and physiological signs of toxicity for short-term effects of 24 hours and, delayed effects of 14 days. Following light ether anesthesia, the mice were euthanized by jugular venesection, and blood was collected into labeled EDTA and plain sample bottles for hematology and serum biochemistry procedures.

2.6. Haematological assessment

The hematological parameters that were assessed were packed cells volume (PCV), hemoglobin concentration (HC), and red and total white blood cell counts (RBC and TWBC) as described by standard procedures (Dacie & Lewis, 1991; Schalm et al., 1975). Blood samples were collected from mice in both the treated and control groups.

2.7. Serum biochemistry

Serum alanine aminotransferase (ALT), aspartate aminotransferase (AST), alkaline phosphatase activity (ALP), albumin (ALB), total protein levels (TP), blood urea nitrogen (BUN) ranges were determined using the Randox assay kit (Randox Laboratories Ltd, Ardmore, Antrim, UK) according to the manufacturer's instructions.

2.8. Histopathological examination

The kidney and liver were harvested from sacrificed mice following the termination of the experiment to check for lesions associated with toxicity such as hemorrhage, shrunken glomerulus, and central vein. The harvested organs were immediately fixed in 10% formalin (Sigma-Aldrich, Inc., St. Louis, MO, USA) solution and then prepared for histopathological examination, viewed under a light microscope, and the microscopic field images were captured (Luna, 1968).

2.9. Data analysis

Data were represented in tables. The quantitative data were presented in the form of a mean ± standard deviation (SD). GraphPad InStat version 3.1 was utilized to analyze data from the acute oral toxicity trial using an independent sample *t*-test. Statistical significance was defined as a $p \leq 0.05$.

3. Results and discussion

3.1. Phytochemical screening

In the methanol extract of *P. tuber-regium*, nine (9) secondary metabolites were found (Table 1). Alkaloids, cardiac glycosides, saponins, phenolic compounds, tannins, steroids, carbohydrates, flavonoids, and terpenoids were among the metabolites discovered. Anthraquinone, on the other hand, was not found in the extract. The result of the phytochemical screening in this study agrees with previous research (Adeyi et al., 2021; Ijeh et al., 2009) on saponins, alkaloids, flavonoids, and steroids.

3.2. Acute oral toxicity study

The acute oral toxicity of the methanol extract of *P. tuber-regium* indicated that at 5000 mg/kg, the extracts caused no mortality in the first 24 hours and then for the next 14 days after being given orally to the mice. No change in clinical or behavioral signs was observed (Table 2). Acute toxicity tests, among other toxicity tests, were used to investigate the safety of herbal products in laboratory animals (Ebbo et al., 2020). Plants produce secondary metabolites for a variety of reasons, including growth regulation, inter- and intra-specific interactions, and defense against predators and pathogens. Many of these natural compounds have been demonstrated to have fascinating biological and pharmacological activity, and they are used as chemotherapeutic agents or as the foundation for the development of modern pharmaceuticals (Ukwuani et al., 2012).

Table 1. Qualitative phytochemical screening of methanol extract of *P. tuber-regium*

No	Phytoconstituents	Test	Inference
1	Alkaloids	Dragendorff test	+
2	Cardiac Glycosides	Keller-Kiliani test	+
3	Saponins	Frothing test	+
4	Phenolic compounds	Lead acetate test	+
5	Tannins	Ferric chloride test	+
6	Steroids	Salkowiski test	+
7	Carbohydrates	Molisch test	+
8	Flavonoids	Shinoda test	+
9	Terpenoids	Liebermann Burchard test	+
10	Anthraquinones	Borntrager's test	-

Keys: (+) = Present, (-) = Absent

Table 2. Acute oral toxicity of methanol extract of *P. tuber-regium* in mice

Experimental mice	Mice label	Dose (mg/kg)	Short-term effect (24 hrs)	Delayed effect (14 days)
A	I	5000	No death	No death
B	II	5000	No death	No death
C	III	5000	No death	No death
D	IV	5000	No death	No death
E	V	5000	No death	No death

At 14 days of observation, a 5000 mg/kg methanol extract of *P. tuber-regium* demonstrated no deleterious influence on the behavioral reactions of the examined rats. There was no death at the tested level which suggests that the plant is relatively safe at the dose used for the study. This is in concert with the work of Adeyi et al. (2021) who reported no death or toxicity sign in rats administered *P. tuber-regium* extract.

3.3. Haematology

There was an observed significant ($p < 0.05$) decrease in the packed cell volume (PCV), hemoglobin concentration (HGB), and total red blood cells (TRBC) in the treated group when compared to the control group. However, there was a significant ($p < 0.05$) increase in the total white blood cell (TWBC), lymphocytes, and monocytes of the treated group (Table 3). The hematopoietic system is one of the most vulnerable systems to hazardous substances, notably in the bone marrow, where red blood cell formation takes place (Kifayatullah et al., 2015). According to Choudhari and Deshmukh (2007), the lower RBC count and Hgb concentration could be due to deteriorated hematopoiesis, restricted erythropoiesis, or an increase in red blood cell breakdown. Haematology revealed a significant change in PCV, Hgb concentration, and RBC in the treated group, which could be due to the type of solvent used for extraction. Methanol extract may have lowered hemoglobin content and PCV count by inhibiting RBC synthesis thereby causing the induction of anemia. An increase in WBCs signals the activation of the immune response, which serves as a protective mechanism against foreign chemicals (Kifayatullah et al., 2015). The ability of the extract to evoke immune status in the mice could explain the substantial increase in total white blood cells and lymphocytes seen in the treated group. The phytochemical constituents present in the extract may be responsible for the protection of the mice against toxicities. According to Oluba et al. (2020), mushroom polysaccharides have been demonstrated to stimulate cellular immunity, increase antibody formation, and boost cytokine release, resulting in a significant shift in neutrophil count. The extract did not affect the other parameters in the hematological examination.

Table 3. Effect of the methanol extract of *P. tuber-regium* on haematological parameters at the limit dose

Parameters	Control	Test
PCV (%)	40.0 ± 1.12	30.7 ± 0.9[a]
HGB (g/dl)	13.2 ± 0.5	10.2 ± 0.3[a]
TWBC (*10^9/l)	7.5 ± 0.5	16.8 ± 1.4[a]
TRBC (*10^9/l)	4.6 ± 0.2	3.6 ± 0.2[a]
NEUT (%)	36.0 ± 0.6	15.0 ± 1.6[a]
LYMPHO (%)	63.0 ± 1.2	81.3 ± 0.9[a]
MONO (%)	1.0 ± 0.6	3.7 ± 2.0[a]
EOSINO (%)	N.D.	N.D.
BASO (%)	N.D.	N.D.
BAND (%)	1.0 ± 0.6	1.0 ± 1.0

Data are expressed as mean ± SD, $n = 5$. [a]:With different superscript across each row are statistically significant ($p < 0.05$) when compared to control. Key: PCV (packed cell volume), HGB (Haemoglobin), TWBC (Total white blood cells), TRBC (Total red blood cells), NEUT (Neutrophils), LYMPHO (Lymphocytes), MONO (Monocytes), EOSINO (Eosinophils), BASO (Basophils), N.D. (Not detected).

Table 4. Effect of the methanol extract of *P. tuber-regium* on blood serum biochemistry at the limit dose

Parameters	Control	Test
AST (u/l)	232.0 ± 15.6	288.0 ± 9.6[a]
ALT (u/l)	78.0 ± 4.04	91.7 ± 2.0[a]
ALP (u/l)	73.0 ± 2.3	111.0 ± 7.5[a]
TP (g/l)	61.0 ± 2.8	69.7 ± 0.3
BUN (mg/dl)	56.7 ± 0.9	81.0 ± 1.2[a]
ALB (g/l)	2.5 ± 0.29	2.9 ± 0.1[a]
CREAT (mg/dl)	0.7 ± 0.1	1.0 ± 0.1[a]

Data are expressed as mean ± SD, $n = 5$. [a]:With different superscript across each row are statistically significant ($p < 0.05$) when compared to control. Key: AST (Aspartate aminotransferase), ALT (Alanine aminotransferase), ALP (Alkaline phosphatase), TP (Total protein), BUN (Blood urea nitrogen), ALB (Albumin), CREAT (Creatinine).

3.4. Serum biochemical analysis

There was an observed significant ($p < 0.05$) increase in the serum aspartate aminotransferase (AST), alkaline phosphatase (ALP), alanine aminotransferase (ALT), blood urea nitrogen, and creatinine in the treated group when compared to the control. Serum albumin and total protein showed no significant changes when the treated group was compared to the control group ($p > 0.05$) (Table 4). The liver and kidney are the two principal organs involved in the detoxification process, with the kidney being more vulnerable to drug-induced toxicity. When tissue is destroyed, liver function marker enzymes (AST, ALT, and ALP) are released into the bloodstream, and their amount is proportional to the extent of hepatic damage (Jisha et al., 2019). The considerable increase in AST, ALT, and ALP levels in the treatment group (Table 4) after receiving a high dose of 5000 mg/kg extract could be due to some of the extract's ingredients. Ojiako and Igwe (2008) produced a similar report. They stated that when saponin, flavonoids, and tannin are consumed by animals, they may cause unfavorable metabolic

reactions. Albumin is the most important protein in plasma generated by the liver in terms of quantity, and it serves as a useful biomarker of hepatic function (Kifayatullah et al., 2015). Albumin synthesis is influenced by a variety of factors, including dietary conditions, hormonal balance, and osmotic pressure. Creatinine, the most extensively used biomarker for assessing renal damage, is a leftover product of creatine produced at a nearly constant rate in the body, which is filtered freely by the glomeruli and not reabsorbed in renal tubules (Sá et al., 2015). When compared to the control group, the results demonstrated a considerable change in creatinine levels in the treated group. Although creatinine is not expected to be reabsorbed, all of the creatinine filtered in the glomerular filtrate travels through the tubular system and is eliminated in urine. Creatinine is reabsorbed rather than expelled in this condition. According to previous reports by Nogaim et al. (2011), mushrooms at higher concentrations tend to evoke an increase in creatinine levels and that was observed in this study.

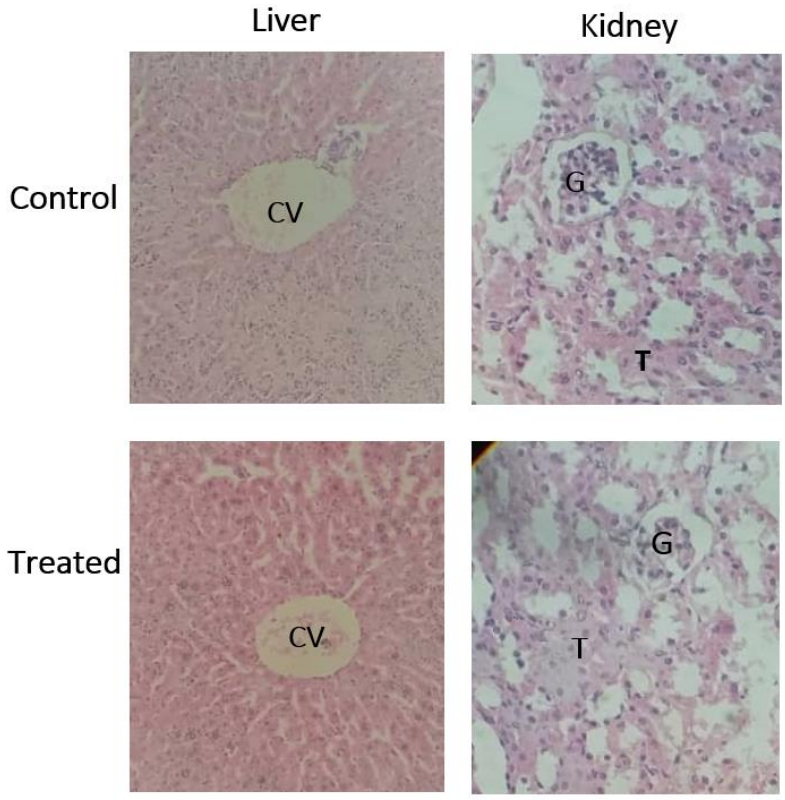

Figure 1. Photomicrograph of liver and kidney from mice showing normal central vein (CV), intact glomerulus (G) and tubules (T) (H & E x 200)

3.5. Histopathological evaluation

On histopathology, the liver section showed a normal central vein without any visible pathology while the examination of the kidney revealed intact glomerulus and tubules (Figure 1). This could be attributed to the mixture of flavonoids and phenols in the plant which has membrane-stabilizing and antioxidant activities, it promotes hepatocyte regeneration, reduces inflammatory reactions, and inhibits fibrogenesis (Soares et al., 2013).

4. Conclusions

In conclusion, qualitative phytochemical screening revealed the presence of nine secondary metabolites. Acute oral toxicity using the up and down procedure showed no deleterious effect at the administered dose of 5000 mg/kg. Significant influence on various hematological and biochemical profiles of *M. musculus* was observed, but not potent enough to cause irreparable liver and kidney damage.

Acknowledgments

None.

Conflict of interest

The authors confirm that there are no known conflicts of interest.

Statement of ethics

All applicable international, national, and/or institutional guidelines for the care and use of animals were followed. All procedures performed in studies involving animals were following the ethical standards of the Ahmadu Bello University, Zaria Committee on Animal Use and Care (ABUCAUC) with the approval number ABUCAUC/2022/011.

Availability of data and materials

All data generated or analyzed during this study are included in this published article.

Funding

The authors declare that the study did not receive any financial support/grant from any public or private organization.

CRediT authorship contribution statement

Sarah Princess Edoh: Conceptualization, Investigation, Writing - original draft
Dahiru Sani: Conceptualization, Investigation, Supervision, Investigation, Writing – review draft
Christian Emeka Mbah: Conceptualization, Investigation, Supervision, Writing – review draft
Hindatu Yusuf: Formal analysis, Data curation, Writing – review draft
Abubakar Nuhu Ishaq: Investigation, Formal analysis, Writing – review draft
Tabita Gaba Sule: Investigation, Writing – review draft
Kalen Ephraim Audu: Investigation, Writing – review draft

ORCID Numbers of the Authors

S. P. Edoh: 0000-0001-5889-3663
D. Sani: 0000-0002-0597-5582
C. E. Mbah: 0000-0002-5638-7545
H. Yusuf: 0000-0002-0089-9963
A. N. Ishaq: 0000-0003-0133-7708
T. G. Sule: 0000-0002-3134-5971
K. E. Audu: 0000-0002-2403-8893

Supplementary File

None.

Publisher's Note

All claims expressed in this article are solely those of the authors and do not necessarily represent those of their affiliated organizations, or those of the publisher, the editors and the reviewers. Any product that may be evaluated in this article, or claim that may be made by its manufacturer, is not guaranteed or endorsed by the publisher.

This is an open-access article distributed under the terms of the Creative Commons Attribution 4.0 International License (CC BY). The use, distribution or reproduction in other forums is permitted, provided the original author(s) and the copyright owner(s) are credited and that the original publication in this journal is cited, in accordance with accepted academic practice. No use, distribution or reproduction is permitted which does not comply with these terms.

References

Adeyi, A. O., Adams, F. A., & Adenipekun, C. O. (2021). *Pleurotus tuber-regium* inclusion in diet ameliorates dyslipidaemia in obese-type 2 diabetic rats. *Clinical Phytoscience, 7*, 84.

Aliyu, U., Awosan, K., Oche, M., Taiwo, A., Jimoh, A., & Okuofo, E. (2017). Prevalence and correlates of complementary and alternative medicine use among cancer patients in usmanu danfodiyo university teaching hospital, Sokoto, Nigeria. *Nigerian Journal of Clinical Practice, 20*(12), 1576-1583.

Choudhari, C., & Deshmukh, P. (2007). Acute and subchronic toxicity study of *Semecarpus anacardium* on Hb% and RBC count of male albino rats. *Journal of Herbal Medicine and Toxicology, 1*, 43-45.

Dacie, J., & Lewis, S. (1991). *Practical haematology, 7th ed.*: London UK: Churchill Livingston.

Ebbo, A., Sani, D., Suleiman, M., Ahmad, A., & Hassan, A. (2020). Acute and sub-chronic toxicity evaluation of the crude methanolic extract of *Diospyros mespiliformis* Hochst ex a. Dc (Ebenaceae) and its fractions. *Toxicology Reports, 7*, 1138-1144.

Ijeh, I. I., Okwujiako, I. A., Nwosu, P. C., & Nnodim, H. I. (2009). Phytochemical composition of *Pleurotus tuber regium* and effect of its dietary incorporation on body/organ weights and serum triacylglycerols in albino mice. *Journal of Medicinal Plants Research, 3*(11), 939-943.

Itodo, J. I., Rekwot, P. I., Aluwong, T., Allam, L., Jolayemi, K. O., Kyari, S., Abah, K. O., Ibrahim, S., Dogara, M. U., *et al.* (2022). *Azanza garckeana* ameliorates Bisphenol A-induced reproductive toxicities in rabbit bucks. *Theriogenology, 192*, 150-165.

Jisha, N., Vysakh, A., Vijeesh, V., & Latha, M. (2019). Anti-inflammatory efficacy of methanolic extract of *Muntingia calabura* L. leaves in Carrageenan induced paw edema model. *Pathophysiology, 26*(3-4), 323-330.

Khandelwal, K. (2005). *Practical book of pharmacognosy*: Pune, India: Nirali Prakashan.

Kifayatullah, M., Mustafa, M. S., Sengupta, P., Sarker, M. M. R., Das, A., & Das, S. K. (2015). Evaluation of the acute and sub-acute toxicity of the ethanolic extract of *Pericampylus glaucus* (Lam.) Merr. in BALB/c mice. *Journal of Acute Disease, 4*(4), 309-315.

Lin, S., Wang, P., Lam, K. L., Hu, J., & Cheung, P. C. (2020). Research on a specialty mushroom (*Pleurotus tuber-regium*) as a functional food: chemical composition and biological activities. *Journal of Agricultural and Food Chemistry, 68*(35), 9277-9286.

Luna, L. G. (1968). *Manual of histologic staining methods of the Armed Forces Institute of Pathology, 3rd ed. pp. 174*: New York: McGraw-Hill.

Muia, B. M., Mbaria, J. M., Kanja, L. W., Gitahi, N., Okumu, P. O., & Okumu, M. O. (2020). Acute and sub-acute toxicity study of the root extracts of *Fagaropsis hildebrandtii* in mice and evaluation of their antimicrobial effects. *F1000Research, 8*, 1444.

Nogaim, Q., Amra, H., & Nada, S. (2011). The medical effects of edible mushroom extract on aflatoxin B1. *Journal of Biological Sciences, 11*(8), 481-486.

OECD (2008). *Guideline for Testing Chemicals 425, Acute Oral Toxicity: Up-and-Down Procedure, Organization for Economic Co-operation and Development (OECD)*: Washington, DC, USA.

Ojiako, O., & Igwe, C. (2008). The nutritive, anti-nutritive and hepatotoxic properties of *Trichosanthes anguina* (snake tomato) fruits from Nigeria. *Pakistan Journal of Nutrition, 7*(1), 85-89.

Okolo, K. O., Orisakwe, O. E., & Siminialayi, I. M. (2020). Dietary supplementation of *Pleurotus tuber regium* in rat feed ameliorates metabolic and hematotoxicity induced by carbon tetrachloride. *Journal of Basic and Clinical Physiology and Pharmacology, 31*(5), 20190188.

Olaniyan, J. M., Muhammad, H. L., Makun, H. A., Busari, M. B., & Abdullah, A. S. (2016). Acute and sub-acute toxicity studies of aqueous and methanol extracts of *Nelsonia campestris* in rats. *Journal of Acute Disease, 5*(1), 62-70.

Oluba, O. M., Akpor, O. B., Adebiyi, F. D., Josiah, S. J., Alabi, O. O., Shoyombo, A. O., & Olusola, A. O. (2020). Effects of co-administration of *Ganoderma* terpenoid extract with chloroquine on inflammatory markers and antioxidant status in *Plasmodium berghei*-infected mice. *Journal of Integrative Medicine, 18*(6), 522-529.

Sá, B. M., Lima, C. S., Silva, U. D. A., Carvalho, H. O., Fernandes, C. P., Resque, R. L., de Oliveria, T. T., & Carvalho, J. C. T. (2015). Subchronic toxicity evaluation of the hydroethanolic extract from *Endopleura uchi* (Huber) Cuatrec in Wistar rats. *African Journal of Pharmacy and Pharmacology, 9*(8), 223-229.

Schalm, O., Jain, N., & Carroll, E. (1975). *Veterinary haematology, 3rd ed.*: Philadelphia, USA: Lea and Febiger Publication; pp. 807.

Shirish, S. (2011). Acute toxicity study for *Tinospora cardifolia*. *International Journal of Research in Ayurveda and Pharmacy, 2*(5), 1571-1573.

Soares, A. A., de Sá-Nakanishi, A. B., Bracht, A., da Costa, S. M. G., Koehnlein, E. A., de Souza, C. G. M., & Peralta, R. M. (2013). Hepatoprotective effects of mushrooms. *Molecules, 18*(7), 7609-7630.

Ukwuani, A., Abubakar, M., Hassan, S., & Agaie, B. (2012). Toxicological studies of hydromethanolic leaves extract of *Grewia crenata*. *International Journal of Pharmaceutical Sciences and Drug Research, 4*(4), 245-249.

Vishwakarma, P., Singh, P., Kushwaha, V., & Tripathi, N. (2018). The effect of aqueous extract of somewild edible macrofungi on in vitro diffusion of glucose. *KAVAKA, 50*, 34-37.

Int. J. Plant Bas. Pharm. (2023) 3(1), 73-85

INTERNATIONAL JOURNAL OF PLANT BASED PHARMACEUTICALS

https://ijpbp.com

RESEARCH ARTICLE

OPEN ACCESS

Biological activities and DNA interactions of aqueous extract of *Phlomis linearis* (Boiss. & Bal.)

Betül Aydın[a*], Lütfiye Yasemin Gönder[b], Nebahat Aytuna Çerçi[c], Yiğit Can Ateş[d], İlayda Sezin Yalçınkaya[a], Nüveyre Canbolat[e], Leyla Açık[a], Nurcan Karacan[e], Emine Akyüz Turumtay[f], Halbay Turumtay[g]

[a] *Gazi University, Faculty of Science, Department of Biology, Ankara, Türkiye*
[b] *The Turkish Sugar Authority, Ankara, Türkiye*
[c] *Kırıkkale University, Scientific and Technological Research Application and Research Center, Kırıkkale, Türkiye*
[d] *Koç University, Faculty of Science, Department of Molecular Biology and Genetics, İstanbul, Türkiye*
[e] *Gazi University, Faculty of Science, Department of Chemistry, Ankara, Türkiye*
[f] *Recep Tayyip Erdogan University, Faculty of Science, Department of Chemistry, Rize, Türkiye*
[g] *Karadeniz Technical University, Faculty of Technology, Department of Energy Systems Engineering, Trabzon, Türkiye*

ARTICLE INFO

Article History:

Received: 29 November 2022
Revised: 21 February 2023
Accepted: 01 March 2023
Available online: 03 March 2023

Edited by: B. Tepe

Keywords:

Phlomis linearis
Biological activity
Cytotoxicity
DNA interaction
Molecular docking

ABSTRACT

Phlomis linearis Boiss. & Bal. of the Lamiaceae family is one of the endemic species in Turkey, i.e., growing in the east, central, and southeast parts of Anatolia and used for herbal tea. This study was designed to identify the biochemical and bioactivity properties of this endemic species by DPPH scavenging activity, metal chelating activity, total phenolic content, HPLC-DAD analysis, and MTT assay. Furthermore, the plant extract was evaluated for its antimicrobial activity against bacteria and fungi by using the microdilution method. The interactions between extract and plasmid DNA and their restriction endonuclease reactions were investigated by agarose gel electrophoresis. To support our hypothesis, we performed a molecular docking analysis. The DPPH scavenging activity of the plant extract was 53.86 ± 0.50 µg/ml in terms of IC_{50} value. The IC_{50} value of the plant extract was determined as 14.71 ± 4.01 mg/ml for metal chelating assay. The phenolic content of the extract was 231.55 ± 2.11 mg/g dry weight expressed as gallic acid equivalents (GAE). HPLC-DAD results revealed that the phenolic compounds were mainly derivatives of rosmarinic acid, chlorogenic acid, luteolin, luteolin-7-glycoside, luteolin derivatives, rutin derivatives, and apigenin derivatives. Besides, the cytotoxic activity of the plant extract against L929 fibroblast, H1299 non-small-cell lung carcinoma, and Caco-2 colorectal adenocarcinoma cell lines was determined by MTT assay. Phenolic content and molecular docking results correlated with each other.

1. Introduction

Physical inactivity, smoking, use of alcohol, infectious agents, aging, and exposure to certain chemicals are contributing to the high incidence rate of cancer (Iqbal et al., 2017). One in six deaths in the world is due to cancer (Kuruppu et al., 2019). Depending upon the stage and subtype of cancer, many of these patients will receive chemotherapy, which is accompanied by certain undesirable side effects. Plant-derived products which are less toxic as compared with conventional treatment methods are significantly considered suitable candidates for anticancer drug development (Iqbal et al., 2017). Antibiotic resistance is one of the biggest threats to public health. Antibiotic resistance leads to higher medical costs and increased mortality. For this reason, scientists are in search of new compounds to treat antimicrobial infections.

Reviewed by:
Ganiyat Oloyede: University of Ibadan, Ibadan, Oyo, Nigeria
Sevim Feyza Erdogmus: Afyonkarahisar Health Science University, Afyonkarahisar, Türkiye

* Corresponding author(s):
E-mail address: barslan@gazi.edu.tr (B. Aydın)
e-ISSN: 2791-7509
doi: https://doi.org/10.29228/ijpbp.19

Please cite this article as: Aydın, B., Gönder, L. Y., Çerçi, N. A., Ateş, Y. C., Yalçınkaya, I. S., Canbolat, N., Açık, L., Karacan, N., Akyüz Turumtay, E., & Turumtay, H. (2023). *Biological activities and DNA interactions of aqueous extract of Phlomis linearis (Boiss. & Bal.)*. *International Journal of Plant Based Pharmaceuticals*, *3*(1), 73-85, https://doi.org/10.29228/ijpbp.19.

Plants have different kinds of secondary compounds as natural protection against microbial attacks and cancer. Many of these compounds have been used as whole plants or extracts for food or medical applications in humans (Wallace, 2004). One group of secondary metabolites is polyphenols in higher plants which have great antioxidant activity. Several studies have shown that plant polyphenols can be used as antioxidants against different oxidative stress-induced diseases such as cardiovascular diseases, diabetes, cancer, and neurodegenerative diseases (Zhou et al., 2019). The human body has a defense system against these oxidative stresses; however, the antioxidant supplement may be helpful for the prevention and/or treatment of these diseases afflicting people worldwide (Stagos, 2019). The flora of Turkey is comprised of approximately 11707 plant species (Davis, 2019), and only a few percent have been studied for the treatment of different diseases. Of these, some of the natural phytochemicals such as taxanes exert their anti-cancer mechanisms by binding to microtubules which are key players for cell division; camptothecin, a topoisomerase poison affects DNA replication; cephalotaxus, an inhibitor of protein synthesis; capsaicin, an activator of caspase 3 and generator of reactive oxygen species leading to apoptosis; cyanidin, an inhibitor of cell growth and division; resveratrol, a modulator of gene expression; rutin and apigenin, inducers of apoptosis and target leptin/leptin receptor activation of caspase-dependent extrinsic apoptosis pathway, inhibit signal transducer, and activate the transcription 3 (STAT3) signaling pathways (Formagio et al., 2015; Heiblig et al., 2014; Kim et al., 2010; Patel et al., 2010; Rahier et al., 2005; Seo et al., 2015; Thakore et al., 2012).

The Lamiaceae family, one of the most important herbal families, incorporates a wide variety of plants with biological and medicinal applications (Uritu et al., 2018). *Phlomis* sp. is one of the genera of Lamiaceae, consisting of 100 species mainly distributed in the Mediterranean and Iran-Turanian phytogeographic region. In Turkey, this genus is represented by 33 species of which 18 are endemics (Dadandı, 2012).

According to World Health Organisation (WHO), antibiotics are becoming increasingly ineffective as drug resistance spreads globally leading to increased difficulty in treating infections and diseases. New antibacterials are therefore urgently needed (WHO, 2015). Also with the increasing mortality rate due to cardiovascular diseases and cancer, it became essential to find alternative leads with fewer side effects for cancer and infectious diseases. Therefore, this study was designed to investigate the antimicrobial, antioxidant, cytotoxic activity, and genotoxicity of the aqueous extract of *Phlomis linearis* with the hope of discovering a new therapeutic agent. The study also determined phenolic acid and flavonoid content using HPLC-DAD and DNA cleavage activity of the extract, in combination with molecular docking simulation of the most profound compounds of the extract.

2. Materials and methods

2.1. Plant material

Plant material collected from Kahramanmaraş province was dried at 35 °C for three days. After drying, 10 g of the dried material was grounded with a homogenizer, and the sample was submerged in 100 ml of water and left to macerate for 1 day. Then, the extract was decanted, and filtered through Whatman No. 1 filter papers, and the filtrate was concentrated to dryness using a standard Buchi rotary evaporator. The resulting dry extracts were resuspended in dimethylsulphoxide (DMSO) (Kim et al., 2011).

2.2. Microorganisms and growth conditions

Gram-positive *Staphylococcus aureus* ATCC 25923, *Bacillus subtilis* ATCC 6633, *Enterococcus hirae* ATCC 9790, *E. faecalis* ATCC 29212, and gram-negative *Klebsiella pneumoniae* ATCC 13883, *Salmonella typhimurium* ATCC 14028, *Proteus vulgaris* RSKK 96029, *Escherichia coli* ATCC 35218, *Pseudomonas aeruginosa* ATCC 27853 and yeast strains *Candida albicans* ATCC 10231 and *C. krusei* ATCC 6258 were used as test microorganisms. The bacterial and yeast cultures were grown on Mueller Hinton Broth at 37 °C and Sabouraud Dextrose Broth at 30 °C, respectively. After incubation, organisms were suspended in 10 ml of physiological saline solution and optical density readings were compared to a 0.5 McFarland standard (1.5×10^8 colony-forming unit/ml).

2.3. Antimicrobial activity

Minimum inhibitory concentrations (MIC), minimum bactericidal concentrations (MBC), and minimum fungicidal concentrations (MFC) of *P. linearis* aqueous extract were determined using sterile 96-well plates according to the Clinical & Laboratory Standards Institute (CLSI) reference methods for bacteria M7-A7 (CLSI, 2018) and yeasts M27-A3 (CLSI, 2008). Standard antimicrobial agents chloramphenicol, ampicillin, and ketoconazole were used as controls for bacteria and fungi, respectively. The analysis was carried out in triplicate.

2.4. Determination of free radical scavenging activity

The free radical scavenging potential of the extracts was determined by diphenyl-2-2-picrylhydrazyl (DPPH) assay comparing the half maximal effective concentration (EC_{50}) value of synthetic antioxidant butylated hydroxytoluene (BHT) with minor modifications according to the method described in Braca et al. (2001). A 0.5 ml extract of varying concentrations was mixed with a methanol solution of DPPH radical (0.1 mM). After 30 minutes of incubation at room temperature in the dark, the absorbance was measured spectrophotometrically at 517 nm against a blank. As a reference standard, BHT was used. The percentage of the DPPH radical scavenging effect of the extract was calculated using the following equation:

$$DPPH\ scavenging\ activity\ (\%\ inhibition) = \frac{Acontrol - Asample}{Acontrol} x\ 100$$

where $A_{control}$ is the absorbance of the control and A_{sample} is the absorbance of the extract.

To determine the concentration of the extract which causes a 50% decrease in DPPH scavenging activity, an extract concentration curve versus percentage inhibition was drawn. The value calculated by linear regression analysis is referred to as EC_{50}. Higher antioxidant activity is indicated by the lower EC_{50} value. All measurements were performed in triplicate.

2.5. Determination of total phenolic content (TPC)

The total phenolic content of the extract was studied according to the method of Folin-Ciocalteu using gallic acid as standard (Afolabi & Oloyede, 2014). 0.1 ml (1 mg/ml) of the extract was mixed with 0.2 ml of diluted Folin-Ciocalteu reagent (1:1 with water). 1 ml of 2% sodium carbonate was added to the reaction mixture after incubation at room temperature for 3 minutes. The absorbance was read at 760 nm by a spectrophotometer (Shimadzu UV-1800, Japan) after 1 h of room temperature incubation in the dark. The total

phenolic content values are expressed as gallic acid equivalent (GAE) in milligrams per gram of dried extract (mg GAE/g extract). All measurements were performed in triplicate.

2.6. Determination of ferrous ion chelating capacity

The ferrous ion chelating capacity of the extract was determined according to the method mentioned by Zhou et al. (2020). 0.5 ml of the extract at varying concentrations was mixed with 1.35 ml of methanol. 0.05 ml of 2 mM $FeCl_2$ was added to the solution and incubated for 5 min. Thereafter, 0.1 ml of 5 mM ferrozine solution was mixed and stayed for 10 min. After incubation, absorbance was measured at 562 nm by spectrophotometer (Shimadzu UV-1800, Japan) against a blank. The percentage of ferrous ion chelating potential of the sample was determined using the following equation:

$$Ferrous\ ion\ chelating\ ability\ (\%) = \frac{Acontrol - Asample}{Acontrol} x\ 100$$

where $A_{control}$ is the absorbance of the control and A_{sample} is the absorbance of the reaction mixture.

The EC_{50} value was determined by a linear regression curve, which is the concentration of the extracts that chelate 50% of the ferrous ion. All measurements were performed in triplicate.

2.7. Cytotoxicity assays

The cytotoxic effect of the plant extract in human L929 fibroblast, H1299 non-small-cell lung carcinoma, and Caco-2 colorectal adenocarcinoma cell lines (cell lines obtained from Kırıkkale University Culture Collection) were determined using 3-(dimethyl-2-thiazolyl)-2,5-diphenyl-2H-tetrazolium bromide (MTT) reduction assay where cisplatin was used as a reference ISO 10993-5 (ISO 10993-5, 2009). Cultures were grown and seeded (10^4 cells per well in the 96-well cell culture plates) in Dulbecco's modified Eagle's medium supplemented with 10% fetal bovine serum (DMEM-10), 1% glutamine, 50 U/ml penicillin, and 50 µg/ml streptomycin. Cells were incubated at 37 °C for 24h in an atmosphere of 5% CO_2 and 100% humidity in the air. The plant extract was dissolved in DMSO (10%) and applied to cells in five different concentrations (beginning from 5 mg/ml and two-fold dilutions). The solvent DMSO (10%), cisplatin (positive), and DMEM medium (blank) were used as controls. After 24 h incubation of cells, 50 µl MTT (1 mg/ml) solution was added to each well and after 2 h of incubation at 37 °C, 100 µl of isopropanol was added to the wells, and the absorbance values of the 96-well plate were read at 570 nm in a microplate reader to determine cell viability. The cytotoxicity studies were made in triplicate and the data were given as mean ± standard deviation (SD). Based on the control groups, the percent viability was calculated by the following formula:

$$Cell\ viability\ (\%) = \frac{Extract\ OD}{Control\ OD}\ x\ 100$$

where OD is the optical density.

2.8. Genotoxicity

The AMES test was performed with the plate incorporation method in the presence and absence of an exogenous metabolic activation system (rat liver postmitochondrial fraction with cofactors-S9mix), by using bacterial reverse mutation test according to the OECD Guideline for testing of chemicals 471 (OECD, 1997). In these experiments, *S. typhimurium* TA97a, *S. typhimurium* TA98, *S. typhimurium* TA100, *S. typhimurium* TA102, and *S. typhimurium* TA1535 strains recommended in OECD 471 standard were used. The plant extract was dissolved in DMSO (10%) and applied in five different concentrations (beginning from non-cytotoxic concentration and serial two-fold dilutions). The strains were incubated at 37 °C for 10-15 hours until the early stationary phase of growth (approximately 10^8 cells per ml in 30 ml nutrient broth in 250 ml flasks). Solvent, negative, and positive controls were established in three replicates using each concentration. For each replicate; 2 ml of histidine-biotin supplemented semi-dissolved (at 43-48 °C) top agar, 0.1 ml of the sample (each concentration)/solvent/positive control solution (mutagen)/negative control solution (phosphate buffer) was transferred to tubes, and 0.1 ml from the bacterial suspension and 0.5 ml of S9mix (5%, v/v), and for the test in the absence of metabolic activation system, phosphate buffer was added instead of S9mix, vortexed and poured on minimal glucose agar plates. The plates were incubated at 37 °C ± 2 for 48 h. Revertant colonies were counted, and statistical analyses were made.

2.9. DNA cleavage activity

Interaction between the water extract of *P. linearis* and pBR322 plasmid DNA was carried out using gel electrophoresis following a method described by Deqnah et al. (2012).

2.10. Restriction enzyme BamHI and HindIII digestion

BamHI and HindIII are restriction endonucleases that bind at the recognition sequence 5'-G/GATCC-3', 5'-A/AGCTT-3' and cut these sequences just after the 5'-guanine and 5'-adenine on each strand, respectively (Binici et al., 2023). The plasmid DNA contains a single restriction site for both enzymes that convert the supercoiled form I and singly nicked circular form II to linear form III DNA. The compounds and the DNA were incubated for 24 and 48 h in an incubator bath at 37 °C and then subjected to restriction enzyme digestion (Okumuş et al., 2016). The mixtures were left in an incubator at 37 °C for another 1 h. The samples were run in an agarose gel. The gel was photographed using Biometra Gel Imaging Systems.

2.11. Determination of phenolic compounds in the plant extract by HPLC-DAD

Phenolic compounds from *P. linearis* were extracted and 0.0971 g dry extract was diluted to a quarter and filtered for HPLC-DAD analysis. The chromatographic analyses were performed using a Dionex (Thermo Scientific, Germering, Germany) Ultimate 3000 HPLC system equipped with an Ultimate 3000 Degasser, an Ultimate LPG-3400SD Pump, an Ultimate WPS-3000TSL Autosampler, an Ultimate 3000 DAD, and an Ultimate TCC-3000SD column compartment.

A Thermo acclaim C30 column (150 mm × 3 mm id × 3 µm pd) was used with Macherey Nagel (3 mm id) guard column. Gradient elution was used with mobile phases of A: 2% acetic acid in water and B: 70% acetonitrile-30% water. The flow rate was 0.35 ml/min and the injection volume was 10 µl. The column temperature was 25 °C. 20 phenolic standards were used for calibration and validation of the HPLC-DAD analysis method as following: gallic acid, protocatechuic acid, *p*-hydroxy benzoic acid (*p*-OH benzoic acid), catechin, chlorogenic acid, caffeic acid, syringic acid, vanillin, epicatechin, *p*-coumaric acid, ferulic acid, rutin, luteolin-7-glucoside, apigenin-7-glucoside, rosmarinic acid, resveratrol, eriodictyol, luteolin, quercetin, and apigenin. They were diluted from their stock

solution into seven different concentrations at 0.3125, 0.625, 1.25, 5, 10, 25, and 40 mg/l in a 1:1 methanol-water solution. The external calibration method (Turumtay et al., 2014) was used, and their regression coefficient (R^2) was found at least 0.999. Repeatability of the retention time and peak areas were measured as coefficient of variation (CV) which was under 0.56 for retention times and 2.55 for areas of the peaks. The limit of detection and quantification values of the peaks were under 0.11 and 0.32 mg/l for all standards. Chromatograms were processed at 254, 280, 315, and 370 nm with a diode array detector that operated 200-400 nm. Identification and quantification of peaks were accomplished by comparison of retention times and UV spectra with those of standard phenolic compounds. With different retention times from the standards, some peaks had the same or very similar UV spectra as some standards. They were identified as the derivatives of the standards with similar UV spectra and quantified as an equivalent of these standards (Turumtay et al., 2014).

Table 1. Minimum inhibitory concentrations (MIC), minimum bactericidal concentrations (MBC), and minimum fungicidal concentrations (MFC) of the *P. linearis* water extract and controls (mg/ml)

Microorganisms		Water extract	Positive controls		
			Ampicillin	Chloramphenicol	Ketoconazole
E. coli ATCC 35218	MIC	500	> 125	> 125	-
	MBC	> 500	> 125	> 125	-
B. subtilis ATCC 6633	MIC	> 500	62.5	3.91	-
	MBC	> 500	62.5	3.91	-
S. aureus ATCC 25923	MIC	> 500	62.5	125	-
	MBC	> 500	62.5	> 125	-
E. faecalis ATCC 29212	MIC	> 500	31.25	62.5	-
	MBC	> 500	125	> 125	-
P. aeruginosa ATCC 27853	MIC	> 500	> 125	> 125	-
	MBC	> 500	> 125	> 125	-
K. pneumoniae ATCC 13883	MIC	> 500	125	15.63	-
	MBC	> 500	125	15.63	-
S. typhimurium ATCC 14028	MIC	> 500	62.5	125	-
	MBC	> 500	62.5	125	-
P. vulgaris RSKK 96029	MIC	> 500	> 125	125	-
	MBC	> 500	> 125	> 125	-
E. hirae ATCC 9790	MIC	> 500	62.5	62.5	-
	MBC	> 500	62.5	> 125	-
C. albicans ATCC 10231	MIC	> 500	-	-	31.25
	MBC	> 500	-	-	62.5
C. krusei ATCC 6258	MIC	> 500	-	-	< 0.98
	MBC	> 500	-	-	15.63

2.12. Molecular docking studies

The docking studies of compounds were carried out using Schrödinger to investigate the binding mode and interactions between ligands and target proteins (Schrödinger Release, 2020-3a, 2020-3b, 2020-3c, 2020-3d, 2020-3e, 2020-3f, 2020-3g, 2020-3h, 2020-3i). The 2D structure of the compounds was downloaded from the ZINC15 database (Irwin & Shoichet, 2005; Irwin et al., 2012). The 3D structures of the compounds were created using MacroModel (Schrödinger Release, 2020-3d) embedded Schrödinger Platform. The LigPrep (Schrödinger Release, 2020-3c) module was used to generate all possible conformers at a pH range of 7 ± 2 and using an OPLS_2005 force field.

The crystal structures of different DNA dodecamers PDB ID: 1BNA (Drew et al., 1981), PDB ID: 2GVR (Morsy et al., 2021), and PDB ID: 2DES (Cirilli et al., 1993), as well as the crystal structures of EGFR tyrosine kinase (PDB ID: 1XKK) (Wood et al., 2004), human basic fibroblast growth factor (PDB: ID 4FGF), cytochrome P450 (PDB ID: 1OG5) (Williams et al., 2003), xanthine oxidase (PDB ID: 3NRZ) (Cao et al., 2010), pro-inflammatory gene COX-2 (PDB ID: 5IKR) (Orlando & Malkowski, 2016), and tyrosine kinase (PDB ID: 1M17) (Stamos et al., 2002) were downloaded from protein databank to further use in molecular docking studies. Structures of the proteins were prepared for docking using the Protein Preparation Wizard of Maestro (Madhavi Sastry et al., 2013; Schrödinger Release, 2020-3e). In this process, the ionization and tautomeric states were generated by Epik (Greenwood et al., 2010; Schrödinger Release, 2020-3a), and the proton states were set by PROPKA. All proteins were finally minimized by the OPLS-2005 force field.

The 3D structure of the ligands was transferred to the Receptor Grid Generation module of Maestro (Schrödinger Release, 2020-3e), and grids were produced using the default parameters: van der Waals scaling factor 1.00 and charge cutoff value 0.25 by using the force field OPLS-2005. Docking simulation was done using the extra precision (XP) scoring function of Glide (Friesner et al., 2004; Friesner et al., 2006; Halgren, 2009; Schrödinger Release, 2020-3b), and only the best scoring fit with docking score was noted for each ligand. Prime (Jacobson et al., 2002; Schrödinger Release, 2020-3f) MM/GBSA calculation was carried out to calculate relative binding free energy for 1XKK. SiteMap (Halgren, 2007; Halgren, 2009; Schrödinger Release, 2020-3i) calculation was performed for 1BNA. QikProp (Schrödinger Release, 2020-3h) module implemented the Schrödinger suite was used for evaluating the ADME properties of the ligands.

3. Results and discussion

3.1. Antimicrobial activity

The results of the antimicrobial screening revealed that the MIC value of *P. linearis* was >500 mg/ml against all bacteria and yeast strains while the MIC value of antibiotics was 3.91 - >125 mg/ml (Table 1). Unlike our high MIC value results, Göger et al. (2021) showed that the MIC value of *P. linearis* EtOAc extracts against *S. aureus* strain was 156.25 µg/ml, *E. coli* and *C. albicans* were 625 µg/ml indicating that the plant was resistant to the EtOAc extract but susceptible to the water extract of *P. linearis*. The different MIC values were attributed to the polarity of the solvent, different stages of growth, and the environment of the plant, which can significantly affect their chemical composition (Koutsoukis et al., 2019).

3.2. Antioxidant activity

Aqueous plant extract exhibited good antioxidant activity (EC_{50} = 53.86 µg/ml) relative to that of BHT as a standard antioxidant (EC_{50} = 96.47 µg/ml) according to the DPPH radical scavenging activity results (Table 2). The EC_{50} value of the *P. linearis* extract is significantly higher than that of the BHT even though both extracts were prepared using aqueous as the extraction solvent. Also, the amount of total phenolic content of the aqueous plant extract was measured and expressed in mg gallic acid equivalent per gram (mgGAE/g). The aqueous extract revealed the presence of total phenols of 231.55 ± 2.11 mgGAE/g extract (Table 2). The metal chelating activity was found at 14.71 ± 4.01 mg/ml. The total phenol content varies depending on the plant species, plant tissue, developmental stage, and environmental factors, such as temperature, water stress, and light conditions (Upadrasta et al., 2011). This paper represents the first report on the antioxidant activities of the aqueous extract of *P. linearis*.

Table 2. The antioxidant properties of *P. linearis* aqueous extract

Parameter	Result	Parameter
Total phenolic content (mg GAE/g extract)	231.55 ± 2.11	Total phenolic content (mg GAE/g extract)
Metal chelating activity (IC_{50}) (mg/ml)	14.71 ± 4.01	Metal chelating activity (IC_{50}) (mg/ml)
DPPH scavenging activity (IC_{50}) (µg/ml)	53.86 ± 0.50	DPPH scavenging activity (IC_{50}) (µg/ml)
BHT (IC_{50}) (µg/ml)	96.47 ± 0.32	BHT (IC_{50}) (µg/ml)

3.3. Cytotoxicity assays

The cytotoxicity of aqueous *P. linearis* extract was determined using MTT assay in mouse fibroblast L929 cell line, human non-small cell lung carcinoma cell line H1299, and human colorectal adenocarcinoma Caco-2 cell lines exposed to 0.16 mg/ml, 0.32 mg/ml, 0.63 mg/ml, 1.25 mg/ml, 2.50 mg/ml, and 5 mg/mL of the extracts at incubation period of 24 h.

MTT test was performed to determine the cytotoxic activity of the aqueous extract of *P. linearis*. The IC_{50} values of the extracts were determined according to cell viability data for cell lines. Figure 1 presents cell viability percentages against applied concentrations for *P. linearis* extract to cell lines. The IC_{50} values of *P. linearis* extract on L929, H1299, and CaCo-2 cells were determined as 5.99 ± 1.19 mg/ml, 2.76 ± 0.04 mg/ml, and 4.85 ± 0.68 mg/ml, respectively.

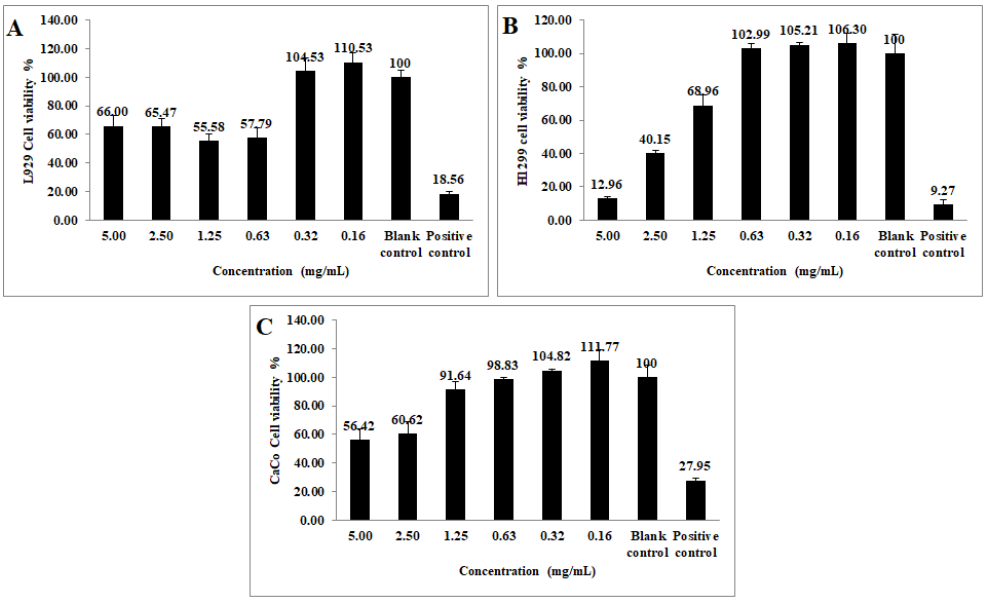

Figure 1. Cell viability percentages for applied concentrations of *P. linearis* aqueous extract on L929 mouse fibroblast cell line (A), H1299 human non-small lung carcinoma cell line (B), and human colorectal adenocarcinoma Caco-2 cell line (C)

Table 3. Genotoxicity test results of *P. linearis* water extract (0.32 mg/ml)

		Plant extract	Negative control
TA97	- S9	81.33 ± 22.5	85.00 ± 9.85
	+ S9	534 ± 38.81	456.67 ± 31.77
TA98	- S9	11.67 ± 2.08	10.67 ± 6.03
	+ S9	505.67 ± 39	431.33 ± 30.09
TA100	- S9	79.33 ± 17.67	74.33 ± 6.81
	+ S9	501.67 ± 34.50	534.67 ± 19.30
TA012	- S9	405.33 ± 28.38	393.33 ± 8.33
	+ S9	704.00 ± 42.33	744 ± 37.36
TA1535	- S9	17.67 ± 1.53	13.67 ± 3.21
	+ S9	456.33 ± 28.36	510.33 ± 47.75

It was observed that the applied doses of the *P. linearis* aqueous extract were unable to demonstrate a potentially toxic effect on L929 cells, but it was effective against H1299 human non-small lung carcinoma cells at high concentrations, as can be seen from the IC_{50} values and viability percentages. The 5 mg/ml concentration of the extract in H1299 cells had almost the same effect as cisplatin, which is widely used in cancer therapy (Ghosh, 2019).

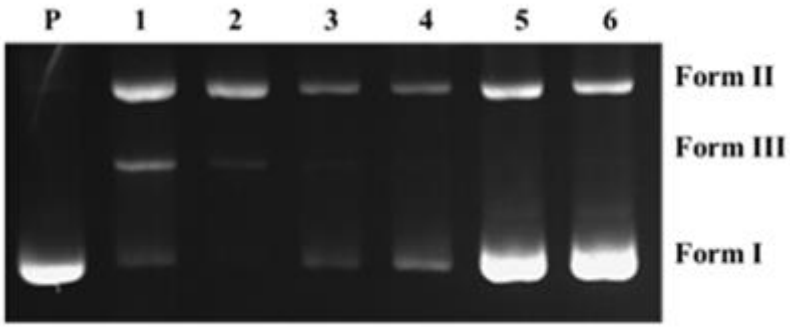

Figure 2. Results of electrophoresis after the incubation of pBR322 plasmid DNA with various concentrations of the extracts for 48 h.
The first line (P) corresponds to untreated pBR322 plasmid DNA as a control, and lines 1-6 correspond to pBR322 plasmid DNA incubated with compounds at concentrations ranging from 1000 µg/ml to 31.25 µg/ml (line 1: 1000 µg/ml; line 2: 500 µg/ml; line 3: 250 µg/ml; line 4: 125 µg/ml; line 5: 62.5 µg/ml; line 6: 31.25 µg/ml).

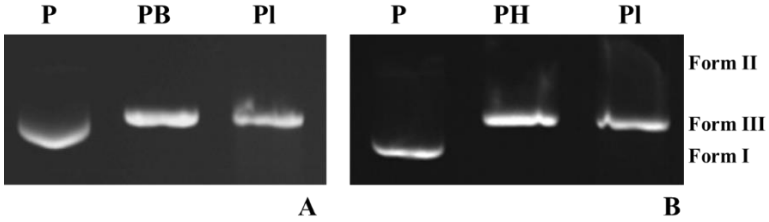

Figure 3. Electrophoretogram for the incubated mixtures of plasmid DNA followed by digestion with BamHI (A) and HindIII (B)
Lane P shows untreated DNA, lanes PB and PH depict untreated but digested plasmid DNA, lane Pl is plasmid DNA treated with the extract and enzyme-digested.

3.4. Genotoxicity

The mutagenicity of plant extract with and without metabolic activation (absence of S9 fraction) was investigated on *S. typhimurium* test strains TA97a, TA98, TA100, TA102, and TA1535. The plant extract was applied at a non-cytotoxic concentration of 0.32 mg/ml for L929 cells as required in the MTT assay results. Induction of *his*$^+$ revertants in *S. typhimurium* strains by *P. linearis* aqueous extracts without (top line) and with (bottom line) metabolic activation (S9mix) are given in Table 3. To determine the statistical significance of the number of *his*$^+$ revertants induced by the plant extract compared to the control, an independent sample *t*-test was done at $p \leq 0.05$.

The results were expressed in the number of revertants/plates of three independent experiments ± SD. Negative control sterile distilled water (100 µl) used as a solvent for the extract.

The use of herbs in recent years in traditional medicine has increased significantly (Sponchiado et al., 2016). However, these plants can be extremely harmful to human health if not administered properly. Studies have revealed that some herbs used even daily are potentially genotoxic (Mendonça et al., 2016). According to the AMES test results, performed both in the absence and presence of metabolic activation, the plant extract did not induce mutagenic effects on any *S. typhimurium* strains tested. There is no data in the literature regarding the genotoxic effect of *Phlomis* species (da Silva Dantas et al., 2020). Moreover, in some studies on the genotoxic effects of species belonging to the Lamiacea family, it was observed that these species also did not have genotoxic effects (Ayubi et al., 2021). It is noteworthy that the species belonging to this family are more effective in terms of anti-genotoxic effects among medicinal plants (da Silva Dantas et al., 2020).

3.5. DNA interaction with plant extract

The agarose gel electrophoresis study was carried out to gather information relating to the structural damaging interactions of the plant aqueous extract with DNA. When pBR322 plasmid DNA was exposed to the plant extract, generally two DNA bands corresponding to forms I and II were observed in both untreated and treated pBR322 plasmid DNA. As the concentration of the compounds was increased, the intensity of form II increased and form I pBR322 plasmid DNA decreased at 48 h incubation, a linear DNA form III band was observed in lane 1-2 corresponding to 1000 µg/mL and 500 µg/mL concentration (Figure 2). The mobility of form I decreased with increasing concentrations of plant extract, and also the presence of linear DNA was observed for other concentrations of the extract rather than two high concentrations indicating double-strand cleavage of the DNA. The changes in mobility and conformations of the DNA bands indicated changes in DNA conformation which may be a result of the covalent binding of some constituents of the aqueous extract with the DNA.

3.5.1. BamHI and HindIII digestion

To obtain further information on changes in DNA conformation, DNA was incubated with the plant extract which was followed by BamHI and HindIII digestion. Figure 3 gives the electrophoretogram

corresponding to the BamHI (A) and HindIII (B) digested incubated mixtures of pBR322 plasmid DNA and plant extract. BamHI and HindIII digestion of pBR322 plasmid DNA incubated with plant extract proved the binding interaction of the extract with A/A and G/G nucleotides of DNA. The compounds may also bind to other nucleotides of DNA. Analysis of phenolic compounds and molecular docking studies were performed to show the initial structural basis of DNA conformational change and DNA cleavage. The discovery of compounds that have the potential to interact with DNA macromolecule, which is the pharmacological target of many drugs currently in clinical use or advanced clinical trials, and determining their mechanism of action are important in terms of developing a new lead compound (Sirajuddin et al., 2013).

3.6. Phenolic content by HPLC-DAD analysis

As can be seen in Table 4 and Figure 4, the majority of phenolic compounds determined in the *P. linearis* aqueous extract are chlorogenic acid, derivatives of rosmarinic acid, rutin, apigenin, and *p*-coumaric acid. Luteolin-7-glycoside, luteolin, and some derivatives of luteolin, *p*-OH benzoic acid, protocatechuic acid, and caffeic acid were also determined as minor compounds.

Table 4. HPLC-DAD analysis of the extracts

No	Retention time	Compound	mg/g extract	µg/g dry plant
1	8.69	Protocatechuic acid	0.23	43.66
2	9.44	*p*-OH benzoic acid der*	0.21	41.40
3	15.54	*p*-OH benzoic acid	0.25	48.40
4	21.87	Chlorogenic acid	2.52	486.29
5	22.87	Caffeic acid	0.17	32.68
6	23.32	Rutin der	0.38	73.82
7	25.16	Apigenin der	0.94	181.00
8	25.63	Protocatechuic acid der	0.36	69.55
9	26.76	*p*-Coumaric acid	0.14	26.38
10	27.17	*p*-Coumaric acid der	0.09	17.00
11	30.22	Rosmarinic acid der	1.71	329.19
12	30.54	Rutin der	3.07	592.26
13	31.13	Rosmarinic acid der	3.38	653.14
14	31.63	Rosmarinic acid der	14.96	2886.62
15	31.85	Chlorogenic acid der	4.94	953.60
16	31.95	Rosmarinic acid der	11.29	2178.14
17	32.39	Luteolin-7-glucoside	0.48	93.04
18	32.56	Rutin der	7.34	1416.57
19	33.29	Rosmarinic acid der	1.30	250.72
20	33.84	Luteolin der	1.95	375.70
21	34.16	*p*-Coumaric acid der	0.19	37.57
22	34.54	Rosmarinic acid der	6.25	1205.75
23	35.36	Rutin der	0.61	117.56
24	35.67	Luteolin der	0.90	174.43
25	36.85	Rosmarinic acid der	0.31	60.55
26	37.636	Rosmarinic acid der	1.51	290.75
27	37.875	Rosmarinic acid der	0.96	186.01
28	38.985	Chlorogenic acid der	0.44	84.52
29	41.398	Luteolin	0.27	52.06
30	43.14	Resveratrol der	1.28	247.80
31	43.483	*p*-Coumaric acid der	0.13	25.97
32	44.53	Chlorogenic acid der	0.24	46.77
33	45.135	Resveratrol der	0.15	29.56
34	46.162	Caffeic acid der	0.41	79.00
35	46.66	Apigenin der	0.99	190.75
36	47.139	*p*-Coumaric acid der	2.84	547.99
37	50.38	*p*-Coumaric acid der	0.21	40.05

*der: derivative

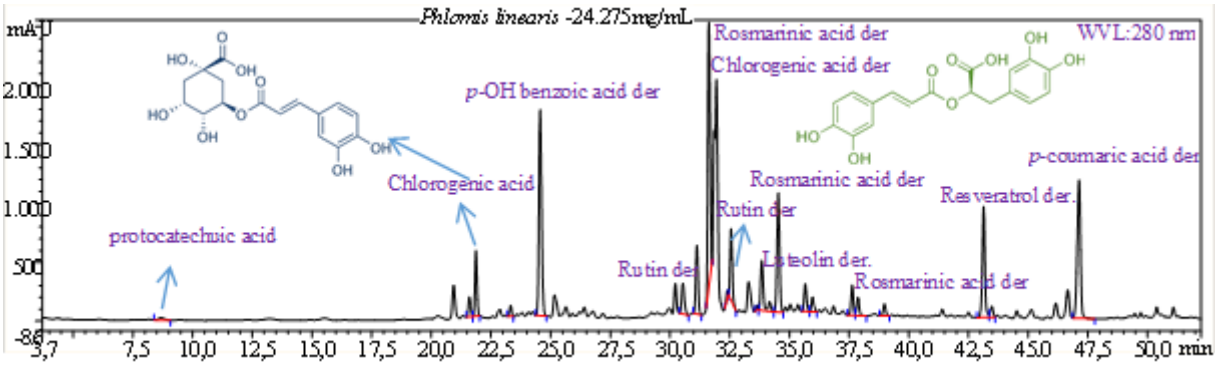

Figure 4. HPLC chromatogram of the *P. linearis* extract with the absorbance monitored at 280 nm

Demirci et al. (2003) reported that the oil of *P. linearis* was found to contain β-caryophyllene (24.2%), germacrene D (22.3%), and caryophyllene oxide (9.2%). Another study showed that the extract contained 14.9% monoterpenes with α-pinene (12.5%) as the major constituent. However, the plant sample collected in Kayseri province did not contain monoterpenes at all. In literature, the essential oil of

Phlomis species was studied. They found mainly sesquiterpene hydrocarbons as the major volatiles with caryophyllene (24.2%), germacrene D (22.3%), and *(Z)*-farnesene (6.6%) (Demirci et al., 2003). Studies regarding the chemical profiles of *P. linearis* were not well-detailed.

Table 5. Ligands in plant extract used in molecular docking*

No	Chemical structure	Chemical name	Molecular weight
1	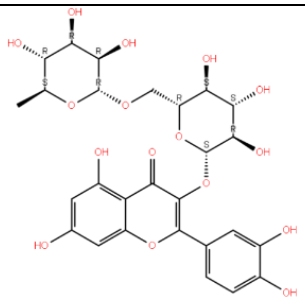	Rutin	610.524
2	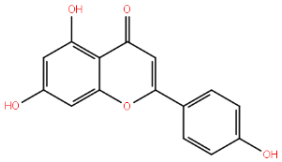	Apigenin	270.241
3	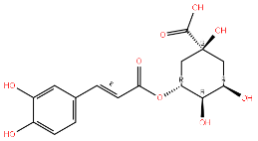	Chlorogenic acid	354.313
4	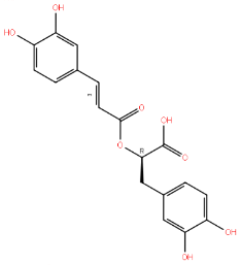	Rosmarinic acid	360.32
5	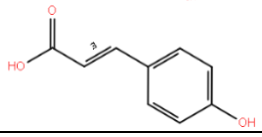	*p*-Coumaric acid	164.16

*Image from ZINC15 database (Irwin & Shoichet, 2005; Irwin et al., 2012)

Table 6. Molecular docking results of DNA with plant extract ligands

PDB IDs	XP docking score (kcal mol^{-1})				
	1	2	3	4	5
1BNA	-8.203	-1.834	-5.115	-6.569	-2.812
2GVR	-9.272	-7.245	-5.969	-7.352	-3.455
2DES	-9.999	-7.710	-9.705	-8.869	-6.021

3.7. Molecular docking studies

According to the HPLC-DAD analysis result, the top five most abundant ligands, *p*-coumaric acid, rosmarinic acid, chlorogenic acid, apigenin, and rutin were selected for molecular docking (Table 5). 2D structure of the ligands was downloaded from the ZINC15 database (Irwin & Shoichet, 2005; Schrödinger Release, 2020-3d). 3D structure, tautomers, and ionic forms of these ligands were prepared by LigPrep (Schrödinger Release, 2020-3c) module embedded in the Schrodinger Platform.

Molecular docking simulations of the plant extract ligands were performed with XP Glide (Friesner et al., 2004; Friesner et al., 2006; Halgren, 2007; Schrödinger Release, 2020-3b), docking protocol of the Schrödinger platform. Obtained XP docking scores were listed in Table 6. DNA dodecamers PDB ID: 1BNA (Drew et al., 1981), PDB ID: 2GVR (Morsy et al., 2021), and PDB ID: 2DES (Cirilli et al., 1993), as well as the other target proteins, were selected for docking studies of the major constituents of plant extract. The DNA sequence of 1BNA is that DNA (5'-D(*CP*GP*CP*GP*AP*AP*TP*TP*CP*GP*CP*G)-3') (Alizadeh et al., 2015; El-Medani et al., 2020; Morsy et al., 2021; Ozkan et al., 2020), 2GVR is that DNA (5'-D(*CP*GP*CP*GP*AP*AP*TP*TP*CP*GP*CP*G)- 3') (Morsy et al., 2021), and 2DES is that DNA (5'-D(*CP*GP*TP*AP*CP*G)-3') (Morsy et al., 2021).

The 3D models of the ligands bonded to 1BNA, and their interactions was given in Figure 5. The docked ligands' conformations were ranked according to the binding energy,

hydrogen bonding, and hydrophobic interactions between the ligands and the DNA (PDB ID: 1BNA, 2GVR, 2DES) (El-Medani et al., 2020). The docking calculations showed that docked compounds generally fit in the DNA minor groove and comprise ionic, and hydrogen bonding interactions with the DNA bases. It was also found that the optimal docking binding interactions have occurred in the G-C region. 1BNA did not have any cognate ligand, therefore, SiteMap (Schrödinger Release, 2020-3i) was used for the docking studies. Compound 1 fits in the DNA major groove as seen in Figure 6a, because it has a larger size rather than other ligands, and it fits in a wider region, i.e., the major groove in the site of 1BNA. Compound 1 has the higher binding interactions (Table 6), because of hydrogen bonding interactions between DG 16, DT 8, DA 6, DA 5, and DA 17, and the aromatic moiety and OH group. The compound 2 has hydrogen bonds between DG 16 and O group in aromatic moiety, DC 15 and OH group of 2. The binding interaction of compound 3 showed hydrogen bonds between DC 9 and OH group of 3, DC 14, and COO-, a group of 3. Also, compounds 4 and 5 shared hydrogen bonds between DG 16 and OH group, and the DT 7 and OH moiety, respectively. The order of XP docking scores is as follows:1 > 4 > 3 > 5 > 2 for 1BNA, 1 > 4 > 2 > 3 > 5 for 2GVR, and 1 > 3 > 4 > 5 > 2 for 2DES.

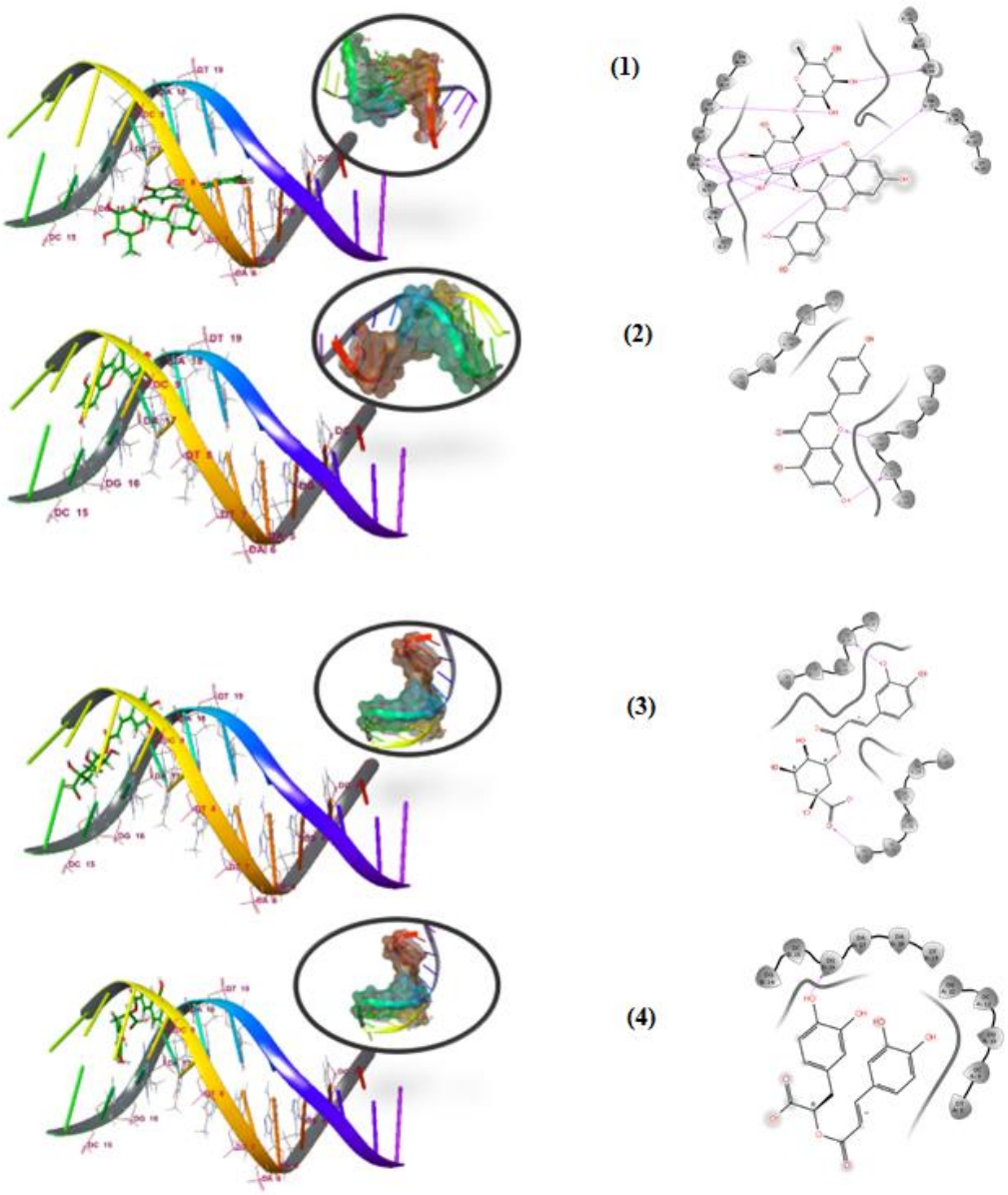

Figure 5. Binding mode of ligands 1, 2, 3, 4, and 5 with 1BNA 3D (left column) and 2D (right column) interactions

Cytochrome P450 (PDB ID: 1OG5) (Williams et al., 2003), xanthine oxidase (PDB ID: 3NRZ) (Cao et al., 2010), and pro-inflammatory gene COX-2 (PDB ID: 5IKR) (Orlando & Malkowski, 2016) were selected as target proteins for the antioxidant property. In addition, EGFR tyrosine kinase (PDB ID: 1XKK) (Wood et al., 2004), and tyrosine kinase (PDB ID: 1M17) (Stamos et al., 2002) were selected for elucidation of the structural basis of cytotoxic properties. Molecular docking studies of the ligands of plant extract and re-docking of cognate ligand was performed using XP Glide (Friesner et al., 2004; Friesner et al., 2006; Halgren, 2007; Schrödinger Release, 2020-3b) docking protocol of Schrödinger platform. Obtained XP Docking scores was listed in Table 7. A 3D model of the compound 1 bonded to the active site of the proteins, i.e., 1OG5 & 1XKK, and their 2D interactions were given in Figure 6. The Prime (Jacobson et

al., 2002; Jacobson et al., 2004; Schrödinger Release, 2020-3f) molecular mechanics/generalized born surface area (MM-GBSA) method was performed only for 1XKK to estimate the relative binding free energy of the ligands to the target protein.

Calculated binding free energy and XP docking score are well correlated. According to the docking score, generally, the antioxidant activities of the compounds were greater than cytotoxic activity, which is consistent with the experimentally obtained data.

Obtained docking score for 1OG5 shows that compounds 1 and 4 bind stronger to the active site of cytochrome P450; in other words, it can be predicted that 1 and 4 may have better antioxidant activity than cognate ligand SWF. Similarly, compound 1 in 3NRZ binds better to the active site of xanthine oxidase than cognate ligand HPA, in other words, compound 1 could have better antioxidant activity than HPA. The docking score of compound 2 for 51KR shows that compound 2 binds better to the active site of the pro-inflammatory gene COX-2, that is, compound 2 could have better antioxidant activity than cognate ligand ID8. Compound 1 was too big for the active site of 5IKR; therefore, it could not form an energetically favorable binding complex in docking calculations.

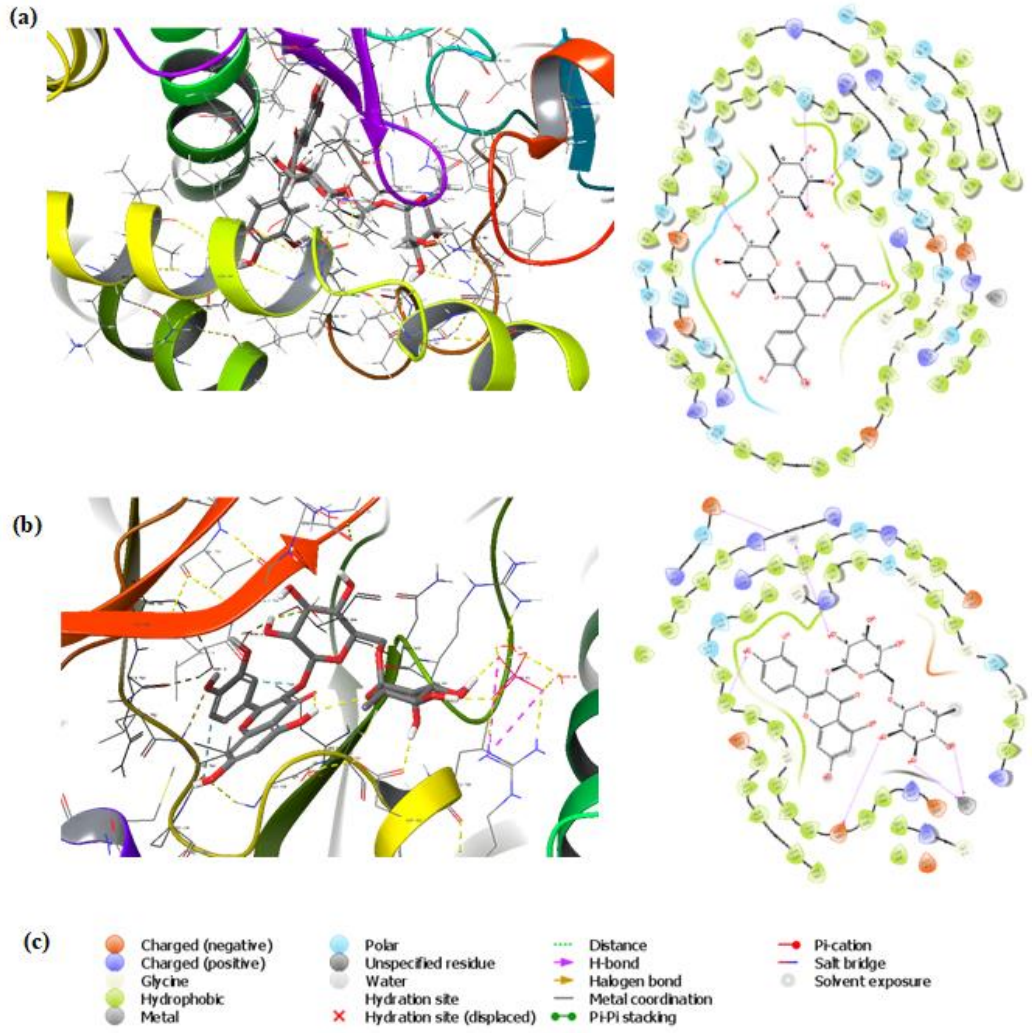

Figure 6. Binding mode of compound 1 with the active site of 1OG5 (a), 1XKK (b), and 2D interactions notations (c)

Tyrosine kinase and fibroblast growth factor were selected to evaluate the cytotoxic activity of the ligands because they are used to describe the cytotoxic activity of L929 mouse fibroblast cells, H1299 human non-small lung carcinoma cells, and human colorectal adenocarcinoma (Caco-2) cells. Tyrosine kinase is also a target enzyme related to oxidative stress. Long-term oxidative damage has been attributed to aging, cancer, neural and cardiovascular disorders, and liver diseases (Arteel, 2003; Guidi et al., 2006; Hyun et al., 2006; Kinnula & Crapo, 2004; Sas et al., 2007; Singh & Jialal, 2006). The docking score of the compounds for 1XKK is not higher than the cognate ligand FMM, that is, the usage of plant extract as an EGFR tyrosine kinase inhibitor is not suitable. The docking score of compound 1, calculated for 1M17 is a little higher than the cognate ligand AQ4, indicating that compound 1 binds stronger than the cognate ligand to the active site of tyrosine kinase. Therefore, it may be predicted that compound 1 could have better cytotoxicity than AQ4.

Compound 1 (rutin) in plant extract has antioxidant and cytotoxicity activity against cytochrome P450 and tyrosine kinase enzyme, respectively. Compound 4 (rosmarinic acid) in plant extract has higher antioxidant activity than cognate ligand SWF. Compound 2 (apigenin) in plant extract has moderate antioxidant and cytotoxic

activity. Consequently, the antioxidant activity of the plant extract is greater than the cytotoxic activity.

Compound 1 has four H-bond interactions with Ala719, Arg817, Asn818, and Asp 831; however, cognate ligand AQ4 has three with Met769, Cys773, and water molecules. Therefore, the polarity and hydrophobicity of compound 1 caused a higher number of non-covalent interactions than AQ4. Moreover, compound 1 has a bigger size compared to SWF. Similarly, compound 1 has more non-covalent interactions in the active site of 1OG5 via three H-bonds (Gln214, Asn217, and Leu208) compared to SWF with two H-bonds (Ala103 and Phe100), one π-π stacking, and one π-cation interaction as seen in Figure 5.

Table 7. Molecular docking results of cognate and plant extract ligands

PDB IDs	XP docking score (kcal mol^{-1})					
	1	2	3	4	5	Cognate
1OG5	-11.624	-7.547	-1.230	-10.555	-5.487	-6.098
3NRZ	-9.248	-7.296	-7.151	-6.440	-6.043	-6.278
5IKR	-	-10.616	-1.981	-6.658	-7.331	-10.132
1XKK	-9.145	-7.850	-6.594	-8.569	-4.901	-12.792
1M17	-12.940	-8.580	-8.122	-3.888	-3.793	-9.611
	Prime MM-GBSA ΔG binding energy (kJ mol^{-1})					
	1	2	3	4	5	
1XKK	-44.81	-39.88	-26.48	-40.60	-16.90	

Table 8. ADME results for selected ligands

No	MW	a	b	c	d	e	f	g	h	i	j
1	610.524	-2.623	9	20.55	3	15	1	-2.272	0.745	-7.436	2
2	270.241	1.635	2	3.75	0	3	3	-3.331	116.767	-3.97	0
3	354.313	-0.287	6	9.65	1	10	1	-2.563	1.652	-6.222	1
4	360.32	1.141	5	7	0	11	1	-3.344	1.512	-5.863	1
5	164.16	1.432	2	2.75	0	4	3	-1.658	62.218	-3.606	0

MW: Molecular weight, a: QPlogPo/w, b: Donor HB, c: Accpt HB, d: Rule of five, e: #rotor, f: Human oral absorption, g: QlogS, h: QPPCaco; i: QPlogKp, j: Rule of three

3.8. ADME/Tox analysis

Theoretical calculations of the ADME (absorption, distribution, metabolism, and excretion) properties of the compounds were carried out by the QikProp (Schrödinger Release, 2020-3h) module. Physically significant descriptors and pharmaceutically relevant properties of the compounds obtained with QikProp (Schrödinger Release, 2020-3h) are given in Table 8. The violation of the number five is acceptable, that is, compounds can be predicted to obey Lipinski's rule (MW < 500, QPlogPo/w < 5, donorHB ≤ 5, accptHB ≤ 10) and to have drug-like properties (Table 8). In addition, compounds are more likely to be orally available because their number of violations of Jorgensen's three rules (QPlogS > -5.7, QP PCaco > 22 nm/s, total primary metabolites < 7) is acceptable (Chen et al., 2020; Duffy & Jorgensen, 2000; Lipinski et al., 2012).

4. Conclusions

The emergence of multiple antibiotic resistance is a worldwide health issue and is motivating an increasing search for active natural and synthetic compounds that can stop antimicrobial resistance. This study showed that *P. linearis* has a more efficient antioxidant capacity compared to reference compounds. *P. linearis* could be a source of new compounds with therapeutic capacity. HPLC-DAD analysis of phenolic content revealed that the species extract is mainly rich in chlorogenic acid, derivatives of rosmarinic acid, rutin, apigenin, and *p*-coumaric acid. The extract had a strong effect on the intensity of form I supercoiled plasmid DNA and caused double-strand breaks indicating DNA cleavage activity. The molecular docking studies revealed that the docked major phytocompounds of *P. linearis* extract are oriented in DNA minor grooves via the formation of ionic, and hydrogen bonding interactions with the DNA bases. Moreover, the antioxidant activity of the plant extract was found greater than its cytotoxic activity, and the major phytocompounds demonstrated their molecular interactions (H-bonding, π-π interactions, etc.) with related target enzymes' active sites. According to ADME results, all 5 compounds showed drug-like properties and were orally available.

Acknowledgments

None.

Conflict of interest

The authors confirm that there are no known conflicts of interest.

Statement of ethics

In this study, no method requiring the permission of the "Ethics Committee" was used.

Availability of data and materials

All data generated or analyzed during this study are included in this published article.

Funding

None.

CRediT authorship contribution statement

Betül Aydın: Conceptualization, Investigation, Visualization, Data curation
Lütfiye Yasemin Gönder: Visualization
Nebahat Aytuna Çerçi: Formal analysis, Investigation, Methodology
Yiğit Can Ateş: Formal analysis, Methodology, Visualization
İlayda Sezin Yalçınkaya: Formal analysis, Investigation
Nüveyre Canbolat: Formal analysis, Investigation, Methodology, Visualization
Leyla Açık: Supervision, Data curation, Conceptualization, Writing - original draft

Nurcan Karacan: Formal analysis, Data curation
Emine Akyüz Turumtay: Formal analysis, Investigation
Halbay Turumtay: Formal analysis, Investigation

ORCID Numbers of the Authors

B. Aydın: 0000-0002-9092-1350
L. Y. Gönder: 0000-0001-6849-3364
N. A. Çerçi: 0000-0002-7864-7213
Y. C. Ateş: 0000-0002-4564-987X
İ. S. Yalçınkaya: 0000-0002-8746-2528
N. Canbolat: 0000-0003-4466-4602
L. Açık: 0000-0002-3672-8429
N. Karacan: 0000-0002-9273-7987
E. Akyüz Turumtay: 0000-0002-1504-4810
H. Turumtay: 0000-0003-4224-8103

Supplementary File

None.

Publisher's Note

All claims expressed in this article are solely those of the authors and do not necessarily represent those of their affiliated organizations, or those of the publisher, the editors and the reviewers. Any product that may be evaluated in this article, or claim that may be made by its manufacturer, is not guaranteed or endorsed by the publisher.

This is an open-access article distributed under the terms of the Creative Commons Attribution 4.0 International License (CC BY). The use, distribution or reproduction in other forums is permitted, provided the original author(s) and the copyright owner(s) are credited and that the original publication in this journal is cited, in accordance with accepted academic practice. No use, distribution or reproduction is permitted which does not comply with these terms.

References

Afolabi, O. B., & Oloyede, O. I. (2014). Antioxidant properties of the extracts of *Talinum triangulare* and its effect on antioxidant enzymes in tissue homogenate of Swiss albino rat. *Toxicology International, 21*(3), 307-313.

Alizadeh, R., Yousuf, I., Afzal, M., Srivastav, S., Srikrishna, S., & Arjmand, F. (2015). Enantiomeric fluoro-substituted benzothiazole Schiff base-valine Cu (II)/Zn (II) complexes as chemotherapeutic agents: DNA binding profile, cleavage activity, MTT assay and cell imaging studies. *Journal of Photochemistry and Photobiology B: Biology, 143*, 61-73.

Arteel, G. E. (2003). Oxidants and antioxidants in alcohol-induced liver disease. *Gastroenterology, 124*(3), 778-790.

Ayubi, Z., Jafari, A., Ayatollahi-Mousavi, S., Jafari, H., & Panddeh, M. (2021). Using Comet assay for genotoxic evaluation of *Zataria multiflora* Boiss., an Iranian endemic plant. *Journal of Food Quality and Hazards Control, 8*, 45-49.

Binici, A., Elmas, G., Okumuş, A., Erden Tayhan, S., Hökelek, T., Şeker, B. N., Açık, L., & Kılıç, Z. (2023). Phosphorus–nitrogen compounds. Part 58. Syntheses, structural characterizations and biological activities of 4-fluorobenzyl-spiro (N/O) cyclotriphosphazene derivatives. *Journal of Biomolecular Structure and Dynamics, 41*(1), 298-318.

Braca, A., De Tommasi, N., Di Bari, L., Pizza, C., Politi, M., & Morelli, I. (2001). Antioxidant principles from *Bauhinia tarapotensis*. *Journal of Natural Products, 64*(7), 892-895.

Cao, H., Pauff, J. M., & Hille, R. (2010). Substrate orientation and catalytic specificity in the action of xanthine oxidase: the sequential hydroxylation of hypoxanthine to uric acid. *Journal of Biological Chemistry, 285*(36), 28044-28053.

Chen, X., Li, H., Tian, L., Li, Q., Luo, J., & Zhang, Y. (2020). Analysis of the physicochemical properties of acaricides based on Lipinski's rule of five. *Journal of Computational Biology, 27*(9), 1397-1406.

Cirilli, M., Bachechi, F., Ughetto, G., Colonna, F. P., & Capobianco, M. L. (1993). Interactions between morpholinyl anthracyclines and DNA: the crystal structure of a morpholino doxorubicin bound to d (CGTACG). *Journal of Molecular Biology, 230*(3), 878-889.

CLSI (2008). Reference method for broth dilution antifungal susceptibility testing of yeasts; approved standard-third edition. In *CLSI document M27-A3, Clinical and Laboratory Standards Institute* Wayne, PA.

CLSI (2018). Methods for dilution antimicrobial susceptibility tests for bacteria that grow aerobically-11th edition. In *CLSI standard M07, Clinical and Laboratory Standards Institute*: Wayne, PA.

da Silva Dantas, F. G., de Castilho, P. F., de Almeida-Apolonio, A. A., de Araujo, R. P., & de Oliveira, K. M. P. (2020). Mutagenic potential of medicinal plants evaluated by the Ames *Salmonella*/microsome assay: A systematic review. *Mutation Research/Reviews in Mutation Research, 786*, 108338.

Dadandı, M. (2012). *Phlomis*. In A. Guner, S. Aslan, T. Ekim, M. Vural, & M. Babac (Eds.), *List of Plants of Turkey (Veinous Plants)*: Nezahat Gökyiğit Botanical Garden and Flora Research Association Publication, İstanbul.

Davis, P. (2019). *Flora of Turkey, Volume 1*: Edinburgh University Press, Edinburgh.

Demirci, B., Dadandı, M. Y., Franz, G., & Başer, K. H. C. (2003). Chemical composition of the essential oil of *Phlomis linearis* Boiss. & Bal., and biological effects on the CAM-assay: a safety evaluation. *Zeitschrift für Naturforschung C, 58*(11-12), 826-829.

Deqnah, N., Yu, J. Q., Beale, P., Fisher, K., & Huq, F. (2012). Synthesis of *trans*-bis-(2-hydroxypyridine) dichloroplatinum (II) and its Activity in Human Ovarian Tumour Models. *Anticancer Research, 32*(1), 135-140.

Drew, H. R., Wing, R. M., Takano, T., Broka, C., Tanaka, S., Itakura, K., & Dickerson, R. E. (1981). Structure of a B-DNA dodecamer: conformation and dynamics. *Proceedings of the National Academy of Sciences, 78*(4), 2179-2183.

Duffy, E. M., & Jorgensen, W. L. (2000). Prediction of properties from simulations: free energies of solvation in hexadecane, octanol, and water. *Journal of the American Chemical Society, 122*(12), 2878-2888.

El-Medani, S. M., Makhlouf, A. A., Moustafa, H., Afifi, M. A., Haukka, M., & Ramadan, R. M. (2020). Spectroscopic, crystal structural, theoretical and biological studies of phenylacetohydrazide Schiff base derivatives and their copper complexes. *Journal of Molecular Structure, 1208*, 127860.

Formagio, A., Vieira, M., Volobuff, C., Silva, M., Matos, A., Cardoso, C., Foglio, M., & Carvalho, J. (2015). In vitro biological screening of the anticholinesterase and antiproliferative activities of medicinal plants belonging to Annonaceae. *Brazilian Journal of Medical and Biological Research, 48*, 308-315.

Friesner, R. A., Banks, J. L., Murphy, R. B., Halgren, T. A., Klicic, J. J., Mainz, D. T., Repasky, M. P., Knoll, E. H., Shelley, M., *et al.* (2004). Glide: a new approach for rapid, accurate docking and scoring. 1. Method and assessment of docking accuracy. *Journal of Medicinal Chemistry, 47*(7), 1739-1749.

Friesner, R. A., Murphy, R. B., Repasky, M. P., Frye, L. L., Greenwood, J. R., Halgren, T. A., Sanschagrin, P. C., & Mainz, D. T. (2006). Extra precision glide: Docking and scoring incorporating a model of hydrophobic enclosure for protein− ligand complexes. *Journal of Medicinal Chemistry, 49*(21), 6177-6196.

Ghosh, S. (2019). Cisplatin: The first metal based anticancer drug. *Bioorganic Chemistry, 88*, 102925.

Göger, G., Türkyolu, Ü., Gürşen, E. N., Yur, S., Karaduman, A. B., Göger, F., Tekin, M., & Özek, G. (2021). Phytochemical characterisation of *Phlomis linearis* Boiss. & Bal and screening foranticholinesterase, antiamylase, antimicrobial, and cytotoxic properties. *Turkish Journal of Chemistry, 45*(2), 387-399.

Greenwood, J. R., Calkins, D., Sullivan, A. P., & Shelley, J. C. (2010). Towards the comprehensive, rapid, and accurate prediction of the favorable tautomeric states of drug-like molecules in aqueous solution. *Journal of Computer-Aided Molecular Design, 24*(6-7), 591-604.

Guidi, I., Galimberti, D., Lonati, S., Novembrino, C., Bamonti, F., Tiriticco, M., Fenoglio, C., Venturelli, E., Baron, P., *et al.* (2006). Oxidative imbalance in patients with mild cognitive impairment and Alzheimer's disease. *Neurobiology of Aging, 27*(2), 262-269.

Halgren, T. (2007). New method for fast and accurate binding-site identification and analysis. *Chemical Biology & Drug Design, 69*(2), 146-148.

Halgren, T. A. (2009). Identifying and characterizing binding sites and assessing druggability. *Journal of Chemical Information and Modeling, 49*(2), 377-389.

Heiblig, M., Sobh, M., & Nicolini, F. (2014). Subcutaneous omacetaxine mepesuccinate in patients with chronic myeloid leukemia in tyrosine kinase inhibitor-resistant patients: Review and perspectives. *Leukemia Research, 38*(10), 1145-1153.

Hyun, D. H., Hernandez, J. O., Mattson, M. P., & de Cabo, R. (2006). The plasma membrane redox system in aging. *Ageing Research Reviews, 5*(2), 209-220.

Iqbal, J., Abbasi, B. A., Mahmood, T., Kanwal, S., Ali, B., Shah, S. A., & Khalil, A. T. (2017). Plant-derived anticancer agents: A green anticancer approach. *Asian Pacific Journal of Tropical Biomedicine, 7*(12), 1129-1150.

Irwin, J. J., & Shoichet, B. K. (2005). ZINC− a free database of commercially available compounds for virtual screening. *Journal of Chemical Information and Modeling, 45*(1), 177-182.

Irwin, J. J., Sterling, T., Mysinger, M. M., Bolstad, E. S., & Coleman, R. G. (2012). ZINC: a free tool to discover chemistry for biology. *Journal of Chemical Information and Modeling, 52*(7), 1757-1768.

ISO 10993-5 (2009). *Biological evaluation of medical devices-Part 5: Tests for in vitro cytotoxicity*: ISO Geneva.

Jacobson, M. P., Friesner, R. A., Xiang, Z., & Honig, B. (2002). On the role of the crystal environment in determining protein side-chain conformations. *Journal of Molecular Biology, 320*(3), 597-608.

Jacobson, M. P., Pincus, D. L., Rapp, C. S., Day, T. J., Honig, B., Shaw, D. E., & Friesner, R. A. (2004). A hierarchical approach to all-atom protein loop prediction. *Proteins: Structure, Function, and Bioinformatics, 55*(2), 351-367.

Kim, I. S., Yang, M. R., Lee, O. H., & Kang, S. N. (2011). Antioxidant activities of hot water extracts from various spices. *International Journal of Molecular Sciences, 12*(6), 4120-4131.

Kim, J. E., Kwon, J. Y., Seo, S. K., Son, J. E., Jung, S. K., Min, S. Y., Hwang, M. K., Heo, Y. S., Lee, K. W., *et al.* (2010). Cyanidin suppresses ultraviolet B-induced COX-2 expression in epidermal cells by targeting MKK4, MEK1, and Raf-1. *Biochemical Pharmacology, 79*(10), 1473-1482.

Kinnula, V. L., & Crapo, J. D. (2004). Superoxide dismutases in malignant cells and human tumors. *Free Radical Biology and Medicine, 36*(6), 718-744.

Koutsoukis, C., Roukos, C., Demertzis, P. G., Kandrelis, S., & Akrida-Demertzi, K. (2019). The variation of the chemical composition of the main plant species in a subalpine grassland in northwestern Greece. *Legume Science, 1*(1), e23.

Kuruppu, A. I., Paranagama, P., & Goonasekara, C. L. (2019). Medicinal plants commonly used against cancer in traditional medicine formulae in Sri Lanka. *Saudi Pharmaceutical Journal, 27*(4), 565-573.

Lipinski, C. A., Lombardo, F., Dominy, B. W., & Feeney, P. J. (2012). Experimental and computational approaches to estimate solubility and permeability in drug discovery and development settings. *Advanced Drug Delivery Reviews, 64*, 4-17.

Madhavi Sastry, G., Adzhigirey, M., Day, T., Annabhimoju, R., & Sherman, W. (2013). Protein and ligand preparation: parameters, protocols, and influence on virtual screening enrichments. *Journal of Computer-Aided Molecular Design, 27*, 221-234.

Mendonça, E. D., da Silva, J., Dos Santos, M. S., Carvalho, P., Papke, D. K. M., Ortmann, C. F., Picada, J. N., Reginatto, F. H., & Ferraz, A. D. B. F. (2016). Genotoxic, mutagenic and antigenotoxic effects of *Cecropia pachystachya* Trécul aqueous extract using in vivo and in vitro assays. *Journal of Ethnopharmacology, 193*, 214-220.

Morsy, N. M., Hassan, A. S., Hafez, T. S., Mahran, M. R., Sadawe, I. A., & Gbaj, A. M. (2021). Synthesis, antitumor activity, enzyme assay, DNA binding and molecular docking of Bis-Schiff bases of pyrazoles. *Journal of the Iranian Chemical Society, 18*, 47-59.

OECD (1997). *Guidelines for the testing of chemicals, section 4 health effects, Test Guideline No. 471, Bacterial Reverse Mutation Test*.

Okumuş, A., Akbaş, H., Kılıç, Z., Yasemin Koç, L., Açık, L., Aydın, B., Türk, M., Hökelek, T., & Dal, H. (2016). Phosphorus–nitrogen compounds part 33: in vitro cytotoxic and antimicrobial activities, DNA interactions, syntheses, and structural investigations of new mono (4-nitrobenzyl) spirocyclotriphosphazenes. *Research on Chemical Intermediates, 42*, 4221-4251.

Orlando, B. J., & Malkowski, M. G. (2016). Substrate-selective inhibition of cyclooxygeanse-2 by fenamic acid derivatives is dependent on peroxide tone. *Journal of Biological Chemistry, 291*(29), 15069-15081.

Ozkan, S. C., Aksakal, F., & Yilmaz, A. (2020). Synthesis of novel calix [4] arene *p*-benzazole derivatives and investigation of their DNA binding and cleavage activities with molecular docking and experimental studies. *RSC Advances, 10*(63), 38695-38708.

Patel, K. R., Brown, V. A., Jones, D. J., Britton, R. G., Hemingway, D., Miller, A. S., West, K. P., Booth, T. D., Perloff, M., *et al.* (2010). Clinical pharmacology of resveratrol and its metabolites in colorectal cancer patients resveratrol in colorectal cancer patients. *Cancer Research, 70*(19), 7392-7399.

Rahier, N., Thomas, C., & Hecht, S. (2005). Camptothecin and its analogs. In G. Cragg, D. Kinston, & D. New (Eds.), *Anticancer agents from natural products* (pp. 5-22): Boca Raton, FL: Taylor and Francis.

Sas, K., Robotka, H., Toldi, J., & Vécsei, L. (2007). Mitochondria, metabolic disturbances, oxidative stress and the kynurenine system, with focus on neurodegenerative disorders. *Journal of the Neurological Sciences, 257*(1-2), 221-239.

Schrödinger Release. (2020-3a). *Epik*: Schrödinger, LLC, New York.

Schrödinger Release. (2020-3b). *Glide*: Schrödinger, LLC, New York.

Schrödinger Release. (2020-3c). *LigPrep*: Schrödinger, LLC, New York.

Schrödinger Release. (2020-3d). *MacroModel*: Schrödinger, LLC, New York.

Schrödinger Release. (2020-3e). *Maestro*: Schrödinger, LLC, New York.

Schrödinger Release. (2020-3f). *Prime*: Schrödinger, LLC, New York.

Schrödinger Release. (2020-3g). *Protein Preparation Wizard*: Schrödinger, LLC, New York.

Schrödinger Release. (2020-3h). *QikProp*: Schrödinger, LLC, New York.

Schrödinger Release. (2020-3i). *SiteMap*: Schrödinger, LLC, New York.

Seo, H., Jo, J., Ku, J., Choi, H., Choi, Y., & Woo, J. (2015). Induction of caspase-dependent extrinsic apoptosis by apigenin through inhibition of signal transducer and activator of transcription 3 (STAT3) signalling in HER2-overexpressing BT-474 breast cancer cells. *Bioscience Reports, 35*(6), e00276.

Singh, U., & Jialal, I. (2006). Oxidative stress and atherosclerosis. *Pathophysiology, 13*(3), 129-142.

Sirajuddin, M., Ali, S., & Badshah, A. (2013). Drug–DNA interactions and their study by UV–Visible, fluorescence spectroscopies and cyclic voltametry. *Journal of Photochemistry and Photobiology B: Biology, 124*, 1-19.

Sponchiado, G., Adam, M. L., Silva, C. D., Soley, B. S., de Mello-Sampayo, C., Cabrini, D. A., Correr, C. J., & Otuki, M. F. (2016). Quantitative genotoxicity assays for analysis of medicinal plants: A systematic review. *Journal of Ethnopharmacology, 178*, 289-296.

Stagos, D. (2019). Antioxidant activity of polyphenolic plant extracts. *Antioxidants, 9*(1), 19.

Stamos, J., Sliwkowski, M. X., & Eigenbrot, C. (2002). Structure of the epidermal growth factor receptor kinase domain alone and in complex with a 4-anilinoquinazoline inhibitor. *Journal of Biological Chemistry, 277*(48), 46265-46272.

Thakore, P., Mani, R. K., & Kavitha, S. J. (2012). A brief review of plants having anti-cancer property. *International Journal of Pharmaceutical Research Development, 3*, 129-136.

Turumtay, E. A., İslamoğlu, F., Çavuş, D., Şahin, H., Turumtay, H., & Vanholme, B. (2014). Correlation between phenolic compounds and antioxidant activity of Anzer tea (*Thymus praecox* Opiz subsp. *caucasicus* var. *caucasicus*). *Industrial Crops and Products, 52*, 687-694.

Upadrasta, L., Mukhopadhyay, M., & Banerjee, R. (2011). Tannins: Chemistry, biological properties and biodegradation. In A. Sabu, S. Roussos, & C. Aguilar (Eds.), *Chemistry and Biotechnology of Polyphenols* (pp. 5-32): Cibet Publishers; Thiruvananthapuram, India.

Uritu, C. M., Mihai, C. T., Stanciu, G. D., Dodi, G., Alexa-Stratulat, T., Luca, A., Leon-Constantin, M. M., Stefanescu, R., Bild, V., *et al.* (2018). Medicinal plants of the family Lamiaceae in pain therapy: A review. *Pain Research and Management, 2018*, 801543.

Wallace, R. J. (2004). Antimicrobial properties of plant secondary metabolites. *Proceedings of the Nutrition Society, 63*(4), 621-629.

WHO (2015). *Global Action Plan on Antimicrobial Resistance*: The WHO Document Production Services, Geneva, Switzerland.

Williams, P. A., Cosme, J., Ward, A., Angove, H. C., Matak Vinković, D., & Jhoti, H. (2003). Crystal structure of human cytochrome P450 2C9 with bound warfarin. *Nature, 424*(6947), 464-468.

Wood, E. R., Truesdale, A. T., McDonald, O. B., Yuan, D., Hassell, A., Dickerson, S. H., Ellis, B., Pennisi, C., Horne, E., *et al.* (2004). A unique structure for epidermal growth factor receptor bound to GW572016 (Lapatinib) relationships among protein conformation, inhibitor off-rate, and receptor activity in tumor cells. *Cancer Research, 64*(18), 6652-6659.

Zhou, J., Yang, Q., Zhu, X., Lin, T., Hao, D., & Xu, J. (2020). Antioxidant activities of *Clerodendrum cyrtophyllum* Turcz leaf extracts and their major components. *PLoS One, 15*(6), e0234435.

Zhou, Y., Jiang, Z., Lu, H., Xu, Z., Tong, R., Shi, J., & Jia, G. (2019). Recent advances of natural polyphenols activators for Keap1-Nrf2 signaling pathway. *Chemistry & Biodiversity, 16*(11), e1900400.

Int. J. Plant Bas. Pharm. (2023) 3(1), 86-94

INTERNATIONAL JOURNAL OF PLANT BASED PHARMACEUTICALS

https://ijpbp.com

RESEARCH ARTICLE

OPEN ACCESS

Development of controlled delivery systems by nanoliposomes of *Hypericum perforatum* L. extracts

Özlem Erdal Altıntaş[a]*, Sevim Feyza Erdoğmuş[b]

[a] *Afyonkarahisar Health Sciences University, Suhut Vocational School of Health Services, Medical Laboratory Techniques Program, 03200, Afyonkarahisar, Türkiye*

[b] *Afyonkarahisar Health Sciences University, Faculty of Pharmacy, Department of Basic Pharmaceutical Sciences, Department of Pharmaceutical Microbiology, 03200, Afyonkarahisar, Türkiye*

ARTICLE INFO

Article History:

Received: 28 February 2023
Revised: 16 March 2023
Accepted: 17 March 2023
Available online: 20 March 2023

Edited by: B. Tepe

Keywords:

Biological activity
Controlled release
Hypericum perforatum L.
Liposomes

ABSTRACT

Hypericum perforatum L. is a popular and widespread medicinal plant used in a wide range of therapy, including gastrointestinal diseases, heart diseases, and skin-related diseases. The rapid development of nanotechnology and its applications in pharmacology have enabled the controlled release of drugs and bioactive components. This study aimed to investigate liposomal formulation for controlled release enriched with methanol and ethanol extract of *H. perforatum*, which has antioxidant, antimicrobial, and proliferative effects. In this context, firstly, the biological activity (antimicrobial, antioxidant, and cell viability) of *H. perforatum* methanol (Hp-MeOH) and ethanol (Hp-EtOH) extracts obtained by ultrasonic extraction method was revealed. Hp-MeOH and Hp-EtOH extracts have a larger zone of inhibition against *Enterococcus faecalis* ATTC 51289 and *Pseudomonas aeruginosa* ATCC 11778, respectively than the positive control amikacin (30mg/ml). Hp-MeOH and Hp-EtOH extracts were found to have a high total antioxidant status and low total oxidant status and oxidative stress index value. Hp-MeOH and Hp-EtOH extracts have a scavenging capacity of DPPH radicals between 23-89% and 27-90%, respectively in the studied concentration range. In addition, the effect of Hp-MeOH and Hp-EtOH extracts on cell viability of dermal fibroblast cells was evaluated for 24, 48, and 72 hours and induction of proliferation of fibroblasts was observed. Highly stable liposomes were successfully developed which encapsulated 82.6 ± 3.63% and 89.8 ± 2.74% Hp-MeOH and Hp-EtOH extracts, respectively. Liposomal structures loaded with Hp-MeOH and Hp-EtOH extracts showed a more controlled and slower release than the free extract.

1. Introduction

In recent years, encapsulation of bioactive compounds and natural plant extracts using nanotechnology has been the focus of pharmaceutical, cosmetic, and food industries and researchers. Encapsulation of plant-based bioactive compounds and crude plant extract may be a useful tool to prevent their degradation and instability due to light, oxygen, and free radicals and to enhance their effective delivery (Tripathy & Srivastav, 2023). Plant extracts contain alkaloids, phenolic acids, polyphenols, proteins, and terpenoids that have important effects and functions such as antioxidant, antimicrobial, anti-inflammatory, and anticancer. Therefore, they have been used as natural therapeutic and complementary substances since ancient times (Sharma et al., 2022). In addition, bioactive plant extracts have significant advantages over synthetic components, such as fewer toxic side effects, high bioavailability, and cheap and easy availability (Parham et al., 2020). To maintain these important properties in a stable form for a long time and to act at the desired site at an effective dose in a controlled manner, plant extracts or their components are combined with biocompatible delivery systems (Rahman et al., 2020). Liposomes, one of the biocompatible and controlled release systems, are small lipid-

Reviewed by:
Muhammad Muddassir Ali: University of Veterinary and Animal Sciences, Lahore, Pakistan
Yasemin Coşkun: Suleyman Demirel University, Isparta, Türkiye

* Corresponding author(s):
E-mail address: ozlem.erdal.ege@gmail.com
(O. Erdal Altıntaş)
e-ISSN: 2791-7509
doi: https://doi.org/10.29228/ijpbp.20

based vesicles with a phospholipid bilayer. These lipid-based vesicles are enormously versatile as they can load several molecules, protect them from degradation, modify their pharmacokinetics and improve the bioavailability profile and eventually improve the therapeutic effect of the incorporated components (Luiz et al., 2023). Liposomes are mainly composed of phospholipids and these components are generally regarded as safe (GRAS) since they are present in the human body, as well as in food products that we consume (Naziris & Demetzos, 2022). Liposomes are prepared using various and combined methods. The choice of method depends on factors such as physicochemical properties, effective concentration and toxicity level, and large-scale production from a pilot plant. The initial loading of the phytochemicals to be encapsulated can be carried out during the preparation of liposomes (passive loading) or by placement across the transmembrane by the carrier (active loading). Liposome production methods include hydration techniques, sonication methods, and solvent evaporation methods (ether injection, ethanol injection, and reverse phase evaporation methods). In addition, micro fluidization and lyophilization are prominent in industrial-scale liposome production (Dua et al., 2012; Maja et al., 2020).

Widely used in folk and modern medicine, *Hypericum perforatum* L. is a perennial herb belonging to the Hypericaceae family. *H. perforatum* is associated with antidepressant, anti-inflammatory, antimicrobial, antiseptic, antioxidant, antitumoral, analgesic, antineoplastic, metabolic syndrome-improving action, and wound-healing activity. Thanks to its essential oils, flavonoids, phenolic acids, naphthodiantrons (hypericin and pseudohypericin), and phloroglucinols (hyperforin and adhyperforin), it has a traditional use in the treatment of wounds, ulcers, and burns (Ali et al., 2018; Nobakht et al., 2022).

Recently, plant extracts have come to the forefront in the development of pharmaceutical formulations to be used in the treatment of many diseases. In this context, this study aimed to produce and characterize liposome structures from *H. perforatum* extract, which has versatile effects and biological activity. Thus, carrier structures with controlled release properties have been created in which this plant, which has a wide range of uses, can be included in pharmaceutical formulations. The pharmacokinetic properties of this lipid carrier system loaded with *H. perforatum* extract can be improved or its therapeutic effects can be increased by combining it with different plant extracts.

2. Materials and methods

2.1. Materials

Dimethyl sulfoxide (DMSO) (D4540), phosphate-buffered saline (PBS) (806552), Folin-Ciocalteu's reagent (47641), 2,2-diphenyl-1-picrylhydrazyl (DPPH) (D9132), gallic acid (91215), and quercetin (Q4951) were all obtained from Sigma-Aldrich (USA). For the cell experiments, a human dermal fibroblast (HDF) cell line was purchased from American Type Culture Collection (Manassas, VA, USA). Dulbecco modified eagle medium (DMEM) (11880028), penicillin/streptomycin (15140122), and fetal bovine serum (FBS) (A3840101) was obtained from GIBCO (Grand Island, NY, USA). For the cell viability and proliferation analyses, an MTT assay kit (M5655) was purchased from Sigma-Aldrich (USA).

2.2. Plant material and extract preparation

H. perforatum (Hp) plants were collected from Afyonkarahisar: Erkmen region (Turkey) in June 2022 and authenticated by Prof. Dr. Mustafa Kargioglu. A voucher specimen (No: AKU-10964) was deposited at the Archives of Afyon Kocatepe University Herbarium. The aerial parts of *H. perforatum* were dried and powdered. The modified ultrasonic extraction method was used to prepare 50% (v/v) aqueous methanol and 50% (v/v) aqueous ethanol extracts of *H. perforatum* (Hp-MeOH and Hp-EtOH) (Latiff et al., 2021).

2.3. Evaluation of antimicrobial activity

2.3.1. Test microorganisms

The antimicrobial tests were performed using referenced strains such as *Listeria monocytogenes* ATCC 1911, *Staphylococcus aureus* ATCC 25923, *Klebsiella pneumoniae* NRRLB 4420, *Pseudomonas aeruginosa* ATCC 11778, *Enterococcus faecalis* ATCC 51289, *Escherichia coli* ATCC 35218, *Bacillus subtilis* NRS-744, *S. aureus* ATCC 6538, *E. coli* ATCC 25922, *P. aeruginosa* ATCC 27853, *S. aureus* ATCC 12600 and *Candida albicans* ATCC 10231.

2.3.2. Antimicrobial activity

The Clinical and Laboratory Standards Institute (CLSI) disc diffusion assay was used to test antimicrobial activity in vitro (CLSI, 2016). Inhibition zone diameters (mm) were measured and evaluated in comparison with the control group. The lowest concentration of a drug that inhibits a microorganism's apparent growth is known as the minimum inhibitory concentration (MIC) value. Microdilution assay following the methods described by the Clinical and Laboratory Standards Institute was used to determine MIC of Hp-MeOH and Hp-EtOH extracts, which leads to inhibition of the growth of the test bacteria (CLSI, 2012) and fungus (CLSI, 2002). The lowest extract concentration that induced 50% cytotoxicities (50% inhibition of microorganism growth) was determined as the MIC value. Penicillin G (10 mg/ml), amikacin (30 mg/ml), and fluconazole (10 mg/ml) were used as positive controls, and distilled water (dH_2O) was used as the negative control.

2.4. Determination of in vitro TAS, TOS, and OSI values

Total antioxidant status (TAS), total oxidant status (TOS), and oxidative stress index (OSI) values of the Hp-MeOH and Hp-EtOH extracts were assessed using commercially available Rel Assay Diagnostic kits (Erel, 2004, 2005). Trolox and hydrogen peroxide standards were used as references for TAS and TOS analyses, respectively. *Eq. 1* was used while calculating the oxidative stress index [OSI (Arbitrary Unit = AU)] value (Erel, 2005).

$$OSI\ (AU) = \frac{TOS\ (\mu mol\ H2O2\ equiv./l)}{TAS\ (mmol\ Trolox\ equiv./l)} x\ 10 \qquad Eq.\ 1$$

2.5. Total phenolic content (TPC)

The total phenolic content of the Hp-MeOH and Hp-EtOH extracts was determined according to the Folin–Ciocalteu method with minor changes (Gamez-Meza et al., 1999) and gallic acid as a standard. 150 µl of suitably diluted extract samples, calibration solutions, and blank solution, as well as 150 µl of Folin-Ciocalteu's reagent, were added to each test tube. The mixture was thoroughly mixed, and after 10 min, 3 ml of Na_2CO_3 solution (2% w/v, in water) was added. The mixture was stored at room temperature for 30 min. After incubation, the absorbance of the mixture was measured at 760 nm in a UV spectrophotometer. The results were calculated using the standard calibration curve of gallic acid (R^2 = 0.9971) and expressed as gallic acid equivalents (mg GAE/g).

2.6. Determination of DPPH radical scavenging capacity

The radical scavenging capacity of Hp-MeOH and Hp-EtOH extracts was measured by the DPPH assay in vitro with minor changes (Blois, 1958). Briefly, a solution of 0.135 mM DPPH radical in methanol was prepared. 100 µl of DPPH radical solution was mixed with increasing concentrations (39.06 - 5000 µg/ml) with 100 µl of plant extracts and incubated for 30 mins at room temperature in the dark. After incubation, the absorbance of the reaction mixture was measured at 517 nm. A mixture of DPPH and methanol were used as the control, a mixture of samples and methanol was used as blank, and quercetin in similar concentrations with samples was used as the positive control. Percentage (%) inhibition was calculated using *Eq. 2*. The DPPH free radical scavenging activity of the plant extracts was determined by the inhibition percentages using the quercetin standard curve (R^2 =0.9787).

$$Inhibition\ (\%) = \frac{Absorbance\ of\ the\ control - Absorbance\ of\ the\ sample}{Absorbance\ of\ the\ control} x\ 100 \qquad Eq.\ 2$$

2.7. In-vitro cell viability assay

In vitro cell viability tests of Hp-MeOH and Hp-EtOH extracts obtained by ultrasonic extraction method were examined using Human Dermal Fibroblast Cell Line (PCS-201-012) at different concentrations for 24, 48, and 72 h. The viabilities of the cells were studied with an MTT assay (Kumar et al., 2018). Briefly, cells at the 70-80% confluency were trypsinized and seeded onto a 96-well plate at the cell/well density of 1 × 10^4. The medium (DMEM complete with 10% FBS and 1% penicillin-streptomycin) was then replaced with a medium containing Hp-MeOH and Hp-EtOH extracts incubated for 24, 48, and 72 hours at 37 °C in humidified air containing 5% CO_2. After the incubation period, the MTT reagent was added to wells and incubated at 37 °C for two more hours at dark in 5% CO_2. After incubation, the MTT reagent was removed from the cells, DMSO was added to each well, and the plate was shaken at low speed for 5 minutes at room temperature. Absorbance values were measured with a microplate reader at a wavelength of 570 nm and cell viability was calculated. Untreated cells were used as the control (cells in wells with no sample other than DMEM medium) and were considered 100% viable. All studies were carried out in triplicate and in vitro test data were statistically analyzed using GraphPad Prism 9 with One-Way ANOVA and Tukey's multiple comparisons tests. The data were presented as a mean with a 95% confidence interval (CI). '*p*' values less than 0.05 were deemed statistically significant.

2.8. Preparation of Hp-MeOH and Hp-EtOH extracts loaded liposomes

Hp-MeOH and Hp-EtOH extracts-loaded liposomes were fabricated using the ethanol injection method (Khoshraftar et al., 2020). 30 ml of ethanol (96%) and 1 g of phosphatidylcholine were constantly agitated at 50 °C for 1 hour until the lecithin was completely dissolved. A rotary evaporator was then used to evaporate the solvent under reduced pressure. Plant extract (1.5 g) was combined with the sample after being dissolved in 36 ml of phosphate buffer at room temperature. Then, the prepared liposomes were subjected to ultrasonication at 40% amplitude for 5 minutes in ultrasonic and after the sample was centrifuged, PBS and liposomes were separated. The samples were refrigerated overnight, followed by centrifugation at 6000 rpm for 10 min. The samples were dried in an oven dryer at 50 °C for 24 h.

2.9. Characterization of Hp-MeOH and Hp-EtOH extracts loaded liposomes

The zeta potential of liposomes was determined (25 °C, 90° angle) by Zeta-Potential and Mobility Meter. Also, the polydispersity index (PDI) and mean size of Hp-MeOH and Hp-EtOH extracts loaded liposomes were measured using the dynamic light scattering (DLS) technique.

2.10. Entrapment efficiency (EE%) of Hp-MeOH extracts loaded liposomes

Assessment of entrapment efficiency (EE%) was carried out using the modified centrifugation method (Khoshraftar et al., 2020). Hp-MeOH and Hp-EtOH extracts were initially measured at 520 nm with UV-Vis spectrophotometry, the wavelength at which the Hp-MeOH extract has the greatest adsorption. To construct a calibration curve, absorbance versus concentration of Hp-MeOH extract at different concentrations dissolved in dH_2O was prepared. The EE (%) was calculated by measuring free Hp-MeOH and Hp-EtOH extracts in the supernatant following liposome centrifugation. The samples were centrifuged for 30 minutes at 4 °C at 4000 rpm. UV/VIS spectrophotometry a 520 nm was used to determine the concentration of free Hp-MeOH and Hp-EtOH extracts in the supernatant.

The EE% of the Hp-MeOH and Hp-EtOH extracts was calculated using *Eq. 3*:

$$EE\ (\%) = \frac{AEa}{AEb} x\ 100 \qquad Eq.\ 3$$

where AEa is the amount of extract (Hp-MeOH and Hp-EtOH) in the liposome found after centrifugation, AEb is the amount of extract (Hp-MeOH and Hp-EtOH) in liposomes found before centrifugation.

2.11. In vitro release kinetics of Hp-MeOH and Hp-EtOH extracts loaded liposomes

In vitro release kinetics of free plant extracts and plant extracts loaded liposomes were carried out utilizing the modified dialysis technique (Khoshraftar et al., 2020). The analysis was carried out in 100 ml of PBS (pH = 7.4) at 37 °C. Extracts loaded liposomes were filled in a cellulose dialysis bag (MW cut-off 12.000). After, the dialysis bag was placed in an isolated environment and mixed with the specified settings. 1 ml of the released content was withdrawn at a specified time and replaced with an equal amount of fresh PBS solution. 1 ml of the release medium was gathered and measured at 520 nm wavelength. The dialysis behavior of free plant extract mixed with PBS was examined using the same method. The free plant extract in the supernatant at each preset period was used to calculate the plant extract release rate from liposomes (*Eq. 4*).

$$In\ vitro\ release\ (\%) = \frac{Total\ amount\ of\ plant\ extract - The\ residue\ of\ plant\ extract}{Total\ amount\ of\ plant\ extract} x\ 100 \qquad Eq.\ 4$$

3. Results and discussion

3.1. Antimicrobial activity of Hp-MeOH and Hp-EtOH extracts

The antimicrobial activity of Hp-MeOH and Hp-EtOH extracts was tested against pathogenic microorganisms (Tables 1 and 2). The results show a significant concentration-dependent antimicrobial activity against a wide range of pathogenic microorganisms. Hp-MeOH extract induced a larger inhibition zone against *S. aureus* ATCC 25923, *E. faecalis* ATCC 51289, *B. subtilis* NRS 744, *S. aureus*

ATCC 6538 and *C. albicans* ATCC 10231 than other pathogens. Hp-EtOH caused a larger inhibition zone against *L. monocytogenes* ATCC 19115, *S. aureus* ATCC 25923, *P. aeruginosa* ATCC 11778, *E. faecalis* ATCC 51289, *E. coli* ATCC 35218, and *E. coli* ATCC 25922 than other pathogens. Among all pathogenic microorganisms tested, Hp-MeOH and Hp-EtOH extracts induced the highest inhibition zone against *E. faecalis* ATCC 51289 (21 mm ± 0.75) and *P. aeruginosa* ATCC 11778 (28 mm ± 0.90), respectively than the positive control amikacin (30mg/ml).

Table 1. Antimicrobial activity of Hp-MeOH extract (mg/ml)*

Test microorganisms	Inhibition zone (mm ± STD)					PC1	PC2	NC
	9.37	18.75	37.5	75	150			
L. monocytogenes ATCC 19115	10 ± 0.25	11 ± 0.25	12 ± 0.35	13 ± 0.25	15 ± 0.50	25 ± 0.80	15 ± 0.60	-
S. aureus ATCC 25923	11 ± 0.20	12 ± 0.25	13 ± 0.25	15 ± 0.33	17 ± 0.50	29 ± 0.90	12 ± 0.10	-
K. pneumoniae NRRLB 4420	-	8 ± 0.10	8 ± 0.25	9 ± 0.20	9 ± 0.25	28 ± 0.50	14 ± 0.40	-
P. aeruginosa ATCC 11778	11 ± 0.20	12 ± 0.25	14 ± 0.40	15 ± 0.33	16 ± 0.70	30 ± 0.80	15 ± 0.20	-
E. faecalis ATCC 51289	13 ± 0.40	15 ± 0.50	18 ± 0.65	20 ± 0.50	21 ± 0.75	24 ± 0.50	14 ± 0.20	-
E. coli ATCC 35218	9 ± 0.25	11 ± 0.50	10 ± 0.25	12 ± 0.15	13 ± 0.15	30 ± 0.50	13 ± 0.40	-
B. subtilis NRS 744	8 ± 0.25	10 ± 0.25	14 ± 0.50	18 ± 0.50	20 ± 0.50	30 ± 0.50	19 ± 0.70	-
S. aureus ATCC 6538	11 ± 0.10	12 ± 0.50	13 ± 0.50	15 ± 0.50	17 ± 0.50	32 ± 0.70	16 ± 0.50	-
E. coli ATCC 25922	8 ± 0.10	9 ± 0.25	11 ± 0.25	14 ± 0.35	15 ± 0.50	30 ± 0.80	16 ± 0.50	-
P. aeruginosa ATCC 27853	11 ± 0.20	12 ± 0.20	13 ± 0.50	14 ± 0.25	16 ± 0.25	21 ± 0.30	14 ± 0.30	-
S. aureus ATCC 12600	11 ± 0.20	12 ± 0.20	13 ± 0.25	15 ± 0.50	16 ± 0.25	38 ± 1.20	15 ± 0.20	-
C. albicans ATCC 10231	13 ± 0.20	14 ± 0.50	15 ± 0.50	16 ± 0.45	18 ± 0.50	30 ± 0.80	-	-

* for *C. albicans* ATCC 10231; PC_1: Fluconazole (10 mg/ml), NC: dH_2O; for other test microorganisms; PC_1: Penicillin G (10 mg/ml), PC_2: Amikacin (30 mg/ml), NC: dH_2O

Table 2. Antimicrobial activity of Hp-EtOH extract (mg/ml)*

Test microorganisms	Inhibition zone (mm ± STD)					PC1	PC2	NC
	9.37	18.75	37.5	75	150			
L. monocytogenes ATCC 19115	12 ± 0.20	19 ± 0.50	21 ± 1.00	23 ± 0.50	26 ± 0.50	25 ± 0.80	15 ± 0.60	-
S. aureus ATCC 25923	9 ± 0.00	15 ± 0.50	18 ± 0.50	20 ± 0.50	23 ± 1.00	29 ± 0.90	12 ± 0.10	-
K. pneumoniae NRRLB 4420	-	-	8 ± 0.00	9 ± 0.00	10 ± 0.30	28 ± 0.50	14 ± 0.40	-
P. aeruginosa ATCC 11778	10 ± 0.50	15 ± 0.40	17 ± 0.60	18 ± 0.30	28 ± 0.90	30 ± 0.80	15 ± 0.20	-
E. faecalis ATCC 51289	10 ± 0.30	17 ± 0.60	20 ± 0.50	23 ± 0.50	25 ± 0.50	24 ± 0.50	14 ± 0.20	-
E. coli ATCC 35218	-	12 ± 0.50	15 ± 0.50	17 ± 0.20	20 ± 0.30	30 ± 0.50	13 ± 0.40	-
B. subtilis NRS 744	8 ± 0.00	14 ± 0.20	15 ± 0.50	16 ± 0.50	18 ± 0.00	30 ± 0.50	19 ± 0.70	-
S. aureus ATCC 6538	10 ± 0.50	12 ± 0.40	14 ± 0.50	15 ± 0.00	17 ± 0.20	32 ± 0.70	16 ± 0.50	-
E. coli ATCC 25922	7 ± 0.00	10 ± 0.30	18 ± 0.70	20 ± 0.50	22 ± 0.20	30 ± 0.80	16 ± 0.50	-
P. aeruginosa ATCC 27853	10 ± 0.10	12 ± 0.80	13 ± 0.50	15 ± 0.50	17 ± 0.50	21 ± 0.30	14 ± 0.30	-
S. aureus ATCC 12600	9 ± 0.50	10 ± 0.00	12 ± 0.40	14 ± 0.20	19 ± 0.30	38 ± 1.20	15 ± 0.20	-
C. albicans ATCC 10231	10 ± 0.30	12 ± 0.20	13 ± 0.50	15 ± 0.50	16 ± 0.40	30 ± 0.80	-	-

* for *C. albicans* ATCC 10231; PC_1: Fluconazole (10 mg/ml), NC: dH_2O; for other test microorganisms; PC_1: Penicillin G (10 mg/ml), PC_2: Amikacin (30 mg/ml), NC: dH_2O

MIC values of Hp-MeOH and Hp-EtOH extracts against pathogenic microorganisms are given in Table 3. When the antimicrobial activity values of the active substances are 0.1 mg/ml or less, it is considered to have high antimicrobial activity, in the range of 0.1 < MIC ≤ 0.625 mg/ml, it shows moderate antimicrobial activity, and when the MIC value is more than 0.625 mg/ml, it is considered to have weak antimicrobial effects (Awouafack et al., 2013; Kuete, 2010). In general; Hp-MeOH extract has low antimicrobial activity on *S. aureus* ATCC 25923, *P. aeruginosa* ATCC 11778, *E. faecalis* ATCC 51289, *S. aureus* ATCC 6538, *P. aeruginosa* ATCC 27853, *S. aureus* ATCC 12600 and *C. albicans* ATCC 10231 (MIC < 5 mg/ml). Hp-EtOH extract has low antimicrobial activity on *L. monocytogenes* ATCC 19115, *S. aureus* ATCC 25923, *P. aeruginosa* ATCC 11778, *E. faecalis* ATCC 51289, *S. aureus* ATCC 6538, *P. aeruginosa* ATCC 27853, and *C. albicans* ATCC 10231 (MIC < 5mg/ml). In a study conducted by Conforti et al. (2005), *H. perforatum* methanol extract was shown to have potent antimicrobial activity on the gram-positive and negative bacteria (*S. aureus* ATCC 29213, *E. faecalis* ATCC 29212 and *E. coli* ATCC 4350) with an MIC value of 50 µg/ml. Besides, Süntar et al. (2016) determined the MIC values of *H. perforatum* ethanol extract against *S. mutans* ATCC 21752, *S. sobrinus* ATCC 6715, and *E. faecalis* ATCC 29912 as 64, 16, 32 and 32 µg/ml, respectively. Eroğlu-Özkan et al. (2019) determined the MIC values of *H. perforatum* methanol extract against *S. aureus* ATCC 6538 and *S. epidermidis* ATCC 12228 as 4.8 and 156 µg/ml, respectively, while the same extract had no antimicrobial effect on *E. coli* ATCC 8739, *K. pneumoniae* ATCC 4352, *P. aeruginosa* ATCC 1539, and *C. albicans* ATCC 10231.

Table 3. MIC values of Hp-MeOH and Hp-EtOH extracts

Microorganisms	MIC values (mg/ml)	
	Hp-MeOH	Hp-EtOH
L. monocytogenes ATCC 19115	9.37	2.34
S. aureus ATCC 25923	4.68	4.68
K. pneumoniae NRRLB 4420	37.50	37.50
P. aeruginosa ATCC 11778	4.68	4.68
E. faecalis ATCC 51289	2.34	4.68
E. coli ATCC 35218	37.50	18.75
B. subtilis NRS 744	18.75	9.37
S. aureus ATCC 6538	4.68	4.68
E. coli ATCC 25922	37.50	18.75
P. aeruginosa ATCC 27853	4.68	4.68
S. aureus ATCC 12600	4.68	9.37
C. albicans ATCC 10231	4.68	2.34

3.2. In vitro TAS, TOS, and OSI values of Hp-MeOH and Hp-EtOH extracts

The antioxidant power of plants or plant extracts is due to their ability to eliminate or transform free radicals. It can be assumed that the higher the antioxidant capacity of a plant or plant extract, the higher its therapeutic potential (Michalak, 2022; Teixeira et al., 2017). TAS, TOS, and OSI values of Hp-MeOH and Hp-EtOH extracts are given in Table 4. It was determined that the Hp-MeOH extract had high total antioxidant status (22.352 ± 0.002 mmol/l), and low total oxidant status (4.753 ± 0.001 µmol/l). In addition, the oxidative stress index (OSI), which is important in evaluating the oxidant/antioxidant ratio of Hp-MeOH extract, was observed to be very low (0.21). Hp-EtOH extract had a high total antioxidant status value (18.804 ± 0.150 mmol/l) and a low total oxidant status value

(4.523 ± 0.120 µmol/l). OSI value of Hp-EtOH was found to be 0.24. In many studies on a plant extract, the TAS value of *Mentha* sp. was observed as 3.628 mmol/l, TOS value was 4.046 µmol/l (Sevindik et al., 2017). The TAS and TOS values of *Salvia multicaulis* Vahl. were 6.434 mmol/l and 22.441 µmol/l, respectively (Pehlivan & Sevindik, 2018). Also, TAS, TOS, and OSI values of *Gundellia tournefortii* L. have been reported as 6.831 mmol/l, 3.712 ± 0.584 µmol/l, and 0.054 ± 0.463 µmol/l, respectively (Saraç et al., 2019). Compared to these studies, TAS values of Hp-MeOH and Hp-EtOH extracts were found higher than these plants. Hp-MeOH extract can be stated as a good source of antioxidants since its extracts have a high antioxidant capacity and low OSI. Hp-MeOH and Hp-EtOH extracts can be expressed as good source of antioxidants since it has a high antioxidant capacity and OSI. Therefore, it can be evaluated in eliminating the negative effects caused by free radicals.

Table 4. TAS, TOS, OSI and TFC values of Hp-MeOH and Hp-EtOH extracts

	Hp-MeOH	Hp-EtOH
TAS (mmol Trolox /l)	22.352 ± 0.002	18.804 ± 0.15
TOS (µmol H_2O_2 /l)	4.753 ± 0.001	4.523 ± 0.12
OSI	0.21	0.24
TFC (mg GAE/g)	38.00 ± 0.02	10.52 ± 0.028

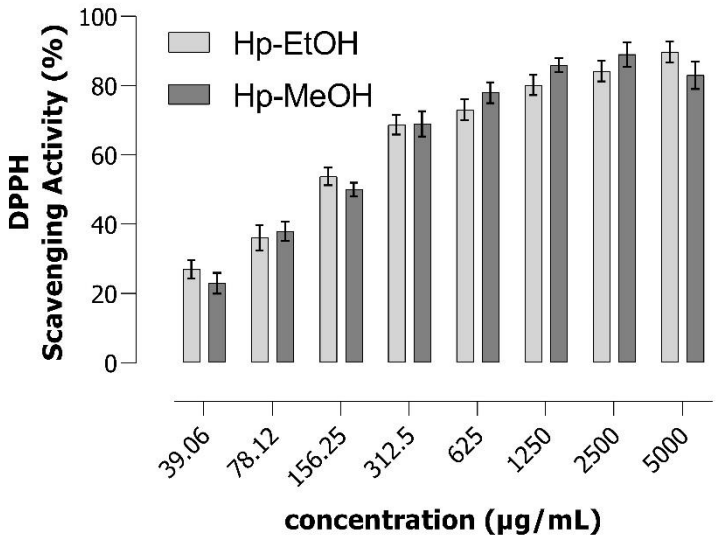

Figure 1. DPPH scavenging activity of Hp-EtOH and Hp-MeOH extracts

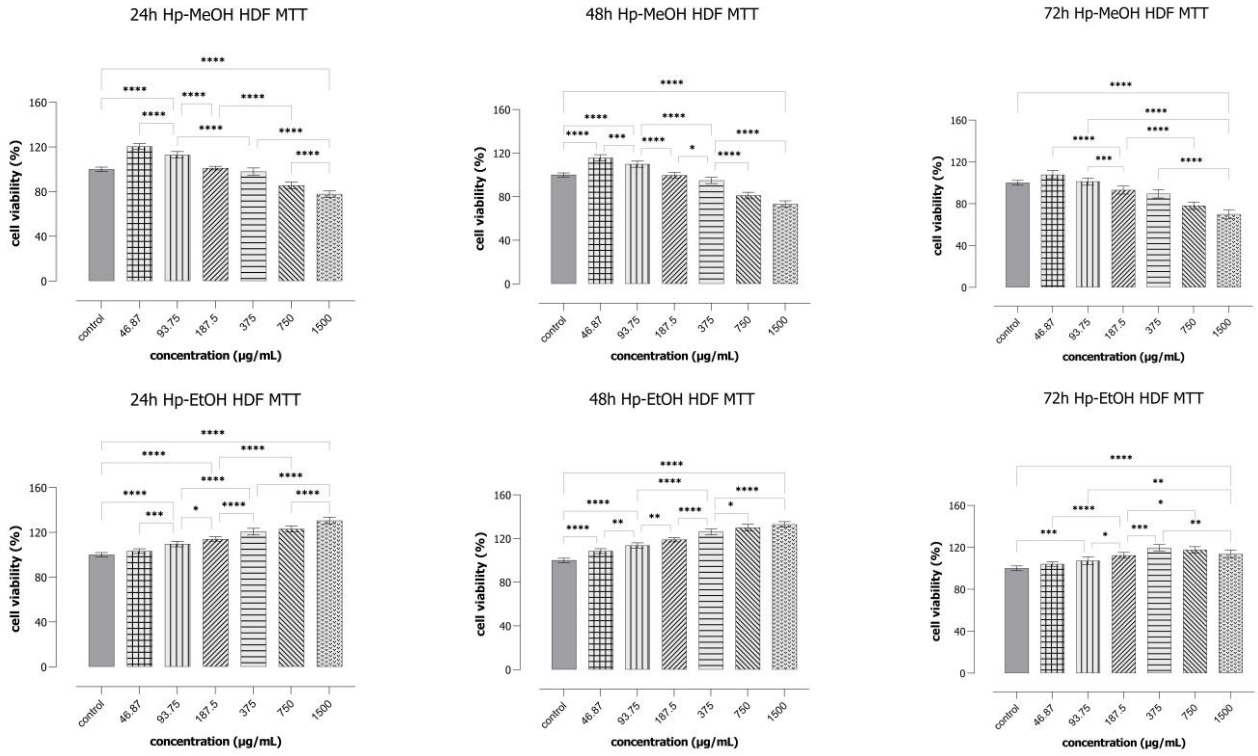

Figure 2. Cell viability (%) of Hp-MeOH and Hp-EtOH extracts (*p* value below 0.05 were considered as statistically significant)

3.3. Total phenolic content of Hp-MeOH and Hp-EtOH extracts

Phenolic compounds are important bioactive components with redox properties responsible for antioxidant activity. Hydroxyl groups in plant extracts help to scavenge free radicals (Soobrattee et al., 2005). The amount of phenolic compounds varies depending on the extraction procedure, solvents, and growing conditions of the plant and plant parts. Phenolic compounds are more soluble in polar organic solvents due to the presence of a hydroxyl group (Isidore et al., 2021). The phenolic content in the Hp-MeOH and Hp-EtOH extracts were measured using the Folin-Ciocalteu reagent and was determined as 38.00 mg GAE/g and 10.52 mg GAE/g, respectively. Comparing the studies in the literature, Sekeroglu et al. (2017) reported the total phenol content (TPC) of the powdered stem, leaves, and flower of *H. perforatum* ethanol and water extract, in which the ethanol extracts from the leaf parts of the *H. perforatum* showed the highest total phenolic content (182.93 mg GAE/g). In another study, the total polyphenolic content of fresh ethanolic extracts of *H. perforatum* was found to be between 9.33 - 50.98 mg GAE/g (Chimshirova et al., 2019). In a study by Brankiewicz et al. (2023), total phenolic content of *H. perforatum* extracts of different origins (both commercially available and laboratory-prepared from wild grown) was evaluated. Both, commercially available and laboratory-prepared *H. perforatum* ethanol extracts showed approximately 8 - 10% of phenolic content in the dry extract.

3.4. DPPH radical scavenging capacity of Hp-MeOH and Hp-EtOH extracts

There are various methods to evaluate the antioxidant capacity of natural plant extracts. The DPPH assays are widely used by many researchers for the rapid evaluation of antioxidant capacity (Pisoschi et al., 2016). The concentration-dependent DPPH scavenging capacity of Hp-MeOH and Hp-EtOH extracts is given in Figure 1. Hp-MeOH and Hp-EtOH extracts had a scavenging capacity of DPPH radicals between 23 - 89% and 27 - 90%, respectively in the studied concentration range (39.06 - 5000 µg/ml). In the study conducted by Mir et al. (2019), the capacity of *H. perforatum* methanolic extract to scavenge DPPH radicals at concentrations of 100, 200, and 300 µg/ml was determined as 35, 55 and 70%, respectively, and ascorbic acid, used as a positive control, inhibited radicals by 68% at a concentration of 300 µg/ml. Moreover, Yilmaz et al. (2021) determined that the DPPH free radical scavenging activity of *H. perforatum* dH_2O extract at 100 µg/ml was 89.3% and gallic acid and trolox used as standards inhibited DPPH radicals by 95.3% and 96.5%, respectively. It is difficult to directly compare the results of the present study with previous studies due to the use of different standards (quercetin equivalent or trolox equivalent, etc.) for the expression of DPPH scavenging capacity. On the other hand, the type of solvent and extraction conditions affect the results.

3.5. Cell viability of Hp-MeOH and Hp-EtOH extracts

The results of cell viability of HDFs upon treatment with the Hp-MeOH and Hp-EtOH extracts are given in Figure 2. When treated with 46.87, 93.75, 187.5, 750, and 1500 µg/ml of Hp-MeOH extract for 24-h, the cell viability of HDF was decreased by 120.58%, 112.99%, 101.12%, 97,95%, 85.58%, and 77.79%, respectively. A similar decrease was also evident by 115.76%, 109.7%, 99.69%, 94.86%, 81.08%, and 73.42% for each concentration at the end of 48th h. Cell viability in HDF cultures for the last time point 72nd h experiment was recorded as 107.83%, 101.24%, 93.11%, 89.58%, 78.15%, and 70.06% after 46.87, 93.75, 187.5, 750, and 1500 µg/ml of Hp-MeOH extract, respectively. In general, the viability of fibroblast cells decreased compared to the control due to the increase in the concentration of Hp-MeOH extract for 24, 48, and 72 hours. At 24th h, cell viability was higher than the control group at concentrations lower than 375 µg/ml. At 48th h, a similar trend was observed. At 72nd h, cell viability at concentrations lower than 187.5 µg/ml was higher than in the control group. Furthermore, % cell viability values at 72nd h were lower than at 24 and 48 hours due to both the decrease in nutrients to be used by the cells and the accumulation of toxic substances in the environment as a result of the metabolic activities of the cells. Dermal fibroblast cell viability of Hp-EtOH extract for 24th, 48th, and 72nd h was enhanced with increasing concentration. Hp-EtOH extract showed higher cell viability than the control group at all three-time points at all concentrations of the extract. Thus, it was determined that Hp-EtOH extract increased fibroblast cell viability and had no cytotoxic effect. The cytotoxic effect of methanolic extract of *H. olympicum* (HOM) (0.5, 1, 1.5, and 2 mg/ml) was evaluated in HDF cells for 24, 48, and 72 hours. It was reported that HOM extract can be safely used up to 2 mg/ml for HDFs without causing any cytotoxicity during the 24, 48, and 72 h of treatment periods. It was also observed that 0.5 and 1.5 mg/ml HOM treatment increased the cell viability of HDFs by 35% and 108%, respectively (Kurt-Celep et al., 2020). In a study, phloroglucinol-enriched fractions (PEF) of *Hypericum* species native to southern Brazil were evaluated for their effect on the proliferation of HaCaT cells. The *H. carinatum* and *H. polyanthemum* PEF demonstrated better results with an increase in cell proliferation (138.7% and 120.6%, respectively) (Bridi et al., 2017).

Table 5. Particle size, PDI value, and ζ-potential of Hp-MeOH and Hp-EtOH extracts-loaded liposomes

Plant extract-loaded liposomes	Average particle size (nm)	PDI value	ζ-potential (mV)
Hp-MeOH	~ 64 nm	0.59	-27.9
Hp-EtOH	~ 15 nm	0.65	-20.0

3.6. Characterization of Hp-MeOH and Hp-EtOH extracts loaded liposomes

Liposomes were used as control delivery systems for the methanol and ethanol extract obtained from the areal parts of *H. perforatum*. The mean diameter and PDI value of the liposomes were measured using the dynamic laser light scattering technique (Table 5). Extract-loaded liposomes were prepared and characterized. The mean diameter of Hp-MeOH and Hp-EtOH extracts loaded liposomes were measured at ~ 64 nm and ~ 15 nm; the PDI values of extracts were found as 0.59 and 0.65, respectively. Hp-MeOH and Hp-EtOH extracts-loaded liposomes were not homogeneously dispersed (polydispersity index > 0.50). The zeta potential is a useful tool for determining the distribution stability of liposomes. Characterizing the surface charge of the particles, provides information about the repulsive forces between them, allowing the stability of dispersions to be predicted. As a general rule, zeta potential values < -30 mV and > 30 mV form stable systems as high surface charges induce repulsion and prevent aggregation. Liposomes with a negative surface charge are beneficial for effective dermal drug delivery (Gharib et al., 2017; Gillet et al., 2011; Rafiee et al., 2017). Hp-MeOH and Hp-EtOH extracts loaded liposomes had highly negative zeta potential values of -27.9 mV and -20.0 mV, respectively (Table 5). In a study, phospholipid vesicles loaded with *H. scruglii* extract were developed and characterized. The *H. scruglii* loaded phospholipid vesicles disclosed mean diameter ranged from 120 to 160 nm, they were homogeneously dispersed (polydispersity index ≤ 0.30), and their zeta potential was highly negative (~ -45 mV). It has been reported to show suitable physicochemical properties for dermal delivery (Allaw et al., 2020). In a study by Pradeep et al. (2019),

liposome structures loaded with *H. hookerianum* extract were developed, and it was reported that highly stable liposome structures were obtained thanks to the properties of the liposomal formulation obtained with a zeta potential of -29.4 mV and an average particle size of 82.33 ± 0.41nm.

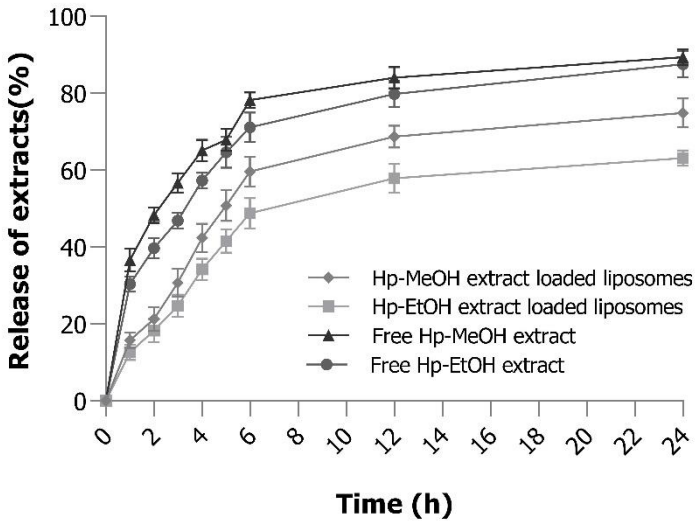

Figure 3. Release profile of Hp-MeOH and Hp-EtOH extracts from liposomes

3.7. Entrapment efficiency (EE%) of Hp-MeOH and Hp-EtOH extracts loaded liposomes

The entrapment efficiency of liposomes loaded Hp-MeOH and Hp-EtOH extracts was determined approximately as 82.6 ± 3.63% and 89.8 ± 2.74%, respectively. The amount of extract incorporated into *H. scruglii*-loaded phospholipid vesicles was found to have a very high entrapment efficiency of ~ 89% (Allaw et al., 2020). In this context, it can be said that liposomes loaded with Hp-MeOH and Hp-EtOH extracts have a high entrapment efficiency.

3.8. Release profile of Hp-MeOH and Hp-EtOH extracts loaded liposomes

During 24th h, the amount of extracts released by the liposomes and the release of extracts in the free state were evaluated and the release profile is given in Figure 3. When the release profile is evaluated, it is seen that extracts-loaded liposomes have a slower and more controlled release profile compared to free extracts. At the end of the first 6th h, 78.20% and 71.10% of the free Hp-MeOH and Hp-EtOH extracts were released, respectively while 59.6% and 48.8% of the Hp-MeOH and Hp-EtOH extracts were released from the liposome structures. At the end of 24th h, a very large amount of free Hp-MeOH and Hp-EtOH extracts were released (89.40% and 87.50%), while 74.9% and 63.1% of the Hp-MeOH and Hp-EtOH extracts loaded in liposome structures were released. When the release of phospholipid vesicles loaded with *H. scruglii* was evaluated, it was reported that a burst release reaching 20% of the initial amount was observed at the 2nd h; then, it became almost constant until the 24th h, reaching ~ 35% (Allaw et al., 2020).

4. Conclusions

The results obtained in this study revealed that *H. perforatum* methanol and ethanol extract encapsulated in liposomes is highly stable and also have the combined advantages of effective antioxidant capacity and maintenance of cell viability on dermal fibroblast cells. The results obtained indicate that liposomal plant extracts can serve as a highly useful, controlled release, and stable release vehicle for novel antioxidant components. Additional information from this study supports the use of *H. perforatum* methanol and ethanol extract as an aid in the treatment of skin diseases. In light of this study, the pharmacokinetic properties of this lipid carrier system loaded with *H. perforatum* extracts can be improved or its therapeutic effects can be increased by combining it with different plant extracts. In this way, it can be incorporated into pharmaceutical formulations for the treatment of many diseases.

Acknowledgments

None.

Conflict of interest

The authors confirm that there are no known conflicts of interest.

Statement of ethics

In this study, no method requiring the permission of the "Ethics Committee" was used.

Availability of data and materials

All data generated or analyzed during this study are included in this published article.

Funding

This study was supported by the scientific research council of Afyonkarahisar Health Science University, Project No. 19.TEMATİK.005.

CRediT authorship contribution statement

Özlem Erdal Altıntaş: Conceptualization, Investigation, Data curation, Formal analysis, Methodology, Writing, Review and Editing
Sevim Feyza Erdoğmuş: Resources, Formal analysis, Methodology, Investigation, Review and Editing

ORCID Numbers of the Authors

Ö. Erdal Altıntaş: 0000-0003-4680-1738
S. F. Erdoğmuş: 0000-0002-4319-7558

Supplementary File

None.

Publisher's Note

All claims expressed in this article are solely those of the authors and do not necessarily represent those of their affiliated organizations, or those of the publisher, the editors and the reviewers. Any product that may be evaluated in this article, or claim that may be made by its manufacturer, is not guaranteed or endorsed by the publisher.

This is an open-access article distributed under the terms of the Creative Commons Attribution 4.0 International License (CC BY). The use, distribution or reproduction in other forums is permitted, provided the original author(s) and the copyright owner(s) are credited and that the original publication in this journal is cited, in accordance with accepted academic practice. No use, distribution or reproduction is permitted which does not comply with these terms.

References

Ali, M., Abdel Motaal, A., Ahmed, M. A., Alsayari, A., & El-Gazayerly, O. N. (2018). An in vivo study of *Hypericum perforatum* in a niosomal topical drug delivery system. *Drug Delivery, 25*(1), 417-425.

Allaw, M., Manconi, M., Aroffu, M., Marongiu, F., Porceddu, M., Bacchetta, G., Usach, I., Rached, R. A., Rajha, H. N., *et al.* (2020). Extraction, characterization and incorporation of *Hypericum scruglii* extract in ad hoc formulated phospholipid vesicles designed for the treatment of skin diseases connected with oxidative stress. *Pharmaceutics, 12*(11), 1010.

Awouafack, M. D., McGaw, L. J., Gottfried, S., Mbouangouere, R., Tane, P., Spiteller, M., & Eloff, J. N. (2013). Antimicrobial activity and cytotoxicity of the ethanol extract, fractions and eight compounds isolated from *Eriosema robustum* (Fabaceae). *BMC Complementary and Alternative Medicine, 13*, 289.

Blois, M. S. (1958). Antioxidant determinations by the use of a stable free radical. *Nature, 181*, 1199-1200.

Brankiewicz, A., Trzos, S., Mrożek, M., Opydo, M., Szostak, E., Dziurka, M., Tuleja, M., Łoboda, A., & Pocheć, E. (2023). Cytotoxic and Antioxidant Activity of *Hypericum perforatum* L. Extracts against Human Melanoma Cells from Different Stages of Cancer Progression, Cultured under Normoxia and Hypoxia. *Molecules, 28*(3), 1509.

Bridi, H., Beckenkamp, A., Ccana-Ccapatinta, G. V., de Loreto Bordignon, S. A., Buffon, A., & von Poser, G. L. (2017). Characterization of phloroglucinol-enriched fractions of Brazilian *Hypericum* species and evaluation of their effect on human keratinocytes proliferation. *Phytotherapy Research, 31*(1), 62-68.

Chimshirova, R., Karsheva, M., Diankov, S., & Hinkov, I. (2019). Extraction of valuable compounds from Bulgarian St. John's wort (*Hypericum perforatum* L.). antioxidant capacity and total polyphenolic content. *Journal of Chemical Technology & Metallurgy, 54*(5), 952-961.

CLSI, C. a. L. S. I. (2002). *Reference method for broth dilution antifungal susceptibility testing of yeasts; approved standard. 2nd ed. Document M27-A2*: Wayne, PA: Clinical and Laboratory.

CLSI, C. a. L. S. I. (2012). *Performance standards for antimicrobial standards institute susceptibility testing, 26 th ed. CLSI supplement M100S*: Wayne, PA: Clinical and Laboratory.

CLSI, C. a. L. S. I. (2016). *Performance standards for antimicrobial standards institute susceptibility testing, 26 th ed. CLSI supplement M100S*: Wayne, PA: Clinical and Laboratory.

Conforti, F., Statti, G., Tundis, R., Bianchi, A., Agrimonti, C., Sacchetti, G., Andreotti, E., Menichini, F., & Poli, F. (2005). Comparative chemical composition and variability of biological activity of methanolic extracts from *Hypericum perforatum* L. *Natural Product Research, 19*(3), 295-303.

Dua, J., Rana, A., & Bhandari, A. (2012). Liposome: methods of preparation and applications. *International Journal of Pharmaceutical Studies and Research, 3*(2), 14-20.

Erel, O. (2004). A novel automated method to measure total antioxidant response against potent free radical reactions. *Clinical Biochemistry, 37*(2), 112-119.

Erel, O. (2005). A new automated colorimetric method for measuring total oxidant status. *Clinical Biochemistry, 38*(12), 1103-1111.

Eroğlu-Özkan, E., Çelik, B. Ö., & Afife, M. (2019). Antimicrobial activities of five endemic *Hypericum* species from Anatolia compared with *Hypericum perforatum*. *Journal of Research in Pharmacy, 23*(1), 114-119.

Gamez-Meza, N., Noriega-Rodriguez, J., Medina-Juarez, L., Ortega-Garcia, J., Cazarez-Casanova, R., & Angulo-Guerrero, O. (1999). Antioxidant activity in soybean oil of extracts from Thompson grape bagasse. *Journal of the American Oil Chemists' Society, 76*, 1445-1447.

Gharib, R., Auezova, L., Charcosset, C., & Greige-Gerges, H. (2017). Drug-in-cyclodextrin-in-liposomes as a carrier system for volatile essential oil components: Application to anethole. *Food Chemistry, 218*, 365-371.

Gillet, A., Compère, P., Lecomte, F., Hubert, P., Ducat, E., Evrard, B., & Piel, G. (2011). Liposome surface charge influence on skin penetration behaviour. *International Journal of Pharmaceutics, 411*(1-2), 223-231.

Isidore, E., Karim, H., & Ioannou, I. (2021). Extraction of phenolic compounds and terpenes from *Cannabis sativa* L. by-products: From conventional to intensified processes. *Antioxidants, 10*(6), 942.

Khoshraftar, Z., Shamel, A., Safekordi, A. A., Ardjmand, M., & Zaefizadeh, M. (2020). Natural nanopesticides with origin of *Plantago major* seeds extract for *Tribolium castaneum* control. *Journal of Nanostructure in Chemistry, 10*, 255-264.

Kuete, V. (2010). Potential of Cameroonian plants and derived products against microbial infections: a review. *Planta Medica, 76*(14), 1479-1491.

Kumar, P., Nagarajan, A., & Uchil, P. D. (2018). Analysis of cell viability by the MTT assay. *Cold Spring Harbor Laboratory Press D, 2018*(15), 464-471.

Kurt-Celep, İ., Celep, E., Akyüz, S., İnan, Y., Barak, T. H., Akaydın, G., Telci, D., & Yesilada, E. (2020). *Hypericum olympicum* L. recovers DNA damage and prevents MMP–9 activation induced by UVB in human dermal fibroblasts. *Journal of Ethnopharmacology, 246*, 112202.

Latiff, N. A., Ong, P. Y., Abd Rashid, S. N. A., Abdullah, L. C., Mohd Amin, N. A., & Fauzi, N. A. M. (2021). Enhancing recovery of bioactive compounds from *Cosmos caudatus* leaves via ultrasonic extraction. *Scientific Reports, 11*, 17297.

Luiz, H., Oliveira Pinho, J., & Gaspar, M. M. (2023). Advancing Medicine with Lipid-Based Nanosystems—The Successful Case of Liposomes. *Biomedicines, 11*(2), 435.

Maja, L., Željko, K., & Mateja, P. (2020). Sustainable technologies for liposome preparation. *The Journal of Supercritical Fluids, 165*, 104984.

Michalak, M. (2022). Plant-derived antioxidants: Significance in skin health and the ageing process. *International Journal of Molecular Sciences, 23*(2), 585.

Mir, M. Y., Kamili, A. N., Hassan, Q. P., Rafi, S., Parray, J. A., & Jan, S. (2019). In vitro regeneration and free radical scavenging assay of *Hypericum perforatum* L. *National Academy Science Letters, 42*, 161-167.

Naziris, N., & Demetzos, C. (2022). Lipid nanoparticles as platforms for theranostic purposes: recent advances in the field. *Journal of Nanotheranostics, 3*(2), 86-101.

Nobakht, S. Z., Akaberi, M., Mohammadpour, A., Moghadam, A. T., & Emami, A. (2022). *Hypericum perforatum*: Traditional uses, clinical trials, and drug interactions. *Iranian Journal of Basic Medical Sciences, 25*(9), 1045-1058.

Parham, S., Kharazi, A. Z., Bakhsheshi-Rad, H. R., Nur, H., Ismail, A. F., Sharif, S., RamaKrishna, S., & Berto, F. (2020). Antioxidant, antimicrobial and antiviral properties of herbal materials. *Antioxidants, 9*(12), 1309.

Pehlivan, M., & Sevindik, M. (2018). Antioxidant and antimicrobial activities of *Salvia multicaulis*. *Turkish Journal of Agriculture-Food Science and Technology, 6*(5), 628-631.

Pisoschi, A. M., Pop, A., Cimpeanu, C., & Predoi, G. (2016). Antioxidant capacity determination in plants and plant-derived products: A review. *Oxidative Medicine and Cellular Longevity, 2016*, 9130976.

Pradeep, P., Manisha, S., Monica Amala Nayaki, J., Sivaraman, D., Selvaraj, R., & Seeni, S. (2019). Potential antioxidant and anti-inflammatory action of *Hypericum hookerianum* extracts in a liposome system evaluated with zebrafish embryos. *Journal of Microencapsulation, 36*(6), 513-522.

Rafiee, Z., Barzegar, M., Sahari, M. A., & Maherani, B. (2017). Nanoliposomal carriers for improvement the bioavailability of high–valued phenolic compounds of pistachio green hull extract. *Food Chemistry, 220*, 115-122.

Rahman, H. S., Othman, H. H., Hammadi, N. I., Yeap, S. K., Amin, K. M., Abdul Samad, N., & Alitheen, N. B. (2020). Novel drug delivery systems for loading of natural plant extracts and their biomedical applications. *International Journal of Nanomedicine, 15*, 2439-2483.

Saraç, H., Demirbaş, A., Daştan, S. D., Ataş, M., Çevik, Ö., & Eruygur, N. (2019). Evaluation of nutrients and biological activities of Kenger (*Gundellia tournefortii* L.) seeds cultivated in Sivas province. *Turkish Journal of Agriculture-Food Science and Technology, 7*(sp2), 52-58.

Sekeroglu, N., Urlu, E., Kulak, M., Gezici, S., & Dang, R. (2017). Variation in total polyphenolic contents, DNA protective potential and antioxidant capacity from aqueous and ethanol extracts in different plant parts of *Hypericum perforatum* L. *Indian Journal of Pharmaceutical Education and Research, 51*(2S), S1-S7.

Sevindik, M., Akgul, H., Pehlivan, M., & Selamoglu, Z. (2017). Determination of therapeutic potential of *Mentha longifolia* ssp. *longifolia*. *Fresenius Environmental Bulletin, 26*(7), 4757-4763.

Sharma, A., Sharma, S., Kumar, A., Kumar, V., & Sharma, A. K. (2022). Plant secondary metabolites: An introduction of their chemistry and biological significance with physicochemical aspect. In A. K. Sharma & A. Sharma (Eds.), *Plant Secondary*

Metabolites: Physico-Chemical Properties and Therapeutic Applications (pp. 1-45): Springer, Singapore.

Soobrattee, M. A., Neergheen, V. S., Luximon-Ramma, A., Aruoma, O. I., & Bahorun, T. (2005). Phenolics as potential antioxidant therapeutic agents: mechanism and actions. *Mutation Research/Fundamental and Molecular Mechanisms of Mutagenesis, 579*(1-2), 200-213.

Süntar, I., Oyardı, O., Akkol, E. K., & Ozçelik, B. (2016). Antimicrobial effect of the extracts from *Hypericum perforatum* against oral bacteria and biofilm formation. *Pharmaceutical Biology, 54*(6), 1065-1070.

Teixeira, T., Vale, R., Almeida, R., Ferreira, T., & Guimarães, L. (2017). Antioxidant potential and its correlation with the contents of phenolic compounds and flavonoids of methanolic extracts from different medicinal plants. *Revista Virtual de Química, 9*(4), 1546-1559.

Tripathy, S., & Srivastav, P. P. (2023). Encapsulation of *Centella asiatica* leaf extract in liposome: Study on structural stability, degradation kinetics and fate of bioactive compounds during storage. *Food Chemistry Advances, 2*, 100202.

Yilmaz, N. A., Yavaser, R., & Karagozler, A. A. (2021). *Hypericum perforatum* L.: A Potent antioxidant source for the treatment of oxidized dentin: An experimental in vitro study. *Journal of Advanced Oral Research, 12*(1), 57-65.

Int. J. Plant Bas. Pharm. (2023) 3(1), 95-103

INTERNATIONAL JOURNAL OF PLANT BASED PHARMACEUTICALS

https://ijpbp.com

RESEARCH ARTICLE

OPEN ACCESS

Essential oil and extracts from *Lavandula angustifolia* Mill. cultivated in Bosnia and Herzegovina: Antioxidant activity and acetylcholinesterase inhibition

Stanislava Talić[a]*, Ilijana Odak[a], Marijana Marković Boras[b], Ante Smoljan[a], Anita Martinović Bevanda[a]

[a] *University of Mostar, Faculty of Science and Education, Department of Chemistry, 88 000 Mostar, Bosnia and Herzegovina*
[b] *University Clinical Hospital Mostar, Department of Laboratory Medicine, 88 000 Mostar, Bosnia and Herzegovina*

ARTICLE INFO

Article History:

Received: 03 February 2023
Revised: 06 April 2023
Accepted: 09 April 2023
Available online: 11 April 2023

Edited by: B. Tepe

Keywords:

Lavandula angustifolia
Essential oil
GC-FID/MS
Antioxidant activity
Acetylcholinesterase inhibition

ABSTRACT

Lavender (*Lavandula angustifolia* Mill.) is a perennial, aromatic, medicinal, and decorative plant widespread in the Mediterranean. Due to the high content of essential oil and numerous beneficial properties, it is an extremely valued plant species. In Bosnia and Herzegovina, lavender is cultivated mainly for the needs of the cosmetic and pharmaceutical industries. In this research, the antioxidant activity and acetylcholinesterase inhibition of essential oil (EO) and extracts isolated from lavender were evaluated. *L. angustifolia* EO was isolated using whole plant material in the flowering period by steam distillation and analyzed by gas chromatography (GC) with flame-ionization (FID) and mass spectrometric (MS) detection. Extracts were prepared by ultrasonic extraction in solvents of different polarities. Total phenolic content in extracts was determined using Folin–Ciocalteu reagent. The antioxidant activity of EO and extracts was examined by two methods, 2,2-diphenyl-1-picrylhydrazil (DPPH) radical scavenging activities and ferric reducing/antioxidant power (FRAP), while the acetylcholinesterase (AChE) inhibitory potential was determined using modified Ellman's method. The EO was high in content of linalool (27.72%) and linalyl acetate (22.82%), followed by α-pinene (9.82%), lavandulol acetate (7.32%), *trans*-caryophyllene (5.70%), and others. In total, 24 components were identified. Total phenol content was highest in water and ethanol extracts (45.3 and 14.40 mg gallic acid equivalent (GAE)/g dry extract). Polar extracts indicate good antioxidant power according to both methods, while EO can be considered as good inhibitor of AChE.

1. Introduction

Lavender, *Lavandula angustifolia* Mill. is an aromatic and medicinal perennial semi-shrub from the Lamiaceae family. The flowers are violet-blue, with an intense aromatic smell, and rich in essential oils (Costea et al., 2019). *L. angustifolia* is indigenous to the mountainous regions of the Mediterranean that are widely cultivated throughout the world. France and Bulgaria are the leading European countries in lavender production (Crișan et al., 2023; Giray, 2018). Since 2000, many lavender plantations have been established in Croatia, Italy, Greece, and the Mediterranean basin in general (Blažeković et al., 2010; Giannoulis et al., 2020; Pistelli et al., 2017). Due to the growing interest in the world market for this plant, plantation cultivation of *L. angustifolia* on small family farms in Bosnia and Herzegovina has become more common in recent years. Lavender is mostly cultivated for the production of essential oil.

Reviewed by:
Sengul Uysal: Selcuk University, Konya, Türkiye
Sidney Augusto Vieira Filho: Universidade Federal de Ouro Preto, Ouro Preto, Brazil

* Corresponding author(s):
E-mail address: stanislava.talic@fpmoz.sum.ba (S. Talić)
e-ISSN: 2791-7509
doi: https://doi.org/10.29228/ijpbp.21

Please cite this article as: Talić, S., Odak, I., Marković Boras, M., Smoljan, A., & Martinović Bevanda, A. (2023). Essential oil and extracts from *Lavandula angustifolia* Mill. cultivated in Bosnia and Herzegovina: Antioxidant activity and acetylcholinesterase inhibition. *International Journal of Plant Based Pharmaceuticals*, *3*(1), 95-103, https://doi.org/10.29228/ijpbp.21.

Commercial lavender essential oil is produced mainly by steam distillation and to a lesser extent by solvent extraction, microwave extraction, supercritical extraction, and hydro-diffusion methods (Kirimer et al., 2017). Lavender essential oil (EO) and extracts show outstanding aroma properties with a pleasant floral note (Guo & Wang, 2020). The lavender essential oil has a long tradition of application in various human activities, such as aromatherapy, traditional medicine, pharmacy, cosmetics, perfume industry, and insecticide industry (Wells et al., 2018). The composition and proportion of individual components in the essential oil significantly depend on the geographical origin, harvest time, and post-harvest processing of lavender. However, most authors listed linalool, linalyl acetate, caryophyllene, and lavandulyl acetate, as the main components of the essential oil (Da Porto et al., 2009; Kirimer et al., 2017; Smigielski et al., 2009; Verma et al., 2010).

L. angustifolia also accumulates phenolic compounds, which contribute to the bioactivity of lavender and its beneficial effect. Positive correlations were observed between the content of total phenols and antioxidant activity. The most present phenolic compounds reported in lavender include gallic acid, rosmarinic acid, caffeic acid, coumaric acid, and other polyphenols (Gallego et al., 2013; Radulescu et al., 2017; Spiridon et al., 2011).

Various studies reported that Lamiaceae species and their phytochemical substances have antioxidant and AChE inhibitory activity and thus could be beneficial in the prevention and treatment of health disorders such as Alzheimer's disease (Da Porto et al., 2009; Odak et al., 2015; Vladimir-Knežević et al., 2014). To the best of our knowledge, *L. angustifolia* phytochemical substances from mountain areas of Bosnia and Herzegovina have not been investigated yet. Hence, this study aimed to determine the chemical composition of the essential oil of *L. angustifolia* from Bosnia and Herzegovina, and examine the antioxidant properties of essential oil and extracts and their inhibitory effects on AChE.

2. Materials and methods

2.1. Chemicals

Acetone, ethyl acetate, ethanol, chloroform, *n*-hexane, acetylcholinesterase (AChE) from *Electrophorus electricus* (electric eel, Type VI-S, lyophilized powder, 200-1.000 units/mg protein), acetylthiocholine iodide (ATChI), galanthamine hydrobromide, 2.2'-diphenyl-1-picrylhydrazyl (DPPH), butylated hydroxytoluene (BHT), 2,4,6-tripyridyl-s-triazine (TPTZ), Folin-Ciocalteu reagent, gallic acid, TRIS-HCl buffer, trizma base, and *n*-pentane were purchased from Sigma-Aldrich (St. Louis, MO, USA). 5,5'-dithio-bis[2-nitrobenzoic acid] (DTNB) was purchased from Zwijndrecht (Belgium). Sodium acetate, acetic acid, hydrochloric acid, iron (III) chloride, and sodium sulfate were purchased from Merck (Germany). All chemicals were of analytical grade purity.

2.2. Plant material

The *L. angustifolia* was harvested in the flowering period at a local plantation (M.T., Goranci, Mostar, Bosnia and Herzegovina; altitude 700 m, 43°25'48.4"N, 17°42'43.2"E) in June 2020. The plant material was identified by a professor of Botany Ph.D. Anđelka Lasić (Department of Biology, Faculty of Science and Education, University of Mostar) and duplicate samples were preserved in the herbarium of the department with number FPMOZ-SB-4-2020.

L. angustifolia essential oil was extracted by steam distillation of whole plant material, for 2 h in a distillery plant for medicinal herbs.

L. angustifolia extracts were prepared using ultrasonic extraction. Dry ground plant material (5 g) and solvent (100 ml) were mixed and submitted to ultrasonic extraction, 35 kHz at 30 °C for 60 min. Solvents of different polarities (water, acetone, ethyl acetate, ethanol, chloroform, and *n*-hexane) were applied. The extracts were filtered and evaporated under reduced pressure to dryness. The experiments were performed in triplicate. All dry extracts were dissolved in TRIS buffer (1; 2.5; 5; 7 and 10 mg/ml) for subsequent analysis.

2.3. Determination of total polyphenols

The total phenolic content in *L. angustifolia* extracts was determined by the conventional spectrophotometric method with the Folin-Ciocalteu reagent (Hernandez et al., 2010). The procedure was described in our previous study (Talić et al., 2019). Data are presented as the average of triplicate analyses for all six different extracts.

2.4. Gas chromatography-mass spectrometry (GC-FID/MS) analysis

The GC-FID/MS analysis of the *L. angustifolia* essential oil was performed on a Shimadzu GC-2010 Plus and a Shimadzu GCMS-QP2010, equipped with an AOC-20i autosampler. Fused silica capillary column Inert Cap (5% diphenyl-95% dimethylpolysiloxane, 30 m × 0.25 mm internal diameter, film thickness 0.25 µm) was used. The solution of essential oil in pentane (1:500 v/v) (1.0 µl) was injected in splitless mode with helium as carrier gas. The operating conditions were as follows: injection temperature 260 °C; helium flow rate, 1.11 ml/min; oven temperature program: 50 °C (2 min), 50-120 °C (2 °C/min), 120-220 °C (5 °C/min). FID conditions: 260 °C, air/H_2 flow: 400/50 ml/min. MS (EI) conditions: ion source temperature: 200 °C, interface temperature: 280 °C, ionization voltage: 70 eV, mass range: m/z 40-400 u; scan time: 0.5 sec. The quantification (%) of each detected component of *L. angustifolia* essential oil was determined by normalizing the peak area in FID analysis. The components in the essential oil were identified via comparison of their retention index on the non-polar column with the *n*-alkane series (C_8-C_{40}). Their mass spectra were compared with the Wiley 7 and NIST spectrum library. The analyses were done in triplicate and the results were represented as mean values ± standard deviation.

2.5. DPPH radical scavenging assay

The antioxidant activity of six different extracts and the essential oil was measured in terms of hydrogen donating or radical scavenging ability, using the stable radical, DPPH (Brand-Williams et al., 1995). Extracts prepared in TRIS buffer (1-20 g/l) and EO prepared in 86% ethanol (75-300 g/l) were tested. The 50 µl of the sample was added in 1 ml of 96% ethanol solution of DPPH (6×10^{-5} M). Post incubation of 30 min the absorbance was measured at 517 nm. The BHT was used as a positive control (1-20 mg/ml). All measurements were performed in triplicate. Inhibition of DPPH was calculated according to the formula below.

$$Inhibition\ (\%) = \frac{A_{C(0)} - A_{A(t)}}{A_{C(0)}} x\ 100$$

where $A_{C(0)}$ is the absorbance of the control at t = 0 min, and $A_{A(t)}$ is the absorbance of the antioxidant at t = 30 min. The results were classified as low: 5-25%; moderate: 25-50%; or good: 50-100%.

2.6. Ferric reducing/antioxidant power (FRAP) assay

The method is based on the ferric-reducing ability of plasma as a measure of antioxidant power (Benzie & Strain, 1996). In this assay, the antioxidant activity of the samples tested was calculated with reference to the reaction signal given by a Fe^{2+} solution of known concentration, representing a one-electron exchange reaction. The preparation of the FRAP reagent and the procedure of measurement was described in a previous study (Talić et al., 2019). The corresponding regression calibration equation for $FeSO^4 \times 7\ H_2O$ (1.0-10.0 mg/ml) was A = 0.1463c + 0.2315 (R^2 = 0.9973). Plant extracts solutions (1.0-10.0 mg/ml, prepared in TRIS buffer) and EO solutions (1.0-10.0 mg/ml, prepared in 86% ethanol) were tested. The BHT was used as the positive control (1.0-10.0 mg/ml). All measurements were performed in triplicate.

2.7. Acetylcholinesterase inhibition assay

The acetylcholinesterase (AChE) inhibitory potentials of *L. angustifolia* extracts and EO were measured by modified Ellman's method (Ellman et al., 1961) as described by Wszelaki et al. (2010). Briefly, 180 µl of TrisHCl buffer (50 mM, pH 8.0), 10 µl of AChE (0.055 U/ml, prepared in 20 mM TrisHCl buffer, pH 7.5), and 10 µl of tested solution (1.0-10.0 mg/ml of plant extracts, 1.0-10.0 mg/ml of EO solutions) were mixed and incubated for 20 minutes (4 °C). The reaction was initiated with the addition of 10 µl of DTNB (0.6 mM) and 10 µl of ATChI (10 mM). Galantamine was used as a positive control (1.0-10.0 mg/ml). Inhibition of AChE was measured using a 96-well microplate reader (IRE 96, SFRI Medical Diagnostics) at 405 nm over a period of 30 minutes at 25 °C. The experiment was run in triplicate. The percentage of enzyme inhibition was calculated according to the formula below.

$$AChE\ inhibition\ (\%) = \frac{A_C - A_T}{A_C} x\ 100$$

where A_C is the activity of the enzyme without the test sample and A_T is the activity of the enzyme with the test sample.

2.8. Statistical analysis

The SPSS (SPSS Inc., Chicago, IL, USA) statistical analysis was applied. All data are expressed as mean ± standard deviation (SD). One Way Analysis of Variance (ANOVA) coupled with Tukey's posthoc tests was used to compare mean values between different extracts, positive control samples, and essential oil. '*p*' value for non-statistical differences was presented. The $p < 0.050$ was defined as statistically significant.

3. Results and discussion

As part of our ongoing research on the properties and possible applications of aromatic herbs from Bosnia and Herzegovina, the extracts at different polarities and essential oil from *L. angustifolia* collected in these regions were studied.

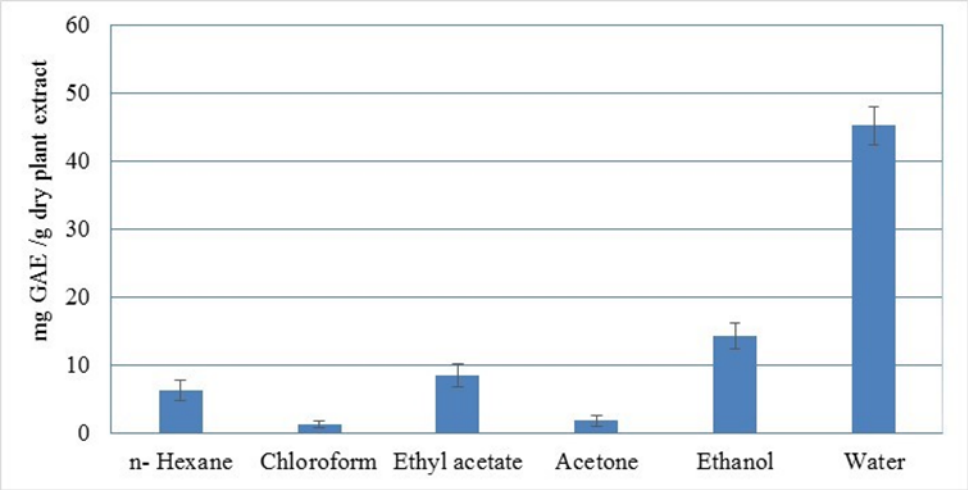

Figure 1. Total polyphenols content in *L. angustifolia* extracts

3.1. Total polyphenols in L. angustifolia extracts

Polyphenols were found in aromatic and medicinal plants, fruits, vegetables, and seeds. In the last few decades, it has been confirmed that polyphenols have several beneficial effects on health, especially due to their antioxidant properties (Hano & Tungmunnithum, 2020). Their role as natural antioxidants is important in the prevention and treatment of inflammatory, cardiovascular, and neurodegenerative diseases and cancer (Quideau et al., 2011). Furthermore, they have a wide range of applications as food supplements, pharmaceutical, and cosmetic additives (Tungmunnithum et al., 2018).

In this study, the total polyphenol content in *L. angustifolia* extracts, prepared in solvents of different polarities, was measured. The total phenolic content, expressed as mg GAE/g dry extract (d.e.) is shown in Figure 1. Water extract was highest in total phenol content (45.30 mg GAE/g d.e.), followed by ethanol (14.40 mg GAE/g d.e.), ethyl acetate (8.50 mg GAE/g d.e.), *n*-hexane (6.40 mg GAE/g d.e.), acetone (1.80 mg GAE/g d.e.) and chloroform (1.20 mg GAE/g d.e.). In general, there is a difference in extracts obtained by polar solvents compared to nonpolar ($p < 0.050$). Pairs of extracts *n*-hexane/ethyl acetate ($p = 0.679$), *n*-hexane/acetone ($p = 0.060$), and chloroform/acetone ($p = 0.998$) displayed no significant differences.

This study confirmed that water as a polar solvent under the given conditions of ultrasonic extraction (35 kHz, 60 min, 30 °C) isolated the highest amount of polyphenolic compounds from *L. angustifolia* extracts. Other similar studies have confirmed that the concentration of total phenols is highly dependent on the solvent and extraction conditions (Radulescu et al., 2017), plant harvesting time (Duda et al., 2015), cultivation conditions, and the parts of a

plant (Adaszyńska-Skwirzyńska & Dzięcioł, 2017; Blažeković et al., 2010). Radulescu et al. (2017) have determined that the use of aqueous alcohol extraction isolated more phenolics compounds, where the main phenolics were gallic acid, umbelliferone, chlorogenic acid, luteolin 7-*O*-glucoside, vitexin, and isoquercitroside. Adaszyńska-Skwirzyńska and Dzięcioł (2017) reported that total phenolics in *L. angustifolia* flowers (1.13-1.14 mg/g dry material) were lower than total phenolics in leafy stalks (3.71-4.06 mg/g dry material). The phenolic content of the whole plant harvested in Romania had 12.44-18.16 mg GAE/g dry plant (Duda et al., 2015). Some studies have confirmed that a higher amount is obtained at the beginning of flowering, than in full bloom, due to the fact that metabolic pathways in the blooming period are activated to produce volatile compounds (Hassiotis et al., 2014).

Table 1. Chemical compositions of *L. angustifolia* essential oil

No	Name of the constituents	RI	Area (%)	Standard deviation (±)
1	β-Myrcene	987	2.15	0.26
2	4-Carene	1009	2.50	0.17
3	α-Pinene	1032	9.82	1.13
4	*trans*-Ocimene	1043	1.40	0.77
5	Linalool	1100	27.72	0.46
6	Alloocimene	1126	1.17	0.12
7	Camphor	1146	0.90	0.03
8	Lavandulol	1161	1.24	0.05
9	Borneol	1171	4.20	0.15
10	Terpinen-4-ol	1179	5.20	0.26
11	Cryptone	1185	0.44	0.02
12	Hexyl butanoate	1190	0.26	0.04
13	α-Terpineol	1193	1.09	0.05
14	*p*-Cumic aldehyde	1240	0.26	0.05
15	Linalyl acetate	1250	22.82	0.33
16	Lavandulol acetate	1281	7.32	0.17
17	Neryl acetate	1355	0.60	0.05
18	Geranyl acetate	1375	1.32	0.12
19	*trans*-Caryophyllene	1418	5.70	0.35
20	β-Farnesene	1449	1.80	0.25
21	Germacrene-D	1478	0.34	0.03
22	γ-Cadinene	1510	0.38	0.03
23	Caryophyllene oxide	1579	1.04	0.12
24	Δ-Cadinene	1638	0.30	0.11
	Total		99.97	

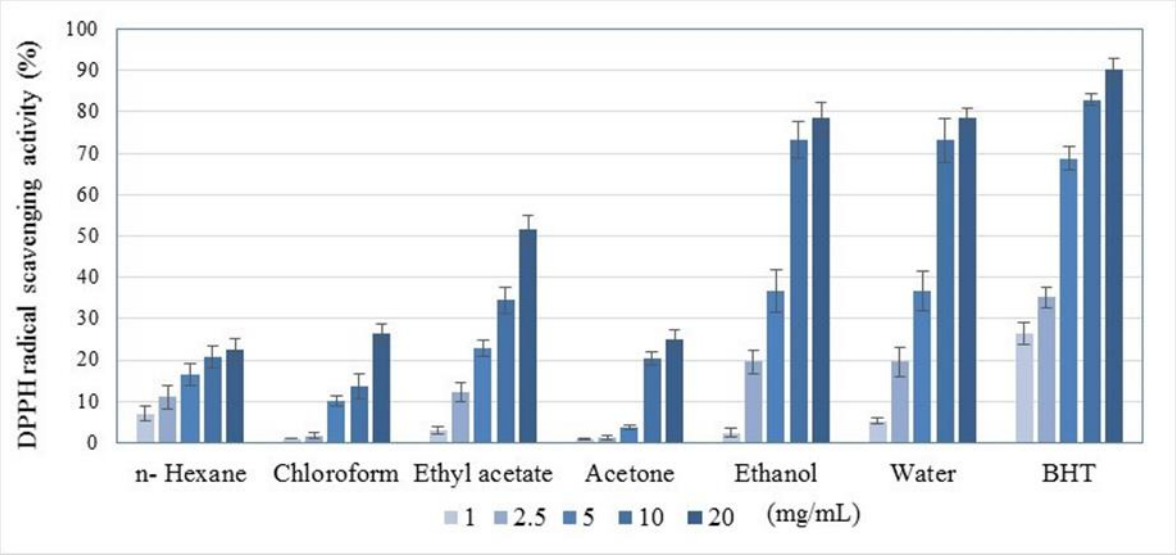

Figure 2. DPPH free radical scavenging activity of BHT and different *L. angustifolia* extracts

3.2. Chemical composition of L. angustifolia essential oil

The *L. angustifolia* EO was obtained by steam distillation and analyzed by GC-FID/MS. The detected compounds of EO are presented in Table 1. In total, 24 compounds were identified in the essential oil, representing 99.97 % of the oil composition. The compounds are presented in order of elution from the nonpolar column. The main detected compounds of *L. angustifolia* EO cultivated in Bosnia and Herzegovina were linalool (27.72%) and linalyl acetate (22.82%), both of which accounted for close to half of the content. The following compounds were α-pinene (9.82%), lavandulol acetate (7.32%), *trans*-caryophyllene (5.70 %), terpinen-4-ol (5.20%), borneol (4.20%), 4-carene (2.50%), and β-myrcene (2.15%).

The biological activity and use of *L. angustifolia* EOs depend on their chemical composition. *L. angustifolia* EO is beneficial for nervousness, insomnia, depression, migraine headaches, sprains, nerve pain, sores, and other diseases (Woronuk et al., 2011). In addition, *L. angustifolia* EO is a medicine used for the treatment of

Alzheimer's disease (Xu et al., 2017). EO rich in linalool and linalyl acetate can be considered as high in quality due to the many beneficial effects of these compounds, such as anti-inflammatory (Peana et al., 2002), anti-bacterial, anti-microbial (Białoń et al., 2019) and different therapeutic properties (Woronuk et al., 2011). According to the literature data, *L. angustifolia* EO has variable chemical composition. *L. angustifolia* cultivated in Poland as the major constituents had linalool (30.6%), linalyl acetate (14.2%), geraniol (5.3%), β-caryophyllene (4.7%), and lavandulyl acetate (4.4%) (Smigielski et al., 2018). *L. angustifolia* cultivated in the mid hills of Uttarakhand (India) had linalyl acetate (47.6%), linalool (28.1%), lavandulyl acetate (4.3%), and α-terpineol (3.7%) as the main compounds (Verma et al., 2010). Linalool and linalyl acetate were also found as the main compounds in *L. angustifolia* EO from Crimean (34.1-52.7%, 23.3-36.6%) (Białoń et al., 2019), and Australia (23.0-57.5%, 4.0-35.4%) (Shellie et al., 2002). However, a completely different composition was found in *L. angustifolia* EO from Iran. The main compounds in this essential oil were carvacrol (26.2%), limonene (19.6%), 1,8-cineole (11.8%), terpinen-4-ol (7.6%), spathulenol (4.9%), α-pinene (4.2%) and *p*-cymene(4.2%) (Bakhsha et al., 2014). Da Porto et al. (2009) investigated the chemical composition of Italian *L. angustifolia* EO, and the main compounds were linalool, linalyl acetate, 1,8-cineole, camphor, and β-caryophyllene. A higher proportion of linalool (54.0%) and a lower proportion of linalyl acetate (11.6%) were found in the essential oil from Croatia (Blažeković et al., 2018) compared to oil from Bosnia and Herzegovina. Both essential oils were characterized by a low amount of camphor (≤ 1%). All these reports suggest that the environmental conditions strongly affect the chemical profile of essential oil either in a quantitative or qualitative extent, which in turn determines their biological activity and application. EO with a high content of linalool and linalyl acetate and a low content of camphor, such as our investigated oil, are among the finest and most desirable lavender oils in the cosmetics and aromatherapy industries (Woronuk et al., 2011).

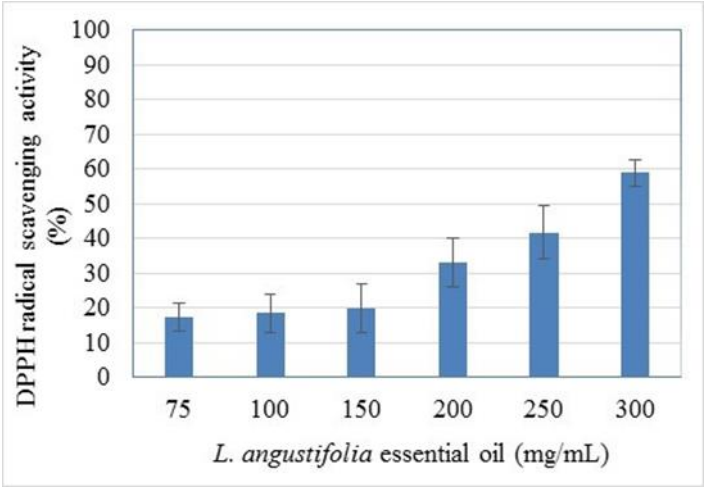

Figure 3. DPPH free radical scavenging activity by *L. angustifolia* essential oil

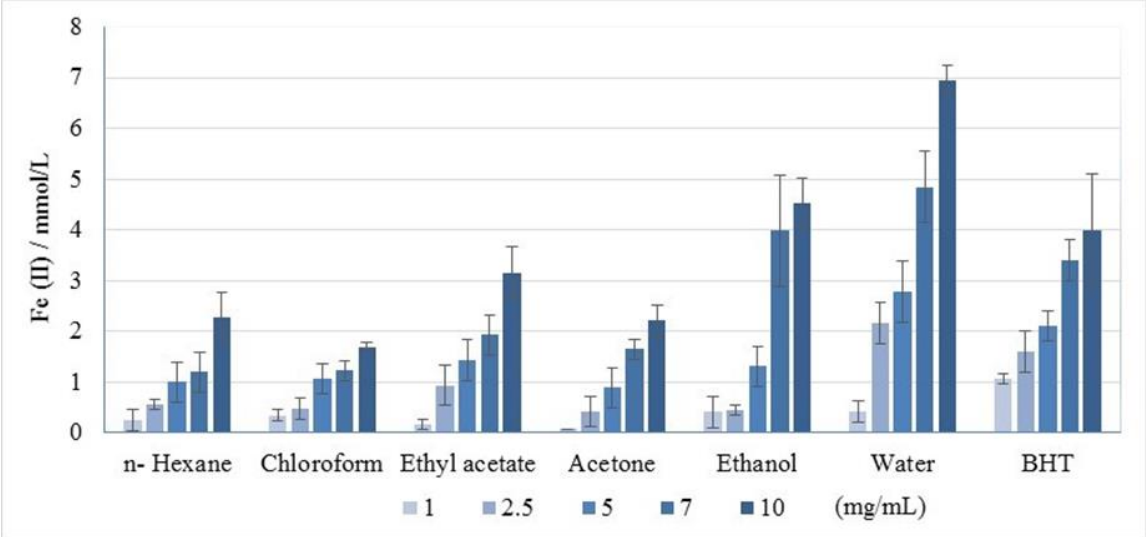

Figure 4. The antioxidant capacity of BHT and different *L. angustifolia* exstracts by FRAP method

3.3. Antioxidant activity

The antioxidant activity of *L. angustifolia* extracts and EO were determined by two methods, DPPH and FRAP. The extracts were prepared in nonpolar and polar solvents.

DPPH radical scavenging activity of *L. angustifolia* extracts is shown in Figure 2. Extracts prepared in *n*-hexane, acetone, and chloroform showed low radical scavenging activity (5-25%). The ethyl acetate extract induced 50% radical scavenging activity at the highest concentration (20 g/l), being considered moderate (25-50%).

However, water and ethanol extracts showed good antioxidant power and reached 73.1-78.5% radical scavenging activity at 10 and 20 mg/ml, respectively (Figure 2). DPPH free radical scavenging activity of BHT compared to each *L. angustifolia* extract was elevated ($p < 0.050$ for all extracts). The difference was also observed in extracts made by polar solvents compared to nonpolar ($p < 0.001$). Pairs of extracts *n*-hexane/chloroform ($p = 0.671$), *n*-hexane/acetone ($p = 0.946$), chloroform/acetone ($p = 0.995$), water/ethanol ($p = 1.00$) displayed no statistically significant difference.

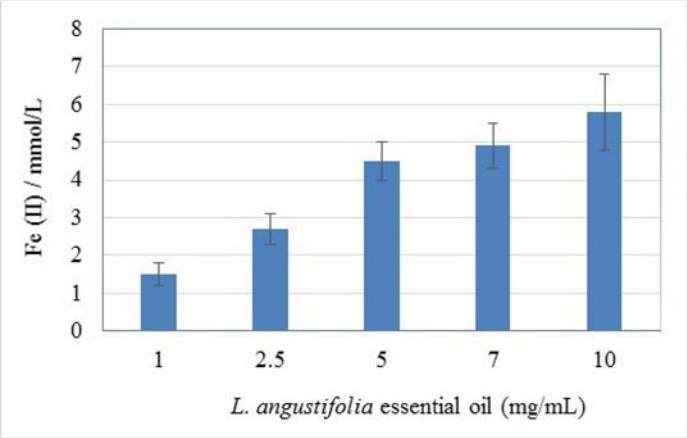

Figure 5. The antioxidant capacity of *L. angustifolia* essential oil by FRAP method

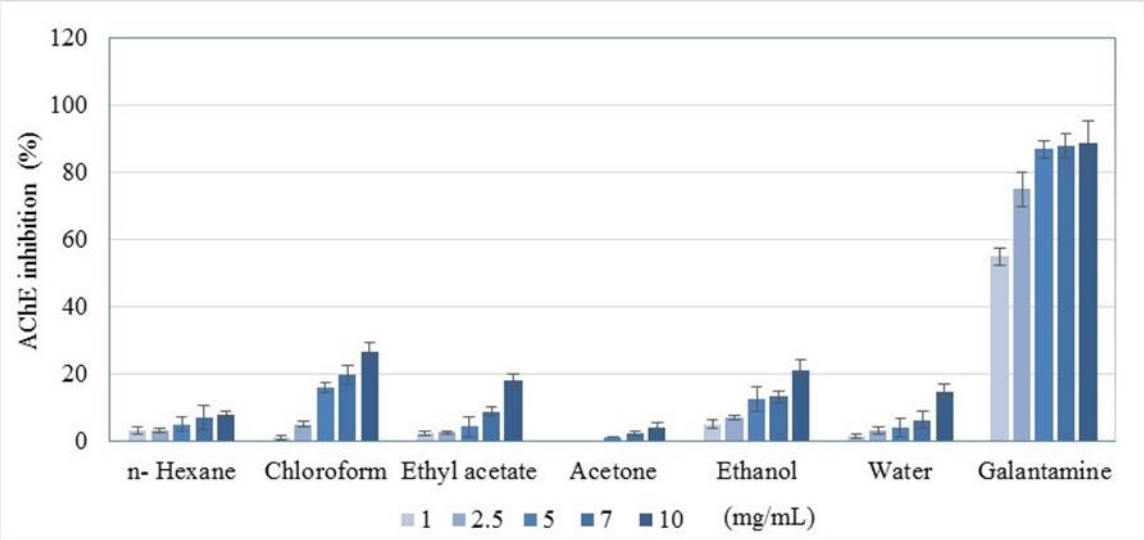

Figure 6. Acetylcholinesterase inhibition by galantamine and different extracts of *L. angustifolia*

DPPH free radical scavenging activity of *L. angustifolia* EO is presented in Figure 3. The EO did not show significant antioxidant activity as only the concentration of 300 mg/ml reached more than 50% free radical scavenging activity. *L. angustifolia* EO also showed weak antioxidant capacity in our previous study for Lamiaceae species (13.3% at 20 mg /ml) according to this method (Odak et al., 2015).

FRAP is the second used method for measuring the antioxidant power of extracts and EO from *L. angustifolia*. All samples used in this assay reduced ferric iron (Fe^{3+}) to ferrous iron (Fe^{2+}). The antioxidant property of *L. angustifolia* extracts by the FRAP method is presented in Figure 4. The BHT was used as a positive control (10 mg/ml is eq. to 4.0 mM Fe^{2+}).

There is a difference in the antioxidant power of extracts obtained using polar solvents compared to nonpolar ones ($p < 0.050$). Acetone, chloroform, and *n*-hexane extracts showed lower antioxidant properties than extracts prepared in ethanol and water. However, there was no difference found in antioxidant capacity between ethyl acetate extract and ethanol extract ($p = 0.274$). Water and ethanol extracts showed the greatest reducing power at 10 mg/ml (4.5 and 6.9 mM Fe^{2+}). Based on both methods used, these two extracts displayed better antioxidant activity than the others. Pairs of extracts *n*-hexane/chloroform ($p = 0.937$), *n*-hexane/ethyl acetate ($p = 0.681$), *n*-hexane/acetone ($p = 1.00$), chloroform/ethyl acetate ($p = 0.149$), chloroform/acetone ($p = 0.975$) and ethyl acetate/acetone ($p = 0.569$) displayed no statistically significant differences. Elevated polyphenols content in aqueous and ethanol extracts of *L. angustifolia* is considered to be responsible for good antioxidant effects. Previous studies confirmed that *L. angustifolia* contains rosmarinic acid, chlorogenic acid, and caffeic acid, which are known as powerful antioxidants (Blažeković et al., 2010). Duda et al. (2015) also reported that ethanolic extracts of *L. angustifolia* possess antioxidant power (2.5 to 8.6 mM Fe^{2+}/100 g dry sample) and correlate well with the total polyphenol content.

Unlike the DPPH method, *L. angustifolia* essential oil showed antioxidant power according to the FRAP method. Reduction to ferrous iron (Fe^{2+}) was dependent on the concentration of essential oils (1-10 mg/ml) and ranged from 1.5 to 5.8 mM Fe^{2+} (Figure 5). In comparison of the antioxidant activity of the essential oil and the extract of similar concentrations, stronger antioxidant activity of the essential oil compared to the extracts was observed ($p < 0.050$), except for ethanol ($p = 0.274$) and water ($p = 0.459$) extracts, and BHT ($p = 0.054$).

3.4. Inhibition of acetylcholinesterase (AChE) activity

AChE inhibitory activity of the EO and extracts of *L. angustifolia* is shown in Figures 6 and 7. Galantamine was used as the reference AChE inhibitor. All the extracts induced low AChE inhibitory activity compared to galantamine ($p < 0.001$). Among them, chloroform extract achieved a slightly greater inhibitory effect of 25% (26.5% at 10 mg/ml). Extracts in polar solvents were compared to nonpolar; water/*n*-hexane ($p = 0.225$), water/ethyl acetate ($p = 0.863$), ethanol/chloroform ($p = 0.456$), ethanol/ethyl acetate ($p = 0.941$) displayed no significant differences. Pairs of extracts *n*-hexane/acetone ($p = 0.790$), and chloroform/ethyl acetate ($p = 0.078$) also displayed no statistically significant AChE inhibitory activity differences.

Similar studies of *L. angustifolia* ethanol extracts confirm a weak to moderate AChE inhibitory effect (Ferreira et al., 2006; Vladimir-Knežević et al., 2014). Research on animal models of Alzheimer's disease showed that the aqueous extract of *L. angustifolia* improves memory (Soheili et al., 2012).

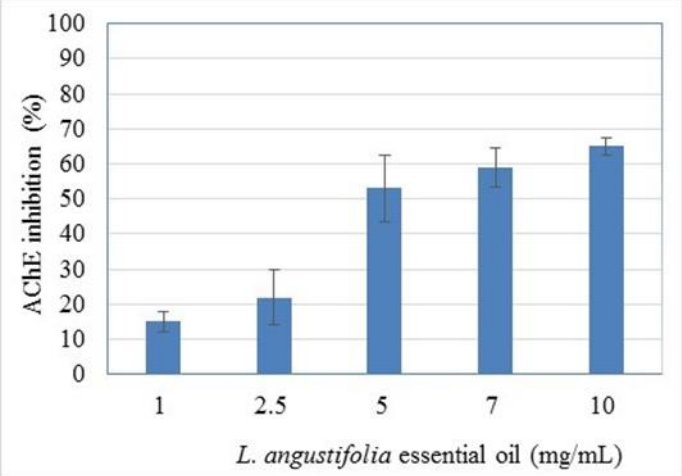

Figure 7. Acetylcholinesterase inhibition by *L. angustifolia* essential oil

L. angustifolia EO showed AChE inhibitory activity as a function of concentration. The results indicated that concentrations 5, 7, and 10 mg/ml achieved over 50% inhibition of AChE activity. Therefore, according to this research, EO can be considered as good inhibitor of AChE at a concentration of 10 g/l. AChE inhibition by EO is elevated compared to all extracts used ($p < 0.001$). Ferreira et al. (2006) also reported that lavender essential oils are good inhibitors (39.5% at 1mg/ml) of AChE.

Cholinesterase inhibition has become the most widely employed clinical approach to treating neurodegenerative diseases. EO and its major component, linalool, have shown multiple bioactivities, especially for Alzheimer's disease (Hancianu et al., 2013; Hritcu et al., 2012; Xu et al., 2017). Numerous studies have confirmed that the accumulation of amyloid beta (Aβ) plaques lead to decreased cognitive function and neurodegenerative disorders such as Alzheimer's disease (Hampel et al., 2010; Querfurth & LaFerla, 2010; Soheili et al., 2012). Aβ plaques are formed due to hyperactivity of AChE and reduction of choline. One possible reason for the accumulation of Aβ in Alzheimer's disease is oxidative stress, mediated by the production of reactive oxygen species (Zuo et al., 2015). Consequently, the antioxidant capacity of essential oils and tested extracts of *L. angustifolia* could contribute to the prevention of plaque formation. Linalool reverses the histopathological hallmarks of AD at mice and restores cognitive and emotional functions via an anti-inflammatory effect (Sabogal-Guáqueta et al., 2016). The chemical composition and biological activity of *L. angustifolia* extracts prepared in water and ethanol should be the subject of future research.

4. Conclusions

Ethanol and water extracts of L. angustifolia are found to contain a high proportion of total polyphenols and have an impressive antioxidant capacity. The main components of the essential oil were linalool, linalyl acetate, α-pinene, and lavandulol acetate. Due to the high content of beneficial health compounds, linalool and linalyl acetate (together over 50%), this oil can be considered as a high-quality oil. In addition, EO showed good inhibitory activity for AChE. It was confirmed that *L. angustifolia* could be used as a source of biologically active compounds and as a valuable raw material for the pharmaceutical and cosmetic industries. The results obtained contribute to the better evaluation and sustainable use of *L. angustifolia* grown in Bosnia and Herzegovina.

Acknowledgments

The authors thank the botanist professor Anđelka Lasić for the identification of the species. Thanks to the Federal Ministry of Education and Science of Bosnia and Herzegovina for supporting this study with the project no. 05-35-1839-1/21.

Conflict of interest

The authors confirm that there are no known conflicts of interest.

Statement of ethics

In this study, no method requiring the permission of the "Ethics Committee" was used.

Availability of data and materials

All data generated or analyzed during this study are included in this published article.

Funding

None.

CRediT authorship contribution statement

Stanislava Talić: Conceptualization, Methodology, Writing - original draft
Ilijana Odak: Visualization, Review & Editing
Marijana Marković Boras: Investigation, Data curation
Ante Smoljan: Investigation, Formal analysis
Anita Martinović Bevanda: Supervision, Resources

ORCID Numbers of the Authors

S. Talić: 0000-0001-7633-4312
I. Odak: 0000-0002-6883-8470
M. Marković Boras: 0000-0002-5575-8893
A. Smoljan: 0000-0001-9396-3372
A. Martinović Bevanda: 0000-0003-0108-3621

Supplementary File

None.

Publisher's Note

All claims expressed in this article are solely those of the authors and do not necessarily represent those of their affiliated organizations, or those of the publisher, the editors and the reviewers. Any product that may be evaluated in this article, or claim that may be made by its manufacturer, is not guaranteed or endorsed by the publisher.

This is an open-access article distributed under the terms of the Creative Commons Attribution 4.0 International License (CC BY). The use, distribution or reproduction in other forums is permitted, provided the original author(s) and the copyright owner(s) are credited and that the original publication in this journal is cited, in accordance with accepted academic practice. No use, distribution or reproduction is permitted which does not comply with these terms.

References

Adaszyńska-Skwirzyńska, M., & Dzięcioł, M. (2017). Comparison of phenolic acids and flavonoids contents in various cultivars and parts of common lavender (*Lavandula angustifolia*) derived from Poland. *Natural Product Research, 31*(21), 2575-2580.

Bakhsha, F., Mazandarani, M., Aryaei, M., Jafari, S. Y., & Bayate, H. (2014). Phytochemical and anti-oxidant activity of *Lavandula angustifolia* mill. essential oil on preoperative anxiety in patients undergoing diagnostic curettage. *International Journal of Women's Health and Reproduction Sciences, 2*(4), 268–271.

Benzie, I. F., & Strain, J. J. (1996). The ferric reducing ability of plasma (FRAP) as a measure of "antioxidant power": the FRAP assay. *Analytical Biochemistry, 239*(1), 70-76.

Białoń, M., Krzyśko-Łupicka, T., Nowakowska-Bogdan, E., & Wieczorek, P. P. (2019). Chemical composition of two different lavender essential oils and their effect on facial skin microbiota. *Molecules, 24*(18), 3270.

Blažeković, B., Vladimir-Knežević, S., Brantner, A., & Štefan, M. B. (2010). Evaluation of antioxidant potential of *Lavandula* x *intermedia* Emeric ex Loisel.'Budrovka': A comparative study with *L. angustifolia* Mill. *Molecules, 15*(9), 5971-5987.

Blažeković, B., Yang, W., Wang, Y., Li, C., Kindl, M., Pepeljnjak, S., & Vladimir-Knežević, S. (2018). Chemical composition, antimicrobial and antioxidant activities of essential oils of *Lavandula* × *intermedia* 'Budrovka' and *L. angustifolia* cultivated in Croatia. *Industrial Crops and Products, 123*, 173-182.

Brand-Williams, W., Cuvelier, M. E., & Berset, C. (1995). Use of a free radical method to evaluate antioxidant activity. *LWT-Food Science and Technology, 28*(1), 25-30.

Costea, T., Străinu, A., & Gîrd, C. (2019). Botanical characterization, chemical composition and antioxidant activity of Romanian lavander (*Lavandula angustifolia* mill.) flowers. *Studia Universitatis Vasile Goldis Arad, Seria Stiintele Vietii, 29*(4), 159-167.

Crișan, I., Ona, A., Vârban, D., Muntean, L., Vârban, R., Stoie, A., Mihăiescu, T., & Morea, A. (2023). Current Trends for Lavender (*Lavandula angustifolia* Mill.) Crops and Products with Emphasis on Essential Oil Quality. *Plants, 12*(2), 357.

Da Porto, C., Decorti, D., & Kikic, I. (2009). Flavour compounds of *Lavandula angustifolia* L. to use in food manufacturing: Comparison of three different extraction methods. *Food Chemistry, 112*(4), 1072-1078.

Duda, S. C., Mărghitaş, L. A., Dezmirean, D., Duda, M., Mărgăoan, R., & Bobiş, O. (2015). Changes in major bioactive compounds with antioxidant activity of *Agastache foeniculum*, *Lavandula angustifolia*, *Melissa officinalis* and *Nepeta cataria*: Effect of harvest time and plant species. *Industrial Crops and Products, 77*, 499-507.

Ellman, G. L., Courtney, K. D., Andres Jr, V., & Featherstone, R. M. (1961). A new and rapid colorimetric determination of acetylcholinesterase activity. *Biochemical Pharmacology, 7*(2), 88-95.

Ferreira, A., Proença, C., Serralheiro, M., & Araujo, M. (2006). The in vitro screening for acetylcholinesterase inhibition and antioxidant activity of medicinal plants from Portugal. *Journal of Ethnopharmacology, 108*(1), 31-37.

Gallego, M. G., Gordon, M. H., Segovia, F. J., Skowyra, M., & Almajano, M. P. (2013). Antioxidant properties of three aromatic herbs (rosemary, thyme and lavender) in oil-in-water emulsions. *Journal of the American Oil Chemists' Society, 90*, 1559-1568.

Giannoulis, K. D., Evangelopoulos, V., Gougoulias, N., & Wogiatzi, E. (2020). Could bio-stimulators affect flower, essential oil yield, and its composition in organic lavender (*Lavandula angustifolia*) cultivation? *Industrial Crops and Products, 154*, 112611.

Giray, F. H. (2018). An analysis of world lavender oil markets and lessons for Turkey. *Journal of Essential Oil Bearing Plants, 21*(6), 1612-1623.

Guo, X., & Wang, P. (2020). Aroma Characteristics of Lavender Extract and Essential Oil from *Lavandula angustifolia* Mill. *Molecules, 25*(23), 5541.

Hampel, H., Shen, Y., Walsh, D. M., Aisen, P., Shaw, L. M., Zetterberg, H., Trojanowski, J. Q., & Blennow, K. (2010). Biological markers of amyloid β-related mechanisms in Alzheimer's disease. *Experimental Neurology, 223*(2), 334-346.

Hancianu, M., Cioanca, O., Mihasan, M., & Hritcu, L. (2013). Neuroprotective effects of inhaled lavender oil on scopolamine-induced dementia via anti-oxidative activities in rats. *Phytomedicine, 20*(5), 446-452.

Hano, C., & Tungmunnithum, D. (2020). Plant polyphenols, more than just simple natural antioxidants: Oxidative stress, aging and age-related diseases. *Medicines, 7*(5), 26.

Hassiotis, C., Ntana, F., Lazari, D., Poulios, S., & Vlachonasios, K. (2014). Environmental and developmental factors affect essential oil production and quality of *Lavandula angustifolia* during flowering period. *Industrial Crops and Products, 62*, 359-366.

Hernandez, M. F., Falé, P. L., Araújo, M. E. M., & Serralheiro, M. L. M. (2010). Acetylcholinesterase inhibition and antioxidant activity of the water extracts of several *Hypericum* species. *Food Chemistry, 120*(4), 1076-1082.

Hritcu, L., Cioanca, O., & Hancianu, M. (2012). Effects of lavender oil inhalation on improving scopolamine-induced spatial memory impairment in laboratory rats. *Phytomedicine, 19*(6), 529-534.

Kirimer, N., Mokhtarzadeh, S., Demirci, B., Goger, F., Khawar, K. M., & Demirci, F. (2017). Phytochemical profiling of volatile components of *Lavandula angustifolia* Miller propagated under in vitro conditions. *Industrial Crops and Products, 96*, 120-125.

Odak, I., Talić, S., & Martinović Bevanda, A. (2015). Chemical composition and antioxidant activity of three Lamiaceae species from Bosnia and Herzegovina. *Bulletin of the Chemists and Technologists of Bosnia and Herzegovina, 45*, 23-30.

Peana, A. T., D'Aquila, P. S., Panin, F., Serra, G., Pippia, P., & Moretti, M. D. L. (2002). Anti-inflammatory activity of linalool and linalyl acetate constituents of essential oils. *Phytomedicine, 9*(8), 721-726.

Pistelli, L., Najar, B., Giovanelli, S., Lorenzini, L., Tavarini, S., & Angelini, L. (2017). Agronomic and phytochemical evaluation of lavandin and lavender cultivars cultivated in the Tyrrhenian area of Tuscany (Italy). *Industrial Crops and Products, 109*, 37-44.

Querfurth, H. W., & LaFerla, F. M. (2010). Alzheimer's disease. *New England Journal of Medicine, 362*(4), 329-344.

Quideau, S., Deffieux, D., Douat-Casassus, C., & Pouységu, L. (2011). Plant polyphenols: chemical properties, biological activities, and synthesis. *Angewandte Chemie International Edition, 50*(3), 586-621.

Radulescu, C., Stihi, C., Ilie, M., Lazurcă, D., Gruia, R., Olaru, O. T., Bute, O. C., Dulama, I. D., Stirbescu, R. M., *et al.* (2017). Characterization of Phenolics in *Lavandula angustifolia*. *Analytical Letters, 50*(17), 2839-2850.

Sabogal-Guáqueta, A. M., Osorio, E., & Cardona-Gómez, G. P. (2016). Linalool reverses neuropathological and behavioral impairments in old triple transgenic Alzheimer's mice. *Neuropharmacology, 102*, 111-120.

Shellie, R., Mondello, L., Marriott, P., & Dugo, G. (2002). Characterisation of lavender essential oils by using gas chromatography–mass spectrometry with correlation of linear retention indices and comparison with comprehensive two-dimensional gas chromatography. *Journal of Chromatography A, 970*(1-2), 225-234.

Smigielski, K., Prusinowska, R., Stobiecka, A., Kunicka-Styczyñska, A., & Gruska, R. (2018). Biological properties and chemical composition of essential oils from flowers and aerial parts of lavender (*Lavandula angustifolia*). *Journal of Essential Oil Bearing Plants, 21*(5), 1303-1314.

Smigielski, K., Raj, A., Krosowiak, K., & Gruska, R. (2009). Chemical composition of the essential oil of *Lavandula angustifolia* cultivated in Poland. *Journal of Essential Oil Bearing Plants, 12*(3), 338-347.

Soheili, M., Tavirani, M. R., & Salami, M. (2012). Clearance of amyloid beta plaques from brain of Alzheimeric rats by *Lavandula angustifolia*. *Neuroscience & Medicine, 3*(4), 26193.

Spiridon, I., Colceru, S., Anghel, N., Teaca, C. A., Bodirlau, R., & Armatu, A. (2011). Antioxidant capacity and total phenolic contents of oregano (*Origanum vulgare*), lavender (*Lavandula angustifolia*) and lemon balm (*Melissa officinalis*) from Romania. *Natural Product Research, 25*(17), 1657-1661.

Talić, S., Odak, I., Bevanda, A. M., Crnjac, N., & Pastar, M. (2019). *Helichrysum italicum* (Roth) G. Don subsp. *italicum* from Herzegovina: Volatile composition, variations during seasons, total polyphenols, acetylcholinesterase inhibition and antioxidant activity. *Croatica Chemica Acta, 92*(1), 69-78.

Tungmunnithum, D., Thongboonyou, A., Pholboon, A., & Yangsabai, A. (2018). Flavonoids and other phenolic compounds from medicinal plants for pharmaceutical and medical aspects: An overview. *Medicines, 5*(3), 93.

Verma, R. S., Rahman, L. U., Chanotiya, C. S., Verma, R. K., Chauhan, A., Yadav, A., Singh, A., & Yadav, A. K. (2010). Essential oil composition of *Lavandula angustifolia* Mill. cultivated in the mid hills of Uttarakhand, India. *Journal of the Serbian Chemical Society, 75*(3), 343-348.

Vladimir-Knežević, S., Blaženković, B., Kindl, M., Vladić, J., Lower-Nedza, A. D., & Brantner, A. H. (2014). Acetylcholinesterase inhibitory, antioxidant and phytochemical properties of selected medicinal plants of the Lamiaceae family. *Molecules, 19*(1), 767-782.

Wells, R., Truong, F., Adal, A. M., Sarker, L. S., & Mahmoud, S. S. (2018). Lavandula essential oils: a current review of applications in medicinal, food, and cosmetic industries of lavender. *Natural Product Communications, 13*(10), 1403-1417.

Woronuk, G., Demissie, Z., Rheault, M., & Mahmoud, S. (2011). Biosynthesis and therapeutic properties of *Lavandula* essential oil constituents. *Planta Medica, 77*(1), 7-15.

Wszelaki, N., Kuciun, A., & Kiss, A. (2010). Screening of traditional European herbal medicines for acetylcholinesterase and butyrylcholinesterase inhibitory activity. *Acta Pharmaceutica, 60*(1), 119-128.

Xu, P., Wang, K., Lu, C., Dong, L., Gao, L., Yan, M., Aibai, S., Yang, Y., & Liu, X. (2017). The protective effect of lavender essential oil and its main component linalool against the cognitive deficits induced by D-galactose and aluminum trichloride in mice. *Evidence-Based Complementary and Alternative Medicine, 2017*, 7426538.

Zuo, L., Hemmelgarn, B. T., Chuang, C. C., & Best, T. M. (2015). The role of oxidative stress-induced epigenetic alterations in amyloid-β production in Alzheimer's disease. *Oxidative Medicine and Cellular Longevity, 2015*, 604658.

Int. J. Plant Bas. Pharm. (2023) 3(1), 104-113

INTERNATIONAL JOURNAL OF PLANT BASED PHARMACEUTICALS

https://ijpbp.com

RESEARCH ARTICLE

OPEN ACCESS

FTIR spectral correlation with alpha-glucosidase inhibitory activities of selected leafy plants extracts

Savani Ulpathakumbura[a,b], Nazrim Marikkar[a*], Lalith Jayasinghe[a]

[a] *National Institute of Fundamental Studies, Hanthana Road, Kandy, Sri Lanka*
[b] *University of Peradeniya, Postgraduate Institute of Science, Kandy, Sri Lanka*

ARTICLE INFO

Article History:

Received: 13 February 2023
Revised: 20 April 2023
Accepted: 24 April 2023
Available online: 26 April 2023

Edited by: B. Tepe

Keywords:

Leafy plants
FTIR
PLS regression analysis
Alpha-glucosidase inhibitory activity

ABSTRACT

Fourier transform infrared spectroscopy (FTIR) is a simple, rapid analytical technique used for the identification of organic functional groups of biomolecules. This study aimed to investigate the use of FTIR spectroscopy method for rapid detection of the α-glucosidase inhibitory activity of crude extracts of edible leafy plants, characterization of functional groups of chemical components present in crude extracts, and identification of possible biomolecules responsible for α-glucosidase inhibitory activity. Powdered leaves of five different plants, namely *Le-kola pala* (LE) (*Premna procumbens*), *Kora kaha* (KK) (*Memecylon umbellatum*), *Koppa* (KO) (*Polyscias scutellaria*), *Stevia* (ST) (*Stevia rebaudiana*), and *Yaki naran* (YK) (*Atlantia ceylanica*) were sequentially extracted with hexane, ethyl acetate (EtOAc) and methanol (MeOH). The FTIR spectra of crude plant extracts were obtained following the KBr pellet method, within the range of 4000-500 cm^{-1}. The plant extracts were subjected to assay the α-glucosidase inhibitory activity. Further, the multivariate predictive models for α-glucosidase inhibitory activity were developed using partial least square (PLS) regression analysis. The highest Rc^2 (0.96), Rcv^2 (0.87), Rp^2 (0.93), and the lowest RMSEC (24.10), RMSECV (41.70), and RMSEP (81.04) values were noticed for spectral region range from 1700 cm^{-1} to 1800 cm^{-1}, indicating the strongest correlation to the α-glucosidase inhibitory activity, while the spectral region range from 1500 cm^{-1} to 1700 cm^{-1} was found to have the lowest Rc^2 (0.71), Rcv^2 (0.52), Rp^2 (0.45) and the highest RMSEC (61.14) and RMSECV (80.21), indicating the lowest correlation to the α-glucosidase inhibitory activity. As the peak appearing in the range of 1700-1800 cm^{-1} is usually ascribed to C=O stretching vibration of ester groups, ketones, and carboxylic acids, there was a strong correlation between α-glucosidase inhibitory activity with those organic functional groups. The present study suggests that FTIR spectral analysis together with PLS regression analysis would be a convenient, rapid tool to determine α-glucosidase inhibitory activity of plant extracts.

1. Introduction

Diabetes Mellitus (DM) is a complex metabolic disorder occurring due to malfunctions in insulin secretion, insulin action, or both. Nowadays, it has become a serious health issue as well as a socioeconomic burden for several countries. Control of hyperglycemia is an important step as diabetes management because if left unchecked it can increase the risk of many macrovascular and microvascular complications such as hypertension, coronary vascular disease, cardiomyopathy, stroke and retinopathy, nephropathy, and neuropathy (Jayaraj et al., 2013). Recent reports pointed out that a high postprandial plasma glucose level could be more deleterious than fasting blood glucose as it can cause serious complications and increase the mortality rate. Hence, patients suffering from diabetes should need to take every possible control measures to minimize their postprandial blood glucose level (Xiao-Ping et al., 2010). One of the effective therapeutic approaches for treating diabetes is to lower the postprandial hyperglycemia level by suppressing glucose absorption through inhibition of the carbohydrate-

Reviewed by:
Walid Elfalleh: Higher Institute of Applied Sciences and Technology of Gabes, Gabes, Tunisia
Mehmet Sabih OZER: Manisa Celal Bayar University, Manisa, Türkiye

* Corresponding author(s):
E-mail address:
nazrim.ma@nifs.ac.lk (N. Marikkar)
e-ISSN: 2791-7509
doi: https://doi.org/10.29228/ijpbp.22

hydrolyzing enzymes, namely α-amylase and α-glucosidase (De Souza Schmidt Goncalves et al., 2010; Nickavar & Abolhasani, 2013). According to Western medical practice, acarbose can help in blunting the postprandial plasma glucose rise by prolonging the enzymatic hydrolysis of complex carbohydrates, thereby delaying glucose absorption (Shobana et al., 2009). To date, some α-amylase and α-glucosidase inhibitors have been isolated from medicinal plants to serve as an orthodox drugs with increased potency and mild side effects when compared to existing synthetic drugs (Kazeem et al., 2013).

For decades, the consumption of several types of leafy plants is advocated for the control and management of postprandial blood glucose. According to a compilation by Ediriweera and Ratnasooriya (2009), edible leafy plants, such as *Kiri anguna* (*Tylophora pauciflora*), *Thebu* (*Costus speciosus*), *Curry plant* (*Murraya koenigii*), *Kowakka* (*Coccinia grandis*), *Adhathoda* (*Adhathoda vasica*), *Mukunuwenna* (*Alternanthera sessilis*), *Ranawara* (*Cassia auriculata*), *Gotukola* (*Cantella asiatica*) are already recognized as effective in controlling diabetes. Aside from these, there are some lesser-known leafy plants, namely *Le-kola pala* (*Premna procumbens*), *Koppa* (*Polyscias scutellaria*), *Stevia* (*Stevia rebaudiana*), *Yaki naran* (*Atlantia ceylanica*), and *Kora kaha* (*Memecylon umbellatum*) which are also believed to have anti-diabetic effect according to traditional knowledge. However, studies are needed to confirm that their anti-diabetic potential is little or insufficient. Currently, various in vitro and in vivo assays are employed in exploratory studies to establish their effectiveness for diabetes. In vitro studies usually adopt parameters that include enzymatic assays related to glucose metabolism while in vivo studies investigate the analysis of anti-diabetic efficacy by biochemical parameters such as blood glucose, insulin, and serum protein (Bhardwaj et al., 2020). The established in vitro methods are, however, rather lengthy, labor-intensive, and require several chemical reagents. Owing to these reasons, there has been a continuous urge in the scientific community to find out simple, cost-effective, and rapid methods to detect α-glucosidase inhibitory activity of emerging foods or plant-based products.

In recent times, FTIR spectroscopy has emerged as a rapid analytical tool for chemical mapping of natural plant extracts and various other products (Gunarathne et al., 2022b). Although this technique was used in the early days for the identification of functional groups in organic molecules, its application range has now broadened to include complex issues related to chemical and biological systems. In food industries, FTIR spectroscopy has been widely investigated for authentication and quality control of food and drugs (Gunarathne et al., 2022a), determination of enzyme activity of sea buckthorn substrate (Adina et al., 2010), and efficacy of herbal medicinal formulations (Ashokkumar & Ramaswamy, 2014; Bunaciu et al., 2011). In comparison to chromatographic techniques, FTIR has become popular due to its rapidity and ease of operation. As it could be applied together with multivariate data analysis, FTIR could help generate predictive models useful for chemical analysis (Easmin et al., 2017). According to some reports, FTIR spectral data combined with multivariate data analysis have been successful to develop predictive models for α-glucosidase inhibitory activity of novel plant extracts (Easmin et al., 2017; Saleh et al., 2018; Umar et al., 2021). The objective of this study was to assess FTIR spectral correlation with α-glucosidase inhibitory activities of selected anti-diabetic leafy plants, namely *Le-kola pala* (LE) (*P. procumbens*), *Koppa* (KO) (*P. scutellaria*), *Stevia* (ST) (*S. rebaudiana*), *Yaki naran* (YK) (*Atlantia ceylanica*), and *Kora kaha* (KK) (*M. umbellatum*). The outcomes of this study would be useful to establish a database of local plant species, which demonstrate moderate to high anti-hyperglycaemic effects.

2. Materials and methods

2.1. Plant materials

Five edible leafy plants, namely *Le-kola pala* (LE) (SULE21004), *Kora kaha* (KK) (SUKK21003), *Koppa* (KO) (SUKO21002), *Stevia* (ST) (SUST21001), and *Yaki naran* (YK) (SUYK21005) were used in this study. Samples were collected from the Central and North Central Provinces of Sri Lanka from March 2021 to May 2021. The plants were cross-checked by Dr. D. S. A. Wijesundera, Senior Taxonomist from the Royal Botanical Garden of Sri Lanka, and their voucher specimens were deposited in Popham's Arboretum of NIFS in Dambulla, Sri Lanka. The collected samples were cleaned under running tap water and dried at 55 °C for 8-10 hours in a forced-convection air-drying oven (Biobase, model-BOV-V230F, China). The dried leaves were ground into powder and stored at 4 °C for further analysis.

2.2. Preparation of crude extracts

Two hundred grams of powdered leaves of each plant species were sequentially extracted with hexane, EtOAc, and MeOH using ultra-sonication (Rocker ultrasonic cleaner, model-Soner 206H) for 30 min. For each solvent type, the extraction was repeated three times. Each plant extract type was concentrated using a rotary evaporator (Heidolph, Laborota 4000) under reduced pressure followed by vacuum drying (vacuum oven, Heraeus instrument, Germany) for 3-4 hours. The crude extracts were stored at -18 °C for further analysis.

2.3. Determination of α-glucosidase inhibitory activity

α-Glucosidase inhibitory activity of crude plant extracts was determined according to the method described by Gunarathne et al. (2022c). Briefly, a concentration series (3.91-1000 ppm) of plant extracts were prepared by dissolving the crude extracts in distilled water with 3% DMSO. Thereafter, 100 µl of 30 mM phosphate buffer (pH 6.5) was added into 96 wells micro-plate, followed by mixing with 25 µl of sample solution (reconstituted crude extract with distilled water). In the next step, 25 µl α-glucosidase enzyme solution (12.5 µl/ml) was added to it and incubated for 5 min at 37 °C. After that, a 50 µl portion of pNPG (*p*-nitrophenyl-α-D-glucopyranoside) solution (0.8 mg/ml) was added and followed by incubation for another 30 min at 37 °C. In the present study, acarbose (Glucobay tablet) was used as the positive control. The absorbance value was measured at 410 nm and the percentage of α-glucosidase inhibitory activity was calculated using the following equation. The IC_{50} values were calculated graphically by plotting the percentage of α-glucosidase inhibition against the sample concentration of each extract.

$$Percentage\ \alpha - glucosidase\ inhibition = \frac{\delta A_{control} - \delta A_{sample}}{\delta A_{control}} x\ 100 \quad \ldots\ldots(1)$$

where;

$\delta A_{control}$ = $Absorbance_{control}$ - $Absorbance_{control\ blank}$

δA_{sample} = $Absorbance_{sample}$ - $Absorbance_{sample\ blank}$

2.4. FTIR measurements

FTIR analysis of crude extracts was performed according to the KBr pellet method as described by Mittal et al. (2020) and Gunarathne et al. (2022b) with some modifications. Initially, approximately 1 mg of each crude extract was mixed with 100 mg of KBr (FT-IR grade, ≥ 99% trace metals basis, Sigma Aldrich) and made into a pellet using a hydraulic press. The spectra were recorded using an FTIR Nicolet iS50 spectrometer (Thermo Nicolet, Madison, WI) equipped with deuterated triglycine sulfate (DTGS) KBr detector and KBr beam splitter. The data were obtained in the mid-infrared region of 4000-500 cm^{-1} by co-adding at 64 scans with resolution, resolution of 8 cm^{-1}. All spectra were ratioed against a background spectrum of pure KBr pallet. The absorbance values were recorded at each data point in triplicate.

2.5. Statistical analysis

α-Glucosidase inhibitory measurements were obtained at least in triplicate data (n=3) and the results were presented as mean ± standard deviation (SD). Data were analyzed statistically by one-way ANOVA using Minitab 17 software package. When the F values were significant, mean differences were compared using Tukey's test at the 5% level of probability.

2.6. Spectral analysis

The manufacturer's software (OMNIC operating system, version 7.0 Thermo Nicolet) was used for spectral pre-processing and qualitative analysis. The raw spectra of each plant extract were subjected to baseline correction and scale normalization, respectively. The mean spectrum of the triplicates was used for qualitative purposes.

2.7. PLS regression analysis

The Unscrambler 9.7 (Camo, USA) software was used to perform the PLS regression analysis for spectral data of crude extracts as described by Gunarathne et al. (2022a). Initially, four replicates of 14 crude extracts were collected and followed by randomly dividing into two sets (i.e., 38 elements to use for calibration and cross-validation and 18 elements to test the predictive models). The predictive models were developed by using the total spectra range (3700-500 cm^{-1}) and different spectra ranges (A: 3700-2800 cm^{-1}; B: 1800-1700 cm^{-1}; C: 1700-1500 cm^{-1}; D: 1500-900 cm^{-1}: E: 900-500 cm^{-1}). The best predictive model for α-glucosidase inhibitory activity was identified by comparing the model parameters including, coefficient of determination of calibration (Rc^2), root mean square errors of calibration (RMSEC), coefficient of determination of prediction (Rp^2), root mean square errors of prediction (RMSEP), coefficient of determination of cross-validation (Rcv^2), root mean square errors of cross-validation (RMSECV).

3. Results and discussion

The spectral overlays given in Figures 1(A), (B), and (C) represent the characteristic bands of the plant extracts obtained from hexane, EtOAc, and MeOH, respectively. The aim of interpreting them was to characterize the organic functional groups as parameters for monitoring α-glucosidase inhibitory activity exhibited by the plants of this study. Assignments of spectral bands falling into different regions of the spectrum (A: 3700-2800 cm^{-1}; B: 1800-1700 cm^{-1}; C: 1700-1500 cm^{-1}; D: 1500-900 cm^{-1}: E: 900-500 cm^{-1}) were made to different organic functional groups based on previous reports listed in Tables 1 and 2.

3.1. Characterization of region A in 3700-2800 cm^{-1}

According to the overview shown in Figure 1(A), the spectral patterns of hexane extracts of the plants differed only slightly in different regions. Broad absorption peaks in the region 3500-3400 cm^{-1} were displayed by all plant extracts. According to Table 1, the broad blunt peak H1 centered at ~3440 cm^{-1} represents the O–H stretching vibration of phenols, alcohols, complex carbohydrates, etc. (Coates, 2000; Nandiyanto et al., 2019). The highest intensity was shown by KO while the lowest intensity was displayed by LE. The high intensity of the H1 peak confirmed the abundance of complex carbohydrates in the hexane extract of KO. On the other hand, the H1 peak appearing as a low-height peak in the hexane extract of LE would indicate a relatively lower amount of the above-mentioned molecules in LE. According to the spectral overlay of EtOAc extracts, as shown in Figure 1(B), the broad blunt peaks (E1) were now centered at ~3400 cm^{-1}, indicating a slight shift in frequency. All EtOAc extracts exhibited an enhancement in the peak intensity when compared to those of hexane extracts. Both KO and ST gave high intensity while others showed low intensity. As mentioned previously in the hexane extract of LE, the broad and low height peak (E1) appearing at 3400 cm^{-1} indicated comparatively lower amount of phenols, alcohols, and carbohydrates in the EtOAc extract of LE. The same was true for the EtOAc extract of KK. Nevertheless, the intensity of peak E1 of KO appearing at ~3400 cm^{-1} was slightly higher than that of peak H1 of KO, indicating the relatively higher abundance of phenols, alcohols, and carbohydrates in EtOAc extracts. The spectral overlay of MeOH extracts in Figure 1(C) shows that all plants exhibited the highest peak intensity for the broad blunt peak (M1), which was centered at ~3410 cm^{-1}. There was a huge enhancement effect on this peak (M1) when compared to those of either hexane or EtOAc extracts. This could be probably due to the fact that the concentration of carbohydrates, phenolics or aliphatic alcohols, etc. would have become high in MeOH extracts due to the effect of sequential extraction.

In the majority of the plant extracts, aliphatic chains occur as components of various biomolecules including lipids, carotenoids, etc. The occurrence of some amount of *cis* and *trans* double bonds as a part of alkenes is common in many cases. The spectral overlay of both hexane and EtOAc extracts as illustrated in Figures 1(A) and (B) gave evidence for the presence of a weak band corresponding to terminal (vinyl) C–H stretching vibration of alkenes. In Figure 1(B), peak E2 appearing at ~3010 cm^{-1} is usually ascribed to terminal (vinyl) C–H stretching of alkenes. Therefore, the high-intense E2 peak in the EtOAc extract of ST could be due to the high-presence of alkenes. According to the spectral overlay of MeOH extracts, as given in Figure 1(C), this weak band was masked due to overlapping caused by the broad blunt peaks (M1) which were centered at ~3410 cm^{-1}. It could also be noted that the influence of lipids with some degrees of unsaturation could be present more in both hexane and EtOAc extracts when compared to MeOH extracts.

The prominent H3 (at ~2925 cm^{-1}) and H4 (~2854 cm^{-1}) peaks in hexane extracts as shown in Figure 1(A) was due to the asymmetrical and symmetrical C–H stretching of methylene groups, respectively (Coates, 2000; Nandiyanto et al., 2019). According to previous studies, these two were quite commonly encountered in the spectra of major edible plant oils and animal fats (Gunarathne et al., 2022b). Among hexane extracts, ST was found to display high-intensity peaks for H3. Meanwhile, among hexane extracts, KK displayed a comparatively high-intense peak for H4. According to spectral overlay as illustrated in Figure 1(B), E3 and E4 peaks of EtOAc extracts were also assigned to the same spectral vibrations.

The prominence of these two peaks was probably due to the heavy presence of aliphatic chains attached to lipids, carotenoids, carbohydrates, and other ester compounds (Table 1). When considering the spectral intensities, the EtOAc extract of LE was found to exert relatively high intensity for peaks E4. As mentioned earlier, E4 confirmed the higher existence of CH_2 groups in the EtOAc extract of LE. A closer look at the spectral patterns illustrated in Figures 1(A) and (B) would suggest that the intensities of these two peaks of hexane extracts were a little higher than those of these two peaks in EtOAc extracts. According to spectral overlay as illustrated in Figure 1(C), the intensities of these two peaks sharply declined in all MeOH extracts. With the prominence of the broad blunt peak (M1) of MeOH extracts centered at ~3410 cm^{-1}, a decline in the intensities of M3 and M4 peaks was noticable. This could be partly due to decreases in the proportion of molecules with aliphatic chains in MeOH extracts after sequential extraction. According to previous studies, extraction with hexane and EtOAc could usually take away most of the lipid biomolecules (Gunarathne et al., 2022b). Among all MeOH extracts, intensities of M3 and M4 peaks of ST and KO were slightly higher than those of the rest of the plant extracts.

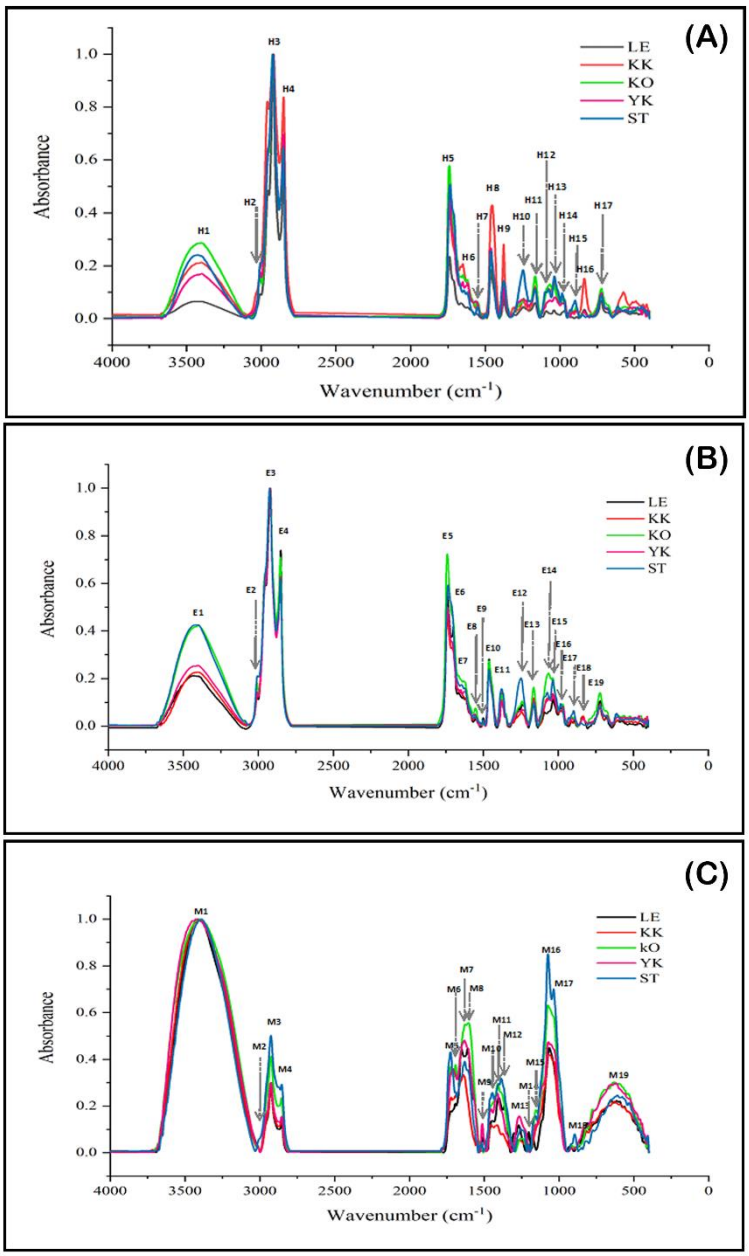

Figure 1. FTIR spectral overlay of hexane (A), ethyl acetate (B) and methanol (C) extracts of leafy plants

3.2. Characterization of region B in 1800-1700 cm^{-1}

The ester groups were always part of various biomolecules present in both hexane and EtOAc extracts. For instance, the majority of oils, fats, waxes, etc. are used to exhibit C=O stretching vibration due to ester groups present in acylglycerol molecules (Coates, 2000; Nandiyanto et al., 2019). According to the spectral overlays in Figures 1(A) and (B), in most of the plant extracts, there appeared the characteristic sharp peaks H5 and E5 centered at ~1742 cm^{-1}. Among hexane extracts, KO showed a high-intense for H5 peak while LE showed a low-intense peak at ~1742 cm^{-1} (H5). Among EtOAc extracts, the high-intense E5 peak denoted the comparatively higher existence of compounds with ester linkage and alkyl carbonates (Figure 1B). This difference could be probably due to the

relative differences in the abundance of compounds with ester linkage in these two types of extracts. According to Figure 1(C), peak M5 at 1730 cm^{-1} was present in all MeOH extracts, but their peak intensities were comparably lower than those of both hexane and EtOAc extracts. This observation suggests that a decrease happened in the proportion of molecules bearing ester functional groups in MeOH extracts with the sequential extraction. By contrast to hexane extracts, EtOAc extracts were found to have an additional peak E6 at ~1706-1712 cm^{-1}. Based on Table 1, this could be assigned to C=O stretching vibration associated with either carboxylic acids or ketones. For instance, a moderate-intense peak of E6 represented the moderate existence of carboxylic acids/ketones in the EtOAc extract of LE. The same is true for MeOH extracts, which also exhibited a peak (M6) at ~1706 cm^{-1} which would indicate the presence of C=O stretching vibration of either carboxylic acids or ketones. However, any peak in this wavenumber range (~1706 cm^{-1}) was not exhibited by the MeOH extract of ST. According to Figure 1(C), this peak in MeOH extracts is represented by M6 which appeared as a high-intense peak for both KO and YK.

Table 1. Characterization of FTIR spectra of hexane and EtOAc extracts of leafy plants

Peak no	Wavenumber range* (cm^{-1})	Mode of vibration	Functional group	Reference
H1, E1	3400-3440	O–H stretching	Carbohydrates/Phenols/Alcohols	(Coates, 2000; Nandiyanto et al., 2019)
H2, E2	3010-3013	Terminal (vinyl) C–H stretching	Alkenes	(Coates, 2000; Nandiyanto et al., 2019)
H3, E3	2925-2928	Methylene C–H asymmetric stretching	(CH_2) Alkanes	(Coates, 2000; Nandiyanto et al., 2019)
H4, E4	2852-2857	Methylene C–H symmetric stretching	(CH_2) Alkanes	(Coates, 2000; Nandiyanto et al., 2019)
H5, E5	1739-1745	C=O stretching	Ester groups/Alkyl carbonates	(Coates, 2000; Nandiyanto et al., 2019)
E6	1706-1712	C=O stretching	Carboxylic acids/Ketones	(Coates, 2000; Nandiyanto et al., 2019)
H6, E7	1630-1658	C=O stretching	Amides	(Coates, 2000; Nandiyanto et al., 2019; Nokhala et al., 2020)
		C=C skeletal stretching	Alkene	
		N-H bending	Primary/Secondary amines	
		–C=N– stretching	Imines	
		–N=N– stretching	Azo compounds	
H7, E8	1550-1565	> N–H bending	Secondary amines	(Coates, 2000; Nandiyanto et al., 2019; Nokhala et al., 2020)
		N=O asymmetric stretching	Aliphatic nitro compounds	
E9	1503-1506	C=C–C stretching	Aromatic rings	(Coates, 2000; Nandiyanto et al., 2019)
		NO_2 asymmetric stretching	Aromatic nitro compounds	
H8, E10	1459-1468	Methyl C–H asymmetric bending	Methyl C–H asymmetric bending-CH_3	(Coates, 2000; Nandiyanto et al., 2019)
		Methylene C–H bending	Methylene C–H bending CH_2	
H9, E11	1380-1383	N=O symmetric stretching	Aliphatic nitro compounds	(Hari & Nair, 2018; Nipun et al., 2020)
H10, E12	1247-1256	Aryl–O stretching	Aromatic ethers	(Coates, 2000; Nandiyanto et al., 2019; Saleh et al., 2018)
		C–N stretching	Aromatic primary amines	
H11, E13	1165-1171	C–N stretching	Secondary amines	(Coates, 2000; Nandiyanto et al., 2019)
H12, E14	1068-1080	C–N stretching	Primary amines	(Coates, 2000; Nandiyanto et al., 2019)
		C–O stretching	Ethers	
		C–O stretching	Cyclic ether	
H13, E15	1035-1044	C–O stretching	Primary alcohols	(Coates, 2000; Nandiyanto et al., 2019)
H14 + H15, E16 + E17	(976-988) + (900-918)	Vinyl C–H out-of-plane bending	Alkenes	(Coates, 2000; Nandiyanto et al., 2019)
H16, E18	838-841	Aromatic C–H out-of-plane bending (C–H 1,4-disubstitution-*para*)	Aromatic ring	(Coates, 2000; Nandiyanto et al., 2019)
H17, E19	723-726	Methylene-$(CH2)_n$-rocking	Hydrocarbon	(Coates, 2000; Nandiyanto et al., 2019)

*Range of variation in wavenumbers at a particular peak among the different edible leafy plants namely; *Le-kola pala, Kora kaha, Koppa, Yaki naran* and *Stevia*

3.3. Characterization of region C in 1700-1500 cm^{-1}

Distinct variations were seen in this range for different plant extracts as shown in Figures 1(A), (B) and (C). The occurrence of H6 and H7 was noticed in hexane extracts while the occurrence of E7, E8, and E9 was observed in EtOAc extracts. According to Figure 1(C), peaks M6, M7, M8, and M9 were found in this range for MeOH extracts. This indicated the effect of sequential extraction on chemical compositional changes of the plant extracts. Based on the information provided in Table 1, most of the hexane extracts were found to have the blunt peak (H6) at ~1655 cm^{-1}, which was attributed to C=O stretching of amides, C=C skeletal stretching of alkenes and C=N stretching of imines. The high-intensity peak of H6 could indicate the relatively high presence of amides and alkenes in the hexane extract of KK. The blunt peak E7 of EtOAc extracts appearing in the range of 1630-1633 cm^{-1} is usually assigned for C=O stretching of amides, C=C skeletal stretching of alkenes, N–H bending of primary and secondary amines, –C=N– stretching of open chain imines and –N=N– stretching of open chain azo compounds (Coates, 2000; Nandiyanto et al., 2019; Nokhala et al., 2020). Among EtOAc extracts, KO exhibited the high-intense peak of E7, indicating the high existence of amides, alkenes, primary amines/secondary amines, imines, and azo compounds. As shown in Figure 1(C), the peak M7 appeared within the range of 1633-1659 cm^{-1} is usually assigned to C=O stretching of amides, C=C skeletal stretching of alkenes, N–H bending of primary and secondary amines, –C=N– stretching of open chain imines (Coates, 2000; Nandiyanto et al., 2019; Nokhala et al., 2020). Among MeOH extracts, KO exhibited the high-intense peak of M7. According to Figure 1(C), among MeOH extracts, KO showed a high-intense peak for M8. The peak M8 is ascribed to the conjugated C=C stretching vibration of alkenes, C=C–C stretching of the aromatic ring, C=O stretching of carboxylates, N–H bending of primary and secondary amines, –C=N– stretching of open chain imines and –N=N– stretching of open chain azo compounds, which exhibited a peak at ~1603-1615 cm^{-1} (Coates, 2000; Nandiyanto et al., 2019; Nokhala et al., 2020). However, this peak did not occur in both hexane and EtOAc extracts.

As shown in Figure 1(A), the peak H7 appearing at ~1559 cm^{-1} is attributed to > N–H bending of secondary amines and N=O stretching of aliphatic nitro compounds (Coates, 2000; Nandiyanto et al., 2019; Nokhala et al., 2020). As illustrated in Figure 1(B), the peak E8 of EtOAc extracts, observed at ~1550 cm^{-1} indicated the presence of > N–H bending of secondary amines and N=O asymmetric stretching of aliphatic nitro compounds (Coates, 2000; Nandiyanto et al., 2019; Nokhala et al., 2020). Among EtOAc extracts, the highest intensity for E8 was displayed by KO, but none

of the crude extracts of MeOH was found to show a peak in the range of 1559-1550 cm^{-1}.

According to Table 1, the peak E9 (~1503 cm^{-1}) is usually ascribed to C=C–C stretching vibration and NO_2 asymmetric stretching vibration of aromatic rings and aromatic nitro compounds, respectively (Coates, 2000). Among EtOAc extracts, this peak appeared as a minute peak, indicating a relatively lower existence of aromatic rings and aromatic nitro compounds in EtOAc extracts. In the case of the MeOH extract of YK, a high-intensity peak was observed for M9. As the peak M9, appearing at ~1515 cm^{-1} would result due to C=C–C stretching of aromatic rings and NO_2 asymmetric stretching of aromatic nitro compounds, the high-intensity peak of M9 would indicate the higher existence of aromatic rings and aromatic nitro compounds in YK (Coates, 2000; Nandiyanto et al., 2019).

3.4. Characterization of region D in 1500-900 cm^{-1}

This particular region of the spectra (1500 cm^{-1}-900 cm^{-1}) is usually known by researchers as the fingerprint region. Hence, it is the region that gives spectral features which are unique to different materials. According to Figure 1(A), the narrow sharp peak (H8) existing at ~1459 cm^{-1} denotes the asymmetric C–H bending of methyl groups and C–H bending vibration of methylene groups in aliphatic chains. Among hexane extracts, KK displayed comparatively high-intense peak for H8. Again, the narrow sharp peak E10 observed among EtOAc extracts at ~1465 cm^{-1} indicates the asymmetric C-H bending of methyl groups and C–H bending vibration of methylene groups in aliphatic chains (Figure 1B). Among the crude EtOAc extracts, LE was found to exert relatively high intens peak for E10. The forgone discussion suggested that the number of lipid biomolecules gets reduced in MeOH extracts as a result of sequential extraction with hexane and EtOAc. Hence, the peak M10 appearing at ~1450 cm^{-1} among MeOH extracts is ascribed to the C=C–C stretching of aromatic rings (Coates, 2000; Nandiyanto et al., 2019). In Figure 1(A), peak M11 existing at ~1403 cm^{-1} would result due to either vinyl C–H in-plane bending vibration of alkenes or O–H bending of phenols/tertiary alcohols. As seen from Figures 1(A) and (C), this peak did not appear to emerge in both hexane or EtOAc extracts. Among MeOH extracts, both KO and ST showed high-intense peaks for M11.

As shown in Figure 1(A), peak H9 appearing at ~1380 cm^{-1} was attributed to the N=O symmetric stretching of aliphatic nitro compounds. This was further confirmed by the presence of aliphatic nitro compounds in hexane extracts of edible leafy plants (Hari & Nair, 2018; Nipun et al., 2020). For instance, a higher abundance of aliphatic nitro compounds in the hexane extract of KO was further confirmed by the high-intense peak H9 appearing at ~1380 cm^{-1}. In the case of EtOAc extracts, peak E11 represented N=O symmetric stretching vibration of aliphatic nitro compounds, in this ST showed a highly intense peak (Figure 1B). Among MeOH extracts, the peak M12 appearing at ~1370 cm^{-1} is attributed to both methyl C–H symmetric bending vibration and N=O symmetric stretching vibration, indicating the presence of alkanes and aliphatic nitro compounds. According to Figure 1(A), peak H10 found at ~1250 cm^{-1} indicates the aryl–O stretching of ethers and C–N stretching of aromatic primary amines in plants (Coates, 2000; Saleh et al., 2018). Among hexane extracts, ST was found to display a high-intense-peak for H10. The presence of a high-intense peak for H10 indicated a higher abundance of aromatic ethers and aromatic primary amines in the hexane extract of ST (White, 1971). Among EtOAc extracts, peak E12 centered at ~1250 cm^{-1} represented the aryl–O stretching of aromatic ethers and C–N stretching of aromatic primary amines in plants (Figure 1B) (Coates, 2000; Saleh et al., 2018). Among the five plants used in this study, ST exhibited the most intense E12 peak. Among MeOH extracts, the peak M13 appearing at ~1270 cm^{-1} is usually ascribed to the aryl–O stretching of aromatic ethers and the C–N stretching of aromatic primary amines. In addition to this, the in-plane blending of O–H of primary and secondary alcohols in plants also contributes to this (Coates, 2000; Saleh et al., 2018). As shown in Figure 1(C), peak M14 existing at 1206 cm^{-1} would result due to the C–O stretching of phenols (Nandiyanto et al., 2019). Among the MeOH extracts, only LE and ST displayed peak M14 (Figure 1C). However, this peak was not seen in any of the plant extracts from hexane and EtOAc (Figure 1B).

As described in Table 1, peak H11 at ~1168 cm^{-1} is generally assigned to the C–N stretching vibration of secondary amines. When compared to other plants, KO displayed a high-intense peak for H11 (Figure 1A). The high-intense peak for H11 would indicate the higher abundance of secondary amine in the hexane extract of KO. Among EtOAc extracts, the corresponding peak representing the presence of secondary amines in all plants is peak E13 (Figure 1B). Concerning E13, KO gave the highest intense peak. Nevertheless, among MeOH extracts, peak M15 appearing within the range of 1159-1174 cm^{-1} represented the C–N stretching of secondary/tertiary amines (Coates, 2000; Nandiyanto et al., 2019). Although all MeOH extracts showed this peak, their signals appeared as a weak-shoulder peak with some overlap.

As shown in Figure 1(A), peak H12 centered within the range of 1074-1080 cm^{-1} is supposed to represent the C–N stretching of primary amines, C–O stretching of alkyl-substituted ethers, and C–O stretching of cyclic ethers. When compared to other plants, the hexane extract of KO displayed high-intense peak for H12. The high-intensity peak of H12 denoted the higher existence of primary amines, alkyl substituted ethers, and cyclic ethers in KO. As elaborated in Table 2, the peak E14 appearing at 1068 cm^{-1} is ascribed to C–N stretching of primary amines, C–O stretching of alkyl substituted ethers, and cyclic ethers (Figure 1B). The low-intense peak E14 in LE at ~1068 cm^{-1} indicated the low levels of primary amines, ethers, and cyclic ethers in LE (Coates, 2000; Nandiyanto et al., 2019). According to Figure 1(C), the peak M16 of MeOH extracts was parallel to H12 of hexane extracts and E14 of EtOAc extracts. As elaborated in Table 2, those occuring within the range of 1068-1079 cm^{-1} would represent C–N stretching of primary amines and C–O stretching of alkyl-substituted ethers and cyclic ethers (Coates, 2000; Nandiyanto et al., 2019). Among MeOH extracts, ST exhibited the high-intense peak for M16.

As illustrated in Figure 1(A), peak H13 at ~1040 cm^{-1} is usually ascribed to the C–O stretching of primary alcohols (Nandiyanto et al., 2019). Among hexane extracts, ST exhibited the high-intense peak for H13, indicating the highest abundance of molecules with primary alcohols. As shown in Figure 1(B), E15 of EtOAc within the spectral region of 1035-1041 cm^{-1} represented the C–O stretching vibration of primary alcohols. Among the plants, both KO and ST displayed the high intense peak for this. According to Figure 1(C), peak M17 of MeOH extracts was parallel to peak H13 and E15 representing the C–O stretching vibration of primary alcohols which is present at the spectral range of 1038-1041 cm^{-1} (Coates, 2000). Among the plants, ST displayed the high-intensity peak for M17 indicating a higher abundance of primary alcohols in ST.

The peaks H14 and H15 within the spectral region from 988 cm^{-1} to 900 cm^{-1} represent the vinyl C–H out-of-plane bending of alkenes (Table 1). For H14 and H15, ST displayed high-intensity peaks while

LE displayed low-intensity minute peaks (Figure 1A). This is indicative of the differences between ST and LE with regard to the abundance of vinyl C–H out-of-plane bending vibration associated with alkenes. Among EtOAc extracts, the occurrence of E16 and E17 peaks within the spectral ranges of 976-988 cm^{-1} and 900-918 cm^{-1} confirmed the existence of vinyl C–H out-of-plane bending vibrations of alkenes (Figure 1B). KK exhibited low-intensity peaks for E16 and E17, indicating the lower abundance of vinyl C–H out-of-plane bending of alkenes. However, the occurrence of the peak corresponding to vinyl C–H out-of-plane bending of alkenes was hardly detected among MeOH extracts (Figure 1C).

Table 2. Characterization of FTIR spectra of MeOH extracts of leafy plants

Peak no	Wavenumber range* (cm^{-1})	Mode of vibration	Functional group	Reference
M1	3400-3440	O–H stretching	Carbohydrates/Phenols/Alcohols	(Coates, 2000; Nandiyanto et al., 2019)
M2	3010-3013	Terminal (vinyl) C–H stretching	Alkenes	(Coates, 2000; Nandiyanto et al., 2019)
M3	2928-2931	Methylene C–H asymmetric stretching	Alkanes (CH_2)	(Coates, 2000; Nandiyanto et al., 2019)
M4	2854-2860	Methylene C–H symmetric stretching	Alkanes (CH_2)	(Coates, 2000; Nandiyanto et al., 2019)
M5	1728-1733	C=O stretching	Esters	(Coates, 2000; Nandiyanto et al., 2019)
M6	1698-1715	C=O stretching	Carboxylic acids/Ketones	(Coates, 2000; Nandiyanto et al., 2019)
M7	1633-1659	C=O stretching	Amides	(Coates, 2000; Nandiyanto et al., 2019; Nokhala et al., 2020)
		C=C skeletal stretching	Alkene	
		N–H bending	Primary/Secondary amines	
		–C=N– stretching	Imines	
M8	1603-1615	Conjugated C=C stretching	Alkenes	(Coates, 2000; Nandiyanto et al., 2019; Nokhala et al., 2020)
		C=C–C stretching	Aromatic rings	
		C=O stretching	Carboxylates	
		N–H bending	Primary/Secondary amines	
		–C=N– stretching	Imines	
		–N=N– stretching of open chain azo compounds	Azo compounds	
M9	1515-1518	C=C–C stretching asymmetric stretching of NO_2	Aromatic rings	(Coates, 2000; Nandiyanto et al., 2019; Nokhala et al., 2020)
			Aromatic nitro compounds	
M10	1450-1459	C=C–C stretching	Aromatic rings	(Coates, 2000; Nandiyanto et al., 2019; Nokhala et al., 2020)
		Methyl C–H asymmetric bending	Alkanes (CH_3)	
		Methylene C-H bending	Alkanes (CH_2)	
M11	1403-1418	Vinyl C–H in-plane-bending	Alkenes	(Coates, 2000; Nandiyanto et al., 2019; Nokhala et al., 2020)
		OH bending	Phenol/Tertiary alcohols	
M12	1370-1390	Methyl C–H symmetric bending	Alkanes (CH_3)	(Hari & Nair, 2018; Nipun et al., 2020)
		N=O symmetric stretching	Aliphatic nitro compounds	
M13	1268-1271	Aryl–O stretching	Aromatic ethers	(Coates, 2000; Nandiyanto et al., 2019; Saleh et al., 2018)
		C–N stretching	Aromatic primary amines	
		OH in-plane bending	Primary or secondary alcohol	
M14	1206	C–O stretching	Phenols	(Nandiyanto et al., 2019)
M15	1159-1174	C–N stretching	Secondary/Tertiary amines	(Coates, 2000; Nandiyanto et al., 2019)
M16	1068-1079	C–N stretching	Primary amines	(Coates, 2000; Nandiyanto et al., 2019)
		C–O stretching	Ethers	
		C–O stretching	Cyclic ethers	
M17	1038-1041	C–O stretching of primary alcohols	Primary alcohols	(Coates, 2000; Nandiyanto et al., 2019)
M18	903-925	C–C skeletal vibration	Alkanes	(Coates, 2000; Nandiyanto et al., 2019)
M19	628-630	Alkyne C–H bending	Aromatic ring	(Coates, 2000; Nandiyanto et al., 2019)
		OH out-of-plane bending	Alcohol	

*Range of variation in wavenumbers at a particular peak among the different edible leafy plants namely; *Le-kola pala, Kora kaha, Koppa, Yaki naran* and *Stevia*

3.5. Characterization of region E below 900 cm^{-1}

As shown in Figure 1(A), peak H16 appearing at ~841 cm^{-1} was due to aromatic C–H out-of-plane bending vibration. Among hexane extracts, KK displayed a relatively high-intense peak for H16, probably due to the high occurence of molecules with aromatic rings in the hexane extract. In the case of the rest of the plant extracts, only a minute peak was seen for H16, indicating the lower abundance of aromatic C–H out-of-plane bending vibration. When considering EtOAc extracts, the peak E18 appearing at ~838 cm^{-1} represented aromatic C–H out-of-plane bending vibration (Figure 1A). However, peak corresponding to aromatic C–H out-of-plane bending of aromatics was not detected among MeOH extracts. According to Figure 1(A), the distinct narrow peak H17 appearing at ~723 cm^{-1} indicated the rocking vibration of the methylene group, confirming molecules with aliphatic hydrocarbon chains in hexane extracts (Coates, 2000; Nandiyanto et al., 2019). Among the plant extracts, KO displayed a high-intense peak for H17, which confirmed the abundance of complex carbohydrates in the hexane extract of KO. The distinct narrow peak E19 of Figure 1(B) existing at ~723 cm^{-1} represented the rocking vibration of the methylene group, confirming the presence of biomolecules with aliphatic hydrocarbon chains in EtOAc extracts (Coates, 2000; Nandiyanto et al., 2019). Here again, KO displayed a high-intense peak for E19 indicating the higher abundance of aliphatic hydrocarbons in the EtOAc extract of KO. However, this particular mode of vibration was non-existent among MeOH extracts. According to Figure 1(C), peak M18 existing at 903-925 cm^{-1} is usually assigned to C–C stretching vibrations of alkanes in the MeOH extracts (Nandiyanto et al., 2019). Among MeOH extracts, both ST and KK showed only a minute peak for M18 (~903-925 cm^{-1}), which indicated the comparatively lower abundance of C–C stretching vibrations of alkanes. Almost all MeOH extracts exhibited peak M19 at ~630 cm^{-1} which would result due to the alkyne C–H bending vibration of aromatic rings and O–H out-of-plane bending of alcohols (Coates, 2000; Nandiyanto et al., 2019). Both KO and YK showed high-intense peaks for M19.

3.6. α-Glucosidase inhibitory activity

The results of α-glucosidase inhibitory activities (IC_{50} values) of all crude plant extracts are presented in Table 3. Except the MeOH extract of KK, all crude plant extracts exerted some inhibitory activity against α-glucosidase. The higher inhibitory potentials, lower IC_{50} values were exhibited by most of the hexane extracts except KO and LE. Significant ($p < 0.05$) differences were exhibited by all hexane extracts for inhibitory activity (IC_{50} values) against α-

glucosidase enzyme, whereas the highest and the lowest activities were displayed by YK (IC_{50} = 7.71 ± 0.40 ppm) and KK (IC_{50} = 56.51 ± 1.26 ppm), respectively. Among EtOAc extracts, the IC_{50} values followed the order of LE < YK < ST < KK < KO, and no significant (p > 0.05) difference was seen between KK and ST. LE exhibited the strongest inhibitory activity against α-glucosidase with an IC_{50} value of 30.97 ± 0.45 ppm, while the lowest activity was exerted by KO. Among MeOH extracts, IC_{50} values followed the order of KO < LE < YK < ST < KK. KO displayed the strongest inhibitory activity (IC_{50} = 18.08 ± 0.27 ppm), while KK (IC_{50} > 2000 ppm) exhibited the weakest inhibitory activity. Establishing correlations between FTIR spectral data and α-glucosidase inhibitory activities of the plant extracts is in line with the objective of this study as to identify functional groups of the chemical constituents, responsible for α-glucosidase inhibitory activity of plant extracts.

Table 3. IC_{50} values of α-glucosidase inhibitory activities of different crude plant extracts[1]

Leafy plant type	IC_{50} value/ppm		
	Hexane	EtOAc	MeOH
LE	$37.58^{d,B}$ ± 1.05	$30.97^{a,A}$ ± 0.45	$42.7^{b,C}$ ± 2.12
KK	$56.51^{e,A}$ ± 1.26	$151.50^{c,B}$ ± 11.84	ND
KO	$31.72^{c,B}$ ± 0.13	$425.98^{d,C}$ ± 14.13	$18.08^{a,A}$ ± 0.27
ST	$21.79^{b,A}$ ± 0.81	$130.85^{c,B}$ ± 0.32	$225.57^{d,C}$ ± 8.85
YK	$7.71^{a,A}$ ± 0.40	$85.24^{b,B}$ ± 2.27	$125.14^{c,C}$ ± 5.41

[1] Each value in the table represents mean of three replicates ± standard deviation. Means that do not share a similar simple superscription letter in the same column and similar capital superscription letter in the same raw are significantly different at 95% confident (α = 0.05). Abbreviations: LE, *Le-kola pala*; KK, *Kora kaha*; KO, *Koppa*; ST, *Stevia*; YK, *Yaki naran*; ND, Not detected.

Table 4. Summary of PLS regression analysis performed for FTIR spectral data and α-glucosidase inhibitory activities of different crude plant extracts[1]

Model no	Region	Rc^2	RMSEC	Rcv^2	RMSECV	Rp^2	RMSEP
1	A	0.81	50.25	0.60	78.24	0.77	46.40
2	B	0.96	24.10	0.87	41.70	0.93	26.04
3	C	0.71	61.14	0.52	80.21	0.45	71.56
4	D	0.95	24.93	0.87	39.12	0.18	87.79
5	E	0.90	35.14	0.61	73.78	0.79	44.32
6	A, B, C, D, E	0.90	36.72	0.75	56.80	0.73	50.20
7	A, C	0.88	39.53	0.72	60.61	0.85	37.35
8	A, C, E	0.90	35.30	0.84	49.41	0.80	43.25
9	A, D, E	0.91	34.56	0.81	50.12	0.77	46.05
10	A, C, D, E	0.91	34.43	0.77	55.13	0.79	44.32
11	B, D, E	0.91	33.72	0.82	49.97	0.69	53.93
12	D, E	0.92	32.67	0.85	45.19	0.74	49.88
13	C, D, E	0.95	26.38	0.85	44.23	0.84	39.10
14	B, E	0.92	32.78	0.77	56.28	0.87	34.91

[1] A: 3700-2800 cm^{-1}, B: 1800-1700 cm^{-1}, C: 1700-1500 cm^{-1}, D: 1500-900 cm^{-1}, E: 900-500 cm^{-1}. Rc^2: Coefficient of determination of calibration, Rp^2: Coefficient of determination of prediction, Rcv^2: Coefficient of determination of cross validation, RMSEC: Root mean square errors of calibration, RMSEP: Root mean square errors of prediction, RMSECV: Root mean square errors of cross validation

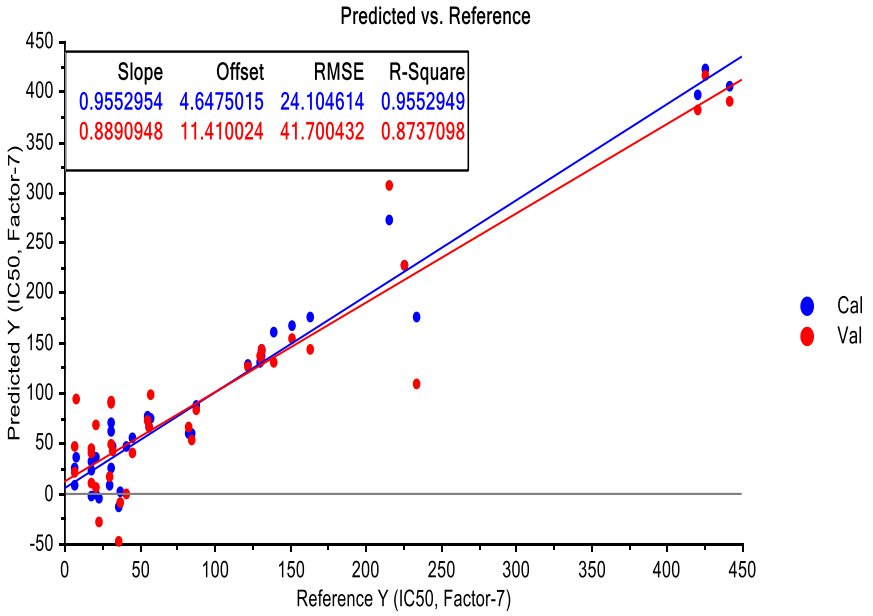

Figure 2. PLS regression (calibration and validation) curves of the best predictive model (Model 2)

3.7. PLS regression analysis

A summary of PLS regression analysis for FTIR spectral data and α-glucosidase inhibitory activities of different crude plant extracts is presented in Table 4. When considering the predictive models developed for individual spectral regions (A, B, C, D, and E), the highest Rc^2 (0.96), Rcv^2 (0.87), Rp^2 (0.93), and the lowest RMSEC (24.10), RMSECV (41.70), and RMSEP (81.04) values were noticed for "Model 2". Meanwhile, "Model 3" was found to show the lowest Rc^2 (0.71), Rcv^2 (0.52), and Rp^2 (0.45), and the highest RMSEC (61.14) and RMSECV (80.21). However, in the case of predictive models developed using selected multiple regions, the highest Rc^2 (0.95), Rcv^2 (0.85), Rp^2 (0.84), and the lowest RMSEC (26.38), and RMSECV (44.23) values were found for "Model 13". The calibration and validation curves for the best PLS regression prediction model "Model 2" are shown in Figure 2. According to PLS regression results, it was evident that the chemical compounds representing spectral region B have had a strong impact on the α-glucosidase inhibitory activity when compared to those of other spectral regions. The spectral region B, ranging from 1700-1800 cm^{-1}, actually represented the presence of chemical constituents with functional groups such as ester linkages, ketone groups, and carboxylic acids as mentioned previously in Tables 1 and 2. Interestingly, compounds with these functional groups which have a higher content of non-polar moieties with ester linkage are mostly present in both hexane and EtOAc extracts.

In these five edible plants, a group of chemical constituents called cinnamic acids, which include sinapic acid, ferulic acid, *p*-coumaric acid, and caffeic acid, are present. They are a common form of phenolic compounds, usually present in plants as esters of sugars and different organic acids (Vermerris & Nicholson, 2008). As described previously, the peak that appeared at ~1740 cm^{-1} would be due to the C=O stretching vibration of ester bonds resulting from these cinnamic acids. According to Pandi and Kalappan (2021), sinapic acid may be present in either the free form or as an ester group; the predominant sinapoyl ester present in leaves is sinapoyl malate. In addition, ferulic acid found in leafy plants can be also conjugated with mono-, di-, and poly-saccharides through ester-linkage (Mancuso & Santangelo, 2014). Ferreira et al. (2019) previously stated that *p*-coumaric acid usually esterifies either with long-chain alkyl alcohols or polysaccharides to produce water-insoluble conjugates of *p*-coumaric acid. In another study Vermerris and Nicholson (2008) found that caffeic acid conjugated with quinic acid through ester linkages to produce chlorogenic acid, which was also previously reported to exist in the five edible leafy plant types (Ulpathakumbura et al., 2023). Vermerris and Nicholson (2008) further mentioned that catechins could also be present in plant extracts in the form of gallic acid esters. Hence, it became evident that the compounds with ester-linkage would have a strong influence on the α-glucosidase inhibitory activity. Further to this, the peak at ~1700 cm^{-1} would results due to the C=O stretching vibration of ketones and carboxylic acids. These carboxylic acids could be hydroxy-benzoic acids present in the leafy plant extracts, which are characterized by the existence of a carboxyl group substituted on a phenol (Vermerris & Nicholson, 2008). The keto groups could also be present in heterocycle flavones such as quercetin, and kaemferol of leafy plants. Hence, it became evident that the compounds with ester-linkage, ketones, and carboxylic acids would have a strong impact on the α-glucosidase inhibitory activity of leafy plant extracts.

4. Conclusions

The FTIR spectral correlations with the anti-hyperglycemic effect of different solvent extracts of selected edible leafy plants of Sri Lanka were explored. All plant extracts exerted inhibitory activity against α-glucosidase except the MeOH extract of KK. Based on PLS regression analysis, a strong correlation was seen between α-glucosidase inhibitory activities of the plant extracts and FTIR spectral data. PLS regression results showed that the chemical constituents represented by the spectral region B (1800-1700 cm^{-1}) of the plants have had a strong relationship with the α-glucosidase inhibitory activity when compared to those of other spectral regions. This particular range (1700-1800 cm^{-1}) is usually ascribed to C=O stretching vibration of ester groups, ketones, or carboxylic acids. This study suggests that FTIR spectroscopic method together with PLS regression analysis can be further explored as an alternative rapid analytical tool for the detection of the anti-hyperglycemic effect of leafy-plant extracts.

Acknowledgments

The expert advice on plant identifcation by Dr. D.S.A. Wijesundera is greatfully acknowledged. The authors also gratefully acknowledge the financial support from National Institute of Fundamental Studies, Sri Lanka for this study.

Conflict of interest

The authors confirm that there are no known conflicts of interest.

Statement of ethics

In this study, no method requiring the permission of the "Ethics Committee" was used.

Availability of data and materials

All data generated or analyzed during this study are included in this published article.

Funding

This study was financially supported by National Institute of Fundamental Studies, Sri Lanka.

CRediT authorship contribution statement

Savani Ulpathakumbura: Formal analysis, Data curation, Methodology, Review & Editing, Writing original draft
Nazrim Marikkar: Conceptualization, Methodology, Project administration, Review & Editing, Writing-reviewing & Editing
Lalith Jayasinghe: Writing-reviewing & Editing

ORCID Numbers of the Authors

S. Ulpathakumbura: 0000-0001-8079-0118
N. Marikkar: 0000-0002-6926-2071
L. Jayasinghe: 0000-0003-1703-4154

Supplementary File

None.

Publisher's Note

All claims expressed in this article are solely those of the authors and do not necessarily represent those of their affiliated organizations, or those of the publisher, the editors and the reviewers. Any product that may be evaluated in this article, or claim that may be made by its manufacturer, is not guaranteed or endorsed by the publisher.

This is an open-access article distributed under the terms of the Creative Commons Attribution 4.0 International License (CC BY). The use, distribution or reproduction in other forums is permitted, provided the original author(s) and the copyright owner(s) are credited and that the original publication in this journal is cited, in accordance with accepted academic practice. No use, distribution or reproduction is permitted which does not comply with these terms.

References

Adina, C., Florinela, F., Abdelmoumen, T., & Carmen, S. (2010). Application of FTIR spectroscopy for a rapid determination of some hydrolytic enzymes activity on sea buckthorn substrate. *Romanian Biotechnological Letters, 15*(6), 5738-5744.

Ashokkumar, R., & Ramaswamy, M. (2014). Phytochemical screening by FTIR spectroscopic analysis of leaf extracts of selected Indian medicinal plants. *International Journal of Current Microbiology and Applied Sciences, 3*(1), 395-406.

Bhardwaj, M., Yadav, P., Dalal, S., & Kataria, S. K. (2020). A review on ameliorative green nanotechnological approaches in diabetes management. *Biomedicine & Pharmacotherapy, 127*, 110198.

Bunaciu, A. A., Aboul-Enein, H. Y., & Fleschin, S. (2011). Recent applications of fourier transform infrared spectrophotometry in herbal medicine analysis. *Applied Spectroscopy Reviews, 46*(4), 251-260.

Coates, J. (2000). Interpretation of infrared spectra, a practical approach. In R. A. Meyers (Ed.), *Encyclopedia of Analytical Chemistry*: US: John Wiley & Sons, Ltd.

De Souza Schmidt Goncalves, A. E., Lajolo, F. M., & Genovese, M. I. (2010). Chemical composition and antioxidant/antidiabetic potential of Brazilian native fruits and commercial frozen pulps. *Journal of Agricultural and Food Chemistry, 58*(8), 4666-4674.

Easmin, S., Sarker, M. Z. I., Ghafoor, K., Ferdosh, S., Jaffri, J., Ali, M. E., Mirhosseini, H., Al-Juhaimi, F. Y., Perumal, V., *et al.* (2017). Rapid investigation of α-glucosidase inhibitory activity of *Phaleria macrocarpa* extracts using FTIR-ATR based fingerprinting. *Journal of Food and Drug Analysis, 25*(2), 306-315.

Ediriweera, E., & Ratnasooriya, W. (2009). A review on herbs used in treatment of diabetes mellitus by Sri Lankan ayurvedic and traditional physicians. *Ayu, 30*(4), 373-391.

Ferreira, P. S., Victorelli, F. D., Fonseca-Santos, B., & Chorilli, M. (2019). A review of analytical methods for *p*-coumaric acid in plant-based products, beverages, and biological matrices. *Critical Reviews in Analytical Chemistry, 49*(1), 21-31.

Gunarathne, R., Marikkar, N., Mendis, E., Yalegama, C., Jayasinghe, L., Liyanage, R., & Jayaweera, S. (2022a). Bioactivity studies of different solvent extracts of partially defatted coconut testa obtained from selected coconut cultivars. *The Journal of Agricultural Sciences-Sri Lanka, 17*(1), 171-184.

Gunarathne, R., Marikkar, N., Mendis, E., Yalegama, C., Jayasinghe, L., & Ulpathakumbura, S. (2022b). Mid-IR Spectral Characterization and Chemometric Evaluation of Different Solvent Extracts of Coconut Testa Flour. *Journal of Food Chemistry and Nanotechnology, 8*(3), 69-75.

Gunarathne, R., Marikkar, N., Yalegama, C., & Mendis, E. (2022c). FTIR spectral analysis combined with chemometrics in evaluation of composite mixtures of coconut testa flour and wheat flour. *Journal of Food Measurement and Characterization, 16*(3), 1796-1806.

Hari, N., & Nair, V. P. (2018). FTIR spectroscopic analysis of leaf extract in hexane in *Jasminum azoricum* L. *Recent Research in Science and Technology, 4*(8), 170-172.

Jayaraj, S., Suresh, S., & Kadeppagari, R. K. (2013). Amylase inhibitors and their biomedical applications. *Starch-Stärke, 65*(7-8), 535-542.

Kazeem, M., Adamson, J., & Ogunwande, I. (2013). Modes of inhibition of α-amylase and α-glucosidase by aqueous extract of *Morinda lucida* Benth leaf. *BioMed Research International, 2013*, 527570.

Mancuso, C., & Santangelo, R. (2014). Ferulic acid: Pharmacological and toxicological aspects. *Food and Chemical Toxicology, 65*, 185-195.

Mittal, P., Goswami, M., & Airi, M. (2020). Phytochemical, FTIR and NMR Analysis of Crude Extract of *Duranta plumieri* leaves. *Journal of Pharmaceutical Sciences and Research, 12*(1), 182-185.

Nandiyanto, A. B. D., Oktiani, R., & Ragadhita, R. (2019). How to read and interpret FTIR spectroscope of organic material. *Indonesian Journal of Science and Technology, 4*(1), 97-118.

Nickavar, B., & Abolhasani, L. (2013). Bioactivity-guided separation of an α-amylase inhibitor flavonoid from *Salvia virgata*. *Iranian Journal of Pharmaceutical Research, 12*(1), 57-61.

Nipun, T. S., Khatib, A., Ahmed, Q. U., Redzwan, I. E., Ibrahim, Z., Khan, A. a. Y. F., Primaharinastiti, R., Khalifa, S. A., & El-Seedi, H. R. (2020). Alpha-glucosidase inhibitory effect of *Psychotria malayana* jack leaf: A rapid analysis using infrared fingerprinting. *Molecules, 25*(18), 4161.

Nokhala, A., Ahmed, Q. U., Saleh, M. S., Nipun, T. S., Khan, A. A. Y. F., & Siddiqui, M. J. (2020). Characterization of α-glucosidase inhibitory activity of *Tetracera scandens* leaves by fourier transform infrared spectroscopy-based metabolomics. *Advances in Traditional Medicine, 20*, 169-180.

Pandi, A., & Kalappan, V. M. (2021). Pharmacological and therapeutic applications of Sinapic acid—An updated review. *Molecular Biology Reports, 48*(4), 3733-3745.

Saleh, M. S., Siddiqui, M. J., Mat So'ad, S. Z., Roheem, F. O., Saidi-Besbes, S., & Khatib, A. (2018). Correlation of FT-IR fingerprint and α-glucosidase inhibitory activity of salak (*Salacca zalacca*) fruit extracts utilizing orthogonal partial least square. *Molecules, 23*(6), 1434.

Shobana, S., Sreerama, Y., & Malleshi, N. (2009). Composition and enzyme inhibitory properties of finger millet (*Eleusine coracana* L.) seed coat phenolics: Mode of inhibition of α-glucosidase and pancreatic amylase. *Food Chemistry, 115*(4), 1268-1273.

Ulpathakumbura, S., Marikkar, N., & Jayasinghe, L. (2023). Anti-oxidative, anti-hyperglycemic and anti-obesity properties of selected edible leafy plants of Sri Lanka. *Food Chemistry Advances, 2*, 100208.

Umar, A. H., Ratnadewi, D., Rafi, M., & Sulistyaningsih, Y. C. (2021). Untargeted metabolomics analysis using FTIR and UHPLC-Q-Orbitrap HRMS of two *Curculigo* species and evaluation of their antioxidant and α-glucosidase inhibitory activities. *Metabolites, 11*(1), 42.

Vermerris, W., & Nicholson, R. (2008). Families of Phenolic Compounds and Means of Classification. In W. Vermerris & R. Nicholson (Eds.), *Phenolic Compound Biochemistry* (pp. 1-34): Springer, Dordrecht.

White, J. L. (1971). Interpretation of infrared spectra of soil minerals. *Soil Science, 112*(1), 22-31.

Xiao-Ping, Y., Chun-Qing, S., Ping, Y., & Ren-Gang, M. (2010). α-Glucosidase and α-amylase inhibitory activity of common constituents from traditional Chinese medicine used for diabetes mellitus. *Chinese Journal of Natural Medicines, 8*(5), 349-352.

Int. J. Plant Bas. Pharm. (2023) 3(1), 114-122

INTERNATIONAL JOURNAL OF PLANT BASED PHARMACEUTICALS

https://ijpbp.com

RESEARCH ARTICLE

OPEN ACCESS

Antioxidant activity of extracts from *Xanthium strumarium* – A medicinal plant from the Kingdom of Lesotho

Manoharan Karuppiah Pillai[a,b*], Potlaki Thebe[b], Rets'epile Paul Matamane[b]

[a] *University of Eswatini, Faculty of Science & Engineering, Department of Chemistry, Kwaluseni Campus, Private Bag 4, Kwaluseni, M201 The Kingdom of Eswatini, Southern Africa*

[b] *National University of Lesotho, Faculty of Science & Technology, Department of Chemistry & Chemical Technology, Roma Campus, P.O. Roma 180, The Kingdom of Lesotho, Southern Africa*

ARTICLE INFO

Article History:

Received: 22 February 2023
Revised: 02 May 2023
Accepted: 10 May 2023
Available online: 23 May 2023

Edited by: B. Tepe

Keywords:

Xanthium strumarium
Asteraceae
DPPH assay
IC_{50} value
Total phenolic contents (TPCs)
Total flavonoid contents (TFCs)

ABSTRACT

Xanthium strumarium L. finds therapeutic applications in traditional medicines. The objective of the current study was to evaluate the antioxidant activity and to determine the total phenolic contents (TPCs) and total flavonoid contents (TFCs) of hexane, chloroform, ethyl acetate, acetone, methanol, and water extracts obtained from the leaves and stem bark of *X. strumarium*. Maceration and hot solvent extraction techniques were used to obtain various solvent extracts. 2,2-Diphenyl-1-picrylhydrazyl (DPPH) radical scavenging and ferric-reducing power assays were used to evaluate the antioxidant activity. Folin-Ciocalteu colorimetric and aluminum chloride colorimetric methods were used to determine the TPCs and TFCs, respectively. The extracts from the leaves and stem bark exhibited radical scavenging activity in the ranges of 18.06 ± 0.3-185.67 ± 11.54% and 9.13 ± 0.54-84.18 ± 0.92%, respectively at a concentration range of 200-3000 µg/ml. The positive control, ascorbic acid, exhibited radical scavenging activity in a range of 56.64 ± 1.26-88.98 ± 0.31% at a concentration range of 200-3000 µg/ml. Additionally, the IC_{50} values of all these extracts were determined. The hexane and chloroform extracts from both leaves and stem bark and methanol leaf extract were found to be the most potent extracts with an IC_{50} value of < 200 µg/ml for each extract. The IC_{50} value of positive control, ascorbic acid was determined to be < 200 µg/ml. Furthermore, in the ferric-reducing power assay, ethyl acetate extract from both leaves and stem bark exhibited the highest ferric-reducing power of 0.996 ± 0.101 and 0.947 ± 0.018 at a concentration of 100 µg/ml. Moreover, the methanol extract from the leaves showed the highest TPCs of 133.41 ± 3.23 mg GAE/g of DW of extract followed by the methanol extract from stem bark and the acetone extract from the leaves with TPCs of 121.21 ± 3.14 and 118.01 ± 1.85 mg GAE/g of DW of extract, respectively. Similarly, the methanol extract from the leaves also showed the highest TFCs of 20.61 ± 1.81 mg QE/g of DW of extract followed by the methanol extract from stem bark with TFCs of 14.90 ± 1.18 mg QE/g of DW of extract. From this study, we concluded that various extracts obtained from the leaves and stem bark of *X. strumarium* exhibited a moderate-to-strong radical scavenging activity and ferric-reducing power and possessed a significant amount of TPCs and TFCs.

1. Introduction

Xanthium strumarium L. belongs to the *Xanthium* genus of the Asteraceae family. *X. strumarium* finds therapeutic applications, which include in the treatment of diabetes, headache, skin itch, arthritis gastric ulcer, nasal sinusitis, bacterial infections, and inflammatory illnesses such as rhinitis and rheumatoid arthritis (Aranjani et al., 2013; Fan et al., 2019; Kamboj & Saluja, 2010; Kumar & Rajkapoor, 2010; Patil et al., 2012). *X. strumarium* has been found to exhibit several biological and pharmacological activities, which include cytotoxicity, anticancer, antitrypanosomal, antiulcerogenic, larvicidal and repellent, antihelmintic, antiarthritic, antinociceptive, antiinflammatory, diuretic, antioxidant, antibacterial and antilipidemic activities

Reviewed by:
Ozlem Erdal Altıntas: Afyonkarahisar Health Science University, Afyonkarahisar, Türkiye
Talha Bin Emran: BGC Trust University Bangladesh, Chittagong, Bangladesh

* Corresponding author(s):
E-mail address:
kmharan@rediffmail.com (M. Karuppiah Pillai)

e-ISSN: 2791-7509
doi: https://doi.org/10.29228/ijpbp.23

(Kim et al., 2005; Lin et al., 2014; Ly et al., 2021; Scherer et al., 2009; Sharifi-Rad et al., 2015; Sharma et al., 2003; Singh et al., 2009; Sridharamurthy et al., 2011; Talakal et al., 1995; Tenguria, 2013). However, some studies showed that *X. strumarium* causes intoxication and is even fatal to humans and cattle (Masvingwe & Mavenyengwa, 1998; Turgut et al., 2005). For example, the seeds of *X. strumarium* cause multiple organ dysfunctions in humans, which include centrilobular hepatic necrosis in the liver, renal proximal tubular necrosis, and cardiac damage (Turgut et al., 2005). The poisonous component isolated and identified in the seeds of *X. strumarium* was carboxyatractyloside (CAT) (Cole et al., 1980; Turgut et al., 2005). Our literature search showed that the antioxidant activity of various extracts from various parts of *X. strumarium* has previously been reported. For example, chloroform, ethanol, and methanol extracts obtained from the roots of *X. strumarium* and 80% methanol, 85% methanol, 98% methanol, 80% ethanol, ethyl acetate, and chloroform/dichloromethane (1:1) extracts obtained from the leaves of *X. strumarium* have previously been reported for their DPPH radical scavenging activity (Guemmaz et al., 2018; Ishwarya & Singh, 2010; Rad et al., 2013; Scherer & Godoy, 2014; Sridharamurthy et al., 2011; Subba & Gaire, 2022). Other solvent extracts such as hexane, acetone, and water extracts of *X. strumarium* have not been investigated so far, especially the species collected in the Kingdom of Lesotho. Therefore, in the present study, we aimed to evaluate the antioxidant activity and ferric-reducing power of various solvent extracts obtained from the leaves and stem bark of *X. strumarium* collected in the Kingdom of Lesotho. Additionally, we also aimed to determine the total phenolic contents (TPCs) and total flavonoid contents (TFCs) of these solvent extracts obtained from the leaves and stem bark of *X. strumarium*. 2,2-Diphenyl-1-picrylhydrazyl (DPPH) radical scavenging assay and ferric reducing power assay were used to evaluate the antioxidant activity. In addition, the IC_{50} values of these solvent extracts were also determined by using DPPH radical scavenging assay. The TPCs and TFCs of these solvent extracts were determined by Folin-Ciocalteu colorimetric method and aluminum chloride colorimetric method, respectively, and the results are summarized in this article.

2. Materials and methods

2.1. Plant material

The plant material viz. fresh leaves and stem bark of *X. strumarium* were collected in January 2022 inside the Roma Campus of the National University of Lesotho (NUL), Lesotho, Southern Africa. Dr. Seleteng-Kose, Department of Biology, NUL, identified the plant material. A voucher specimen viz. Potlaki/XSLS/2022 and Potlaki/XSSB/2022 for leaves and stem bark, respectively, were kept separately at Organic Research Laboratory, Department of Chemistry & Chemical Technology, Faculty of Science & Technology (FoST), NUL, Roma Campus, Maseru, the Kingdom of Lesotho, Southern Africa.

2.2. Processing of plant material

The plant material was air-dried separately at room temperature for two weeks and then ground into powder using a blender (Waring Blender, Model HGB2WT93, 240V AC, 3.5 AMPs). Approximately, 1.850 and 1.800kg of powdered leaves and stem bark, respectively, were obtained.

2.3. Preparation of plant extracts

A mass of 250 g of powdered leaves was extracted with hexane for 24 hours at room temperature using a mechanical shaker. Using a vacuum filter (ATB, Model: 284065-H, Power: 230V 3.0A, 1320/min 50 Hz), the solution was filtered and the solvent was removed using a Buchi rotavapor. The hexane crude extract thus obtained was transferred to a pre-weighed beaker. The leaf powder was recovered from the above process and was extracted again with hexane at reflux conditions for 24 hours. A total mass of 4.576 g of combined hexane crude extract was obtained. The same procedure was followed separately to obtain crude extracts from other solvents. A mass of 8.098, 62.687, 6.262, 26.371, and 26.612 g chloroform, ethyl acetate, acetone, methanol, and water crude extracts was obtained, respectively, from 250, 250, 250, 250, and 95 g of powdered leaves. Similarly, 1.224, 0.865, 4.547, 2.242, 34.414, and 8.994 g of hexane, chloroform, ethyl acetate, acetone, methanol, and water stem-bark crude extracts were obtained, respectively, from 250, 250, 250, 250, 250 and 90 g of powdered stem-bark.

2.4. Chemicals used

Analytical reagents (AR) grades of solvents viz. methanol, ethyl acetate, chloroform, and hexane, AR grades of chemicals such as gallic acid *tris*-(hydroxymethyl) aminomethane and Folin-Ciocalteu reagent were obtained from Sigma-Aldrich. 2,2-Diphenyl-1-picrylhydrazyl and ascorbic acid were obtained from Prestige Laboratory Supplies. Sodium hydroxide, disodium hydrogen carbonate, and sodium dihydrogen phosphate were purchased from Minema Ltd. Aluminium chloride and sodium carbonate were obtained from Associated Chemical Enterprises. Trichloroacetic acid and ferric chloride were purchased from BDH Chemicals Ltd. Sodium phosphate and sodium nitrite was obtained from Saarchem Pty Ltd. Potassium ferricyanide, quercetin, and sodium carbonate was purchased respectively from Holpro Analytics Pty Ltd, Acros Organics and Radchem Laboratory Supplies.

2.5. DPPH radical scavenging activity and determination of IC_{50} values

The evaluation of antioxidant activity and the determination of IC_{50} values of various extracts obtained from the leaves and stem bark of *X. strumarium* were achieved DPPH radical scavenging assay by using the method described in the literature (Pillai & Magama, 2020; Pillai et al., 2018; Sixtus & Pillai, 2022). The preparation of stock solutions of each extract and positive control, ascorbic acid (3.0 mg of each extract or ascorbic acid in 1.0 ml of 50% methanol, v/v) and further dilutions from each of these stock solutions (3000, 2000, 1500, 1000, 800, 500, and 200 µg/ml), the preparation of negative control (50% methanol blank solution, v/v) and rest of the experimental procedure were as per the details outlined in the literature (Sixtus & Pillai, 2022). Briefly, 3.94 mg of DPPH dissolved in 100 ml of methanol was served as an oxidant solution. The test solution consisted of 0.1 ml of each extract solution or positive control, 1.0 ml of 0.1 mM DPPH antioxidant solution, and 0.45 ml of 50 mM Tris-HCL buffer at pH 7.4. The absorbance of the mixture was measured at 517 nm after 30 min incubation. All experiments were conducted in triplicates and the results were reported as the average value of three experiments. The percentage of DPPH radical scavenging activity was calculated by the equation:

$$DPPH\ Scavenged\ (\%) = \frac{A_{Cont} - A_{Test}}{A_{Cont}} x\ 100$$

where A_{test} = Absorbance of extract solution or positive control, A_{cont} = Absorbance of negative control. The IC_{50} value of each extract and positive control were also determined as per the procedure outlined in the literature (Sixtus & Pillai, 2022), i.e. by plotting extract concentrations versus the percentage inhibition of DPPH radical,

which was obtained by averaging three experimental values (Sixtus & Pillai, 2022).

2.6. Ferric reducing power assay

The evaluation of the ferric-reducing power of various extracts obtained from the leaves and stem bark of *X. strumarium* was carried out using a method described in the literature (Sixtus & Pillai, 2022). The preparation of stock solutions of each extract and positive control, ascorbic acid (0.2 mg of each extract or ascorbic acid in 1.0 ml of methanol), further dilutions from each of these stock solutions (5, 10, 20, 40, 80, and 100 µg/ml), the preparation of negative control (50% methanol blank solution, v/v) and rest of the experimental procedure were as per details outlined in the literature (Sixtus & Pillai, 2022). Briefly, the reaction mixture consisted of 2.0 ml of each solution of extract or ascorbic acid, 2.0 ml of 0.2 M phosphate buffer at pH 6.6, and 2.0 ml of 0.01% potassium ferricyanide solution. A volume of 2.0 ml of 0.1% trichloroacetic acid was added to the reaction mixture after 20 minutes of incubation at 50 °C. The supernatant was collected separately after centrifugation of the mixture at 3000 rpm for 10 minutes. An aliquot of each supernatant was mixed separately with 2.0 ml of freshly prepared 0.1% ferric chloride solution and then 2.0 ml of distilled water was added. The absorbance of the content was measured at 700 nm after allowing the reaction mixture to stand for 10 minutes. Ferric reducing power is the ability of an extract or pure compound to reduce Fe (III) to Fe (II) (Sixtus & Pillai, 2022). The ability of this ferric-reducing power is indicated by the formation of Prussian blue coloration and is measured at 700 nm. All experiments were conducted in triplicates and the results were reported as the average value of three experiments. The higher value of absorbance means a higher ferric reducing the power of an extract or pure compound and vice versa.

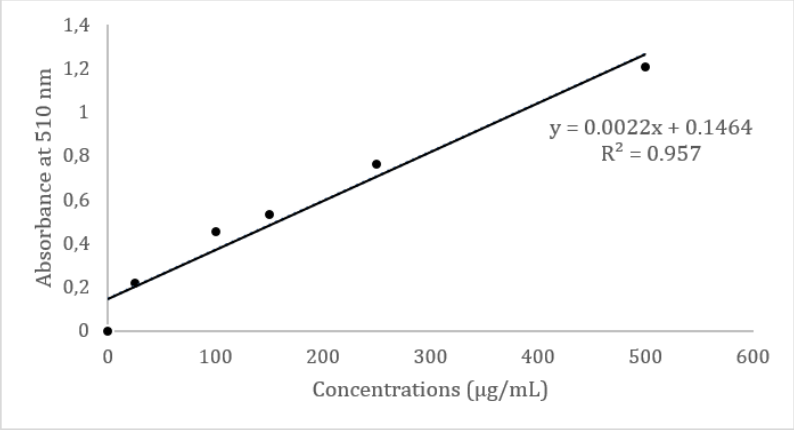

Figure 1. Calibration curve of gallic acid used to determine TPCs of various extracts

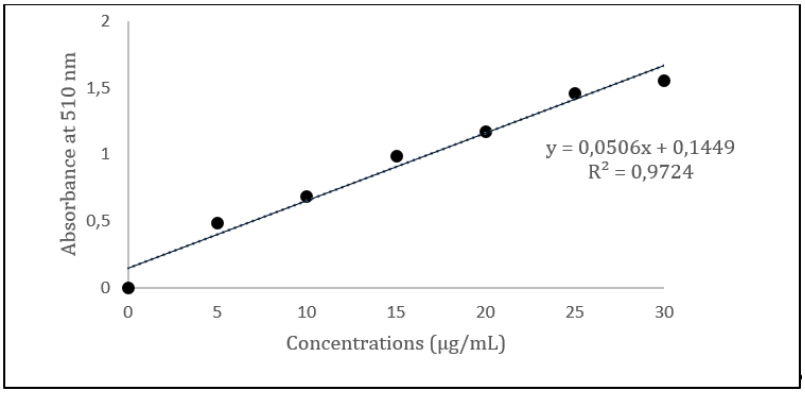

Figure 2. Calibration curve of quercetin used to determine TFCs of various extracts

2.7. Determination of total phenolic contents (TPCs)

Folin-Ciocalteu colorimetric method was employed to determine the TPCs of various extracts obtained from the leaves and stem-bark of *X. strumarium* as per literature (Sixtus & Pillai, 2022). Gallic acid served as a standard to get a calibration curve (Figure 1). The preparation of a test solution of each extract (10 ml at a concentration of 1000 µg/ml in 50% methanol, v/v), a stock solution of gallic acid (1000 µg of gallic acid in 1.0 ml of 50% methanol, v/v), further dilutions from the stock solution of gallic acid (750, 500, 250, 150, 100 and 25 µg/ml), the preparation of negative control (50% methanol blank solution, v/v) and rest of the experimental procedure were as per details outlined in the literature (Sixtus & Pillai, 2022). Briefly, an aliquot of 0.3 ml of each extract solution or gallic acid solution was mixed separately with 2.5 ml of 10% (v/v) Folin-Ciocalteu reagent followed by the addition of 5 ml of 7.5% sodium carbonate. The reaction mixture was incubated at room temperature in the dark for a period of 2 hours. The absorbance of each of these mixtures was measured at 510 nm. All experiments were carried out in triplicates and the results were reported as the average value of three determinations. The gallic acid calibration plot was employed to estimate the total phenolic contents of each extract and is expressed as mg GAE/g DW. The calibration curve of

gallic acid (y = 0.0022x + 0.1454; R^2 = 0.957) in a concentration range of 100-600 µg/ml is given in Figure 1.

2.8. Determination of total flavonoid contents (TFCs)

The aluminum chloride colorimetric method was employed to determine the TFCs of various extracts obtained from the leaves and stem bark of *X. strumarium* as per the literature (Sixtus & Pillai, 2022). Quercetin served as a standard to get a calibration curve (Figure 2). The preparation of a test solution of each extract (10 ml at a concentration of 1000 µg/ml in 50% methanol, v/v), a stock solution of quercetin (100 µg in 1.0 ml of, 50% methanol, v/v), further dilutions from this quercetin stock solution (30, 25, 20, 15, 10 and 5 µg/ml), the preparation of negative control (50% methanol blank solution, v/v) and the rest of the experimental procedure were as per the details outlined in the literature (Sixtus & Pillai, 2022). Briefly, an aliquot of 0.3 ml of each extract solution or quercetin solution was mixed separately with 0.3 ml of 5% sodium nitrite followed by the addition of 0.3 ml of 10% aluminum chloride after a 5 minutes interval. The reaction mixture was allowed to stand for a minute and a volume of 2 ml of 1.0 M sodium hydroxide and 6 ml of deionized water was added. The absorbance of each mixture was measured at 510 nm. All experiments were carried out in triplicates and the results were reported as the average value of three determinations. The quercetin calibration curve was employed to determine the total flavonoid contents of each extract and is expressed as mg QE/g DW. The calibration curve of quercetin (y = 0.0506x + 0.1449; R^2 = 0.9724) in a concentration range of 5-30 µg/ml is given in Figure 2.

2.9. Statistical analysis

Statistical analysis was performed using SPSS software version 28.0.0.0 for DPPH radical scavenging assay and SPSS v23.0 two-way analysis of variance (ANOVA) for ferric reducing power assay. The differences were statistically significant when $p \leq 0.05$.

3. Results and discussion

3.1. Evaluation of various extracts for their DPPH radical scavenging activity and determination of their IC_{50} values

The following twelve extracts were prepared from leaves and stem bark of *X. strumarium*. Hexane leaf extract (E1), chloroform leaf extract (E2), ethyl acetate leaf extract (E3), acetone leaf extract (E4), methanol leaf extract (E5), water leaf extract (E6), hexane stem bark extract (E7), chloroform stem bark extract (E8), ethyl acetate stem bark extract (E9), acetone stem bark extract (E10), methanol stem bark extract (E11) and water stem bark extract (E12). The result of the DPPH radical scavenging activity of all these twelve extracts (E1-E12) and the positive control, ascorbic acid are summarised in Tables 1 and 2. Ascorbic acid showed the highest radical scavenging activity of 88.98 ± 0.31% at a concentration of 3000 µg/ml (Tables 1 and 2). The leaf extracts showed the following order of scavenging activity: E1 > E2 > E5 > E4 > E3 > E6 (Tables 1 and 2). Extract, E1 showed the highest scavenging activity followed by E2 and E5, E4, E3, and E2 at a concentration of 3000 µg/ml (Tables 1 and 2). Similarly, the stem bark extracts exhibited the following order of scavenging activity: E8 > E10 > E7 > E9 > E11 > E12 (Tables 1 and 2). Extract, E8 showed the highest scavenging activity followed by E7, E10, E9, E11, and E12 at a concentration of 3000 µg/ml (Tables 1 and 2). Overall, all extracts (E1-E12) showed a moderate-to-significant radical scavenging activity albeit relatively lower than the positive control, ascorbic acid. Extracts, E1, E2, E5, and E8 showed > 80% scavenging activity at a concentration of 3000 µg/ml, which was comparable to positive control. The radical scavenging potential of these twelve extracts (E1-E12) and ascorbic acid are also shown in the bar diagrams for ease of comparison (refer to Figure 3 and Figure 4).

Additionally, the IC_{50} values of E1-E12 and ascorbic acid were determined and are summarised in Tables 1 and 2. The IC_{50} values of E1-E12 were determined to be < 200, < 200, 1856.02, 212.14, < 200, < 200, 2465.21, < 200, < 200, 1575.34, 256.74, 1939.04, and > 3000 µg/ml, respectively. The IC_{50} value of positive control, ascorbic acid, was determined to be < 200 µg/ml. This result showed that the leaf extracts viz. E1, E2, and E5 were found to be the most potent and their IC_{50} values were found to be < 200 for each extract, which was similar to positive control. Extracts, E4, E3, and E6 showed IC_{50} values of 212.14, 1856.02, and 2465.21 µg/ml, respectively. Similarly, the stem bark extracts viz. E7 and E8 were found to be the most potent and their IC_{50} value was found to be < 200 for each extract, which was similar to positive control. Extracts, E10, E9, E11, and E12 showed IC_{50} values of 212.14, 1856.02, 2465.21, and > 3000 µg/ml, respectively. Extract, E12 showed the lowest scavenging activity among all extracts with an IC_{50} value of > 3000 µg/ml. Overall, E1, E2, E5 E7, and E8 were identified as the most potent extracts with IC_{50} value of < 200 for each extract (Tables 1 and 2).

Various solvent extracts obtained from various parts of *X. strumarium* collected in different locations in several countries have previously been investigated for their DPPH free radical scavenging activity. For example, in a previous study, the dried roots of *X. strumarium* have been procured from a local market in the Karnataka State of India (Sridharamurthy et al., 2011). Chloroform and 90% ethanolic crude extracts have been obtained from these dried roots by cold maceration and Soxhlet apparatus methods, respectively (Sridharamurthy et al., 2011). The IC_{50} values of the chloroform and 90% ethanolic extracts have been determined to be 29.81 ± 0.95 and 24.85 ± 2.49 µg/ml, respectively in the DPPH radical scavenging assay (Sridharamurthy et al., 2011). Similarly, in another study, the roots of *X. strumarium* have been collected in the Tambaram area of Chennai, India (Ishwarya & Singh, 2010). Chloroform and methanolic crude extracts have been obtained from the dried roots by cold percolation and Soxhlet apparatus methods, respectively. The IC_{50} values of the chloroform and methanolic crude extracts have been determined to be 10.28 ± 0.69 and 40.40 ± 0.19 µg/ml, respectively in the DPPH radical scavenging assay (Ishwarya & Singh, 2010). Additionally, several fractions obtained from these chloroform and methanolic crude extracts have exhibited IC_{50} values in the ranges of 51.05 ± 3.61-180.40 ± 2.69 and 63.83 ± 0.23-184 ± 2.69 µg/ml, respectively in the DPPH radical scavenging assay (Ishwarya & Singh, 2010). In another study, the leaves of *X. strumarium* were collected in 2021 in the Arghakhanchi District of Nepal (Subba & Gaire, 2022). A methanolic crude extract has been obtained from the dried leaves by cold percolation method at room temperature and this methanolic extract exhibited an IC_{50} value of 258.10 µg/ml in the DPPH radical scavenging assay (Subba & Gaire, 2022). In another study, the leaves of *X. strumarium* were collected between August and September 2012 in the Baluchestan Province of Iran (Rad et al., 2013). An 85% methanolic extract has been obtained from the dried leaves by heating the content in a water bath at 25 °C for 24 hours with the help of a mechanical shaker (Rad et al., 2013). This 85% methanolic extract exhibited an IC_{50} value of 90 ± 0.01 µg/ml in the DPPH radical scavenging assay (Rad et al., 2013). In another study, the leaves of *X. strumarium* were collected in April 2014 on the farm of the Faculty of Agricultural Engineering, State University of Campinas, Campinas, Sao Paulo, Brazil (Scherer & Godoy, 2014). 80% ethanol, 80%

methanol, ethyl acetate, and chloroform/dichloromethane (1:1) extracts have been obtained from the air-dried leaves using static maceration, dynamic maceration and Soxhlet apparatus methods (Scherer & Godoy, 2014). The 80% ethanol extracts obtained from the static maceration, dynamic maceration, and Soxhlet apparatus methods were found to exhibit IC_{50} values of 47.83 ± 1.40, 53.01 ± 1.20 and 53.34 ± 1.52 µg/ml, respectively in the DPPH radical scavenging assay (Scherer & Godoy, 2014). However, the 80% methanol extracts obtained from the static maceration, dynamic maceration, and Soxhlet apparatus were found to demonstrate IC_{50} values of 44.94 ± 1.06, 45.05 ± 1.15 and 43.53 ± 1.61 µg/ml, respectively in the DPPH radical scavenging assay (Scherer & Godoy, 2014). Furthermore, the ethyl acetate extracts obtained from the static maceration, dynamic maceration, and Soxhlet apparatus methods showed IC_{50} values of 346.35 ± 16.50, 369.83 ± 13.58 and 423.97 ± 22.27 µg/ml, respectively in the DPPH radical scavenging assay (Scherer & Godoy, 2014). On the other hand, the chloroform/dichloromethane (1:1) extracts obtained from the static maceration and dynamic maceration presented IC_{50} values of 657.10 ± 24.01 and 674.61 ± 28.57 µg/ml, respectively (Scherer & Godoy, 2014). In another study, the leaves of *X. strumarium* were collected in July-August 2013 in Beni Aziz (Setif), Algeria (Guemmaz et al., 2018). A 98% methanolic crude extract has been obtained from the dried leaves by cold percolation method at room temperature and this 98% methanolic extract showed an IC_{50} value of 84.00 ± 0.0003 µg/ml in the DPPH radical scavenging assay. The chloroform, ethyl acetate, and aqueous fractions obtained from this 98% methanolic extract have demonstrated IC_{50} values of 234.00 ± 0.017, 17.00 ± 0.0004 and 46.00 ± 0.0006 µg/ml, respectively in the DPPH radical scavenging assay (Guemmaz et al., 2018).

Table 1. Percentage inhibition of DPPH radical scavenging activity of various extracts from leaves and stem-bark of *X. strumarium*

Extracts	Concentrations (µg/ml)/Inhibition (%)						
	200	500	800	1000	1500	2000	3000
E1	48.11 ± 3.86^{c}	53.04 ± 1.28^{e}	56.32 ± 2.18^{f}	62.15 ± 6.30^{f}	70.92 ± 2.99^{e}	76.48 ± 2.64^{d}	85.67 ± 11.54^{f}
E2	63.21 ± 0.09^{a}	65.57 ± 0.05^{b}	70.92 ± 0.09^{b}	74.94 ± 0.14^{a}	80.48 ± 0.14^{a}	82.26 ± 0.09^{a}	84.89 ± 0.27^{b}
E3	18.06 ± 0.31^{b}	26.77 ± 0.18^{a}	34.10 ± 1.03^{b}	43.76 ± 0.27^{b}	46.39 ± 0.34^{a}	55.59 ± 0.09^{a}	62.59 ± 0.09^{a}
E4	47.87 ± 0.09^{a}	52.60 ± 0.18^{b}	56.41 ± 0.14^{a}	58.75 ± 0.34^{a}	68.38 ± 0.34^{a}	74.05 ± 0.14^{a}	78.46 ± 0.18^{a}
E5	53.58 ± 0.14^{a}	60.37 ± 0.18^{a}	71.87 ± 0.18^{a}	73.94 ± 0.09^{a}	76.60 ± 0.09^{a}	80.28 ± 0.14^{a}	84.54 ± 0.27^{b}
E6	20.27 ± 0.22^{b}	23.20 ± 0.14^{a}	29.55 ± 0.27^{b}	36.79 ± 0.09^{a}	42.26 ± 0.14^{a}	48.08 ± 0.14^{a}	51.57 ± 0.18^{a}
E7	51.50 ± 1.01^{c}	57.39 ± 1.25^{d}	61.08 ± 0.35^{a}	62.80 ± 1.24^{c}	65.07 ± 0.41^{c}	66.05 ± 0.23^{b}	67.67 ± 2.09^{d}
E8	50.98 ± 0.46^{a}	56.29 ± 0.46^{b}	62.41 ± 0.31^{a}	71.07 ± 0.36^{a}	80.03 ± 0.10^{a}	82.99 ± 0.20^{b}	84.18 ± 0.92^{c}
E9	20.26 ± 0.44^{a}	35.93 ± 0.22^{a}	38.21 ± 0.23^{a}	46.01 ± 0.55^{a}	49.94 ± 0.44^{b}	63.03 ± 0.54^{c}	65.72 ± 0.18^{a}
E10	47.16 ± 0.49^{b}	47.99 ± 0.22^{a}	56.86 ± 0.14^{a}	62.23 ± 0.09^{b}	68.41 ± 0.14^{b}	73.73 ± 0.18^{a}	76.98 ± 0.59^{b}
E11	17.97 ± 0.41^{b}	27.22 ± 0.15^{a}	33.75 ± 0.18^{b}	41.78 ± 0.22^{d}	47.78 ± 0.09^{c}	54.26 ± 0.09^{a}	59.84 ± 0.09^{a}
E12	9.13 ± 0.54^{c}	12.12 ± 0.28^{c}	18.20 ± 0.14^{a}	21.69 ± 0.14^{a}	27.01 ± 0.18^{a}	35.52 ± 0.18^{b}	43.03 ± 0.18^{a}
Asc. acid	56.64 ± 1.26^{d}	65.69 ± 0.39^{a}	74.29 ± 0.09^{a}	77.33 ± 1.33^{d}	82.89 ± 0.09^{a}	84.78 ± 0.14^{a}	88.98 ± 0.31^{b}

E1 = hexane leaf extract, E2 = chloroform leaf extract, E3 = ethyl acetate leaf extract, E4 = acetone leaf extract, E5 = methanolic leaf extract, E6 = water leaf extract, E7= hexane stem bark extract, E8 = chloroform stem bark extract, E9 = ethyl acetate stem bark extract, E10 = acetone stem bark extract, E11 = methanolic stem bark extract, E12 = water stem bark extract, Asc. acid = Ascorbic acid, TFCs = Total flavonoid contents, TPCs = Total phenolic contents, N/A = Not applicable. Values with different superscript letters are statistically different within column.

Table 2. IC_{50} values, TPCs and TFCs of various extracts from leaves and stem-bark of *X. strumarium*

Extracts	IC_{50} (µg/ml)	TPCs (mg GAE/g DW)	TFCs (mg QE/g DW)
E1	< 200	4.03 ± 0.34	0.73 ± 0.03
E2	< 200	54.11 ± 1.16	5.04 ± 1.08
E3	1856.02	59.98 ± 2.01	3.01 ± 1.16
E4	212.14	118.01 ± 1.85	11.63 ± 2.32
E5	< 200	133.41 ± 3.23	20.61 ± 1.81
E6	2465.21	35.92 ± 5.00	1.20 ± 0.34
E7	< 200	6.89 ± 1.73	1.00 ± 0.78
E8	< 200	38.04 ± 0.88	3.76 ± 1.26
E9	1575.34	61.46 ± 1.11	3.91 ± 1.17
E10	256.74	60.80 ± 6.17	7.08 ± 2.35
E11	1939.04	121.21 ± 3.14	14.90 ± 1.18
E12	> 3000	29.42 ± 2.31	3.23 ± 0.79
Asc. acid	< 200	N/A	N/A

E1 = hexane leaf extract, E2 = chloroform leaf extract, E3 = ethyl acetate leaf extract, E4 = acetone leaf extract, E5 = methanolic leaf extract, E6 = water leaf extract, E7= hexane stem bark extract, E8 = chloroform stem bark extract, E9 = ethyl acetate stem bark extract, E10 = acetone stem bark extract, E11 = methanolic stem bark extract, E12 = water stem bark extract, Asc. acid = Ascorbic acid, TFCs = Total flavonoid contents, TPCs = Total phenolic contents, N/A = Not applicable. Values with different superscript letters are statistically different within column.

From the above discussions, we noticed that cold maceration or cold percolation, or hot solvent extraction techniques have been utilized to obtain various solvent extracts from various parts of *X. strumarium* collected at different locations in several countries and these solvent extracts have been evaluated for their antioxidant activity by DPPH radical scavenging assay (Guemmaz et al., 2018; Ishwarya & Singh, 2010; Rad et al., 2013; Scherer & Godoy, 2014; Sridharamurthy et al., 2011; Subba & Gaire, 2022). However, in the present study, the combination of maceration and hot solvent extraction techniques was used to obtain various solvent extracts from the leaves and stem bark of *X. strumarium* collected in the Kingdom of Lesotho. The maceration technique was first used to extract compounds as much as possible from the plant materials and the sample recovered from the maceration technique was further subjected to hot solvent extraction at reflux conditions to extract the remaining compounds. In other words, the optimal extraction of compounds from the plant materials was achieved by the combination of these two extraction techniques. Additionally, these solvent extracts from the leaves and stem bark of *X. strumarium* obtained from the above extraction techniques were evaluated for their DPPH radical scavenging activity. We noticed that the methanol and ethyl acetate extracts obtained from the leaves of *X. strumarium* were common both in the previous and present studies (Scherer & Godoy, 2014; Subba & Gaire, 2022). As

discussed previously that the methanolic extract obtained from the leaves of *X. strumarium* collected in 2021 in Nepal by cold percolation method was found to exhibit an IC_{50} value of 258.10 µg/ml in the DPPH radical scavenging assay (Subba & Gaire, 2022). Similarly, the ethyl acetate extract obtained from the leaves of X. *strumarium* collected in April 2014 in Brazil by static maceration, dynamic maceration, and Soxhlet apparatus methods showed IC_{50} values of 346.35 ± 16.50, 369.83 ± 13.58 and 423.97 ± 22.27 µg/ml, respectively in the DPPH radical scavenging assay (Scherer & Godoy, 2014). However, in the present study, the methanol and ethyl acetate extracts obtained from the leaves of *X. strumarium* collected in January 2022 in the Kingdom of Lesotho exhibited IC_{50} values of < 200 and 1856.02 µg/ml, respectively in the same DPPH radical scavenging assay. In other words, in the present study, the methanolic extract from the leaves of *X. strumarium* demonstrated significantly higher radical scavenging activity compared to the previous report (Subba & Gaire, 2022) and therefore, it displayed a lower IC_{50} value. On the other hand, in the present study, the ethyl acetate extract obtained from the leaves of *X. strumarium* possessed much lower scavenging activity compared to the previous report (Scherer & Godoy, 2014) and therefore, it exhibited a much higher IC_{50} value. This observation revealed a fact that there was a discrepancy in the IC_{50} values of methanol and ethyl acetate extracts reported in the previous studies (Scherer & Godoy, 2014; Subba & Gaire, 2022) and the determined IC_{50} values in the present study. This discrepancy can be attributed to the facts that the quantity, variety, and variation of active compounds that could be extracted from the plant materials are dependent on the geographic locations and seasons in which the plant materials are collected as well as the extraction techniques used to obtain various extracts from the collected plant materials. The discrepancy in the IC_{50} values of methanol and ethyl acetate extracts in the previous (Scherer & Godoy, 2014; Subba & Gaire, 2022) and present studies might be due to these factors.

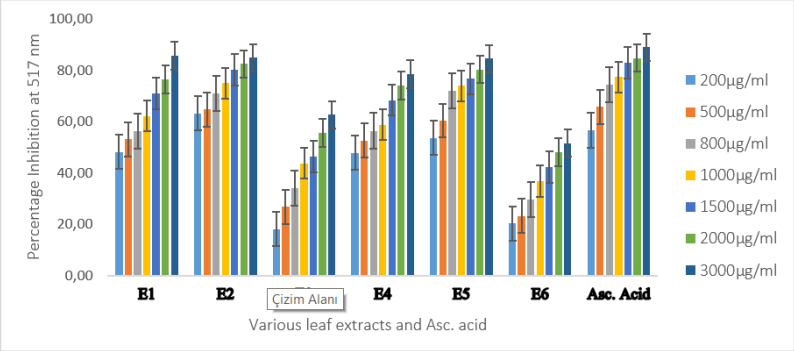

Figure 3. Percentage of DPPH radical scavenging activity of various extracts from leaves of *X. strumarium* and ascorbic acid at various concentrations

E1 = hexane leaf extract, E2 = chloroform leaf extract, E3 = ethyl acetate leaf extract, E4 = acetone leaf extract, E5 = methanolic leaf extract, E6 = water leaf extract, Asc. acid = Ascorbic acid

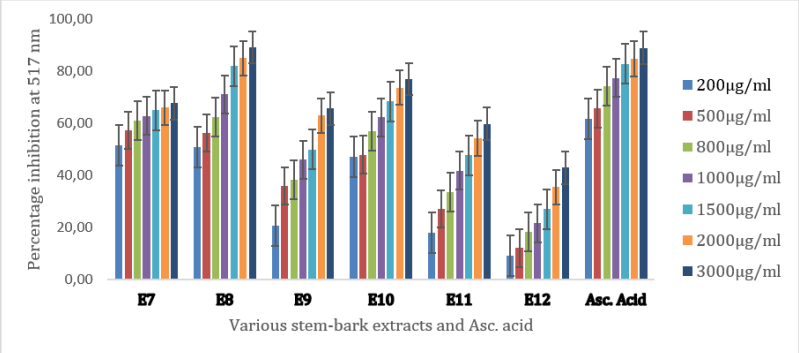

Figure 4. Percentage of DPPH radical scavenging activity of various extracts from stem-bark of *X. strumarium* and ascorbic acid at various concentrations

E7 = hexane stem-bark extract, E8 = chloroform stem-bark extract, E9 = ethyl acetate stem-bark extract, E10 = acetone stem-bark extract, E11 = methanolic stem-bark extract, E12 = water stem-bark extract. Asc. acid = Ascorbic acid

3.2. Evaluation of various extracts for their ferric-reducing power

The result of the ferric-reducing power of all twelve extracts (E1-E12) is summarised in Table 3. Ascorbic acid served as the positive control. For clarity and comparison purposes, the dose-response curve of ferric-reducing power of various leaves extracts (E1-E6) and stem bark extracts (E7-E12) are given in Figures 5 and 6, respectively together with the dose-response curve for positive control, ascorbic acid. In general, the stem bark extracts (E7-E12) showed higher ferric-reducing power than leaf extracts (E1-E6). The ferric-reducing power of the leaf extracts was observed in the following order: E3 > E5 > E4 > E1 > E6 > E2. Extract, E3 exhibited the highest reducing power of 0.996 ± 0.101 at a concentration of 100 µg/ml. Similarly, the ferric-reducing power of the stem bark extracts was observed in the following order: E9 > E10 > E11 > E12 > E7 > E8. Extract E9 showed the highest ferric-reducing power of 0.947 ± 0.018 at a concentration of 100 µg/ml. Extracts E10 and E11 also showed comparable ferric-reducing power as that of E9. However, all extracts (E1-12) showed lower ferric-reducing power than the positive control, ascorbic acid at higher concentrations. In a

previous report, a methanolic crude extract and its chloroform, ethyl acetate, and aqueous fractions obtained from the leaves of *X. strumarium* have exhibited EC_{50} values of 0.059 ± 0.001, 0.120 ± 0.0045, 0.017 ± 0.00015 and 0.036 ± 0.0016 mg/ml, respectively in the ferric-reducing power assay (Guemmaz et al., 2018).

Table 3. Ferric reducing power of various extracts from leaves and stem bark of *X. strumarium**

Extracts	Concentrations (µg/ml)/Ferric reducing power					
	5	10	20	40	80	100
E1	0.125 ± 0.034^{c}	0.186 ± 0.003^{a}	0.280 ± 0.012^{a}	0.384 ± 0.065^{e}	0.502 ± 0.027^{c}	0.611 ± 0.073^{e}
E2	0.083 ± 0.010^{a}	0.114 ± 0.018^{b}	0.178 ± 0.002^{a}	0.290 ± 0.041^{d}	0.312 ± 0.007^{a}	0.394 ± 0.045^{d}
E3	0.361 ± 0.007^{a}	0.397 ± 0.004^{a}	0.455 ± 0.044^{c}	0.691 ± 0.023^{b}	0.884 ± 0.078^{f}	0.996 ± 0.101^{f}
E4	0.224 ± 0.052^{d}	0.296 ± 0.043^{d}	0.383 ± 0.008^{a}	0.472 ± 0.038^{b}	0.567 ± 0.057^{e}	0.709 ± 0.064^{e}
E5	0.302 ± 0.046^{d}	0.366 ± 0.001^{a}	0.444 ± 0.074^{e}	0.678 ± 0.029^{c}	0.753 ± 0.035^{c}	0.922 ± 0.005^{a}
E6	0.111 ± 0.012^{a}	0.143 ± 0.093f	0.194 ± 0.003^{a}	0.298 ± 0.000^{a}	0.346 ± 0.041^{d}	0.412 ± 0.009^{a}
E7	0.138 ± 0.037^{c}	0.176 ± 0.082^{f}	0.266 ± 0.015^{a}	0.352 ± 0.013^{a}	0.498 ± 0.032^{c}	0.593 ± 0.001^{a}
E8	0.093 ± 0.004^{a}	0.125 ± 0.000^{a}	0.155 ± 0.012^{a}	0.226 ± 0.019^{b}	0.302 ± 0.019^{b}	0.361 ± 0.024^{b}
E9	0.241 ± 0.034^{a}	0.317 ± 0.008^{a}	0.478 ± 0.053^{e}	0.513 ± 0.002^{a}	0.728 ± 0.034^{c}	0.947 ± 0.018^{b}
E10	0.192 ± 0.006^{a}	0.290 ± 0.012^{a}	0.368 ± 0.042^{d}	0.552 ± 0.001^{a}	0.800 ± 0.013^{a}	0.911 ± 0.089f
E11	0.202 ± 0.063^{e}	0.287 ± 0.004^{a}	0.406 ± 0.013^{a}	0.623 ± 0.030	0.764 ± 0.011^{a}	0.885 ± 0.004^{a}
E12	0.103 ± 0.016^{b}	0.152 ± 0.007^{a}	0.238 ± 0.007^{a}	0.426 ± 0.017^{b}	0.576 ± 0.014a	0.660 ± 0.034^{c}
Asc. acid	0.326 ± 0.005^{a}	0.485 ± 0.040^{c}	0.518 ± 0.057^{e}	0.597 ± 0.046^{d}	0.905 ± 0.071^{e}	1.213 ± 0.078^{e}

* Refer to footnotes of Tables 1 and 2

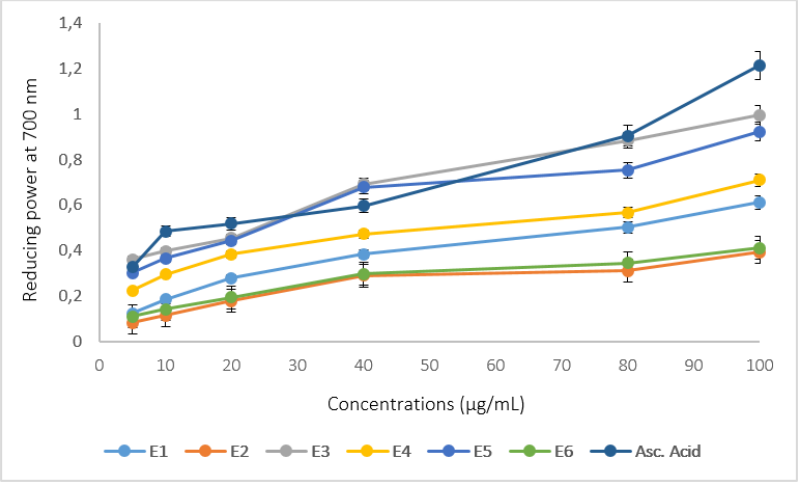

Figure 5. Dose-response curve for various extracts (E1-E6) obtained from leaves of *X. strumarium* for their ferric reducing power
Refer the footnotes of Figure 3

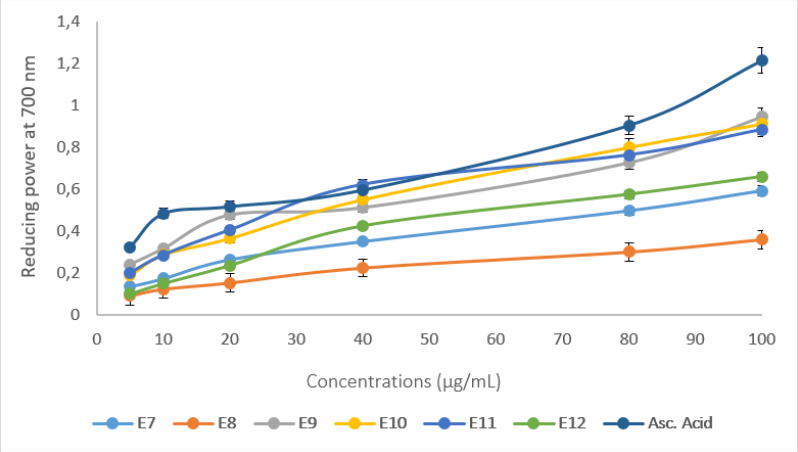

Figure 6. Dose-response curve for various extracts (E7-E12) obtained from stem-bark of *X. strumarium* for their ferric reducing power
Refer the footnotes of Figure 4

3.3. Determination of TPCs and TFCs of various extracts

The TPCs of E1-E12 were determined by Folin-Ciocalteu colorimetric method and the results are summarized in Tables 1 and 2. Gallic acid served as a standard to estimate the TPCs of various extracts and the calibration curve of gallic acid is given in Figure 1. The TPCs of extracts from leaves (E1-E6) were found to be 4.03 ± 0.34, 54.11 ± 1.16, 59.98 ± 2.01, 118.01 ± 1.85, 133.41 ± 3.23 and 35.92 ± 5.00 mg of GAE/g DW, respectively. This result showed that E5 exhibited the highest TPCs among leaf extracts followed by E4, E3, E2, E6, and

E1 (Table 3). The TPCs of extracts from stem bark (E7-E12) were found to be 6.89 ± 1.73, 38.04 ± 0.88, 61.46 ± 1.11, 60.80 ± 6.17, 121.21 ± 3.14 and 29.42 ± 2.31 mg of GAE/g DW, respectively. This result indicated that E11 showed the highest TPCs among stem bark extracts followed by E9, E10, E8, E12, and E7 (Tables 1 and 2).

The TFCs of E1-E12 were determined by the aluminum chloride colorimetric method and the results are summarized in Tables 1 and 2. Quercetin served as a standard to estimate the TFCs of various extracts and the calibration curve of quercetin is given in Figure 1. The TFCs of extracts from leaves (E1-E6) were found to be 4.03 ± 0.34, 54.11 ± 1.16, 59.98 ± 2.01, 118.01 ± 1.85, 133.41 ± 3.23 and 35.92 ± 5.00 mg of QE/g DW, respectively. This result showed that E5 exhibited the highest TFCs among leaf extracts followed by E4, E3, E2, E6, and E1 (Tables 1 and 2). The TFCs of extracts from stem bark (E7-E12) were found to be 6.89 ± 1.73, 38.04 ± 0.88, 61.46 ± 1.11, 60.80 ± 6.17, 121.21 ± 3.14 and 29.42 ± 2.31 mg of QE/g DW, respectively. This result indicated that E11 showed the highest TPCs among stem bark extracts followed by E10, E9, E8, E17, and E7 (Tables 1 and 2).

The TPCs and TFCs of various extracts obtained from various parts of the *X. strumarium* have previously been reported. For example, in a previous study, as discussed previously that the aerial parts of *X. strumarium* have been collected in May 2018 in Ho Chi Minh City, Vietnam (Ly et al., 2021). An ethanolic extract has been obtained from these aerial parts by cold percolation technique at room temperature. The TPCs and TFCs of this ethanolic extract have been determined to be 84.86 ± 5.13 mg of GAE/g DW and 3.66 ± 0.08 mg of QE/g DW, respectively (Ly et al., 2021). Similarly, in another study, as discussed previously that the leaves of *X. strumarium* were collected in July-August 2013 in the Beni Aziz (Setif), Algeria (Guemmaz et al., 2018). A 98% methanolic crude extract has been obtained from the dried leaves by cold percolation method at room temperature and the chloroform, ethyl acetate, and aqueous fractions have been obtained from this 98% methanolic crude extract (Guemmaz et al., 2018). The 98% methanolic crude extract, the chloroform, ethyl acetate, and aqueous fractions demonstrated TPCs of 85.77 ± 4.98, 0.58 ± 3.3, 166.26 ± 27.98 and 75.24 ± 13.31 mg of GAE/g DW, respectively (Guemmaz et al., 2018). Similarly, the 98% methanolic crude extract, the chloroform, ethyl acetate, and aqueous fractions displayed TFCs 11.76 ± 1.39, 17.26 ± 2.75, 29.037 ± 3.14 and 10.60 ± 1.615 mg of QE/g DW, respectively (Guemmaz et al., 2018). In another study, the leaves of *X. strumarium* were collected in April 2014 in Sao Paulo, Brazil (Scherer & Godoy, 2014). 80% ethanol, 80% methanol, ethyl acetate, and chloroform/dichloromethane (1:1) extracts have been obtained from the air-dried leaves using static maceration, dynamic maceration and Soxhlet apparatus methods (Scherer & Godoy, 2014). The TPCs of 80% ethanol extract obtained from the static maceration, dynamic maceration, and Soxhlet apparatus methods have been determined to be 64.51 ± 1.0, 70.07 ± 1.6 and 69.38 ± 1.3 mg GAE/g DW, respectively (Scherer & Godoy, 2014). Similarly, the TPCs of 80% methanol extract obtained from the static maceration, dynamic maceration, and Soxhlet apparatus methods have been determined to be 93.68 ± 2.1, 78.23 ± 0.9 and 81.35 ± 1.3 mg GAE/g DW, respectively (Scherer & Godoy, 2014). Additionally, the TPCs of ethyl acetate extract obtained from the static maceration, dynamic maceration, and Soxhlet apparatus methods have been determined to be 21.98 ± 3.6, 27.19 ± 1.0 and 23.19 ± 0.3 mg GAE/g DW, respectively (Scherer & Godoy, 2014). Furthermore, the TPCs of chloroform/dichloromethane (1:1) extract obtained from the static maceration and dynamic maceration have been determined to be 13.30 ± 0.8 and 18.85 ± 2.4 mg GAE/g DW, respectively (Scherer & Godoy, 2014). In the present study, we determined the presence of significant amounts of TPCs and TFCs in various extracts obtained from the leaves and stem bark of *X. stramarium*, and particularly, the methanolic extracts from both leaves and stem bark showed higher TPCs and TFCs. Moreover, we noticed that the ethyl acetate extracts obtained from the leaves of *X. strumarium* were common both in the previous and present studies. As discussed previously that the TPCs of ethyl acetate extract obtained from the leaves of *X. strumarium* collected in Brazil by static maceration, dynamic maceration, and Soxhlet apparatus methods have been determined to be 21.98 ± 3.6, 27.19 ± 1.0 and 23.19 ± 0.3 mg GAE/g DW, respectively. On the other hand, in the present study, TPCs of ethyl acetate extract obtained from the leaves of *X. strumarium* collected in the Kingdom of Lesotho were determined to be 59.98 ± 2.01 mg of GAE/g DW. In other words, the TPCs of ethyl acetate extract in the present study were found to be much higher than in the previous report. Again, this discrepancy might be due to the same factors that the quantity, variety, and variation of active compounds that could be extracted from the plant materials are dependent on the geographic locations and seasons in which the plant materials are collected as well as the extraction techniques used to obtain various extracts from the collected plant materials.

4. Conclusions

Various solvent extracts obtained from the leaves and stem bark of *X. strumarium* were evaluated for their DPPH radical scavenging activity and ferric-reducing power. The extracts from the leaves and stem bark exhibited radical scavenging activity in the ranges of 18.06 ± 0.3-185.67 ± 11.54% and 9.13 ± 0.54-84.18 ± 0.92%, respectively at a concentration range of 200-3000 µg/ml. The positive control, ascorbic acid exhibited radical scavenging activity in a range of 56.64 ± 1.26-88.98 ± 0.31% at the same concentration range of 200-3000 µg/ml. The hexane, chloroform, and methanol extracts from leaves and the chloroform extract from stem bark showed higher radical scavenging activity compared to other extracts at a concentration of > 3000 µg/ml. Additionally, the IC_{50} values of all these extracts were determined using the same DPPH radical scavenging assay. The hexane and chloroform extracts from both leaves and stem bark and the methanol extract from leaves were found to be the most potent extracts with an IC_{50} value of < 200 µg/ml for each extract. The positive control, ascorbic acid also showed an IC_{50} value of < 200 µg/ml. Furthermore, in the ferric-reducing power assay, the ethyl acetate extract from both leaves and stem bark exhibited the highest reducing power of 0.996 ± 0.101 and 0.947 ± 0.018 at a concentration of 100 µg/ml. Additionally, the methanol extract from the leaves showed the highest TPCs of 133.41 ± 3.23 mg GAE/g of DW of extract followed by the methanol extract from the stem bark and then the acetone extract from the leaves with TPCs of 121.21 ± 3.14 and 118.01 ± 1.85 mg GAE/g of DW of extract, respectively. Similarly, the methanol extracts from both leaves and stem bark also showed the highest TFCs of 20.61 ± 1.81 and 14.90 ± 1.18mg QE/g of DW of extract, respectively. Based on our findings, it can be concluded that diverse extracts derived from the leaves and stem bark of *X. strumarium* displayed a moderate-to-strong radical scavenging activity and ferric-reducing power, along with substantial levels of total phenolic compounds (TPCs) and total flavonoid contents (TFCs). Since *X. stramarium* has been used in traditional medicine to treat a variety of diseases, further studies on this plant are recommended to commercialize products from this plant.

Acknowledgments

The authors thank the National University of Lesotho for its overall support. One of the authors, Manoharan K. Pillai, also thanks the

University of Eswatini for the support. A part of this paper has been extracted from the report of Potlaki Thebe's undergraduate research project.

Conflict of interest

The authors confirm that there are no known conflicts of interest.

Statement of ethics

In this study, no method requiring the permission of the "Ethics Committee" was used.

Availability of data and materials

All data generated or analyzed during this study are included in this published article.

Funding

This study was supported by National University of Lesotho.

CRediT authorship contribution statement

Manoharan Karuppiah Pillai: Conceptualization, Supervision, Investigation, Data analysis, Compilation and writing the original draft
Potlaki Thabe: Conceptualization, Investigation, Data analysis and writing a draft
Rets'epile Paul Matamane: Conceptualization, Investigation, Data analysis and writing a draft

ORCID Numbers of the Authors

M. Karuppiah Pillai: 0000-0001-7425-6509
P. Thebe: 0009-0001-4566-9598
R. P. Matamane: 0000-0002-4110-4119

Supplementary File

None.

Publisher's Note

All claims expressed in this article are solely those of the authors and do not necessarily represent those of their affiliated organizations, or those of the publisher, the editors and the reviewers. Any product that may be evaluated in this article, or claim that may be made by its manufacturer, is not guaranteed or endorsed by the publisher.

This is an open-access article distributed under the terms of the Creative Commons Attribution 4.0 International License (CC BY). The use, distribution or reproduction in other forums is permitted, provided the original author(s) and the copyright owner(s) are credited and that the original publication in this journal is cited, in accordance with accepted academic practice. No use, distribution or reproduction is permitted which does not comply with these terms.

References

Aranjani, J. M., Manuel, A., Mallikarjuna Rao, C., Udupa, N., Rao, J. V., Joy, A. M., Gandhi, P., & Radhakrishnan, E. K. (2013). Preliminary evaluation of in vitro cytotoxicity and in vivo antitumor activity of *Xanthium strumarium* in transplantable tumors in mice. *The American Journal of Chinese medicine, 41*(1), 145-162.

Cole, R. J., Stuart, B. P., Lansden, J. A., & Cox, R. H. (1980). Isolation and redefinition of the toxic agent from cocklebur (*Xanthium strumarium*). *Journal of Agricultural and Food Chemistry, 28*(6), 1330-1332.

Fan, W., Fan, L., Peng, C., Zhang, Q., Wang, L., Li, L., Wang, J., Zhang, D., Peng, W., *et al.* (2019). Traditional uses, botany, phytochemistry, pharmacology, pharmacokinetics and toxicology of *Xanthium strumarium* L.: A review. *Molecules, 24*(2), 359.

Guemmaz, T., Zerargui, F., Boumerfeg, S., Arrar, L., Aouachria, S., Khennouf, S., Charef, N. E., & Baghiani, A. (2018). Anti-hemolytic, anti-lipid peroxidation, antioxidant properties and acute toxicity of *Xanthium strumarium* leaves extracts. *Annual Research & Review in Biology, 24*(3), 1-12.

Ishwarya, S., & Singh, M. K. (2010). Evaluation of antioxidant and in vitro cytotoxicity of crude fractions from the roots of *Xanthiuim strumarium*. *International Journal of PharmTech Research, 2*(4), 2219-2223.

Kamboj, A., & Saluja, A. K. (2010). Phytopharmacological review of *Xanthium strumarium* L. (Cocklebur). *International Journal of Green Pharmacy (IJGP), 4*(3), 129-139.

Kim, I. T., Park, Y. M., Won, J. H., Jung, H. J., Park, H. J., Choi, J. W., & Lee, K. T. (2005). Methanol extract of *Xanthium strumarium* L. possesses anti-inflammatory and anti-nociceptive activities. *Biological and Pharmaceutical Bulletin, 28*(1), 94-100.

Kumar, K. S., & Rajkapoor, B. (2010). Evaluation of Anti-epileptic Activity of *Xanthium strumarium* L. *Pharmacologyonline, 2*, 850-855.

Lin, B., Zhao, Y., Han, P., Yue, W., Ma, X.-Q., Rahman, K., Zheng, C.-J., Qin, L.-P., & Han, T. (2014). Anti-arthritic activity of *Xanthium strumarium* L. extract on complete Freund' s adjuvant induced arthritis in rats. *Journal of Ethnopharmacology, 155*(1), 248-255.

Ly, H. T., Truong, T. M., Nguyen, T. T. H., Nguyen, H. D., Zhao, Y., & Le, V. M. (2021). Phytochemical screening and anticancer activity of the aerial parts extract of *Xanthium strumarium* L. on HepG2 cancer cell line. *Clinical Phytoscience, 7*(1), 1-8.

Masvingwe, C., & Mavenyengwa, M. (1998). Toxicological evaluation of the plant *Xanthium strumarium* in Pigs in Zimbabwe. *Journal of Venomous Animals and Toxins, 4*, 113-119.

Patil, M. V. K., Kandhare, A. D., & Bhise, S. D. (2012). Anti-arthritic and anti-inflammatory activity of *Xanthium srtumarium* L. ethanolic extract in Freund's complete adjuvant induced arthritis. *Biomedicine & Aging Pathology, 2*(1), 6-15.

Pillai, M. K., & Magama, S. (2020). DPPH radical scavenging activity of extracts from *Urtica urens* (Urticaceae). *Journal of Medicinal Plants Research, 14*(5), 232-238.

Pillai, M. K., Matela, K. S., George, M. J., & Magama, S. (2018). Antioxidant activity of extracts from *Schinus molle* L. and *Gleditsia triacanthos* L. *Journal of Medicinal Plants Research, 12*(24), 369-374.

Rad, J. S., Alfatemi, S. M. H., Rad, M. S., & Iriti, M. (2013). In vitro antioxidant and antibacterial activities of *Xanthium strumarium* L. extracts on methicillin-susceptible and methicillin-resistant *Staphylococcus aureus*. *Ancient Science of Life, 33*(2), 109-113.

Scherer, R., Duarte, M., Catharino, R., Nachtigall, F., Eberlin, M., Teixeira Filho, J., & Godoy, H. (2009). *Xanthium strumarium* L. antimicrobial activity and carboxyatractyloside analysis through electrospray ionization mass spectrometry. *Revista Brasileira de Plantas Medicinais, 11*, 159-163.

Scherer, R., & Godoy, H. (2014). Effects of extraction methods of phenolic compounds from *Xanthium strumarium* L. and their antioxidant activity. *Revista Brasileira de Plantas Medicinais, 16*, 41-46.

Sharifi-Rad, J., Hoseini-Alfatemi, S. M., Sharifi-Rad, M., Sharifi-Rad, M., Iriti, M., Sharifi-Rad, M., Sharifi-Rad, R., & Raeisi, S. (2015). Phytochemical compositions and biological activities of essential oil from *Xanthium strumarium* L. *Molecules, 20*(4), 7034-7047.

Sharma, S., Singh, D., Khan, F., Swarankar, C., & Bhagwan, P. (2003). Anthelmintic activity of *Xanthium strumarium* against *Haemonchus contortus* infection in sheep. *Indian Journal of Animal Sciences (India), 73*(3), 342-344.

Singh, S., Raghavendra, K., & Dua, V. (2009). Evaluation of Larvicidal and Repellent Activity of *Xanthium strumarium* (Asteraceae) Ethanol Extract agaist Mosquito Vectors. *Portal Regional da BVS, 41*(4), 263-269.

Sixtus, S. T., & Pillai, M. K. (2022). Evaluation of antioxidant activity of extracts from *Leucosidea sericea*. *Herba Polonica, 68*(1), 10-18.

Sridharamurthy, N., Yogananda, R., & Srinivas, U. (2011). In vitro Antioxidant and Antilipidemic Activities of *Xanthium strumarium* L. *Current Trends in Biotechnology and Pharmacy, 5*(3), 1362-1371.

Subba, B., & Gaire, S. (2022). Analysis of phyto-constituents, antioxidant and antidiabetic activities of some medicinal plants of Nepal. *Scientific World, 15*(15), 44-50.

Talakal, T., Dwivedi, S., & Sharma, S. (1995). In vitro and in vivo antitrypanosomal activity of *Xanthium strumarium* leaves. *Journal of Ethnopharmacology, 49*(3), 141-145.

Tenguria, M. (2013). Estimation of Total Polyphenolic Content and Antibiogram Studies of Leaf and Fruit Aqueous Extracts of *Xanthium strumarium* L. *Science Secure Journal of Biotechnology, 2*(3), 83-88.

Turgut, M., Alhan, C. C., Gürgöze, M., Kurt, A., Doğan, Y., Tekatli, M., Akpolat, N., & Aygün, A. D. (2005). Carboxyatractyloside poisoning in humans. *Annals of Tropical Paediatrics, 25*(2), 125-134.

Int. J. Plant Bas. Pharm. (2023) 3(1), 123-130

INTERNATIONAL JOURNAL OF PLANT BASED PHARMACEUTICALS

https://ijpbp.com

RESEARCH ARTICLE

OPEN ACCESS

Ameliorative effect of lycopene alone and in combination with co-enzyme Q10 in streptozotocin-induced diabetic nephropathy in experimental rats

Pooja B. Rasal[a], Gaurav N. Kasar[a], Manoj S. Mahajan[a], Aman B. Upaganlawar[a]*, Chandrashekhar D. Upasani[a]

[a] *SNJB's Shriman Sureshdada Jain College of Pharmacy, Department of Pharmacology, Chandwad Dist: Nashik, India*

ARTICLE INFO

Article History:

Received: 18 April 2023
Revised: 06 June 2023
Accepted: 14 June 2023
Available online: 15 June 2023

Edited by: B. Tepe

Keywords:

Antioxidants
CoQ10
Diabetic nephropathy
Lycopene
Oxidative stress
Streptozotocin

ABSTRACT

Diabetic nephropathy (DN) has become an utmost reason for long-standing renal dysfunction and end-stage renal disease globally. Oxidative stress induced by persistent hyperglycemia is considered a fundamental element in the evolution of DN. The goal of this research was to discover the outcome of appendages of natural antioxidants such as lycopene and co-enzyme Q10 (CoQ10) in DN rats and to observe the preventive effects in DN. A diabetes model was developed in a Wistar strain of male rats (200–250 g) by subcutaneous injection of streptozotocin (55 mg/kg). Development of nephropathy was assessed by renal function tests including blood glucose, creatinine, albumin, total protein, total bilirubin, uric acid, total cholesterol, triglycerides, and CRP level. Oxidative stress markers such as LPO and GSH content and activity of membrane-bound Na^+/K^+ ATPases were measured in kidney homogenate. Renal damage was assessed by performing a histopathological analysis. DN rats showed a significant elevation in creatinine, albumin, total protein, total bilirubin, uric acid, total cholesterol, triglycerides, CRP, and LPO levels whereas a significant reduction in creatinine clearance and GSH level. Treatment with antioxidants such as lycopene (5 mg/kg/p.o.) and CoQ10 (10 mg/kg/p.o.) along with their combination for 4 weeks notably altered the level of renal function biomarkers and oxidative stress markers. These antioxidants and their combination also protected the kidney from abnormal morphological changes. The present findings suggest that the combined administration of lycopene and CoQ10, which are antioxidants, exhibits synergistic effects in mitigating renal injury by reducing hyperglycemia, oxidative stress markers, and histopathological alterations.

1. Introduction

Diabetes mellitus (DM) patients have poor glycemic control and experience some microvascular consequences involving diabetic nephropathy (DN) (Balakumar et al., 2009; Marcovecchio et al., 2011). DN is specified by anatomical and physiological abnormalities in the kidney (Forbes et al., 2008).

The hallmarks of DN comprise buildup of extracellular matrix, stiffness of the basal membrane, scarring of the glomerulus, podocyte mislaid, enlargement of mesangial cells, and tubular abnormalities (Arora & Singh, 2013; Horie et al., 1997; Ritz, 2013). These modifications lead to changes in urinary albumin excretion, glomerular filtration rate (GFR), microalbuminuria, uremia, creatinine clearance rate, etc. Cumulatively all the above alterations in pathogenesis lead to End-Stage Renal Disease (ESRD) (Ritz et al., 2011; Schena & Gesualdo, 2005; Sudamrao Garud & Anant Kulkarni, 2014).

Reviewed by:
Stephen Chijioke Emencheta: University of Nigeria, Nsukka, Nigeria
Poonguzhali Subramanian: Taylor's University, Subang Jaya, Selangor, Malaysia

* Corresponding author(s):
E-mail address:
amanrxy@gmail.com (A. B. Upaganlawar)
e-ISSN: 2791-7509
doi: https://doi.org/10.29228/ijpbp.24

Please cite this article as: Rasal, P. B.., Kasar, G. N., Mahajan, M. S., Upaganlawar, A. B., & Upasani, C. D. (2023). Ameliorative effect of lycopene alone and in combination with co-enzyme Q10 in streptozotocin-induced diabetic nephropathy in experimental rats. *International Journal of Plant Based Pharmaceuticals*, *3*(1), 123-130, https://doi.org/10.29228/ijpbp.24.

Hyperglycemia, hyperlipidemia, and proteinuria are the key players that cause renal injury in DN. Hyperglycemia triggers many renal cells for the stimulation of humoral mediators and cytokines. These substances lead to many changes in the kidney such as increased ECM deposition, buildup of advanced glycation end products (AGEs), and alteration in permeability of the basal membrane which promotes glomerular fibrosis and aggravates DN (Schena & Gesualdo, 2005).

Oxidative stress (OS) markedly takes part in the genesis of DN and hyperglycemia-produced oxidative stress is strongly indicated in various studies (Ighodaro, 2018; Kashihara et al., 2010). Elevated OS in a hyperglycemic state causes activation of various pathways such as P38-MAPK, AKT, and Rheb pathway which promote fibrosis and inflammation of tissue in the kidney that is attributable to DN (Bhattacharjee et al., 2016; Fakhruddin et al., 2017; Platé et al., 2020).

Reports suggested that anti-oxidative therapy has shown promising results in reducing and delaying the signs and symptoms associated with animal models of streptozotocin-induced DN in rats (Akbar et al., 2011; Mahmoodnia et al., 2017; Rojas-Rivera et al., 2012; Tavafi, 2013).

Lycopene is a bioactive carotenoid, generally found in tomatoes. It is a powerful oxygen quencher among other carotenoids and could effectively lower the formation of reactive oxygen species (ROS) (Shi et al., 2004; Zhu et al., 2020). It reduces the likelihood of developing many chronic diseases including cardiovascular disorders (Sayahi & Shirali, 2017), diabetes (Zhu et al., 2020), anti-inflammatory (Puah et al., 2021), kidney diseases (Zhu et al., 2011) and asthma (Leh & Lee, 2022).

Another important antioxidant is Coenzyme Q10 (CoQ10), an internally produced hydrophobic substance, commonly found in mitochondria and essential in ATP production during oxidative phosphorylation (Hodgson et al., 2002; Mahajan et al., 2020). It inhibits the peroxidation of protein and lipid along with free radical scavenging action and thus, guards tissue from oxidative injury (Rosenfeldt et al., 2007).

Several studies have revealed that the combination of antioxidants shows synergistic effects in the conditions such as myocardial infarction (Upaganlawar & Gandhi, 2010), inflammation (Fuller et al., 2006), hepatorenal toxicity (Elsayed et al., 2021), neuropathy (Esu et al., 2022), migraine (Parohan et al., 2021), prostate cancer (Gunasekera et al., 2007), atherosclerosis (Li et al., 2019), and autoimmune disease (Vetvicka & Vetvickova, 2018). Considering the available literature, no study to date investigated the concomitant results of lycopene and CoQ10 in DN. The current work was outlined to assess the effectiveness of lycopene and CoQ10 combination in diabetic nephropathy in laboratory rats.

2. Materials and methods

2.1. Drugs and chemicals

Lycopene and CoQ10 were obtained from Universal Industries, Nashik, and Zydus Cadila, India respectively. Streptozotocin (STZ) was purchased from Sigma Aldrich (USA). All chemical and necessary diagnostic kits were of standard class.

2.2. Experimental animals

Healthy male rats of the Wistar strain were split into five groups each consisting of six rats. The rats were obtained from Wockhardt Ltd. Aurangabad, India. They were housed as per CPCSEA guidelines. The study methods were permitted by the IAEC of the organization, (SSDJ/IAEC/2021-22/03).

2.3. Induction of DN using STZ

DN was developed by a single dose of STZ (55 mg/kg) prepared in 0.2 ml of citrate buffer (0.1 M, pH 4.5). Diabetes was confirmed 72 h after the STZ dosing and the blood glucose level (BGL) was measured by digital Glucometer (ACCU-CHEK, Roche Diabetes Care, Germany). Then rats were tested for four weeks for the progression of nephropathy.

2.4. Experimental design

Five groups of rats were formed, with each group comprising six rats. The descriptions of the groups are as follows:

Group I: Control rat treated with vehicle alone (0.2 ml/kg/s.c.)
Group II: Rats administered with STZ (55 mg/kg/s.c.) (Mahajan et al., 2020)
Group III: Rats treated with lycopene (5 mg/kg/p.o./day) dissolved in distilled water (Pansare et al., 2021)
Group IV: Rats treated with CoQ10 (10 mg/kg/p.o./day) (Mahajan et al., 2020)
Group V: Rats treated with lycopene (5 mg/kg/p.o./day) plus CoQ10 (10 mg/kg/p.o./day) simultaneously in combination

All drug treatment was given for 4 weeks.

2.5. Estimation of body weight, kidney weight, and kidney hypertrophy index

In the 4th week, rats were sacrificed and kidneys were removed. The body and kidney weight of the rats were measured by electronic weighing balance and the kidney index was evaluated as per the given formula (Liu et al., 2010):

$$Kidney\ hypertrophy\ index\ (\%) = \frac{Kidney\ weight}{Body\ weight} x\ 100$$

2.6. Estimation of biochemical parameters in serum and urine

In the 4th week of the study, rats were individually kept in metabolic cages for one day, and urine sample collection was done. Blood was obtained from the retro-orbital nerve by employing ether anesthesia using micro-capillary and the serum was separated using high-speed centrifugation. Urine and serum samples were kept at –20 °C and used for various biochemical estimations. Blood glucose was measured using a glucometer. Total protein, total bilirubin, uric acid, total cholesterol, triglycerides, and C-reactive protein (CRP) were analyzed in serum and the level of albumin and creatinine were determined in urine samples using commercial diagnostic kits. Creatinine clearance was calculated by the given formula (Lavender et al., 1969):

$$Creatinine\ clearance\ \left(\frac{ml}{min}\right) = Urinary\ creatinine\ x\ \frac{Urine\ volume}{Serum\ creatinine}$$

2.7. Tissue homogenization

At the end of treatment, the rats were sacrificed via the decapitation method and the kidney was excised, and washed in cold physiological saline. One kidney was stored for histopathological examination in 10% formalin solution while the other kidney was used for the estimation of antioxidant enzyme. The kidney was finely chopped into small pieces in a chilled sucrose solution (0.25 M). The renal tissues were homogenized in 10% w/v *tris*-hydrochloride buffer (10 mM, pH 7.4). The homogenate was centrifuged at 10000 rpm for 15 minutes at 0 °C using a cooling centrifuge (Jain, 2015). The supernatant was utilized to determine the concentration of lipid peroxidation (LPO) and reduced glutathione (GSH), while the assessment of Na^+/K^+ ATPases was conducted using a sediment-based method.

2.8. Evaluation of OS markers

2.8.1. Determination of lipid peroxidation (LPO)

2.0 ml homogenate was mixed with 2.0 ml of 10% (w/v) TCA and cooled for 15 minutes. The precipitate was separated by centrifugation. 2.0 ml of thiobarbituric acid (TBA) was added to a clear supernatant and the solution was heated. The pink color formed by the reaction of TBA with MDA was read at 532 nm against the blank. Standard malondialdehyde in a different concentration (0-23 nM) was used. The values were expressed as nM of MDA/mg protein (Slater & Sawyer, 1971).

2.8.2. Determination of reduced glutathione (GSH)

The deproteinization of kidney homogenate (supernatant) was made by using 20% TCA and then centrifugation was performed. 0.25 ml of supernatant, 2 ml of DTNB reagent, and phosphate buffer were added. The yellow color produced was measured at 412 nm. Different concentrations (10-50 µg) of standard glutathione were prepared. The concentration of GSH was mentioned as GSH mg/g protein (Moron et al., 1979).

2.8.3. Determination of Na^+/K^+ ATPase

In 0.2 ml homogenate, 1 ml of *tris*-hydrochloride buffer, and 0.2 ml each of sodium chloride, magnesium sulfate, EDTA, potassium chloride, and ATP were added. The mixture was incubated for 15 minutes at 36 °C. The reaction was arrested by 1.0 ml of TCA (10%), and centrifuged. The phosphorus content of the solution was measured and the enzymatic activity was expressed as nM of IP liberated/gm protein/min (Lowry et al., 1951).

2.9. Histopathological examination

A 5 µm portion was prepared, after which the sections were stained with hematoxylin and eosin (H&E), and assessed for general morphological alteration under the light microscope (400× magnification) and the photographs were taken.

2.10. Statistical analysis

All variables were analyzed by Graph Pad Prism (version 5.01), after implementing ANOVA with Dunnett's post-hoc test. Data was given in terms of mean ± standard error of mean (SEM) (n = 6). Among all tested groups, a statistical difference at the level of $p < 0.05$ was considered statistically significant.

3. Results and discussion

Antioxidants have been investigated for their potential therapeutic effects in diabetes and DN. Antioxidants are substances that reduce oxidative stress and thereby free radical production. Hyperglycemia leads to renal tissue damage by modifications of many hemodynamic factors (Ashrafi et al., 2017). Oxidative stress generated during DN is responsible for the apoptosis of renal tissue (Kukner et al., 2009).

The injection of STZ into the experimental rats in this study resulted in permanent diabetes due to the toxic effects of STZ on the pancreatic beta cells, leading to their dysfunction and subsequent disruption of insulin production, and, in turn, contributed to the development of hyperglycemia and OS in the renal tissue (Daniel et al., 2015; Wang et al., 2016).

Hyperglycemia is a vital tool for monitoring DN development (Wang et al., 2016). As indicated in Figure 1, at the end of the 4th week, fasting BGL was estimated. DN rats demonstrated markedly elevated levels of BGL ($p < 0.001$) as compared to control rats indicating severe destruction of beta cells. Administration of lycopene and CoQ10 alone as well as in combination markedly reduced the BGL ($p < 0.001$) compared to DN rats by inhibiting activation of hemodynamic pathways. The result was matched with the formerly reported research work (Pansare et al., 2021).

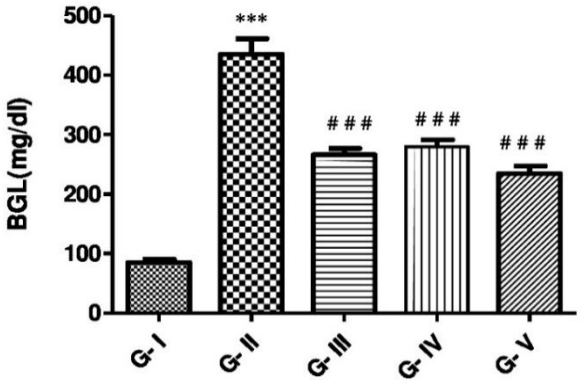

Figure 1. Lycopene, CoQ10, and its combined effects on BGL
Data was mentioned in terms of mean ± SEM (n=6).
ANOVA was applied with the Dunnett t-test for analysis.
$^{*}p < 0.05$, $^{**}p < 0.01$, $^{***}p < 0.001$ compared to normal and $^{\#}p < 0.05$, $^{\#\#}p < 0.01$, $^{\#\#\#}p < 0.001$ compared to DN.

STZ-induced diabetic rats showed a remarkable loss in body weight. Depletion in body weight after STZ injection might be due to the oxidation of tissue proteins, disruption of muscle tissue, and gluconeogenesis (Daniel et al., 2015). It is considered that renal hypertrophy is the main pathological indicator of diabetes-induced renal dysfunction (Ghule et al., 2012). In the present research, the kidney hypertrophy index of STZ-treated rats was notably raised due to alteration in kidney and body weight as compared with normal rats ($p < 0.01$). This could be due to structural damage to renal tissue. It is previously reported that kidney hypertrophy has been linked to increased kidney weight in DM because of excessive usage of glucose, and an elevated synthesis of protein and phospholipids in the renal tissue (Mogensen, 2004; Teoh et al., 2010). In DN rats treated with lycopene, the kidney hypertrophy index was markedly decreased as expected ($p < 0.05$). When compared to the STZ rats, rats treated with the combination of CoQ10 and lycopene showed

markedly decreased levels of kidney hypertrophy index ($p < 0.01$) than rats treated with only lycopene (Figure 2).

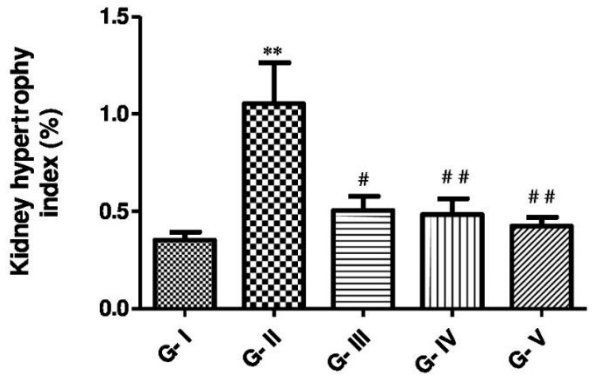

Figure 2. Lycopene, CoQ10, and its combined effects on kidney hypertrophy index

Data was mentioned in terms of mean ± SEM (n=6).
ANOVA was applied with the Dunnett t-test for analysis.
$^{*}p < 0.05$, $^{**}p < 0.01$, $^{***}p < 0.001$ compared to normal and $^{\#}p < 0.05$, $^{\#\#}p < 0.01$, $^{\#\#\#}p < 0.001$ compared to DN.

Long-term hyperglycemia leads to polyuria in DM. In the current research, it was noticed that DN rats displayed a remarkable increase in urine volume (24 h) ($p < 0.001$). It was demonstrated that the level of renal function biomarkers i.e. creatinine, albumin, total protein, total bilirubin, and uric acid were notably increased in DN rats ($p < 0.001$) indicating abnormalities in the excretory and regulatory function of the kidney leading to interstitial atrophy, necrosis of epithelial cells due to oxidative damage (Akinnuga et al., 2019; Lee & Ku, 2008; Nakagawa et al., 2005; Yokozawa et al., 2005). These alterations in biomarkers level were due to the accumulation of glucose in blood and urine (Sangar & Singh, 2016). Microalbuminuria and creatinine are the key indicators of renal failure. DN rats showed remarkable reduction in creatinine clearance due to damage to the tubule cells ($p < 0.001$). The present reports indicated that DN rats treated with antioxidants lycopene and CoQ10 showed markedly decreased levels of urine output ($p < 0.01$), renal biomarkers such as creatinine, albumin, total protein, total bilirubin, and uric acid whereas rats administered with their combination showed a marked reduction in these levels ($p < 0.001$) compared with single treatments with these agents. The creatinine clearance also increased significantly after treatment with both antioxidants ($p < 0.001$) (Table 1).

Table 1. Lycopene, CoQ10, and its combined effects on biochemical parameters

Parameters	Group I	Group II	Group III	Group IV	Group V
Urine volume (ml/day)	24.4 ± 1.04	90.0 ± 1.45***	59.0 ± 2.39###	61.6 ± 1.43###	45.5 ± 1.93###
Urine creatinine (mg/dl)	1.09 ± 0.15	3.31 ± 0.40***	1.85 ± 0.33#	1.76 ± 0.27#	1.39 ± 0.31##
Creatinine clearance (ml/min)	1.49 ± 0.14	0.30 ± 0.03***	0.66 ± 0.04###	0.79 ± 0.03###	1.10 ± 0.06###
Urine albumin (g/dl)	1.66 ± 0.115	4.68 ± 0.210***	3.51 ± 0.185##	2.93 ± 0.265###	2.43 ± 0.170###
Total protein (g/dl)	6.79 ± 0.651	13.81 ± 1.073***	9.69 ± 0.998##	10.08 ± 0.663#	8.35 ± 0.642###
Total bilirubin (mg/dl)	0.81 ± 0.20	2.31 ± 0.37**	1.08 ± 0.26##	1.31 ± 0.16#	1.07 ± 0.15##
Uric acid (mg/dl)	2.21 ± 0.244	7.77 ± 0.296***	5.53 ± 0.415##	5.33 ± 0.445##	4.36 ± 0.479###
Total cholesterol (mg/dl)	75.44 ± 4.87	144.3 ± 4.59***	112.5 ± 6.64##	106.4 ± 6.67###	83.07 ± 2.87###
Triglyceride (mg/dl)	71.33 ± 7.97	165.3 ± 4.61***	107.3 ± 2.95###	110.1 ± 4.01###	92.63 ± 2.38###

Data was mentioned in terms of mean ± SEM (n=6).
ANOVA was applied with the Dunnett t-test for analysis.
$^{*}p < 0.05$, $^{**}p < 0.01$, $^{***}p < 0.001$ compared to normal and $^{\#}p < 0.05$, $^{\#\#}p < 0.01$, $^{\#\#\#}p < 0.001$ compared to DN.

It was found that chronic hyperglycemia causes significant dyslipidemia in DN rats due to abnormal insulin regulation ($p < 0.001$). Insulin deficiency causes high serum lipid levels by the mobilization of free fatty acids. It also hydrolyzes triglycerides by stimulating lipoprotein lipase (Raghunathan et al., 2014; Wang et al., 2011). Research has proclaimed the relationship between aberrant lipid levels and the risk of the succession of DN (Marcovecchio et al., 2011). In this investigation, increased levels of total cholesterol and triglycerides in diabetic rats were remarkably lowered with the 4-week therapy of lycopene, CoQ10 alone, and a combination of both, which may be added to its renoprotective effects in DN ($p < 0.001$) (Table 1).

CRP appears in blood during an inflammatory process, which increases significantly in diabetes conditions ($p < 0.001$) due to tissue injuries. It was found that after the treatment, lycopene significantly declined the CRP level ($p < 0.01$). STZ-exposed rats treated by CoQ10 alone remarkably showed reduced levels of CRP ($p < 0.05$). Whereas simultaneous treatment with lycopene and CoQ10 of DN rats more remarkably declined the CRP level than single treatments ($p < 0.001$) (Figure 3).

STZ-treated animals show declined defense mechanisms of antioxidants in OS (Orhan et al., 2006) (Figure 4). In this investigation, excessive ROS generated in DN rats led to the oxidation of biomolecules, particularly lipid peroxidation and significantly increased its level ($p < 0.001$). LPO is considered a pivotal indicator of OS. Excessive LPO is responsible for high glucose levels by damaging the beta cells (Patel et al., 2014). Antioxidants prevent the interaction between free radicals and biological substances (Arora et al., 2002). It was found that after a 4-week treatment of lycopene, CoQ10, and their simultaneous dose to the STZ rats, they demonstrated a notable reduction in LPO level as correlated with DN groups ($p < 0.001$) (Figure 4a).

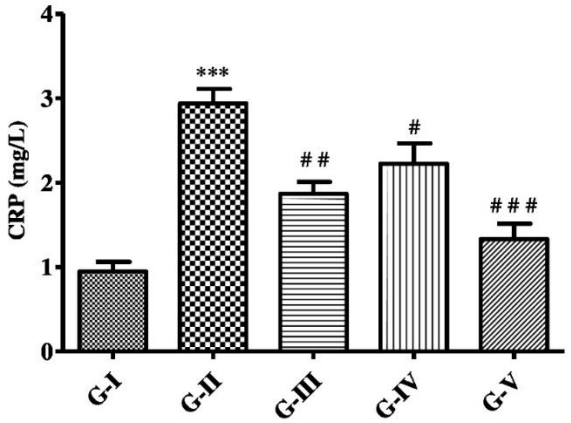

Figure 3. Lycopene, CoQ10, and its combined effects on serum CRP level

Data was mentioned in terms of mean ± SEM (n=6).
ANOVA was applied with the Dunnett t-test for analysis.
$^{*}p < 0.05$, $^{**}p < 0.01$, $^{***}p < 0.001$ compared to normal and $^{\#}p < 0.05$, $^{\#\#}p < 0.01$, $^{\#\#\#}p < 0.001$ compared to DN.

Reduced glutathione (GSH) is an endogenous antioxidant having a major function in numerous biological activities such as cellular growth, protein synthesis, and metal chelation (Bartoli et al., 2017) and maintains redox balance in the cells. GSH has the property to redevelop another hydrophobic antioxidant (Sharma et al., 2012). The significant decline of GSH levels in the kidney tissue of DN rats hastens OS ($p < 0.001$) (Patel et al., 2014) (Figure 4b). This result was in line with earlier recorded studies (Jain et al., 2020; Suvarchala Reddy et al., 2019). Rats that received lycopene showed a remarkable raise in GSH levels than CoQ10 ($p < 0.001$) but a combination of both showed a more beneficial elevation in GSH levels compared with the DN rats ($p < 0.001$).

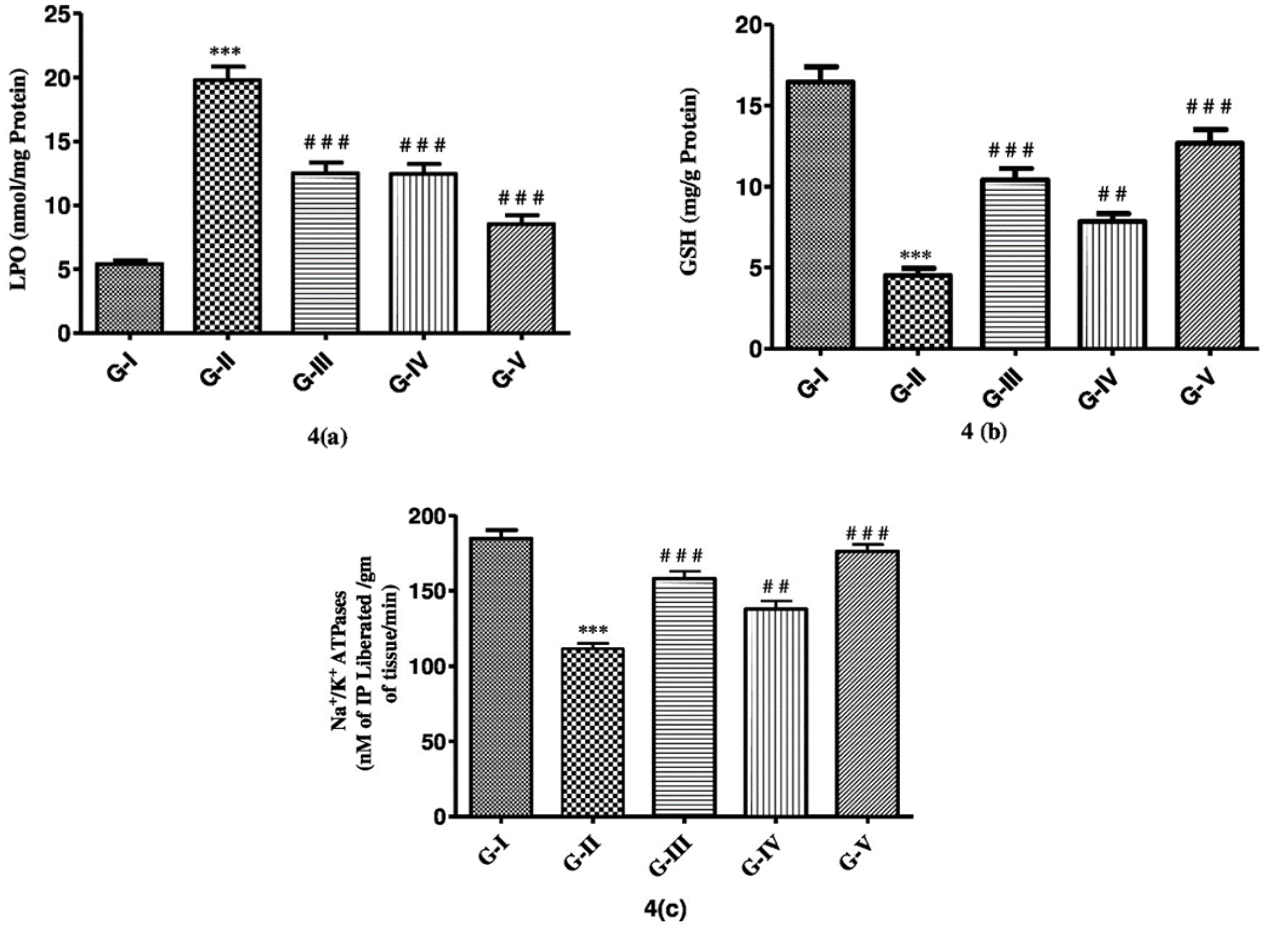

Figure 4. Lycopene, CoQ10, and its combined effects on markers of oxidative stress in the renal tissue

4(a) LPO, 4(b) GSH, 4(c) Na^+/K^+ ATPases

Data was mentioned in terms of mean ± SEM (n=6).

ANOVA was applied with the Dunnett t-test for analysis.

$^{*}p < 0.05$, $^{**}p < 0.01$, $^{***}p < 0.001$ compared to normal and $^{\#}p < 0.05$, $^{\#\#}p < 0.01$, $^{\#\#\#}p < 0.001$ compared to DN.

The activity of the membrane-bound ATPase i.e. Na^+/K^+ ATPase was notably declined in DN rats ($p < 0.001$) when compared with control rats. This might be due to changes in the ionic homeostasis of membrane-bound enzymes (Senthil et al., 2007). In this study, it was noticed that treatment with lycopene alone more effectively improved membrane-bound enzyme activity ($p < 0.001$) than CoQ10 but the combination exerted a more potent increase in levels of membrane-bounded enzymes ($p < 0.001$). This finding provides elucidation regarding the concurrent administration of antioxidants, highlighting their synergistic functionality when used in combination (Figure 4c).

A histopathological study of the kidney was performed to figure out whether these biochemical changes in renal function biomarkers cause structural alterations at the microscopic level. This analysis conceded that long-term diabetes was responsible for pronounced morphological alteration in the anatomy of the glomerulus and tubular cells of the kidney. It was noticed that DN groups showed structural modification such as the rise in the stiffness of the glomerular basement membrane, and degeneration of tubular cells that hastened vacuole formation in the tubule (Figure 5b). Rats administered with antioxidants such as lycopene and CoQ10 alone showed lesser glomeruli impairment with minimal tubular cell degeneration (Figure 5c and 5d). Whereas, treatment with the combination of both antioxidants more effectively decreased abnormal morphological changes in glomeruli and tubular cells of DN rats, and protected renal tissue from diabetes-associated injury (Figure 5e). The histological findings cleared that these structural changes were due to the abnormal excretory and regulatory function of the kidney and this alterations were markedly reversed by antioxidant therapy.

4. Conclusions

The present investigation suggested that natural antioxidants such as lycopene and CoQ10 can modulate hyperglycemia and oxidative stress generated due to DM. The simultaneous treatment of both lycopene and CoQ10 displayed a remarkable renoprotective effect

by improving the function of the renal antioxidant system and altering morphological changes. The findings of this investigation demonstrated that the combined effect of lycopene and CoQ10 were due to their antioxidant property which attenuate the development of DN.

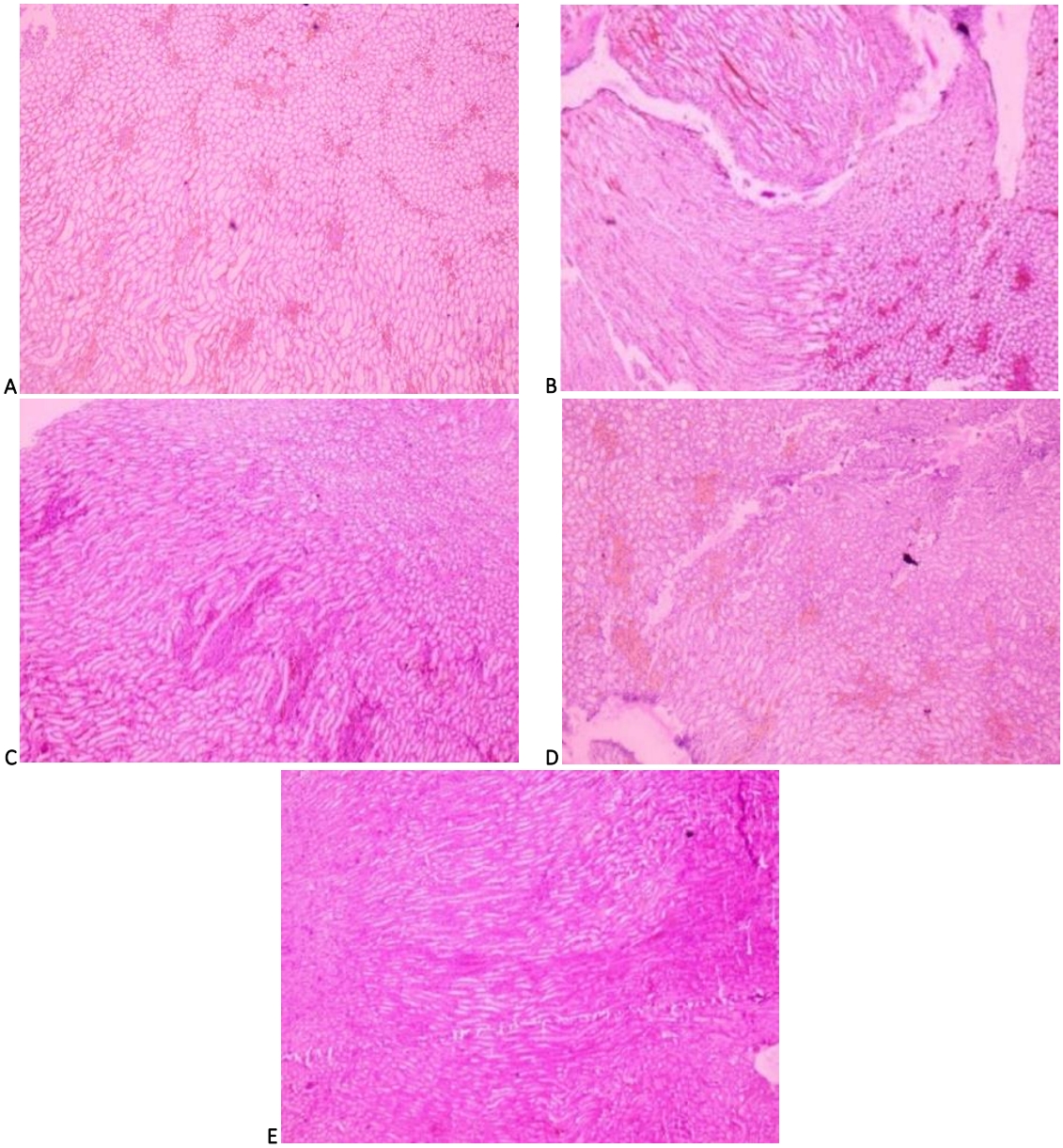

Figure 5. Photomicrographs of histopathological analysis of renal tissue of rats by H & E staining

A) Group- I, B) Group- II, C) Group- III, D) Group- IV, E) Group- V

A) Group-I: The renal tissue section of control rats showed a normal structure of the glomerulus and renal tubules.

B) Group-II: Diabetic rats showed a raised thickness of the basement membrane of glomeruli and degeneration of some tubular epithelial cells, which are prone to glomerulosclerosis and tubular atrophy.

C) Group-III: Rats treated with lycopene show lesser glomeruli impairment and tubular cell degeneration.

D) Group-IV: Tissue section showing fewer tubular vacuole formation.

E) Group V: The renal section treated with the simultaneous dose of lycopene and CoQ10 shows a normal appearance of glomeruli with improvement in tubular degeneration.

Acknowledgments

All the authors are grateful to Universal Industries, Sinnar (Nashik) for providing lycopene drug and Zydus Cadila, Ahmedabad, (India) for CoQ10 drug samples.

Conflict of interest

The authors confirm that there are no known conflicts of interest.

Statement of ethics

The methods in this study was permitted by IAEC of the organization, (SSDJ/IAEC/2021-22/03) and carried according to the CPCSEA guidelines.

Availability of data and materials

All data generated or analyzed during this study are included in this published article.

Funding

None.

CRediT authorship contribution statement

Pooja B. Rasal: Conceptualization, Investigation, Writing original draft
Gaurav N. Kasar: Conceptualization, Investigation, Writing original draft
Manoj Mahajan: Investigation, Supervision, Review and editing, Software
Aman Upaganlawar: Investigation, Supervision, Review and editing, Software
Chandrashekhar Upasani: Formal analysis, Methodology, Validation and supervision

ORCID Numbers of the Authors

P. B. Rasal: 0009-0003-3138-7340
G. N. Kasar: 0000-0001-6098-2956
M. Mahajan: 0000-0003-4204-2666
A. Upaganlawar: 0000-0003-4122-5081
C. Upasani: 0000-0003-4446-1557

Supplementary File

None.

Publisher's Note

All claims expressed in this article are solely those of the authors and do not necessarily represent those of their affiliated organizations, or those of the publisher, the editors and the reviewers. Any product that may be evaluated in this article, or claim that may be made by its manufacturer, is not guaranteed or endorsed by the publisher.

This is an open-access article distributed under the terms of the Creative Commons Attribution 4.0 International License (CC BY). The use, distribution or reproduction in other forums is permitted, provided the original author(s) and the copyright owner(s) are credited and that the original publication in this journal is cited, in accordance with accepted academic practice. No use, distribution or reproduction is permitted which does not comply with these terms.

References

Akbar, S., Bellary, S., & Griffiths, H. R. (2011). Dietary antioxidant interventions in type 2 diabetes patients: a meta-analysis. *The British Journal of Diabetes & Vascular Disease, 11*(2), 62-68.

Akinnuga, A. M., Bamidele, O., & Adewumi, A. J. (2019). Evaluation of kidney function parameters in diabetic rats following virgin coconut oil diet. *Folia Medica, 61*(2), 249-257.

Arora, A., Sairam, R., & Srivastava, G. (2002). Oxidative stress and antioxidative system in plants. *Current Science, 82*(10), 1227-1238.

Arora, M. K., & Singh, U. K. (2013). Molecular mechanisms in the pathogenesis of diabetic nephropathy: an update. *Vascular Pharmacology, 58*(4), 259-271.

Ashrafi, M., Nazifi, S., Namazi, F., Kazemipour, N., Karimi, B., Goudarzi, T., & Talebanzadeh, S. (2017). Renal protective effect of saffron aqueous extract in streptozotocin induced diabetic rats. *International Journal of Medical Research and Health Sciences, 6*, 151-161.

Balakumar, P., Arora, M. K., & Singh, M. (2009). Emerging role of PPAR ligands in the management of diabetic nephropathy. *Pharmacological Research, 60*(3), 170-173.

Bartoli, C. G., Buet, A., Gergoff Grozeff, G., Galatro, A., & Simontacchi, M. (2017). Ascorbate-glutathione cycle and abiotic stress tolerance in plants. In M. Hossain, S. Munné-Bosch, D. Burritt, P. Diaz-Vivancos, M. Fujita, & A. Lorence (Eds.), *Ascorbic Acid in Plant Growth, Development and Stress Tolerance* (pp. 177-200): Springer, Cham.

Bhattacharjee, N., Barma, S., Konwar, N., Dewanjee, S., & Manna, P. (2016). Mechanistic insight of diabetic nephropathy and its pharmacotherapeutic targets: an update. *European Journal of Pharmacology, 791*, 8-24.

Daniel, E., Mohammed, A., Tanko, Y., & Ahmed, A. (2015). Effects of lycopene on kidney antioxidant enzyme activities and functions in streptozotocin-induced diabetic Wistar rats. *Cell Biology, 3*(1), 1-13.

Elsayed, A., Elkomy, A., Elkammar, R., Youssef, G., Abdelhiee, E. Y., Abdo, W., Fadl, S. E., Soliman, A., & Aboubakr, M. (2021). Synergistic protective effects of lycopene and N-acetylcysteine against cisplatin-induced hepatorenal toxicity in rats. *Scientific Reports, 11*(1), 1-10.

Esu, K. D., Bakare, A. O., & Owoyele, B. V. (2022). Effects of co-administration of vitamin E and lithium chloride on chronic constriction injury-induced neuropathy in male Wistar rats: Focus on antioxidant and anti-inflammatory mechanisms. *Pain Practice, 22*(2), 148-158.

Fakhruddin, S., Alanazi, W., & Jackson, K. E. (2017). Diabetes-induced reactive oxygen species: mechanism of their generation and role in renal injury. *Journal of Diabetes Research, 2017*, 8379327.

Forbes, J. M., Coughlan, M. T., & Cooper, M. E. (2008). Oxidative stress as a major culprit in kidney disease in diabetes. *Diabetes, 57*(6), 1446-1454.

Fuller, B., Smith, D., Howerton, A., & Kern, D. (2006). Anti-inflammatory effects of CoQ10 and colorless carotenoids. *Journal of Cosmetic Dermatology, 5*(1), 30-38.

Ghule, A. E., Jadhav, S. S., & Bodhankar, S. L. (2012). Trigonelline ameliorates diabetic hypertensive nephropathy by suppression of oxidative stress in kidney and reduction in renal cell apoptosis and fibrosis in streptozotocin induced neonatal diabetic (nSTZ) rats. *International Immunopharmacology, 14*(4), 740-748.

Gunasekera, R. S., Sewgobind, K., Desai, S., Dunn, L., Black, H. S., McKeehan, W. L., & Patil, B. (2007). Lycopene and lutein inhibit proliferation in rat prostate carcinoma cells. *Nutrition and Cancer, 58*(2), 171-177.

Hodgson, J., Watts, G., Playford, D., Burke, V., & Croft, K. (2002). Coenzyme Q10 improves blood pressure and glycaemic control: a controlled trial in subjects with type 2 diabetes. *European Journal of Clinical Nutrition, 56*(11), 1137-1142.

Horie, K., Miyata, T., Maeda, K., Miyata, S., Sugiyama, S., Sakai, H., De Strihou, C. V. Y., Monnier, V. M., Witztum, J. L., *et al.* (1997). Immunohistochemical colocalization of glycoxidation products and lipid peroxidation products in diabetic renal glomerular lesions. Implication for glycoxidative stress in the pathogenesis of diabetic nephropathy. *The Journal of Clinical Investigation, 100*(12), 2995-3004.

Ighodaro, O. M. (2018). Molecular pathways associated with oxidative stress in diabetes mellitus. *Biomedicine & Pharmacotherapy, 108*, 656-662.

Jain, M. D. (2015). Silibinin, a bioactive flavanone, prevents the progression of early diabetic nephropathy in experimental type-2 diabetic rats. *International Journal of Green Pharmacy, 9*(2), 118-124.

Jain, P. G., Patil, D. J., Nayase, P., Surana, S. J., & Patil, P. P. (2020). Protective effect of diosgenin on streptozotocin induced diabetic nephropathy in experimental rats. *International Journal of Pharmaceutical Sciences and Drug Research, 12*(2), 201-207.

Kashihara, N., Haruna, Y., K Kondeti, V., & S Kanwar, Y. (2010). Oxidative stress in diabetic nephropathy. *Current Medicinal Chemistry, 17*(34), 4256-4269.

Kukner, A., Colakoglu, N., Ozogul, C., Naziroglu, M., & Firat, T. (2009). The effects of combined vitamin C and E in streptozotocin-induced diabetic rat kidney. *Clinical Reviews and Opinions, 1*(2), 29-36.

Lavender, S., Hilton, P., & Jones, N. (1969). The measurement of glomerular filtration-rate in renal disease. *The Lancet, 294*(7632), 1216-1219.

Lee, H. S., & Ku, S. K. (2008). Effect of *Picrorrhiza rhizoma* extracts on early diabetic nephropathy in streptozotocin-induced diabetic rats. *Journal of Medicinal Food, 11*(2), 294-301.

Leh, H. E., & Lee, L. K. (2022). Lycopene: A potent antioxidant for the amelioration of type II diabetes mellitus. *Molecules, 27*(7), 2335.

Li, X., Xiao, H., Lin, C., Sun, W., Wu, T., Wang, J., Chen, B., Chen, X., & Cheng, D. (2019). Synergistic effects of liposomes encapsulating atorvastatin calcium and curcumin and targeting dysfunctional endothelial cells in reducing atherosclerosis. *International Journal of Nanomedicine, 14*, 649-665.

Liu, W., Zhang, X., Liu, P., Shen, X., Lan, T., Li, W., Jiang, Q., Xie, X., & Huang, H. (2010). Effects of berberine on matrix accumulation and NF-kappa B signal pathway in alloxan-induced diabetic mice with renal injury. *European Journal of Pharmacology, 638*(1-3), 150-155.

Lowry, O. H., Rosebrough, N. J., Farr, A. L., & Randall, R. J. (1951). Protein measurement with the Folin phenol reagent. *Journal of Biological Chemistry, 193*, 265-275.

Mahajan, M., Upasani, C., Upaganlawar, A., & Gulecha, V. (2020). Renoprotective effect of co-enzyme Q10 and N-acetylcysteine on streptozotocin-induced diabetic nephropathy in rats. *International Journal of Diabetes and Clinical Research, 7*(2), 1-12.

Mahmoodnia, L., Mohammadi, K., & Masumi, R. (2017). Ameliorative effect of lycopene effect on cisplatin-induced nephropathy in patient. *Journal of Nephropathology, 6*(3), 144-149.

Marcovecchio, M. L., Lucantoni, M., & Chiarelli, F. (2011). Role of chronic and acute hyperglycemia in the development of diabetes complications. *Diabetes Technology & Therapeutics, 13*(3), 389-394.

Mogensen, C. E. (2004). Microalbuminuria, blood pressure and diabetic renal disease: origin and development of ideas. In C. E. Mogensen (Ed.), *The Kidney and Hypertension in Diabetes Mellitus* (pp. 905-960): CRC Press.

Moron, M. S., Depierre, J. W., & Mannervik, B. (1979). Levels of glutathione, glutathione reductase and glutathione S-transferase activities in rat lung and liver. *Biochimica et Biophysica Acta (BBA)-General Subjects, 582*(1), 67-78.

Nakagawa, T., Yokozawa, T., Yamabe, N., Goto, H., Shibahara, N., Rhyn, D. Y., & Shimada, Y. (2005). Long-term treatment with Hachimi-jio-gan attenuates kidney damage in spontaneously diabetic WBN/Kob rats. *Journal of Pharmacy and Pharmacology, 57*(9), 1205-1212.

Orhan, N., Aslan, M., Orhan, D. D., Ergun, F., & Yeşilada, E. (2006). In-vivo assessment of antidiabetic and antioxidant activities of grapevine leaves (*Vitis vinifera*) in diabetic rats. *Journal of Ethnopharmacology, 108*(2), 280-286.

Pansare, K., Upasani, C., Upaganlwar, A., Sonawane, G., & Patil, C. (2021). Pre-clinical study of lycopene alone and in combination with olive oil in streptozotocin-induced diabetic nephropathy. *Vidyabharati International Interdisciplinary Research Journal, 5*(Special Issue on International Virtual Conference on Innovation in Multidisciplinary Studies-IVCIMS 2021), 320-332.

Parohan, M., Sarraf, P., Javanbakht, M. H., Foroushani, A. R., Ranji-Burachaloo, S., & Djalali, M. (2021). The synergistic effects of nano-curcumin and coenzyme Q10 supplementation in migraine prophylaxis: A randomized, placebo-controlled, double-blind trial. *Nutritional Neuroscience, 24*(4), 317-326.

Patel, A. N., Bandawane, D. D., & Mhetre, N. K. (2014). Pomegranate (*Punica granatum* Linn.) leaves attenuate disturbed glucose homeostasis and hyperglycemia mediated hyperlipidemia and oxidative stress in streptozotocin induced diabetic rats. *European Journal of Integrative Medicine, 6*(3), 307-321.

Platé, M., Guillotin, D., & Chambers, R. C. (2020). The promise of mTOR as a therapeutic target pathway in idiopathic pulmonary fibrosis. *European Respiratory Review, 29*, 200269.

Puah, B. P., Jalil, J., Attiq, A., & Kamisah, Y. (2021). New insights into molecular mechanism behind anti-cancer activities of lycopene. *Molecules, 26*(13), 3888.

Raghunathan, S., Tank, P., Bhadada, S., & Patel, B. (2014). Evaluation of buspirone on streptozotocin induced type 1 diabetes and its associated complications. *BioMed Research International, 2014*, 948427.

Ritz, E. (2013). Clinical manifestations and natural history of diabetic kidney disease. *Medical Clinics, 97*(1), 19-29.

Ritz, E., Zeng, X. X., & Rychlík, I. (2011). Clinical manifestation and natural history of diabetic nephropathy. *Diabetes and the Kidney, 170*, 19-27.

Rojas-Rivera, J., Ortiz, A., & Egido, J. (2012). Antioxidants in kidney diseases: the impact of bardoxolone methyl. *International Journal of Nephrology, 2012*, 321714.

Rosenfeldt, F. L., Haas, S. J., Krum, H., Hadj, A., Ng, K., Leong, J. Y., & Watts, G. F. (2007). Coenzyme Q10 in the treatment of hypertension: a meta-analysis of the clinical trials. *Journal of Human Hypertension, 21*(4), 297-306.

Sangar, C., & Singh, J. (2016). Effects of Streptozotocin-induced Type I Diabetes Mellitus on Cation contents in Urinary Bladder tissues of the rat. *International Journal of Pharmaceutical Sciences and Research, 7*(2), 789-797.

Sayahi, M., & Shirali, S. (2017). The antidiabetic and antioxidant effects of carotenoids: a review. *Asian Journal of Pharmaceutical Research and Health Care, 9*(4), 186-191.

Schena, F. P., & Gesualdo, L. (2005). Pathogenetic mechanisms of diabetic nephropathy. *Journal of the American Society of Nephrology, 16*(3), S30-S33.

Senthil, S., Sridevi, M., & Pugalendi, K. (2007). Cardioprotective effect of oleanolic acid on isoproterenol-induced myocardial ischemia in rats. *Toxicologic Pathology, 35*(3), 418-423.

Sharma, P., Jha, A. B., Dubey, R. S., & Pessarakli, M. (2012). Reactive oxygen species, oxidative damage, and antioxidative defense mechanism in plants under stressful conditions. *Journal of Botany, 2012*, 217037.

Shi, J., Kakuda, Y., & Yeung, D. (2004). Antioxidative properties of lycopene and other carotenoids from tomatoes: synergistic effects. *Biofactors, 21*(1-4), 203-210.

Slater, T., & Sawyer, B. (1971). The stimulatory effects of carbon tetrachloride and other halogenoalkanes on peroxidative reactions in rat liver fractions in vitro. General features of the systems used. *Biochemical Journal, 123*(5), 805-814.

Sudamrao Garud, M., & Anant Kulkarni, Y. (2014). Hyperglycemia to nephropathy via transforming growth factor beta. *Current Diabetes Reviews, 10*(3), 182-189.

Suvarchala Reddy, V. N., Ganga Raju, M., Alekhya, B., & Subrahmanyam, C. (2019). Attenuation of Diabetic Nephropathy In Streptozotocin Induced Diabetic Rats By Methanolic Extract Of Bougainvillea Spectabilis Aerial Parts. *International Journal of Pharmaceutical Sciences and Drug Research, 11*(1), 16-21.

Tavafi, M. (2013). Diabetic nephropathy and antioxidants. *Journal of Nephropathology, 2*(1), 20-27.

Teoh, S., Latiff, A. A., & Das, S. (2010). Histological changes in the kidneys of experimental diabetic rats fed with *Momordica charantia* (bitter gourd) extract. *Romanian Journal of Morphology and Embryology, 51*(1), 91-95.

Upaganlawar, A., & Gandhi, H. (2010). Effect of vitamin E alone and in combination with lycopene on biochemical and histopathological alterations in isoproterenol-induced myocardial infarction in rats. *Journal of Pharmacology and Pharmacotherapeutics, 1*(1), 24-31.

Vetvicka, V., & Vetvickova, J. (2018). Combination therapy with glucan and coenzyme Q10 in murine experimental autoimmune disease and cancer. *Anticancer Research, 38*(6), 3291-3297.

Wang, G. G., Lu, X. H., Li, W., Zhao, X., & Zhang, C. (2011). Protective effects of luteolin on diabetic nephropathy in STZ-induced diabetic rats. *Evidence-Based Complementary and Alternative Medicine, 2011*, 323171.

Wang, S., Yang, Z., Xiong, F., Chen, C., Chao, X., Huang, J., & Huang, H. (2016). Betulinic acid ameliorates experimental diabetic-induced renal inflammation and fibrosis via inhibiting the activation of NF-κB signaling pathway. *Molecular and Cellular Endocrinology, 434*, 135-143.

Yokozawa, T., Nakagawa, T., Oya, T., Okubo, T., & Juneja, L. R. (2005). Green tea polyphenols and dietary fibre protect against kidney damage in rats with diabetic nephropathy. *Journal of Pharmacy and Pharmacology, 57*(6), 773-780.

Zhu, J., Wang, C. G., & Xu, Y. G. (2011). Lycopene attenuates endothelial dysfunction in streptozotocin-induced diabetic rats by reducing oxidative stress. *Pharmaceutical Biology, 49*(11), 1144-1149.

Zhu, R., Chen, B., Bai, Y., Miao, T., Rui, L., Zhang, H., Xia, B., Li, Y., Gao, S., *et al.* (2020). Lycopene in protection against obesity and diabetes: A mechanistic review. *Pharmacological Research, 159*, 104966.

ijpbp.com